



LAWRENCE
LIVERMORE
NATIONAL
LABORATORY

International Symposium on Systems and Human Science - SSR2005

K. J. Addison

March 17, 2005

International Symposium on Systems and Human Science
San Francisco, CA, United States
March 9, 2005 through March 11, 2005

Disclaimer

This document was prepared as an account of work sponsored by an agency of the United States Government. Neither the United States Government nor the University of California nor any of their employees, makes any warranty, express or implied, or assumes any legal liability or responsibility for the accuracy, completeness, or usefulness of any information, apparatus, product, or process disclosed, or represents that its use would not infringe privately owned rights. Reference herein to any specific commercial product, process, or service by trade name, trademark, manufacturer, or otherwise, does not necessarily constitute or imply its endorsement, recommendation, or favoring by the United States Government or the University of California. The views and opinions of authors expressed herein do not necessarily state or reflect those of the United States Government or the University of California, and shall not be used for advertising or product endorsement purposes.

SSR2005: March 9-11, 2005, San Francisco
International Symposium on Systems and Human Science



Proceedings for SSR 2005

UCRL-PROC-210181

[Conference Program](#)[Papers by Author](#)[Send E-mail](#)

Contact Information

[By Name](#)[By Affiliation](#)

This document was prepared as an account of work sponsored by an agency of the United States Government. The United States Government nor the University of California nor any of their employees, makes any warrant express or implied, or assumes any legal liability or responsibility for the accuracy, completeness, or usefulness of any information, apparatus, product, or process disclosed, or represents that its use would not infringe privately owned rights. Reference herein to any specific commercial product, process, or service by trade name, trademark, manufacturer, or otherwise, does not necessarily constitute or imply its endorsement, recommendation, or favor by the United States Government or the University of California. The views and opinions of authors expressed herein do not necessarily state or reflect those of the United States Government or the University of California, and shall not be used for advertising or product endorsement purposes.

This work was performed under the auspices of the U.S. Department of Energy by University of California, Livermore National Laboratory under Contract W-7405-Eng-48.

SSR2005 Symposium Program

Wednesday, March 9th

8:00	Conference Registration	Sequoia Foyer
8:30	Continental Breakfast	Sequoia Foyer

9:00	Opening Comments Ed Jones- <i>Lawrence Livermore National Laboratory</i> , Prof. Tatsuo Arai- <i>Osaka University</i>	Sequoia Room
9:30-10:15	Session 1 M. Makowski – “ <i>Model-based Decision Making Support for Problems with Conflicting Goals</i> ” C. Kaskiris – “ <i>Mobile Agents: A Ubiquitous Multi-Agent System for Human-Robotic Planetary Exploration</i> ”	Sequoia Room
10:15-10:30	Break	Sequoia Foyer
10:30-12:00	Session 1 (cont) H. Niho- <i>Excavation and Recovery of Non-stockpile Munitions in China</i> ” S. Nishide – “ <i>Wide Area Recognition for Safety and Security Preserving Robots</i> ” T. Takimoto- “ <i>Active Compensation for Oscillatory Motions in Human Control Behavior</i> ”	Sequoia Room

Wed., March 9th continued

12:00-1:00	Lunch		Bayshore Ballroom
1:00-3:00	Session 2		Sequoia Room
	<p>Sandia Speaker TBD</p> <p>T. Umetani – <i>“Identification and Localization of Buried Metal Object – High-Speed Model Matching Using Genetic Algorithm-“</i></p> <p>K. Inoue – <i>“Evaluation of Human Sense of Security for Coexisting Robots Using Virtual Reality 2nd Report: Evaluation of Humanoid Robots Passing by Humans in Corridors”</i></p> <p>J. Iio – <i>“Human Detection System Using Robust Silhouette Extraction from Surveillance Image”</i></p>		
3:00-3:15	Break		Sequoia Foyer
3:15 -5:00	Session3A	Sequoia Room	Session 3B Poplar Room
	<p>Y. Mae – <i>“ Person Identification by Color Pattern Acquired in Visual Tracking”</i></p> <p>S. Kawabata – <i>“Real-time Background Estimation from Occluded Image Using Iterative Optimal Projection Method”</i></p> <p>T. Hirayama – <i>“Development of Biometric Authentication API Based on Face Recognition – BioAPI++ ”</i></p> <p>K. Ohara – <i>“Application on Ubiquitous function for Human Life”</i></p> <p>K. Sakata – <i>“Wheelchair User Support System Using Humanoid robots – User Interface using Smart Handy Device-“</i></p> <p>Y. Miura – <i>“Value Judgment for Evaluating Sense of Security Provided by Nursing Care Robots Based on Prospect Theory Under Uncertainty”</i></p>		
5:15 -5:30	Break		
5:30-9:30	Reception		Bayshore Ballroom
	6:00 Guest Speaker TBD		

SSR2005 Symposium Program

Thursday, March 10th

8:00 Continental Breakfast Sequoia Foyer

8:30-10:15	<p>Session 4</p> <p>Keynote Speech– Prof. Hiroyuki Tamura, “<i>Structural Modeling and Decision Support for Dissolving Uneasiness Using Revised DEMATEL Methods</i>”</p> <p>T. Kanno – “<i>Integrated Simulation of Emergency Response of Related Organizations and Resident’s Behavior in Nuclear Disaster</i>”</p> <p>M. Nagase – “<i>Assessment of Safety Regulation by Social Simulation</i>”</p> <p>L. Wu – “<i>Construction Productivity Loss and Worker ss Behavior caused by Workspace Conflict</i>”</p>	Sequoia Room
------------	--	--------------

10:15-10:30 Break Sequoia Foyer

10:30-12:00	<p>Session 4 (cont)</p> <p>K. Hipel – “<i>Modeling Trust Using a Fuzzy Logic Approach</i>”</p> <p>T. Wu – “<i>An Approximate Dynamic Programming Approach for the Military Airlift Problem</i>”</p> <p>T. Moritani – “<i>Tracking Multiple Objects Occluding each Other Without Feature Extraction</i>”</p>	Sequoia Room
-------------	---	--------------

Thurs., March 10th continued

12:00-1:00	Lunch		Bayshore Ballroom	
1:00-3:00	<p>Session 5</p> <p>C. Kirchsteiger – <i>“Probabilistic Reliability Assessment for Complex Systems in the Absence of Operating Experience Data”</i></p> <p>K. Suzuki – <i>“Malfunction Diagnosis of the Feedback System Based on the Gap Metric”</i></p> <p>Y. Tanno – <i>“Distribution and the Information Security of Archive Contents”</i></p> <p>S. Mamada – <i>“A Polynomial Time Algorithm for the Two-Sink Location Problem in a Tree Dynamic Network”</i></p>		Sequoia Room	
3:00-3:15	Break			
3:15 -5:00	<p>Session6A</p> <p>T. Shimizu – <i>“Human Modeling of Residents’ Response in Nuclear Disaster”</i></p> <p>M. Tsai – <i>“The Human Related Issues of Knowledge”</i></p> <p>T. Ishii – <i>“Development of a Support System for Consensus Building with Elicitation of Concerns and Conflicts”</i></p>	Sequoia Room	<p>Session 6B</p> <p>Y. Hijikata – <i>“Distributed Video Data Management System of Monitoring Cameras for Security and Safety”</i></p> <p>T. Mashita – <i>“Error Analysis in HyperOmni Vision”</i></p> <p>T. Hirayama – <i>“Face Authentication System with Facial Personation Prevention by Using Infrared Images”</i></p>	Poplar Room

SSR2005 Symposium Program

Friday, March 11th

8:00 Continental Breakfast Sequoia Foyer

8:30-10:15	<p>Session 7</p> <p>D. Price – <i>“Vulnerability and Risk Assessment Using the Homeland-Defense Operational Planning System (HOPS)”</i></p> <p>Y. Iino – <i>“Development of a Support Tool for Risk Analysis in Health Care Process by HFMEA Method”</i></p> <p>M. Lee – <i>“The Organization Relationship for Construction Enterprise Resource Planning Project – Lessons Learned in Taiwan”</i></p>	Sequoia Room
------------	---	--------------

10:15-10:30 Break Sequoia Foyer

10:30-11:00	<p>Session 7 (cont)</p> <p>J. You – <i>“A Dispatch Model for Fire Fighting”</i></p>	Sequoia Room
11:00-11:30	<p>Closing Comments</p> <p>Prof. Tatsuo Arai-<i>Osaka University</i>, Ed Jones-<i>Lawrence Livermore National Laboratory</i></p>	

12:00-1:00 Box Lunches Sequoia Foyer

1:00-5:00 NIF Tour LLNL

SSR2005: March 9-11, 2005, San Francisco International Symposium on Systems and Human Science



Contact Listing by Affiliation

Institute for Energy:

Kirchsteiger, Christian
European Commission
DG-JRC
Institute for Energy
Probabilistic Risk & Availability Assessment of
Energy Systems
Westerduinweg 3 - 1755 Le Petten
The Netherlands
Phone: 31-224-56-5118 / Fax: 31-224-56-5641
E-mail: christian.kirchsteiger@jrc.nl

International Institute for Applied Systems Analysis (IIASA):

Makowski, Marek
International Institute for Applied Systems Analysis
A-2361 Laxenburg Austria
Phone: 43-2236-807-561 / Fax: 43-22236-71-313
E-mail: marek@iiasa.ac.at

Kansai University:

Tamura, Hiroyuki
Department of Electrical Engineering and Computer
Science
Faculty of Engineering
Kansai University
3-3-35 Yamate-cho, Suita, Osaka 564-8680, Japan
Phone: 81-6-6368-0829 / Fax: 81-6-6368-0829
E-mail: H.Tamura@kansai-u.ac.jp

Osaka University (con't):

Nishida, Shogo
Osaka University
1-3 Machikaneyama
Toyonaka, Osaka 560-8531 Japan

Nishide, Shun
Department of Systems Innovation
Graduate School of Engineering Science
Osaka University
1-3 Machikaneyama
Toyonaka, Osaka 560-8531 Japan
Phone: 81-6-6850-6366 / Fax: 81-6-6850
E-mail: nishide@arai-lab.sys.es.osaka-u.ac.jp

Nonaka, Seri
Department of Systems Innovation
Graduate School of Engineering Science
Osaka University
1-3 Machikaneyama
Toyonaka, Osaka 560-8531 Japan
Phone: 81-6-6850-6366 / Fax: 81-6-6850

Sakaguchi, Yukinobu
Department of Systems Innovation
Graduate School of Engineering Science
Osaka University
1-3 Machikaneyama
Toyonaka, Osaka 560-8531 Japan
Phone: / Fax:
E-mail: sakaguchi@arai-lab.sys.es.osaka-u.ac.jp

Sakata, Kotaro
Department of Systems Innovation
Graduate School of Engineering Science
Osaka University
1-3 Machikaneyama
Toyonaka, Osaka 560-8531 Japan

Kyoto University:

Fujishige, Satoru

Research Institute for Mathematical Science
Kyoto University
Sakyo-Ku, Kyoto 606-8502 Japan
Phone: 81-75-753-7250 / Fax: 81-75-753-7276
E-mail: fujishig@kurims.kyoto-u.ac.jp

Phone: 81-6-6850-6367 / Fax: 81-6-6850
E-mail: sakata@arai-lab.sys.es.osaka-u.ac

Sato, Kosuke

Department of Engineering Science
Osaka University
1-3 Machikaneyama
Toyonaka, Osaka 560-8531 Japan
Phone: 81-6-6850-6371 / Fax: 81-6-6850

Lawrence Livermore National Laboratory:

Durling, Ron

P.O. Box 808, L-182
Livermore, CA 94551
Phone: 925-422-1467 / Fax: (925) 422-3821
E-mail: durling1@llnl.gov

Suzuki, Keita

Graduate School of Engineering Science
Department of Systems Innovation
Osaka University
1-3 Machikaneyama
Toyonaka, Osaka 560-8531 Japan
Phone: 81-6-6850-6358 / Fax: 81-6-6850
E-mail: suzuki@ft-lab.sys.es.osaka-u.ac.jp

Price, David

P.O. Box 808, L-182
Livermore, CA 94551
Phone: 925-422-3980 / Fax: (925) 422-3821
E-mail: price16@llnl.gov

Takimoto, Takashi

Department of Systems Innovation
Osaka University
1-3 Machikaneyama
Toyonaka, Osaka 560-8531 Japan
Phone: 81-6-6850-6388 / Fax: 81-6-6850
E-mail: takimoto@hopf.sys.es.osaka-u.ac

Spero, Kimberlee

P.O. Box 808, L-182
Livermore, CA 94551
Phone: 925-422-7913 / Fax: (925) 422-3821
E-mail: spero2@llnl.gov

Takubo, Tomohito

Department of Systems Innovation
Graduate School of Engineering Science
Osaka University
1-3 Machikaneyama
Toyonaka, Osaka 560-8531 Japan
Phone: 81-6-6850-6366 / Fax: 81-6-6850

Matsushita Electric Industrial Co., Ltd:

Maehara, Fumio

Matsushita Electric Industrial Co., Ltd
2-15 Matsuba-Cho.Kadoma-Shi
Osaka, Japan

Tanno, Yoshikazu

Osaka University
Yamagata Digital Content Center for Research
Promotion
1-3-8 Matsuei
Yamagata-shi, Yamagata 990-2473 Japan
Phone: 81-23-647-8121 / Fax: 81-23-647
E-mail: tan@archive.gr.jp

Mitsubishi Research, Inc.:

Hiyane, Kazuo

Information Technology Research Dept.
Mitsubishi Research Institute Inc.
2-3-6 Otemachi, Chiyoda-ku Tokyo, 100-8141

Ujii, Yoshihiro

Department of Systems Innovation
Graduate School of Engineering Science

Japan
 Phone: 81-3-3277-0750 / Fax: 81-3-3277-3473
 E-mail: hiya@mri.co.jp

Osaka University
 1-3 Machikaneyama
 Toyonaka, Osaka 560-8531 Japan
 Phone: 81-6-6850-6366 / Fax: 81-6-6850

Iio, Jun

Information Technology Research Dept.
 Mitsubishi Research Institute, Inc.
 2-3-6 Otemachi, Chiyoda-ku Tokyo, 100-8141
 Japan.
 Phone: 81-3-3277-0750 / Fax: 81-3-3277-3473
 E-mail: iiojun@mri.co.jp

Umetani, Tomohiro

Graduate School of Engineering Science
 Osaka University
 1-3 Machikaneyama
 Toyonaka, Osaka, 560-8531 Japan
 Phone: 81-6-6850-5368 / Fax: 81-6-6850
 E-mail: umetani@sys.es.osaka-u.ac.jp

Nara Institute of Science and Techlogy:

Sasao, Naoki

Graduate School of Information Science
 Nara Institute of Science and Techlogy
 8916-5 Takayama
 Ikoma, Nara 630-0192 Japan
 E-mail: naoki-sa@is.naist.jp

Wang, Yiqun

Osaka University
 1-3 machikaneyama
 Toyonaka, Osaka 560-8531 Japan
 Phone: 81-6-6850-6382 / Fax: 81-6-6850
 E-mail: wang@nishilab.sys.es.osaka-u.ac.j

Yachida, Masahiko

Graduate School of Engineering Science
 Osaka University
 1-3 Machikaneyama
 Toyonaka, Osaka 560-8531 Japan
 Phone: 81-6-6850-6361 / Fax: 81-6-6850
 E-mail: yachida@yachi-lab.sys.es.osaka-u

NASA Ames Research Center:

Clancey, William

NASA Ames Research Center, Computational
 Sciences Division
 MS 269-3, Moffet Field, CA 94035

Institute for Human and Machine Cognition, UWF,
 Pensacola, FL 32514.
 Phone: 650-604-2526 / Fax: 650-604-4036
 E-mail: william.j.clancey@nasa.gov

Yamamoto, Shigeru

Department of Systems Innovation
 Osaka University
 1-3 Machikaneyama
 Toyonaka, Osaka 560-8531, Japan
 Phone: 81-6-6850-6388 / Fax: 81-6-6850
 E-mail: yamamoto@sys.es.osaka-u.ac.jp

Sierhuis, Maarten

RIACS
 NASA Ames Research Center
 Moffett Field, CA 94035
 Phone: 650-604-4917 / Fax: 650-6047-4954
 E-mail: msierhuis@mail.arc.nasa.gov

Princeton University:

Powell, Warren

Department of Operations Research and Fi
 Engineering
 Princeton University
 Princeton, NJ 08544
 E-mail: powell@princeton.edu

Van Hoof, Ron

QSS
 NASA Ames Research Center
 Moffett Field, CA 94035
 Phone: 732-632-9459 / Fax: 732-632-9607
 E-mail: rvhoof@optonline.net

Wu, Tongqiang

Department of Operations Research and Fi
 Engineering
 Princeton University

National Taiwan University:

Guo, Sye-Jye

National Taiwan University
 Dep. Of Civil Engineering Construction Engineering
 & Management
 1, Sec.4 Roosevelt Road
 Taipei, 106 Taiwan, R.O.C.

Lee, Meng-Hsueh

National Taiwan University
 1, Sec. 4 Roosevelt Road
 Taipei, 106 Taiwan, R.O.C.
 E-mail: d92521016@ntu.edu.tw

Liu, Shu-Shun

Dept. Civil Engineering
 National Taiwan University 1,
 1, Sec. 4 Roosevelt Road
 Taipei, 106 Taiwan, R.O.C.

Tsai, Ming Da

National Taiwan University
 1, Sec. 4 Roosevelt Road
 Taipei, 106 Taiwan, R.O.C.
 Phone: 886-02-23630231-3380-20 / Fax: 886-02-
 23661640
 E-mail: miketsai@ce.ntu.edu.tw

Tserng, H. Ping

Dept. Civil Engineering
 National Taiwan University 1,
 1, Sec. 4 Roosevelt Road
 Taipei, 106 Taiwan, R.O.C.
 Phone: 886-2-2758-9568 / Fax: 886-2-2758-7477
 E-mail: hptserng@ce.ntu.edu.tw

Wu, Li-Wen

National Taiwan University
 Dept. Of Civil Engineering Construction Engineering
 & Management
 1, Sec.4 Roosevelt Road
 Taipei, 106 Taiwan, R.O.C.
 Phone: (886)928592269 / Fax: (886)2366-1640
 E-mail: d92521009@ntu.edu.tw

Princeton, NJ 08544

E-mail: twu@princeton.edu

Project Management Consultant PCI/JGC Jc Venture:

Niho, Hiroshi

Project Management Consultant PCI/JGC Jc
 Venture
 23 Building 1-23-7 Toramon
 Minatoku, Tokyo 105-0001 Japan
 Phone: 81-3-3501-0544 / Fax: 81-3-3501
 E-mail: nihoh@pcitokyo.co.jp

Research Institute for Sci and Techlogy for Society (RISTEX):

Kanno, Taro

RISTEX
 2-5-1 Atago
 Minato-Ku, Ttokyo 105-6218 Japan
 Phone: 81-3-5404-2893 / Fax: 81-3-6402
 E-mail: kan@diras.q.t.u-tokyo.ac.jp

The National Institute of Advanced Industrial Scier and Techlogy:

Hirai, Shigeoki

AIST Central
 2-1-1 Umezo
 Tsukuba, Ibaraki 305-8564, Japan
 Phone: 81-29-861-7264 / Fax: 81-29-861
 E-mail: s.hirai@aist.go.jp

Kuen, Kim Bong

AIST Central
 2-1-1 Umezo
 Tsukuba, Ibaraki 305-8564, Japan
 Phone: 81-29-861-7264 / Fax: 81-
 E-mail: bk.kim@aist.go.jp

You, J. Juh

Dept. Civil Engineering
National Taiwan University
1, Sec. 4. Roosevelt Road
Taipei, 106 Taiwan, R.O.C.
Phone: 886-2-2758-9568 / Fax: 886-2-2758-7477
E-mail: d91521026@ntu.edu.tw

Ohba, Kohtaro

AIST Central
2-1-1 Umezo
Tsukuba, Ibaraki 305-8564, Japan
Phone: 81-29-861-7264 / Fax: 81-29-861
E-mail: k.ohba@aist.go.jp

Osaka University:**Arai, Tatsuo**

Osaka University
Department of Systems Innovation
1-3 Machikaneyama
Toyonaka-shi, Osaka 560-8531 Japan
Phone: 81-6-6850-6367 / Fax: 81-6-6850-6367
E-mail: arai@sys.es.osaka-u.ac.jp

Fujii, Takao

Graduate School of Engineering Science
Department of Systems Innovation
Osaka University
1-3 Machikaneyama
Toyonaka, Osaka 560-8531 Japan
Phone: 81-6-6850-6358 / Fax: 81-6-6850-6341
E-mail: fujii@sys.es.osaka-u.ac.jp

Hijikata, Yoshinori

Graduate School of Engineering Science
Osaka University
1-3 machikaneyama
Toyonaka, Osaka 560-8531 Japan
Phone: 81-6-6850-6382 / Fax: 81-6-6850-6341
E-mail: hijikata@sys.es.osaka-u.ac.jp

Hirayama, Takatsugu

Graduate School of Engineering Science
Osaka University
1-3 Machikaneyama
Toyonaka, Osaka, 560-8531 Japan
Phone: 81-6-6850-6361 / Fax: 81-6-6850-6341
E-mail: hirayama@yachi-lab.sys.es.osaka-u.ac.jp

Hiura, Shinsaku

Graduate School of Engineering Science
Osaka University
1-3 Machikaneyama
Toyonaka, Osaka 560-8531 Japan
Phone: 81-6-6850-6371 / Fax: 81-6-6850-6341

Tanie, Kazuo

AIST Central
2-1-1 Umezo
Tsukuba, Ibaraki 305-8564, Japan
Phone: 81-29-861-7264 / Fax: 81-29-861
E-mail: tanie.k@aist.go.jp

**University of California,
Berkeley:****Kaskiris, Charis**

SIMS
University of California, Berkeley
Berkeley, CA 94720
Phone: 510-858-4599 / Fax: 510-642-581
E-mail: kaskiris@sims.berkeley.edu

University of Fukui:**Mae, Yasushi**

Faculty of Engineering
University of Fukui
3-9-1 Bunkyo
Fukui 910-8507 Japan

University of Tokyo:**Furuta, Kazuo**

Division of Environmental Studies
University of Tokyo
Furuta Laboratory, Faculty of Engineering
Bldg.12, 7-3-1 Hongo
Bunkyo-ku, Tokyo 113-0033 Japan
Phone: 81-3-5841-6965 / Fax: 81-3-5841
E-mail: furuta@q.t.u-tokyo.ac.jp

Iino, Yuji

Graduate school of Frontier Sciences
University of Tokyo

E-mail: shinsaku@sys.es.osaka-u.ac.jp

Inoue, Kenji

Department of Systems Innovation
Graduate School of Engineering Science
Osaka University
1-3 Machikaneyama
Toyonaka, Osaka 560-8531 Japan
Phone: 81-6-6850-6366 / Fax: 81-6-6850-6366
E-mail: iue@sys.es.osaka-u.ac.jp

Inuiguchi, Masahiro

Graduate School of Engineering Science
Osaka University
1-3 Machikaneyama
Toyonaka, Osaka 560-8531 Japan
Phone: 81-6-6850-6350

Iwai, Yoshio

Graduate School of Engineering Science
Osaka University
1-3 Machikaneyama
Toyonaka, Osaka 560-8531 Japan
Phone: 81-6-6850-6361 / Fax: 81-6-6850-6341
E-mail: iwai@sys.es.osaka-u.ac.jp

Kaneko, Osamu

Department of Systems Innovation
Graduate School of Engineering Science
Osaka University
1-3 Machikaneyama
Toyonaka, Osaka 560-8531 Japan
Phone: 81-6-6850-6358 / Fax: 81-6-6850-6341
E-mail: kaneko@sys.es.osaka-u.ac.jp

Kawabata, Satoshi

Graduate School of Engineering Science
Osaka University
1-3 Machikaneyama
Toyonaka, Osaka 560-8531 Japan
Phone: 81-6-6850-6371 / Fax: 81-6-6850-6341

Kumeno, Hironori

Graduate School of Engineering Science
Osaka University
1-3 Machikaneyama
Toyonaka, Osaka 560-8531 Japan
Phone: 81-6-6850-5368 / Fax: 81-6-6850-6341
E-mail: kume@arai-lab.sys.es.osaka-u.ac.jp

Furuta Lab, Faculty of Engineering
Bldg.12, 7-3-1 Hongo
Bunkyo-ku, Tokyo 113-0033 Japan
Phone: 81-3-5841-8923 / Fax: 81-3-5841
E-mail: ii@cse.k.u-tokyo.ac.jp

Ishii, Takari

University of Tokyo
Furuta Lab, Faculty of Engineering
Bldg.12, 7-3-1 Hongo
Bunkyo-ku, Tokyo 113-0033 Japan
Phone: 81-3-5841-8923 / Fax: 381--5841
E-mail: ishii@cse.k.u-tokyo.ac.jp

Nagase, Masaya

Division of Environmental Studies
University of Tokyo
Furuta Laboratory, Faculty of Engineering
Bldg.12, 7-3-1 Hongo
Bunkyo-ku, Tokyo 113-0033 Japan
Phone: 81-3-5841-8923 / Fax: 81-3-5841
E-mail: nagase@cse.k.u-tokyo.ac.jp

Shimizu, Tatsuya

Graduate School of Frontier Sciences
5-116-3 Kariya-chou
Ushiku-shi, IBARAKI, 300-1235 Japan
Phone: 03-5841-8923 / Fax: 03-5841-892
E-mail: shimeji@amber.plala.or.jp

University of Tsukuba:

Ohara, Kenichi

University of Tsukuba
1-1-1 Tendai
Tsukuba-Shi, Ibaraki-Ken 305-8568 Japan
Phone: 81-29-853-2111 / Fax: 81-29-853
E-mail: k-ooohara@aist.go.jp

University of Waterloo:

Al-Mutairi, Mubarak

Department of Systems Design Engineering
University of Waterloo
Waterloo, Ontario N2L 3G1 Canada
Phone: 1(519) 888-4567 ext. 7736 / Fax:
746-4791
E-mail: malmutai@uwaterloo.ca

Makino, Kazuhisa

Division of Mathematical Science for Social Systems
Graduate School of Engineering Science
Osaka University
1-3 Machikaneyama
Toyonaka, Osaka 560-8531 Japan
Phone: 81-6-6850-6351 / Fax: 81-6-6850-6341
E-mail: maki@sys.es.osaka-u.ac.jp

Hipel, Keith

Department of Systems Design Engineering
University of Waterloo
Waterloo, Ontario N2L 3G1 Canada
Phone: 1(519) 888-4567 ext. 2830 / Fax:
746-4791
E-mail: kwhipel@uwaterloo.ca

Mamada, Sakato

Division of Mathematical Science for Social Systems
Graduate School of Engineering Science
Osaka University
1-3 Machikaneyama
Toyonaka, Osaka 560-8531 Japan
Phone: 81-6-6850-6353 / Fax: 81-6-6850-6341
E-mail: mamada@inulab.sys.es.osaka-u.ac.jp

Kamel, Mohammed

Department of Electrical and Computer En
University of Waterloo.
Waterloo, Ontario N2L 3G1 Canada
Phone: 1(519) 888-4567 ext. 7736 / Fax:
746-4791
E-mail: malmutai@uwaterloo.ca

Mashita, Tomohiro

Yachida Lab
Graduate School of Engineering Science
Osaka University
1-3 Machikaneyama
Toyonaka, Osaka 560-8531 Japan
Phone: 81-6-6850-6363 / Fax: 81-6-6850-6341
E-mail: mashita@yachi-lab.sys.es.osaka-u.ac.jp

Miura, Yoshitomo

Graduate School of Engineering Science
Osaka University
1-3 Machikaneyama
Toyonaka, Osaka 560-8531 Japan
Phone: 81-6-6368-0829 / Fax: 81-6-6368-0829
E-mail: miura@inulab.sys.es.osaka-u.ac.jp

Moritani, Takayuki

Graduate School of Engineering Science
Osaka University
1-3 Machikaneyama
Toyonaka, Osaka 560-8531 Japan

[Send e-mail](#)

[Main Page](#)

SSR2005: March 9-11, 2005, San Francisco

International Symposium on Systems and Human Science



Proceedings

Al-Mutairi, Mubarak

Department of Systems Design Engineering
University of Waterloo
Waterloo, Ontario N2L 3G1 Canada
Phone: 1(519) 888-4567 ext. 7736 / Fax: 1(519) 746-4791
E-mail: malmutai@uwaterloo.ca

Arai, Tatsuo

Osaka University
Department of Systems Innovation
1-3 Machikaneyama
Toyonaka-shi, Osaka 560-8531 Japan
Phone: 81-6-6850-6367 / Fax: 81-6-6850-6367
E-mail: arai@sys.es.osaka-u.ac.jp

Clancey, William

NASA Ames Research Center,
Computational Sciences Division MS 269 -3,
Moffet Field, CA 94035

Institute for Human and Machine Cognition, UWF,
Pensacola, FL 32514.
Phone: 650-604-2526 / Fax: 650-604-4036
E-mail: william.j.clancey@nasa.gov

Durling, Ron

P.O. Box 808, L-182
Livermore, CA 94551
Phone: 925-422-1467 / Fax: (925) 422-3821
E-mail: durling1@lnl.gov

Fujii, Takao

Graduate School of Engineering Science
Department of Systems Innovation
Osaka University
1-3 Machikaneyama
Toyonaka, Osaka 560-8531 Japan
Phone: 81-6-6850-6358 / Fax: 81-6-6850-6341
E-mail: fujii@sys.es.osaka-u.ac.jp

Fujishige, Satoru

Research Institute for Mathematical Science

Mashita, Tomohiro

Yachida Lab
Graduate School of Engineering Science
Osaka University
1-3 Machikaneyama
Toyonaka, Osaka 560-8531 Japan
Phone: 81-6-6850-6363 / Fax: 81-6-6850-6341
E-mail: mashita@yachi-lab.sys.es.osaka-u.ac.jp

Miura, Yoshitomo

Graduate School of Engineering Science
Osaka University
1-3 Machikaneyama
Toyonaka, Osaka 560-8531 Japan
Phone: 81-6-6368-0829 / Fax: 81-6-6368-0829
E-mail: miura@inulab.sys.es.osaka-u.ac.jp

Moritani, Takayuki

Graduate School of Engineering Science
Osaka University
1-3 Machikaneyama
Toyonaka, Osaka 560-8531 Japan

Nagase, Masaya

Division of Environmental Studies
University of Tokyo
Furuta Laboratory, Faculty of Engineering
Bldg.12, 7-3-1 Hongo
Bunkyo-ku, Tokyo 113-0033 Japan
Phone: 81-3-5841-8923 / Fax: 81-3-5841-8923
E-mail: nagase@cse.k.u-tokyo.ac.jp

Niho, Hiroshi

Project Management Consultant PCI/JGC Joint Ve
23 Building 1-23-7 Toramon
Minatoku, Tokyo 105-0001 Japan
Phone: 81-3-3501-0544 / Fax: 81-3-3501-0809
E-mail: nihoh@pcitokyo.co.jp

Nishida, Shogo

Osaka University
1-3 Machikaneyama
Toyonaka, Osaka 560-8531 Japan

Kyoto University
Sakyo-Ku, Kyoto 606-8502 Japan
Phone: 81-75-753-7250 / Fax: 81-75-753-7276
E-mail: fujishig@kurims.kyoto-u.ac.jp

Furuta, Kazuo
Division of Environmental Studies
University of Tokyo
Furuta Laboratory, Faculty of Engineering
Bldg.12, 7-3-1 Hongo
Bunkyo-ku, Tokyo 113-0033 Japan
Phone: 81-3-5841-6965 / Fax: 81-3-5841-6965
E-mail: furuta@q.t.u-tokyo.ac.jp

Guo, Sye-Jye
National Taiwan University
Dept. Of Civil Engineering Construction Engineering &
Management
Sec.4, Roosevelt Road
Taipei, 106 Taiwan, R.O.C.

Hijikata, Yoshinori
Graduate School of Engineering Science
Osaka University
1-3 Machikaneyama
Toyonaka, Osaka 560-8531 Japan
Phone: 81-6-6850-6382 / Fax: 81-6-6850-6341
E-mail: hijikata@sys.es.osaka-u.ac.jp

Hipel, Keith
Department of Systems Design Engineering
University of Waterloo
Waterloo, Ontario N2L 3G1 Canada
Phone: 1(519) 888-4567 ext. 2830 / Fax: 1(519) 746-
4791
E-mail: kwhipel@uwaterloo.ca

Hirai, Shigeoki
AIST Central
2-1-1 Umezo
Tsukuba, Ibaraki 305-8564 Japan
Phone: 81-29-861-7264 / Fax: 81-29-861-7201
E-mail: s.hirai@aist.go.jp

Hirayama, Takatsugu
Graduate School of Engineering Science
Osaka University
1-3 Machikaneyama
Toyonaka, Osaka, 560-8531 Japan
Phone: 81-6-6850-6361 / Fax: 81-6-6850-6341
E-mail: hirayama@yachi-lab.sys.es.osaka-u.ac.jp

Hiura, Shinsaku
Graduate School of Engineering Science
Osaka University
1-3 Machikaneyama
Toyonaka, Osaka 560-8531 Japan
Phone: 81-6-6850-6371 / Fax: 81-6-6850-6341
E-mail: shinsaku@sys.es.osaka-u.ac.jp

Nishide, Shun
Department of Systems Innovation
Graduate School of Engineering Science
Osaka University
1-3 Machikaneyama
Toyonaka, Osaka 560-8531 Japan
Phone: 81-6-6850-6366 / Fax: 81-6-6850-6367
E-mail: nishide@arai-lab.sys.es.osaka-u.ac.jp

Nonaka, Seri
Department of Systems Innovation
Graduate School of Engineering Science
Osaka University
1-3 Machikaneyama
Toyonaka, Osaka 560-8531 Japan
Phone: 81-6-6850-6366 / Fax: 81-6-6850-6366

Ohara, Kenichi
University of Tsukuba
1-1-1 Tendai
Tsukuba-Shi, Ibaraki-Ken 305-8568 Japan
Phone: 81-29-853-2111 / Fax: 81-29-853-2111
E-mail: k-oohara@aist.go.jp

Ohba, Kohtaro
AIST Central.
2-1-1 Umezo .
Tsukuba, Ibaraki 305-8564 Japan
Phone: 81-29-861-7264 / Fax: 81-29-861-7201
E-mail: k.ohba@aist.go.jp

Powell, Warren
Department of Operations Research and Financial
Engineering
Princeton University
Princeton, NJ 08544
E-mail: powell@princeton.edu

Price, David
P.O. Box 808, L-182
Livermore, CA 94551
Phone: 925-422-3980 / Fax: (925) 422-3821
E-mail: price16@llnl.gov

Sakaguchi, Yukinobu
Department of Systems Innovation.
Graduate School of Engineering Science.
Osaka University.
1-3 Machikaneyama.
Toyonaka, Osaka 560-8531 Japan
Phone: / Fax:
E-mail: sakaguchi@arai-lab.sys.es.osaka-u.ac.jp

Sakata, Kotaro
Department of Systems Innovation
Graduate School of Engineering Science
Osaka University
1-3 Machikaneyama
Toyonaka, Osaka 560-8531 Japan
Phone: 81-6-6850-6367 / Fax: 81-6-6850-6341

Hiyane, Kazuo

Information Techlogy Research Dept.
Mitsubishi Research Institute, Inc.
2-3-6 Otemachi,
Chiyoda-ku Tokyo, 100-8141 Japan
Phone: 81-3-3277-0750 / Fax: 81-3-3277-3473
E-mail: hiya@mri.co.jp

Iino, Yuji

Graduate school of Frontier Sciences
University of Tokyo
Furuta Lab, Faculty of Engineering
Bldg.12, 7-3-1 Hongo
Bunkyo-ku, Tokyo 113-0033 Japan
Phone: 81-3-5841-8923 / Fax: 81-3-5841-8923
E-mail: ii@cse.k.u-tokyo.ac.jp

Iio, Jun

Information Techlogy Research Dept.
Mitsubishi Research Institute, Inc.
2-3-6 Otemachi,
Chiyoda-ku Tokyo, 100-8141 Japan.
Phone: 81-3-3277-0750 / Fax: 81-3-3277-3473
E-mail: iiojun@mri.co.jp

Inoue, Kenji

Department of Systems Innovation
Graduate School of Engineering Science
Osaka University
1-3 Machikaneyama
Toyonaka, Osaka 560-8531 Japan
Phone: 81-6-6850-6366 / Fax: 81-6-6850-6366
E-mail: iue@sys.es.osaka-u.ac.jp

Inuiguchi, Masahiro

Graduate School of Engineering Science
Osaka University
1-3 Machikaneyama
Toyonaka, Osaka 560-8531 Japan
Phone: 81-6-6850-6350

Ishii, Takanori

University of Tokyo
Furuta Lab, Faculty of Engineering
Bldg.12, 7-3-1 Hongo
Bunkyo-ku, Tokyo 113-0033 Japan
Phone: 81-3-5841-8923 / Fax: 381--5841-8923
E-mail: ishii@cse.k.u-tokyo.ac.jp

Iwai, Yoshio

Graduate School of Engineering Science
Osaka University
1-3 Machikaneyama
Toyonaka, Osaka 560-8531 Japan
Phone: 81-6-6850-6361 / Fax: 81-6-6850-6341
E-mail: iwai@sys.es.osaka-u.ac.jp

Kamel, Mohammed

Department of Electrical and Computer Engineering

E-mail: sakata@arai-lab.sys.es.osaka-u.ac.jp

Sasao, Naoki

Graduate School of Information Science
Nara Institute of Science and Techlogy
8916-5 Takayama
Ikoma, Nara 630-0192 Japan
E-mail: naoki-sa@is.naist.jp

Sato, Kosuke

Department of Engineering Science
Osaka University
1-3 Machikaneyama
Toyonaka, Osaka 560-8531 Japan
Phone: 81-6-6850-6371 / Fax: 81-6-6850-6341

Shimizu, Tatsuya

Graduate School of Frontier Sciences
5-116-3 Kariya-chou
Ushiku-shi, IBARAKI 300-1235 Japan
Phone: 03-5841-8923 / Fax: 03-5841-8923
E-mail: shimeji@amber.plala.or.jp

Sierhuis, Maarten

RIACS
NASA Ames Research Center
Moffett Field, CA 94035
Phone: 650-604-4917 / Fax: 650-6047-4954
E-mail: msierhuis@mail.arc.nasa.gov

Spero, Kimberlee

P.O. Box 808, L-182
Livermore, CA 94551
Phone: 925-422-7913 / Fax: (925) 422-3821
E-mail: spero2@lnl.gov

Suzuki, Keita

Graduate School of Engineering Science
Department of Systems Innovation
Osaka University
1-3 Machikaneyama
Toyonaka, Osaka 560-8531 Japan
Phone: 81-6-6850-6358 / Fax: 81-6-6850-6341
E-mail: suzuki@ft-lab.sys.es.osaka-u.ac.jp

Takimoto, Takashi

Department of Systems Innovation
Osaka University
1-3 Machikaneyama
Toyonaka, Osaka 560-8531 Japan
Phone: 81-6-6850-6388 / Fax: 81-6-6850-6388
E-mail: takimoto@hopf.sys.es.osaka-u.ac.jp

Takubo, Tomohito

Department of Systems Innovation
Graduate School of Engineering Science
Osaka University
1-3 Machikaneyama
Toyonaka, Osaka 560-8531 Japan

University of Waterloo.
Waterloo, Ontario N2L 3G1 Canada
Phone: 1(519) 888-4567 ext. 7736 / Fax: 1(519) 746-4791
E-mail: malmutai@uwaterloo.ca

Kaneko, Osamu
Department of Systems Innovation
Graduate School of Engineering Science
Osaka University
1-3 Machikaneyama
Toyonaka, Osaka 560-8531 Japan
Phone: 81-6-6850-6358 / Fax: 81-6-6850-6341
E-mail: kaneko@sys.es.osaka-u.ac.jp

Kanno, Taro
Research Institute of Science and Techlogy for Society
(RISTEX).
2-5-1 Atago
Minato-ku, Tokyo 105-6218, Japan
Phone: 81-3-5404-2893 / Fax: 81-3-6402-7578
E-mail: t-can@sea.sannet.ne.jp

Kaskiris, Charis
SIMS
University of California, Berkeley
Berkeley, CA 94720
Phone: 510-858-4599 / Fax: 510-642-5814
E-mail: kaskiris@sims.berkeley.edu

Kawabata, Satoshi
Graduate School of Engineering Science
Osaka University
1-3 Machikaneyama
Toyonaka, Osaka 560-8531 Japan
Phone: 81-6-6850-6371 / Fax: 81-6-6850-6341

Kirchsteiger, Christian
European Commission
DG-JRC
Institute for Energy
Probabilistic Risk & Availability Assessment of Energy
Systems
Westerduinweg 3 - 1755 Le Petten
The Netherlands
Phone: 31-224-56-5118 / Fax: 31-224-56-5641
E-mail: christian.kirchsteiger@jrc.nl

Kuen, Kim Bong
AIST Central
2-1-1 Umezo
Tsukuba, Ibaraki 305-8564, Japan
Phone: 81-29-861-7264 / Fax: 81-
E-mail: bk.kim@aist.go.jp

Kumeno, Hironori
Graduate School of Engineering Science
Osaka University
1-3 Machikaneyama

Phone: 81-6-6850-6366 / Fax: 81-6-6850-6366

Tamura, Hiroyuki
Department of Electrical Engineering and Comput
Science
Faculty of Engineering
Kansai University
3-3-35 Yamate-cho,
Suita, Osaka 564-8680, Japan
Phone: 81-6-6368-0829 / Fax: 81-6-6368-0829
E-mail: H.Tamura@kansai-u.ac.jp

Tanie, Kazuo
AIST Central
2-1-1 Umezo
Tsukuba, Ibaraki 305-8564 Japan
Phone: 81-29-861-7264 / Fax: 81-29-861-7201
E-mail: tanie.k@aist.go.jp

Tanno, Yoshikazu
Osaka University
Yamagata Digital Content Centerfor Research & P
1-3-8 Matsuei
Yamagata-shi, Yamagata 990-2473 Japan
Phone: 81-23-647-8121 / Fax: 81-23-647-8122
E-mail: tan@archive.gr.jp

Tsai, Ming Da
National Taiwan University
1, Sec. 4, Roosevelt Road
Taipei, 106 Taiwan, R.O.C.
Phone: 886-02-23630231-3380-20 / Fax: 886-0-
23661640
E-mail: miketsai@ce.ntu.edu.tw

Tserng, H. Ping
Dept. Civil Engineering
National Taiwan University
1, Sec. 4 Roosevelt Road
Taipei, 106 Taiwan, R.O.C.
Phone: 886-2-2758-9568 / Fax: 886-2-2758-747
E-mail: hptserng@ce.ntu.edu.tw

Ujiie, Yoshihiro
Department of Systems Innovation
Graduate School of Engineering Science
Osaka University
1-3 Machikaneyama
Toyonaka, Osaka 560-8531 Japan
Phone: 81-6-6850-6366 / Fax: 81-6-6850-6366

Umetani, Tomohiro
Graduate School of Engineering Science
Osaka University
1-3 Machikaneyama
Toyonaka, Osaka, 560-8531 Japan
Phone: 81-6-6850-5368 / Fax: 81-6-6850-6341
E-mail: umetani@sys.es.osaka-u.ac.jp

Toyonaka, Osaka 560-8531 Japan
 Phone: 81-6-6850-5368 / Fax: 81-6-6850-6341
 E-mail: kume@arai-lab.sys.es.osaka-u.ac.jp

Lee, Meng-Hsueh

National Taiwan University
 Sec. 4, Roosevelt Road
 Taipei, 106 Taiwan, R.O.C.
 E-mail: d92521016@ntu.edu.tw

Liu, Shu-Shun

Dept. Civil Engineering
 National Taiwan University
 Sec. 4, Roosevelt Road
 Taipei, 106 Taiwan, R.O.C.

Mae, Yasushi

Faculty of Engineering
 University of Fukui
 3-9-1 Bunkyo
 Fukui 910-8507 Japan

Maehara, Fumio

Matsushita Electric Industrial Co., Ltd
 2-15 Matsuba-Cho.
 Kadoma-Shi, Osaka Japan

Makino, Kazuhisa

Division of Mathematical Science for Social Systems
 Graduate School of Engineering Science
 Osaka University
 1-3 Machikaneyama
 Toyonaka, Osaka 560-8531 Japan
 Phone: 81-6-6850-6351 / Fax: 81-6-6850-6341
 E-mail: maki@sys.es.osaka-u.ac.jp

Makowski, Marek

International Institute for Applied Systems Analysis
 A-2361 Laxenburg, Austria
 Phone: 43-2236-807-561 / Fax: 43-22236-71-313
 E-mail: marek@iiasa.ac.at

Mamada, Sakato

Division of Mathematical Science for Social Systems
 Graduate School of Engineering Science
 Osaka University
 1-3 Machikaneyama
 Toyonaka, Osaka 560-8531 Japan
 Phone: 81-6-6850-6353 / Fax: 81-6-6850-6341
 E-mail: mamada@inulab.sys.es.osaka-u.ac.jp

Van Hoof, Ron

QSS
 NASA Ames Research Center
 Moffett Field, CA 94035
 Phone: 732-632-9459 / Fax: 732-632-9607
 E-mail: rvhoof@optonline.net
 Osaka University.1-3 machikaneyama, Toyonaka
 560-8531
 Phone: 81-6-6850-6382 / Fax: 81-6-6850-6341
 E-mail: wang@nishilab.sys.es.osaka-u.ac.jp

Wang, Yiqun

Osaka University
 1-3 machikaneyama
 Toyonaka, Osaka 560-8531 Japan
 Phone: 81-6-6850-6382 / Fax: 81-6-6850-6341
 E-mail: wang@nishilab.sys.es.osaka-u.ac.jp

Wu, Li-Wen

National Taiwan University
 Dep. Of Civil Engineering Construction Engineerin
 Management
 1, Sec.4, Roosevelt Road
 Taipei, 106 Taiwan, R.O.C.
 Phone: (886)928592269 / Fax: (886)2366-1640
 E-mail: d92521009@ntu.edu.tw

Wu, Tongqiang

Department of Operations Research and Financia
 Engineering
 Princeton University
 Princeton, NJ 08544
 E-mail: twu@princeton.edu

Yachida, Masahiko

Graduate School of Engineering Science, .Osaka
 University.1-3 Machikaneyama, Toyonaka, Osaka
 8531, Japan.
 Phone: / Fax:
 E-mail:

Yachida, Masahiko

Graduate School of Engineering Science
 Osaka University
 1-3 Machikaneyama
 Toyonaka, Osaka 560-8531 Japan
 Phone: 81-6-6850-6361 / Fax: 81-6-6850-6341
 E-mail: yachida@yachi-lab.sys.es.osaka-u.ac.jp

Yamamoto, Shigeru

Department of Systems Innovation
 Osaka University
 1-3 Machikaneyama
 Toyonaka, Osaka 560-8531, Japan
 Phone: 81-6-6850-6388 / Fax: 81-6-6850-6388
 E-mail: yamamoto@sys.es.osaka-u.ac.jp

You, J. Juh

Dept. Civil Engineering

National Taiwan University
1, Sec. 4, Roosevelt Road
Taipei, 106 Taiwan, R.O.C.
Phone: 886-2-2758-9568 / Fax: 886-2-2758-747
E-mail: d91521026@ntu.edu.tw

[Send e-mail](#)

[Main Page](#)

An Approximate Dynamic Programming Approach for the Military Airlift Problem

Tongqiang Tony Wu and Warren B. Powell
Department of Operations Research and Financial Engineering
Princeton University, Princeton, NJ 08544
twu@princeton.edu and powell@princeton.edu

Abstract

We introduce an approximate dynamic programming model for the military airlift problem which is categorized as a stochastic dynamic asset management problem. The approximate dynamic programming model owns both the flexibility of simulation models and the intelligence of optimization models while it avoids the curse of dimensionality in typical stochastic programming models. We implement both a rule based simulation model and the approximate dynamic programming model in the numerical experiments for the purpose of comparison. The solution of the approximate dynamic programming model is better than that of the simulation model. The result of the approximate dynamic programming model also shows that the value function approximations bring the global information into the local optimization problems and help the model make better decisions.

1: Introduction

Air Mobility Command's (AMC) primary mission is rapid, global mobility for America's armed forces by military airlift. The command also plays a crucial role in providing humanitarian support at home and around the world. The military airlift problem faced by the AMC is then effectively routing a fleet of aircraft to deliver requirements (troops, equipment, food and other forms of freight) from origins to destinations all over the world as quickly as possible under a variety of constraints. However, various random events may prevent AMC to finish their job efficiently. One of the biggest operational challenges of these aircraft is that their probability of a failure of sufficient severity to prevent a timely takeoff ranges between 10 and 25 percent. A failure can result in a delay or even require an off-loading of the freight to another aircraft.

There are two existing classes of approaches to the military airlift problem: simulation models (such as MASS (Mobility Analysis Support System) and AMOS, which are heavily used within the AMC) as well as

optimization models (Morton et al. (1996), Rosenthal et al. (1997), Baker et al. (2002)). Bridging these approaches are stochastic programming models (Goggins (1995), Morton et al. (2003)). In general, simulation models are flexible but are governed by simple rules while optimization models are intelligent (in the sense that they react in a reasonable way on data changes) but less flexible. The stochastic programming models try to get robust solutions while they handle the uncertainties in the system. Usually a stochastic programming model for a real application is too big to be solved easily.

In this paper, some of the limitations of simulation have been overcome by using an approximate dynamic programming algorithm. This technology is a form of intelligent simulation. Instead of using one large math program (as would be used in a pure optimization approach) the model in this paper solves sequences of smaller local math programs in an iterative fashion. We use the value function approximation to bring the global information into the local problem. The models step through time just as any (discrete time) simulator would do, allowing us to apply classical simulation strategies to capture complex system dynamics. However, the models in this paper solve sequences of small optimization problems (covering one time period at a time) just as an optimization model would. As a result, the behavior of the system is guided by a contribution (negative cost) function rather than rules, which are used in many simulation models.

In section 2, we give a literature review on the military airlift problem. Our model for the problem is in section 3. The approximate dynamic programming technique is introduced in section 4. Section 5 is the numerical experiments and section 6 is the conclusions.

2: Literature Review

A number of simulation models have been proposed for airlift problems (and related problems in military logistics). Schank et al. (1991) reviews several deterministic simulation models. Burke et al. (2004) develops a model called TRANSCAP (Transportation System Capability) to simulate the deployment of forces

from Army bases. Perhaps the most widely used model at the Air Mobility Command is MASS (Mobility Analysis Support System) which is a discrete-event worldwide airlift simulation model used in strategic and theater operations to deploy military and commercial airlift assets. MASS simulates the flows of aircraft moving a set of requirements, where the requirements are specified in a “time-phased force deployment dataset” (TPFDD). As an analysis methodology, MASS/AMOS offers the flexibility to incorporate the complex dynamics of these systems and the ability to explicitly control the behavior of the system through the specification of the rules used to manage the aircraft. At the same time, these models struggle with the challenge of juggling multiple aircraft. As a result, they resort to simple rules to reduce the dimensionality of the problem. Simulation has been criticized by optimization specialists in the academic community because the behavior is not “optimal,” but also by the practitioner community for the noise inherent in the behavior of even deterministic simulations, which complicates the analysis of small changes in rules and inputs.

In Figure 1, we give an algorithm that employs a simple rule based policy (RB) in the simulation for the military airlift problem. It does not use a contribution function to make the decision.

- | |
|---|
| <p>Step 1: Pick the first available remaining requirement in the TPFDD.</p> <p>Step 2: Pick the first available remaining aircraft.</p> <p>Step 3: Do the following feasibility check:
 Can the aircraft handle the requirement?
 Can the en-route and destination airbases accommodate the aircraft?</p> <p>Step 4: If the answers are all yes in Step 3, deliver the requirement by that aircraft and update the remaining weight of that requirement.</p> <p>Step 5: If that requirement is not finished, go to Step 2.</p> <p>Step 6: If there are remaining requirement, go to Step 1.</p> |
|---|

Figure 1: An algorithm with the rule based policy (RB) in the simulation

Development efforts focusing on the optimization models for the airlift problem had paralleled the development of simulation models. Mattock et al. (1995) describe several mathematical modeling formulations for military airlift operations. According to Baker et al. (2002), research on air mobility optimization at the Naval Postgraduate School (NPS) started with the Mobility Optimization Model (MOM). Described in Wing et al. (1991), this model is time-dependent and concentrates on both sealift and airlift operations. THRUPUT, a general airlift model developed by Yost (1994), captures the specifics of airlift operations but is static. The MOM and THRUPUT models are combined into THRUPUT II (Rosenthal et al. (1997)) that is time dependent and also

captures the specifics of airlift operations. During the development of THRUPUT II at NPS, a group at RAND developed a similar model called CONOP (CONcept of OPERations), described in Killingsworth & Melody (1997). The THRUPUT II and CONOP models each possessed several features that the other lacked. Therefore, the NPS and the RAND Corporation merged the two models into NRMO (NPS/RAND Mobility Optimizer), described in Baker et al. (2002).

Optimization offers the theoretical appeal of providing “optimal” solutions. Also, small changes in the input data tend to produce small, and reasonable, changes in the objective function. Optimization, however, suffers from some limitations. Perhaps the most apparent is the difficulty in modeling complex operational problems in a realistic way. The inability to incorporate uncertainty is also an issue, complicating, for example, the modeling of aircraft failures. More problematic is the difficulty in modeling the evolution of the system over time.

One feature of simulation models is their ability to handle uncertainty, and as a result there has been a steady level of academic attention toward incorporating uncertainty into optimization models, resulting in stochastic programming models. Dantzig & Ferguson (1956) is one of the first to study uncertain customer demands in the airlift problem. Midler & Wollmer (1969) also takes into account stochastic cargo requirements. Goggins (1995) extended Throughput II to a two-stage stochastic linear program to address the uncertainty of aircraft reliability. Niemi (2000) expands the NRMO model to incorporate stochastic ground times through a two-stage stochastic programming model. Granger et al. (2001) compared the simulation model and the network approximation model for the impact of stochastic flying times and ground times on a simplified airlift network. Morton et al. (2003) developed the Stochastic Sealift Deployment Model (SSDM), a multi-stage stochastic programming model to plan the wartime, sealift deployment of military cargo subject to stochastic attack.

A stochastic programming model is even larger than the corresponding optimization model since it needs to handle the random events. In general, it will have one more dimension to denote the different scenarios. In multi-period problems, the number of scenarios grows exponentially with the number of time periods. Even if we only use a small sample of outcomes (as an example, 20 outcomes), the resulting model is usually computationally intractable.

3: A mathematic model for the military airlift problem

In this paper, the time is modeled as depicted in Figure 2. Time $t = 0$ is special such that it represents “here and now” with the information that is available now. The

discrete time period t refers to the time interval from $t - 1$ to t . This means that the first new information arrives during time period 1. Thus, during time period t , random information comes in continuously. At the end of time period t (it is also the beginning of the next time period), a decision is made with all the information known. In fact, any function indexed by t is assumed to be measured at discrete time t , which therefore implicitly means that the function has access to the information that has arrived during time interval t (between $t - 1$ and t). Throughout this paper, indexing by t tells us that the variable or function includes information up through time t .

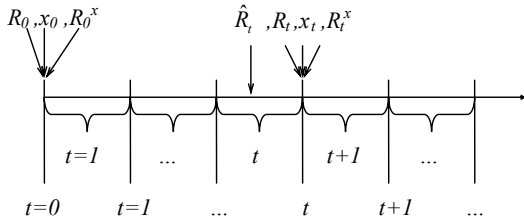


Figure 2: The modeling of time and the system evolution

We use the superscript A to denote the flavor of aircraft and superscript R to denote that of requirements. To model the military airlift problem, we define:

J = The set of airbases. Airbase $j \in J$.

T^h = The simulation horizon.

$T = \{0, 1, \dots, T^h\}$, the set of time periods. Time $t \in T$.

A = The attribute space of resources (aircraft and requirements).

A^A = The attribute space of aircraft.

A^R = The attribute space of requirements.

a/a' = The notation for attribute vector of resources. If $a \in A^A$, then a is the attribute vector of an aircraft. If $a' \in A^R$, then a' is that of a requirement. As an example,

$$a = \begin{bmatrix} \text{C-17(aircraft type)} \\ 50 \text{ Tons(capacity)} \\ \text{EDAR(current airbase)} \\ 40 \text{ Tons(loadedweight)} \end{bmatrix} \in A^A \quad a' = \begin{bmatrix} 2(\text{requirement ID}) \\ 200 \text{ Tons(weight)} \\ \text{KBOS(origin airbase)} \\ \text{OEDF(destination)} \end{bmatrix} \in A^R$$

$R_{tt'a'}$ = The number of resources that are knowable at the end of time t (before the decision at time t is made) and will be actionable with attribute vector $a' \in A$ at time $t' \geq t$. Here, t is the knowable time and t' the actionable time. For the aircraft, the unit of R is the pounds of capacity. For requirements, the unit is the pounds of goods.

$$R_{tt'a'} = \{R_{tt'a'} : a' \in A\}$$

$$R_t = \{R_{tt'a'} : t' \geq t\}$$

W_t = The exogenous information processes at time $t \in T$.

\hat{R}_t in the following is an example of W_t .

Ω = The set of possible outcomes of exogenous information $\{W_t, t \in T\}$.

ω = One sample of the exogenous information ($\omega \in \Omega$).

$\hat{R}_{tt'a'}$ = The number of new resources that first become known during time t , and will first become actionable with attribute vector $a' \in A$ at time $t' \geq t$.

$$\hat{R}_{tt'} = \{\hat{R}_{tt'a'} : a' \in A\}$$

$$\hat{R}_t = \{\hat{R}_{tt'a'} : t' \geq t\}$$

$d_{aa'}$ = The decision to couple aircraft $a \in A^A$ to requirement $a' \in A^R$ (load or pick up).

D_a^A = The set of decisions that can be applied to an aircraft with attribute vector $a \in A^A$. It includes the decisions to couple aircraft to requirements ($d_{aa'}$), move aircraft to airbases $j \in J$ or do nothing on aircraft (hold).

x_{tad} = The number of times that we apply a decision $d \in D_a^A$ to an aircraft with attribute vector $a \in A^A$ at time t .

$$x_t = \{x_{\text{tad}} : a \in A^A, d \in D_a^A\}$$

$$\delta_{tt'a'}(t, a, d) = \begin{cases} 1 & \text{If decision } d \text{ acting on an aircraft} \\ & \text{with attribute vector } a \in A^A \text{ at time } t \\ & \text{produces an aircraft with attribute} \\ & \text{vector } a' \in A^A \text{ at time } t' \\ 0 & \text{Otherwise} \end{cases}$$

I_t = The information available at time t .

Π = The set of policies. Policy $\pi \in \Pi$.

$X_t^\pi(I_t)$ = Under policy $\pi \in \Pi$, the function that determines the set of decisions x_t at time t based on the information I_t .

$R_{tt'a'}^x$ = The number of resources that are knowable at the end of time period t (after the decision x_t is made) and will be actionable with attribute vector $a' \in A$ at time t' . It is the post-decision state variable at time t .

$$R_{tt'a'}^x = \{R_{tt'a'}^x : a' \in A\}$$

$$R_t^x = \{R_{tt'a'}^x : t' \geq t\}$$

c_{tad} = The contribution of applying decision d to an aircraft with attribute $a \in A^A$ at time t .

$$c_t = \{c_{\text{tad}} : a \in A^A, d \in D_a^A\}$$

$C_t(x_t)$ = The total contribution due to x_t in time period t . If the contribution is linear, then

$$C_t(x_t) = c_t x_t = \sum_{a \in A^A} \sum_{d \in D_a^A} c_{\text{tad}} x_{\text{tad}}$$

The decisions x_t are returned by our decision function $X_t^\pi(I_t)$, so our challenge is not to choose the best decisions but rather to choose the best policy. At this moment, the information at time t consists of the resources R_t , that is $I_t = R_t$. Thus, our optimization problem is given by:

$$(1) \max_{\pi \in \Pi} E \left[\sum_{t \in T} C_t(X_t^\pi(R_t)) \right]$$

$x_t \in \chi_t, \forall t \in T$, where χ_t is the feasible set at time t :

$$\begin{aligned}
(2) \quad & \sum_{d \in D_a^A} x_{tad} = R_{ta} \quad \forall a \in A^A \\
(3) \quad & \sum_{a \in A^A: d=d_{aa'}} x_{tad} \leq R_{ta'} \quad \forall a' \in A^R \\
(4) \quad & x_{tad} \geq 0 \quad \forall a \in A^A, d \in D_a^A \\
(5) \quad & R_{t'a'}^x = R_{t'a'} + \sum_{a \in A^A} \sum_{d \in D_a^A} \delta_{t'a'}(t, a, d) x_{tad} \quad \forall t' > t, a' \in A^A \\
(6) \quad & R_{t'a'}^x = R_{t'a'} + 1_{\{t'=t+1\}} (R_{ta'} - \sum_{a \in A^A: d=d_{aa'}} x_{tad}) \quad \forall t' > t, a' \in A^R \\
(7) \quad & R_{t+1, t'a'} = R_{t'a'}^x + \hat{R}_{t+1, t'a'} \quad \forall t' > t, a' \in A^A \cup A^R
\end{aligned}$$

Equation (2) is the flow balance constraint for aircraft. Equation (3) is the requirement bundling constraint which states that the total weight of a requirement is not less than the sum of the weights of that requirement assigned to aircraft. It is this constraint that causes the model not to be a network flow problem. Equation (4) is the non-negativity constraint for the aircraft. Equation (5), (6) and (7) are system dynamics. Equation (5) (for aircraft) and Equation (6) (for requirements) mean that the post-decision system state at time t consists of what we know about the pre-decision status of resources for time t' at the end of time period t and the endogenous changes (the decisions) to resources for time t' that are made at time t . Equation (7) means that the pre-decision system state at time $t+1$ consists of the post-decision state at time t and the exogenous changes to resources for time t' that arrives during time period $t+1$.

At the beginning of time period t , we have the post decision resources, R_{t-1}^x , from the end of previous time period. As new information at time t , \hat{R}_t , arrives, we have the pre-decision system state R_t . We make decisions x_t over R_t . After decisions are made, the post decision resources, R_t^x , will be available at the end of time period t . Thus, the evolution of information as in Figure 2 is $\{R_0, x_0, R_0^x, \dots, \hat{R}_{t-1}, R_{t-1}, x_{t-1}, R_{t-1}^x, \hat{R}_t, R_t, x_t, R_t^x, \dots\}$, where, $\{\hat{R}_1, \dots, \hat{R}_{t-1}, \hat{R}_t, \dots\}$ is a sample realization of the random processes $\{W_t : t \in T\}$.

4: An approximate dynamic programming policy

Approximate dynamic programming is any technique which converges to an (approximately) optimal policy over time in a stochastic decision problem (Si (2002)). The technical challenge in approximate dynamic programming is how to use learning-based approaches to develop general purpose designs to maximize the sum of expected contribution over future time, in a stochastic environment, without simulating all of the future scenarios. Bertsekas & Tsitsiklis (1996) is the first major reference that gives a general introduction to a variety of

methods. Sutton & Barto (1998) studies the subject from the view of reinforcement learning. Sutton (1988) introduces temporal-difference learning that is a form of stochastic approximation procedure. Tsitsiklis & Van Roy (1997) studies the convergence properties of temporal-difference methods using continuous approximations of value functions. Cheung & Powell (2000) introduces a stochastic hybrid approximation procedure (SHAPE) for two-stage stochastic programs. The linear value function approximations are based on stochastic approximation methods by Robbins & Monro (1951) and Blum (1954). Kushner & Yin (1997) gives a thorough review of these techniques. Cheung & Powell (1996) is the first to study separable, piecewise linear value function approximations. Godfrey & Powell (2001) proposes an adaptive learning algorithm for piecewise linear, separable value function approximations for two-stage resource allocation problems. Godfrey & Powell (2002a) extends it to multistage, single commodity problems.

Re-writing the optimization problem (1) recursively, we get the optimality equations of dynamic programming which are introduced in section 4.1. The classic backward dynamic programming techniques are only suitable for a small problem. For real and large applications, we need to switch to forward (approximate) dynamic programming techniques that are discussed in section 4.2.

4.1: The optimality equations

Define,

$V_t(R_t)$ = The value function that captures the total contribution to the system from time t and afterwards if the system is in state R_t at time t .

$V_t^x(R_t^x)$ = The (post-decision) value function if the system is in post-decision state R_t^x at time t .

If the system is in state R_t and we make decision x_t , the system will be in some post-decision state R_t^x . Since the post-decision value function $V_t^x(R_t^x)$ tell the total contribution from time t for the post-decision variable, we may make decision x_t^* as,

$$(8) \quad x_t^*(R_t) = \arg \max_{x_t \in \mathcal{X}_t} [C_t(R_t, x_t) + V_t^x(R_t^x(R_t, x_t))]$$

The value of being in state R_t is then the value of using the optimal decision $x_t^*(R_t)$. That is:

$$(9) \quad V_t(R_t) = \max_{x_t \in \mathcal{X}_t} [C_t(R_t, x_t) + V_t^x(R_t^x(R_t, x_t))]$$

$$(10) \quad = \max_{x_t \in \mathcal{X}_t} [C_t(R_{t-1}, \omega_t, x_t) + V_t^x(R_t^x(R_{t-1}, \omega_t, x_t))]$$

Since the new information at time $t+1$, W_{t+1} , is random at time t , the value function of the post-decision state R_t^x is then the expectation of the pre-decision value functions at time $t+1$,

$$(11) \quad V_t^x(R_t^x) = E\{V_{t+1}(R_{t+1}(R_t^x, \omega_{t+1})) \mid R_t^x\}$$

$$(12) \quad = E\{V_{t+1}(R_{t+1}(R_t, x_t, \omega_{t+1})) \mid R_t\}$$

Combining equation (9) and (12), we get the optimality equations (Bellman's equation) (Bellman (1957), Bellman & Dreyfus (1959) and Denardo (1982)),

$$(13) \quad V_t(R_t) = \max_{x_t \in \mathcal{X}_t} [C_t(R_t, x_t) + E\{V_{t+1}(R_{t+1}(R_t, x_t, \omega_{t+1})) | R_t\}]$$

Equation (13) is used for a classic backward dynamic programming algorithm that is suitable for a small problem. When the problem size is large, we would adopt the approximate dynamic programming techniques. For this purpose, we substitute equation (10) into equation (11), and get the optimality equations using the post-decision state variables,

$$(14) \quad V_{t-1}^x(R_{t-1}^x) = E\{\max_{x_t \in \mathcal{X}_t} [C_t(R_{t-1}^x, \omega_t, x_t) + \bar{V}_t^x(R_t^x(R_{t-1}^x, \omega_t, x_t))] | R_{t-1}^x\}$$

4.2: Approximate dynamic programming

The classic backward dynamic programming algorithm for solving a finite horizon problem is straightforward. We start at the last time period, compute the value function for each possible state R_T , and then step back another time period. This way, at time period t we have already computed $V_{t+1}(R_{t+1})$. Employing equation (13) recursively, we could compute $V_t(R_t) \forall t \in T$. However, the backward dynamic program is not suitable for the real applications with high dimensions. There are three curses of dimensionality in the dynamic programming formula for a real problem: the state variable, outcomes and decisions all tend to be high dimensional. As a result, methods which depend on discrete representations of these variables are computationally intractable.

To solve the three curses of dimensionality, approximate dynamic programming using the post-decision optimality equation (14) is adopted. When stepping forward through time, we need to have at hand an approximation of the value function that can be used to make decisions. This approximation will then have to be updated iteratively. At iteration n , let:

$\bar{V}_t^{x,n}(R_t^x)$ = Approximate post-decision value function for time t at iteration n

Assume that we have found a suitable approximation for the value functions. We can find a decision x_t by sampling the information that would be available before we make the decision, denoted by $\omega_t = W_t(\omega)$, and then choosing x_t by solving:

$$(15) \quad x_t(R_{t-1}^x, \omega_t) = \arg \max_{x_t \in \mathcal{X}_t} [C_t(R_{t-1}^x, \omega_t, x_t) + \bar{V}_t^x(R_t^x(R_{t-1}^x, \omega_t, x_t))]$$

Since the post-decision state variable is used, we could choose a single sample realization (the information that we would know anyway before making decision x_t).

Step 0. Initialize an approximation for the value function $\bar{V}_t^{x,0}(R_t^x) \forall t \in T$ and R_t^x . Let $n = 1$.

Step 1. Set $t = 0$ and choose ω^n .

Step 2a. Let $\omega_t^n = W_t(\omega^n)$ and solve:

$$x_t^n(R_{t-1}^{x,n}, \omega_t^n) = \arg \max_{x_t \in \mathcal{X}_t} [C_t(R_{t-1}^{x,n}, \omega_t^n, x_t) + \bar{V}_t^{x,n-1}(R_t^x(R_{t-1}^{x,n}, \omega_t^n, x_t))]$$

Step 2b. Compute $R_t^{x,n} = R_t^{x,n}(R_{t-1}^{x,n}, \omega_t^n, x_t^n)$

Step 2c. Set $t = t + 1$. If $t = T^h$ go to step 3. Else go to step 2a.

Step 3. Update the approximation $\bar{V}_t^{x,n}(R_t^x) \forall t \in T$.

Step 4. Let $n = n + 1$. If $n < N$ go to step 1. Else stop.

Figure 3: Approximate dynamic programming (ADP) using the post-decision state variable

Figure 3 gives an algorithm of the approximate dynamic programming policy (ADP) using the post-decision state variables. If the value function approximation is a linear approximation of the resource vector:

$$\bar{V}_t^x(R_t^x) = \sum_{t' > t} \sum_{a'} \bar{v}_{t'a'} R_{t'a'}^x$$

where $\bar{v}_{t'a'}$ means the value of one more unit of resource with attribute a' at time t' , then, the updating strategies in the step 3 of the approximate dynamic programming algorithms could be as following. Let \hat{v}_{ta}^n be the dual variable for the resource constraint (2). \hat{v}_{ta}^n is a sub-gradient of $\bar{V}_t^{x,n}(R_t^x)$, and therefore forms the basis of a linear approximation for the value function. Because the gradient can fluctuate from iteration to iteration, we perform smoothing:

$$(16) \quad \bar{v}_{ta}^n = (1 - \alpha^n) \bar{v}_{ta}^{n-1} + \alpha^n \hat{v}_{ta}^n \quad \forall a \in A^A$$

In principle, the step size should satisfy the standard conditions from stochastic approximation theory that $\sum_{n=1}^{\infty} \alpha^n = \infty$ and $\sum_{n=1}^{\infty} (\alpha^n)^2 < \infty$. In practice, we have found that a constant step size works well, or the McClain step size: $\alpha^{n+1} = \alpha^n / (1 + \alpha^n - \bar{\alpha})$ which declines arithmetically to the limit point $\bar{\alpha}$ which might be a value such as 0.05.

If the value function approximation is a piece-wise linear (non-linear) approximation of the resource vector, the updating strategies in the step 3 could be concave adaptive value estimation (CAVE, Godfrey & Powell (2001), Godfrey & Powell (2002a) and Godfrey & Powell (2002b)) and separable projective approximation routine (SPAR, Powell et al. (2002) and Topaloglu & Powell (2003)).

5: Numerical experiments

To test the feasibility of the approximate dynamic programming policy (ADP) (as in Figure 3) for the military airlift problem, we use an unclassified TPFDD data set for the problem. The results of the rule based policy (RB) (as in Figure 1, a simple version of the current military practice) are also given for a comparison. The problem is to manage six aircraft types (C-5A, C-5B, C-17, C-141B, KC-10A and KC-135) to move a set of requirements between the USA and Saudi Arabia, where the total weight of the requirements is about four times the total capacities of all the aircraft. The simulation horizon is 50 days, divided into four hour time intervals. Moving a requirement involves being assigned to a route which will bring the aircraft through a series of intermediate airbases for refueling and maintenance. One of the biggest operational challenges of these aircraft is their probability of failure that can result in a delay. To make the model interesting, we assume that an aircraft of type C-141B (empty or loaded) has a 20% probability of failure, and needs five days to be repaired if it fails at an airbase in Northern Europe. All other aircraft types or airbases are assumed to be able to repair the failures without delay.

We assume that there are three types of costs involved in the military airlift problem: transportation costs (0.02 cent per mile per pound of capacity of an aircraft), aircraft repair costs (6 cents per period per pound of capacity of a broken aircraft.) and penalties for late deliveries (4 cents per period per pound of requirement delivered late).

We run 20 iterations in the (ADP) policy while the (RB) policy only needs a single iteration. We use two measures of solution quality. The first is the traditional measure of costs. It is important to emphasize that this is an imperfect measure, since some behaviors may not be reflected in a cost (negative contribution) function. The second measure is throughput which is of considerable interest in the study of airlift problems.

Cost (\$)	(RB)	(ADP) n=19
Travel	313,665,964	127,203,532
Late	113,488,411	56,379,632
Repair	8,736,184	1,609,297
Total	435,890,559	185,192,461

Table 1: Costs of (RB) and (ADP) solutions

Table 1 reports the costs of policy (RB) and policy (ADP) at the last iteration. The total cost is the sum of transportation costs, late delivery costs, and aircraft repair costs. It is clear that the result of (ADP) policy dominates that of the (RB) policy in terms of all the costs.

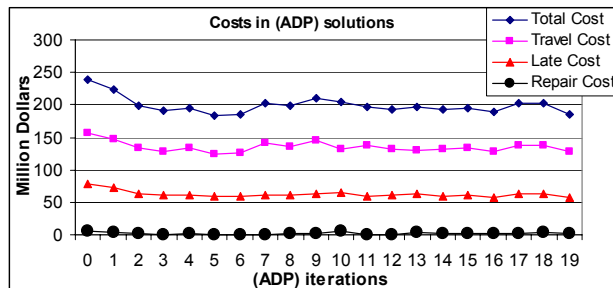


Figure 4: Costs of the (ADP) policy in iterations

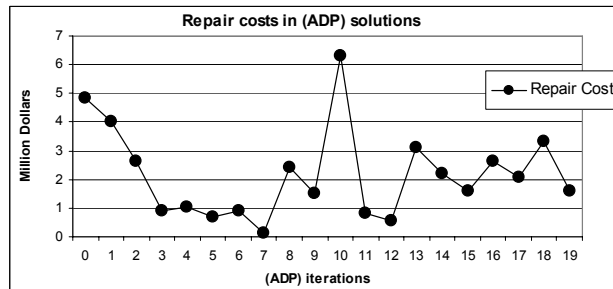


Figure 5: Repair costs of the (ADP) policy in iterations

We plot the total, travel, late and repair costs of all iterations of the (ADP) policy in Figure 4. Since the repair costs are relatively small, we re-plot them in Figure 5 for legibility. The travel and late costs are decreasing in the first a few iterations and then remain at their levels although there are some fluctuations. The repair costs observe the same pattern with relatively big fluctuations after the first a few iterations since the randomness in this experiment is caused by the aircraft breakdown. The result shows that the value function approximations in the (ADP) policy do bring the global information into the local optimization problem and help the model make better decisions after a few learning iterations. The fluctuations are inherent and caused by the stochastic feature of the military airlift problem.

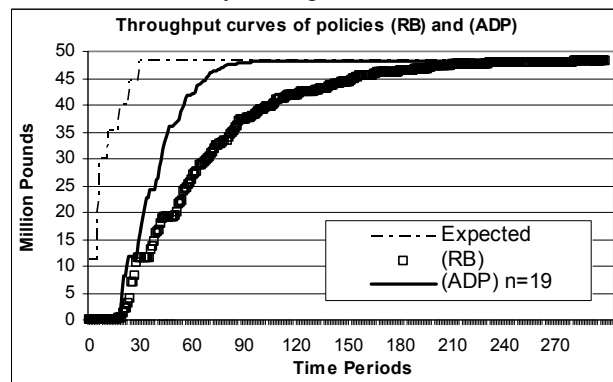


Figure 6: Throughput curves of policies (RB) and (ADP), showing cumulative pounds delivered over the simulation.

The throughputs of policy (RB) and policy (ADP) at the last iteration, as well as the cumulative expected throughput are plotted in Figure 6. It is clear that the (ADP) policy produces a faster delivery than the (RB) policy.

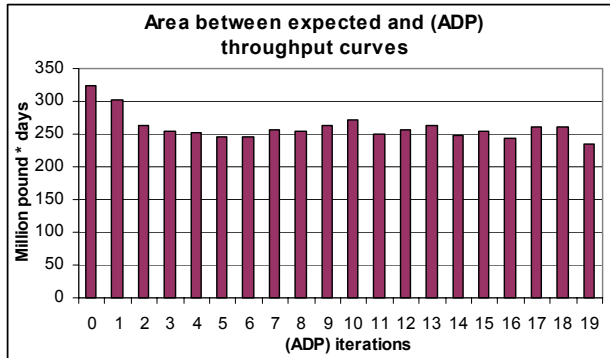


Figure 7: The late delivery in policy (ADP) in iterations

We calculate the area between the expected throughput and the throughput curves of different iterations of the (ADP) policy and plot them in Figure 7. These areas actually measure the lateness of the delivery in iterations. The smaller the area is, the faster the delivery is. We may see that the areas are decreasing in the first a few iterations and then remain at that level with some fluctuations. It has the same pattern as the costs. Once again, the result shows that the (ADP) policy do help the model make better decisions after a few learning iterations. The fluctuations are natural and caused by the random feature inherent in the military airlift problem.

6: Conclusions

This paper demonstrates that we can build an approximate dynamic programming model for the military airlift problem, a dynamic stochastic asset management problem. The approximate dynamic programming model is an intelligent simulator. It combines the flexibility of the simulation models with the intelligence of the optimization models.

Our experimental work shows that the results of the (ADP) policy overcome that of the (RB) policy both in terms of the costs and throughput. In the (ADP) policy, we show that the costs are decreasing and the throughputs become faster in the first a few iterations and then remain at their levels with some fluctuations caused by the stochastic nature in the military airlift problem. The result shows that the value function approximations in the (ADP) policy bring the global information into the local optimization problem and help the model make better decisions after a few learning iterations. We note that the (ADP) policy can be warm-started, which means that we

can perform a series of training iterations after which the results are stored. Then, the analysis of new scenarios can be performed with a small number of iterations.

7: References

- Baker, S., Morton, D., Rosenthal, R. & Williams, L. (2002), 'Optimizing military airlift', *Operations Research* 50(4), 582–602.
- Bellman, R. (1957), *Dynamic Programming*, Princeton University Press, Princeton.
- Bellman, R. & Dreyfus, S. (1959), 'Functional approximations and dynamic programming', *Mathematical Tables and Other Aids to Computation* 13, 247–251.
- Bertsekas, D. & Tsitsiklis, J. (1996), *Neuro-Dynamic Programming*, Athena Scientific, Belmont, MA.
- Blum, J. (1954), 'Multidimensional stochastic approximation methods', *Annals of Mathematical Statistics* 25, 737–744.
- Burke, J. F. J., Love, R. J. & Macal, C. M. (2004), 'Modelling force deployments from army installations using the transportation system capability (TRANSCAP) model: A standardized approach', *Mathematical and Computer Modelling* 39(6-8), 733–744.
- Cheung, R. & Powell, W. B. (1996), 'An algorithm for multistage dynamic networks with random arc capacities, with an application to dynamic fleet management', *Operations Research* 44(6), 951–963.
- Cheung, R. K.-M. & Powell, W. B. (2000), 'SHAPE: A stochastic hybrid approximation procedure for two-stage stochastic programs', *Operations Research* 48(1), 73–79.
- Dantzig, G. & Ferguson, A. (1956), 'The allocation of aircrafts to routes: An example of linear programming under uncertain demand', *Management Science* 3, 45–73.
- Denardo, E. V. (1982), *Dynamic Programming*, Prentice-Hall, Inc., Englewood Cliffs, NJ.
- Godfrey, G. & Powell, W. (2001), 'An adaptive, distribution-free algorithm for the newsvendor problem with censored demands, with applications to inventory and distribution', *Management Science* 47(8), 1101–1112.
- Godfrey, G. & Powell, W. B. (2002a), 'An adaptive, dynamic programming algorithm for stochastic resource allocation problems I: Single period travel times', *Transportation Science* 36(1), 21–39.
- Godfrey, G. & Powell, W. B. (2002b), 'An adaptive, dynamic programming algorithm for stochastic resource allocation problems II: Multi-period travel times', *Transportation Science* 36(1), 40–54.

- Goggins, D. A. (1995), Stochastic modeling for airlift mobility, Master's thesis, Naval Postgraduate School, Monterey, CA.
- Granger, J., Krishnamurthy, A. & Robinson, S. M. (2001), Stochastic modeling of airlift operations, in B. A. Peters, J. S. Smith, D. J. Medeiros & M. W. Rohrer, eds, 'Proceedings of the 2001 Winter Simulation Conference'.
- Killingsworth, P. & Melody, L. J. (1997), Should C-17's be deployed as theater assets?: An application of the CONOP Air Mobility Model, Technical report RAND/DB-171-AF/OSD, Rand Corporation.
- Kushner, H. J. & Yin, G. G. (1997), Stochastic Approximation Algorithms and Applications, Springer-Verlag, New York.
- Mattock, M. G., Schank, J. F., Stucker, J. P. & Rothenberg, J. (1995), New capabilities for strategic mobility analysis using mathematical programming, Technical report, RAND Corporation.
- Midler, J. L. & Wollmer, R. D. (1969), 'Stochastic programming models for airlift operations', Naval Research Logistics Quarterly 16, 315–330.
- Morton, D. P., Rosenthal, R. E. & Lim, T. W. (1996), 'Optimization modeling for airlift mobility', Military Operations Research pp. 49–67.
- Morton, D. P., Salmeron, J. & Wood, R. K. (2003), 'A stochastic program for optimizing military sealift subject to attack', (in review.) Available at Stochastic Programming E-Print Series, <http://dochoost.rz.huberlin.de/speps/> (1), 36.
- Niemi, A. (2000), Stochastic modeling for the NPS/RAND Mobility Optimization Model, Department of Industrial Engineering, University of Wisconsin-Madison, Available: <http://ie.engr.wisc.edu/robinson/Niemi.htm>.
- Powell, W. B., Ruszczyński, A. & Topaloglu, H. (2002), Learning algorithms for separable approximations of stochastic optimization problems, Technical report, Princeton University, Department of Operations Research and Financial Engineering.
- Robbins, H. & Monro, S. (1951), 'A stochastic approximation method', Annals of Math. Stat. 22, 400–407.
- Rosenthal, R., Morton, D., Baker, S., Lim, T., Fuller, D., Goggins, D., Toy, A., Turker, Y., Horton, D. & Briand, D. (1997), 'Application and extension of the Thruput II optimization model for airlift mobility', Military Operations Research 3(2), 55–74.
- Schank, J., Mattock, M., Sumner, G., Greenberg, I. & Rothenberg, J. (1991), A review of strategic mobility models and analysis, Technical report, RAND Corporation.
- Si, J. (2002), Welcome and introduction, 2002 NSF Workshop on Learning and Approximate Dynamic Programming, Playacar, Mexico, Available: [http://ebrains.la.asu.edu/~nsfadb/presentations/JennieSi opening.ppt](http://ebrains.la.asu.edu/~nsfadb/presentations/JennieSi%20opening.ppt).
- Sutton, R. (1988), 'Learning to predict by the methods of temporal differences', Machine Learning 3, 9–44.
- Sutton, R. & Barto, A. (1998), Reinforcement Learning, The MIT Press, Cambridge, Massachusetts.
- Topaloglu, H. & Powell, W. B. (2003), 'An algorithm for approximating piecewise linear concave functions from sample gradients', Operations Research Letters 31(1), 66–76.
- Tsitsiklis, J. & Van Roy, B. (1997), 'An analysis of temporal-difference learning with function approximation', IEEE Transactions on Automatic Control 42, 674–690.
- Wing, V., Rice, R. E., Sherwood, R. & Rosenthal, R. E. (1991), Determining the optimal mobility mix, Technical report, Force Design Division, The Pentagon, Washington D.C.
- Yost, K. A. (1994), The thruput strategic airlift flow optimization model, Technical report, Air Force Studies and Analyses Agency, The Pentagon, Washington D.C.

**Identification and Localization of Buried Metal Object
- High-Speed Model Matching using Genetic Algorithm -**

Tomohiro UMETANI*, Yasushi MAE**, Tatsuo ARAI*, Hironori KUMENO*
Kenji INOUE*, Tomohito TAKUBO*, and Hiroshi NIHO***

* Division of Systems and Applied Informatics, Department of Systems Innovation,
Graduate School of Engineering Science, Osaka University
1-3 Machikaneyama, Toyonaka, Osaka, 560-8531, JAPAN
Tel: +81-6-6850-6368, FAX: +81-6-6850-6341
{umetani, kumeno, takubo}@arai-lab.sys.es.osaka-u.ac.jp
{arai, inoue}@sys.es.osaka-u.ac.jp

** Faculty of Engineering, University of Fukui
3-9-1 Bunkyo, Fukui, 910-8507, JAPAN
mae@rc.his.fukui-u.ac.jp

***PCI

TOPIC: Measurement, monitoring, and reliable control

Identification and Localization of Buried Metal Object - High Speed Model Matching using Genetic Algorithm -

Abstract

This paper describes a method of automated identification of partially exposed metal objects such as abandoned chemical weapon to excavate hazardous objects safely and quickly. In order to excavate the metal objects safely and quickly, the identification method should have high-accuracy of shape and pose (position and orientation) identification. In addition, the identification method should determine the object shape and pose with reasonable cost. The paper focuses on a method of high-speed model matching method using genetic algorithm. The paper introduces a method of setting of initial search area of object matching to obtain accurate pose and shape of the metal objects with reasonable calculating cost. Experimental results show feasibility of our proposed method since the object poses and shapes are obtained accurately and stably with reasonable calculation cost for automated excavation.

1: Introduction

It is desired that removal of hazardous materials such as abandoned chemical weapons from burial pits should be completed safely in a short span of time [1][2][3]. An automated excavation system has been proposed to excavate metal objects from the burial pit [3][4]. The system removes soil around the metal objects safely and quickly to achieve the excavation task. The system identifies shape and pose (position and orientation) of the metal object. After the identification, the manipulator excavates the metal objects.

The excavation system should identify shape and pose of metal objects with good accuracy and reasonable calculation cost. Since the objects are hazardous, the system

should manipulate the object carefully. In addition, there are many metal objects in the burial pits and they lie in the pit unevenly and densely. It is required to distinguish each metal object and identify the shape and pose of the object.

This paper describes an automated identification method for shape and pose of partially exposed metal objects [7]. The method extracts areas of the several objects from the captured range image. Shape and pose of the metal object are determined by matching the target area to the reference shape model of the object given beforehand. The method provides the shape and pose of metal object for automated excavation.

The paper focuses on improvement of the pose accuracy and the calculation cost. It is required to enlarge the search area of the object since there is an orientation error of the principal axis, a division error of the extracted object area, and the range data that is not belong to the object is consisted in the detected object area. On the other hand, even if the search area of the object is enlarged, a method that it takes so much cost for identification of the objects is useless. It is necessary to identify the shape and pose of the objects with reasonable calculation cost since there are many metal objects in the burial pit.

The proposed method applies a genetic algorithm to identify the metal objects quickly. The paper introduces a method of setting of initial search area of object matching to obtain accurate pose and shape of the partially exposed objects with reasonable calculating cost. We have carried out the measurement of the object pose under the several conditions of the target object. Experimental results show feasibility of the shape and pose identification of the partially exposed object.

2: Automated Excavation System

2.1: Characteristics of Metal Object

We introduce characteristics of buried metal objects to show feasibility of the automated excavation system. First, we derive feasibility of the system from the characteristics of metal objects. Buried metal objects have several characteristics shown as follows:

- (1) The shapes of metal objects are few since an object is mass-product materials.
- (2) Metal objects have rotary-symmetrical shape.
- (3) Object color has changed for a long term by corrosion and rust.
- (4) Objects have been deformed because of corruption and rust of the surface of the object.

From the characteristics (1) and (2), there is feasibility of the automated identification system for safe excavation. An automated pattern matching method is useful for identification since there are few types of objects. Rotary-symmetrical shape decreases the degrees of the freedom of the object pose.

On the other hand, it is difficult to the color data and precise shape data for identification because of the characteristics (3) and (4). In addition, color data is not useful for this automated excavation system since the change of light source influences this data strongly. These problems make the automated identification difficult since it is difficult to distinguish between the object area and that of surroundings of objects.

Next, we derive the sensory data for identification from buried conditions of metal objects. Buried conditions of the metal objects are shown as follows:

- (1) Metal objects are partially exposed in the identification part of the excavation process.
- (2) Metal objects are laid densely in the burial pit.

From the condition (1), the vision data captured by the camera and range data is useful for identification. In the

excavation process, the system removes the soil around the metal objects [3]. A part of the metal object is visible. From the condition (2), it is difficult to distinguish and identify each metal object with a metal finder or GPR.

We use the three-dimensional range data as the sensory data for identification of the metal objects. Other sensory data captured by the metal finder [5] or GPR [6] may be useful for excavation by the manipulator. The sensory-data fusion is important issue to realize a safe manipulation, but it is future work.

2.2: Prototype identification system

Figure 1 shows the overview of automated excavation system. A data capture system such as three-eye camera or a laser range finder obtains the three-dimensional range data of the buried pit. The robot arm removes the soil around the objects and handles the objects. The data capture system, the robot arm and the operation server are connected each other by the Internet.

We use range data captured by a three-eye camera or a laser range finder for identification part of the excavation task. The shape and pose of the object are estimated by the operation server. The robot arm removes and recovers the metal object using the sensory data. If the server cannot determine object pose, the server interprets the identification result is doubtful. Then, the server makes a plan of the removal of the soil around the objects again.

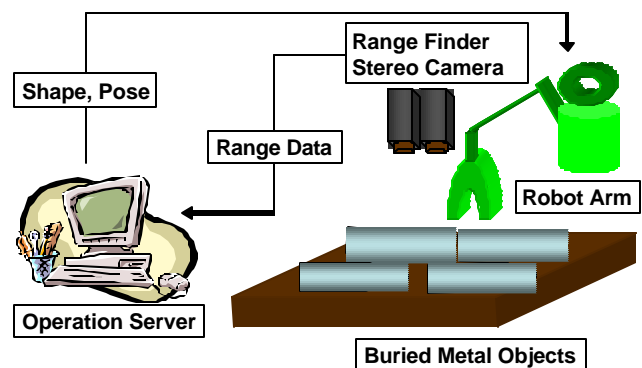


Figure 1: Systems overview.

Figure 2 shows the experimental setup in our laboratory. Three-eye camera are fixed about 700 [mm] above the target area vertically. The camera directs to the target area. We use Digiclops (focal range $f = 3.8$ [mm], the range of capturing is more than about 50 [cm]) as the three-eye camera. The coordination frames of the robot arm and three-eye camera are set as shown in Fig. 2.

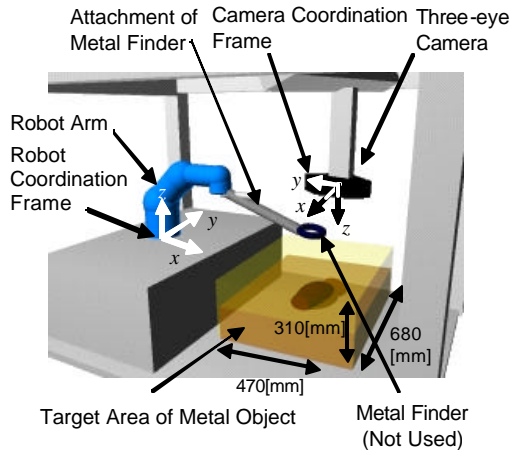


Figure 2: Automated identification system.

The distance to the target area is obtained by the triangulation based on the stereo vision. The distance can be measured in the area that the view of at least two cameras are overlapped. The size of the image data for range image is 640×480 pixels and the distance is obtained by each pixel. The matching between the image pixels of each camera is obtained by correlation centering on the target pixel defined beforehand. The correlation is obtained based on the Sum of Absolute Difference (SAD) matching method. The size of the SAD mask is 15×15 pixels.

3: Procedure of Automated Identification

We describe a procedure of identification of pose and shape of metal object using the three-dimensional captured range data [7]. The camera captures data of surroundings of the metal object and makes a range image of the exposed area of the object from the captured data. The computer estimates and detects a part of the target object using

the range image data. The shape and pose of the metal object are determined by the matching to the reference shape model of the object given beforehand. The procedure of this process is shown as follows:

- (1) Obtain a range image using a three-eye camera.
- (2) Extract the area of target object from the range data.
- (3) Obtain the principal axis of the object.
- (4) Obtain the ridgeline of the metal object.
- (5) Match the object ridgeline to the model of the metal object. The pose that is matched to the model best is regarded as the estimated pose of the object.

The procedure of the identification is shown in Fig. 3. This paper focuses on the improvement of pose accuracy using the object ridgeline and a quick matching method using a genetic algorithm. We introduce a method of obtaining the object ridgeline and setting an initial search area of object pose in the following sections precisely.

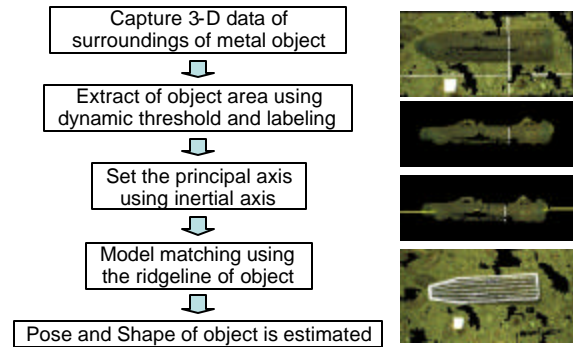


Figure 3: Procedure of object identification.

4: Shape and Pose Identification using Object Ridgeline

4.1: Object Ridgeline

For each set of range data corresponding to the object area, the system defines the ridgeline of the metal object. The ridgeline is obtained stably since the ridgeline is a set of the highest position of object data on the plane that is perpendicular to the principal axis of the object. In addition, the ridgeline of the metal object is defined as one line

since the metal object has a rotary-symmetrical shape. A ridgeline of the metal object is shown as the white-dotted shape in Fig. 4. The procedure of acquisition of a ridgeline is shown as follows:

- (1) The system estimates the horizontal orientation of the metal object ϕ . This orientation is obtained using the principal axis of the object.
- (2) The system supposes multiple planes that are perpendicular to the horizontal orientation of the object and are parallel to the vertical axis of the three-dimensional volume.
- (3) The system extracts a set of the object area corresponding to the plane. The system extracts the object data that is near the plane. The system searches the highest position of the range data corresponding to the plane.
- (4) The system regards the set of the highest position of the range data as the ridgeline of the metal object.

When the metal object is directed vertically, the system cannot obtain the ridgeline of the object. In this case, it is required that the system checks that the object is directed vertically and the system identifies the shape and pose of the metal object using the other method.



Figure 4: Object ridgeline.

4.2: Object Matching using Object Ridgeline

The system can identify the shape and pose of the object by fitting the object model to the ridgeline of the metal object. We suppose an evaluation function to the summation of the distance between each point of the ridgeline and the nearest point of the object model. The object model is set variously. The summation of the distance is zero when each point of the ridgeline is fitted to the object

model. However, a part of the metal object is buried and the shape of the ridgeline and that of the object model has its errors. Therefore, we regard the object pose that the summation of the distance is minimized as the object pose. The system determines the object shape using the criterion that the summation of the distance between the ridgeline and each object model is minimized.

We set the search area for object matching using the characteristics of the captured data of the metal object to estimate the accurate pose and correct shape of the metal object with a reasonable calculation cost. It is required that the number of estimated parameter of the object should be increased and search area of the metal object should be enlarged in order to improve the accuracy of identification of shape and pose of the object. However, the enlargement of search area causes the increase of the calculation cost.

Figure 5 shows the estimated parameters of the metal object. Coordinate (x, y, z) indicates the position of the center of gravity. Object orientation Ω_y and Ω_z are rotational angles about y -axis and z -axis, respectively. Coordinate (dX, dY, dZ) indicates the translational displacement of the center of gravity with respect to the object coordinate frame.

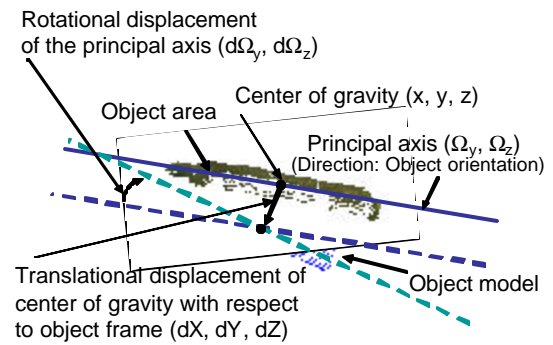


Figure 5: Estimated parameters in object matching.

The system estimates the pose of the metal object by matching the object model to the object ridgeline about the displacement of the center of gravity of the object. If the

principal axis of the metal object is level and the exposed part of the object is large, the object principal axis and the center of gravity are estimated with good accuracy. On the other hand, if the metal object is inclined or the exposed part of the object is small, the error of the principal axis is large, and the estimated position of the center of the gravity of the metal object is far from that of the real object. However, if the system extracts the exposed area of the metal object correctly, it is clear that there is a metal object near the extracted object area.

We apply a genetic algorithm to the object-matching algorithm. Since the parameters of the object are various, the size of the search area is very large. This algorithm does not estimate the most optimized object pose perfectly, however, the algorithm estimates approximately suitable object pose in the reasonable cost.

The translational and rotational displacements of the principal axis from the center of gravity are used as the estimated parameters in the object matching method. It may be reasonable that we apply the object pose $(x, y, z, \Omega_y, \Omega_z)$ as the estimated parameter of the metal object since the object pose can be estimated directly. However, the system can reduce the search area by estimating the center of gravity, the principal axis and the ridgeline of the object beforehand so that the system estimates the suitable object pose stably and quickly.

5: Identification Experiment

5.1: Object Setting

We have various conditions of the object setting about object shape, the ratio of the exposed area of the object, vertical and horizontal orientation of the object, and position of the neighborhood objects.

(1) Object Shape

The target object is 75[mm] and 90[mm] object.

(2) Ratio of the exposed area of the object

The ratio of the exposed area of the target object is defined as the area ratio of the object area projected to the horizontal plane. This ratio of the exposed area is 1 if the object is perfectly exposed.

(3) Horizontal and vertical orientation of the object

The horizontal orientation ϕ is defined as the angle about the vertical direction. The vertical orientation θ is defined as the angle about the horizontal direction. We set the several patterns of vertical orientation.

(4) Position of neighborhood objects

The number of the neighborhood object is one. The relative relationships between each object are defined two parameters d and ϕ .

We have identified the metal pose under the several conditions shown in Fig. 6. Experimental Conditions are shown as follows. There are nine patterns of setting of metal objects. In the case (1), (2), (7) and (8), the metal objects are level. In the case (2), the metal object is buried partly. In the case (3), (4), (5), (6) and (9), the metal objects are inclined. In the case (3), (4) and (9), the vertical orientation θ is 15 [deg]. In the case (5), the vertical orientation θ is 45 [deg]. In the case (6), the vertical orientation θ is 90 [deg].

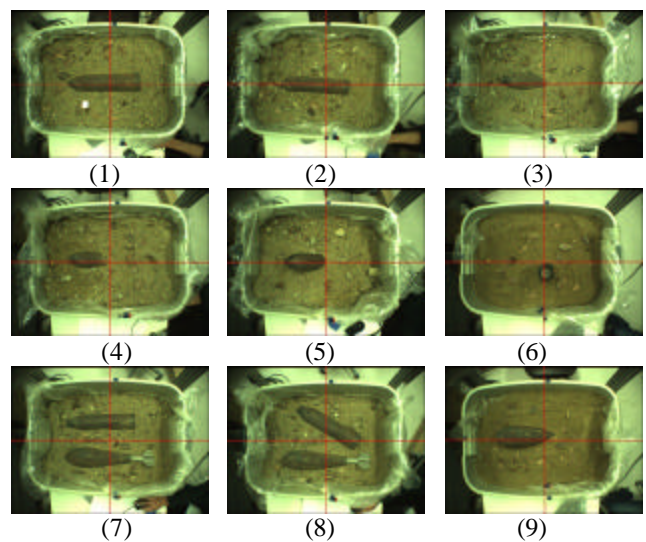


Figure 6: Object setting.

5.2: Range of Matching Algorithm

The parameters of matching algorithm are translational displacement of center of gravity, rotational displacement of principal axis, and translational displacement of the metal object along the shifted principal axis. The range of the estimation parameters is set from the result of the conventional identification method [8].

The translational displacement of center of gravity depends on the conditions of the object. The center of gravity and the principal axis of object are estimated beforehand so that the range of each translational displacement of the center of gravity is set ± 512 [mm] about the direction of the principal axis and ± 64 [mm] about the perpendicular direction to the principal axis, respectively. The exposed area of metal object is extracted stably, and the width of the metal object is less than 100 [mm]. The metal object shapes has the rotary symmetrical and elongated shape so that the principal axis is estimated stably.

The range of rotational displacement of the principal axis depends on the accuracy of the estimated principal axis. The horizontal orientation ϕ is estimated accurately since the object area of the metal object is extracted stably. On the other hand, the vertical orientation θ is estimated inaccurately when the metal object is inclined. The ranges of rotational displacements of principal axis are set ± 0.256 [rad] about ϕ and ± 0.512 [rad] about θ , respectively.

There are two patterns of the object direction about the same principal axis. The system estimates the object pose for each pattern of the direction, the system regards more suitable object pose as the estimated object pose.

We apply the parameter-free genetic algorithm [8] to the object matching since the parameters of the algorithm are only the evaluation function, the gene length for each parameter, and the number of the evaluation. Each parameter is encoded 10 bits. The number of the evaluation is set 6.0×10^4 . This number is illustrated that the number of individuals is 300 and the number of evaluation is 200

in the general genetic algorithm. The adaptation value of the algorithm is the negative value of the summation of the distance between each point of the object ridgeline and the most nearest point of the object model.

5.3: Experimental Result

We have estimated the object pose 10 times for each object shape and condition. Figure 7 shows the experimental results of the pose estimation. White-dotted shape is the estimation result. The parameters of objects are average of identification results for each condition. The system cannot estimate the condition (6). In this case, the system cannot estimate the principal axis of the object and the object ridgeline, either. The proposed method identifies the object pose accurately. The required time of the pose identification is about 1 minute.

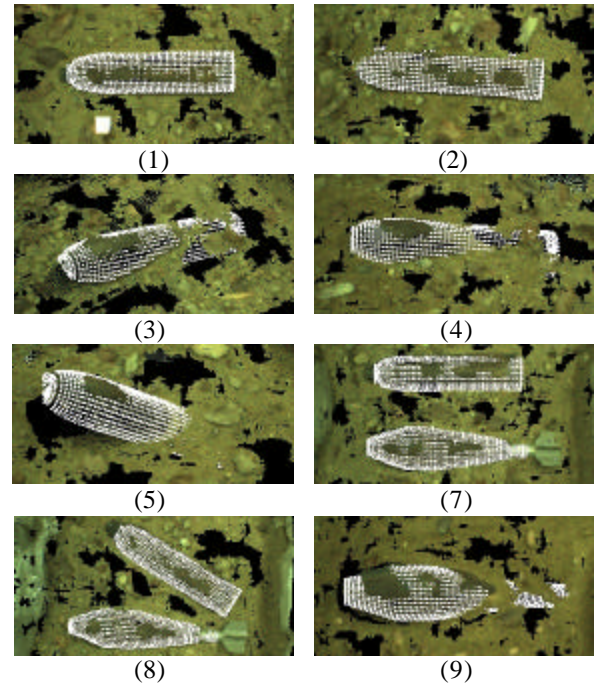


Figure 7: Experimental results.

We evaluate the standard deviation of the object pose by the identification algorithm and the identification result of the object shape. The shape identification result is evaluated by the comparison of the adaptation value of the

identification result for each shape. The identification results in Fig. 7 are the results using the correct shape.

The matching results show feasibility of automated identification of shape and pose using the ridgeline of the metal object. Table 1 shows the standard deviation of the object pose. From table 1, the system obtains the object pose stably. In addition, the standard deviation about the direction of the principal axis is larger than the standard deviation about the perpendicular directions to the principal axis. The standard deviation about the perpendicular directions to the principal axis influences the clearance between the object and the manipulator.

Table 1: Standard deviation of object pose

Condition	Standard Deviation				
	Translational [mm]		Rotational [deg]		
	Along	Perpendicular	Vertical	Horizontal	
(1)	2.189	1.319	0.632	0.553	0.843
(2)	11.370	0.320	0.785	0.949	0.356
(3)	3.187	0.539	0.961	1.262	0.380
(4)	1.915	0.528	0.649	0.657	0.298
(5)	3.807	1.401	2.153	2.425	0.952
(7)	13.308	0.038	0.870	0.864	0.189
	3.586	0.614	0.515	0.496	0.409
(8)	4.220	0.071	0.056	0.646	0.172
	2.262	0.624	0.331	0.283	0.301
(9)	8.510	0.941	2.918	2.466	0.481

The object shape is correct by the result of the Mann-Whitney U test about the median of the adaptation value for each shape, except the case (3) and (5). In the case (3) and (5), we cannot conclude that the adaptation value for correct shape is larger than that for incorrect shape.

Figure 8 shows the relation between the number of the evaluation and the adaptation value of the most adapted individual in the matching method in the case (5). The vertical axis indicates the adaptation value. The horizontal axis indicates the number of the evaluation. The system obtains the final estimated result in the 23000 evaluation times in the latest case. It is required more evaluation times to estimate the most suitable object pose.

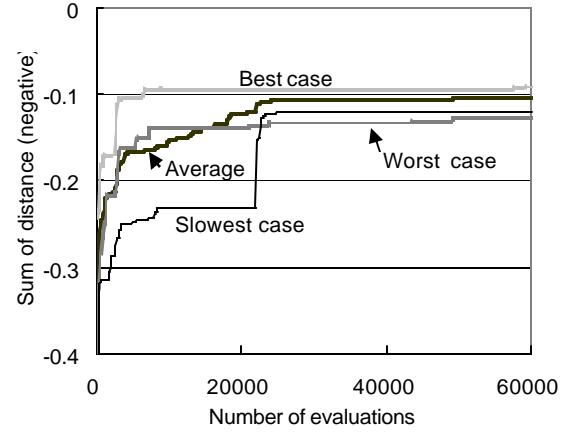
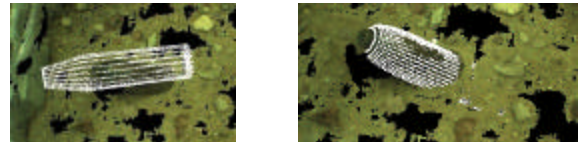


Figure 8: Adaptation value of the most adapted individual.

We discuss the calculation cost using the required time to estimate the object pose. The span of the object matching is 5 [mm] and 0.005 [rad], respectively. We have carried out the full-range search with 1 parameter (translational displacement of the center of gravity along the principal axis, conventional method [8]), and 3 parameters (translational displacement about the principal axis and rotational displacement of the principal axis). We use an object setting the case (5) in this examination.



(a) Conventional method (b) Full-range search (3 axes)



(c) Proposed Method

Figure 9: Identification results using full-range search with less parameter.

The estimated result of each condition is shown in Fig. 9. The system estimates the object pose with much error in the case the full-range search with 1 parameter. It is required several search parameters to pose identification of the metal object. The range of the parameters is set as the same of the proposed method. We have the identification

experiment using the PC (Pentium 4, 3[GHz]). The required time in the case (5) is 0.0047 [sec] for 1 parameter, 900 [sec] for 3 parameters, 32 [sec] for the proposed method, respectively. The proposed method can estimate the suitable pose within a reasonable calculation cost.

6: Conclusions

This paper describes an automated identification method of shape and pose of partially exposed metal objects based on the range image data. The method uses the characteristics of exposed metal object, rotary symmetrical shape, a few shapes of the object. By estimating the center of gravity of an object, the principal axis, and ridgeline of the object, the system identifies the shape and pose of metal object stably with reasonable calculation cost. Experimental results show feasibility of the identification of the metal objects using the three-dimensional distance data.

This method cannot estimate the shape and pose of standing vertically object since the system cannot estimate the ridgeline in this case. It is required the other process to identify this kind object. This method estimates the approximate object pose with the reasonable cost using the genetic algorithm. However, this algorithm does not ensure the optimized object pose and the length of the calculation is not determined. The more examinations of the shape and pose identification are required to apply the proposed method to the real excavation system.

More robust and accurate method of extracting the area of the metal object is required in order to apply to the real excavation system. The paper does not discuss the absolute error of the identification result. The discussion of absolute error and standard deviation for the identification is required to realize the automated excavation system.

The development of more accurate and robust automated identification method, and to apply the automated identification to the real excavation system are future works of our study.

References

- [1] T. Arai and H. Niho, "Teleoperation and Automation for Excavating Abandoned Chemical Weapons," *Proc. 2002 SICE System Integration Div. Ann. Conf.*, vol. 1, 2002, pp. 157 – 158 (in Japanese).
- [2] C. Christensen, "Technologies for Removal of Hazardous Materials from the Subsurface Environment," *Proc. 1st Int'l Symp. System and Human Science – For Safety, Security, and Dependability –*, 2003, pp. 119 – 132.
- [3] H. Niho, "Technologies for Removal of Hazardous Materials from the Subsurface Environment," *Proc. 1st Int'l Symp. System and Human Science – For Safety, Security, and Dependability –*, 2003, pp. 113 – 118.
- [4] H. Hara and M. Nakajima, "Robotic Grip-system-test for Recovery of Non-stockpile Munitions," *Proc. 2002 SICE System Integration Div. Ann. Conf.*, vol. 1, 2002, pp. 159– 160 (in Japanese).
- [5] X. Huang, D. Bernd and L. E. Bernold, "Innovative Technology Development for Safe Excavation," *J. Construction Engineering and Management*, vol. 122, no. 1, 1996, pp. 91 – 96.
- [6] H. Herman and S. Singh, "First Results in autonomous retrieval of buried objects," *Automation in Construction*, vol. 4, no. 2, 1995, pp. 111 – 123.
- [7] T. Umetani et al., "Identification of Partially-Exposed Metal Object," *Proc. 21st Int'l Symp. Automation and Robotics in Construction (ISARC)*, 2004, pp. 274 – 279.
- [8] H. Sawai et al., "Parameter-free Genetic Algorithm (PfGA)," *IEICE Trans. Information and Systems*, vol. J81-D-II, no. 2, 1998, pp. 450 – 452 (in Japanese).

TOPIC: Human and organizational behavior and errors

Active Compensation for Oscillatory Motions in Human Control Behavior

Author's information:

Takashi Takimoto *1
Graduate Student
Dept. Systems Innovation, Osaka University
Machikaneyama, Toyonaka, Osaka 560-8531, JAPAN
Phone: +81-6-6850-6354
Fax: +81-6-6850-6341
Email: takimoto@hopf.sys.es.osaka-u.ac.jp

Shigeru Yamamoto *2
Associate Professor
Dept. Systems Innovation, Osaka University
Machikaneyama, Toyonaka, Osaka 560-8531, JAPAN
Phone/Fax: +81-6-6850-6388
Email: yamamoto@sys.es.osaka-u.ac.jp

*1 Speaker

*2 Corresponding Author

Active Compensation for Oscillatory Motions in Human Control Behavior

Takashi Takimoto¹, Shigeru Yamamoto¹

¹ Graduate School of Engineering Science, Osaka University
Machikaneyama, Toyonaka, Osaka 560-8531, Japan

Abstract

Generally, limitations of human accuracy in manual manipulation hinder the quality of work performed by human operators of manual control systems. Therefore, to enhance accuracy, undesired motions must be effectively suppressed. In this paper, we propose active feedback control methods based on the so-called delayed feedback control and washout filters to suppress harmful oscillatory motions in such systems. Moreover, we implemented the proposed methods for manual control of an inverted pendulum system. The experimental set has a pole attached to a moving cart; a human operator controls the movements of the cart to keep the pole upright. The effectiveness of the proposed techniques is illustrated with experimental data indicating that oscillations of the pole are suppressed.

1. Introduction

In this paper, we focus on the class of manual control systems in which a human operator manipulates an unstable object. In such systems, human operators' skills affect the achievement of the control purpose of the control system. Additionally, operator-induced vibration occurs due to the limits of human accuracy in performing manual operations [1, 2]. A hand tremor is an example of such vibration. In a system controlled by manual manipulation such as microsurgery, unnecessary vibration in the system caused by the movements of the operator is undesirable. Therefore, effective suppression of undesired motion during manual manipulation is required to enhance the accuracy of control systems.

In this paper, we propose additional automatic control to suppress the harmful vibration in manual control systems. The proposed additional automatic control is different from the direct application of automatic control to the systems for human operators in the usual sense. In the usual control method, an operator's intention is not

taken into account. Hence, the important flexibility of manual operations will be lost. Therefore, additional automatic control that can incorporate operators' intentions and thus support their work is required.

In this paper, we introduce an active feedback controller as an additional automatic control; this additional control can suppress vibration by stabilizing the equilibrium point of a manual control system. The equilibrium points in a manual control system depend on the kind of operations to be performed and the human operators' intentions. Therefore, the points may vary due to the intentions of human operators. In addition, they are generally uncertain.

In order to achieve automatic control that supports human operators, the proposed controller should stabilize a manual control system without changing its equilibrium points. Therefore, we adopt robust control methods that preserve the targeted equilibrium point of an open-loop manual control system and facilitate automatic following of the targeted equilibrium point when the open-loop system changes.

In this paper, we propose and investigate two feedback

mechanisms. One is based on the so-called delayed feedback control (DFC) [3]; the other is based on washout filters [4, 5]. The main benefit of using these mechanisms is that they do not affect the steady state of control systems. Hence, they are robust against the uncertainty of equilibrium points [6, 7].

Moreover, to illustrate the effectiveness of the proposed technique, we describe our experiment with an inverted pendulum system (See Figure 2) as an unstable system controlled by manual operation. A human operator stabilizes a pendulum by manipulating a cart that is part of this system. Thus, we illustrate how the proposed controllers can suppress oscillatory motions in a manual control system.

2. Manual Control System

The manual control system considered in this section is diagrammed in Figure 1. In this manual control system, depicted by a dotted line, a human operator determines the amount of operations based on the observed output of an unstable object. Then, because of the limits of human operator accuracy in manual operations, the controlled output may oscillate. In this paper, we consider the control problem of finding an appropriate input $u(t)$ to stabilize the manual control system and support operation by using the proposed control methods based on measured output, $y(t)$.

Then, we assume the following for the manual control system.

Assumption 1 The manual control system under consideration can be described, however unknown, by the nonlinear differential equation;

$$\begin{aligned} \dot{x}(t) &= f(x(t), u(t)) \\ y(t) &= g(x(t)), \end{aligned} \quad (1)$$

where $x(t) \in \mathfrak{R}^n$ is the state vector, $u(t) \in \mathfrak{R}^r$ is the input vector, and $y(t) \in \mathfrak{R}^m$ is the measured output.

Assumption 2 At least one equilibrium point exists in the manual control system.

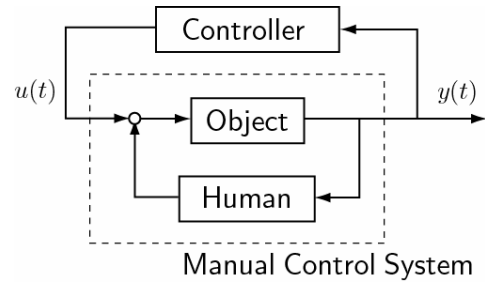


Fig.1 Manual control system with active feedback controller

3. Proposed Control Methods

To identify the systems unknown dynamics (1), we apply the so-called reconstruction method to the original manual control system (1). We adopt the reconstruction method by using the delay-time coordinate, which is the (ml) th-order vector,

$$z(t) = \begin{bmatrix} y(t) \\ y(t-\mathbf{t}) \\ \vdots \\ y(t-(l-1)\mathbf{t}) \end{bmatrix} \in \mathfrak{R}^{ml} \quad (2)$$

in which \mathbf{t} is the time delay. That $z(t)$ can reconstruct the original dynamics if $ml > 2n$ is known, (Takens' embedding theorem) [8]. Since the manual control system contains a human operator, the order of the original system is generally unknown. Therefore, l is determined by trial and error. Then, the reconstructed dynamics can be described by

$$\dot{z}(t) = F(z(t), u(t)). \quad (3)$$

By using the reconstructed dynamics (3), we can identify the linearized system around the equilibrium point z_f which is given by

$$d\dot{z}(t) = A dz(t) + Bu(t), \quad (4)$$

where

$$A = \left. \frac{\partial F(z, u)}{\partial z} \right|_{z=z_f, u=0}, \quad B = \left. \frac{\partial F(z, u)}{\partial u} \right|_{z=z_f, u=0},$$

$$dz(t) = z(t) - z_f.$$

In this study, we adopt delayed feedback control and washout filters to stabilize the unknown equilibrium point z_f that exists in the system (3) when $u(t) = 0$.

3.1 Delayed Feedback Control

Delayed feedback control (DFC) is given by

$$u(t) = -K(z(t) - z(t-T)),$$

where K is a constant gain and T is a time delay. These DFC parameters are determined such that the linearized closed-loop system around z_f is asymptotically stable. A method to find stabilizing parameters K and T from Jacobian matrices A and B was developed by H. Kokame *et al.* [7].

3.2 Washout Filters

A washout filter is a high pass filter that washes out steady state inputs. The transfer function of the washout filter used in this work is given by

$$G(s) = \frac{s}{s+d},$$

where d is the reciprocal of the filter time constant. Hence, the output of the washout filter vanishes in steady states. Therefore, feedback controllers based on this washout filter can stabilize without changing the equilibrium points of the open-loop system.

The generalized washout filter-aided feedback control [4, 5] is given by

$$\dot{\hat{z}}(t) = P(\hat{z}(t) - z(t))$$

$$u(t) = K(\hat{z}(t) - z(t)),$$

where P is a nonsingular matrix and K is a feedback gain. Parameters P and K are determined such that the linearized closed-loop system around z_f is asymptotically stable [4, 5].

4. Experiment with Inverted Pendulum System

To demonstrate the effectiveness of the proposed technique, we applied it to manual control of the inverted

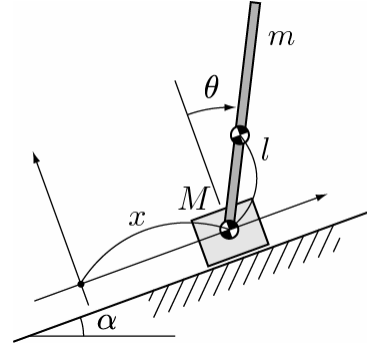


Fig. 2 Inverted pendulum system

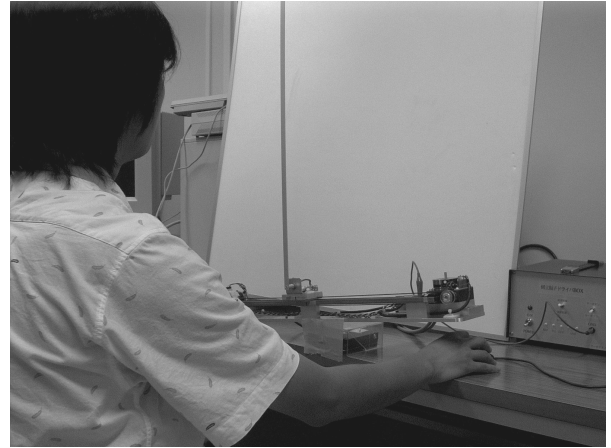


Fig. 3 View of experimental setup

pendulum system with an inclined rail shown in Figure 2. In the manual control system, the task of a human operator is to stabilize the pendulum by controlling the cart in this system. Here are the parameters of the system. The length from the joint to the gravity center of the pendulum l is 0.5 m, the mass of the pendulum m is 0.056 kg, the mass of the cart M is 0.235 kg and the angle of the slope α is 15 deg. In the experiment, the parameters are assumed to be unknown. Therefore the control purpose is to stabilize the unknown equilibrium point z_f of the manual control system. In this experiment, we used a mouse as the operator's input device. By operating the mouse, we can move the cart to right or left as shown in Figure 3.

Figure 4 shows the time response of the displacement

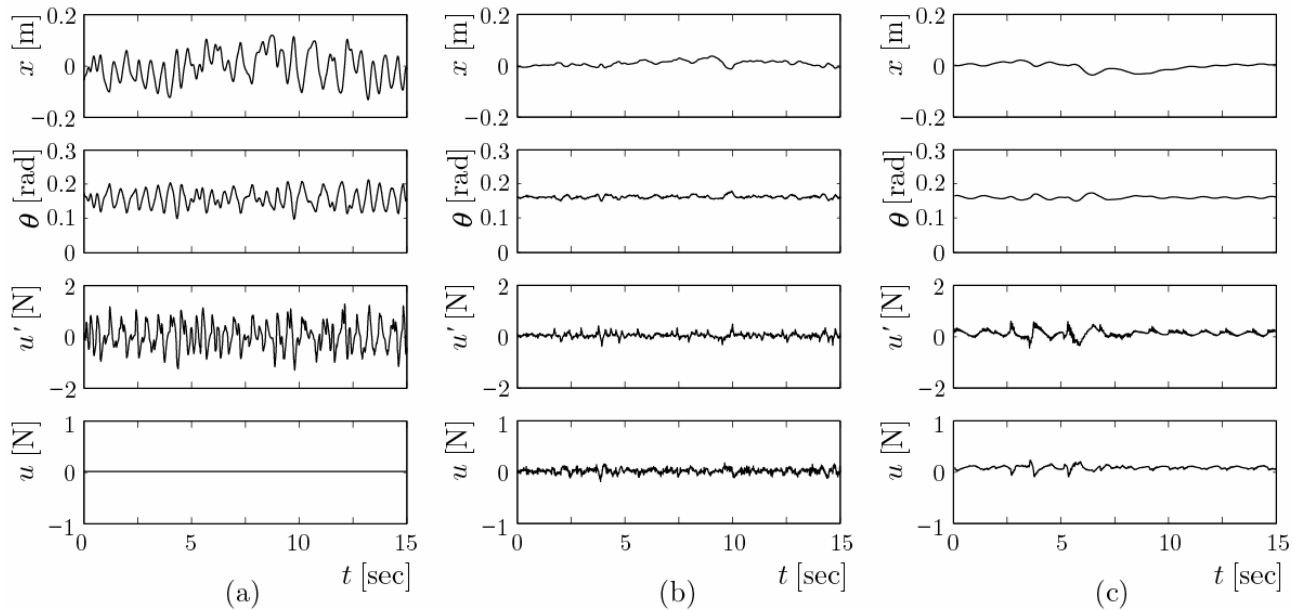


Fig. 4 Time responses of the inverted pendulum system with (a) only manual control, (b) manual control with DFC, and (c) manual control with washout filters

of the cart $x(t)$, the angle of the pendulum $q(t)$, the control input by the human operator $u'(t)$, and the control input $u(t)$ by the proposed control method. Figure 4 (a) is a result obtained with only manual control, whereas Figure 4 (b) and (c) are results by manual control with the DFC method and manual control with the washout filters, respectively. Although the upright state of the pendulum is maintained as shown in Figure 4 (a), vibration occurs. Moreover, the vibration of the control input by manual manipulation is large. On the other hand, the vibrations are suppressed by the DFC method as shown in Figure 4 (b), and by washout filter-aided control as shown in Figure 4 (c). Therefore, by using the proposed control method, the control input of manual manipulation is suppressed and the load of manual operation is reduced.

5. Conclusion

In this paper, we have proposed an active control method, and have shown that it can suppress vibration in a manual control system. Since the method is for the

purpose of supporting the operations of human operators, it can only stabilize systems that require human operators. By using the proposed techniques and this method, control systems for supporting human operators can be achieved.

Acknowledgement

This research was supported by the Japan Society for the Promotion of Science under Grant-in-Aid for Creative Scientific Research (Project No. 13GS0018).

References

- [1] Y. Kawazoe, T. Ota, K. Tanaka, and K. Nagai, "Nonlinear behavior in stabilizing control of an inverted pendulum on a cart by human operator," *Proceeding of the 5th MOVIC*, No. 97-31, 1997, pp. 395-398. (in Japanese).
- [2] C. Riviere, W. Ang, and P. Khosla, "Toward active tremor canceling in handheld microsurgical instruments," *IEEE Trans. Robotics and Automation*, Vol. 19, No. 5, 2003, pp. 793-800.

- [3] K. Pyragas, "Continuous control of chaos by self-controlling feedback," *Physics Letters A*, Vol. 170, 1992, pp. 421-428.
- [4] M. A. Hassouneh, H.-C. Lee, and E. H. Abed, "Washout filters in feedback control: Benefits, limitations and extensions," *ISR, University of Maryland, College Park, Tech. Rep. TR 2004-16*, 2004.
- [5] M. A. Hassouneh, H.-C. Lee, and E. H. Abed, "Washout filters in feedback control: Benefits, limitations and extensions," *Proceeding of the American Control Conference*, 2004, pp. 3950-3955.
- [6] H. Kokame, K. Hirata, K. Konishi and T. Mori, "State difference feedback for stabilizing uncertain steady states of non-linear systems," *Int. J. of Control*, Vol. 74, No. 6, 2001, pp. 537-546.
- [7] H. Kokame, K. Hirata, K. Konishi and T. Mori, "Difference feedback can stabilize uncertain steady states," *IEEE Trans. Automatic Control*, Vol. 46, No. 12, 2001, pp. 1908-1913.
- [8] F. Takens, "Detecting strange attractors in turbulence, Dynamical Systems and Turbulence," *Lecture Notes in Mathematics Vol. 898 (Eds. D. Rand, L.S. Young)*, Springer Verlag, 1981, pp. 366-381.

Title

Distribution and the information security of archive contents

Author' s information

Yoshikazu TANNO

Osaka University , 1 Machikaneyama-cho Toyonaka-shi Osaka, Japan

Fumio MAEHARA

Matsushita Electric Industrial Co., Ltd. , 2-15 Matsuba-cho Kadoma-shi Osaka, Japan

Tatsuo ARAI

Osaka University , 1 Machikaneyama-cho Toyonaka-shi Osaka, Japan

Topic

Network and systems security

Author information

Yoshikazu TANNO

Yamagata Digital Content Center for Research and Promotion, 1-3-8 Mtsuei Yamagata-shi Yamagata, Japan,990-2473

Phone: +81-23-647-8121

FAX: +81-23-647-8122

E-mail: tanno@archive.gr.jp

URL: <http://www.archive.gr.jp>

Distribution and the Information Security of Archive Contents

Yoshikazu Tanno^{*1,*2}, *Fumio Maehara*^{*3} and *Tatsuo Arai*^{*1}

*1 Osaka University, 1 Machikaneyama-cho Toyonaka-shi Osaka, Japan

*2 Yamagata Digital Content Center for Research and Promotion, 1-3-8 Mtsuei Yamagata-shi Yamagata, Japan

*3 Matsushita Electric Industrial Co., Ltd., 2-15 Matsuba-cho Kadoma-shi Osaka, Japan

E-mail: tanno@archive.gr.jp URL: <http://www.archive.gr.jp>

Abstract: According to the rapid expansion of the broadband digital network and terrestrial broadcasting, the contents distribution and their security are becoming the important issues expanding. Here we introduce the large scale archive and the distribution system for education and disaster security. The contents management and security issues on this are also discussed. Especially the issues about the harmful information, network virus and illegal copy will be discussed based on ISO17799 and 15408 recommendation. New watermark technology and Meg7 metadata index are introduced to the unified management of video contents and additional information. The validity of the system is cleared throughout the experiments.

Keywords: Archive, Security, Contents ID, Watermark, ISO17799

1. Introduction

With the rapid progress in broadband network and the digital terrestrial broadcasting, new type of digital content creation and their distribution become increasingly indispensable [1]. Digital video archive is one of the solutions for this issue. Conventional major contents are entertainment, music and news category etc; on the other hand the social safety information such as disaster, crime or social security are newly remarked.

To archive previous information such as disaster, accident and earthquake as audiovisual information is also very important activity for the social security.

In this case embedding the relating informs on video signal is one of the important issue to be solved for unified management of video and its relating information and also prevent dispersing these information.

Watermark technology and standard contents Identification (ID), the other words metadata embedding, is on of the important solution of this.

Large-scale archive and contents distribution system had been developed in Yamagata Video Archive Research Center (YRC). Which archive has 7200 digital videocassettes robot and DVD, HD server. Optical fiber channel had been connected two-research point, YRC and Tohoku University of art and design, which distance is 10Km to utilize transmission experiments with High Definition Video signal for remote editing and watermark ID embed.

About 3000 archive contents had been made for utilize the network distribution experiments.

There are several issues to be solved on such archive and distribution; which are visual and easy retrieval, copyright protection remote and convenient editing and security protection [2].

The wide range security policy is needed in such video and information archive such as security organization, physical security assurance, information security and copy right, metadata security.

To solve these issues, large-scale archive system had been made in YRC, and three major research activities had been done through 1999 to 2002. These are research of expandability of archive robot to 5million cassettes, visual retrieval interface by using multi motion thumbnail icon, remote editing and watermark. Later new theme has added on these 4 themes. These new themes are contents ID as embed by water mark and archive security.

Here we report the overview of the archive system, security activity based on ISO17799, contents ID with watermark based on MPEG-7 coding for distribution channel security. This paper describes the brief overview of the archive and distribution system in section 2, security management of the system in section 3, watermark technology is in section 4, Mpeg-7 over contents ID in section 5, the application for the prevention of disaster archive and education system in section 6 and finally concluded in section 7.

2. Archive System

Four research activity have been done in the Yamagata Video Archive Research Center (YRC, 1999-2003.3) which is currently handed over to Yamagata Digital Contents Center for Research and Promotion (YDCC, 2003.4 - now). YRC was one of the research center in the Telecommunication Advancement Organization (TAO) belonged to Ministry of Pubic Management, Home Affairs, Posts and Telecommunications. Four research themes, which represent the aspects of preservation, content creation, copyright protection and security, have been

carried on. Security is the new issue proposed now by the authors. The diagram of the system is shown in Fig.1.

In the aspect of preservation, large-scale digital video archive robot had been developed, which outlook is shown in Fig.2. The capacity of the robot is 7200 digital cassettes and the architecture is designed expandable to approximately 5million cassettes. Professional use Vide Cassette Recorder (DVC-PRO) with DV (Digital Video) codec format is used. DVD and Hard Disk server are also utilized. 16 sub-divided video thumbnail icons are utilized for easy retrieve interface for this large-scale archive for quick retrieval [3-6].

Video contents stored in the archive are about 3000 title made by YDCC, which include culture, history, scenery and education etc.

In the aspect of copyright protection, watermark technology had been developed. New method named spatial frequency distribution method had been proposed and several experiments have been done. The third issue is remote editing and editing information preservation in the combination with remote fiber network and time code preservation by watermark. The fourth issue (New issue) is security. Here security organization, physical security environment, information security and distribution channel securities have been discussed.

In the aspect of information security ISO 17799 and 15408 guideline is considered on the archive security. The distribution channel security, standard contents ID (cID) is proposed by cIDf (contents ID forum), and embedding method of cID on the audiovisual data by watermarking is proposed and several experiments have been done.

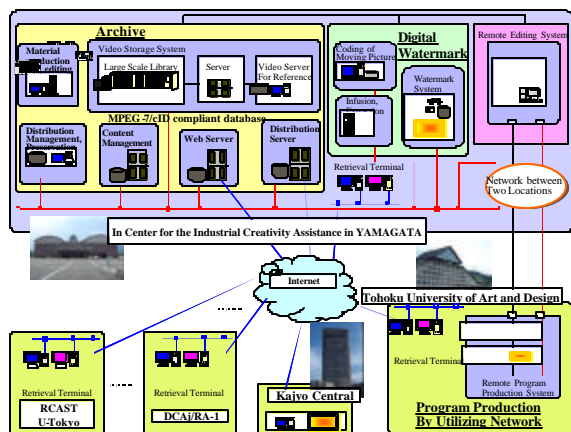


Fig. 1 Archive and contents distribution system

3. Archive Security

In such archive and this content distribution, security management is one of the very important issues. Security management includes several issues, which are organization management, physical protection, and information protection and delivery channel management. Organization management, physical protection and information protection is described by ISO 17799 guideline and products security is mentioned by ISO 15408.

Contents distribution channel security includes illegal copy, change and delivery.

The security in the content distribution channel is now discussed by contents ID forum (cIDf) in which standard guideline for the contents ID and the embedding methods are discussed and proposed. Watermark is one of the recommended methods to embed ID information on the video and audio contents in the aspects of immutability of edit and copy operation.

ISO15408 and 17799 are the recommendation, which guide the information security system and products, which include the networks or various information security devices. ISO15408 guides final products include system and 17799 guides the managements system for produce such products or system [7,8].

These criteria established in Dec. 1999 by ISO (International Standard Organization) and introduced to Japan in July 2000 as JIS X5070.

Major point of the recommendation Security Target (ST) is required, which is the specification document of security design, security design structure and logical design. And also requires source program codes and testing method description.

The approach for the information security includes

1. Exclusiveness: Clearing the security problem and Remove the occurrence.
2. Minimization: Decrease the influences of the security To the capable level.
3. Supervising: Detecting beforehand the security problem And eliminate the security loss.

The security issued are described below and the security protection done in YRC (YDCC) is underlined and some protection method is also described.

[Security Organization]

1. Clarify director's responsibility
2. Establish Common Criteria (CC) and Security Target (ST)
3. Personnel management and training

[Physical Security environment]

1. Fire Prevention management and Fire proof building and equipment
2. Building Structure for prevention disasters
3. Prevention for crime (Security door etc.)
4. 24 hours online monitor by the security guard company
5. Deiced security zones and equips fireproof safe

[Information Security]

1. Install Firewall and cipher
2. Anti-virus operation
3. 24 hour supervise on network

[Distribution Channel Security] (Proposing Now)

1. Illegal copy protection
2. Illegal change and edit protection
3. Illegal delivery protection

Information security has very much aspect such as virus, frequent attack, disguising IP address, illegal copy of contents and credit card number, sending harmful or obscene contents address etc. Firewall and vaccination program are one of the power full solution. You can find the solution in the homepage of Trend micro Corp. or

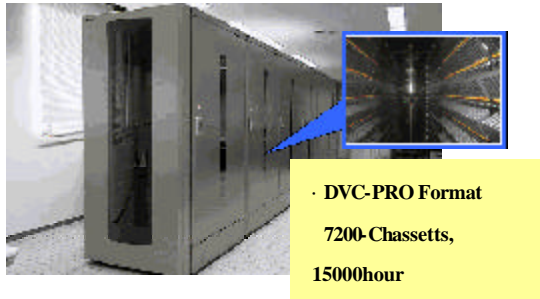


Fig. 2 The outlook of the tape archive robot

Microsoft corp. But many other problems can't be solved in the simple way, you should take measures depend on the situation. Frequent change of password, 24 monitor of the network can be the other solution.

Objective Security Target should be settled and Common Criteria should also be cleared.

Strict management on organization and personnel on the security is done by National Government and prefecture in YRC (YDCC). The archive is located in tough structure building which has 2nd floor height obeyed by architecture low and fire protection low. 24 online guard system by Security Guard Company is done and electric security doors are equipped. No fire facilities such as cooking are inside.

The Internet delivery channel is completely separated to internal archive data channel physical and also protocol separation. Outside invasion through network is completely protected.

The issue of security by the distribution channel is under discussion. Several propose have been done in the content ID forum. The standard content ID proposal and Watermark embed technology, and several organizational structures for the distribution channel. These are reported in the following section.

4. Contents ID and watermark

Another important issue is distribution security in the contents market. This includes several points, such as illegal copy, illegal change and illegal delivery etc.

Disappearing and dispersing caused by the separate store of the audiovisual information and code information is also the point. Database separation sometime cause human error of retrieval and distribution.

Fig.3 shows the Graphic User Interface of Mpeg-7 metadata based retrieval system.

The difference of indexing data in different database causes the mismatch of the database, which prevent the uniqueness and exchangeability of the database.

Two important issues are proposed. One is the proposal for the unified ID format, which is done in ISO as MPEG-7 and 21 and also done contents ID forum in Japan. These two organizations are closely related and working together.

New watermark technology named "Spatial Frequently Distribution Embed Method" is newly proposed in research at YRC [9-12].

The cID is embedded in audio and visual data by watermark. This enable unified management of audiovisual data and code ID data in the same database.

Unified ID also enables the easy retrieve to the database, which is,



Fig. 3 GUI of Mpeg-7 based retrieval system

distributed world widely such as Internet homepage data retrieval.

The digital watermark technology is one of the important issues to embed additional information to the video data. In the large amount of video database, separate database manager such as oracle system or SQL server are used. But in such system, the data mismatch caused by human dispersing or human operation error. One of the effective method to preserve the additional information relate to the video data is digital watermarking. In this method additional data, called cID or metadata, time-code, and copyright information are added on the video data themselves on the lower bit area of the DCT coefficient of the video data.

Fig. 4 shows the watermarking method used in YRC[9,10], in which low space frequency area on DCT is aimed at the data embedding as well as high frequency area as same as high frequency area. An example of embedded video data and extraction result is shown in Fig. 5.

Fig. 5 shows the evaluation of S/N ratio versus cutting frame. The watermark is embedded in each video frame. Cutting frame represents one example of the part in the continuous video frame (1 to 14). About 45dB in average is obtained in S/N ratio.

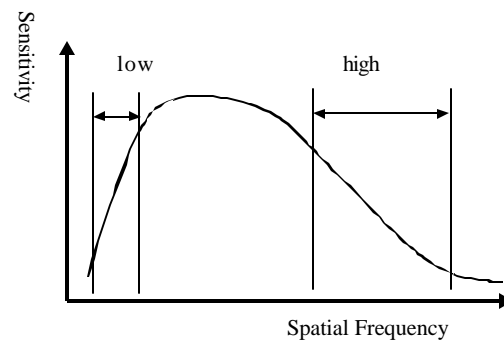


Fig. 4 The spatial frequency of human eye property for the watermark

5. MPEG-7 OVER Content ID

5.1 Mpeg-7

ID data, which is embedding by watermark, include copyright information such as author, producer etc,

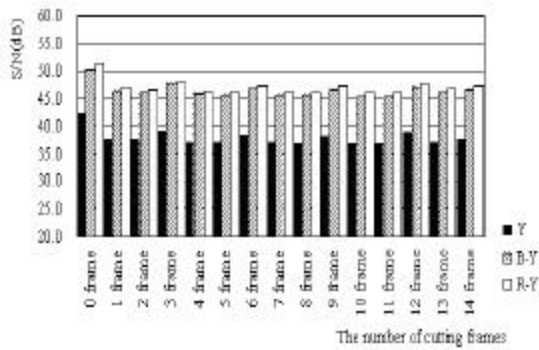


Fig 5 S/N ration of watermark with the number of cutting frames

remarked time, place, explanation, keyword etc. Mpeg7, 21 and Metadata are global standard disruption format of ID, which are worked in ISO as international Standard Guideline. Contents ID forum is working on this issue in Japan. Metadata include huge amount of category [13-17].

Fig. 6 shows the example of ID which only include Material ID data, and time-code, which is the detail information of time information of video data. Detail information data is linked to this header information. ID number will supposedly given by the authorized ID Management Center shown in Fig. 8.

Record of disaster will be the one of the ID information of this. Disaster information management center will be needed in the near future.

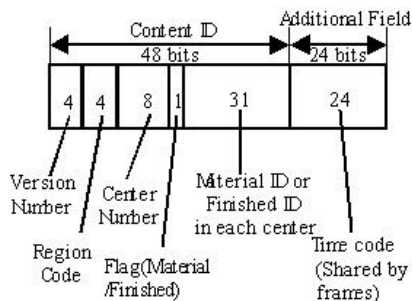


Fig. 6 cID format

The benefit of cID is as following

- Realize easy, unified and global database management and retrieve.
- Prevent disappearing or separation of ID data and audiovisual data.
- Identify copyright information and protect copy right
- Realize cipher operation
- Assure the trace-ability in the market by recording ID number distribution history, such as products number or telephone number of mobile phone.

MPEG-7 over cID is almost the same idea as MPEG -21. MPEG-21 is still under discussion and not settled yet, hence we introduce the idea of MPEG-7 over id originally in Yamagata. Which is suitable method for the contents distribution flow of the from creation to end user. Database discribed by MPEG -7 has small data rate and open to the

public. On the other hand contents ID database has higher bit rate and includes closed data. This is suitable for large database. We considered the merit of both system and proposed MPEG-7 over cID.

5.2 Verification Tests

The system being built to adopt MPEG -7 and Content ID using existing equipment for research and development purpose in YRC. The purpose of the verification tests here YRC are as follows:

- Feasibility test for contents folder, secondary use of the contents held in **YDCC**.(Contents bushiness purpose)
- Possibility of building future content ID management Center and assessment and verification of this Center (Practical operation study)
- Verification of platform system for content distribution and delivery

We conducted two types of verification tests as followings. One is proposed by public organization, and the other is original planning test on **YRC**.

- Verification test proposed by public government supported organization. DCAj(Digital Contents Association Japan) mainly led this verification test and this was conducted in a large scale. YRC participated in this official test and then conducted our original planning test added in this official test.

This test started from confirmation of the target content except for retrieval and finished by obtaining metadata Thus this test centers on resolution of watermark and management ID.

5.3 Experimental Results

The Following is the results of verification tests:

- Verification test propounded by public organization
 - Basic system of ID management center has been established by building database compliant to cIDf condition.
 - Basic system of digital watermark center has been established by building automatic system for embedding and extracting digital watermark which aims to develop for research system in order to adopt practical application.
 - Fundamental basis for YRC original test aiming to establish the business model has been built.
- YRC Original V erification test
 - Profile development original to YRC using MPEG-7 has been built and implemented.
 - Retrieval application software using MPEG -7 newly developed for the test has been implemented and that made retrieval from Web possible.
 - Conventional retrieval of text -base and flat-type was compared with new retrieval of high-level description with scalability using MPEG-7 and confirmed so that new method contributed to efficient retrieval.
 - Remote editing from Web site by referring to original time code produced at archive registration was verified.

(v) Extraction of required Meta information and creation of profile in editing process were completed.

6. The prevention of disaster and education archive and distribution system

6.1 Prevention of disaster system

The requirements of the specifications for the index format of the prevention of the disaster is urgency (speed) and global. Here we use the Mpeg-7 over cID to describe the index format of the prevention of the disasters to realize high speed retrieval and unified management.

Each video frame comes to the unique code in the world and remote edit in far distance place is also realized.

The characteristics of the ID is as followings:

- (1) 2 billion contents management and frame unit management is realized.
- (2) The distinguishing of the clip and program is realized.
- (3) Mpeg-7 Part 5 MDs scheme can be adapted

The categories such as earthquake or typhoon and their occurrence place, time can be embedded. Watermark ID of them is embedded. The free link of the several section of the metadata format of the prevention of the disaster is shown in Figure 7. The most important point of this is the management of original time code to show the exact date, time and the circumstances of the disaster corresponding to the time code. In such archive and distribution system, the security assurance based on ISO 17799 and 15408 guidelines is highly needed.

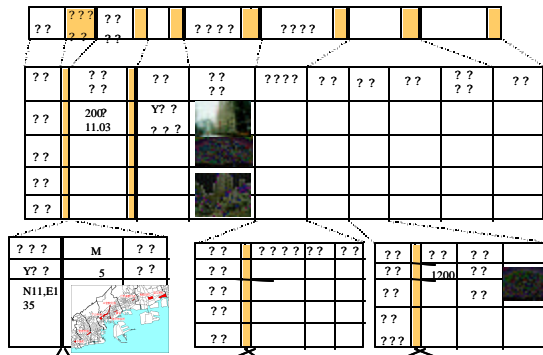


Fig. 7 Hazard metadata format



Fig. 8 An example of the interfaced of Government Information system open to the citizens

Disaster information is input by the portable telephone to the center disaster information system which is in part of Government Information System (GIS) and these information is transmitted to the personal computer at home by internet. Portable telephone transmission service is also currently under planning. The user interface of GIS is shown in Figure 8

6.2 Education system

The other example is school network. 51 primary school and junior high school are connected by intranet and 560 clips are provided as the educational video to apply the national social study textbook. Educational clip is almost 2 minutes each and the metadata is attached by HTML description which includes creator information, copy right information, contents information and so on. Figure 9 shows the user interface of education clip library. Beside of them metadata includes application purpose, clipped place, performance right in play clip, time limit of usage, on off of watermark etc. Figure 10 shows the user interface of metadata information.



Fig. 9 The home town vide library

ジャンル	制作年度	制作場所	放送年度	収録場所	放送局
01エーサ情報	01エーサ情報	06	01エーサ情報	01エーサ情報	06
制作年度情報	制作年度	2001-3-18	制作場所	制作場所	制作場所
02エーサ情報	02エーサ情報	06	02エーサ情報	02エーサ情報	06
制作年度情報	制作年度	2001-3-18	制作場所	制作場所	制作場所
03エーサ情報	03エーサ情報	06	03エーサ情報	03エーサ情報	06
制作年度情報	制作年度	2001-3-18	制作場所	制作場所	制作場所

Fig. 10 The contents of the metadata with cIDf base

7. Conclusion

Here we reported large-scale video archive system and the security in four aspects. These are security organization, physical security environment, and information security

and distribution channel security. Distribution channel security includes network and media delivery on the market. The security system was mentioned in the relation with ISO17799 (15408) guideline. In the aspect of distribution security standard contents ID format proposed by id f is introduced. The new watermark method named "Spatial frequency separation embedding method is also newly introduced [15, 16]. Several watermark experiments has been done and the result and S/N ration has been shown. The validity of the proposal has been clarified through the experiment. Distribution simulation experiments have also been done and the validity of the cIDf proposal has been proved

The next issue of the security settles the Common Criteria (CC) and Security Target (ST). And also get the approval by the authorized Security Assurance Organization.

In the aspect of distribution security, we plan to utilize the verified "MPEG -7 over Content ID" and make structure to consolidate the retrieval profile unique to YRC, and to adapt the control and management method of content and database using the method to the requirement of wider content distribution world. Future verification will handle issues below:

Production of meta-information with MPEG-7 description, reduction of workload and cost upon content registration and checking influence on retrieval efficiency are the next issue to be urged.

Improving efficiency of visual retrieval by MPEG-4 reference video and practical application of IP based remote editing.

Robustness of digital watermark when the content is tampered and subject of assessment of influence digital watermark to picture quality

Our goal will be the unified content management that can meet to both professional and private creators need. And also establish the system model that verifies secure content distribution. Thus we commit to contribute the de content base businesses and also the safety society.

Acknowledgement: Authors thanks to the member of TAO(NIEST), Yamagata city and prefecture government, Mitsubishi Electric Corporation, Sony Corporation, Osaka University and University of Tokyo of their kind corporation.

REFERENCES

- [1] Ministry of Public Management, Home Affairs, Posts and Telecommunications: 2001 White Paper Information and Communications in Japan, p138-141, 2001.
- [2] Fumio Maehara, Masaru Kawabata, Haruo Hiki, Yoahikazu Tanno, Manabu Ito and Fumio Hasegawa, "Broadcasting Program Production System by using Peta-byte Class Large Scale Archive", Trans of IEICE Vol., J84 No.4 , pp.809-817
- [3] Fumio Maehara, Yukiko Inoue, Jun Ikeda, Manabu Ito, Fumio Hasegawa, "Visual Data Retrieve Method for the Large scale Video Archie System, Trans. of Video, Inf. Media Society , Vol.54, No.4, pp.601~608
- [4] Fumio Maehara, Masaru Kawabata, Haruo Hiki Yoshikazu Tanno, Manabu Ito and Fumio Hasegawa.: "Peta-byte Class Video Archive System By Large-scale Automatic Robot", Proc. IEICE Fall Conf., Sept.1?
- [5] Fumio Hasegawa, Fumio Maehara, Masaru Kawabata, Haruo Hiki, Yoshikazu Tanno, Manabu Ito: "Program production system utilizing large-scale archive", Technical Report of IEICE, IIE99-83, Nov.1999.
- [6] Haruo Hiki, Fumio Maehara, Yoshikazu Tanno, Manabu Ito, Fumio Hasegawa: "Remote Retrieval and Editing System for Large-scale archive", Technical Report of IEICE, EID99-137, IE99-13, Feb.2000.
- [7] ISO/IEC, "Information technology -Code of practice for information security management"
- [8] ISO/IEC, "15408-1,2 1999,: Information technology -Security techniques- Evaluation criteria for IT security, Part1,2"
- [9] Haruo Hiki, Masaru Kawabata, Youichi Isibashi and Fumio Hasegawa, "Peta-byte Video Archive with Content ID and Original Time Code" SMPTE Journal, Feb./Mar. 2002 pp.80-84
- [10] Yuji Akahori, et al.: "Proposal on automatic editing method of video image by estimating filming condition", Technical Report of IEICE, IE94-117, 1995-01.
- [11] Eiichi Iwanari, et al.: "Clustering and Cut Detection of scene using DCT element", Technical Report of IEICE, PRU93-119, 1994.01
- [12] Hiroyuki Ueda, et al.: "Proposal on conversational type of editing method applying recognition technology", IEICE Transaction, D-II vol.75-D-II, no.2 pp.216-225, 1992.2
- [13] MPEG -7: <http://www.itscj.ipsj.or.jp/mpeg7/>
- [14] cIDf: <http://www.cidf.org/>
- [15] Hirokazu Ishizaki et. al. ,"Evaluation for Logical Filtering Method of Digital watermarking", SCIS99 , Jan. 1999
- [16] Masaru Kabata, et. Al , "A study for picture-quality Distribution by Digital watermarking" Proceeding of 2002 ITE Annual Convention
- [17] Manabu Ito, Koichi Ito, Yoichi Ishibashi, Takuyo Kogure, Fumio Hasegawa: "Retrieval Profile Using MPEG7/MDS for the Large Scale Video Archive", Proc. IEICE Conf., SD-3-6, pp385, March 2002.

MODELING TRUST USING A FUZZY LOGIC APPROACH

Name: Mubarak S. AL-Mutairi.

Title & Institution: PhD Candidate in the Department of Systems Design Engineering at the University of Waterloo.

Address: Department of Systems Design Engineering
University of Waterloo
200 University Avenue West
Waterloo, ON
Canada N2L 3G1

Telephone: +1(519) 888-4567 ext. 7736

Fax: +1(519) 746-4791

E-mail: malmutai@uwaterloo.ca

Name: Keith W. Hipel.

Title & Institution: Professor and Coordinator of the Conflict Analysis Group in the Department of Systems Design Engineering at the University of Waterloo.

Address: Department of Systems Design Engineering
University of Waterloo
200 University Avenue West
Waterloo, ON
Canada N2L 3G1

Telephone: +1(519) 888-4567 ext. 2830

Fax: +1(519) 746-4791

E-mail: kwhipel@uwaterloo.ca

Name: Mohamed Kamel.

Title & Institution: Professor of Electrical and Computer Engineering, Canada Research Chair in Cooperative Intelligent Systems, and Director of the Pattern Analysis and Machine Intelligence Group.

Address: Department of Electrical and Computer Engineering
University of Waterloo
200 University Avenue West
Waterloo, ON
Canada N2L 3G1

Telephone: +1(519) 888-4567 ext. 5761

Fax: +1(519) 746-3077

E-mail: mkamel@pami.uwaterloo.ca

Modeling Trust Using a Fuzzy Logic Approach

Mubarak AL-Mutairi, Keith Hipel, and Mohammed Kamel

Abstract

A fuzzy logic procedure is developed for formally modeling trust in Multiagent Systems. A great deal of e-commerce over the net relies on a certain degree of trust. With the growing e-market, trust is going to play a major role in successful transactions. In order to allow such trust reasoning, one has to embed the concept of trust into an agent. A first step in this direction is the development of a comprehensive operational model of trust which is executable by the agent. While the decision to trust bears some risks due to the uncertainty and the loss of control, not trusting means giving up potential benefits. The literature on trust from Sociology, Philosophy and elsewhere is surveyed to better understand how it is formed, maintained and destroyed. Fuzzy logic is effective for modeling some graded phenomena like trust that are subjective and difficult to estimate experimentally. Because it is able to work with vague, ambiguous, imprecise, noisy, or missing information, the fuzzy logic approach is ideal for modeling trust in such large, open, dynamic, and unpredictable environments.

1.0 Introduction

Due to risks and uncertainty in an electronic environment, the issue of trust is frequently raised. Different components of the electronic realm tend to act in autonomous ways in order to achieve their goals. In such an open and dynamic environment, the agents tend to behave in an irrational and unpredictable manner. With no central authority controlling such an environment and no agent being able to know everything about other agents, trust plays a great role in agent interactions. Hence, embedding the concept of trust into agents will enable them to make better decisions about whom to trust and cooperate with.

The higher the trust value, the more reliable an agent is, and the lower the chances of loss. Most of the current trust models are based on theories from sociology. Researchers envision trust as being the same across different disciplines and they think of it as trust or don't trust situation. Traditional trust models tend to utilize quantitative tools (Esfandiari 2001, Falcone 2003, and Marsh 1994). Trust decisions should be based on a set of criteria like reputation, risk, and the uncertainty of the

situation. The proposed model is able to handle large, open, dynamic, and unpredictable environments with vague, ambiguous, imprecise, noisy, or missing information.

Fuzzy set theory (Zadeh 1973) is a powerful tool when dealing with decisions where the situation is vague or imprecise. It tolerates blurred boundaries of definitions bringing the hope of incorporating qualitative factors into the decision making process with unclear or vaguely defined boundaries. In this model, the values and weights of each criterion are expressed in normal linguistic terms. Then, those terms are converted into appropriate fuzzy values. Simple arithmetic fuzzy operations are employed to incorporate these values to get the Fuzzy Attractiveness Ratio (FAR) (Lin and Chen 2004). Finally, FAR is converted back into linguistic terms to assist the trust decision.

In the following sections, trust definitions are summarized and assessed across the different disciplines to come up with a comprehensive definition. This definition will form the basis for our proposed model. The main contribution of this paper is the global view of trust among the different disciplines and aggregating them together to come up with a robust and comprehensive model of trust.

2.0 Trust Definition from Different Disciplines

Different disciplines handle trust differently according to their own perceptions and what fits their specific goals. In order to consolidate a global view of trust, we need to step back and analyze why different disciplines see trust differently and bring them together into one robust comprehensive model. The following sections examine trust from different points of view.

2.1 Trust in Sociology

The sociology of trust has been investigated from different angles: rational choices, culture, functionality, symbolic interaction, and others. Trust is a social relationship subject to its own special system of rules (Luhmann 1979). Trust occurs within interactions that are influenced by both personality and social systems (Lahno

2001). Most sociologists agree with: “the clear and simple fact that, without trust, the everyday social life which we take for granted is simply not possible” (Good 2000, p. 32). We always find ourselves in a condition of uncertainty about and uncontrollability of future actions. We have no way of knowing and controlling what others will do independently of our own actions and we are not even sure how they will react to ours. In summary, uncertainty and risk are integral components of human interactions that can’t be ignored or avoided.

In situations in which we have to act in spite of uncertainty and risk, the third orientation that comes to the fore is that of trust (Sztompka 1999). Trusting becomes a crucial strategy for dealing with an uncertain and uncontrollable future. Since there is no way of knowing what is in the minds of others, we need trust to deal with an unknown future and others’ uncontrollable actions.

When participating in uncertain and uncontrollable conditions, we take risks, we gamble, and we make bets about the future and the actions of the others. A simple and general definition of trust is: “trust is a bet about the future contingent actions of others” (Sztompka 1999, p. 25). In this sense, trust consists of two main components: beliefs and commitments. First, it involves specific expectations: “trust is based on an individual’s theory as to how another person will perform on some future occasion” (Good 2000, p. 33). When placing trust we behave as if we know the future. Secondly, trust involves commitment through action or roughly speaking, placing a bet. Thus: “trust is the correct expectations about the actions of other people that have a bearing on one’s own choice of action when that action must be chosen before one can monitor the actions of those others” (Gambetta 2000, p. 51). In order to have a better and deeper understanding of trust, we need to pay attention to the mental and subjective attitudes of the trusting person. It is important to focus on what happens in an individual’s mind when trusting someone else.

2.2 Trust in Philosophy

Trust and distrust are subjective attitudes that affect our thinking and feelings (Hardin 2002). When trusting, we are more likely to let ourselves be vulnerable to others and allow ourselves to depend on others. Trust is a cooperative activity in which we engage so that we can assist one another in the care of goods (Baier 1986). We trust others when we allow them the opportunity to care for something we value. We trust things as well as people. While trusting things is based on the properties of the things that we know in advance, trusting people is based on past experiences. When we trust, we hold expectations toward another person. To expect is to look forward to something without anticipating disappointment. When

holding expectations of another, we project into the future, making an inference about the sort of person someone is going to be in the future. When trusting, the expectations alone are not enough but we must anticipate that the other has good intentions and the ability to carry out what is expected of him or her.

In order to trust someone, we need to have a sense of his or her values. A person who lacks commitment to any values or principles doesn’t give us the ability to predict either good or bad intentions or treatment. Knowing the other’s values, commitments, and loyalty will help us to decide to what extent risk would be involved if we count on that person. We trust others more fully when we believe that they have positive feelings towards us personally and not just as members of some group. Trust is a risky business because people whom we trust can let us down and we are vulnerable to harm when they do so. It is important to accept the risks of trust and try to handle them rather than taking the simplistic view that trust is always good. Sometimes we trust too easily and risk a great deal in doing so (Cvetkovih and Lofstedt 1999, Hardin 2002). Our trust is generally based on experiences with other people. On the basis of those experiences, we construct a characterization or picture of them but in reality they are free agents with different characterizations that go beyond our beliefs about them.

2.3 Trust in Computer Science

Computer scientists tried to formalize the corpus of knowledge derived from sociology and psychology into agents’ architectures. We can understand trust as an attitude of an agent who believes that another agent has a given property. Therefore, we can analyze the meaning of trust as a function of the attributed properties. For instance, the property may be that the agent we trust fulfills his obligations, like the case of a buying agent. Properties we consider are the ability of the agent to do the job, ability to make decisions, or the ability just to deliver information (Demolombe 2001).

With the emergence of Electronic Commerce, trust issues became important for so many people. Generally speaking, it is agreed that in order for Electronic Commerce to become successful, most people have to trust it. The person's trust in a transaction is determined by the trust in the counter party and the trust in the transaction media assuming that party and media trust supplement each other. If there is not sufficient party trust, then the media trust and its control protocols should be brought in to supplement the party trust. Trust in the counter party can be defined as "The subjective probability by which an individual A expects that another individual B performs a given action on which its welfare depends" (Falcone and Castelfranci 2001, p. 56).

According to this definition, it could be argued that trust has both objective and subjective attributes. The first depends on the media structure, such as the functionality of the control mechanisms in place. The second depends on personal experiences in dealing with a specific party, or with specific procedures and control protocols.

2.4 Trust in Psychology

In his 1973 book, M. Deutsch defines trust as confidence that one will find what is desired from another person rather than what is feared. Many researchers find this definition to be a specific characteristic of a relationship. Deutsch, however, presents many other aspects of trust in his 1973 work. He presents trust as being despair, innocence, social conformity, virtue, gambling, risk-taking and faith, among others.

From a psychological perspective, risk in trust is approached as one of the characteristics of individuals. While some people are willing to take risks, there are some who are too cautious and distrustful to take any chances. Trusting behavior depends on how individuals perceive an ambiguous path or unclear situation. In such cases, the occurrence of a good or bad result is dependant on other's actions. Knowing that a negative result is more harmful than a good one, a trusting decision should be made.

The use of the word 'perceive' in the previous paragraph is to emphasize the subjective nature of trust. If trust is based on individual perception, it is likely that the same situation will be seen differently by different individuals. Estimates of chances and expected gains or losses are subjective. Thus, some individuals might make unwise risks, thereby acting as if they are taking chances while, in fact, they are trusting unwisely.

2.5 Trust as a Global View

Gambetta (2000) attempted to gather different thoughts regarding trust from many areas. The most important aspect of his work is the use of values. On the other hand, using explicit values for trust can be problematic due to the subjectivity of trust that the same value could be seen differently by different agents. Yet the use of values for measuring trust allows us to talk more precisely about certain circumstances or behaviors concerning trust. Also, it allows a straightforward implementation of the formulation.

In his research, Gambetta (2000, p. 217) defines trust as "a particular level of subjective probability with which an agent assesses that another agent or group of agents will perform a particular action both before he can monitor such action or independently of his capacity ever

to be able to monitor it and in a context in which it affects his own action". This definition excludes certain aspects which are important to trust like referring only to the trust relationship between the agents themselves and not, for example, the agents and the environment. It also excludes those agents whose actions have no effect on the decision of the truster, despite the fact that trust is present. An interesting point in Gambetta's work is the concern regarding competition and cooperation. In some cases, cooperation is not good such as the cooperation among thieves or drug dealers while it is very desirable among policemen. Then, it is good to find "the optimal mixture of cooperation and competition rather than deciding at which extreme to converge" (Gambetta 2000, p. 215). In competitive situations cooperation is of great importance since "even to compete in a mutually non-destructive way one needs at some level to trust one's competitors to comply with certain rules" (Gambetta 2000, p. 215). Despite the importance of using values for trust, Gambetta didn't develop the idea in any concrete fashion (Marsh 1994).

3.0 Proposed Model

With rapidly growing electronic commerce applications involving agent systems, the issue of trust is increasing in importance. Scientists pay a great deal of attention to social values like trust and emotions (Lahno 2001), and their possible applications in their fields of interest. Most of the current work on trust envisions trust as being uni-dimensional. As discussed in the previous sections, studying trust among the different disciplines helps in capturing the multidimensionality and the complexity of trust. It enables researchers to conceptualize the different components of trust like risk, uncertainty, and dependence, and how they interact and affect each other. Accordingly, it is time to step back and examine why the different disciplines view trust differently. The main contribution of this paper is to construct a global view of trust among the different disciplines and aggregate them together to come up with a robust and comprehensive model of trust.

3.1 Preliminaries

Following the procedure of Chen and Chen (2003) and based on the concepts of fuzzy numbers and their arithmetic (Chen and Pham 2001, Nguyen 1997), a generalized trapezoidal fuzzy number is represented as $A = (a, b, c, d; w)$, where $0 < w \leq 1$, and $a, b, c, \text{ and } d$ are real numbers. If $w=1$, then the generalized fuzzy number A is called a normal trapezoidal fuzzy number denoted as $A = (a, b, c, d)$. If $a = b$

and $c = d$, then A is called a crisp interval. If $b = c$, then A is called a generalized triangular fuzzy number. If $a = b = c = d$ and $w = 1$, then A is called a real number.

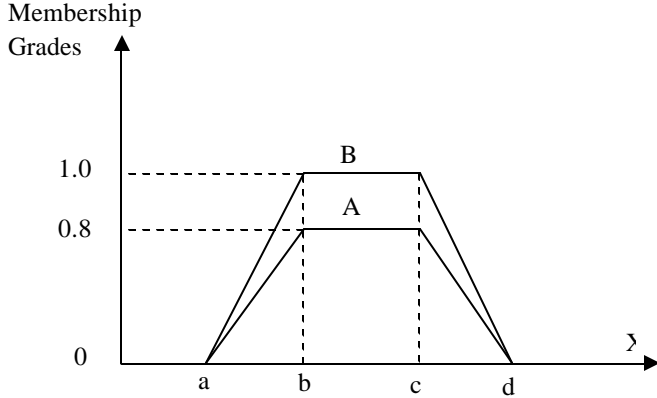


Figure 1. Two generalized trapezoidal fuzzy numbers A and B (Chen and Chen 2003).

Figure 1 shows two different generalized trapezoidal fuzzy numbers for the cases $A = (a, b, c, d; w_1)$ and $B = (a, b, c, d; w_2)$, which denote two different decision makers' opinions. The values of w_1 and w_2 represent the degrees of confidence of the opinions of the two decision makers where $w_1 = 0.8$ and $w_2 = 1.0$.

3.2 Fuzzy Numbers and their Arithmetic Operations

The arithmetic operations between the generalized trapezoidal fuzzy numbers A_1 and A_2 are as follows:

1. Fuzzy number addition:

$$\begin{aligned} A_1 \oplus A_2 &= (a_1, b_1, c_1, d_1; w_1) \oplus (a_2, b_2, c_2, d_2; w_2) \\ &= (a_1 + a_2, b_1 + b_2, c_1 + c_2, d_1 + d_2; \min(w_1, w_2)), \end{aligned} \quad (1)$$

where $a_1, b_1, c_1, d_1, a_2, b_2, c_2,$ and d_2 are any real numbers.

2. Fuzzy number subtraction:

$$\begin{aligned} A_1 \ominus A_2 &= (a_1, b_1, c_1, d_1; w_1) \ominus (a_2, b_2, c_2, d_2; w_2) \\ &= (a_1 - a_2, b_1 - b_2, c_1 - c_2, d_1 - d_2; \min(w_1, w_2)), \end{aligned} \quad (2)$$

where $a_1, b_1, c_1, d_1, a_2, b_2, c_2,$ and d_2 are any real numbers.

3. Fuzzy number multiplication:

$$A_1 \otimes A_2 = (a, b, c, d; \min(w_1, w_2)), \quad (3)$$

where $a = \min(a_1 \times a_2, a_1 \times d_2, d_1 \times a_2, d_1 \times d_2)$,
 $b = \min(b_1 \times b_2, b_1 \times c_2, c_1 \times b_2, c_1 \times c_2)$,

$c = \max(b_1 \times b_2, b_1 \times c_2, c_1 \times b_2, c_1 \times c_2)$, and
 $d = \max(a_1 \times a_2, a_1 \times d_2, d_1 \times a_2, d_1 \times d_2)$. It is obvious that if $a_1, b_1, c_1, d_1, a_2, b_2, c_2,$ and d_2 are all positive real numbers, then

$$A_1 \otimes A_2 = (a_1 \times a_2, b_1 \times b_2, c_1 \times c_2, d_1 \times d_2; \min(w_1, w_2))$$

4. Fuzzy number division:

The inverse of the fuzzy number A_2 is $1/A_2 = (\frac{1}{d_2}, \frac{1}{c_2}, \frac{1}{b_2}, \frac{1}{a_2}; w_2)$, where

$a_2, b_2, c_2,$ and d_2 are all nonzero positive real numbers or all nonzero negative real numbers. If $a_1, b_1, c_1, d_1, a_2, b_2, c_2,$ and d_2 are all nonzero positive real numbers, then the division of A_1 and A_2 is

$$\begin{aligned} A_1 \div A_2 &= (a_1, b_1, c_1, d_1; w_1) \div (a_2, b_2, c_2, d_2; w_2) \\ &= (\frac{a_1}{d_2}, \frac{b_1}{c_2}, \frac{c_1}{b_2}, \frac{d_1}{a_2}; \min(w_1, w_2)) \end{aligned} \quad (4)$$

3.3 Model Framework

The general framework for this model is displayed in Figure 2. It consists of three main modules: the decision maker, the trustworthy assessment, and the fuzzy evaluation. The decision maker tries to collect as much information as possible about the agent of concern. This could come from a third party, past history (reputation), or by observation. The criteria for the trustworthy agent and their minimum acceptable thresholds must be defined in advance. Those thresholds could be expressed in natural language phrases where they are assigned corresponding fuzzy weights and values. Based on the computed value for Fuzzy Attractiveness Ratio (FAR) and the judgment of the decision maker, the final trust decision can be made.

3.4 Trust Criteria

Based on a comprehensive and thorough study of trust among different disciplines, it has been decided that the three main criteria for trust are the available information about the agent of concern, the circumstances for that issue in regard to that specific agent, and the judgment of the agent in charge of making the trust decision. Each of those criteria are classified further and split into sub-criteria as shown in Figure 3.

3.5 Fuzzy Values and Weights

Due to the subjective nature of the evaluation criteria as well as the vague and imprecise nature of the available

information, it is easier to express the values and the weights in natural language terms rather than specifying crisp values. These linguistic terms could be assessed through the use of fuzzy logic. A hypothetical example of the linguistic terms and their corresponding fuzzy values for the weights and trust values are given in Tables 1 and 2, respectively.

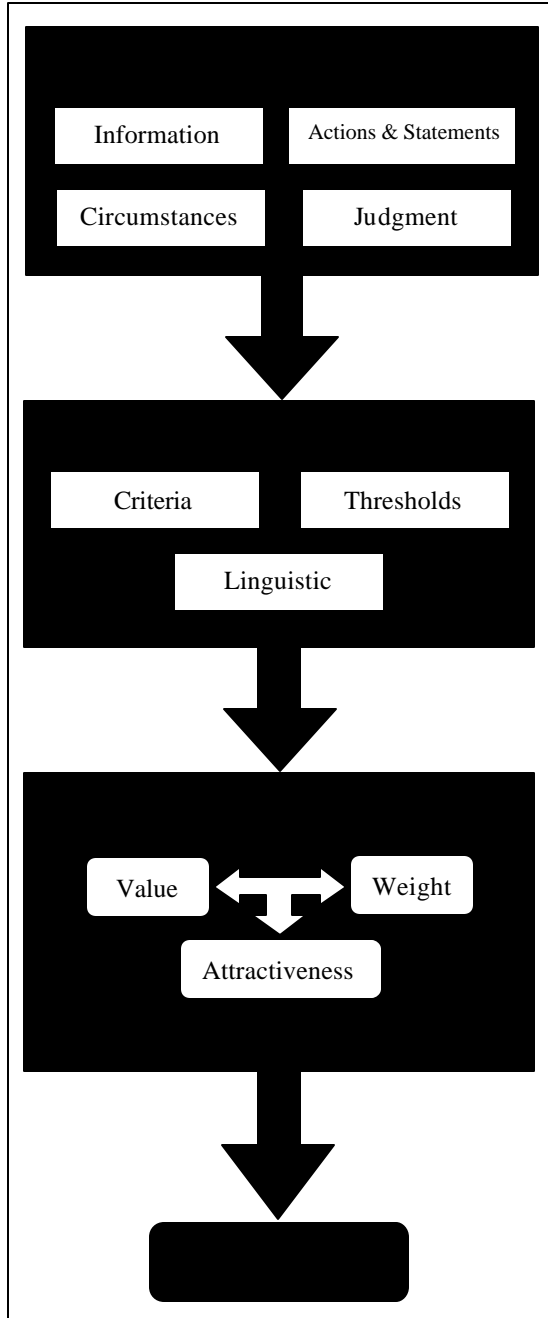


Figure 2. Fuzzy trust model framework

3.6 Trust Computation

To consolidate the fuzzy values and fuzzy weights of all the important trust factors into one Fuzzy Attractiveness Ratio (FAR), we follow the procedure of (Lin and Chen 2004). The higher the FAR value, the more trustworthy the agent is. Let R_j and W_j , where $j = 1, 2, \dots, n$, respectively be the fuzzy rating and fuzzy weighting given to factor j . Then, the fuzzy attractiveness ratio is computed as

$$FAR = \sum_{j=1}^n (W_j \otimes R_j) / \sum_{j=1}^n W_j \quad (5)$$

Once the FAR has been computed, this value could be approximated by a similar close linguistic term from the Trust Level (TL, see Table 2). Several methods for matching the FAR with the corresponding TL have been proposed. The Euclidean distance will be used since it is the most intuitive from the human perception of approximation and the most commonly used method. The distance between FAR and each fuzzy number member of TL can be calculated as follows:

$$d(FAR, TL_i) = \left\{ \sum_{x \in p} (f_{FAR}(x) - f_{TL_i}(x))^2 \right\}^{1/2} \quad (6)$$

Where $p = \{x_0, x_1, \dots, x_m\} \subset [0, 1]$ such that $0 = x_0 < x_1 < \dots < x_m = 1$. For simplicity, let $p = \{0, 0.1, 0.2, 0.3, 0.4, 0.5, 0.6, 0.7, 0.8, 0.9, 1.0\}$, then the distance from FAR to each of the members of the set TL can be calculated and the closest linguistic expression is the one with minimal distance value.

Table 3 shows the main criteria and sub-criteria for trust along with their corresponding values and weights. Using the information in this table and Equation 5, we obtain the fuzzy values for main criteria as follows:
 Information = (0.240321, 0.473871, 0.702241, 1.332143)
 Circumstances = (0.320318, 0.545564, 0.764603, 1.272021)
 Judgment = (0.170945, 0.351068, 0.568247, 1.039452)

Computing the Fuzzy Attractiveness Value using Equation 1, we got: FAR = (0.169475, 0.440821, 0.706578, 1.746069) By using Equation 2, the Euclidean distance from FAR to each member in set TL at a-cut = 0 was calculated as:

$D(FAR, AL) = 1.94197$, $D(FAR, VL) = 1.87186$, $D(FAR, L) = 1.64586$, $D(FAR, FL) = 1.38833$, $D(FAR, M) = 1.11402$, $D(FAR, FH) = 0.99907$, $D(FAR, H) = 1.03242$, $D(FAR, VH) = 1.22953$, and $D(FAR, AH) = 1.28260$.

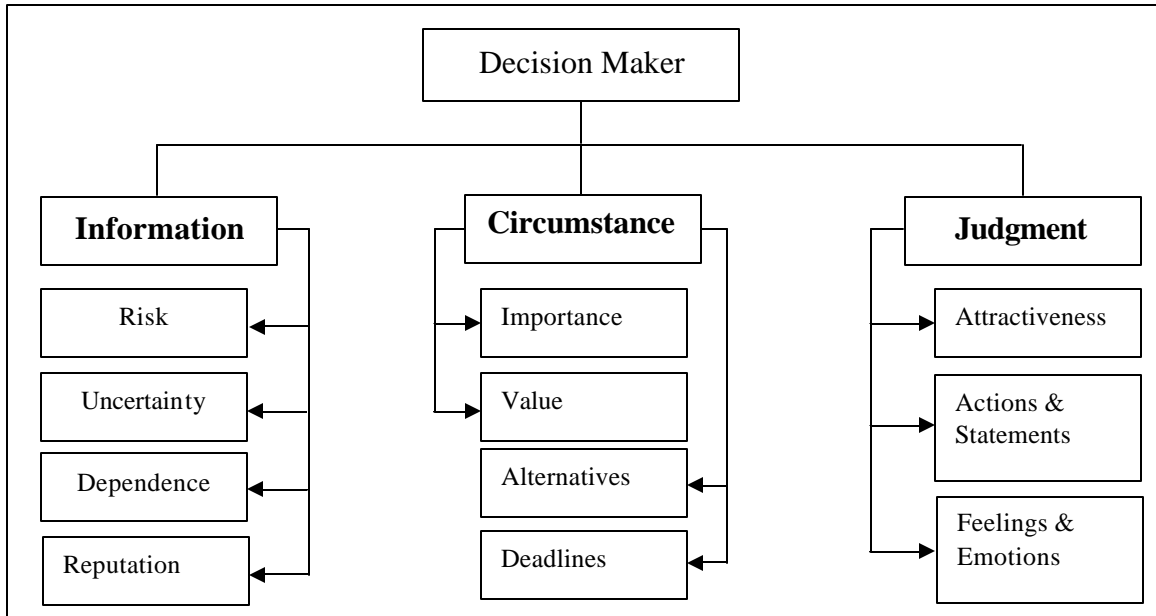


Figure 3. Trustworthy criteria and sub-criteria

Linguistic Terms	Generalized Fuzzy Numbers
Very High	(0.82, 0.98, 1.0, 1.0; 1.0)
High	(0.62, 0.78, 0.82, 0.98; 1.0)
Fairly High	(0.42, 0.58, 0.62, 0.78; 1.0)
Fairly Low	(0.22, 0.38, 0.42, 0.58; 1.0)
Low	(0.0, 0.18, 0.22, 0.38; 1.0)
Very Low	(0.0, 0.0, 0.02, 0.18; 1.0)

Table 1. Fuzzy weights for linguistic terms and their values

Linguistic Terms	Generalized Fuzzy Numbers
Absolutely low	(0.0, 0.0, 0.0, 0.0; 1.0)
Very low	(0.0, 0.0, 0.02, 0.07; 1.0)
Low	(0.04, 0.1, 0.18, 0.23; 1.0)
Fairly low	(0.17, 0.22, 0.36, 0.42; 1.0)
Medium	(0.32, 0.41, 0.58, 0.65; 1.0)
Fairly high	(0.58, 0.63, 0.80, 0.86; 1.0)
High	(0.72, 0.78, 0.92, 0.97; 1.0)
Very high	(0.93, 0.98, 1.0, 1.0; 1.0)
Absolutely high	(1.0, 1.0, 1.0, 1.0; 1.0)

Table 2. Fuzzy trust linguistic terms and values

Criteria	Sub-Criteria	Fuzzy Values	Fuzzy Weights
Information			(0.82, 0.98, 1.0, 1.0; 1.0)
	Risk	(0.32, 0.41, 0.58, 0.65; 1.0)	(0.22, 0.38, 0.42, 0.58; 1.0)
	Uncertainty	(0.58, 0.63, 0.80, 0.86; 1.0)	(0.22, 0.38, 0.42, 0.58; 1.0)
	Dependence	(0.17, 0.22, 0.36, 0.42; 1.0)	(0.62, 0.78, 0.82, 0.98; 1.0)
	Reputation	(0.72, 0.78, 0.92, 0.97; 1.0)	(0.62, 0.78, 0.82, 0.98; 1.0)
Circumstances			(0.62, 0.78, 0.82, 0.98; 1.0)
	Importance	(0.72, 0.78, 0.92, 0.97; 1.0)	(0.82, 0.98, 1.0, 1.0; 1.0)
	Value	(0.32, 0.41, 0.58, 0.65; 1.0)	(0.42, 0.58, 0.62, 0.78; 1.0)
	Alternatives	(0.17, 0.22, 0.36, 0.42; 1.0)	(0.22, 0.38, 0.42, 0.58; 1.0)
	Deadlines	(0.58, 0.63, 0.80, 0.86; 1.0)	(0.42, 0.58, 0.62, 0.78; 1.0)
Judgment			(0.62, 0.78, 0.82, 0.98; 1.0)
	Attractiveness	(0.32, 0.41, 0.58, 0.65; 1.0)	(0.62, 0.78, 0.82, 0.98; 1.0)
	Actions & Statements	(0.32, 0.41, 0.58, 0.65; 1.0)	(0.62, 0.78, 0.82, 0.98; 1.0)
	Feelings & Emotions	(0.17, 0.22, 0.36, 0.42; 1.0)	(0.22, 0.38, 0.42, 0.58; 1.0)

Table 3. Trust main and sub-criteria and their fuzzy values and weights

Then, by matching the linguistic term with the minimum D, the trust value is fairly high though it is not so far from being high value. Expressing the trust value over a set of values rather than a single crisp value gives the decision maker a greater flexibility and fewer chances for making a wrong trusting decision.

4.0 Conclusions

Due to the complex, multidimensional, and subjective nature of trust, conventional mathematical modeling might not be able to handle it. Hence, fuzzy-based trust modeling approach is proposed in this research. In this model, a thorough review of trust across different disciplines is carried out. To come up with a universal definition of trust, we need to understand why different disciplines perceive trust differently. This allows us to bring them together within a robust comprehensive model. In this model, the natural linguistic terms are used to assign the weights and values of the vague or imprecise defined trust criteria. This approach is designed to handle subjective, vague or imprecise situations. It gives us accurate and easy to interpret results over a range of values to allow for minor shifts rather than trying evaluating it with a single crisp value.

References

- [1] A. Baier, "Trust and Antitrust," *Ethics*, vol. 96, pp. 231-260, 1986.
- [2] G. Chen and T. Pham, *Introduction to Fuzzy Sets, Fuzzy Logic, and Fuzzy Control Systems*. RCR Press, New York, 2001.
- [3] S. Chen and S. Chen, "Fuzzy Risk Analysis Based on Similarity Measures of Generalized Fuzzy Numbers," *IEEE Transactions on Fuzzy Systems*, vol. 11, no.1, pp. 45-56, 2003.
- [4] G. Cvetkovih and R. Lofstedt, *Social Trust and the Management of Risk*, Earthscan Publications, London, 1999.
- [5] R. Demolombe, "To Trust Information Sources: a Proposal for a Modal Logic Framework," in *C. Castelfranchi and Y-H Tan (eds), Trust and Deception in Virtual Societies*, Kluwer Academic Publisher, pp. 111-124, 2001.
- [6] M. Deutsch, *The Resolution of Conflict*. New Haven, Yale University Press, 1973.
- [7] B. Esfandiari and S. Chandrasekharan, "On How Agents Make Friends: Mechanisms For Trust Acquisition," in *Proceedings of Fourth*

- Workshop on Deception Fraud and Trust in Agent Societies*, pp. 27-34, 2001.
- [8] R. Falcone and C. Castelfranci, "Social Trust: a Cognitive Approach," in: *C. Castelfranci and Yao-Hua (eds), Trust and Deception in Virtual Societies*, Kluwer Academic Publisher, pp. 55-90, 2001.
- [9] R. Falcone, G Pezzulo, and C. Castelfranchi, "A Fuzzy Approach to a Belief-Based Trust Computation," in: *R. Falcone, S. Barber, L. Korba, M. Singh (eds.), Trust, Reputation, and Security: Theories and Practice*, Springer-Verlag, pp. 73-86, 2003.
- [10] D. Gambetta, "Can We Trust Trust?," in *D. Gambetta (ed.), Trust: Making and Breaking Cooperative Relations*, electronic edition, Department of Sociology, University of Oxford, Chapter 13, pp. 213-237, 2000.
- [11] D. Good, "Individuals, Interpersonal Relations, and Trust," in *D. Gambetta (ed.), Trust: Making and Breaking Cooperative Relations*, electronic edition, Department of Sociology, University of Oxford, Chapter 3, pp. 31-48, 2000.
- [12] R. Hardin, *Trust and Trustworthiness*. Russell Sage Foundation, New York, 2002.
- [13] B. Lahno, "On The Emotional Character of Trust," *Ethical Theory and Moral Practice*, vol. 4, pp. 171-189, 2001.
- [14] C. Lin and Y. Chen, "Bid/no-bid decision-making – a fuzzy linguistic approach," *International Journal of Project Management*, vol. 22, pp. 585-593, 2004.
- [15] N. Luhmann, *Trust and Power*, Wiley, New York, 1979.
- [16] S. Marsh, *Formulizing Trust as a Computational Concept*, PhD thesis, Dept. Computer Science and Mathematics, Univ. Stirling, London, 1994.
- [17] H. Nguyen, *A First Course in Fuzzy Logic*, CRC Press, Boca Raton, 1997.
- [18] P. Sztompka, *Trust: A Sociological Theory*, Cambridge University Press, New York, 1999.
- [19] L. Zadeh, "Outline of a New Approach to the Analysis of Complex Systems and Decision Processes," *IEEE Transactions Systems, Man and Cybernetics*, vol. 3, pp. 28-44, 1973.

TOPIC: Human and organizational behavior and errors

Distributed Video Data Management System of Monitoring Cameras for Security and Safety

Author's information:

Yoshinori Hijikata *1
Research Associate
Dept. Systems Innovation, Osaka University
Machikaneyama, Toyonaka, Osaka 560-8531, JAPAN
Phone: +81-6-6850-6382
Fax: +81-6-6850-6341
Email: hijikata@hopf.sys.es.osaka-u.ac.jp

Yiqun Wang *2
Doctoral Student
Dept. Systems Innovation, Osaka University
Machikaneyama, Toyonaka, Osaka 560-8531, JAPAN
Phone: +81-6-6850-6382
Fax: +81-6-6850-6341
Email: wang@nishilab.sys.es.osaka-u.ac.jp

Shogo Nishida *2
Professor
Dept. Systems Innovation, Osaka University
Machikaneyama, Toyonaka, Osaka 560-8531, JAPAN
Phone: +81-6-6850-6382
Fax: +81-6-6850-6341
Email: nishida@sys.es.osaka-u.ac.jp

*1 Speaker

*2 Corresponding Author

Distributed Video Data Management System of Monitoring Cameras for Security and Safety

Yoshinori Hijikata¹, Yiqun Wang¹ and Shogo Nishida¹

¹ Graduate School of Engineering Science, Osaka University
Machikaneyama, Toyonaka, Osaka 560-8531, Japan

Abstract

Monitoring cameras with the capability of connecting to the Internet are increasing. This paper proposes a system which manages the distributed video data efficiently and has an interface which can be operated easily. For managing video data, the raw video data is stored in a local PC which directly connects to the camera and only the recording information is managed in the server by using a spatio-temporal indexing algorithm. The data communication is conducted through HTTP and the search input and output is realized in Web browser. As spatio-temporal indexing algorithm, we can apply any existing general algorithm like 3D R-tree, 2+3 R-tree and HR-tree. The camera's recording direction is dispersed into 8 directions, and in every direction a spatio-temporal data structure is constructed. For the search interface, we propose an input method of search key which does not insist users to care the locations of cameras by introducing the idea of virtual wall. The user searches for the video data, which records the virtual wall in a certain direction. The virtual wall (x_s, y_s, x_e, y_e) and the recording direction d in the user's search key, are transformed to the spatial search range (x_1, y_1, x_2, y_2) of the search key for the spatio-temporal data indexing structure. The method is to arrange rectangles in front of the virtual wall.

1. Introduction

Recently, monitoring cameras can be seen in our daily life. We can find them in entrances of buildings, stations, highways and so on. Although these monitoring cameras are generally used for security, the recorded video data from monitoring cameras can also be utilized for disaster prevention and marketing analysis. For instance of disaster prevention, when a large-scale disaster occurs, an operator in a disaster center checks the video data to investigate the cause of the disaster and checks on the damage situation of the scene. As to the marketing analysis, a worker in a company analyzes the confluence of people to find some common significant features in the people (ex. whether there are many business men or there

are many children). With these purposes, it is necessary to analyze the video data by human. With the widespread of net cameras, many video data can be available in the future, and the above task will become hard for people to do. Hence, the search function for video data by computer is important.

In our research, we propose a video data management system, which handles video data in a distributed environment and allows users to search video data intuitively from a web browser from the viewpoints of time and space. Here, we will introduce an idea of virtual wall, which enables intuitive search of video data without being conscious of cameras positions and their recording directions. In the system, the indexing information of video data and the video data itself are managed separately, and the data communication and search

interface are actualized in the web environment. These two points can be considered as the novelty of our research.

Firstly, we explain our motivation of the intuitive search of video data. When we attach indexes to video data automatically by the system, the location information is for the camera not for the object that the camera recorded. This is because the sensor to know the location information is equipped with the cameras and it is difficult to measure the location of the target object at the current level of sensing technologies. A range search is the most popular method for spatial search. However, if the cameras record wide range like monitoring cameras at street corners, the search result includes video data which are out of the search range, but are recorded by cameras which are in the search range. Users may be confused of the search result. It may be a big burden for users to use this type of search in consideration of the gap between the camera's position and the target object's position.

Here, we propose a new search method of video data recorded by monitoring cameras in a city. Here we suppose a large virtual wall in the city, and the user searches for the video data, which records the virtual wall in a certain direction. This query is practical to perform the demands like "How bad the disaster scene is if we watch from the seaside?", "How is the situation of the back of the building?" and so on. We also design the user interface of the system. To let the user easily input the virtual wall of the search-key, the system displays a GIS map data on a window and allows the user to draw the virtual wall on it. In addition, the system does not show the user the whole video data of the search result all at once, but firstly searches for the video data recorded farther from the virtual wall, which is easy to grasp the whole scene, and allows the user to request the closer video data by interactive operations on the interface.

Secondly, we explain our motivation of managing distributed video data in the web environment. It is effective to search for data in a centralized management system. However if the video data recorded from many cameras are transmitted to one server on real time, it will exceed the network bandwidth of the server.

Hata proposed a video data management system to

manage distributed video data effectively [1]. The basic idea is to store the video data itself in local cameras and transmit the recording information of the video data to the server instead. However, the data communication in the proposed system is realized on TCP level, and the search is performed on an original application built on the server. A firewall prevents the data communication, and it does not allow several users to search the video data from their own PCs.

Additionally, as the spatio-temporal information of video data is not used to make the index, the system will cost long time in the search process if the system handles many video data.

In our research, we store the video data in local cameras and manage the recording information on the server like Hata's system. However, the data communication is performed through HTTP, and the search interface is realized in the web environment.

Concretely, to allow users to input the virtual wall interactively on the GUI, we make the function to set a search key work on a java applet through a web browser. Also the video data of the search result will be displayed to the users on a web browser. The server returns a HTML document of the search result, in which the URLs of the video data are inserted. Function buttons for narrowing down video data are also inserted in this HTML document. In this way, the user does not have to go to the place where the server is set, and can search for video data through a web browser without installing an original software on his computer. Furthermore, he can use his familiar web browser and media player which is installed by default. Moreover, in order to minimize the time cost in the search process, the recording information of video data are managed by a spatio-temporal data structure. This can mitigate the degree of decrease of the system's performance in the search process even if the system handles many video data.

In this paper, Section 2 describes the objective our system structure. Section 3 describes the management method of the recording information of the video data and the design of the search interface. Also the screenshots of the system will be shown in this section. Section 4 examines the performance and the usability of the system.

After mentioning the related works in Section 5, we offer some conclusions in Section 6.

2. System structure

This section describes the objective to use video data, the hardware structure of the local camera, and the system structure.

2.1 Objective to use video data

People search for the video data related to the occurred problem for investigating the cause of the problem or the influence of the problem. Our research aims to build a video data management system for this user's purpose. The follows are some examples of the objectives to use the video data. In the investigation of the influence or damage of a problem, it is important to check the video data that records the place from where the report of the problem was sent, the place where the sensor alarmed, or the place where some important buildings like hospitals and schools exist. Furthermore, by analyzing the recorded contents of the video data for every certain time since the problem occurred, we can understand the change of the area. As to the investigation of the cause of the problem, it is necessary to analyze the video data, which recorded the place where the problem occurred, and sometimes we have to check the video data that are recorded several minutes ago, hours ago or days ago before the problem occurred. We focus on the case for analyzing problems by using video data, and target the situation in which the user repeats the search and confirms what happened there.

2.2 Hardware of the local camera

In recent years, there are many types of commercial network cameras. Since most of them can be connected to LAN and are equipped with some server functions, the video stream of those cameras can be acquired through the web browser of PC.

The network camera we suppose for our system is shown in Fig.1. A commercial network camera is

connected to a local PC through the Ethernet, and the

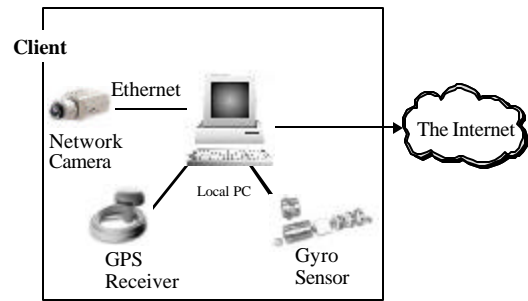


Fig.1 Network camera for our system

local PC acquires the video stream from the network camera and saves it as files at regular time intervals. The local PC is connected to GPS and Gyro sensors.

2.3 Overview of system

The overview of the system is depicted in Fig.2. The

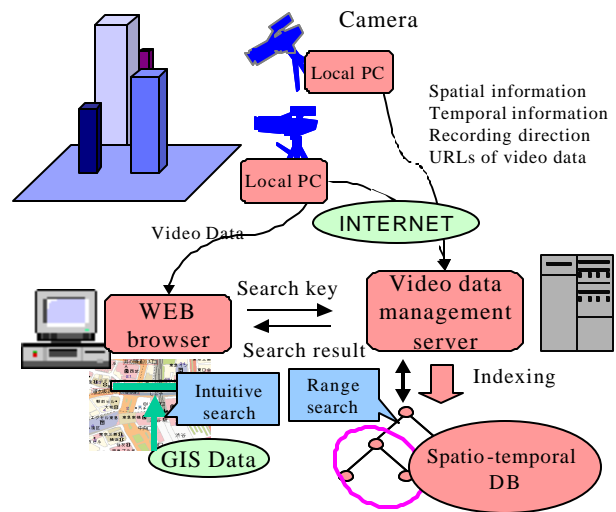


Fig.2 System structure

local PCs of the net cameras transmit the recording information of the video data (camera's position, recording time and recording direction) to the server through the Internet, and these information will be managed by a spatio-temporal data structure in the server. To search for video data, the user gives the user's search-key and views the search result through the web browser. The user can input the search key by a mouse on the GIS's map displayed on the web browser. The video data of the search result will be displayed on a new window of the web

browser. When the server receives the user's search key, it transforms the user's search key to the search key for the spatio-temporal data structure, and calls the data structure to perform the search. After the search is done, the server inserts the acquired URLs of the video data in a HTML document of the search result, and then returns this page to the web browser. After the web browser displays this web page, it will download and play the target video data as video stream from the local PC.

Note that our research defines the user's search key as "search for the video data, which are recorded during a period ($t1, t2$), and records a virtual wall (xs, ys, se, ye) in a certain direction (d)". However, our proposed search-key is different of the search key for a general spatio-temporal data structure. The most popular search key in spatio-temporal database is range search. The search key for range search is "search for the objects which existed in a period ($t1, t2$), and in a rectangle area ($x1, x2, y1, y2$)". Thus it is necessary to transform the user's search key to the search key for the spatio-temporal data structure.

2.4 Module structure of system

Fig.3 shows the module structure of the system. Flow (a) - (b) represent the process flow that the video data are transmitted from local PCs, and Flow (1) - (7) show the process flow of the search process requested by the user. The server side modules are the "request manager", the "spatio-temporal DBMS" and the "map DB". At the time of data registration, the request manger receives the recording information from local PCs, and then sends the information to the spatio-temporal DBMS. In the search process, the request manger takes charge of the message exchange between the client PC and the server, the generation of the HTML document which are inserted the URLs of the video data of the search result. The spatio-temporal DBMS is a module to make index of the spatio-temporal data, and the map DB is to store the GIS's map data.

The client PC has a web browser, on which the map viewer implemented in a Java applet runs. The map viewer downloads the map data from the map DB in the

server, and then displays the map. The user inputs the

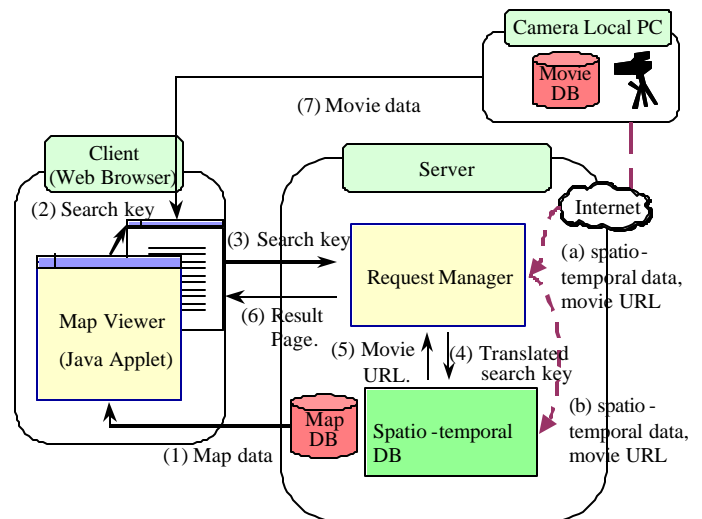


Fig.3 Module structure of the system

search key on the displayed map with a mouse. The web browser of the user's PC will display the HTML document of the search result, and then requests the video data based on the URLs from the local PCs which connects to the cameras.

3. Data structure and design of user interface

In this section, we will describe the spatio-temporal data structure, the method of search key transformation, the method for displaying the video data of the search result, and screenshots of the system.

3.1 Data structure

Our system applies an existing basic spatio-temporal data structure to manage the video data. The camera's recording direction is dispersed into 8 directions, and in every direction a spatio-temporal data structure is constructed. To search for video data, the input data of the spatio-temporal data structure is the temporal search range ($t1, t2$), the spatial search range ($x1, y1, x2, y2$) and the recording direction of the camera (d). The URLs of the video data are outputted. Here, the spatial search range of the input data can be acquired by transforming from the user's search key; the virtual wall (xs, ys, xe, ye) and the projective direction d . The transformation method will be

explained in Section 3.3. After receiving the search key for the spatio-temporal data structure, a data structure will be selected according to the recording direction (d) of the input data, and then the spatio-temporal range search is performed in this data structure. As spatio-temporal data structure, we know there are 3D R-tree [2], 2+3 R-tree [3], HR-tree[4] and so on. 3D R-tree is used in our system, which can handle dynamic data and provide a stable search performance.

3.2 Method for displaying video data

In our system, the interface of the search result page firstly displays the video data which are recorded farther from the virtual wall. The user can narrow down these video data and request the closer video data. Moreover, the system does not search all the video data that record the virtual wall, but firstly searches for the video data taken farther point. It searches closer data interactively according to the user's operation. Here, we will describe the interface of the search result page

It is important for the system to show a limited number of video data to the user at a time, so that the user can browse the search result. It is also important that to correlate the arrangement of the video data displayed on the screen with their actual recording time and position information. By this means, the user can narrow down the

video data intuitively by refining the spatial search range and the temporal search range on the screen.

The interface of the search result page is shown in Fig.4. On the search result page, the screen is divided into $M * L$ displaying areas to display video data. Video data is played in each displaying area. The number of the displaying areas is within the number that the user can look through the whole displayed video data easily. The search result page has two modes to display the video data of the search result: the spatial-ordering mode and the temporal-ordering mode.

In the spatial-ordering mode, the horizontal direction of the screen matches the horizontal direction to the virtual wall. The video data displayed in the n -th column of the screen are recorded from the cameras, whose real positions are in the n -th region when the spatial search range is divided into N regions in the vertical direction to the virtual wall uniformly. In the bottom of the screen, there is a $[>>]$ button under each column of the displaying areas. The function of the button is to narrow down the video data into the video data in the selected area. If the user pushes the $[>>]$ button, and the whole screen will be used to display the video data which are recorded in the equivalent region.

Furthermore, the interface provides a function to set the spatial search range to search for the closer video data or farther video data. Concretely, if the user pushes the [Forward] button, the system will search for the video data in a closer region to the virtual wall which record more detailed information. If the user selects the [Back] button, the system will search for the video data in a farther region which record the overview of the scene.

In the temporal ordering mode, the horizontal direction of the screen is equivalent to the time axis. The video data displayed in the n -th column of the displaying areas are recorded in the n -th period when the temporal range is divided into N periods. Under every column of the displaying areas, a time indicator is used to show the recording time information of the video data in this column. If the user pushes the $[>>]$ button under a time indicator, the system will narrow down the video data in the equivalent period, and the whole screen will display the

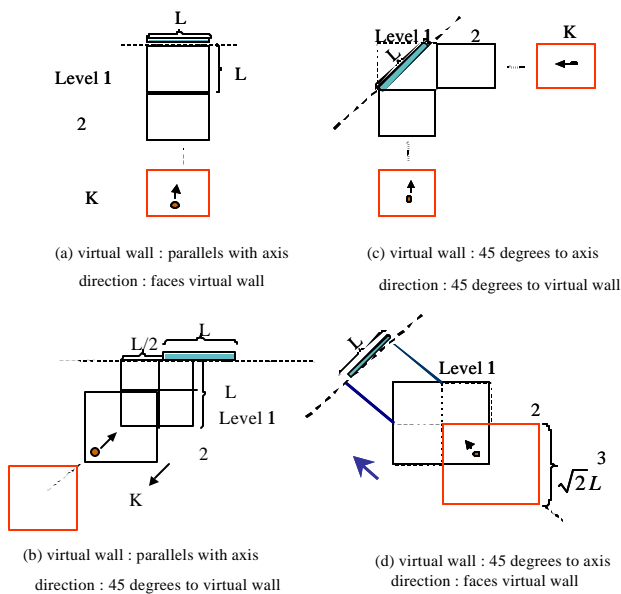


Fig.5 Transformation of spatial key

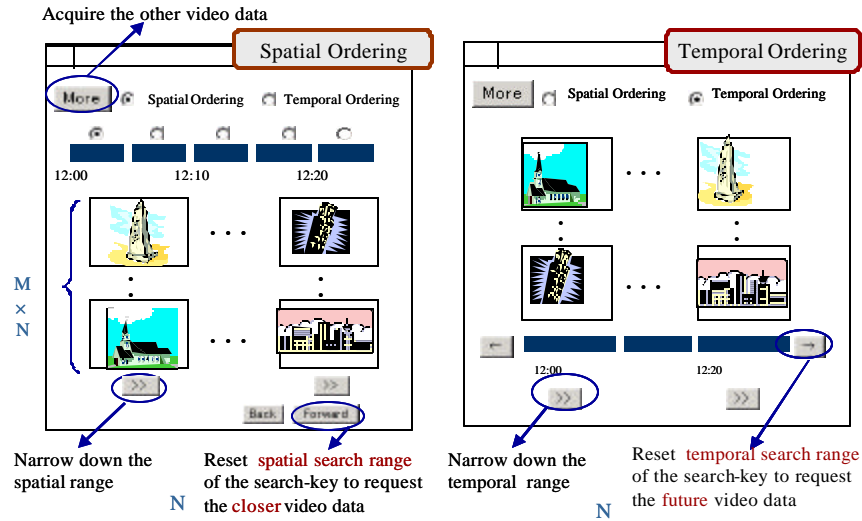


Fig.4 Interface of the search result page

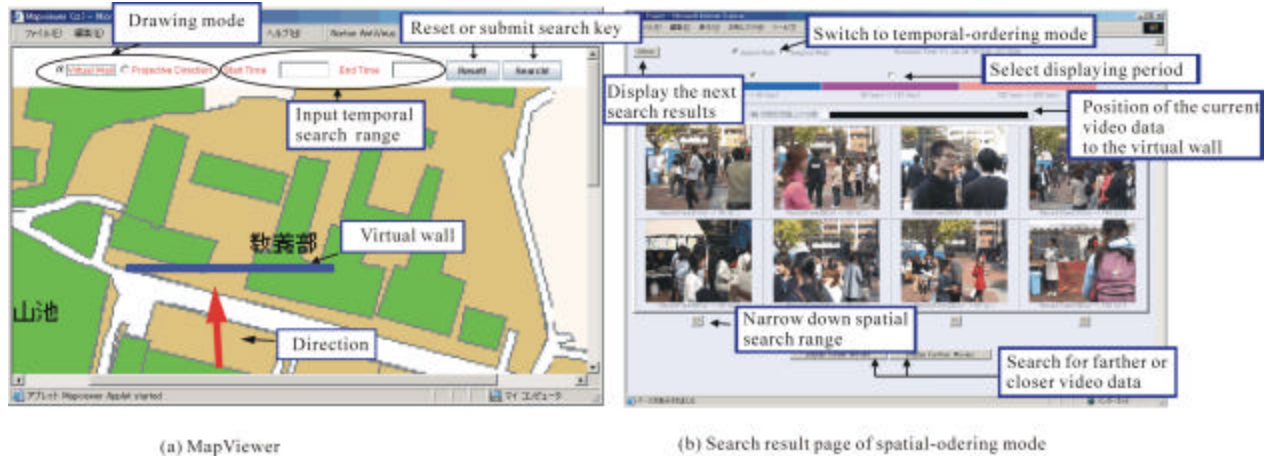


Fig.6 Screenshot of the system

video data which are recorded in this period.

3.2 Method of search key transformation

The virtual wall (x_s, y_s, x_e, y_e) and the recording direction d in the user's search key, are transformed to the spatial search range (x_1, y_1, x_2, y_2) of the search key for the data structure. Fig.5 shows the method of the search key transformation. Note that Fig.5 (a)-(b) show the case that the virtual wall is parallel with the axis, and Fig.5 (c)-(d) show the case that the virtual wall is set in the direction of 45 degrees to the axis. The range inside of the heavy lines is the range where the system should find the solutions. Since the spatial search range for the

spatio-temporal data structure is a region whose edges are parallel with the X axis or Y axis, our method gives approximate solutions by arranging K spatial search ranges in front of the virtual wall. In Fig.5, the range is a square, and the length of the edge is equal to the length of the virtual wall. When the user's search key is transformed to the search key for the data structure, the square of $k=K-1$ level will be selected firstly to perform the search. After displaying the search result, if the user requests for the closer video data to get more detailed information, the system will reset the spatial search range as the square of $k=K-1-1$ level and perform the new search.

3.3 Screenshot of system

Fig.6-(a) shows the screenshot of the map viewer, and Fig6-(b) shows the page of the search result. In the map viewer, firstly the user draws the virtual wall by the mouse, and then he draws the projective direction which he wants to watch the wall. After inputting the temporal search range, the user pushes the [Search] button, and he will view the search result from the server on a new window of the web browser. In Fig6 -(b), the page is set as the spatial ordering mode. The video data, displayed on the screen from left to right, are recorded by the cameras which are also set from left to right to the virtual wall in the actual space.

4. Summary

This paper proposed a distributed video data management system with an intuitive search interface. For the search interface, we proposed an input method of search key which does not insist users to care the locations of cameras by introducing the idea of virtual wall. We also provided a search result interface that allows users to narrow down the spatial search range and the temporal search range of the video data in the search result, in which the horizontal direction of the screen corresponds to the horizontal direction of the actual space and the time axis. Moreover, for managing the video data in the distributed environment effectively, the system manages only the recoding information in the server, and stores the raw video data itself in a local PC which directly connects to the camera. The data communication is realized through HTTP, and the user can search for the video data interactively through the web browser. Hence the user can use our system without the influence of a firewall, and use his familiar web browser and media player. The future work of our research is to design a hybrid search interface with a virtual wall and ith conventional range search.

Acknowledgement

This research was supported by the Japan Society for the Promotion of Science under Grant-in-Aid for Creative Scientific Research (Project No. 13GS0018 and No. 15300034).

References

- [1] H. Toshihiko, T. Akihiro, O. Minoru and B. Satoru, "Effective Search and Replay Methods for Distributed Historical Video Data and Their Implementation", *Journal of IEICE*, Vol.J82-D-I, No.1, 1999, pp.234-246 (in Japanese).
- [2] X. Xu, J. Han and W. Lu: "RT-tree: An Improved R-tree Index Structure for Spatiotemporal Databases", *Proc. of the 4th Intl. Symposium on Spatial Data Handling*, 1990, pp. 1040-1049.
- [3] M.A. Nascimento, J.R.O. Silva and Y. Theodoridis: "Evaluation of Access Structure for Discretely Moving Points", *Proc. of International Workshop on Spatio-temporal Database Management*, 1999, pp. 171-188.
- [4] M.A. Nascimento, J.R.O. Silva and Y. Theodoridis: "Access Structures for Moving Points", 1998, *TimeCente*, Technical Report 33.
- [5] W.W. Chu, A.F. Cardenas and R.K. Taira: "A Knowledge-based Multimedia Medical Distributed Database System", *Information Systems*, Vol.20, No.2, 1995, pp.75-96.
- [6] M. Donderler, et al.: "A Rule-based Video Database System Architecture", *Information Sciences*, Vol.143, No.1, 2002, pp. 13-45.
- [7] M.E. Donderler, O. Ulusoy and U. Gudukbay: "Rule-based Spatiotemporal Query Processing for Video Databases", *The VLDB Journal*, Vol.13, 2004, pp. 86-103.
- [8] L. Chen and T. Ozsu: "Modeling of Video Objects in a Video Database", *Proc. of IEEE International Conference on Multimedia*, 2002, pp. 217-221.
- [9] W.C. Feng, et al.: "Panoptes: Scalable Low-power Video Sensor Networking Technologies", *Proc. of ACM Multimedia*, 2003, pp.562-571.



LAWRENCE
LIVERMORE
NATIONAL
LABORATORY

VULNERABILITY AND RISK ASSESSMENT USING THE HOMELAND-DEFENSE OPERATIONAL PLANNING SYSTEM (HOPS)

Ronald L. Durling, Jr., David E. Price, Kimberlee K. Spero

March 9, 2005

International Symposium on Systems Safety Security and
Reliability, March 9-11th 2005
San Francisco, CA

Disclaimer

This document was prepared as an account of work sponsored by an agency of the United States Government. Neither the United States Government nor the University of California nor any of their employees, makes any warranty, express or implied, or assumes any legal liability or responsibility for the accuracy, completeness, or usefulness of any information, apparatus, product, or process disclosed, or represents that its use would not infringe privately owned rights. Reference herein to any specific commercial product, process, or service by trade name, trademark, manufacturer, or otherwise, does not necessarily constitute or imply its endorsement, recommendation, or favoring by the United States Government or the University of California. The views and opinions of authors expressed herein do not necessarily state or reflect those of the United States Government or the University of California, and shall not be used for advertising or product endorsement purposes.

Auspices Statement

This work was performed under the auspices of the U.S. Department of Energy by University of California, Lawrence Livermore National Laboratory under Contract W-7405-Eng-48.

VULNERABILITY AND RISK ASSESSMENT USING THE HOMELAND-DEFENSE OPERATIONAL PLANNING SYSTEM (HOPS)

ABSTRACT

For over ten years, the Counterproliferation Analysis and Planning System (CAPS) at Lawrence Livermore National Laboratory (LLNL) has been a planning tool used by U.S. combatant commands for mission support planning against foreign programs engaged in the manufacture of weapons of mass destruction (WMD). CAPS is endorsed by the Secretary of Defense as the preferred counterproliferation tool to be used by the nation's armed services.

A sister system, the Homeland-Defense Operational Planning System (HOPS), is a new operational planning tool leveraging CAPS expertise designed to support the defense of the U.S. homeland.

HOPS provides planners with a basis to make decisions to protect against acts of terrorism, focusing on the defense of facilities critical to U.S. infrastructure. Criticality of facilities, structures, and systems is evaluated on a composite matrix of specific projected casualty, economic, and sociopolitical impact bins. Based on these criteria, significant unidentified vulnerabilities are identified and secured. To provide insight into potential successes by malevolent actors, HOPS analysts strive to base their efforts mainly on unclassified open-source data. However, more cooperation is needed between HOPS analysts and facility representatives to provide an advantage to those whose task is to defend these facilities.

Evaluated facilities include: refineries, major ports, nuclear power plants and other nuclear licensees, dams, government installations, convention centers, sports stadiums, tourist venues, and public and freight transportation systems.

A generalized summary of analyses of U.S. infrastructure facilities will be presented.

BACKGROUND

The Counterproliferation Analysis and Planning System (CAPS) at Lawrence Livermore National Laboratory (LLNL) has been a planning tool used by U.S. combatant commands for mission support planning against foreign programs engaged in the manufacture of weapons of mass destruction (WMD) over the past twelve years. CAPS is endorsed by the Secretary of Defense as the preferred counterproliferation tool to be used by the nation's armed services. The CAPS Program provides a powerful database and engineering tools for assessing various processes (chemical, biological, nuclear, metallurgical, etc.) that proliferants use to build weapons of mass destruction and their delivery systems. By analyzing a country's specific approach to weapons production, we can pinpoint critical processing steps or production facilities which, if denied, would prevent that country from acquiring weapons of mass destruction, and we can pinpoint vulnerabilities which can then be exploited. The CAPS Program also assesses the consequences of a decision to interfere with suspected weapons development facilities.

There are four steps in creating the CAPS database. CAPS analysts: 1) model the set of chemical, biological, nuclear and missile manufacturing processes used to generate WMD and their delivery systems; 2) analyze a country's specific approach to WMD production from the possible sets; 3) pinpoint critical processing steps or production facilities which, if denied, would prevent that country from producing WMD; and 4) assess the health and environmental consequences of intervention actions.

If a consequence analysis is required, CAPS uses state-of-the-art software, climatology and terrain data to model the effects of the dispersal of toxic materials. Real-time data is a keystone of CAPS. For example, analysts can access a particular location and request a depiction of a plume release affected by winds blowing at that moment at the site.

CAPS consequence assessments provide military planners credible, documented estimates of collateral damage and include near real-time crisis action planning requests with little or no advanced notice. The system uses a secure communications network that transmits its critical data, analyses, and consequence assessments directly to military users worldwide. It comprises more than ten thousand web pages of information. During the early stages of Operation Iraqi Freedom, the number of hits increased to over one million per month.

STRUCTURE OF CAPS ANALYSES

CAPS analyses are categorized based on the degree of detail in the analysis

- A Level 1 analysis is a country-level identification of all sites that contribute to a specific WMD program
- A Level 2 (site-level) analysis identifies the layout and function of buildings on a particular site.
- A Level 3 (country program) analysis integrates the Level 1 and Level 2 analyses to identify the critical path for a country's WMD program by process, precursor, import, or technology.
- A Level 4 (building-level) analysis provides identification of the key components inside the most important building or buildings of an evaluated facility.
- A Level 5 (Criticality, Accessibility, Recuperability, Vulnerability, Effect, and Recognizability, or CARVER) analysis identifies the vulnerabilities of the key components identified in the Level 4 analysis.
- A Level 6 analysis identifies direct and indirect precision and network-centric effects on the processes analyzed in the Level 4 and 5 analyses.

CAPS has a potential for applications far beyond its original mission, especially in service to homeland security. This analysis and information system offers the possibility of assisting civil government in activities ranging from deliberate planning to disaster relief to emergency response. A sister system, the Homeland-Defense Operational Planning System (HOPS), is being used to support homeland defense activities in several states.

THE HOMELAND-DEFENSE OPERATIONAL PLANNING SYSTEM

The Homeland-Defense Operational Planning System (HOPS) is a new operational planning tool based on the CAPS structure and leverages CAPS expertise in exploiting vulnerabilities for protection of critical infrastructure to support the defense of the U.S. homeland. The close organizational connection between CAPS and HOPS permits managers in both programs to readily leverage CAPS analytic expertise as well as technologies and

analytic tools as they become available. The analyses that HOPS requires have their own specific attributes, and additional experts have been brought into the organization to meet these demands.

HOPS is sponsored by the California National Guard and has been vetted in several state and national level exercises. HOPS has also been recognized by multiple organizations as being superior to existing planning tools.

HOPS provides planners with the basis to make decisions to defend against acts of terrorism, focusing on the defense of facilities critical to the infrastructure of the United States and its territories. HOPS is currently involved in assisting multiple states as they establish their Protection of Critical Infrastructure plans. The program further provides strategic planners with a means to seamlessly communicate with other elements associated with defense and emergency response, and provides computer-based tools to support planning and response activities. HOPS has been an integral part of several exercises involving response to postulated WMD events in the United States.

STRUCTURE OF HOPS ANALYSES

There are four major aspects to the program:

- Criticality assessments of high value facilities. These assessments provide high-resolution analyses that identify the specific attributes of a facility that make it critical as well as its impact to the nation or state were it to be compromised.
- Vulnerability assessments of critical infrastructures associated with industry, agriculture, transportation, government/military installations, and large public structures such as sports arenas and convention centers. When appropriate, these assessments involve systematic analyses of the infrastructure to identify single points of failure and other critical nodes.
- A robust communications network that enables strategic planners engaged in homeland-defense to access the HOPS database to make decisions for strategic planning, and to communicate with subordinate and parallel organizations engaged in homeland-defense and to emergency responders in the event of an attack. HOPS is designed to reach its analysts directly at their work desks by operating on whatever classified or unclassified networks are required, including JWICS and SIPRNet (secure communications networks used by the Department of Defense).

- Analytic tools, such as three dimensional atmospheric plume modeling that utilizes real time wind conditions and conflict simulations that model the effectiveness of security plans. HOPS is also able to integrate with current data sets maintained by cities, counties or other jurisdictions. In this way organizations can leverage data that is already being maintained without requiring additional effort or resources.

HOPS analyses are generally equivalent to a Level 4 analysis in CAPS, but there are several distinct differences. Most significantly, while CAPS looks at the criticality of a site in terms of stopping or delaying the process for building WMD, criticality of sites within HOPS is evaluated on a composite matrix of specific projected casualty, economic, and sociopolitical impact bins. Another significant difference is that HOPS analysts strive to base their efforts initially on unclassified open-source data to provide insight into potential successes by malevolent actors.

CRITICALITY ANALYSIS METHODOLOGY

Criticality analysis attempts to prioritize infrastructure elements within a given area or sector of interest by the magnitude of the impacts created by the element's destruction or disablement. The ranking is performed based on "element criticality," defined as a function of the magnitude of potential casualties, economic impacts, and sociopolitical impacts.

In reality, the element's criticality is affected, to some degree, by the cause of damage – for example, the sociopolitical effects of a terrorist attack resulting in the destruction of an airport terminal will be very different from those same effects resulting from the collapse of the terminal due to poor structural design. However, one must also keep separate the magnitude of effect due to the specific attack mode compared to the effect posed by the element. Any attack has an effect. Criticality analysis attempts to identify those elements that by their very nature magnify the effect of attack. Examples include national monuments and facilities storing large quantities of hazardous materials.

Vulnerability is a function of accessibility, attack deterrence capability (security measures, protective force), and the element's "hardness" or physical ability to withstand the attack or contingency stress. In a HOPS analysis, the criticality of an element is not influenced by its vulnerability. For example, a sports arena is always critical as a high value terrorist target

because of the potentially high casualty rate regardless of the security and protective measures deployed.

It is assumed that a terrorist organization will consider the vulnerability of a target in a way that matches their available resources and capabilities with feasible interdiction or defeat modes. This would be done separately from assessing the criticality or value of the target that is, in turn, dependent only on the extent of potential casualties, economic impacts, and sociopolitical impacts, as discussed below.

Facilities deemed to be highly critical yet invulnerable, as well as facilities not critical but highly vulnerable, may not be of significant concern to homeland defenders. In both cases the interest may not be relevant, but it is the broad mix between these two extremes upon which HOPS focuses its efforts.

Casualties

Typically, the extent of casualties is thought of as “body count” resulting from explosion, fire, flood, structural collapse, or exposure to toxic chemical, radiation, chemical warfare agent, or biological agent.

A separate consideration is to distinguish between the casualties related to the type of a terrorist assault device used and the casualties that are related to the inherent characteristics of the infrastructure element. In a HOPS analysis, the focus is primarily on the effects stemming from the inherent characteristics of the infrastructure element being analyzed and not on the effects of different types of assault devices or modes of interdiction.

Key considerations in assessing the potential extent of casualties are:

- Type and quantity of hazardous materials stored or processed onsite, or those used in the attack
- Presence of materials that, upon purposeful contamination and subsequent consumption, can result in significant health impacts to offsite population – for example, a food processing plant could be of high value as a target for a surreptitious terrorist attack involving poisoning of the food or its ingredients.
- Number of people or workers present in the immediate impact area
- Proximity to population centers downwind of the impact area
- Population density of the affected downwind areas

Some cases may require additional modeling of thermal effects, blast overpressure effects, or atmospheric dispersion. A wealth of information that is needed for casualty assessment is available in open source literature and the public domain.

Economic Impacts

In the HOPS analyses, a distinction is made between the direct and indirect economic consequences of an attack.

Key considerations in assessing direct economic impacts are as follows:

- Damage repair/restoration cost
- Lost revenue and profit due to disruption of element's operations
- Value of lost inventory or intrinsic value of damaged goods

Key considerations in assessing indirect economic impacts are:

- Duration of damage restoration effort
- Upstream and downstream ripple effects
- Effects of changes in customer spending patterns
- Loss of jobs
- Healthcare costs
- Government expenditures (emergency services, security, protection, etc.)
- Loss of efficiencies in patterns (road detours, makeshift offices etc.)

Indirect impacts also include changes in purchasing or spending patterns resulting from public fear – for example, both airline and tourism industries were severely impacted worldwide by the events of 9/11. In the nuclear power industry, direct costs associated with damage or destruction of a nuclear power plant will include the cost of replacement part procurement, installation and reconstruction. Indirect costs primarily include the cost of replacement power, which could be on the order of a million dollars per day.

While direct costs can be estimated with fair accuracy for most cases using standard techniques, the indirect costs are generally more difficult to estimate owing to the complexities involved and current unavailability of reliable models.

Sociopolitical Impacts

One of the main objectives of a terrorist organization is to instill widespread fear, anxiety, or outrage leading to instabilities and disruptions in the normal functioning of a society. Such instabilities and disruptions may take the form of reduced productivity, introduction of freedom-curtailing security measures, pressure on government to conform to the terrorists demands, and attendant changes in the laws, political climate, foreign policy, and even military actions abroad.

Assessing sociopolitical impact is the most difficult aspect of criticality because of the complexity and uncertainties involved in determination of specific potential consequences (especially long-term consequences), lack of clear metrics, and inherent reliance on subjective judgment of the analyst(s) in dealing with many intangible factors. In assessing sociopolitical consequences, the analyst must also consider loss of life and economic effects, past societal responses, political climate, and symbolic value of a target to the society and to terrorists.

Criticality Assessment Methodology

The criticality assessment methodology encompasses the following steps:

- 1) Gather and review relevant information about the competing infrastructure elements within a given venue.
- 2) Eliminate those elements that are clearly of negligible criticality (i.e., those elements where the potential casualty rate, economic impacts, and sociopolitical impacts would be insignificant).
- 3) Systematically assess the remaining elements using both qualitative and, if at all possible, quantitative arguments.
- 4) Conduct a critical review of the draft assessment by qualified peer reviewers.

Each element is assessed and rated with regard to each category (casualties, economic impacts, and sociopolitical impacts) in terms of high, moderate, low, or minor impact. The following table provides example criteria for these categories:

METRIC	HIGH	MODERATE	LOW	MINOR
Casualty	= 5000 deaths	200 – 5000 deaths	1 - 200 deaths	No deaths
Economic	= \$1 billion	\$100 m - \$ 1 billion	\$10 m - \$100 m	= \$10 million

METRIC	HIGH	MODERATE	LOW	MINOR
Sociopolitical	Detriment to national security, government, or military readiness or functionality; Large multi-region/country impact; Unique, world-wide recognition, #1-3 in nation or world; Nationwide fear	Threat to national security, government, military; Multi-state impact; 3m – 10m people directly affected Regional landmark or government building, Top 10 in nation; Terrorism directed at national interest; Regional fear	Multi-city impact; 3m - 100,000 people directly affected Not unique, Not widely known; Widely known but not highly reported in media. Terrorism but locally directed; Limited fear	Local impact; = 100,000 people directly affected Not unique, Not widely known; Low media coverage

A short narrative documents each assessment and provides the rationale and supporting discussion for the ratings assigned. The overall criticality of the element is then based on the individual criteria ratings and is generally the same as the highest individual criteria rating.

Field of Inquiry

The field of inquiry defines how the three factors that influence criticality (i.e., casualties, economic impacts, and sociopolitical impacts) are applied. At the venue or regional level, the task is to rate each individual facility in terms of its criticality relative to the other facilities within the venue or region of interest. Hence, it becomes important to consider and compare facility-specific indirect economic impacts and sociopolitical impacts.

Facilities that are assessed as highly critical are then subjected to analysis at the facility level to identify those specific systems, equipment, or elements that, upon failure, would disable the functioning of the entire facility over a long time, cause the release of hazardous materials, cause fire or explosion, or instill widespread public fear. The focus of a facility-level analysis is to identify the critical equipment or systems within the facility that result in greatest impact or effect.

ANALYSES

The facilities considered in HOPS are grouped into five major categories:

- Agriculture
- Industry

- Military/Government
- Sports/Civic
- Transportation

These categories were derived from Department of Homeland Security Sectors and Department of Commerce listings. They were consolidated and grouped into the five sectors based on input from the State level Critical Infrastructure lists.

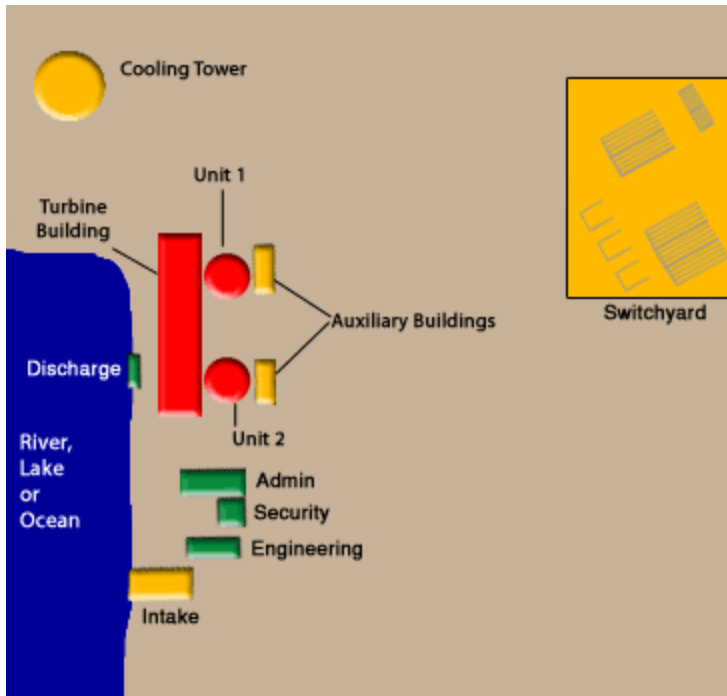
EXAMPLE ANALYSIS SUMMARIES

Facilities evaluated to date include refineries, major ports, nuclear plants and other nuclear material users, convention centers, sports stadiums, dams, transportation facilities, government installations, and public transportation.

Typically, risk and reliability analyses of nuclear power plants have focused on prevention of damage to the reactor core and resultant releases of radioactive material, and vulnerability analyses focus on physical security measures, i.e., “gates and guards”. However, this approach fails to recognize the high symbolic value resulting from an attack on a nuclear power plant, regardless of actual damage caused by the attack. Furthermore, any disruption of plant operation would result in a significant economic impact due to factors such as repair costs, replacement power costs, etc.

As introduced above, our analyses of domestic nuclear power plants were based solely on open source data found on the internet and other publicly available resources. This material included basic descriptions of the facilities, documents from public hearings regarding environmental and regulatory issues, up to a complete set of operator system training guides. A generic analysis summary is presented below to illustrate the HOPS structure and methodology.

The analysis presentation starts with an overview of the facility listing major components, as well as a satellite image and color-coded schematic that summarizes the criticality analysis for the facility, with red signifying the most critical. If there are important subsystems or structures in the facility, the schematic also allows the user to navigate to the desired analysis.



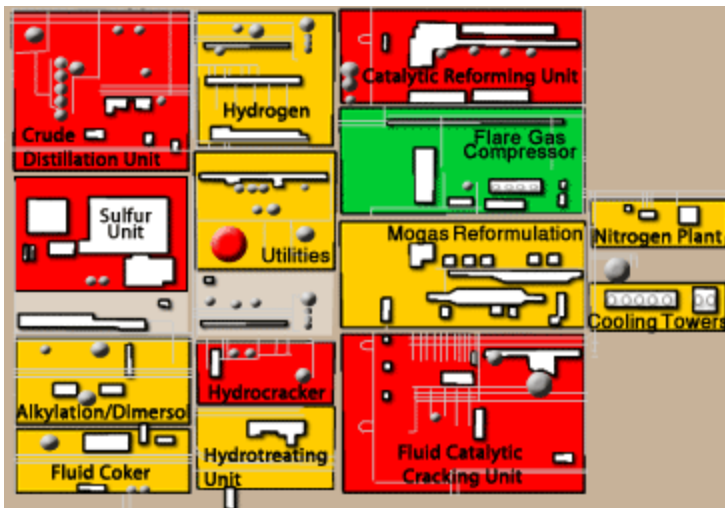
In the case of the generic nuclear facility depicted above, the two reactor containment buildings are deemed highly critical structures. Most would expect this to be the case from a casualty standpoint. However, although irradiated fuel is extremely hazardous, the robustness of the reactor vessel and the containment buildings themselves leads to a moderate criticality rating from a casualty standpoint. Rather, it is the economic impact that leads to high criticality. If the containment structures and major systems within them were damaged, the replacement time is judged to be significantly longer than other structures and systems at the plant, and the resultant costs for replacement power – on the order of a million dollars a day – would be significant. The turbine building is also highly critical, primarily due to economic concerns.

Once the most important structures have been identified, protective actions and other mitigation measures may be put in place. In some cases, structures and systems that were not previously identified as important may need additional security and mitigation measures.

In addition to nuclear power plants, HOPS has provided analyses of convention centers. Again the analysis presentation starts with an overview of the system showing floor plans and major components of the facility, such as utilities, air intakes and emergency generators. In the case of a convention center, criticality is a function of the event it is hosting, thereby leading the analysis to look at potential attacks on the population. An understanding of the facility's systems

and how they affect each room of the center is provided. In this way defenders can understand what they need to protect and responders have a path to follow show an event occur.

Criticality of refineries is similar to that of nuclear plants, in that economic criticality contributes significantly to overall criticality. However, due to the presence of large quantities of hazardous materials, such as anhydrous ammonia or amines (monoethanol amine, diethanol amine, and methyl diethanol amine) used for sulfur extraction and recovery, health consequences also contribute significantly to overall facility criticality. In the example refinery below, the crude distillation unit, fluid catalytic cracking unit, catalytic reforming unit, and hydrocracker are assigned a high criticality rating based on economic considerations. Additionally, failure of the anhydrous ammonia tank and the sulfur unit would each result in significant casualties due to the toxic release, thus they are also considered highly critical. Of the remaining areas, the hydrotreating unit is a moderately critical area due to potential consequences of a release of hydrogen sulfide from the unit. The remaining moderate criticality areas are identified based on economic impacts.



Our analyses have in many instances identified vulnerabilities not previously identified. Unfortunately, although the specifics are based on unclassified data, the results are sensitive, thus we cannot discuss them in any detail in any public forum.

CONCLUSIONS AND RECOMMENDATIONS

Many of the facilities we have evaluated, whether they be nuclear power plants, refineries, or seaports, are generally unwilling to share their information, even with a nationally recognized institution such as a National Laboratory. In many cases, there are concerns about releasing

proprietary information, but there is also the concern of inadvertent public dissemination for fear of incurring potential legal liability.

However, as we have repeatedly demonstrated, terrorists have access to the same information, and could conceivably reach the same conclusions with regard to heretofore unidentified vulnerabilities.

In addition, most facilities focus on physical security, while their true vulnerability may lie in the process or technology of their facility. While facilities are unwilling to unveil their physical security plans, they are often completely willing to talk about their processes. Thus, we strongly encourage more cooperation between HOPS analysts and facility representatives, either through sharing of additional information that may not be generally available to the public or by participating in the review process of HOPS analyses, such that we can provide a measurable advantage to those whose task is to defend these facilities.

We also encourage the facilities as they complete their risk and vulnerability assessments to focus on the technology and engineering aspects of their area, not simply the perimeter defense.

Title: Face Authentication System with Facial Personation Prevention by Using Infrared Images

Authors: Takatsugu Hirayama, Yoshio Iwai, and Masahiko Yachida

TOPIC: Integration of systems and human sciences

Affiliation: Graduate School of Engineering Science, Osaka University

Address: 1-3 Machikaneyama-cho, Toyonaka, Osaka 560-8531, JAPAN

Phone number: +81-6-6850-6361

Fax number: +81-6-6850-6341

E-mail: {hirayama, iwai, yachida}@yachi-lab.sys.es.osaka-u.ac.jp

Face Authentication System with Facial Personation Prevention by Using Infrared Images

Takatsugu Hirayama¹, Yoshio Iwai¹, and Masahiko Yachida¹

¹ Graduate School of Engineering Science, Osaka University
1-3 Machikaneyama-cho, Toyonaka, Osaka 560-8531, JAPAN
{hirayama, iwai, yachida}@yachi-lab.sys.es.osaka-u.ac.jp

Abstract

Conventional face authentication systems cannot prevent personation by face photos. We propose a face authentication system which distinguishes between a person and a face photo from infrared images. The system can detect a facial region robust for background variations by simple image processing methods because of the characteristic of infrared images. A face photo is distinguished from a person by using our efficient method based on the photometric stereo. The method can detect a curvature photo which is not dealt with in previous researches. Face authentication is based on our effective method which performs fine estimation of facial position in parallel with person identification.

1. Introduction

Security systems using face authentication technology will be effective for various high-security situations. Some researchers have developed the systems such as PASSFACE[1], FacePass_{TM}[2], FaceIt^(R)[3], FaceKey[4], and FACELOCK[5]. FacePass_{TM}, FaceIt^(R), and FaceKey have been put to practical use. However, these systems cannot prevent personation by face photos. This is an important problem. In this work, we propose a face authentication system which can distinguish between a person and a face photo.

There are some concavities and convexities on human faces. They do not exist on photos. Therefore, face authentication systems can distinguish between a person

and a face photo by measuring three-dimensional shape of an authentication subject. The photometric stereo method[6] is one of three-dimensional measurements. The method uses multiple images which are taken by switching multiple light sources. Tsuda et al. proposed a person-photo distinction technique[7] based on this method. The technique generates an illumination differential image from two infrared (IR) images taken by alternately irradiating IR light from the right and the left sides of an authentication subject, and calculates the surface normal of the subject. The photometric stereo method can be applied to visible images. However, strong visible light to generate the illumination differential image causes user's stress because human perceives visible light. It is possible for a user to find out the architecture of a face authentication system, if the user notices the system turning on/off the light sources. Tsuda et al. used IR light in order to solve these problems with visible light. The person-photo distinction technique has some problems. First, they proposed the technique without the assumption that impostor wears a mask made of the curved face photo. Then, the technique has low computational efficiency because it completely estimates the surface normal of face.

Using IR light is also effective for face detection. Conventional face detection methods[8][9] and general background subtraction method[10] which improves the performance of face detection are sensitive to illumination variations. Generally, this problem can be

solved by preparing models that correspond to illumination variations. However, using multiple models incurs a high computational cost. There is the trade-off between accuracy and efficiency of face detection. If the face authentication system is used in doors, we can solve the trade-off by using IR light. There is no strong IR light in doors. We can increase the contrast between the authentication subject and the background by adjusting IR light to irradiate the subject only, and detect a facial region efficiently. Using IR light is more effective than the general background subtraction method because background variations do not affect appearance of IR images.

Some researchers have proposed face detection methods using IR light. Dowdall et al. have proposed a face detection technique which uses two images taken by irradiating lower band near-IR light and upper band near-IR light respectively[11]. The technique capitalizes on the unique reflectance characteristics of human skin and human hair in the near-IR spectrum[12]. A weak point of the technique is that it detects a face in an image generated by frame subtraction. In order to capture a frontal face for face authentication, the technique must require user to translate his face looking to camera. It is onerous task for a user. Eveland et al. have proposed a face detection technique using thermal-IR light[13]. The technique cannot capture detailed texture of a face because thermal-IR images are measurement data of thermal emission from an object. It is difficult to authenticate a face from the thermal-IR image. Considering face authentication, near-IR images are more effective than thermal-IR images because of the similarity of visible images.

In this work, we solve some problems with the above techniques, and propose a new technique which performs more efficient face detection and more stable person-photo distinction than the previous techniques. We also propose a face authentication system based on the technique and our face authentication method [14] which is optimum for 1 vs. N matching. The method

performs

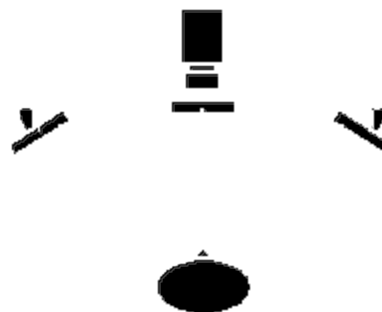


Figure 1: Proposed system .

fine estimation of facial position in parallel with person identification. We can solve the trade-off between accuracy and computational efficiency of face authentication by using the parallelization method.

2. Face Authentication System with Facial Personation Prevention

2.1 System Overview

When the face authentication system takes face photos of user, we assume the following three situations: (1) a user gets still with expressionless, (2) a user stands in front of a camera and maintains a roughly constant distance from a camera, (3) a user shows his frontal face to a camera. We propose a face authentication system with facial personation prevention in consideration of these assumptions.

The photometric stereo method introduced into the proposed system needs multiple light sources. The system uses two near-IR illuminators in order to simplify the system architecture. The two illuminators are set on both side of the IR camera as shown in Fig.1. By using the right and left light sources, the system can measure the largest convexity on the face surface. The convexity is ridge of the nose. The process flow of the proposed system is summarized in Fig.2. The system is composed of the face detection module and the face authentication module. The system takes two images (left-illuminated image I_L and right-illuminated image I_R) of the

authentication subject by irradiating IR light from the

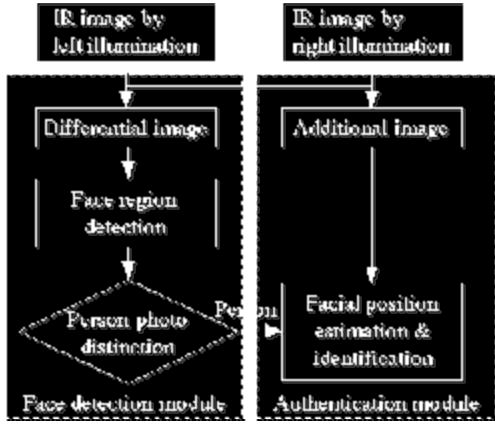


Figure 2: Process flow of proposed system.



Figure 3: IR images.

right and the left sides of him alternately. The illumination differential image I_D is generated by measuring the difference between I_L and I_R :

$$I_D(x,y) = |I_L(x,y) - I_R(x,y)| \quad (1)$$

I_L , I_R , and I_D are shown in Fig.3.

First, the facial region detection and the person-photo distinction in the face detection module are performed in sequence for the differential image. The face detection module is based on the proposed method in this work. If the module judges the authentication object as a person, the system generates an illumination additional image I_A

from I_L and I_R :



Figure 4: Process flow of facial region detection.

$$I_A(x,y) = I_L(x,y) + I_R(x,y). \quad (2)$$

The system performs the face authentication module based on our face authentication method and authenticates the person in the additional image.

2.2 Face Detection Module

The face detection module performs facial region detection process that is shown in Fig.4 and person-photo distinction process.

2.2.1 Facial region detection

First, the system binarizes the illumination differential image and generates a binary image I_B . The threshold of binarization is determined by the p-tile method. We assume that face size in I_D hardly changes, i.e. a facial region has a roughly constant size. Therefore, the facial region in I_B is separated from the other region by the binarization. If luminance distribution of hair and clothes is similar to that of the facial region, a human region with the facial region is extracted. Noise components are also extracted in the background. The system then measures size of each region by labeling in order to remove the noise components, i.e. the system measures size S_l of region R_l with label l in a labeled image L . We apply the water flood algorithm to labeling and introduce

sampling at intervals j pixel into the algorithm for faster process. The noise components are removed by Eq.(3) which changes the label of larger-than- t_S ($=j \times j$) region to A_{person} . The region with A_{person} is defined as the human region R_{person} by Eq.(4).

$$L(x,y) = A_{person} \quad \text{if } S_l \geq t_S, \quad (x,y) \in R_l. \quad (3)$$

$$R_{person} = \overset{D}{\{ (x,y) | L(x,y) = A_{person} \}} \quad (4)$$

Next, head region R_{head} , facial region R_{face} , and eyes region R_{eyes} are estimated in the human region in sequence. We define the head region R_{head} as a region between top position y_{top} of the human region and neck position y_{neck} (Eq.(5)). Width of the head region is not limited. The neck position is estimated by measuring human region width W_{person} , and it is position with the minimum W_{person} between ear position y_{ear} and bottom position y_{bottom} of the human region (Eq.(6)). The ear position is estimated as the position that y-position of human contour (i.e. edge of human region) changes most significantly (Eq.(7)).

$$R_{head} = \overset{D}{\{ (x,y) | y_{top} \leq y \leq y_{neck}, (x,y) \in R_{person} \}} \quad (5)$$

$$y_{neck} = \arg \min_{y_{ear} \leq y \leq y_{bottom}} W_{person}(y),$$

$$W_{person}(y) = x_R(y) - x_L(y),$$

$$x_R(y) = \max \{ x | (x,y) \in R_{person} \}$$

$$x_L(y) = \min \{ x | (x,y) \in R_{person} \} \quad (6)$$

$$y_{ear} = y_{counter}(x_{ear}),$$

$$y_{counter}(x) = \min \{ y | (x,y) \in R_{person} \}$$

$$x_{ear} = \arg \min_x \{ y_{counter}(x) - y_{counter}(x-1) - y_{bottom} \}. \quad (7)$$

We define the facial region R_{face} as a region between eyebrows position $y_{eyebrow}$ and the neck position (Fig.5).

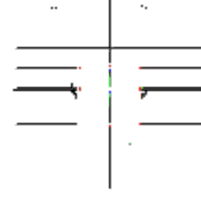


Figure 5: Facial region.

Facial region width W_{face} is equal to the distance between the eyebrows position and the neck position. Bisection point x_{center} of the width is defined as the centroid of the head region (Eq.(8)). Before the eyebrows position estimation, nose position y_{nose} is estimated as the position with the maximum value of the horizontal integral projection $P(y)$ in the head region (Eq.(9)). The system then measures the local minimum $Y_{localmin}$ of $P(y)$ between the top position and the nose position, and estimates the eyebrows position as the position with the minimum of $Y_{localmin}$ (Eq.(10)).

$$R_{face} = \overset{D}{\{ (x,y) | y_{eyebrow} \leq y \leq y_{neck},$$

$$x_{center} - \frac{W_{face}}{2} \leq x \leq x_{center} + \frac{W_{face}}{2} \}},$$

$$W_{face} = y_{neck} - y_{eyebrow},$$

$$x_{center} = \frac{\sum_{(x,y) \in R_{head}} x}{\sum_{(x,y) \in R_{head}} P(y)},$$

$$P(y) = \sum_{(x,y) \in R_{person}} I_B(x,y). \quad (8)$$

$$y_{nose} = \arg \max_{y_{top} \leq y \leq y_{neck}} P(y). \quad (9)$$

$$y_{eyebrow} = \arg \min_{y \in Y_{localmin}, y_{top} \leq y \leq y_{nose}} P(y). \quad (10)$$

The eyes region R_{eyes} is defined as a region between the eyebrows position and the nose position. Eyes region width W_{eyes} is equal to the facial region width. Bisection point x_{center} of the width is the centroid of the head region (Eq.(11)). The largest concavity and convexity in

the facial region is in the eyes region. The system distinguishes between a person and a face photo by measuring concavity-convexity degree in the eyes region.

$$R_{eyes}^D = \left\{ (x, y) \mid y_{eyebrow} \leq y \leq y_{nose} \right. \\ \left. x_{center} - \frac{W_{eyes}}{2} \leq x \leq x_{center} + \frac{W_{eyes}}{2} \right\}, \\ W_{eyes} = W_{face}. \quad (11)$$

2.2.2 Person-photo Distinction

If the system takes images of face photos, appearance of the illumination differential images depends on paper quality (gloss paper or standard paper), curvature degree (flatness or curvature), and color (monochrome or color) of the face photo. For example, the illumination difference between right-illuminated image and left-illuminated image of the flat photo is very little, and face texture appears on the illumination differential images of a monochrome photo with standard paper only. The illumination differential images of face photo are shown in Fig.6 and Fig.7. We analyzed difference between the illumination differential images of a face photo and a person and achieved the following two properties: (1) the head region is separated into right and left regions distantly, or does not exist in the illumination differential images of a face photo, while it is separated at short intervals or is not separated in the images of a person; this property depends on the curvature degree of a photographic subject, (2) streaky textures appear in the eyes region of the illumination differential images of a person because there are concavities and convexities on the face surface, while it does not appear on the images of a face photo. We introduce two features (1) curvature degree and (2) concavity-convexity degree based on two properties into the system in order to distinguish between a face photo and a person. We define curvature degree D_{curve} as a distance between right and left human regions at nose position y_{nose} (Eq.(12)), and measure the concavity-convexity degree D_{bamp} on the basis of the



Figure 6: Illumination differential images of face photo with gloss paper.

Figure 7: Illumination differential images of face photo with standard paper.

vertical integral projection $P(x)$ in the eyes region (Eq.(13)). The system performs the person-photo distinction for the authentication subject Z by using the threshold process according to Eq.(14).

$$D_{curve} = v_R(y_{nose}) - v_L(y_{nose}), \\ v_L(y_{nose}) = \max_{x \leq x_{center}} \{x \mid (x, y_{nose}) \in R_{person}\} \\ v_R(y_{nose}) = \min_{x \geq x_{center}} \{x \mid (x, y_{nose}) \in R_{person}\} \quad (12)$$

$$D_{bamp} = \sum_{x \in R_{eyes}} 1 \quad \text{if } P(x) = P_{th} \cap P(x-1) \neq P_{th}, \\ P(x) = \sum_{(x,y) \in R_{eyes}} I_B(x, y), \\ P_{th} = \frac{\max_{x \in R_{eyes}} P(x) - \min_{x \in R_{eyes}} P(x)}{2}. \quad (13)$$

$$Z = \begin{cases} 'photo' & \text{if } D_{curve} > C \cap D_{bamp} < B \\ 'person' & \text{otherwise} \end{cases}. \quad (14)$$

2.3 Face Authentication Module

First, the facial region R_{face} estimated in the face detection module is projected into the illumination additional image. Our face authentication method which performs fine estimation of facial position in parallel

with person identification is then applied to the region. The method represents a face as a graph where 30 nodes are placed on the facial feature points (Fig. 8). Each node has the Gabor features extracted from an image at the corresponding location. The method is composed of five states: position estimation by global scanning, position estimation by local scanning, scale estimation, personal model estimation, and verification as shown in Fig.9. The facial position, scale, and personal model are estimated by changing these states. The facial position estimation is based on the coarse-to-fine algorithm using two scanning states. The global scanning state has a low computational cost, although it does not provide stable estimation. We regard the positions estimated in this state as central positions for a detailed search of a face. The position estimation by local scanning performs a detailed search around the central positions. The local scanning state has a higher computational cost than the global scanning state, although it can estimate more accurately. The scale estimation state estimates the facial scale by using our scale conversion method, and the personal model estimation state uses the hierarchical model database and a priority queue. The verification state verifies the validity of a graph generated from the estimated position, scale, and model. The method performs more accurate estimation by updating positions, scales, and models stored in the top ranks of the queue. Finally, the method selects a personal model from the cluster, and we can regard the model as a person identification result. Details of the method are described in [14].

Figure 8: Face graph.

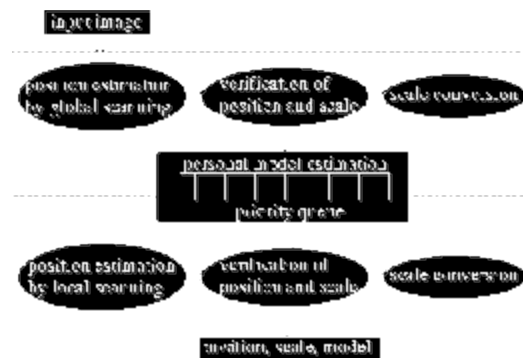


Figure 9: Process flow of face authentication module.

3. Evaluation Experiments

We conducted face authentication experiments to verify whether the proposed system is effective. The system for the experiments was constructed on SGI Origin300 (8CPU R14000 500MHz, MEMORY 4GB). The IR camera introduced into the system was HITACHI KP-M2R which has peak of wavelength sensitivity at about 600 nm. We mounted the camera with the IR pass filter because wavelength sensitivity range of the camera covers the visible band. The IR illuminator radiated near-IR ray of 880 nm. The right and left illuminators were turned on/off manually.

We took 50 person model images from 50 different experimental subjects by setting distance between a user and the camera to 35 cm. When the system is put into practice, it is impossible for a user to control the distance completely though we assume that the user stands at a roughly constant distance from the camera. Therefore, we took 3 person test images per subject by setting the distance to 28cm, 42cm and 35cm respectively. We call face images taken at 35cm the standard face (100% size). The facial region width of the standard face was 138 pixels on an average. The face images taken at 28cm and 42cm were 120% and 80% size of the standard face respectively. We also prepared 8 different face photos per subject and then took 48 photo model images and 144 photo test images from 48 face photos of 6 different subjects. The 8 different face photos were created by combining the following three parameters: paper quality

(gloss paper or standard paper), curvature degree (flatness or curvature), and color (monochrome or color) of the face photo. The faces of all images were expressionless and in frontal pose according to our assumptions. Each image was 512×512 pixels in size and 8 bits grayscale. In the face detection module, the image was reduced 16 times from its original size because size of the image does not affect accuracy of processes. The following parameters were used in this experiment: $j = 5$, $B = 5$, $C = 5$. We derived parameters B and C from all model images experimentally.

3.1 Facial Region Detection Performance

The estimation results of the facial region are shown in Fig.10. We confirmed that the system accurately estimates the facial region regardless of whether the photographic subject is a person or a face photo. We conducted face detection experiment on 150 person test images. The estimation accuracy of the facial region is shown in Table 1. We verified the accuracy indicating the position error, the size error, and face detection rate. The position error is the average distance between centroid of true facial region extracted by hand and centroid of the facial region estimated by the system. The true facial region is generally defined as a square region which includes eyebrows and mouth. The size error is the ratio of the facial region width estimated by the system to the width of the true facial region. The face detection rate is probability that both eyes and mouth are completely included in the estimated facial region. We confirmed that the system did not achieve high accuracy in all indicators. We believe this result occurs because the system defines a region between the eyebrows position and the neck position that may be above the mouth position as the facial region. The processing time for the facial region detection was 0.027 seconds on an average. The system has enough performance to perform preprocessing of fine facial position estimation because of high efficiency.

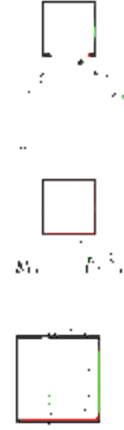


Figure 10: Facial region detection results.

Table 1: Accuracy of facial region detection.

Test set	Position error (pix)	Scale error (%)	Detection rate (%)
80%	18.3	100 ± 17.9	78.0
100%	17.6	100 ± 20.6	82.0
120%	16.8	100 ± 17.8	70.0

Table 2: Accuracy of person-photo distinction.

Test set	FRR (%)	FAR (%)
80%	6.0	0
100%	6.0	0
120%	6.0	0

3.2 Person-photo Distinction Accuracy

We conducted a person-photo distinction experiment on all test images. The distinction accuracy is verified by the false rejection rate (FRR) and the false acceptance rate (FAR) as shown in Table 2. FRR is error rate which the system judges a person as a face photo. FAR is error rate which the system judges a face photo as a person and is more important than FRR in face authentication situation. We appreciate the system because FAR is 0%. Error related to FRR often occurs when a user wears glasses. The glasses also cause deterioration of the



Figure 11: Face graph matching results.

estimation accuracy of the facial region.

3.3 Face Authentication Performance

We regarded 25 of 50 experimental subjects as the registered person, and we registered their model images and model graphs in the personal model database. The other experimental subjects were unregistered persons. We conducted face authentication experiment on 150 person test images. Some results of the face graph matching in the face authentication module are shown in Fig.11. These results indicate that the system could accurately estimate facial position and scale. We confirmed that the system could also accurately detect facial feature points as a result of the personal model estimation.

We show the estimation accuracy of facial position and scale in Table 3, indicating the average error between the estimated position and the ground truth, the average of the estimated scale. We confirmed that the accuracy deteriorated as facial scale varies. The person identification accuracy is represented by the ROC curves of FRR and FAR in Fig.12. We confirmed that the system did not achieved high identification accuracy and the accuracy deteriorated as facial scale varies. The equal error rate (EER), defined as the point where FRR=FAR, was 26% for test set 80%, 12% for test set 100%, and 16% for test set 120%. Security systems based on face authentication need EER less than 1%. We consider that it is possible for identification using IR image to be difficult. We also consider that distortion and rotation of facial image arose as distance between the camera and the experimental subject varies. We must introduce image feature with high performance for IR image and

Table 3: Accuracy of face graph matching.

Test set	Position error (pix)	Estimated scale (%)
80%	5.6	80 ± 11.2
100%	2.7	100 ± 3.2
120%	4.2	120 ± 4.5

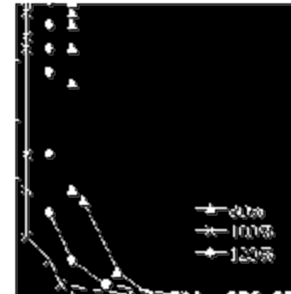


Figure 12: Accuracy of face authentication.

authentication process robust for variations of facial appearance into our method. The processing time for the face authentication was 33 seconds on an average.

4. Conclusion

We proposed a new face authentication system that prevents facial personation by using infrared images. We verified the system can accurately distinguish between a person and a face photo with a small computational cost through evaluation experiments. However, the system did not achieve high accuracy of the person identification. We need to improve the proposed system.

Acknowledgment

This research was partially supported by the Japan Society for the Promotion of Science under Grant -in-Aid for Creative Scientific Research (Project No. 13GS0018).

References

[1] M. Doi, Q. Chen, A. Matani, O. Oshiro, K. Sato, and

- K. Chihara, "Lock control system based on face identification," *IEICE Trans. Information and System D-II*, vol. J80-DII, no. 8, pp. 2203-2208 (1997).
- [2] H. Dobashi, A. Okazaki, and K. Takagi, "FacePassTM face recognition security system," *TOSHIBA REVIEW*, Vol. 57, No. 8, pp. 48-51 (2002).
- [3] <http://www.faceit.com/>.
- [4] <http://www.society.omron.co.jp/faceid/2/f2.html>.
- [5] T. Hirayama, Y. Iwai, and M. Yachida, "FACELOCK-Lock control security system using face recognition," *IEEJ Trans. EIS*, vol. 124, no. 3, pp. 784-797 (2004).
- [6] K. Shinmoto, T. Honda, and S. Kaneko, "A formalization of photometric stereo method using two lights sources and its application to reconstruction of human skin replicas," *IEICE Trans. Information and System D -II*, vol. J82-D-II, no. 1, pp. 10-18 (1999).
- [7] T. Tsuda, K. Yamamoto, and K. Kato, "A proposal of the distinguish technique between a real person and a photograph," *Proc. 6th Asian Conf. on Computer Vision*, vol. 1, pp. 539-544 (2004).
- [8] H. Rowley, S. Baluja, and T. Kanade, "Neural network-based face detection," *Proc. IEEE Conf. Computer Vision and Pattern Recognition*, pp. 203-208 (1996).
- [9] P. Viola and M. Jones, "Rapid object detection using a boosted cascade of simple features," *Proc. IEEE Conf. Computer Vision and Pattern Recognition*, pp. 511-518 (2001).
- [10] T. Mitsuyoshi, Y. Yagi, and M. Yachida, "Real time human feature acquisition and human tracking by omnidirectional image sensor," *Proc. IEEE Conf. Multisensor Fusion and Integration for Intelligent Systems*, pp. 258-263 (2003).
- [11] J. Dowdall, I. Pavlidis, and G. Bebis, "Face detection in the near-IR spectrum," *Image and Vision Computing*, vol. 21, pp. 565-578 (2003).
- [12] I. Pavlidis and P. Symosek, "The imaging issue in an automatic face disguise detection system," *Proc. IEEE Workshop on Computer Vision beyond the Visible Spectrum: Methods and Applications*, pp. 15-24 (2000).
- [13] C. K. Eveland, D. A. Socolinsky, and L. B. Wolff, "Tracking human faces in infrared video," *Image and Vision Computing*, vol. 21, pp. 579-590 (2003).
- [14] T. Hirayama, Y. Iwai, and M. Yachida, "Parallelization between face localization and person identification," *Proc. 6th IEEE Conf. on Automatic Face and Gesture Recognition*, pp. 183-188 (2004).

**Development of a Support System
for Consensus Building with Elicitation of Concerns and Conflicts**

Takanori Ishii¹ and Kazuo Furuta²
Institute of Environmental Studies, The University of Tokyo

7-3-1 Hongo, Bunkyo-ku, Tokyo 113-0033 Japan
TELEPHONE/FAX: +81-3-5841-8923 / +81-3-5841-8923
E-mail: ¹ishii@cse.k.u-tokyo.ac.jp, ²furuta@q.t.u-tokyo.ac.jp

Topic: Concepts, formalisms, methods and tools

Development of a Support System for Consensus Building with Elicitation of Concerns and Conflicts

Abstract

Since conflicts among stakeholders usually exist in development projects, assessment of the conflicts is vitally needed. For helping this process, we developed a method to elicit stakeholders' concerns and conflicts effectively.

In this study stakeholders describe their concerns by using a semi-IBIS method, which helps them to introspect logically. After several times of interactions among concerns described, "Conflicts Map" representing the situation of conflicts is generated.

In addition, we implemented this method as a web-based system and tested the feasibility of this method through a real conflict case. In this case we acquired structured concerns of participants and visualized the conflicts.

This system will help people in conflicting situation by giving them structured argument based on their well elicited concerns.

1: Introduction

Recently social assets such as highways and waste treatment facilities cannot be successfully developed without mutual understanding among stakeholders. Therefore, public involvement (PI) has become inevitable in consensus building and thereby social needs for conflict assessment have also arisen. Conflict assessment [1] is the first stage of PI process, where stakeholders' concerns about a certain subject are elicited and a facilitator who is in charge of dispute resolution embodies and clarifies their conflicts. Along with popularization of PI, needs for conflict assessment have become increased these days and this tendency will probably go on in the future.

The aim of this study is twofold: to develop a method to elicit stakeholders' concerns and conflicts effectively, and to implement the methodology as a web-based system and test its feasibility.

2: Developed methods and systems

2.1: Overview of the method

We assume that the users of this method and system are those who have to reach agreement respecting a certain topic, that is, *Stakeholders*. In this method such a topic is called *Subject*. Needless to say, each of them has his or her own assumption or idea around Subject. Now we define *Concerns* as a collection of what one can conceive from a certain Subject. And we also define *Conflicts* as a collection of all stakeholders' Concerns. The elicitation method of their Concerns is as follows.

First, each stakeholder describes his/her Concerns logically based on a *semi-IBIS method*, which is a modified version of the *IBIS method*. This semi-IBIS method we propose here helps stakeholders to build their Concerns all by themselves. Along with the description, stakeholders edit their Concerns by using two editing methods: *Equivalence Link* and *Quotation*. These methods are introduced for the purpose of enabling stakeholders to broaden and enrich their Concerns via mutual reference of each other's Concerns.

After several times of description and editing mentioned above, it is assumed that stakeholders' Concerns come to be elicited further in comparison with those at the beginning. By collecting these "well elicited" Concerns, *Conflicts Map* that represents the Conflicts among stakeholders can be obtained. Conflicts Map is a commonly accepted achievement in a usual conflict assessment, but any de facto standard of its format has not yet been established. In this study, we

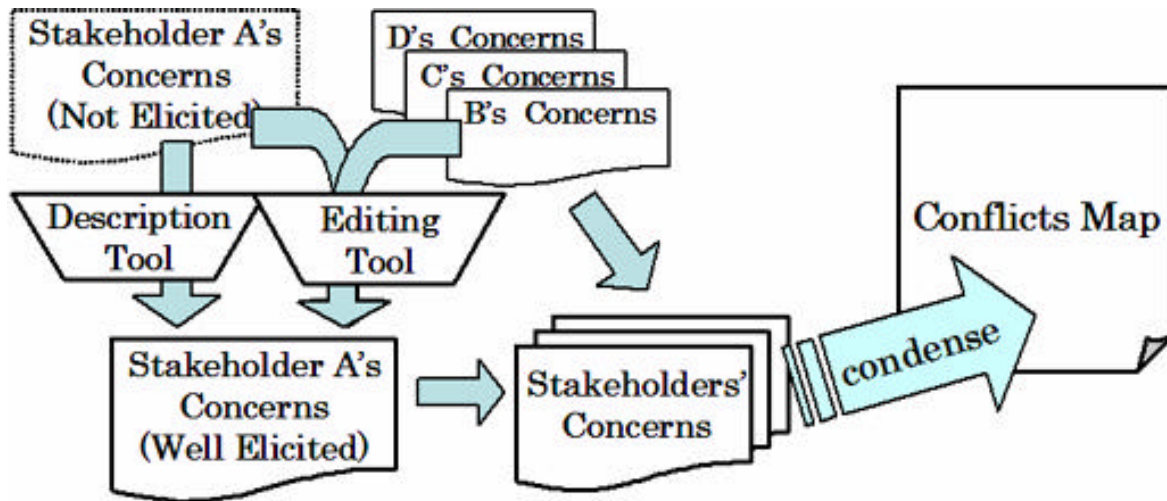


Fig. 1 Elicitation of Concerns and Conflicts

propose an *Issue-Position Cluster* to visualize a conflict situation. An overall scheme proposed here is shown in Fig.1.

2.2: Method for describing Concerns

In Fig.2 the *IBIS method* is shown. The IBIS method was developed by Horst Rittel in IBIS (Issue Based Information Systems) [2], in which logical and structured argumentations are held around some design topics among experts. In this method, only three types of statement are allowed: *Issue*, *Position*, and *Argument*, and each of them are connected by one of nine kinds of links that define the relation among three statement nodes, where an Issue represents problems or questions regarding some topic, a Position represents a statement or assertion to an Issue, and an Argument represents a support or an objection to a Position.

There are no stop rules in the IBIS method, and every statement node can be an edge. As a consequence, an argumentation held in IBIS comes to be a directed graph. This method has been used successfully in various areas such as architectural design, city planning, and planning at World Health Organization [3].

One study shows more detailed aspects of the IBIS method [3]. In that study, two significant results are obtained from observations where the IBIS method is implemented into a hypertext system with a graphical

user interface. One is that there is an explicit tendency in link usage. For example, Supports are much more posted than Object-to, and so are Specializes than Generalizes.

Another is that the IBIS usage itself falls into some patterns: one usage is for an isolated hypertext tool for structured thinking in which one particular person continuously posted his/her issues, positions, and arguments.

Based on those results mentioned above, we make minor revisions to the IBIS method and propose the *semi-IBIS method*, which is aimed at use in logical and structured description of one's Concerns (Fig. 3). In the semi-IBIS method, argument nodes are eliminated, because every argument posted to his/her own position essentially supports it; there are no meanings any longer. Accordingly, four types of links connected to argument nodes are also removed. Furthermore, the types of links seldom used such as Generalizes are also removed so as to simplify the method and ease its usage.

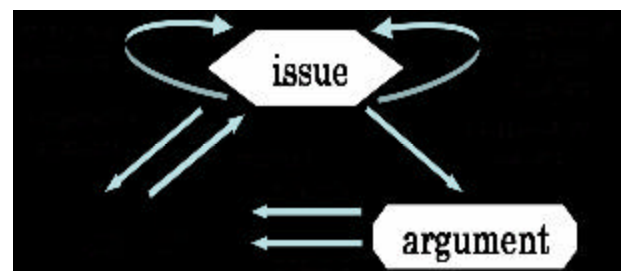


Fig. 2 IBIS method

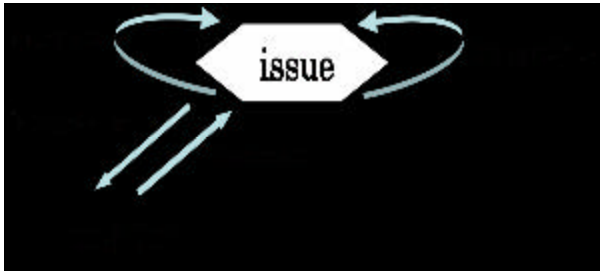


Fig. 3 Semi-IBIS method

2.3: Method for editing Concerns

Along with the description of the Concerns, we offer stakeholders two editing methods (Fig.4). One is *Quotation*. After referring others' Concerns, a stakeholder is allowed to "copy" whatever he/she wants to adopt and "paste" it as his/her own Concerns. This series of operation is defined as Quotation. By using Quotation, stakeholders are assumed that their Concerns become broad and better-elicited.

Another is *Equivalence Link*. This is a declaration of having an issue which is similar to or almost the same as a certain issue posted in other stakeholders' Concerns. Although the Equivalence Link does not change the structure of Concerns, it plays an important role in generating the Conflicts Map.

2.4: Method for generating Conflicts Map

After several times of description and editing, and if

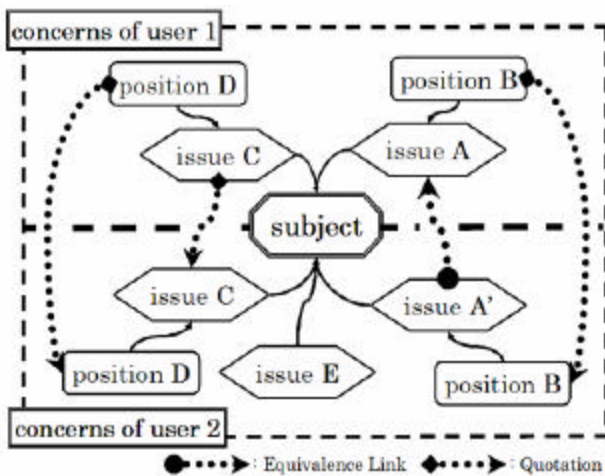


Fig.4 Quotation and Equivalence Link

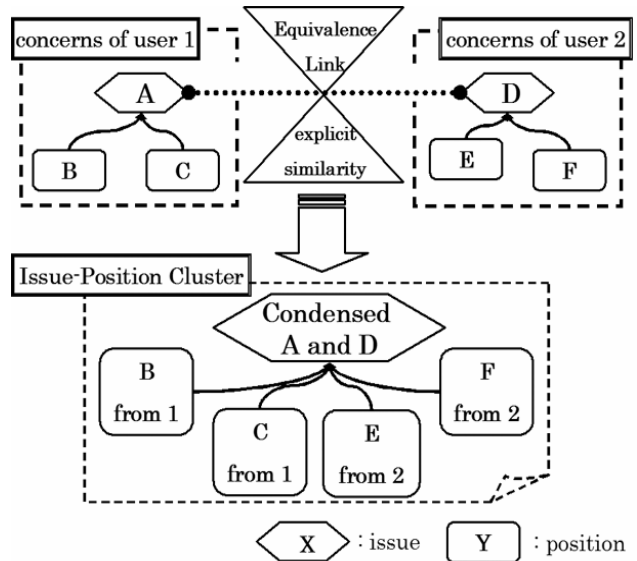


Fig.5 Generation of Issue-Position Cluster

every stakeholder acknowledges that his/her Concerns are well elicited, a *Conflicts Map* is to be generated.

Using Equivalence Links and explicit similarities as criteria, similar issues are gathered and integrated into a *Condensed Issue*. Around the Condensed Issue, stakeholders' positions are still linked. This aggregation which consists of Condensed Issue and its former positions is defined as an *Issue-Position Cluster* (Fig.5).

Each Cluster represents a conflict situation respecting a certain topic. Conflicts Map is formed as a collection of such clusters.

2.5: Implementation of the methods

We implemented the methods stated above as a web-based system. It has two windows; one is *My Concerns Window*, and another is *Others' Concerns Window*. The former is for viewing Concerns of a stakeholder who currently uses it, and the latter is for viewing those of other stakeholders. These Concerns shown on the windows are in tree view where a Subject node is a root node, several Issue nodes are linked to it and then other Issue and Position nodes are linked to them and so forth. Any linkage which does not correspond to the semi-IBIS method is prohibited.

This system offers to users a visual interface for description and editing Concerns. As to the description, it

provides user with functions for posting, deleting and modifying nodes representing Issue and Position in My Concerns Window. As to the editing, it provides users with a function for quoting others' Issue and Position nodes from Others' Concerns Window to My Concerns Window with a mouse. Also, to facilitate the quotation, it is equipped with a function for searching similar Issue nodes posted by others. Japanese Morphological Analysis System "ChaSen" [4] is used in this search function where contents of each node are segmented out morphologically and compared with each other by using the number of common nouns between them as criteria.

Users can use this system on a web browser with Macromedia Flash Player 7, which is freely available. All data including described Concerns is preserved in a server. Therefore, in use of this system, users just access the web site, enter their names and passwords, and then they are ready to describe their Concerns. Fig. 6 shows a screenshot of the system after log-in.

3: Case study

3.1: Abnormal red tide in the Ariake Sea

Between 2000 and 2001, an abnormal red tide has

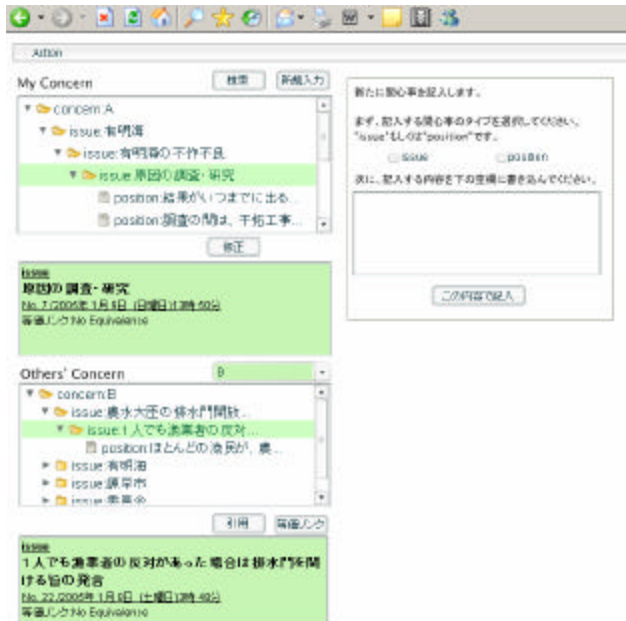


Fig.6 Web-based system

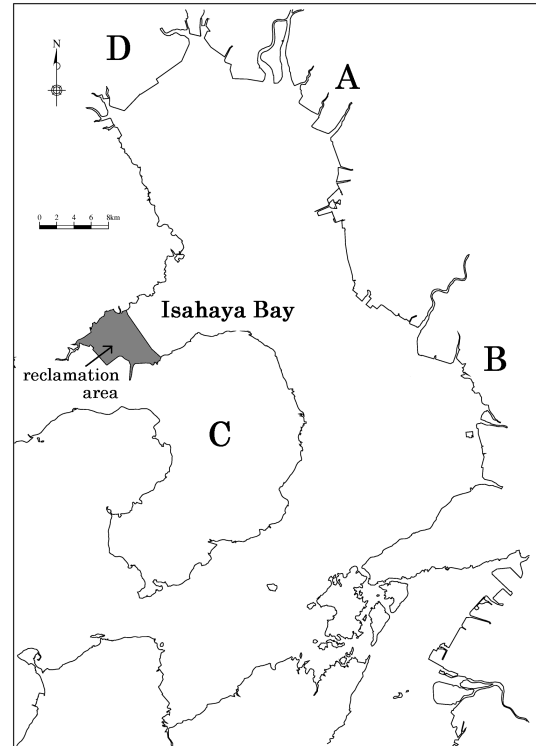


Fig.7 Ariake Sea and Isahaya Bay

broken out in the Ariake Sea, Kyushu, Japan, and the seaweed cultivation and other fishery products has been damaged around the same time. Seaweed farmers and fishermen blamed the Isahaya Bay reclamation project in Nagasaki Prefecture, because the project had been doubted to have an adverse effect on the environment of the Ariake Sea from its start in 1997 (Fig.7).

Against the background of the complaint of the fishermen who doubt the relevance between the reclamation project and the red tide, the Ministry of Agriculture, Forestry and Fisheries of Japan (MAFF) formed a study committee for the bad harvest of seaweed and others in the Ariake Sea in February 2001 [5]. The committee mainly consisted of local fishermen, local citizens, researchers, and government officials. Committee meetings were held 10 times from March 2001 to March 2003.

3.2: Analysis of the minutes

The methods we propose are aimed at an elicitation of stakeholders' Concerns and, as a consequence of it, the

My Concern

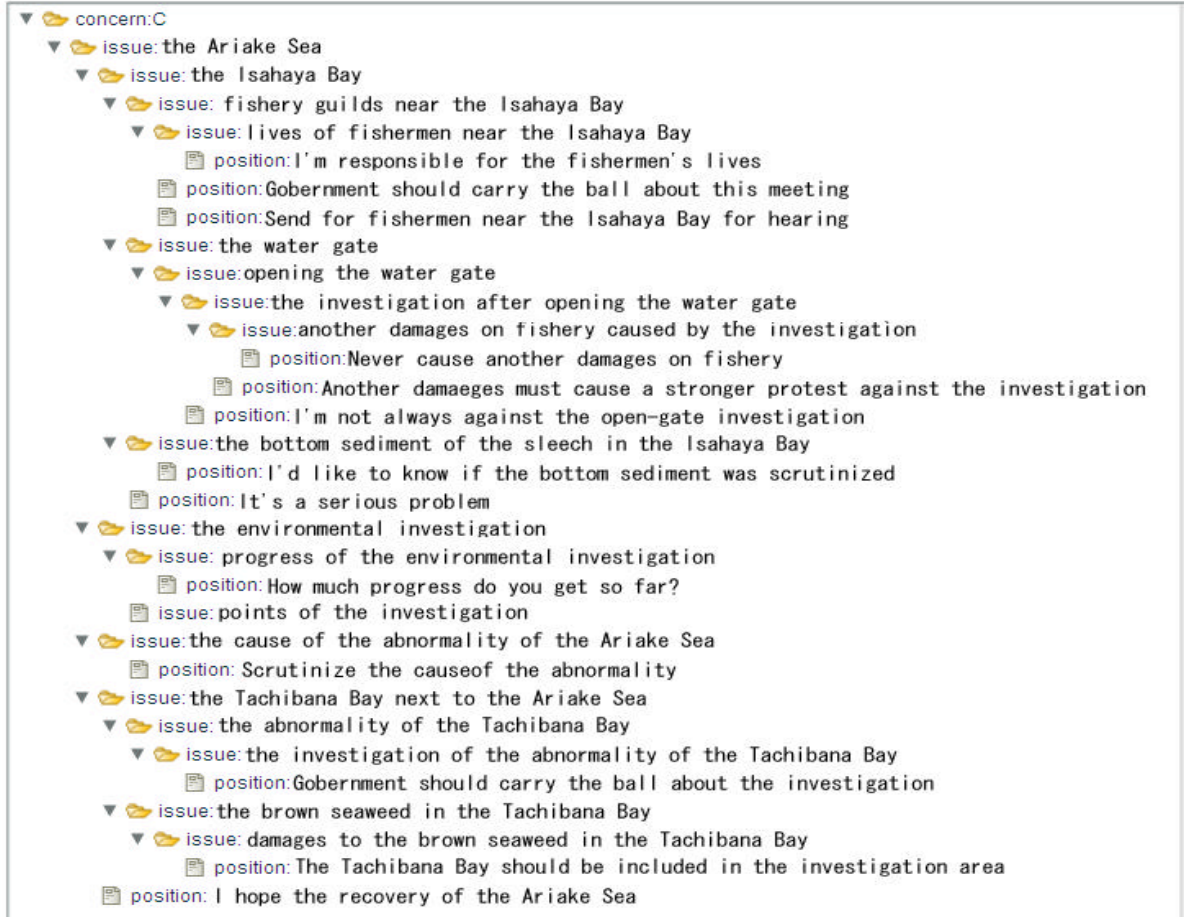


Fig.8 Elicited Concerns by semi-IBIS method

Conflicts, not through several times of discussions among them but through up-front introspections and mutual references among what they have in mind.

The objective of this case study is to test the feasibility of the elicitation strategy by the semi-IBIS method and an elicitation of Conflicts, that is, how well an initial conflict situation gets visualized.

We just chose the first three committee meetings as the samples of the analysis because stakeholders' Concerns are assumed to remain the same as those at the initial state due to fewer interactions and less elapsed time and hereby statements in the minutes are thought to well represent their "real" Concerns without any compromise.

Among the participants, we selected 4 fishermen each of whom represents a fishery guild in the respective prefectures; A, B, C and D (Fig.7). Since the guilds had

commonly shared the wealth provided by the Ariake Sea for a long time and also suffered considerable damage from the red tide, we previously assumed that the structures of their Concerns are similar to each other. Fig.8 shows the Concerns of the representative of C prefecture. Other three Concerns had similar structures regarding Issues.

After describing their Concerns based on the semi-IBIS method, we found out the assumption was almost correct. The dominant Issues among them are as follows:

- Opening / closing the water gate (the dike)
- Environmental investigation of the Ariake Sea

They all have in mind the necessity of the environmental investigation of the Ariake Sea to clear up the causes of

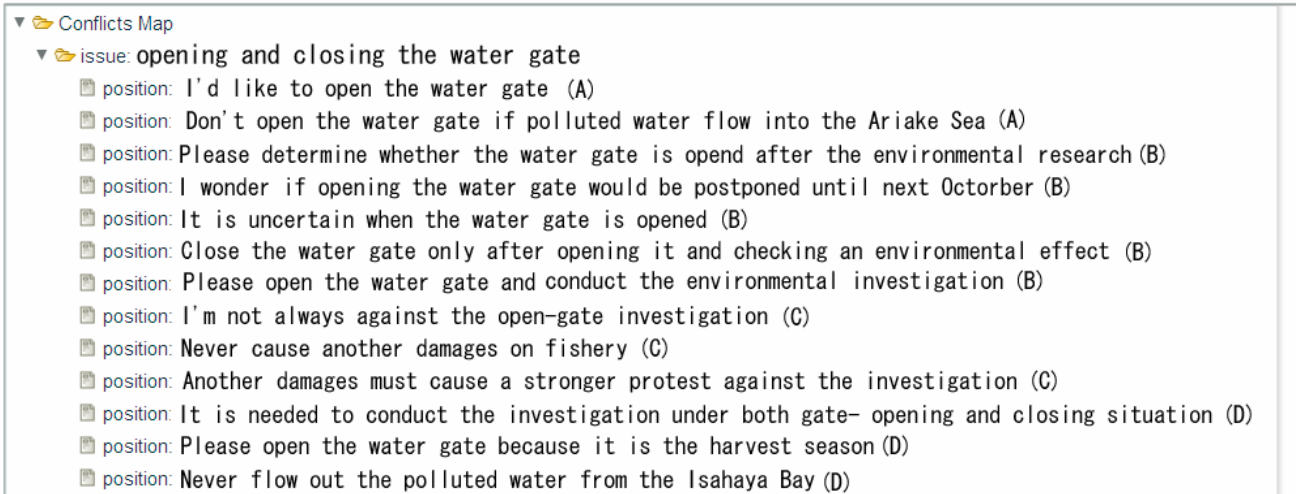


Fig.9 Issue-Position Cluster

the abnormality. Some differences, however, can be found regarding the attitudes towards opening and closing the water gate (the dike). While the rep B strongly claims his Position that the water gate should be opened as early as possible, the rep A and D have an additional Position that the situation where polluted water in the reclamation area of the Isahaya Bay would flow into the Ariake Sea should be carefully avoided. Though the rep C has a similar Position to that of the rep A and D, his Position is clearer. C prefecture has the Isahaya Bay, therefore if another damages on fishery due to opening the water gate happen, it is certain that fishermen near the Isahaya Bay will seriously suffer from it. Based on this concern, the rep C has a Position about a scrutiny of the bottom sediment of the Isahaya Bay. Fig.9 shows the Issue-Position Cluster (part of the Conflicts Map) where the Condensed Issue is *opening and closing the water gate* and each Position is printed with a name who posted it.

4: Conclusion

We proposed a method for describing and editing stakeholders' concerns logically and for generating a map representing conflicts among them. From the result of the case study, the semi-IBIS method works well in describing and structuralizing Concerns of stakeholders in a conflict situation. Also we developed a web-based

system for facilitating this process using visual aids.

Further researches have to be done among stakeholders who are currently in a conflict situation with actual operations of the web-based system. Especially, a comparison between elicited Concerns and "real" Concerns should be carefully studied. Several usability issues such as operability are also left uninvestigated.

References

- [1] Lawrence Susskind, Sarah McKernan, Jennifer Thomas-Larmer, *The Consensus Building Handbook: A Comprehensive Guide to Reaching Agreement*, 1999.
- [2] Rittel, H. and Kunz, W. "Issues as elements of information systems." Working Paper #131. Institut für Grundlagen der Planung I.A. University of Stuttgart, 1970.
- [3] Jeff Conklin and Michael L. Begeman: "gIBIS: A Hypertext Tool for Exploratory Policy Discussion", *Proceedings of CSCW88*, pp.140-152, 1988.
- [4] NAIST Computational Linguistics Lab., "Japanese Morphological analysis system Chasen", <http://chasen.naist.jp/hiki/ChaSen/> (in Japanese).
- [5] The Ministry of Agriculture, Forestry and Fisheries of Japan, "The study committee for the bad harvest of seaweed and others in the Ariake Sea", <http://www.jfa.maff.go.jp/ariakenori/> (in Japanese).

**Evaluation of Human Sense of Security for
Coexisting Robots Using Virtual Reality
2nd Report: Evaluation of Humanoid Robots Passing by Humans in Corridors**

Kenji Inoue, Seri Nonaka, Yoshihiro Ujiie, Tomohito Takubo, Tatsuo Arai

Department of Systems Innovation
Graduate School of Engineering Science
Osaka University
1-3 Machikaneyama, Toyonaka, Osaka 560-8531, Japan
Phone: +81-6-6850-6366
Fax: +81-6-6850-6366
Email: inoue@sys.es.osaka-u.ac.jp

TOPIC: coexisting robot, sense of security, virtual reality, humanoid robot

Evaluation of Human Sense of Security for Coexisting Robots Using Virtual Reality

2nd Report: Evaluation of Humanoid Robots Passing by Humans in Corridors

Abstract

When robots coexisting with humans are designed, it is important to evaluate the psychological influence of the shape, size and motion of the robots on the humans. For this purpose, an evaluation system of human sense of security for coexisting robots using virtual reality is discussed. Virtual robots are visually presented to a human subject using CAVE system; the subject and the robots coexist in the virtual world. The subject answers the questionnaire about his impression on the robots and their motions, and his sense of security is evaluated. Because of using virtual reality, the shape, size and motion of the robots can be easily changed and tested, and it is also possible to experiment in various situations and environments. In the present report, a humanoid robot passing by a human subject in a corridor is evaluated. The subject stands in the CAVE, and the virtual humanoid robot is walking from the front. The distance between the robot's walking path and the subject is changed. Three motion patterns of the robot head---facing forward, facing the subject and looking around---and four patterns of walking speed---fast, slow, speed-up and slowdown---are compared. The psychologically acceptable distance between the robot and the subject is measured, and the subject answers his impression on these motions. As the experimental results, the acceptable distance is little influenced by the head motion or walking speed. But different patterns of them give the subjects different impression whether the robot is aware of the subjects or is coming toward them.

1: Introduction

In the near future, it is expected that robots will be introduced into our living space and help us in our daily life. For this purpose, it is necessary to design the robots and their motions considering the interaction between the robots and humans: ``physical safety" and ``mental safety". Physical safety means that robots do not injure humans. Mental safety will be said that humans do not feel fear of or surprised at robots. In addition, it is important that humans do not feel unpleasant to or disgusted at robots. There are several ways to realize physical safety: robots avoid humans by measuring the distance between them with some kinds of sensors, or robots are covered with some kind of soft material so as not to injure humans. It is possible to evaluate physical safety quantitatively, and the evaluation could be used for designing robots and planning their motions. On the other hand, mental safety is not yet fully discussed. This is because which parameters of robots (shape, size, motion, etc.) may affect human mentality is not clarified, the method of measuring human emotion is not established, and how to evaluate human sense of security for coexisting robots quantitatively is not defined. There are some researches on the evaluation of human emotions against coexisting robots or the interaction between robots and humans[1-7]. These researches did not evaluate the shape, size and motion of robots comprehensively or different types of robots were not compared.

For these problems, we have already proposed an

evaluation system of human sense of security for coexisting robots using virtual reality[8]. Virtual robots are visually presented to a human subject through a head mounted display (HMD); the subject and the robots coexist in the virtual world. The subject answers the questionnaire about his impression on the robots and their motions, and his sense of security is evaluated. Because of using virtual reality, the shape, size and motion of the robots can be easily changed and tested, and it is also possible to experiment in various situations and environments. In this report, we use CAVE system instead of the HMD, because it can give high realistic sensation to humans. Humanoid robots will be one of the candidates for coexisting robots. Thus a humanoid robot passing by a human subject in a corridor is evaluated using this system.

2: Evaluation of Human Emotions for Coexisting Robots Using Virtual Reality

For designing robots with mental safety, it is necessary to investigate and compare human emotions for various kinds of robots and many patterns of their motion. Different motions of the same robot may give different impressions on humans, and different types of robots doing the same task may give different influences on human emotions. Hence it is necessary to evaluate them comprehensively. Comparing different types of robots is also important. For example, humanoid robots seem to be more suitable as coexisting robots than other types of robots; it has not yet been ascertained. It is, however, quite difficult to evaluate many types of robots and their various motions using real robots, because making and controlling real robots requires much cost and time.

Future robots will be used not only indoors but also outdoors. Human emotions for the robots may depend on the situations. Hence evaluation tests in various situations

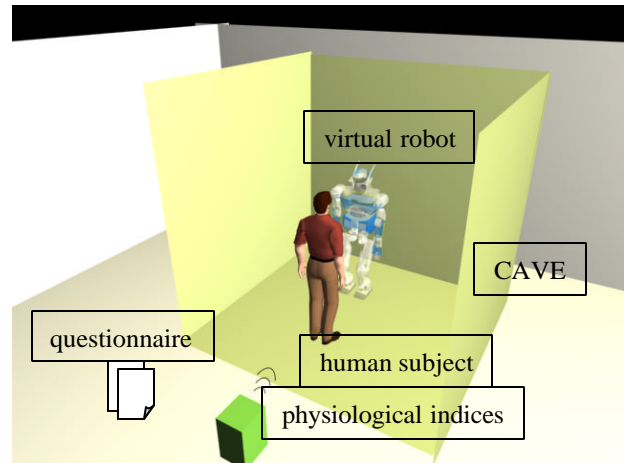


Figure 1: Evaluation system of human sense of security for robots using virtual reality

or environments are also required. But preparing various real environments for the tests is difficult, and some situations (e.g. on-street) are dangerous.

For these reasons, we propose to evaluate human emotions for coexisting robots using virtual reality. As shown in **Figure 1**, virtual robots are visually presented to a human subject using CAVE system; the subject and the robots coexist in the virtual world. The subject answers the questionnaire about his impression on the robots and their motions, and his sense of security is evaluated. We are also planning to measure some kinds of physiological indices of the subject for quantitative evaluation; that will be a future work. CAVE is one of immersive visualization systems. It consists of four screens and a projector for each. The screens are placed on the front, left, right, and on the ceiling or the floor. A subject wears stereoscopic glasses and stands inside the CAVE; it allows a stereoscopic view. As a result, the subject feels like existing inside the virtual world. CAVE can give higher realistic sensation to humans than the HMD which we used in the previous study[8].

Odashima et al. developed a system where a human subject and a virtual robot coexist in the virtual world

using CAVE[9]. The robot is a humanoid robot. Its motion is generated by capturing and simulating the motion of a human operator in another room and is presented to the subject in the CAVE. Generating humanoid robot motion from human motion is easy. But this method is only applicable to humanoid robots, and the motion is limited to what humans can do. Furthermore, it is impossible to adjust the motion trajectory precisely.

Because we do not have to make real robots, the proposed system allows us to test and compare various kinds of robots and their different motions. It is possible to experiment in various situations and environments, including the cases which are difficult in the real world. The trajectories of the robots can be programmed and easily modified. We do not have to measure the locations of the robots. Because virtual robots do not physically conflict with subjects, they can experiment in safe. On the other hand, this system cannot deal with the situations where the subject has physical contact with the robot: for example, a nursing-care robot. The movable area of the subject is limited inside the CAVE. Whether human emotions for virtual robots indicate a similar tendency to those for real robots is an important issue.

3: Evaluation of Humanoid Robots Passing by Humans in Corridors

We can predict other person's motion quite naturally. In the same way, humanoid robots will be able to let us predict their motions naturally, if they behave like humans. Furthermore, human-like behaviors of humanoid robots will make us feel comfortable. This will be one of the merits of humanoid robots. In other words, this is an effective usage of the redundant degrees of freedom of humanoid robots.

In this report, a humanoid robot passing by a human

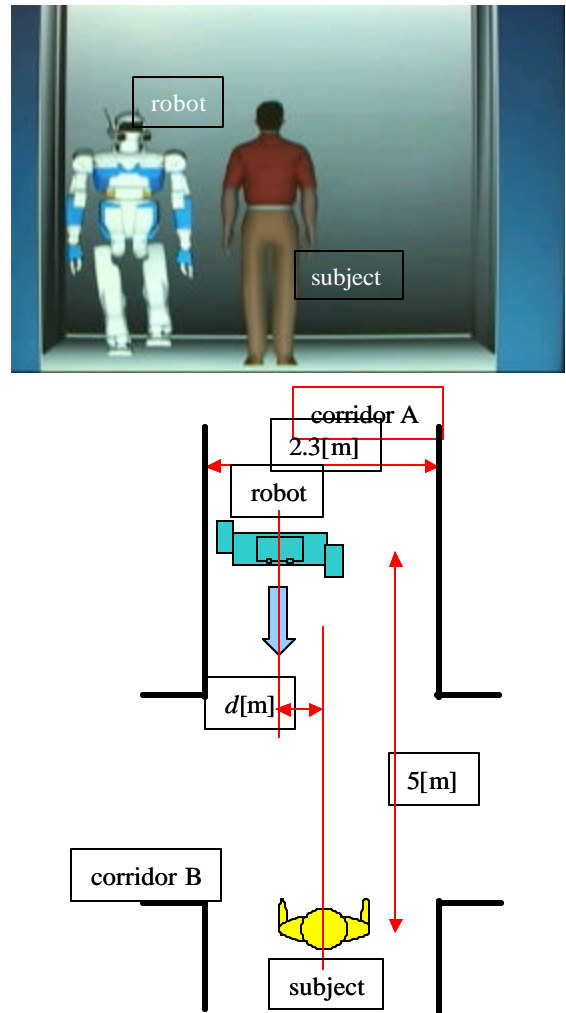


Figure 2: Experiment of humanoid robot passing by human subject in corridor

subject in a corridor is evaluated; this situation will often happen in the future human-robot coexisting society. If the subject can know that the robot is aware of him, he will feel secure for the robot. As the sign of this awareness, we consider the head motion and walking speed, on the analogy of human motions.

3.1: Experimental Method

The used model of humanoid robot is “HRP2”, which was developed in “Humanoid Robotics Project”[10]. It is

1.54[m] in height and 0.62[m] in width. As shown in **Figure 2**, a human subject stands inside the CAVE and sees the animation of the virtual humanoid robot walking from the front. The sound of the robot's walking, which is the recording of a real HRP2, is also presented. Two corridors A and B intersect, and the robot walks along the corridor A. The width of the corridors is 2.3[m]. The subject stands at the entrance of the intersection and the center of the corridor A, facing the robot. The initial distance between the robot and the subject is 5[m]. The subject pushes a button when he wants to avoid the robot, and the location of the robot at this moment is recorded. When the subject pushes the button or the robot passes by the subject, one trial is finished. After each trial, the subject answers the questionnaire.

12 men in the age between 22 and 30, who have little seen real robots, are experimented.

3.2: Motion Patterns

First, the distance between the robot's walking path and the subject (d [m] in Figure 2) is changed: 0.0[m], 0.2[m] and 0.5[m]. Second, as the sign of awareness, the head motion is changed:

- (H1) facing forward,
- (H2) facing the subject, and
- (H3) looking around (repeatedly shaking the head from side to side).

These patterns are illustrated in **Figure 3**. The walking speed is also changed as the sign of the awareness:

- (S1) constant 0.15[m/s],
- (S2) constant 0.225[m/s],
- (S3) speed-up from 0.15[m/s] to 0.225[m/s], and
- (S4) slowdown from 0.225[m/s] to 0.15[m/s].

In the patterns (S3) and (S4), the speed changes in the half way to the subject.

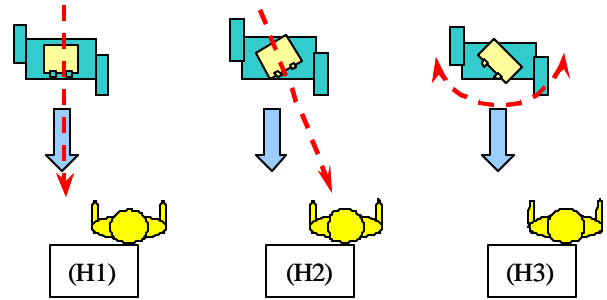


Figure 3: Head motion patterns

Table 1: Combined motion patterns of robot

pattern	distance[m]	head motion	walking speed
1	0.0	H1	S1
2	0.0	H3	S1
3	0.2	H1	S1
4	0.2	H2	S1
5	0.2	H3	S1
6	0.5	H1	S1
7	0.5	H2	S1
8	0.5	H3	S1
9	0.0	H1	S2
10	0.0	H1	S3
11	0.0	H1	S4
12	0.2	H1	S2
13	0.2	H1	S3
14	0.2	H1	S4
15	0.5	H1	S2
16	0.5	H1	S3
17	0.5	H1	S4

Combining these patterns, we prepare 17 motion patterns summarized in **Table 1**. In order to cancel out the order factor, these are presented to human subjects in randomized order. It takes about 30[min.] for one subject.

3.3: Evaluation

The subject pushes a button when he wants to avoid the robot; the location of the robot at this moment is recorded. After each trial, he answers the following questionnaires about the reason why he pushes the button in 6 levels: from 1 ("never") to 6 ("very much").

- 1: The subject thinks that the robot will not be able to

avoid him if it does not begin avoidance now.

- 2: The robot seems to be unaware of the subject.
- 3: The robot shows little intention of avoiding the subject.
- 4: The robot seems to be about to fall down.
- 5: The robot seems to be about to stagger.
- 6: The robot seems to be coming toward the subject.
- 7: The subject cannot guess where the robot is going.
- 8: The subject finds the robot intimidating.
- 9: The robot seems to be about to run suddenly.
- 10: The subject feels fear of the robot's appearance.

These questionnaires are written in Japanese.

3.4: Results and Discussions

Figure 4(a) shows the average score of the major questionnaire answers when the robot head is facing forward (H1) and the walking speed is different; **Figure 4(b)** shows the average score when the walking speed is constant 0.15[m/s] (S1) and the head motion is different. **Figure 5** illustrates the locations of the robot when three subjects pushed the button.

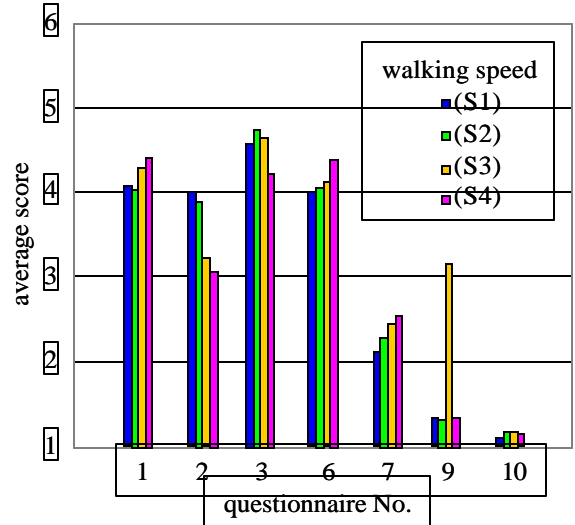
From these results, we can draw the following conclusions:

On the effect of the walking speed (Figure 4(a)):

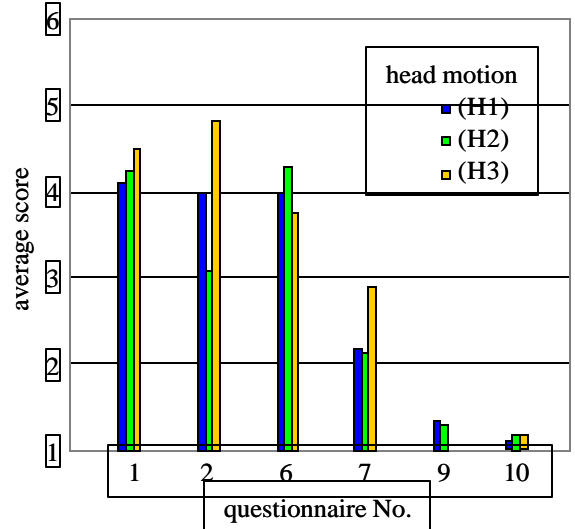
- (a) The average scores of the 2nd questionnaire answer when the walking speed is constant are higher than those when the speed changes. It means that changing walking speed could be a sign to inform humans that the robot is aware of them.

On the effect of the head motion (Figure 4(b)):

- (b) The score of the 2nd answer when the robot head is facing the subject is the lowest, and that when the robot is looking around is the highest. The score of the 6th answer shows countertendency. It means that directing the head to humans is effective to inform them that the robot is aware of them; but they also



(a) Robot head is facing forward (H1)



(b) Walking speed is constant 0.15[m/s] (S1)

Figure 4: Average score of questionnaire answers

think that the robot is coming toward them.

- (c) The score of the 7th answer when the robot is looking around is higher than those the other head motions. Hence looking around confuses humans even if the robot is walking straight and constantly.

On the psychologically acceptable distance (Figure 5):

- (d) The psychologically acceptable distance between the robot and humans depends on individuals more strongly, rather than the motion patterns of the robot.

4: Conclusion

An evaluation system of human sense of security for coexisting robots using virtual reality is discussed. Using this system, a humanoid robot passing by a human subject in a corridor is evaluated. As the results, different patterns of the head motion and walking speed give the subjects different impression whether the robot is aware of the subjects or is coming toward them. These will be an effect of the human-like motion of humanoid robots.

In the future works, we will measure some physiological indices for quantitative evaluation of human sense of security. The comparison between human emotions for virtual robots and real robots is now under experiment. Finally, we will experiment with many types of robots and their motions and compare them. That will give a hint to design coexisting robots.

Acknowledgment

This work was supported by MEXT under Grant-in-Aid for Creative Scientific Research (Project No. 13GS0018).

References

- [1] S. Suzuki, et al., "A Study on Emotional Influence of Shapes of Care-Worker Support Robot", Proc. ROBOMECH2003, 1P1-2F-C7, 2003 (*in Japanese*).
- [2] N. Takamatsu, et al., "Measurement of Mental Load Received by a Robot Motion", Proc. ROBOMECH 97, pp.969-970, 1997 (*in Japanese*).
- [3] H. Mizoguchi, et al., "Generating Sense of Security by Behaviour of Human Symbiosis Robot", Proc. ROBOMECH 97, pp.561-562, 1997 (*in Japanese*).
- [4] T. Mitsui, et al., "Psychophysiological Effects by Interaction with Mental Commit Robot", Proc. IROS2001, pp.1189-1194, 2001.
- [5] P. Rani, et al., "Affect-Sensitive Human-Robot Cooperation -Theory and Experiments", Proc. 2003 IEEE ICRA, pp.2382-2387, 2003.
- [6] S. Kajikawa, et al., "Motion Planning for Hand-Over between Human and Robot", Proc. IROS1995, pp.193-199, 1995.
- [7] T. Nakata, et al., "Synthesis of Robot-to Human Expressive Behavior for Human-Robot Symbiosis", Proc. IROS1996, pp.1608-1613, 1996.
- [8] S. Nonaka, et al., "Evaluation of Human Sense of Security for Coexisting Robots using Virtual Reality (1st report: Evaluation of Pick and Place Motion of Humanoid Robots)", Proc. 2004 IEEE ICRA, pp.2770-2775, 2004.
- [9] T. Odashima, et al., "A PC-based 3D Dynamic Simulation Environment for Developing Human Interactive Robot Systems", Proc. SI2002, pp.59-60, 2002 (*in Japanese*).
- [10] K. Kaneko, et al., "Humanoid Robot HRP-2", Proc. 2004 IEEE ICRA, pp.1083-1090, 2004.

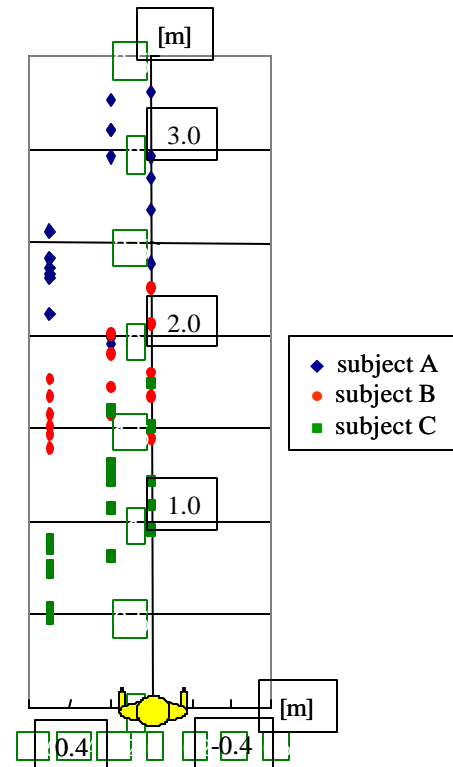


Figure 5: Psychologically acceptable distance between robot and subject

Human Detection System using Robust Silhouette Extraction from Surveillance Images

Jun Iio,

3-6, Otemachi 2-chome, Chiyoda-ku, Tokyo, 100-8141 Japan

Tel: +81-3-3277-0750 / Fax: +81-3-3277-3473

iiojun@mri.co.jp

Information Technology Research Department,

Mitsubishi Research Institute, Inc.

Kazuo Hiyane,

3-6, Otemachi 2-chome, Chiyoda-ku, Tokyo, 100-8141 Japan

Tel: +81-3-3277-0750 / Fax: +81-3-3277-3473

hiya@mri.co.jp

Information Technology Research Department,

Mitsubishi Research Institute, Inc.

Topic: Measurement, monitoring, and reliable control

Human Detection System using Robust Silhouette Extraction from Surveillance Images

Abstract:

In this paper, we report an implementation of human image detecting system. The system is able to detect the human objects in image sequences from surveillance camera, and store the images into mass storage devices.

The system is based in our robust human silhouette extraction method, which uses disparity information from the stereoscopic camera to distinguish between objects from the background image.

In general, the environmental condition such as lighting condition and camera location tend to affect the recognition rate in image processing within optical wavelength. Even if an algorithm shows a good result in the laboratory, it can not be usable in the real field.

Because we put weight on robustness and tractability of the system, we adopted the stereo based method as the human detection algorithm.

Detecting human image and tracking method is following . 1. The candidate of human region is separated by statistical background subtraction. 2. The head image is tracked by dynamic tracking method. 3. The whole human silhouette is extracted if the tracking process is continued for a certain period.

We conducted an experiment of our prototype system for 24 hours. The system recorded human image with 92.6% accuracy rate.

Strong points of this work are followings. 1. It is easy to set up the proposed system because it does not require any calibration. 2. This system shows steady performance of human detection under anything but ideal circumstances.

1. Introduction

There are many type of human image tracking such as surveillance camera, intruder detection system, human behavior monitoring, and so on. For those applications, especially considering head point tracking as human information measurement, we are developing a novel information input device [1].

Various image capture devices are proposed to work efficiently in many applications described above. Though it is the best way to choose the most suitable one among them for the application, it is the most common case that image capturing is implemented by optical wavelength cameras. Recently the most of cellular phones have the small camera. And because of volume efficiency, the cost of camera devices rapidly dropped down. It helps the camera system to be widely used.

We have to consider about some conditions if we use an off-the-shelf camera for the specific application. Efficiency of the system, such as recognition rate, highly depends on its lighting condition and any condition of camera position. Therefore it is commonly believed that even though an algorithm shows a good result in the laboratory, when it is implemented in some product, it might not work well if the algorithm is implemented to the product without any workaround.

In addition, an environmental condition such as background information has significant impact on the result of recognition system. So we developed a method to separate an object image from background image. Our method works stably in various environments. And we tried to apply it to human detection system.

2. Related work

In our proposed system, disparity images from a stereoscopic camera are used as basic input images. Our system is very robust for the changes of environment condition because of the analysis based on the disparity image. Although similar implementations of people counting system are proposed in [2] and [3], they are using some models. In [2], the system tries to fit human models, under the assumption that the disparity image is taken by cameras looking down to the floor. On the other hand, our system do not have any human models, therefore our system has higher flexibility on setting camera and it can be usable in various situation.

In addition, face recognition is adopted to detect human images in [3]. Extracting face region from captured image on the basis of skin color has some kind of weakness, that is, it is very sensitive to environmental change. And besides, it cannot work correctly when someone wearing skin-color-like dresses comes into its viewing range.

An adaptive background subtraction proposed in [4] is similar to our approach. In [4], they report robust background subtraction by statistical processing to the sequences of disparity images. Our algorithm is the refinement of [4]. In [4], conditions of each pixel are estimated using binomial distribution constructed from the sequence of previous pixel values. Parameters of binomial distribution are updated every time so that the system is acceptable to the change of background information. Our algorithm is improved version with regard to the noise eliminating process and the background updating criteria. In these processes we use not only temporal information but spatial one to make background separation more stable.

3. Overview of algorithm

The process of eliminating background information from disparity image and extracting objects from separated region is shown in figure 1.

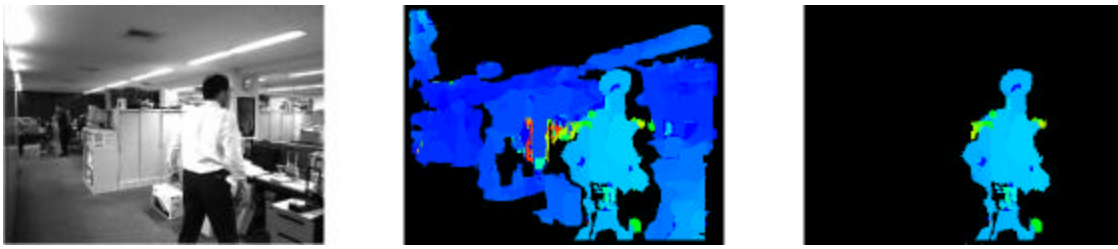


Figure 1 (a) input image, (b) disparity image, (c) extracted region

In our system, firstly, input image which include a human silhouette (a) is modified to disparity image (b), in real time. And then the human silhouette is extracted by the statistical background subtraction (c).

Conventional background subtraction has its background image as known information beforehand. And to extract some objects in an input image, it takes the difference of the input image and the background image. This background subtraction is very simple and powerful under some situation. However, it has following problems;

- It needs to prepare a reliable background image. Camera has to be set strictly. If the camera position moves even a little, we have to take another background image for the new camera view.
- It cannot follow the environmental change. The background image readily changes according to surrounding illumination condition. Especially if the camera has auto gain control function, the gain level of whole image is immediately changes when anything enters into the view of camera. It means the background image also changes drastically and simple background subtraction cannot work correctly.

The implementation for the real environ ment requires some robustness against these conditions.

3.1. Adaptive background subtraction

To make stable recognition system, we used an adaptive learned background image and separate it by means of statistical information. It is also important point that the background separation is based on disparity images from the stereoscopic camera. It enables us to take advantage of the independence from the lighting condition.

Each pixel consisting of the disparity image has a buffer memory, which keeps values of some dozens of previous frames. The longer the length of this buffer, the more stable the system would be. But throughput of whole system drops down because processing time is proportional to the rate of the frame length. In our prototype system, we prepared 64 byte long ring buffers for each pixel. Thus we can use information from previous 64 frames. Since this system can handle 10 to 12 frames per second, information during the last five seconds can be recorded into the buffer.

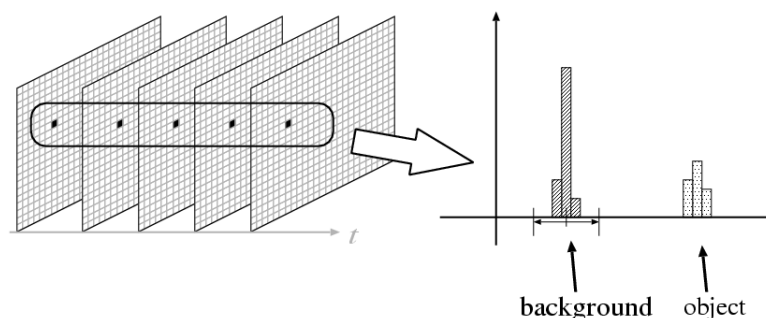


Figure 2 Background separation

Next we describe background separation process based on the statistical information.

The system enters background information learning phase just after it is activated. In this phase, disparity values are stored into the buffers for each pixel. Even if the sequence of disparity images contains some object which is not a part of background, it would not be problem because update process can get rid of it from background information.

1. After the learning phase, the system enters running phase. In this phase, the system creates histograms on values in each buffer. These histograms play a role for judging whether a pixel value is a part of background or not. A pixel value of input disparity image is compared with this histogram. Because the distance between camera and background is invariant, the histogram has a peak if the pixel is a part of background image. In consideration of measurement error, we assumed some margins around the peak value, and if the input pixel value falls in this range, it is decided as a part of background image.
2. Additionally, the disparity image created by correlation stereo matching contains much image noise. So we employ labeling process to eliminate such noise. In this stage, conjunctive region which has pixels above a certain numbers is decided as an object image separated from background image.
3. Buffers keep previous information is updated every time, unless any objects are detected. This is a special case to avoid embedding the image of any object into the background image.
4. The system has resetting process by way of exception. This is used when the whole environmental condition is completely changed, such as at the case of turning off all the lights, putting on the lights, or the case of persistent changes are added into the background information. This process prevents from making update dead-locking.

3.2. Tracking human silhouette

The background separating method described before is not using the fact that is whether the object is a candidate of human or not. To make it suitable to human tracking application, this system applies a head position tracking algorithm proposed in [1].

Overview of the head tracking algorithm is as follows;

Suppose that the region which shows the head position is already determined at a given time. How to decide initial region is described later on.

The center of head position $\bar{X}_t \in \mathcal{R}^2$ at time t is updated to \bar{X}_{t+1} by following equation.

$$\bar{X}_{t+1} = \frac{\sum_{p \in D(\bar{X}_t)} w(p)p}{\sum_{p \in D(\bar{X}_t)} w(p)} \quad (1)$$

We note the region I_m as extracted human silhouette at the time t . $D(\bar{X}_t)$ in the equation (1) means product set of the region around \bar{X}_t and I_m . And variable p runs over the region $D(\bar{X}_t)$. $w(p)$ is a weight function used at calculating the weighted average point.

In this calculation, it is important how the weight function $w(p)$ should be chosen. In our algorithm, to emphasize importance of pixels placed at higher area of captured image, we chose $w(p)$ as follows;

$$w(p) = w(x, y) = H - y \quad (2)$$

In equation (2), H means the height of input image.

According to the equations (1) and (2), the region that are tracking a head position (we call this as “the tracking region”) sequentially moves upward. Since the human has the head at the top of its body, the movement of the tracking region reaches equilibrium at some point and the region will stop at the highest position of extracted human silhouette. This algorithm enables stable head position tracking because it is independent of any textual information of input image.

We are also able to measure average values of disparity at the center point of the tracking region. So the system can report not only person's location but tells us the movement of person passing in front of the camera.

3.3. Initial point of the tracking region

In [1], since there was an assumption that a user was sitting in front of the camera, it was no matter even though the initial point of the tracking region was set at the center of the image. However this system requires more general approach.

At the stable situation, that is, any object is not entering the area viewed by surveillance camera, the image after adaptive background subtraction process would not have any objects. Tracking process can be started as soon as someone enters the monitoring area. Although it is ideal to detect multiple regions at the same time, we propose a single person tracking system in order to validate the stability of our algorithm in this paper.

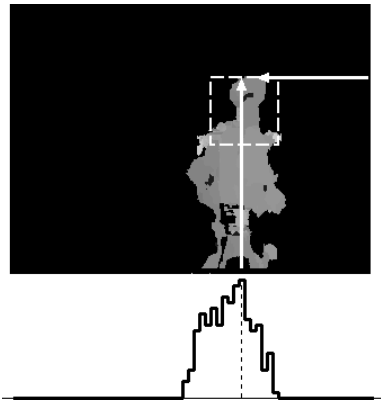


Figure 3 Initial point of tracking region

Figure 3 shows how to determine the initial point of the tracking region. With regard to the extracted human silhouette, a histogram is created by projection along with X axis. Mode value of this histogram is selected as x -coordinate of the initial point. Y -value of the initial point is the least value of y -coordinate in the region of extracted region. The initial position of the tracking region is placed under the point calculated by the criteria described above.

4. Experiment

We implement a passerby recording system as a prototype system to examine the efficiency of this algorithm.

4.1. Passerby recording system

This prototype system extracts a human silhouette and tracks it by the algorithm described in the previous section, and records the image into mass storage with its time stamp when system can decide that the tracking is stable. Practically if the system can follow a candidate of human object during the sequential 15 frames, it records the image at that time. When the system stores the image into the mass storage, it assumes the whole of extracted region as the human silhouette. Then a rectangle surrounding the region is drawn in the captured image as the result of passerby detection.

We had set up the system in our office as shown in figure 4 and the experiment was conducted for 24 hours.

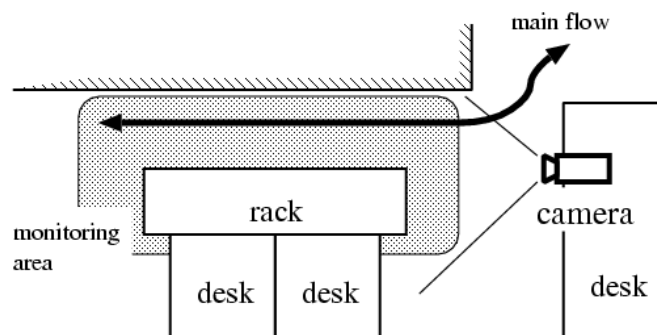


Figure 4 Experimental system installation in the office

Since the location where the camera is placed corresponds to passageway in our office, many persons pass along with the direction shown by the arrow in the figure 4. However, because there are workplaces at the left side of the image, there is possibility that someone stays at the monitoring area. And from the condition of making disparity image by correlation stereo, the area of where we can measure the distance correctly is restricted in a certain range. The shaded region in figure 4 shows the monitoring area.

4.2. Result of the experiment

The experiment was conducted from 15:30 to the same time of the next day. It should be strongly commented

that the environmental condition was extraordinarily changed because there are no lights at the midnight.
The system recorded 472 images through the whole experiment. Figure 5 shows a part of recorded images.



Figure 5 Examples of captured images

Recognition rate and error rate is shown in table 1.

Table 1 Experimental result

	Cases	Rate (%)
Correctly detected	437	92.6
Detected region was improper	11	2.3
Misdetected (the case that multiple persons were in the image)	13	2.8
Misdetected (the case that no person was in the image)	11	2.3
Total	472	100.0

We note that the system counts one person as multiple persons redundantly if one person is staying in front of the camera for a long time; for instance, the image sequence of 000037 to 000039 in the figure 5.

As shown in many images in figure 5, accuracy of recognition of human silhouette is high. The rate of correctly recording human silhouette was 92.6%. Although we could find the case that the part of human silhouette could be detected or detected region contained the area other than human body, the rate of that was 2.3%. And almost of all the case that the error occurred, the target person was much closed to the camera and input image did not contain whole of the silhouette of the target. We did not consider such a special case. It should be eliminated from the candidate of recording images.

And because the system has only one tracking region, it could not track multiple objects if more than two persons enter the monitoring area. Regarding this error, we found 13 cases had occurred at the experimental result. Typical example is shown in figure 6.

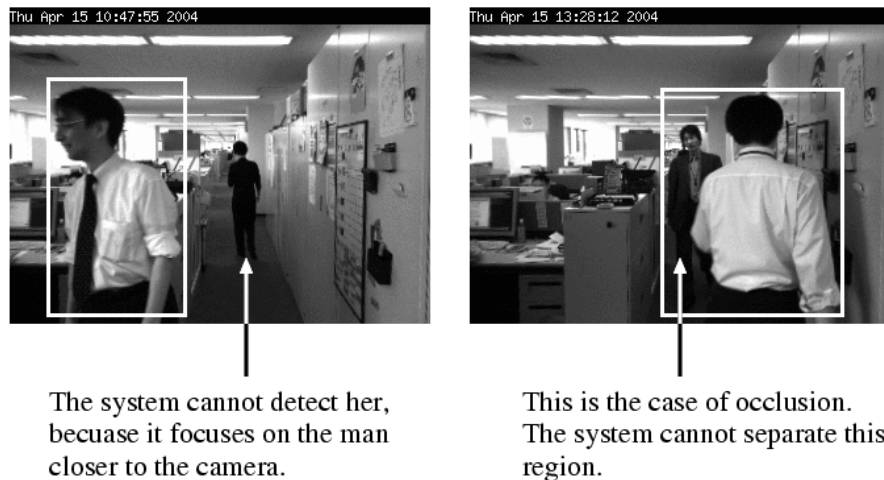


Figure 6 Typical examples of failure

We can deal with the left image in figure 6 by preparing the multiple tracking regions. On the other hand, some prediction process regarding the velocity and distance of moving objects has to be introduced, when the occlusion occurred as if the image shown in the right side of figure 6.

We found 11 error cases that there was nobody in the captured image. Most of the cases was caused by the false in learning process from the fact that there were somebody was staying in front of the camera. In addition, similar error occurred when the environmental condition was drastically changed. Even if this algorithm is based on disparity image, it is difficult to follow such a fast and furious change of environmental condition. The reason is because the enormous change affects the calculation of creating disparity image and the base of this algorithm is the stability of the disparity. However, it would be easy to distinguish this situation as a special case and reset the system to work correctly, by means of detecting the change of brightness of whole image.



Figure 7 human recognition under the different condition

Figure 7 shows two examples under the significantly different lighting condition. The left one was taken under the daylights, and the right one was taken at the early morning. The person captured in the right image was the first one who came into the office, therefore the light of the office was still off at that time.

These two images illustrate the robustness of this system. Since background separation based on disparity image and statistical background subtraction whose background information is updated every time, the combination of two approach get the system very stable. Figure 7 shows this system recognizes the human image under the various conditions without any changes of its parameters.

On the subject of the throughput, we could get about 10 to 12 frames per second on this prototype system. This prototype was implemented on GNU/Linux OS running on the IBM/PC compatible, with Pentium IV 2.6 GHz CPU and 1GB memories. We note that all process from making disparity image to background separation, head point tracking, and human silhouette estimation are executed without any hardware acceleration.

5. The merit of this algorithm, and future work

The prototype system, which was implemented just for this experiment, does not require any strict distance information. Therefore we can omit a calibration process while the camera is placed at some appropriate location. If the user of this system would like to take up the more correct information on the distance between the camera and the object, or if anyone would like to improve capability of this system to cope with multiple persons tracking, it might be required that the strict camera calibration is made and build the relationship between the camera coordinates and the world coordinates. Although that strictness is meaningful for some cases, the convenience from the fact that the user need not care about the complicated camera calibration could take much advantage for its easy operation, just like the case explained in this experiment.

The sequence of captured image is just stored into the hard disk drive as a simple image file but also system could have the three-dimensional information of the human position tracking, internally. Therefore it is possible to calculate the direction of passing by and the speed of that. Furthermore, it is also able to analyze the time of the object staying in the monitoring area, if anyone has been staying in the area for a while.

There remains some room for improvement in the prototype system implemented for this experiment. It has only one tracking region to make it clear on our problem. As a result of that, when more than two persons enter into the monitoring area, the system is unable to make correct tracking, at best it can track only one person. In order to produce this function practically, we have two problems. One is to develop the way of determining the initial point of multiple tracking regions, and another is just adding a management mechanism of tracking regions into the current tracking system. However the latter is not so simple. It must be considered to manage two tracking regions under the case when two persons make crossing or some kind of occlusion.

Basically, two regions can be tracked simultaneously by using not only horizontal and vertical but also depth information. This three-dimensional tracking process seems possible to be implemented because our tracking algorithm is based on disparity image. In addition, if the system can record the speed and direction of tracking target, and if it has the prediction of the movement of persons, it would be able to support the tracking under the condition that the multiple moving persons are crossing at any point.

There are similar human detection and recording systems which are also using an infrared camera or ultrasonic sensors. In comparison with this system, it could be easier to configure of the whole system. Because detecting the position of persons and recording its image are both produced via one camera device in this system.

6. Conclusion

We proposed disparity image based human tracking system and its experimental result. It showed a good result for surveillance application in the real environment. In the human tracking system embedded with proposed

algorithm, basically it does not require the camera calibration nor the configuration of any parameters for environmental condition. It enables us to extract human regions from easily located camera. Furthermore, since we can get spatial information of human location as additional information in the real time, it is able to apply some kind of human behavior observation. It is usable for a survey in marketing field such as flow research, circulation planning, and so on.

Development of some new methods for multiple human tracking is still remains for our future work. We have to make the system more stable using the velocity of the tracking region. And we would like to establish more general and steady human tracking system with managing more than two tracking regions simultaneously.

References

[1] J. Iio et al., "Detection of the User Position using Disparity Map and its Application to a 3D Interface," *Information Technology Letters*, vol.2, 2003, pp.271-272 (in Japanese).

[2] K. Hayashi et al., "Counting Pedestrians using Projected Histogram of Stereo Depth," *IEICE Technical Report on Pattern Recognition and Media Understanding (PRMU2002 146-168)*, vol. 102, no. 532, Dec. 2002, pp.146-168 (in Japanese).

[3] Y. Ishii et al., "A Marketing Information System using Stereovision and Frontal Face Detection," *Proc. of 8th Symp. Sensing via Image Information (SII2002)*, 2002, pp.197-202 (in Japanese).

[4] C. Eveland et al., "Background Modeling for Segmentation of Video-Rate Stereo Sequences," *Proc. IEEE Conf. Computer Vision and Pattern Recognition (CVPR98)*, 1998, pp.266-272.

Concepts, formalisms, methods, and tools

**Development of a Support Tool for Risk Analysis
in Health Care Processes by HFMEA Method**

Yuji Iino*₁, Kazuo Furuta*₂

Graduate school Frontier Science, The University of Tokyo *₁

The University of Tokyo *₂

Furuta-Lab., Faculty of Engineering Blg.12 7-3-1 *₁, *₂

Tel: +81-358-41-8923 *₁, *₂

Fax: +81-358-2475 *₁, *₂

iino@cse.k.u-tokyo.ac.jp *₁ furuta@q.t.u-tokyo.ac.jp *₂

Development of a Support Tool for Risk Analysis in Health Care Processes by HFMEA Method

Yuji Iino, University of Tokyo, Kazuo Furuta, University of Tokyo

Abstract

A set of classes is defined for all target tasks in health care so that possible error modes for each task can be raised. In addition, knowledge on cause-effect relations of human cognitive process enables the analysts to search for the root causes of errors. These classes and relations are originated in Cognitive Reliability and Error Analysis Method (CREAM), but some adjustment has been done for the domain. The user can raise possible error modes and their causes by choosing alternatives give by the support system step by step.

A series of processes of injection at one hospital was analyzed for demonstration of the proposed method. Our tool can provide useful guidelines to users who have insufficient knowledge on human factors.

1: Introduction

1.1: Risk Management in Medical Processes

In recent years, the press reported a large number of accidents in medical treatment, and people request medical facilities to take some remedial actions for patient safety[1]. To resolve this issue, Ministry of Health, Labour and Welfare gave guidelines for making up a risk management standard manual in 2000. And Japan Medical Association has opened many training sessions to bring up risk managers every year from 2001[2]. Risk managers in medical facilities are required four tasks: (i) re-design of health care processes safer,

(ii) risk management, (iii) coordination to accomplish accountability in case any trouble occurred, and (iv) monitoring of the patient safety system of their own medical facilities. In many cases, doctors become risk managers at Japanese medical facilities[2]. In other words, risk managers who have enough knowledge on human factors are few in Japan.

1.2: Risk Analysis Method - HFMEA

Health Care Failure Mode and Effect Analysis (HFMEA) was designed by the Veterans Affairs (VA) National Center for Patient Safety specifically for healthcare[3]. Hazard analysis steps in HFMEA are based on the traditional steps of Failure Modes and Effects Analysis (FMEA). A risk priority number; however, is to be calculated with a hazard score that is read directly from the Hazard Matrix Table.

Five steps of HFMEA are as follows.

STEP1 - Define the HFMEA topic.

STEP2 - Assemble an analyst team. This team is to be multidisciplinary including Subject Matter Experts and an advisor.

STEP3 - Graphically describe the target process. This step is divided into five sub-steps (from step3-a to step3-e). In step3-a, a flow diagram of the process is drawn and verified. In step3-b, each process step in the flow diagram is numbered. In step3-c, if the process is complex, the area of the process to focus on is identified. In step3-d, all sub processes under each block of the flow diagram

are identified. These sub-steps are consecutively lettered, i.e., 1a, 1b, and so on. In step3-e, a flow diagram composed of each sub process is created.

STEP4 - Conduct hazard analysis. In this step, all possible/potential failure modes under the sub-processes identified in STEP3 are listed. Severity and probability of each potential failure mode are determined, and hazard scores for all of the failure modes are calculated.

STEP5 - Action and outcome assessment. What the team to do is determined: to eliminate, control, or accept the cause of a failure mode. Actions to eliminate or control each failure mode are to be described. Particular measures of outcome assessment are identified that will be used to analyze and test redesigned processes. A single individual who is responsible by title to complete the recommended action is identified. Commitment by the top management to the recommended action is certified.

HFMEA is used in VA hospitals actually, and it is effective for analyzing risks in healthcare processes.

For conducting HFMEA, an analyst team needs to be assembled with experts of multi-professions, a doctor, a nurse, a pharmacist, and or a technical staff in medical facilities. The analyst team has to do brainstorming to list up all possible/potential failure modes in STEP4. If members of the team have insufficient knowledge on human factors, the brainstorming is sometimes ineffective. Training for patient safety, however, is not enough to all of medical staffs in the present situation. There are small medical facilities with a few members; it is hard for these facilities to employ human factor specialists as risk managers. The support tool developed in the present work enables them to omit the brainstorming, which depends on team members'

personal knowledge.

This paper is intended to report development of a support tool for HFMEA. Target users are staffs of medical facilities who have enough knowledge of their own domains but not enough of human factors.

2: Overview of the new approach

2.1: Work Unit

In STEP3 of HFMEA, the process to be studied is decomposed into minimum works like sub-steps or sub-sub-steps. Those works that cannot be decomposed further are called "work units" in this study. Every medical process can be expressed as a chain of work units. Generally the order of work units is fixed, and a wrong order can be a cause of error. For example, a chain of work units is as follows.

- (1) Get instruction from the doctor to prepare injection for the patient.
- (2) Search for the prescription of injection.
- (3) Check the drug name, dose, and date.
- (4) Sign in the prescription.
- (5) Check the syringe and needle.

In Step (3) the letters written on papers are confirmed. In Step (5) the syringe is confirmed by size, weight, and the letters printed on its surface. Since work units are characterized by actions themselves, the general and skeletal form of the above example is obtained by extracting key actions as follows

- (1') Get instruction ...
- (2') Search for ...
- (3') Check ...
- (4') Sign in ...
- (5') Check ...

Since Step (3') is similar to Step (5'), they have same possible/potential root causes.

To search for possible/potential error modes and root causes, work units are classified by the classification scheme of Cognitive Reliability and Error Analysis Method (CREAM)[4].

2.2: Classification and Search Scheme in CREAM

The classification scheme of CREAM is shown in Table 1. It consists of three categories and twelve groups of human erroneous actions.

Table1 Classification scheme of CREAM

Category	Group
Person Related Genotypes	Observation
	Interpretation
	Planning
	Temporary
	Person related functions
	Permanent person related Functions
Technology Related Genotypes	Equipment failure
	Procedures
	Temporary interface problems
	Permanent interface problems
Organization Related Genotypes	Communication
	Organization
	Training
	Ambient conditions
	Working conditions

The first category, "Person Related Genotypes", is related to the specific human cognitive functions.. The second category is "Technology Related Genotypes", which includes everything that can be traced directly to

technological parts of the system. It contains issues of procedures and interface.. The last category is "Organization Related Genotypes", which concerns about the environment surrounding workers and technical systems. A part of them belongs to sociotechnical systems.

All classification groups may be linked to others. The connections are called consequent-antecedent relations, which will describe that the groups can be related each other. The principle of the consequent-antecedent relation of CREAM is illustrated in Fig.1.

There are two kinds of antecedents: general and specific antecedents. General antecedents can have further links to other groups. Specific antecedents are terminals with no further links. In Fig.1, antecedents A2, A3, B3 and C1 are general , while antecedents A1, B1, B2 and C2 are specific. Consequent-antecedent relations can be established by providing a list of likely candidates of antecedents for each general consequent.

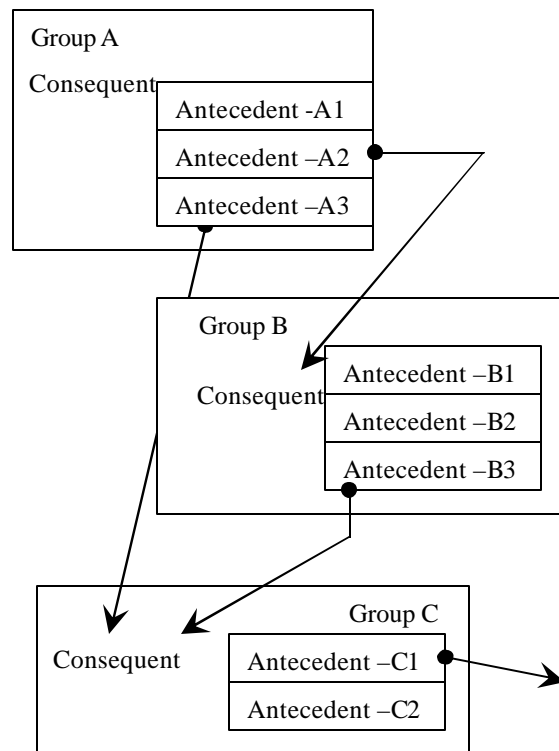


Fig.1: Consequent-antecedent relation

Each antecedent may either appear as a consequent of another classification group or may be a root cause. As for the case shown in Fig.1, Group B is an antecedent of Group A, and Group C is an antecedent of Group A, and B. Linking between groups means that the analysis can be carried out as far as one likes. In the original search scheme of CREAM specific stop rules are required. Stop rules are not considered, however, in this study for simplicity.

2.3: Development of support tool

The support tool developed in this study is based on the two above-mentioned methods: the work unit classification, and the retrospective analysis with consequent-antecedent relation. The tool was programmed in JavaScript and Hypertext Markup Language (HTML). The user can browse the web pages of the tool with several kinds of standard web browsing software of the latest version, such as MS Internet Explorer, Netscape Navigator, and so on. When the all HTML and JavaScript files are saved in a local stand-alone PC, the user can use this tool locally without access to the Internet.

Technical terms on human factors were substituted for ordinary terms as much as possible. Target users of this tool are non-experts on human factors but staffs of medical facilities. We referred to the translation of the NCPS Triage Cards(TM) for Root Cause Analysis to make texts in our tool[5] [6]. Fig.2 is an example of screen shot of the tool. The window is divided into three frames. Frame A in Fig.2 is a history frame, where the history of choices is displayed. The history is recorded as Cookie files. The user is able to check the history any time he/she wants during analysis. If the user wishes to

go back to any past point to try other choices, he/she can move the pointer cursor over the designated item, and a short message of the past item with the Branch Button appear in Frame C. The Branch Button will be explained later.

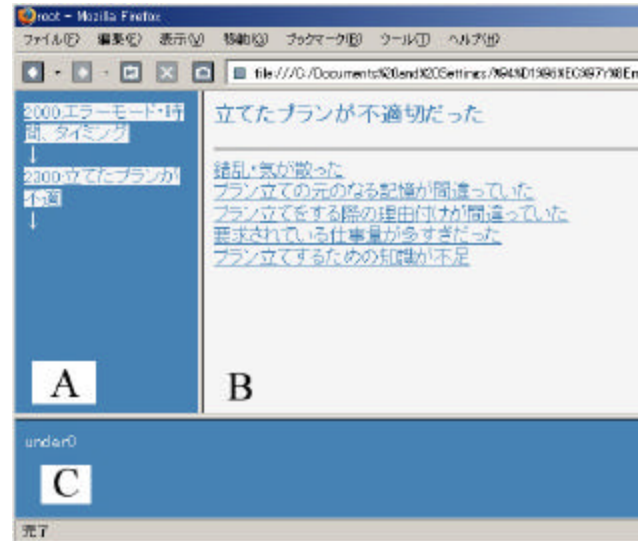


Fig. 2: Main window of the support tool

Frame B shown in Fig. 3 is an example of main texts in the display field.

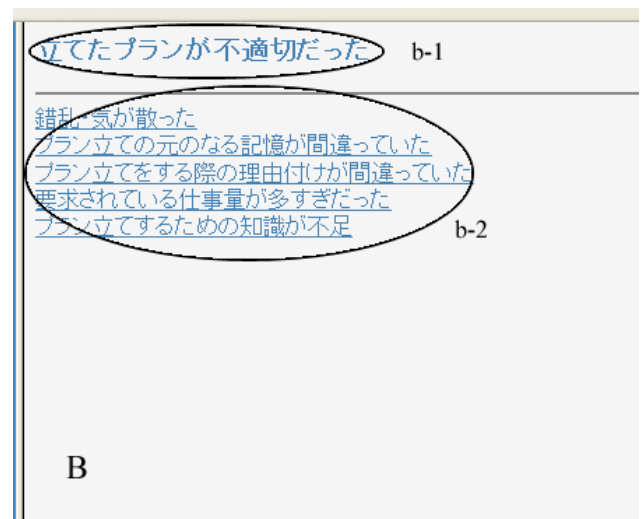


Fig. 3: Main frame of the support tool

Text b-1 is a label for the consequent currently under analysis. A short text about consequent under analysis is

sometimes shown here. Text b-2 is a list of candidate antecedents for the item in b-1. The user can click and select one antecedent from the list in b-2, and then the analysis goes on to the next step. The history of choices in Frame A is modified and a new HTML file is loaded onto Frame B.

The selected antecedent becomes a new consequent, so that the user is able to analyze the causal factors of erroneous actions in a retrospective manner by clicking CREAM classification groups step by step. Frame C is a footnote field. When the pointer cursor is located over one of history item in Frame A, a note about the selected intermediate cause is shown here. The Branch Button will appear at the same time. If the user clicks the button, a new window will open. The original window is called the parent, and the first window is called the root window. The branch window inherits a part of the history data of its parent. The user can thereby analyze multiple routes consequent-antecedent links in parallel as shown in Fig.4. In this figure, the user, who chose B as the antecedent of A at first, returned and chose another antecedent C. A new branch window then opened, the history data of which was inherited from the parent window.

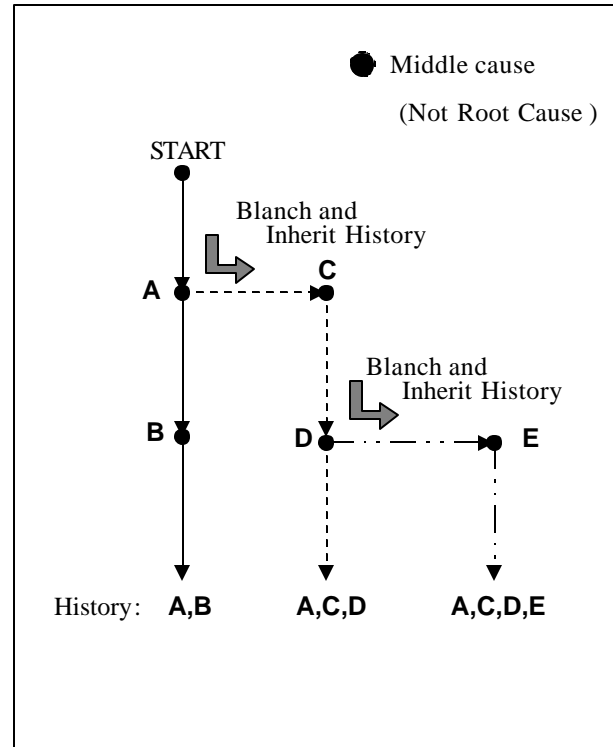


Fig. 4: Analysis in a tree structure.

3: Result and discussion.

In this chapter, our tool is examined by applying it to practical processes of medical treatment in a hospital. The target is an injection process by a doctor, a nurse, and a pharmacist. The reason of this choice from various processes is that this process has a clearly flow of works as well as variation of tasks in three positions. Two analyses were conducted, one with the support tool, and the other by conventional brainstorming without the support tool.

3.1: Work unit classification.

Firstly, the work unit classification method described in Section 2.2 was done. The process of a doctor consists of three parts, eight tasks, and 22 work units. These parts

are “Diagnosis”, “Planning of medical treatment” and “Make instruction paper for injection”. These work units were classified into 10 classes.

The nurse’s process is composed of five parts, 20 tasks, and 41 work units. The parts include “Check instruction paper”, “Exchange injection carts”, “Preparation of injection”, “Injection”, and “After injection report”. Nurse’s work units were classified into 9 classes.

The process of a pharmacist consists of five parts, ten tasks, and 28 work units. The five parts are “Accept instruction for injection”, “Inspection of the instruction”, “Printout of syringe label”, “Collect and set bottles of drug”, “Inspection of the bottles”

There are 28 work units of three processes of injection, and these work units are classified into 9 classes.

The number of all work units of a doctor, a nurse and a pharmacist was 85. They were classified into 15 classes. The number of classes is less than one fifth of single work unit. This means that this classification method is effective to organize and simplify a large number of work units.

3.2: Searching for failure modes.

In the next step, searching of possible/potential failure modes for all of the work units was done. Using our tool, the work units were classified into failure modes. Out of 71 work units, the most possible failure mode selected by brainstorming was included in the choices shown by this tool. It means the correct candidate of possible failure modes can be searched for by this tool

3.3: Searching for root causes

At last, root causes of each failure modes were analyzed. Each root cause analyzed by brainstorming is shown as an analysis tree in Fig.4. This result shows that our method did not restrict the range of search sufficiently, but it is required to search for root causes..

4: Conclusion

In the present work a new risk analysis method, which supports brainstorming in HFMEA steps was proposed, and a support tool based on the method was developed. A test of analyzing real processes of medical treatment in a hospital shows that the effectiveness of this tool is not enough for practical use, because antecedent-consequent relations are to be more adjusted to medical treatment processes. This requires future works on a new set of antecedent-consequent relations and more user-friendly interface. Nonetheless, the newly developed tool will allow us to decrease the difficulty in using the HFMEA method.

References

- [1] Ministry of Health, Labour and Welfare JAPAN. “A Health, Labour and Welfare White Paper 2004”2004:104-105
- [2] Japan Medical Association, “Patient Safety” <http://www.med.or.jp/anzen/>
- [3]VA National Center for Patient Safety ”Healthcare Failure Mode and Effect Analysis” 12, June, 2002 <http://www.patientsafety.gov/HFMEA.html>
- [4] E. Hollnagel, *Cognitive Reliability and Error Analysis Method*, Elsevier, 1998
- [5] T. Yanagawa “Improved Reporting Systems Analyzing Events and RCA (Root Cause Analysis)”J.Natl.Inst.Public Health, vol.5 Ino.3, 2001, pp.147-149

[6] VA National Center for Patient Safety, "*Concept Definitions for Triggering and Triage Questions*"
<http://www.patientsafety.gov/concepts.html>

Title: Development of Biometric Authentication API Based on Face Recognition— BioAPI++

Authors: Yoshio Iwai¹ , Takatsugu Hirayama¹ , and Masahiko Yachida¹

TOPIC: Network and systems security

Development of Biometric Authentication API Based on Face Recognition

— BioAPI++

Yoshio Iwai¹, Takatsugu Hirayama¹, and Masahiko Yachida¹

¹ Graduate School of Engineering Science, Osaka University
Toyonaka, Osaka 560-8531, JAPAN
{iwai,hirayama,yachida}@yachi-lab.sys.es.osaka-u.ac.jp

Abstract

Face is one of biometric information for identifying a person. Many researches on security systems using biometric information have been done in the recent decade. Biometric information has the advantage that it is unlikely to be forged, robbed, and lost, so it can be used for high security systems. Personal identification using facial images has the advantage that a system can capture personal biometric information without contact. In addition, BioAPI consortium defines BioAPI recently, and applications based on BioAPI have been developed on the MS Windows platform. In this work, we develop a biometric identification API, BioAPI++, based on BioAPI using by facial image recognition, and present a sample implementation that can be compiled on the various UNIX-like platform such as Linux, MacOS X, and IRIX. Our implementation system is a client-server system and has network transparency, so it looks like a local system from applications. To achieve network transparency, we make and improve SFAP (Simple Face Authentication Protocol) version 1.1. SFAP is a simple and secure protocol because it uses OpenSSL as a sub layer of communication module. We have conducted experiments on an IRIX system for checking the performance of our BioAPI++ implementation.

1. Introduction

In recent years, the development of computer systems

is necessary for us to have a safe life. Such a system would need facilities to detect unusual situations automatically and inform system administrators of unusual situations by sensing and recognizing our environment. Cameras have usually been utilized as environmental sensors because they do not make us feel uncomfortable. By using cameras, we can easily recognize the surroundings and can have much information of the surroundings in an instant.

Many researchers have developed security systems using biometric person authentication technologies. These systems may be able to attain a high performance because biological information such as facial features, retinas, and so on cannot easily be copied, stolen, manipulated, nor lost. Security systems based on face authentication have the advantages described above. Some researchers have developed face authentication systems such as PASSFACE[1], FacePassTM[2], FaceIt^(R)[3], and FaceKey[4]. PASS-FACE, FacePassTM, FaceIt, and FaceKey are based on template matching[5], constrained mutual subspace method[6], local feature analysis[7], and elastic bunch graph matching[8, 9] respectively. The elastic bunch graph matching matches a face model graph (reference graph) with a face image and has the highest recognition performance of the four previous methods[10, 11].

So far, many biometric security systems have been developed, and there are the growing needs of combination of biometric security systems. To meet the

needs, the BioAPI Consortium was founded to develop a biometric API that brings platform and device independence to application programmer. BioAPI has developed a specification for a standardized API that will be compatible with a wide range of biometric application[12]. However, BioAPI has some problems that some types are undefined or out-of-range of specification¹. A reference implementation was released, but this implementation depends on the CSSM (Common Security Service Manager) for management of loadable modules. Therefore, module management of BioAPI will be affected by changes of CSSM specification.

In this work, we develop a biometric identification API, BioAPI++, based on BioAPI using by facial image recognition, and present a sample implementation that can be compiled on the various UNIX-like platforms such as Linux, MacOS X, and IRIX. Our sample implementation system is a client-server system and has network transparency, so it looks like a local system from applications. To achieve network transparency, we make and improve SFAP (Simple Face Authentication Protocol).

2. Development of Biometric Authentication API based on Face Recognition _ BioAPI++

The target systems of BioAPI++ are the various UNIX-like platforms such as Linux, MacOS X and IRIX. In experiments, we confirmed that our sample implementation could be run on these platforms. In this section, we briefly explain the architecture, process model, and plug-in module of BioAPI++. We also explain the FACELOCK plug-in.

2.1 Architecture of BioAPI++

The architecture of BioAPI++ is shown in Fig. 1. In general, most of all security APIs have three layers[13]. BioAPI and BioAPI++ also have three layers. Bio::API class provides an interface for application layer, and Bio::SPI class provides an interface for service provider layer. A biometric authentication service provider can make their modules inheriting Bio::SPI class that provides the common interface of modules. Bio::Framework class manages plug-in modules. The reference implementation of BioAPI used the CSSM library for managing loadable plug-in modules. BioAPI++ use the standard dynamic loading library for loading plug-in modules in order to enhance module independence.

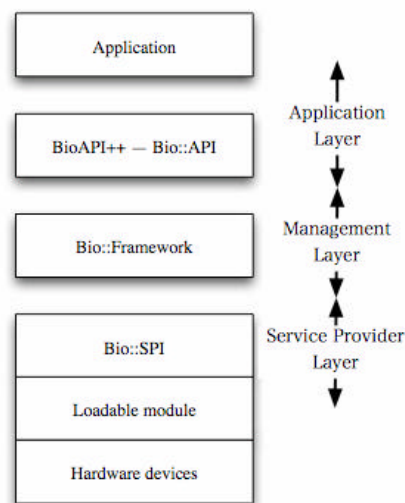


Figure 1: Architecture of BioAPI++

2.2 Process Model and Matching Mode of BioAPI++

The process model of BioAPI++ and BioAPI is shown in Fig. 2[12]. BIR means Biometric Identification Record, and contains various data used for biometric authentication. The inner information of BIR is usually closed, so BIR is accessed via BIR handles. BioAPI divides authentication process into three stages: capture, process, and match. A biometric data are captured by

¹ For example, STRING is one of undefined types; the maximum length of path name is also undefined.

sensors at the capture stage. Quality enhancement and feature extraction from the sensor data are performed at the process stage, and matching process is done at the match stage. BioAPI also provides an API for calling these stages individually.

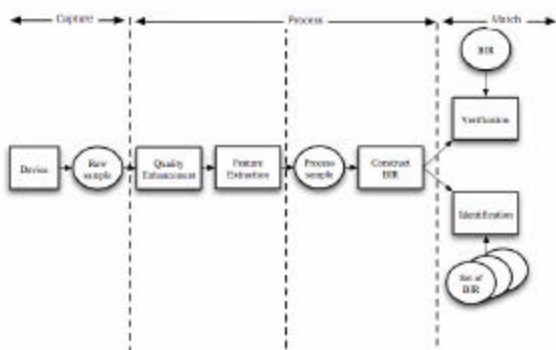


Figure 2: process model

As shown in Fig. 2, BioAPI++ has two matching modes: verification and identification. Verification is one-to-one matching performed by calling `Bio::API::Verify` and `Bio::API::VerifyMatch`. The difference between two functions is whether the captured BIR is matched with BIR database (`Verify`) or with BIR template provided as an argument (`VerifyMatch`). Identification is one-to-N matching performed by calling `Bio::API::Identify` and `Bio::API::IdentifyMatch`.

2.3 Module Interface

`Bio::SPI` provides a module interface. The fundamental functions are shown as follows:

Memory operations :

FreeBIRHandle frees a memory assigned for a BIR by a handle

GetBIRFromHandle gets a BIR from a handle

GetHeaderFromHandle gets a header of BIR from a handle

Biometric operations :

Capture captures a biometric data from a sensor

CaptureTemplate captures a biometric data as a template from a sensor

Process extracts features from a captured data (depend on each module)

VerifyMatch performs verification

IdentifyMatch performs identification

Database operations :

DbOpen opens a database

DbClose closes a database

DBStoreBIR stores a BIR into a database

DBGetBIR retrieves a BIR from a database

Memory operations are used for allocating a memory for a BIR and for reading data from a BIR. Main functions of `Bio::SPI` are biometric operations based on the process model of BioAPI. Capture inputs a biometric data from a sensor, Process extracts features and enhances qualities of data, and then the matching is performed by calling `VerifyMatch/IdentifyMatch`. Some modules have database functions that store and retrieve BIRs from a database. A module need not have all functions. When a function that is not implement is called, the module returns an error.

2.4 FACELOCK plug-in module

Each plug-in is provided as a loadable module by a service provider. In this section, we briefly explain the FACELOCK plug-in module inherited from `Bio::SPI` class.

The architecture of FACELOCK plug-in module is shown in Fig. 3. `FACELK` class inherited from `Bio::SPI` class provides the interface of `Bio::SPI` instead of the face identification library provided by the FACELOCK. Though the FACELOCK is a client-server system, `FACELK` class looks like a local plug-in module from `Bio::Framework`. To achieve network transparency, we make and improve SFAP (Simple Face Authentication Protocol). We explain the protocol in the next section in detail.

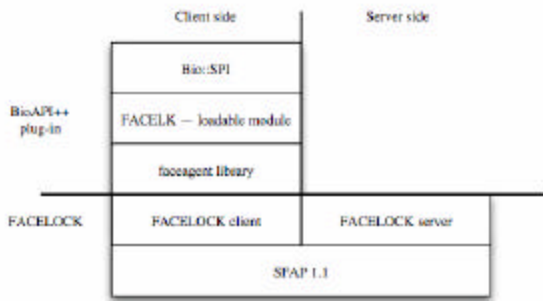


Figure 3: Architecture of FACELOCK plug-in module

3. Face Authentication Protocol

3.1 Protocol Stack

The protocol stack is shown in Fig.4. Our proposed protocol stack is called SFAP (Simple Face Authentication Protocol). We assume that the encryption equivalent to SSL/TLS is provided at a lower layer than that of SFAP. In our implementation, we use OpenSSL [14] for encryption. An SFAP server on open networks like the Internet needs countermeasures against DoS (Denial of Service) attacks, but we assume that an SFAP server is used on closed networks such as a LAN in consideration of the server's service characteristics. Consequently, we do not consider the countermeasures in this paper.

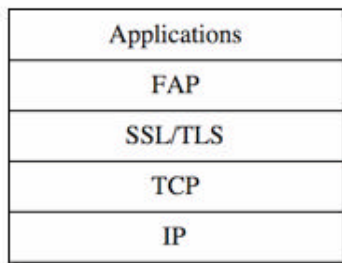


Figure 4: Protocol Stack

3.2 Data Representation

In recent years, XML form has been used as data

representation for interoperability. However, we use frame form as data representation of SFAP because of the compactness and simplicity of packets. The SFAP's packet consists of a fixed-size header and additional variable-length data as shown in Fig.5.

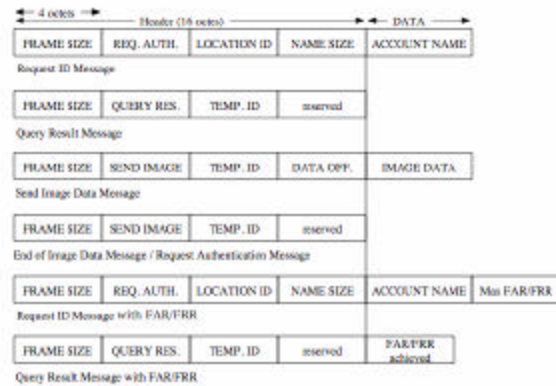


Figure 5: message format

We briefly explain each field as follows:

FRAME SIZE: size of message frame

REQUEST AUTH: request for connection to the authentication server

LOCATION ID: location of a lock

TEMPORAL ID: ID for temporal use issued by the server

NAME SIZE: length of user's account name

ACCOUNT: user's account name

QUERY RESULT: request for the authentication result

SEND IMAGE: transfer image data to the server

DATA OFFSET: offset of image data

IMAGE DATA: a part of a user's image

Max FAR/FRR: maximum value of FAR and FRR

FAR/FRR achieved: FAR and FRR values achieved by the server

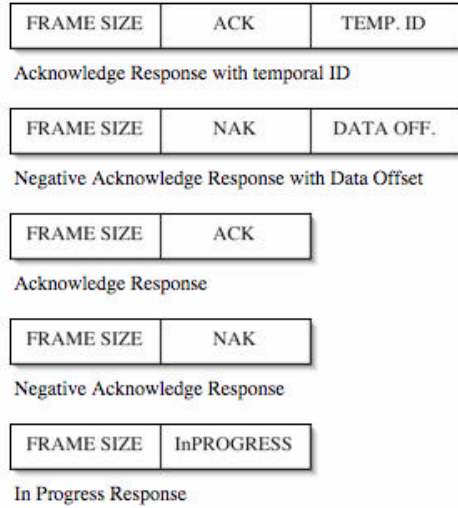


Figure 6: response format

Next, we show response messages in Fig.6. The message, "Acknowledge response with temporal ID," is a positive response for acknowledgment and is added to a temporal ID used for this session. The messages, "ACK and NAK," are used in the usual senses of "ACK/NAK." The message, "In Progress Response," is given when the "Query Result" message is sent by a client and the process for the user's authentication is still running on the server. The client who receives this response message issues a "Query Result" and again waits for a certain time determined by a random number in order to avoid congestion.

3.3 Protocol Overview

The overview of the basic protocol is shown in Fig.7. The protocol consists of four stages.

REQUEST AUTHENTICATION STAGE: A client requests authentication from the SFAP server. The server that receives the request opens an SSL connection and permits the client to use the server. At this point, the server checks the ID and IP address of the client and can restrict clients to use the server. When the SSL connection is established, the server issues a temporal ID to the client and the client uses

this temporal ID for this session hereafter.

SEND IMAGE STAGE: The client successfully connected to the server sends an image used for authentication. The image is divided into some fixed-size frames and transferred to the server. In the case of transfer error while sending the image, the server sends a NAK and a data offset of the error frame to the client.

END OF IMAGE DATA: The client informs the server that the client has completed the data transfer by sending an "end of image data" message. The server receiving this message sends an ACK if all data are received successfully; otherwise the server sends a NAK. After the successful transfer, the server forks a child process to perform an authentication procedure using the image.

QUERY RESULT: After the client has finished sending an image, the client waits for a certain number of seconds determined by a random number, and then the client requests an authentication result. If the server has finished the authentication process, the server sends an ACK message as a positive response or a NAK message as a negative response. If the server is still performing the authentication process, the server sends an "In Progress Response" message. When the client receives this message, the client sends a "Query Result" message again after waiting for a certain time determined by a random number, in order to avoid congestion.

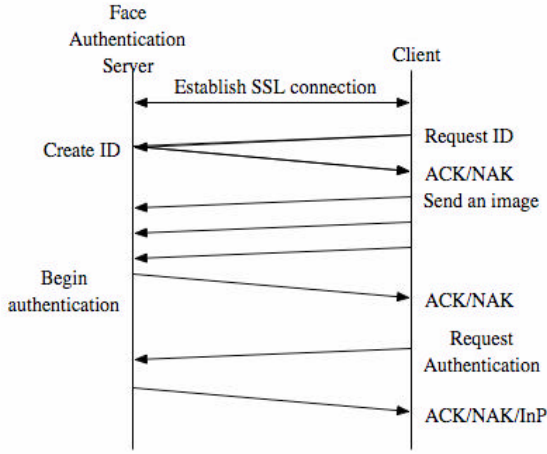


Figure 7: message interchanges of SFAP

3.4 Implementation of Protocol

We have implemented the proposed protocol described above on UNIX systems (Solaris, IRIX, Linux). State transition of a server and a client are shown in Fig.8. In general, implementation of a server system is divided into two classes: iterative server and concurrent server. An iterative server has the disadvantage that a high-load server's response is slow but has the advantage that the implementation of an iterative server is easy. Therefore, in the proposed system we construct most modules of the server as iterative and the face recognition module of the server, a highest-load module, as concurrent by forking a child process.

3.5 Models for Protocol Evaluation

To accurately evaluate the performance of the proposed protocol, in this section we model each process. The operations conducted at the request authentication phase are shown in Fig.9. The mean time for processing at this phase, T_R , is expressed as follows:

$$T_R \equiv T_{SSL} + T_{REQ} + T_{com} + T_{res} + 2d, \quad (1)$$

where T_{SSL} is the mean time to open an SSL connection, T_{REQ} is the mean time to process a request authentication packet, T_{com} and T_{res} are the mean

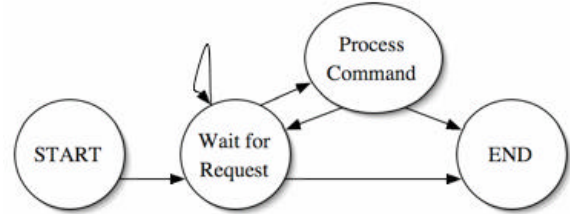
times for a packet to send a message or a response, and d is the mean time delay through the network. Similarly, the mean time for processing at the query result phase, T_Q , is expressed by the following equation:

$$T_Q \equiv T_{QUE} + T_{com} + T_{res} + 2d, \quad (2)$$

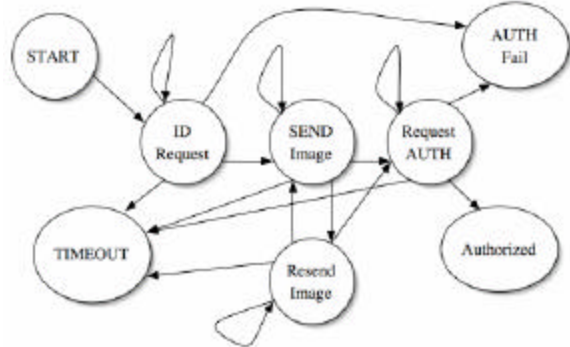
where T_{QUE} is the mean time to process a query result packet (see Fig.10). Here, we assume that T_{com} is the same in all messages, and that T_{res} is the same in all responses. The mean time for processing at the send image phase, T_I , is expressed as follows:

$$T_I \equiv \left\lfloor \frac{N_I}{N_{mess}} \right\rfloor T_{IMG} + T_{CLS} + 2d, \quad (3)$$

where N_I is the size of an input image, N_{mess} is the data size of a message, T_{IMG} is the mean time for processing messages excluding the last message, and T_{CLS} is the mean time for processing the last message. The last message is treated as an exception because T_{CLS} includes the time required for server's forking a child process to perform face recognition.



(a) state transition of server



(b) state transition of client

Figure 8: State transition of SFAP

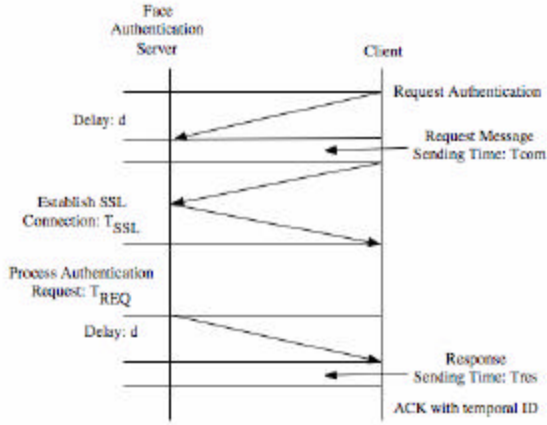


Figure 9: Request Authentication Phase

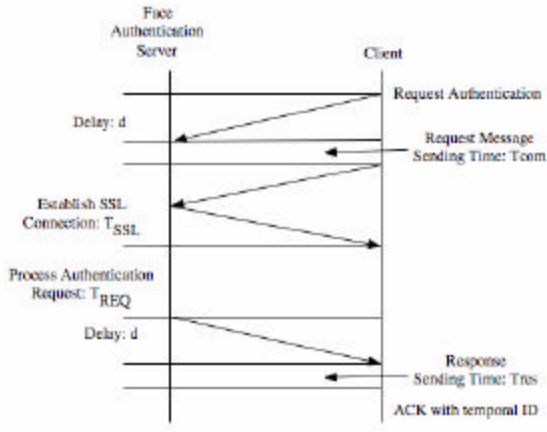


Figure 10: Query Result Phase

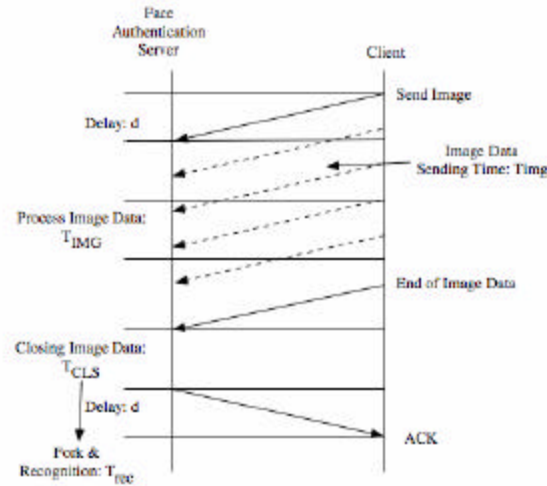


Figure 11: Send Image Data Phase and End of Image Data Phase

3.6 The Worst Response Time

The worst response time for a message is expressed by the following equation, because our experimental SFAP server is constructed as an iterative server:

$$T_{worst} = \max(T_R, T_Q, T_{IMG}). \quad (4)$$

3.7 Throughput

The mean of throughput, $N_{throughput}$ (issues/sec), is expressed by the following equation:

$$N_{throughput} = \frac{1}{\max(T_{rec}/M, T_R + T_I + N_Q T_Q)},$$

where T_{rec} is the mean time for processing face recognition, M is the multiplexity of recognition processes, and N_Q is the average number of query result messages issued by a client during a session.

4. Evaluation Experiments

We conducted experiments to verify the performance of communication module. In our experiments, we used two workstations (SGI Origin 300, 8 CPU, 2 GB memory as a server, and SGI Origin 300, 4 CPU, 1 GB memory as a client) interconnected by an Ethernet switch (Cabletron Smart Switch SSR2000). The input image size used for authentication is 512 pixels x 512 pixels x 8 bits, and 256 KB in total. The workstations are connected by Fast Ethernet (100 Mbps) via SSR2000.

4.1 Mean Time for Message Transfer

The mean time for message transfer and the mean time for processing face recognition are shown in Table 1. Each data is the average of 10,000 trials. The transfer delay is about 1.53 ms. The transfer delay is slightly longer than other protocols of the network layer because SFAP is an application layer protocol. The overhead time for encryption of request and query messages is short

because the size of these messages is very small, but the overhead time for encryption of an image is about 500 ms. For a 256 KB image, the overhead rate for encryption can be estimated at 2 ms/KB.

(ms)	d	T_R	T_Q	T_I	T_{rec}
Encryption	23.5	37.9	6.56	1666.2	26200
No encryption	1.53	32.9	4.57	1108.5	26200

Table 1: Mean time for message transfer

4.2 Throughput

The relationship between throughput and multiplexity is shown in Fig.12. The line plots are made from theoretical and ideal values calculated from the data in the previous section. The line plot of $T_{rec} = 26.2$ (sec) is made from real data collected by the server, while $T_{rec} = 26.2$ is the average value of the face recognition process. The plot corresponds closely with the simulated plot of $T_{rec} = 26.2$.

The maximum throughput is restricted to 31 clients/min due to network performance, but the actual maximum throughput is only limited by the number of CPUs in the server; if the face recognition process is faster, the maximum throughput is greater. In this paper, there is room for improvement in the server's throughput. Within ten seconds after the face recognition process finishes, throughput of a server connected with Fast Ethernet will reach 30 clients/min. This performance is enough for small offices and small groups, but not enough for large enterprise servers. To apply our protocol to such an enterprise server, we need to make some improvements such as server clustering, load-balancing, and image data compression.

5. Conclusion

We have developed a biometric C++ API based on BioAPI using a face recognition system called

FACELOCK. We have also extended an original communication protocol, SFAP, to construct a server-client system for biometric authentication. We have conducted experiments to verify the performance of the server. We have modeled our server performance by using various mean times and showed the theoretical limits of server's performance. In addition, we have estimated the actual values of the various mean times of the server performance and confirmed that the server performance corresponds to the theoretical performance. In future work we will verify the stability of the proposed protocol for error recovery.

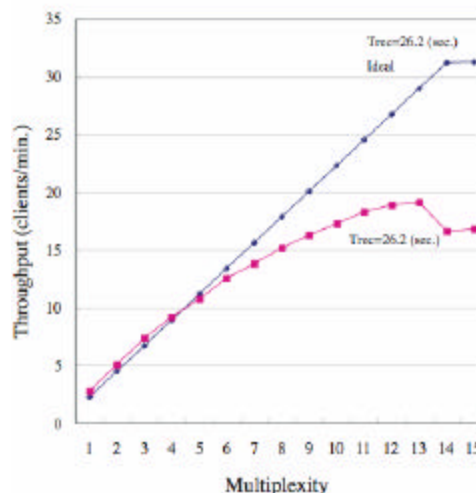


Figure 12: Server throughput

Acknowledgment

This research was partially supported by the Japan Society for the Promotion of Science under Grant-in-Aid for Creative Scientific Research (Project No. 13GS0018).

References

- [1] M. Doi, Q. Chen, A. Matani, O. Oshiro, K. Sato, and K. Chihara, "Lock control system based on face identification," *IEICE Trans. on Information and System*, Vol. J80-DII, No. 8, Aug. 1997, pp. 2203-2208.

- [2] H. Dobashi, A. Okazaki, and K. Takagi, "FacePassTM face recognition security system," *TOSHIBA REVIEW*, Vol. 57, No. 8, 2002, pp. 48-51.
- [3] <http://www.faceit.com/>.
- [4] <http://www.society.omron.co.jp/faceid/2/f2.html>.
- [5] X. Song, C. Lee, G. Xu, and S. Tsuji, "Extracting facial features with partial feature template," *Proc. Asian Conf. Computer Vision*, 1994, pp. 751-754.
- [6] K. Fukui, O. Yamaguchi, K. Suzuki, and K. Maeda, "Face recognition under variable lighting condition with constrained mutual subspace method-learning of constraint subspace to reduce influence of lighting changes," *IEICE Trans. on Information and System*, Vol. J82-DII, No. 4, Apr. 1999, pp. 613-620.
- [7] P. Penev and J. Atick, "Local feature analysis: A general statistical theory for object representation," *Neural Systems*, Vol. 7, No. 3, 1996, pp. 477-500.
- [8] L. Wiskott, J. M. Fellous, N. Krüger, and C. von der Malsburg, "Face recognition and gender determination," *Proc. Int'l Workshop on Automatic Face- and Gesture-Recognition*, 1995, pp. 92-97.
- [9] L. Wiskott, J.-M. Fellous, N. Krüger, and C. von der Malsburg, "Face recognition by elastic bunch graph matching," *IEEE Trans. on PAMI*, Vol. 19, No. 7, July 1997, pp. 775-779.
- [10] E. Hjelm and B. K. Low, "Face detection: A survey," *Computer Vision and Image Understanding*, Vol. 83, No. 3, 2001, pp. 236-274.
- [11] O. Ayinde and Y. -H. Yang, "Face recognition approach based on rank correlation of Gabor-filtered images," *Pattern Recognition*, Vol. 35, No. 6, 2002, pp. 1275-1289.
- [12] BIOAPI consortium, "BIOAPI specification version 1.1", <http://www.bioapi.org/>.
- [13] NPO Japan Network Security Association, "Technical report for security API," *Technical Report*, 15 Jokei No. 1516, IPA, 2004. http://www.ipa.go.jp/security/fy15/reports/sec_api/.
- [14] <http://www.openssl.org/>.

**Title: Integrated Simulation of Emergency Response of Related Organizations and Residents'
Behavior in Nuclear Disaster**

Author1: Taro Kanno

Address: 2-5-1, Atago, Minato-Ku, Tokyo, 105-6218, Japan

Phone&Fax: +81-3-6402-7578(fax), +81-3-5404-2893 (phone)

Email: kanno@diras.q.t.u-tokyo.ac.jp

Affiliation: Research Institute of Science and Technology for Society, Japan

Author2: Tatsuya Shimizu

Address: 2-11-16, Yayoi, Bunkyo-ku, Tokyo, 113-0033, Japan

Phone&Fax: +81-3-5841-2475(fax), +81-3-5841-8923(phone)

Email: shimizu@cse.k.u-tokyo.ac.jp

Affiliation: Institute of Environmental Studies, the University of Tokyo, Japan

Author3: Kazuo Furuta

Address: 2-11-16, Yayoi, Bunkyo-ku, Tokyo, 113-0033, Japan

Phone&Fax: +81-3-5841-6965(phone)

Email: furuta@q.t.u-tokyo.ac.jp

Affiliation: Institute of Environmental Studies, the University of Tokyo, Japan

Topic: Human and organizational behavior and errors

Integrated Simulation of Emergency Response of Related Organizations and Residents' Behavior in Nuclear Disaster

Taro Kanno*, Tatsuya Shimizu**, and Kazuo Furuta**

* Research Institute of Science and Technology for Society, Japan

** Institute of Environmental Studies, the University of Tokyo, Japan

Abstract

We are now developing an integrated simulation system of emergency response (MASTERD: Multi-Agent Simulation sysTem of Emergency Response in Disasters) for design and assessment support of emergency response system (ERS). The target domain of a prototype of MASTERD is nuclear disaster. The main components of it are an organizational activity simulator (OAS) and an evacuation simulator (ES). OAS simulates activities of related organizations participating in emergency response, such as national and local governments, disaster prevention agencies, medical agencies, mass media, and so on. Each organization is implemented as one agent with a rule-based decision-making model based on emergency response plans and manuals. An evacuation simulator simulates residents' situation assessment and decisions influenced by information provided by OAS agents of mass media and municipality governments, or other people (ES agents). We constructed a conceptual model of resident behavior by analysis of past disaster cases and implemented it on a probabilistic reasoning model. OAS and ES are implemented as distributed objects with a common message protocol on a CORBA platform. It was confirmed that OAS could simulate a current ERS by a reconstruction simulation of emergency response exercises.

It was also confirmed that ES can simulate qualitative features of residents' behaviors. We plan to conduct integrated simulations under various conditions and closely assess total performance of ERS.

1. Introduction

Disaster emergency response is the last line of defense to protect both social safety and public sense of security against disasters. It is therefore important to carefully design an emergency response system (ERS) and assess the total function and vulnerability of it. For the purpose of design and assessment of ERS, various types of emergency drills, such as blind, desktop, full-scale drills, are currently designed and conducted. However, even though such an exercise is deliberately planned and designed, it is virtually impossible to conduct it under as many conditions as possible. In such a case where experiments or drills are unfeasible in real-life settings, computer simulation can be a valuable alternative to understand and assess the performance of ERS.

We are now developing an integrated simulation system of emergency response (MASTERD: Multi-Agent Simulation sysTem of Emergency Response in Disasters)

for design and assessment of ERS (Kanno et al, 2004). MASTERD has a distributed-object architecture and is composed of six basic components: a simulation kernel, an organizational activity simulator (OAS), an evacuation simulator (ES), GIS sever, disaster phenomena simulators, and presentation tools. This paper introduces a prototype of MASTERD for nuclear disasters, and describes two major components of it: an organizational activity simulator and an evacuation simulator.

In the next section, we present the basic architecture of a prototype of MASTERD. In Section 3 and 4, we describe the details of OAS and ES. In Section 5, we explain how these two components are integrated and discuss on the applications of the integrated simulation. Then conclusion is given in Section 6.

2. System Architecture

Figure 1 shows a conceptual design of MASTERD. It is composed of six basic components. The brief explanation of each component is given below.

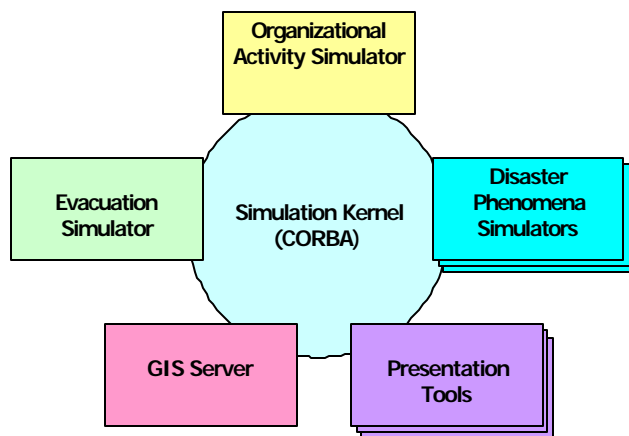


Figure 1 Architecture of MASTERD

Simulation Kernel developed with CORBA controls the whole simulation process and message transfers in/among

the components. CORBA is an open distributed object-computing infrastructure and automates many common network-programming tasks. APIs of the simulation kernel enables an easy integration of various components .

Organizational Activity Simulator (OAS) simulates activities of organizations participating in emergency response operations, such as national and local government, police and fire department, medical agencies, mass media. Many works have been done on simulation of disaster situations, but most of them have focused on disaster phenomena or residents' evacuation. As shown in the past disasters, emergency response activities significantly influence mitigation and moderation of harmful effects of disasters. This kind of simulation therefore is important to evaluate the total performance of ERS.

Evacuation Simulator (ES) simulates residents' behavior in disasters. Simulation studies of resident behavior in disasters so far have focused on how people evacuate; however, the simulator of the prototype of MASTERD deals with not only actions but also decision-making process. It is necessary to consider it because residents cannot recognize the threats or necessity of evacuation in a nuclear disaster.

GIS provides geographical and time-space information of disaster environment. It also provides several methods such as shortest path search or storage and mapping calculated results of other components.

Disaster Phenomena Simulators simulates physical phenomena of disaster environment, for example plant behavior, dispersion of hazardous materials, fire spread, and so on. We implemented a diffusion simulator as this component to a prototype of MASTERD for nuclear disasters.

Presentation Tools provide various input/output interfaces for each component. We developed a viewer and a scenario manager in the prototype. The viewer visualizes task and communication flows in OAS, and the scenario manager configures simulation conditions and inputs trigger information to the diffusion simulator and OAS.

3. Organizational Activity Simulator

This simulator simulates activities (communications and task executions) of related organizations participating in emergency response activities in nuclear disasters. 95 agents were implemented in the prototype. The details of the agent model of OAS are explained in this section.

3.1 Organizational Behavior Model

Figure 2 shows a schematic diagram of the agent model of OAS. It is a rule-based decision-making model and has an input-decision-action cycle: gets information or resource from the environment or other agents, selects proper responses referring to knowledge base, and then execute it. Some rules are normative extracted from the current emergency response plans and manuals, and some are general or empirical rules in emergency response. This model uses domain specific knowledge but is itself domain independent.

3.1.1 Knowledge Base stores plans and point-of-contact (POC) extracted from the current emergency response plans and manuals. Most of the plans are situation-triggered; they are initiated when some key information on situations is received. POC is a communication path among different sections or organizations. We can simulate different ERS by editing the contents of the plans and POC. Knowledge base also stores acquired information and request-query history,

which are used for re-request or re-query.

3.1.2 Action is a primitive task class required in emergency response and defined as a set of required resources, duration, and contents. For example, “call” requires unoccupied phones and workforces at both sender and receiver, and sends a message after the defined duration is over. We implemented 13 basic actions necessary for emergency response by reviewing several scenario of full-scale emergency exercises..

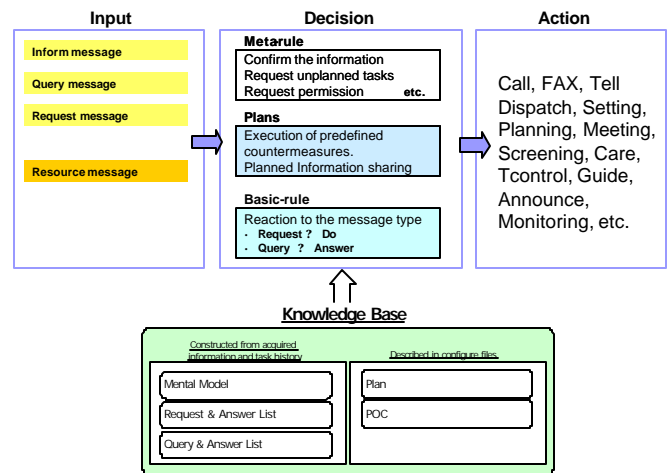


Figure 2 Agent Model

4. Evacuation Simulator

This simulator simulates resident’s decision-making and actions influenced by information provided by mass media, municipality government, and other people. We constructed a conceptual model of resident behavior by analysis of 57 documents on past disasters and implemented it on a probabilistic reasoning model.

4.1 Resident Behavior Model

Figure 3 shows an overview of the model. The bottom part of Figure. 3 shows the conceptual model of resident behavior based on the conventional

Stimulus-Organism-Response model of a human information processor, which consists of three steps: information input, situation judgment, and action. The influencing factors of each step of S-O-R model (attributes of information, recipient, and situation) have been extracted from the case analysis (Furuta et al, 2003). The upper shows the computational model of the S-O-R model. We implemented the decision-making process on Bayesian Belief Network (BBN) in which situation assessment and the contributions of the influencing factors are reflected in the structure of the BBN and its probabilities. Actions are determined by the balance between the need for evacuation obtained by the probabilistic reasoning and mental barriers.

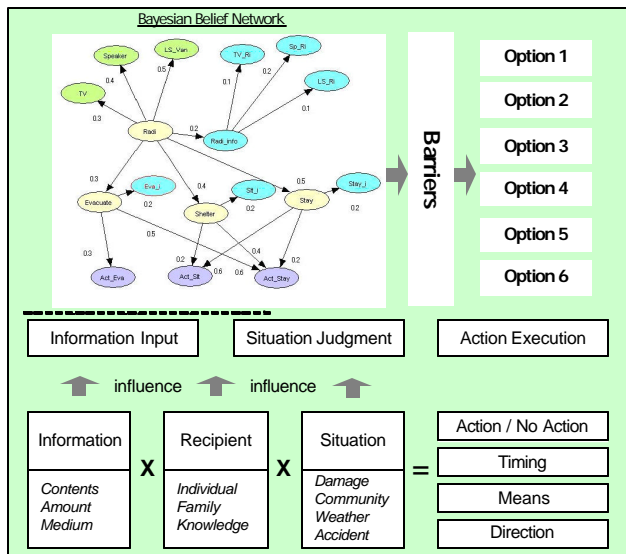


Figure 3 Overview of the Resident Behavior Model

5. Integration of OAS and ES

Because coordination and announcement by related organizations greatly influence the behavior of residents, especially in nuclear disasters where disaster information cannot be directly perceived by residents, it is important to simulate and assess the total process from the outbreak of

an accident to evacuation of residents. Both OAS and ES were implemented as distributed objects on the simulation kernel, it is therefore easy to integrate these two components. We integrated them by using common message format and protocol: resident agents can directly receive messages from OAS agents. Figure 4 shows a schematic diagram of how OAS and ES are integrated.

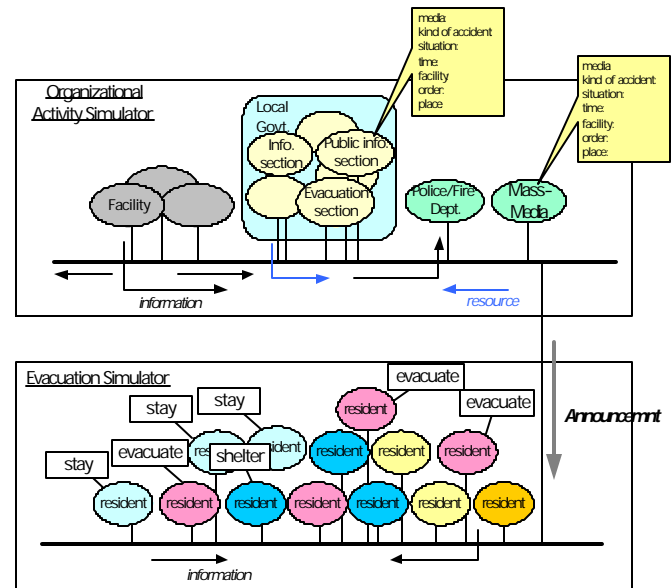


Figure 4 Integration of OAS and ES

5.1 Message Format and Protocol

Messages used in OAS and ES have hierarchical structure based on FIPA-ACL (Agent Communication Language), and are classified into four types: inform, query, request, and resource. Table 1 shows the format of these three types of message. When an agent receives an inform message, it will initiate plan or communication if necessary, and is stored in its knowledge base. When an agent receives a query message, then the agent will answer to it based on its knowledge base. If an agent receives request message, then the agent will do the requested task if possible. If a resource message is received, then the number of the object will increase.

Table 1 Format of a Message

type	contents
inform	sender, receiver, time, media, titles, contents
query	sender, receiver, time, media, title, content
request	sender, receiver, time, media, action, object, quantity, quality, means
resource	sender, receiver, time, object, quality, quantity

5.2 Announcement

A mental model of OAS agent is a storage of the inform message obtained from environment or other organizations, and is represented as a slot-filer (title-content) frame. The titles were prepared to cover all the information exchanged in several scenarios of a full-scale nuclear disaster emergency drill of a local government. An example of the mental model used in the prototype is shown in Figure 5.

The organizations that have responsibility to make announcement, such as municipality governments or mass media, appropriately create a message for announcement based on their own mental model and announce it. In a reconstruction simulation of the emergency drill, we implemented a rule according to the exercise scenario to make an announcement 1) when the first accident report is receive from the facility, 2) after the meeting, 3) when an evacuation is initiated. Figure 6 shows the content of an announcement created by an OAS agent of the public information section of the local government after the first meeting of the disaster headquarters.

5.3 Input to ES

Resident agents who satisfy necessary conditions to receive it, for example level of awareness, location, available media, and so on, can get the message. The received information is parsed and if there is corresponding contents to the nodes of the BBN, then the

belief of them increase and the values of all nodes are updated.

■ Accident (level1-5, increase, continue, decrease, end)	■ EvacuationArea (km)
■ Emission (on, increase, decrease, off)	■ ShelteringArea (km)
■ Victim (level1-3, etc.)	■ TControlArea (route)
■ Weather (N,W,S,E)	■ Iodine (use, no-use, etc.)
■ Radiation1~ 7 (mSv/h)	■ Food (on, off, etc.)
■ MaxArea (km)	■ National (gathering, setting, etc.)
■ MaxRadiation (mSv/h)	■ Pref (level1-3, setting, etc.)
■ ProjectionE, ProjectionS (km)	■ City1 -(setting, established, etc.)
■ Declaration (nothing, nuclear_emergency, lifting, etc)	■ OFC (gathering, established, etc.)
■ Evacuation (planning, start, started, finish, lifting, etc)	■ OFCMeeting (ready, finished, etc.)
■ Sheltering (planning, start, started, finish, lifting, etc)	■ EMC (gathering, established, etc.)
■ TrafficControl (planning, start, started, finish, lifting, etc)	■ EMDC (gathering, established, etc.)
■ EMedical (dispatching, 1 st -3 rd _start, etc)	■ AidStation1- (setting, established, screening, etc.)
■ EMonitoring (planning, initial, 1 st _start, etc.)	
■ Announce (stay, evacuation, sheltering, etc.)	

Figure 5 Mental Model

```

<inform>
  <sender>/Pref/Ibaraki/Saitai/Kouhou</sender>
  <receiver>/City/Tokai/Tokai</receiver>
  <content>
    <kouhou>
      <title>PrefAnnounce</title>
      <time>270</time>
      <kind>radiation</kind>
      <situation>Continue3</situation>
      <radiation>0</radiation>
      <facility>jnc1</facility>
      <action>stay</action>
      <region>>null</region>
      <meetpoint>>null</meetpoint>
    </kouhou>
  </content>
  <media>BMusen</media>
</inform>

```

Figure 6 an Example of the Content of Announcement

5.4 Applications of Integrated Simulation

Emergency response plans and manuals are usually designed on a task-by-task basis, such as emergency medical activity, evacuation, announcement, and so on. It is therefore difficult to understand and assess the total performance of ERS in an actual emergency. Full-scale emergency exercise may be the only way to know how an ERS works, however, it is difficult to conduct exercises under various conditions and those based on designed scenarios are far from actual emergencies. Computer simulation considering various factors of disasters is a

valuable tool and highly needed.

5.4.1 Design and Assessment of Evacuation Scheme

Most of the emergency plans and manuals concerning on announcement to residents describe what should be announced and how. In real situations, however, it is necessary to make an announcement based on available information considering the current residents' behaviors. OAS and ES can simulate under various conditions of both what and how to announce and residents' behaviors, and assess the effectiveness and efficiency of evacuation scheme under different conditions.

5.4.2 Support for Education and Training

One of the serious problems of local municipalities or other organizations participating in emergency response is personnel rotation, which makes difficult for officers to accumulate knowledge and experience to cope with an emergency. Computer simulation on emergency response can easily provide opportunities to learn how ERS works under different situations and is expected to contribute to resolve such problems. We are now developing a trainee console for integrated simulation of MASTERD and trainees. This tool is constructed on the simulation kernel and enables trainees to command other OAS agents. They can learn how to cope with ongoing situations in a different way than emergency drills.

5.4.3 Risk Education and Dialogue

While officers of local municipalities suppose that residents will follow their evacuation order, the residents are not necessarily willing to do so. In JCO accident, 15% people in evacuation area did not evacuate and 50% people in non-evacuation area did (Umemoto et al, 2000). One of the reasons of this can be a lack of knowledge on evacuation schema and reliance on the local government.

OAS and ES can show the performance of the current ERS and enable to share it among different stakeholders, and is expected to encourage and promote risk education and dialogue.

6. Conclusion

We are developing an integrated simulation system of emergency response in disasters (MASTERD). In this paper, the two major components of a prototype for nuclear disasters, organizational activity simulator and evacuation simulator, are introduced. These components were developed on the same simulation kernel and integrated by message transfer between them; therefore, it is possible to simulate interactions between activities of related organizations and residents behavior. We have carried out test simulations separately so far, and plan to confirm the validity of each simulation model. At the next step, we will conduct integrated simulations with all components of MASTERD and assess the total performance of ERS under various conditions.

References

- K. Furuta, T. Kanno, E. Yagi, and Y. Shuto, "Socio-Technological Study for Establishing Comprehensive Nuclear Safety System, Proc. 11th. Int'l Conf. Nuclear Engineering (ICONE11), 2003.
- T. Kanno, Y. Morimoto, and K. Furuta, "Multi-agent Simulation System of Emergency Response in Nuclear Disaster", Proc. 7th. Int'l Conf. Probabilistic Safety Assessment and Management(PSAM7),2004,pp. 389-394.
- M. Umemoto, K. Kobayashi, T. Ishigami, and M. Watanabe, "The Inhabitants' Receiving Disaster Information and Their Reaction at the JCO Criticality Accident in Tokai-mura", Proc. Symp. Inst. Social Safety Science, 2000, Vol.10, pp 113-116 (in Japanese).

Mobile Agents: A Ubiquitous Multi-Agent System for Human-Robotic Planetary Exploration

Integration of Systems and Human Sciences

Charis Kaskiris

kaskiris@sims.berkeley.edu

SIMS, University of California, Berkeley, CA 94720

RIACS, NASA Ames Research Center, Moffett Field, CA 94035

Phone: (510) 858-4599 Fax: (510) 642-5814

Maarten Sierhuis

msierhuis@mail.arc.nasa.gov

RIACS, NASA Ames Research Center, Moffett Field, CA 94035

Phone: (650) 604-4917 Fax: (650) 604-4954

William J. Clancey

william.j.clancey@nasa.gov

Computational Sciences Division, MS 269-3, Moffett Field, CA 94035

Institute for Human and Machine Cognition, UWF, Pensacola, FL, 32514

Phone: (650) 604-2526 Fax: (650) 604-4036

Ron van Hoof

rvhoof@optonline.net

QSS, NASA Ames Research Center, Moffett Field, CA 94035

Phone: (732) 632 9459 Fax: (732) 632 9607

Mobile Agents: A Ubiquitous Multi-Agent System for Human-Robotic Planetary Exploration

Abstract

Future human planetary exploration creates challenges both for technology and mission management. Ubiquitous computing principles and applied artificial intelligence are promising approaches in making planetary surface missions safer and more effective. Architectures which integrate both approaches and facilitate the interaction and collaboration between astronauts, robots, systems, and remote science teams are necessary to achieve these goals. The Mobile Agents project uses a real-time distributed multi-agent architecture and system to provide model-based real-time distributed support for human-robotic collaboration, science data collection, mission-plan tracking, and health monitoring. The Brahms agent-oriented modeling environment provides a layer of abstraction for enabling a diversity of software, hardware, and humans to be integrated into data management and workflow. Brahms agents facilitate the communication between different mission participants and interact through voice interfaces with astronauts, remote science teams, and mission control. This paper presents the astronaut-robotic planetary exploration environment as an example of ubiquitous computing. It also discusses an area largely unexplored in the ubiquitous/pervasive literature, namely human-robotic interaction through a localized or tele-operated ubiquitous computing system. The Mobile Agents Architecture is presented and the agent-layer aspects which related to human-robotic pervasive systems are further discussed. We conclude with remarks about evaluation of the architecture through field testing.

1. Introduction

Future human planetary exploration provides increased challenges for both technology and human mission management. These challenges necessitate closer collaboration between humans, robots, and systems to achieve the science objectives of these missions. Planetary exploration, and in particular Mars, poses additional requirements for mission execution and coordination. The inter-planetary time-delay makes real-time mission management from Earth infeasible. This necessitates localized mission control of extra-vehicular activities (EVA). Access to the planet's surface is also limited by crew size and the allowable numbers of EVA in which each can participate. Expertise on exploration activities might not be on site but rather remotely located in a Mars-based habitat or Earth. At the same time, remote science teams (RST) need to be able to actively participate with the exploration astronauts to maximize scientific work. Finally, EVA astronauts' cognitive focus should be spent on scientific data collection, rather than on mundane support functions. Hazardous exploration missions further necessitate mobility of systems which provide localization and contextual-awareness which can be assisted by remote tele-operation and collaboration.

Advances in mobile devices, protocols, sensors, and systems have enabled the advancement of architectures which can support pervasive¹ computational applications envisioned by Weiser [23] His notion of disappearing technology which becomes part of the fabric of work practice could prove critical in answering the challenges of planetary exploration. Such systems require new paradigms of interaction and control. Artificial intelligence has been successfully used to deal with smart interfaces, location and situation awareness, and resource control [16]. At the same time, ubiquitous computing has produced an array of technologies, algorithms, and devices to deal with location-awareness [19]² and context-awareness [18][14]. Wearable computing applications [21] further explored mobile computing capabilities. Agent architectures have also been used to provide contextual awareness with localization services [11].

Agent architectures may further provide the interfaces between disparate components and participants with such missions, linking devices, sensors, and humans with each other. The agent layer of the Mobile Agents Architecture (MAA) provides such integration capabilities to a mobile computing ubiquity system. The Mobile Agents project's main objective has been to develop a model-based, distributed agent architecture which integrates diverse components in a system designed for lunar and planetary

surface operations [6, 7, 8, 9]. The agent architecture provides interfaces between humans, robots, systems, sensors; provides relational storage of science data; and provides intelligent assistance to the mission's local and remote participants.

In the next section we discuss how the MAA integrates many different aspects of ubiquitous computing in an integrated way different from other systems. We further discuss assumptions used in the model and how they relate to existing ubiquitous systems. The integration of these different research approaches allows Mobile Agents to investigate their interaction. We then present the agent layer of the MAA, and discuss the three main tasks that the agents perform: (a) plan management, (b) science data management, and (c) mission data management. Each task's agent responsibility is further discussed in the context of mission objectives and constraints. We then conclude.

2. Mobile Agents as a Multi-Agent Ubiquitous Computing Environment

Different ubiquitous computing environments and systems³ have been implemented, each of which deals with a particular aspect of ubiquitous computing research, namely, location-awareness, context-awareness, security, privacy, interfaces, ambient displays, smart objects, collaboration and information sharing. Most projects deal directly with a problem of limited scope and few provide general solutions to more complex problems. The complexity of planetary exploration missions, however, requires that the MAA takes into consideration a diverse set of research questions and provide holistic solutions.

Given the diversity of data sources and components to be integrated, the agent-oriented language Brahms [5][20] has been used as a common communication and computation layer in integrating these diverse systems. It serves as a common programming layer to control devices and to integrate and manipulate captured information.

The Mobile Agents project is one of the few projects that draw on diverse ubiquitous computing and distributed artificial intelligence ideas and approaches into an integrated system for planetary surface exploration. Previous work in the context of campus-based systems for localization and services [11][17] have taken similar but less general models. The ubiquitous computing characteristics implemented in Mobile Agents are described below:

- **Context-Awareness:** The distributed agents have knowledge of other agents in the system and their work practice expectations for performing mission operations and monitoring. Mission plan

¹ Ubiquitous computing and Pervasive computing have been used in the literature interchangeably for extensions of computation beyond the computer. We will use the terms interchangeably.

² See references in related work in [12].

³ An extensive list of projects was started by McCarthy, Jenkins, and Hendry [17] <http://www.ucrp.org/>

knowledge allows the agents to provide assistance in monitoring mission status.

- **Location-Awareness:** The MAA uses GPS tracking devices⁴ on all-terrain vehicles (ATV), astronaut suits and the EVA robotic assistant (ERA) to keep track of GPS coordinates of astronauts, created locations, science data collected, robots. The agents have situational knowledge in reference to static locations. Localization knowledge is further exploited by monitoring agents to provide guidance to humans and robots with regards to deviations from mission transversal paths and time-to-completion.
- **Remote Interaction:** The habitat communicator (HabCom) can monitor, communicate, and command EVA components remotely, given the ability to have situational awareness of the mission through the agent architecture. Remote Science Teams are also able to model the scientific data collection process through data communicated from the field by the agents.
- **Data Storage:** Agent belief-states serve as data storage for all mission-related data. This approach has been previously used, utilizing agents as data storage devices [22].
- **Mobility:** Mobile ubiquitous systems can be thought of as static monitoring environments with sensors, or mobile environments integrated to the clothing of a human (wearable computing applications [21]). The astronauts have integrated computing systems in their suits with connections to health-monitoring sensors. Wireless connectivity enables teams of astronauts to perform similar activities in different locations.
- **Multi-modal Interfaces:** Astronauts can communicate with the agent system through the use of naturalistic speech recognition - a list of commands and responses is listed in [7, 8]. The speech interface is also used for creation of science data (i.e. voice notes) as well as for mission management (i.e. request current location) and for commanding other components (i.e. robot take a picture of me). The HabCom monitors agent interactions through a variety GUI monitoring interfaces and may also perform tasks using the human speech-computer interface.

The MAA consists of layers of functionality which enable agents to collect information from local and remote components and devices. Agents reside with particular

systems and devices which are part of astronaut space-suits, all-terrain vehicle computers, robotic assistants, biomedical monitors, and mission control operations. Some of these components have fixed geographic locations, i.e. the habitat mission control commander, and others are inherently mobile, i.e. the astronauts performing the planetary transversal. The agent layer provides a common language and decision management for coordinating disparate devices, humans, and robots.

Given the scope of its problem domain, the MAA had further requirements and features which are not commonly addressed in ubiquitous computing projects. These assumptions are further challenged and investigated with each natural experiment during field tests [7, 8] and new considerations and problems which arise provide future research endeavors. These qualitative differences and assumptions are listed below:

- **Hybrid Ubiquity:** The MAA system is a combination of static and mobile components. This allows the propagation of a persistent computational environment which moves with the components which need it the most, e.g. astronauts. At the same time, stationary remote science teams and mission control participate through science data exchange, EVA plan development and execution monitoring. This necessitates the ability of the system to have situational knowledge of static and dynamic components. Furthermore, the expectation is that the EVA teams will operate in environments where there is minimal outside infrastructure to support operations. The only assumption is of a habitat in a fixed location and a localization system (at this point an Earth-based GPS system). Wireless network connectivity is provided from the habitat through the use of repeaters with satellite connection to the internet to communicate with earth-based remote science teams.
- **Heterogeneity of Components:** The MAA system provides a common interface and language for robots, astronauts, remote scientists, HabCom, sensors, and systems to collaborate in the context of their shared work practice information.
- **Persistent Monitoring:** The MAA system provides persistent monitoring of mission progress, astronaut and system health, and provides alerting for potentially dangerous situations. Unlike ubiquitous systems that have strong privacy concerns [15] monitoring is at the heart of the MAA, as the movement, health, and activity of astronauts is persistently tracked. This is necessitated by the context of operating in hazardous environments. Similar monitoring has

⁴ We assumed the existence of a localization service. This is an active area of research outside the scope of this project, for example [13].

been applied to ubiquitous multi-agent location-specific contexts [2].

- **Integrated Data Collection:** The MAA system integrates data from different input devices and pushes them to remote science collectors, enabling the collaboration between local and remote human teams. The systems described in [17] usually deal with a restricted set of data or have multiple collection points which do not integrate the information collected. One of MAA's advantages is to enable the local and remote integration and correlation of mission data from disparate sources. Furthermore, new types of devices can be easily integrated into the system through the use of the Brahms Java Application Programming Interface (JAPI).
- **Expansion through Agent Models:** Additional astronauts and robots can be added to the system with minimal integration work, by replicating the agent models. Unlike traditional multi-agent environments which integrate atomic agents, the MAA integrates agent models, which consist of many agents.
- **Resource Management:** Currently the MAA provides basic monitoring of battery power-levels, health-data, and plan workflow data, which can be used in resource management. At this stage, the assumption is that the EVA mission is performed within the energy constraints of the devices utilized. This assumption, however, is qualitatively different than issues explored in the literature with regards to sensors [4]. The role of agents in resource management has been previously investigated through economic mechanisms [10]. Applying resource allocation mechanisms into is a topic of future research for the MAA.

The ability to collect and integrate information from multiple audiovisual input sources is facilitated through the use of the distributed agent environment which takes advantage of the KaOS architecture [1]. The advantage of using a common language to integrate data and functionality is in allowing the use of basic modeling ideas to deal with semantically dissimilar data. Designing an agent to command the robot is semantically equivalent to designing an agent to create a voice annotation from the speech of an astronaut. It also allows the use of common abstractions for performing particular tasks (i.e. Speech Act Theory for communication using FIPA-compliant protocols). In the next section we describe the components of the agent layer in the MAA focusing on the aspects which are directly handled by the community of agents.

3. The Agent Layer in the MAA

The distributed agent community in the MAA is separated into independent Brahms models running on networked computing devices. Figure 1 shows a schematic of the MAA. Each Brahms model consists of a group of agents in each of the work practice components, i.e. astronaut models, robot models, HabCom models. Each human is supported by its own personal agent in each model. Personal agents perform tasks on behalf of the human or device they represent. Their primary function is to translate commands and responses from the astronauts to the MAA. Human input is facilitated through dialog agents, which translate human speech to Brahms beliefs and vice a versa. Brahms inter-agent communication is facilitated through FIPA-compliant communicative SpeechAct definitions. Brahms agents further interact with software logic on other systems and robots through java-based communication agents. All data recorded during the science mission is kept in belief sets of agents. Data may include biomedical information from the biovest sensors, images from digital cameras, voice notes from the speech system, GPS location from the MEX system, and plan tracking information. The belief information is in effect metadata of actual data and/or images further propagated to applications which handle science data.

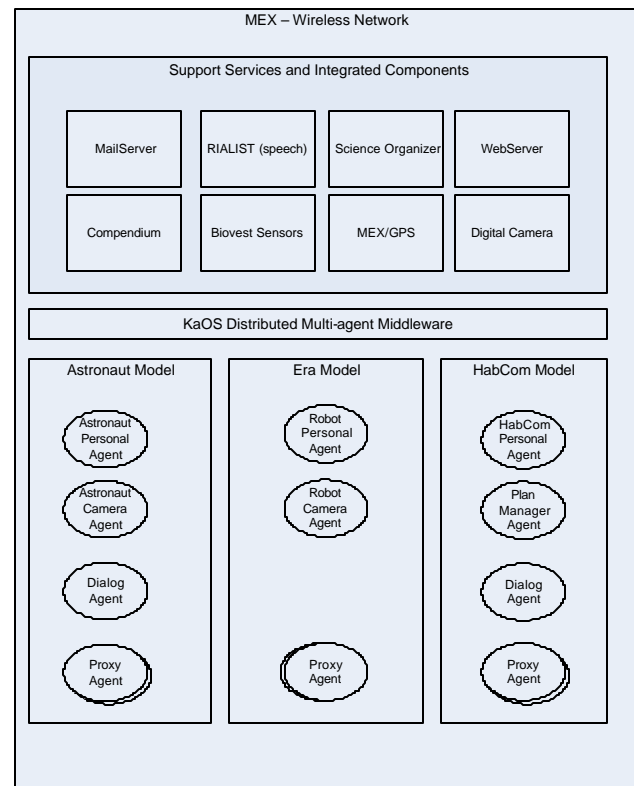


Figure 1: Mobile Agents Architecture

Figure 1 shows a schematic of the mobile agents architecture. There are three types Brahms models, each one running on its own Brahms virtual machine. One

model supporting each astronaut exploring, one controlling the EVA Robotic Assistant, and finally a model supporting HabCom and providing mission monitoring, system monitoring, and data management

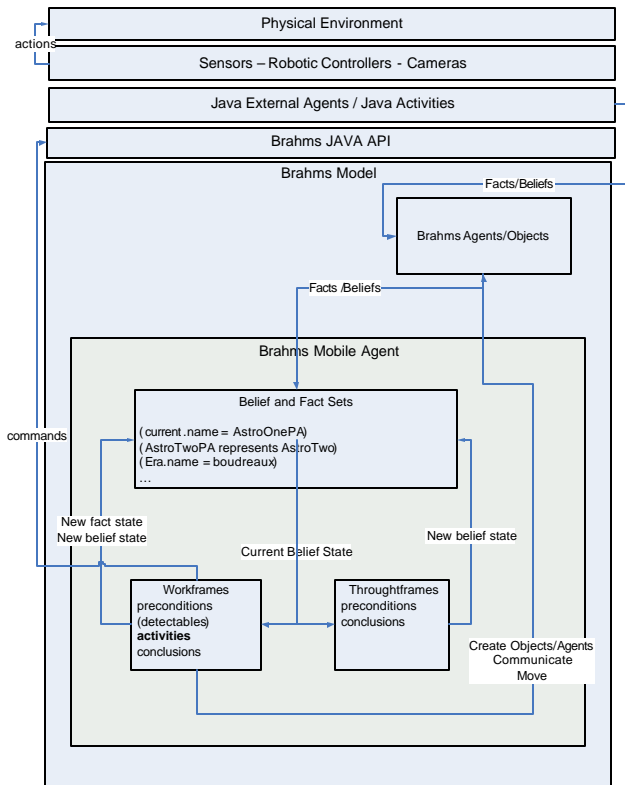


Figure 2: Anatomy of a Brahms Mobile Agent

Brahms agents maintain knowledge of their current state of the world through beliefs and facts⁵. Beliefs represent the information that an agent has about its own state, the state of other agents, and the state of the physical environment as perceived through sensors. An agent may receive beliefs from another agent, from sensors, or from making conclusions based on its own beliefs and results of its own actions. The activities that agents are predominately involved in are communication activities. Their purpose is to update other systems, humans, and robots about their own state of the world. They are also used for commanding and subsequent responses. They also create conceptual objects to represent scientific data collected and generate associations between different sources of data and context based on the agent's beliefs. Figure 2 shows the anatomy of a Brahms mobile agent. The agent receives beliefs about the physical environment from sensors which in turn use the Brahms JAPI to insert beliefs into the agent's belief set. The new beliefs may be preconditions for *workframes* or *throughframes*

⁵ In this exposition we use facts and beliefs interchangeably. See discussion in (Clancey, Sachs, Sierhuis & van Hoof, 1998) for explanation of modeling differences.

(production rules) which in turn trigger conclusions about new beliefs and/or trigger activities. In some cases *workframes* are triggered by *detectables* which are activated when a particular fact is inserted into a Brahms model. An agent's activities may generate interaction with other agents and objects within the Brahms model or across models utilizing the KaOS infrastructure. The infrastructure allows for locating and communicating with other agents on separate Brahms virtual machines across a TCP/IP network.

They may also generate a command to sensors, systems, or robots for commanding or retrieving information through Java activities or through a Java Agent who is integrated with such a system.

We further elaborate on the role of agent models in three functional areas of interest: human-robotic collaboration, plan management, science data management.

3.1 Plan Management

Plan and activities are represented graphically using Compendium⁶. The mission plan delineates which activities will be performed by whom, their duration, location, and thresholds for deviations from standard operating conditions. The plan is uploaded by plan-monitoring agents, who reside within the astronaut personal agents in their respective models. As such, the personal agents provide monitoring capabilities of the state of the mission and provide appropriate alerts to the local and remote mission participants. The alerts are generated when astronauts fail to progress to activities assigned in the plan.

The agent system keeps track of mission data and reacts to the actual mission progress with respect to plan duration and localization constraints. Hence, personal agents keep track of current mission status. Each activity has attributes which denote the limits of the activity instantiation: time limits and location limits. The personal agents provide alerting services when these limits are exceeded. For example, if the astronaut deviates by more than 10 meters from the direction of transversal, a voice warning will be generated by the personal agent tracking location data.

Personal agents can also modify the starting location and/or duration of an activity as per astronaut command. At the same time they keep track of the new plan activities and provide alerts for deviations. The dynamic configuration of plans is facilitated through local agent commands and remote communications with the HabCom who oversees the mission. Currently, during a mission, all astronauts are involved in the same activity. In future scenarios, we will investigate coordination amongst

⁶ For a detailed description of the software and methodology behind compendium visit: <http://www.compendiuminstitute.org/>.

astronauts who are performing overlapping yet separate activities and how their personal agents can assist such coordination.

Keeping track of mission scientific tasks, health status, and localization is a rather formidable set of activities for astronauts. Alerting astronauts of deviations is monitored by agents who can more easily track GPS data and compute when a deviation has happened. Astronauts are informed about the plan and what activity they should be participating in. They are also informed about the expected duration of each activity and get warnings when an activity's projected duration is over. Monitoring the plan is critical given the limited life-support and energy resources available and radiation exposure limits. Plan parameters, such as activity location and duration, can be changed dynamically through the agent layer therefore allowing for the distribution of new plans.

3.2 Science Data Management

The primary objective of all planetary exploration missions is the collection of scientific data. Given the high levels of radiation exposure, astronauts need to be rotated for EVA missions. This necessitates maximizing the scientific data collection during EVAs. The agent system performs science data management including tracking separate sources of information and data files as well as generating associations between them. These data is communicated to the science organizer and remote science teams enabling them to evaluate the science data collected as the EVA is being performed. The data collection and handling is completely transparent to the astronaut performing the EVA. The science data collection requirements include the capture of images of geologically important locations and artifacts, voice-annotations, localization of activities and science data collection, and sample-bag creation and tracking.

The personal agents communicate with remote science team agents whose purpose is to populate a science database shared with the Remote Science Team. The Remote Science Team is comprised of scientists who analyze the results of the EVA. The information is stored in the science organizer, a knowledge management database system for scientific data management. The purpose of having the agents deal with the repeated task for generating, keeping track, and associating science data, has to do with the principle of maximizing astronaut science activity time. Had the astronaut have to do all the aforementioned tasks for every science observation, then the length and mass of data collected would be less. At the same time, the agents provide the necessary communication with the RST, who may also make requests with regards to the science data collection. In that instance, the astronauts may serve as an extension of the RST on to exploration site. This is facilitated through the agent layer which permits remote interaction.

3.3 Mission Data Management

There are different levels of mission data that are kept track of using the multi-agent environment. At each location that an astronaut is, she can give a voice command to its own personal agent who in turn creates objects in the multi-agent system and populate the object with the object's meta data.

Agents monitor the state of the wireless network, the GPS tracking status, the battery levels and issue alerts when needed. These are monitored by the personal agents of the astronauts who are responsible for keeping track of vital systems for the astronaut they represent. Thresholds for maximum and minimum readings are integrated into the logic of the agents, who in turn generate alerts when the GPS tracking goes down, when a command has not been responded for a long time, when the heart-rate or respiration rate of the astronaut is too high, or when batteries are critical. These warnings are critical both for safety and for re-planning given changing environmental and system conditions.

The purpose of pushing mission data management tasks to agents stems from the complexity of tasks that astronauts on EVA are entailed in. It would be cognitively taxing for an astronaut to monitor her health status, battery levels of her computers and perform all mission related work. Since safety is the primary concern with missions, having the agents provide remote information to the mission control at the habitat, further allows remote and local monitoring for critical information. Off-loading these tasks to automated agents brings issues of when and how to provide information regarding health and system status. We expect future field tests to provide us answers to these questions.

4. Conclusions

We have presented the mobile agents architecture as one which integrates many ubiquitous computing and multi-agent approaches into a system which deals with the challenges of planetary exploration. The agent layer of the MAA provides a way for integrating human activity and monitoring devices with data and workflow management systems in an effort to off-loading tasks from human participants. Agents collect, associate, and distribute mission and science data, and manage the mission plan. In order to achieve this, the MAA makes use of different ubiquitous computing technologies and ideas, which are integrated together. The integration of these different research approaches allows Mobile Agents to investigate their interaction through an iterative work-practice analysis approach, with field tests being an integral part of it. This approach resonates with ideas voiced in the ubiquitous computing literature [14] of naturalistic experiments. Requirements collected during the last

MDRS field test (April 2004) are forming the basis for the improvement of the current MAA. Extensions, including autonomous robotic collaboration and human-robotic teamwork models are integrated into the new architecture to be field tested in April 2005.

Acknowledgements

The Mobile Agents project is funded by the NASA/Ames Intelligent Systems Program, Human-Centered Computing area managed by Mike Shafto. The project's PI is Bill Clancey, and the overall project lead is Maarten Sierhuis. The project is a collaboration of eight research teams with more than twenty researchers at NASA Ames Research Center, NASA Johnson Space Center, NASA Glenn Space Center, KMi, Open University, and the University of Southampton in the UK.

Every year the Mobile Agents team tests a new version of the software and hardware at the Mars Dessert Research Station (MDRS) in the Utah dessert. The MDRS is a prototype Mars habitat designed and developed by the Mars Society. Every year, a crew of six lives and works at the MDRS to simulate living and working on Mars supported by MAA, in 2003 as Rotation 16 and in 2004 as Rotation 29. We like to thank the Mars Society for their support in letting us use their facility as out simulation and test environment.

References

- [1] Bradshaw, J. M. et. al. "Representation and Reasoning for DAML-Based Policy and Domain Services in KaOS and Nomads" 2nd IJCAAMS Melbourne, Australia (2003).
- [2] Brueckner, Sven A. and H. Van Dyke Parunak "Swarming Agents for Distributed Pattern Detection and Classification." *AAMAS, Workshop on ubiquitous agents on embedded, wearable, and mobile devices*. Bologna, Italy (2002).
- [3] Barkhuss, L. and Dey, A. "Is Context-Aware Computing Taking Control away from the User? Three Levels of Interactivity Examined." *Proceedings of the 5th International Conference on Ubiquitous Computing*, Seattle, WA (2003).
- [4] Chakravorty, R., Vidales, P., Dragovic, B., Policroniades, C. and Patanapongpibul, L. "Ubiquity in Diversity - A Network-Centric Approach." *In Adjunct Proceedings, 5th International Conference on Ubiquitous Computing*, Seattle, WA (2003).
- [5] Clancey, W. J., Sachs, P., Sierhuis, M., and Hoof, R. v. "Brahms: Simulating practice for work systems design." *International Journal of Human-Computer Studies* (49) (1998): 831-865.
- [6] Clancey, W. J., Sierhuis, M., Kaskiris, C., and Hoof, R. v., "Brahms Mobile Agents: Architecture and Field Tests.," presented at *AAAI Fall Symposium*, North Falmouth, MA, 2002.
- [7] Clancey, W. J., Sierhuis, M., Kaskiris, C., and Hoof, R. v. "Advantages of Brahms for Specifying and Implementing a Multiagent Human-Robotic Exploration System." *The 16th International FLAIRS Conference*, St. Augustine, FL, (2003).
- [8] Clancey, W. J., Sierhuis, M., Alena, R., Crawford, S., Dowding, J., Graham, J., Kaskiris, C., Tyree, K., and Hoof, R. v. "The Mobile Agents Integrated Field Test: Mars Desert Research Station April 2003." *The 17th International FLAIRS Conference*, ST. Augustine, FL, (2004a).
- [9] Clancey, W. J., Sierhuis, M., Alena, R., Crawford, S., Dowding, J., Graham, J., Kaskiris, C., Tyree, K., and Hoof, R. v. "The Mobile Agents: A Distributed Voice-Commanded Sensory and Robotic System for Surface EVA Assistance." *9th ASCE Aerospace Division International Conference*, Houston, TX, (2004b).
- [10] Clearwater, S. (ed.): *Market Based Control*, World Scientific (1996)
- [11] Griswold, W. G., et. al. "UCSD ActiveCampus - Mobile Wireless Technology for Community-Oriented Ubiquitous Computing." *In Adjunct Proceedings, 5th International Conference on Ubiquitous Computing*, Seattle, WA (2003).
- [12] Harle, R. K. and Hopper A. "Building World Models by Ray-Tracing with Ceiling-Mounted Positioning Systems." *Proceedings of the 5th International Conference on Ubiquitous Computing*, Seattle, WA (2003).
- [13] Huntsburger, Terry et al. "Sensory Fusion for Planetary Surface Robotic Navigation, Rendezvous, and Manipulation Operations," *Proceedings of ICAR The 11th International Conference on Advanced Robotics*, Coimbra, Portugal (2003)
- [14] Intille, S., Munguia, M. T., Rondoni, J., Beaudin, J., Kukla, C., Agarwal, S., Bao, L., and Larson, K. "Tools for Studying Behavior and Technology in Natural Settings." *Proceedings of the 5th International Conference on Ubiquitous Computing*, Seattle, WA (2003).
- [15] Kaskiris, C. "Socially-Informed Privacy-Enhancing Solutions: Economic Privacy and the Negotiated Privacy Boundary" *Workshop on Socially Informed Design of Privacy-enhancing Solutions in Ubiquitous Computing, 5th International Conference on Ubiquitous Computing*, Seattle, WA (2003).
- [16] Kruger, A. and Malaka, R. "AIMS2003 Artificial Intelligence in Mobile Systems," *In Adjunct*

- Proceedings, 5th International Conference on Ubiquitous Computing*, Seattle, WA (2003).
Adjunct Proceedings,” *5th International Conference on Ubiquitous Computing*, Seattle, WA (2003).
- [18] Schilit, B., Adams, N., and Want, R. “Context-aware Computing Applications,” *In Proceedings of the Workshop on Mobile Computing Systems and Applications*. (1994).
- [19] Scott, J. and Hazas M. “User-Friendly Surveying Techniques for Location-Aware Systems,” *Proceedings of the 5th International Conference on Ubiquitous Computing*, Seattle, WA (2003).
- [20] Sierhuis, M. “Modeling and Simulating Work Practice,” PhD Thesis. Social Science and Informatices (SWI). University of Amsterdam, The Netherlands, ISBN 90-6464-849-2.(2001).
- [17] McCarthy, J.F., Jenkins, J.R., and Hendry, D. G.: “The Ubiquitous Computing Resource Page. In Sparacino, F. “Sto(ry)chastics: A Bayesian Network Architecture for User Modeling and Computational Storytelling for Interactive Spaces,” *Proceedings of the 5th International Conference on Ubiquitous Computing*, Seattle, WA (2003).
- [21] Villate, Y., Illarramendi, A., and Pitoura E. “Mobile and External Storage Space Using Agents for Users of Mobile Devices,” *AAMAS, Workshop on Ubiquitous Agents on Embedded, Wearable, and Mobile Devices*. Bologna, Italy (2002).
- [22] Weiser, M.: “The Computer for the 21st Century.” *Scientific American*, 265(3):94-104 Sept (1991).

Real-Time Background Estimation from Occluded Image using Iterative Optimal Projection Method

Satoshi KAWABATA, Shinsaku HIURA and Kosuke SATO

Graduate School of Engineering Science, Osaka University

1-3 Machikaneyama, Toyonaka, Osaka 560-8531 Japan

tel : +81-6-6850-6371

fax : +81-6-6850-6341

e-mail : shinsaku@sys.es.osaka-u.ac.jp

Topics : Measurement, monitoring, and reliable control

Real-Time Background Estimation from Occluded Image using Iterative Optimal Projection Method

Satoshi KAWABATA, Shinsaku HIURA and Kosuke SATO
Graduate School of Engineering Science, Osaka University

Abstract

We have proposed an intrusion detection system which calculates the shape of intersection of intruders on sensitive planes using silhouette-based shape reconstruction. Our system has advantages of efficiency against the other systems which reconstructs whole shape of intruder because it is enough for detection of intrusion to watch only on the surface of regions to be monitored. However, we have assumed that there are no moving objects except intruders in the observing space. In this paper, we propose the iterative optimal projection method to estimate a varied background in real time from a dynamic scene with intruders. At first, the background images are collected for a while, because we assume that the motion of background is well known. Then, the background images are compressed using eigenspace method to form a database. While the monitoring of the scene, new image is taken by a camera, and the image is projected onto the eigenspace to estimate the background. But however, the estimated image is much affected by the intruders, so that the region of intruder is calculated by using background subtraction using former estimated background. Then eigenspace projection is executed using the image whose region of the intruder is replaced by the former background and we have updated background. We proved that the cycle converges to a correct background image and we confirmed we can calculate the right region of the object through some experiments.

1 Introduction

Nowadays a lot of cameras are used at shops, museums, banks, roads and so on, but taken images are only recorded and mainly used for evidence for post-mortem. In the case of very critical missions which requires real-time responses, human would watch many monitors tiled on a wall. To save such labor and cost for monitoring, special sensors are often used. Light beam detectors are used to find undesirable intrusion, but the sensitive lines are not flexible because it is

strictly related to the arrangement of the equipments. Passive infra-red sensor which detects the heat of human body is also widely used, but it will detect only the existence of the human body and detailed observation of monitoring area is impossible.

For replacing human observer with a computer, image-based surveillance and monitoring method is extensively researched. For example, DARPA VSAM project[1] and ISPS CDV project[2] are intensively attacked to the problem and produced many successful results. However, most methods proposed by these projects are complicated and difficult to use because they tried to understand the action of the object. Therefore, we focused to find the objects intruding to the 3-D restricted area. To make it possible, we proposed silhouette-based planar view-volume intersection method which watches only the surface of restricted area. In experiments, it works well when the silhouette is extracted from input image correctly. Since we used background subtraction[3] to calculate the silhouette, the background must be static. Therefore we developed new background subtraction algorithm to cope with the dynamic but known object using eigenspace-based method. In the latter half of this paper, we describe and evaluate our approach.

2 Detection of Intruders

As a first step of autonomous monitoring, we aimed to only detect the intruder who goes across critical surfaces which is arranged by a supervisor. It is very simple but generic and easy to understand, and we believe that it is enough satisfactory to the most applications. In this paper we propose a practical intrusion detection system based on a contour-based multi-planar visual hull method. The system consists of several sets of a camera and a PC connected via network. Prior to the monitoring, a system manager will set up several sensitive planes in the world using a GUI. Input image taken by the camera is shown on the display, and the manager simply set the boundary of the sensitive planes as shown in Figure 1. To detect

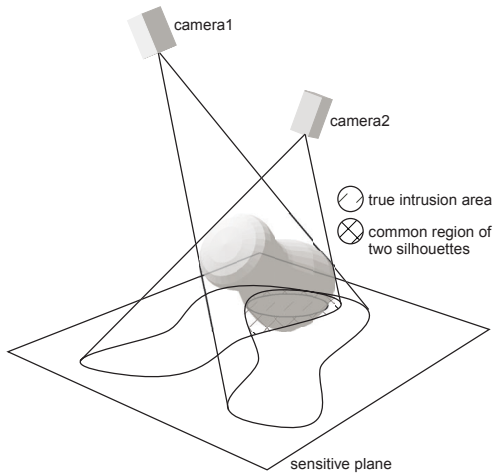


Figure 1: Planar view-volume intersection method.

the intruding objects, images taken by the cameras are compared with a maintained background image using PISC method[3] which is an object detection method based on background subtraction, and is very robust against shadows and changes of illumination. Then the contour of the object region on a image is traced and transformed to the coordinate of sensitive plane. It much accelerates the data transfer via network, because the data of the traced contours are much more compact than the raw binary images. The contours are collected to a single PC and the shape of the common regions are calculated. If the intruding object exceeds the sensitive plane, the contours from each PC would have some common regions as shown in Figure 1. If the intruder occludes the critical point on the sensitive planes from the all cameras to avoid observation, the system also alerts to the user. This system does not reconstruct the shape of the object, but the system is able to handle 3-D restricted volumes because multiple sensitive planes can be set arbitrarily. This system does not require us to calibrate the camera because this system is based on 2-D homography.

The important properties of actual monitoring system are as follows: 1) easy to install, 2) robustness, 3) responsibility to the unexpected events. In fact, our system does not restrict the shape of the critical surfaces (sensitive planes) and it is not related to the location of the cameras. The cameras are not necessary to be calibrated in advance, and the sensitive planes can be set on the input image displayed on a GUI interface. Since our system is based on the background subtraction method, we employed robust PISC algorithm. It is robust to the change of illumination or shadow of the object. Our system will alert

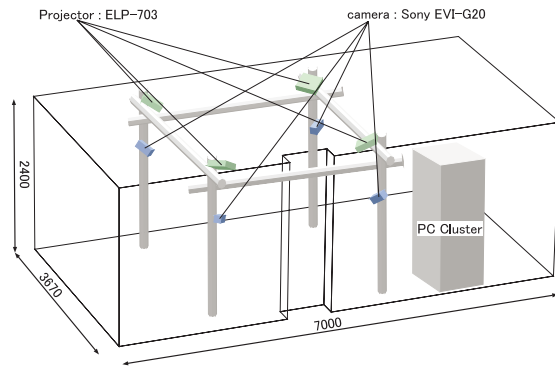


Figure 2: Experimental setup of monitoring system.

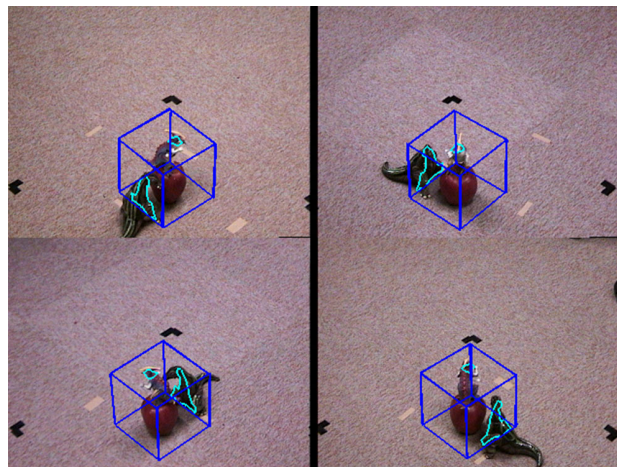


Figure 3: Result of detected intrusion.

when the critical point (intersection of the object and sensitive planes) is occluded by the other object. This characteristic is preferable to the monitoring system.

We made a system for experiment with four cameras set on the each corner of the ceiling as shown in figure 2. We used four Sony EVI-G20 cameras which is connected to a PC cluster. PC cluster consists of eight PCs connected via 100Mbps Ethernet. We achieved real-time detection of object intrusion with four sensitive planes around the object as shown in figure 3.

3 Detection of Object Region in front of Dynamic Background

Background subtraction uses static background captured before monitoring, therefore it can not handle the moving object as a background. Real-time background maintainance, such as median filter, is

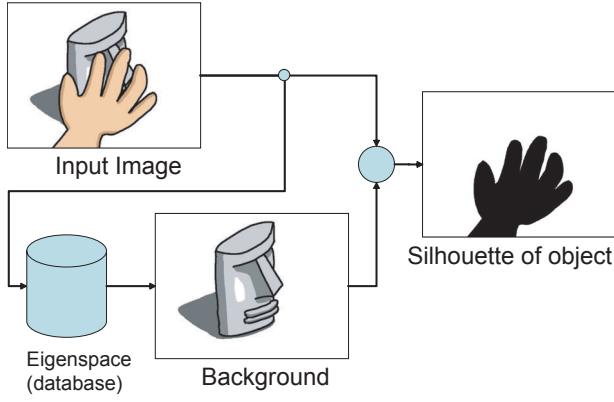


Figure 4: Eigenspace-based dynamic background subtraction.

widely used to solve this problem, but fast motion of the background object will be detected as a intruder. Therefore, we used a sequence of background to make a database of known scene, and then the background subtraction is executed using varing background estimated from the database as shown in Figure 4.

3.1 Image Reconstruction using Eigenspace

When we have s background images $\mathbf{x}_1, \dots, \mathbf{x}_s$, one of background images \mathbf{x}_i can be approximated using matrix $E = [e_1 \dots e_d]$ ($d < s$) which consist of orthonormal basis e_1, \dots, e_s calculated using principal component analysis (PCA), as

$$\mathbf{x}_i \approx E\mathbf{p}_i + \bar{\mathbf{x}} \quad (1)$$

where e_1, \dots, e_s is called as eigenvectors. To simplify the equation, we omit the average image $\bar{\mathbf{x}}$ because it is constant.

$$\mathbf{x}_i \approx E\mathbf{p}_i \quad (2)$$

Inversely, we can calculate the point \mathbf{p} in an eigenspace which corresponds to the background image \mathbf{x} as

$$\mathbf{p} = E^T \mathbf{x} \quad (3)$$

where $(E^T E)^{-1} E^T = E^T$, because E is orthonormal. If we have the point \mathbf{p} , the background image \mathbf{x} can be reconstructed using eigenvectors.

$$\mathbf{x} \approx E\mathbf{p} \quad (= EE^T \mathbf{x}) \quad (4)$$

3.2 Estimation of Background

As described above, we can reconstruct the background image if we can estimate the point in an eigenspace, \mathbf{p} . In this paper, we propose the method to estimate \mathbf{p} from a image $\tilde{\mathbf{x}}$ a part of which is occluded by unknown objects. BPLP method[5] calculates the point to minimize the difference between input and estimated image except the occluded region. This method can be represented using diagonal matrix Σ whose diagonal element is 0 when the corresponding pixel is occluded and 1 not occluded, as

$$\varepsilon^T \varepsilon \xrightarrow{\mathbf{p}} \min. \quad (5)$$

$$\varepsilon = (\tilde{\mathbf{x}} - E\mathbf{p})^T \Sigma^T \Sigma (\tilde{\mathbf{x}} - E\mathbf{p}) \quad (6)$$

and the solution $\hat{\mathbf{p}}$ is given as follows.

$$\hat{\mathbf{p}} = (E^T \Sigma^T \Sigma E)^{-1} E^T \Sigma^T \Sigma \tilde{\mathbf{x}} \quad (7)$$

But however, equation (7) takes much time because d^2 times multiplication of image by image must be calculated. So that, we propose an iterative projection method as follows. Instead of equation (7), we use a recurrence equation,

$$\hat{\mathbf{p}}_n = E^T \hat{\mathbf{x}}_{n-1} \quad (8)$$

and we can calculate n^{th} estimated point $\hat{\mathbf{p}}_n$ using $n - 1^{th}$ estimated background. The background image $\hat{\mathbf{x}}_{n-1}$ is a composition of former estimated background and input image $\tilde{\mathbf{x}}$,

$$\hat{\mathbf{x}}_{n-1} = \Sigma \tilde{\mathbf{x}} + (I - \Sigma) E \hat{\mathbf{p}}_{n-1} \quad (9)$$

where the occluded region of input image is replaced by the former estimated background.

From these equations, general term can be lead out as

$$\begin{aligned} \hat{\mathbf{p}}_n &= \{I - (I - E^T \Sigma^T \Sigma E)\}^{-1} \\ &\quad \left\{ I - (I - E^T \Sigma^T \Sigma E)^n \right\} E^T \Sigma^T \Sigma \tilde{\mathbf{x}} \\ &\quad + (I - E^T \Sigma^T \Sigma E)^n \hat{\mathbf{p}}_0 \end{aligned} \quad (10)$$

In addition, if $\|I - E^T \Sigma^T \Sigma E\|_2 < 1$ is satisfied, the limit of recurrence equation converges to

$$\lim_{n \rightarrow \infty} \hat{\mathbf{p}}_n = (E^T \Sigma^T \Sigma E)^{-1} E^T \Sigma^T \Sigma \tilde{\mathbf{x}}. \quad (11)$$

This equation shows that our method converges to the optimal solution which is same as BPLP described above.

3.3 Updating Occlusion Mask

Both BPLP and our method needs information of the region occluded by intruders, Σ . Unfortunately, this diagonal matrix is unknown because the objective of our research is to estimate the silhouette of the unknown object. Therefore, we calculate the mask Σ by using simple background subtraction as

$$\Sigma(j) = \begin{cases} 1, & \text{for } |\hat{\mathbf{x}}(j) - \mathbf{x}(j)| < th \\ 0, & \text{for } |\hat{\mathbf{x}}(j) - \mathbf{x}(j)| \geq th \end{cases} \quad (12)$$

where th is a threshold and (j) denotes each pixel or element of diagonal matrix. Of course, the estimated background $\hat{\mathbf{x}}$ is varied when the occlusion mask Σ changes, therefore, background estimation described in section 3.2 and background subtraction by equation (12) must be iterated. The sequence of simultaneous estimation of background and object region is summarized as follows.

BPLP:

1. capture new image $\tilde{\mathbf{x}}$,
2. equation (7) for background estimation using old object region Σ ,
3. equation (12) to update object region Σ ,
4. go to 1.

Proposed method:

1. capture new image $\tilde{\mathbf{x}}$,
2. equation (9) to combine input image and old background using old object region Σ ,
3. equation (8) to estimate new background image,
4. equation (12) for update object region Σ ,
5. go to 1.

Evidently our method has faster frame rate of background subtraction, and it has a potential to faster convergence to the correct region and background.

4 Experiments

4.1 Evaluation using CG images

To compare our method to BPLP equally, we used synthetic images for background and input images. Figure 5(a) shows the background image (ground truth) and 5(b) input image generated by POV-Ray 3.6. In both figures, star-shaped background object rotates just three-sixty through 256 images. The dimension of eigenspace is 58 when accumulation contributing ratio is 95%.

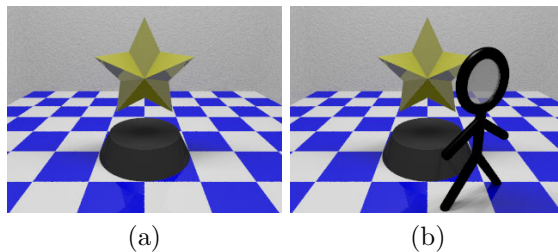


Figure 5: Rendered CG image. (a) background image, (b) input image with moving intruder. In both images, centered star-shaped object rotates.

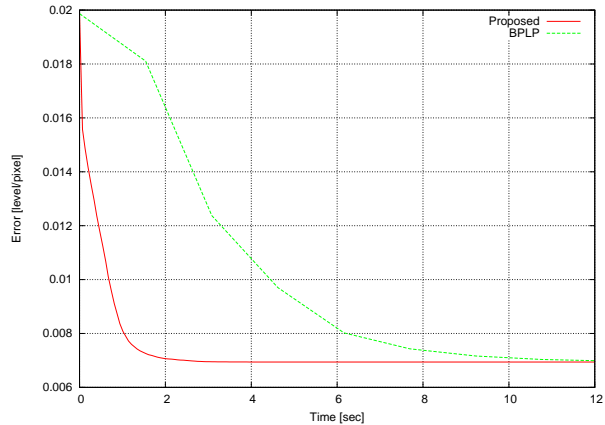


Figure 6: Convergence for fixed image

4.1.1 Experiment 1 : Convergence for Fixed Image

In this experiment, we compare the speed of convergence using fixed input image. We used an average image as an initial value.

Figure 6 shows the result of convergence. The error is a variance between estimated image and ground truth. By this result, it is better to update the object region mask rapidly than the slow calculation of the optimal value.

4.1.2 Experiment 2 : Error for real-time sequence

In this experiment, we checked the error for a stream of images. We assumed all 256 images as a sequence of images of 30frames/sec, therefore the period of all images is 8.53sec. Figure 7 shows the sequence of error value for both method. In this figure, vertical line indicates the time of updating background image.

For real-time sequence, our result shows not only less error but also faster cycle of estimation. Table 1 shows the average of the error through the se-

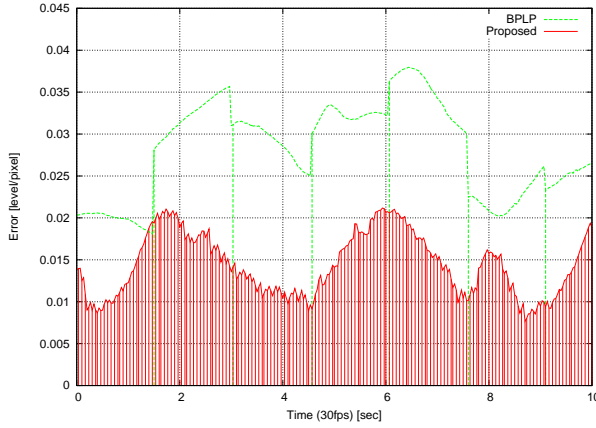


Figure 7: Error for real-time sequence

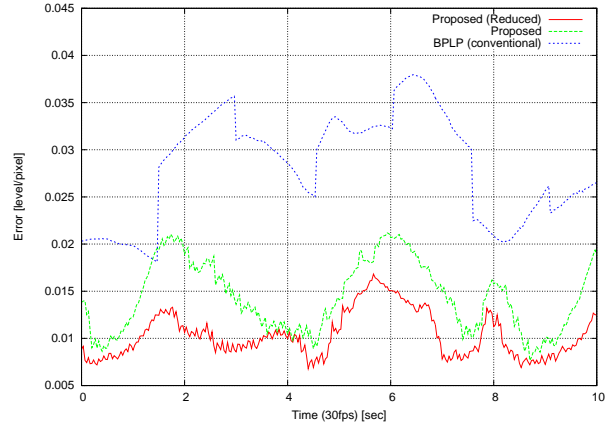


Figure 8: Improvement by exclusion of static pixels

Table 1: Average of error of estimated background

without object region exclusion	0.090839
BPLP	0.028175
Our method	0.014375
Our method (excludes static pixels)	0.010365

quence. This results shows our method has better performance for real-time sequence.

4.1.3 Static Pixel Exclusion

In actual, a part of background image stays static while the background includes dynamic object. Therefore, we exclude such pixels from the estimation. Figure 8 shows the effect of exclusion of static pixels. Since the cycle time of estimation is shorter, the error of estimation becomes smaller. The frame rate of this method is 20fps to 30fps.

4.2 Evaluation using real images

We used equipments for this experiment as follows.

- PC : Dual Xeon (HT) 3.6GHz, RAM 2GB
- Graphics : GeForce Quadro FX 3400
- Camera : Sony DFW-VL500 (IEEE 1394)

Figure 9 shows the screenshot of our system. The background is a miniature of dinosaur rotating on a chair, and the intruding object is a miniature of white cat. The dimension of eigenspace is 46 when the number of background image is 256 and accumulation contributing ratio is 95%. In Figure 9, top-left is input image($\hat{\mathbf{x}}$), top-right estimated background



Figure 9: Background Estimation using real images

($E\hat{\mathbf{p}}_n$), bottom-left mask image (Σ) and bottom-right combined image ($\hat{\mathbf{x}}_n$), respectively. The region of the intruding object is extracted correctly while the background object is moved.

5 Conclusions

In this paper, we described a method to achieve autonomous scene monitoring system. At first, we proposed a practical intrusion detection system based on a view-volume intersection method. The system consists of four sets of a camera and a PC connected via network and several sensitive planes in the world is defined by the system administrator using a GUI. This system does not require us to calibrate the camera because this system is based on 2-D homography.

To detect intrusion, the object is extracted us-

ing improved background subtraction method named PISC. Then the contour of the object silhouette is traced and transferred to the server PC. The collected contours are transformed to the coordinate of sensitive plane. The server PC judges the existence of a common region. If the intruding object crosses the sensitive plane, the contours from each PC would have some common regions.

In the latter half of our paper, we proposed novel background subtraction method for dynamic scene. A sequence of background is used to make a database based on eigenspace method, and the background is estimated from the input image which includes unknown objects. Compared to the previous work, our method is not only faster but also more precise to estimate both background and occluded region.

References

- [1] DARPA VSAM (Video Surveillance and Monitoring) Project, <http://www-2.cs.cmu.edu/vsam/OldVsamWeb/vsamhome.html>
- [2] T. Matsuyama: Cooperative Distributed Vision: - Dynamic Integration of Visual Perception, Action, and Communication-, 23rd Annual German Conference on Artificial Intelligence and 21st DAGM-Symposium, September 1999.
- [3] S. Kaneko, Y. Satoh and S.Igarashi: Robust Object Detection in Image Sequence Using Peripheral Increment Sign Correlation, Proc. of 5th Japan-France Congress on Mechatronics, pp.287-292, 2001.
- [4] Satoshi Kawabata, Shinsaku Hiura and Seiji Inokuchi : Intrusion Detection System using Contour-based Multi-Planar Visual Hull Method, IEEE Conference on Multisensor Fusion and Integration for Intelligent Systems (MFI2003), pp. 293-298 (Jul. 2003)
- [5] Toshiyuki Amano, Yukio Sato: Image Interpolation using BPLP Method on the Eigenspace IEICE Journal D-II, Vol.J85-DII No.3 pp.457-465, 2002(in Japanese).

Topic: "Evaluation and diagnosis of complex systems"

**Probabilistic Reliability Assessment for Complex Systems
in the Absence of Operating Experience Data**

Christian Kirchsteiger

European Commission, Directorate-General Joint Research Centre (DG JRC),

Institute for Energy, Westerduinweg 3, 1755 LE Petten, The Netherlands

christian.kirchsteiger@jrc.nl

<http://www.energyrisks.jrc.nl>

Probabilistic Reliability Assessment for Complex Systems in the Absence of Operating Experience Data

Christian Kirchsteiger

European Commission, Directorate-General Joint Research Centre,
Institute for Energy, Westerduinweg 3, 1755 LE Petten, The Netherlands

Abstract: The objective of this paper is to show how probabilistic reliability can be assessed for complex systems in the absence of statistical data on their operating experience, based on performance evaluation of the dominant underlying physical processes. The approach is to distinguish between *functional* and *performance* probabilities when dealing with the quantification of the overall probability of a system to perform a given function in a given period of time (reliability). In the case of systems where sufficient statistical operating experience data are available, one can focus the quantitative evaluation entirely on the assessment of the functional probability for a given active item (e.g. a pump) by assuming that the specification, layout, construction and installation is such that the item is providing the assigned performance, e.g. in the form of generating the required flow rate. This is how traditional Probabilistic Safety Assessments (PSAs) focus the reliability analysis for the various safety features on the calculation of values for the availability per demand. In

contrast, for various systems relevant in advanced technical applications, such as passive safety features in innovative reactor designs, it is essential to evaluate both functional and performance probabilities explicitly and combine the two probabilities later on. This is of course due to the strong reliance of passive safety systems on inherent physical principles. In practice, this means that, for example, in case of a passive cooling system based on natural circulation of a given medium, one has to evaluate and to assess the probability to have a medium condition and a flow rate such that a cladding temperature, represented by a probability distribution, can be hold at a required level. A practical example of this method is given for the case of the reliability assessment of a residual passive heat removal system. General conclusions are drawn regarding reliability estimation of complex, interconnected systems in the absence of statistical performance data, such as for infrastructures.

1. Introduction

Innovative reactor concepts make use of passive safety features to a large extent in combination with active safety or operational systems. A "passive system" does not need external input, such as energy, to operate. This is why it is expected that passive systems combine the advantages of simplicity, reduction of the need for human interaction, reduction or avoidance of external electrical power or signals.

However, to be able to judge their overall performance, special aspects such as missing operating experience over the wide range of conditions, lack of data on some phenomena and the smaller driving forces as compared to active safety systems have to be taken into account.

This is especially true for so-called Category B passive systems (following IAEA classification [1]), i.e. those which rely on natural forces and whose accident prevention and mitigation functions are, once the systems are started, not provided by means of external power sources.

Theoretically, a passive system should be much more reliable than an active one as

it does not need any external input or energy to operate and it relies only upon

- the natural laws of physics (e.g. gravity, natural circulation, convection, etc.) and/or
- inherent characteristics (properties of materials, internally stored energy, etc.) and/or
- "intelligent" use of the energy that is inherently available in the system (e.g. decay heat, chemical reactions, etc.).

Historically, in the 1980's when passive safety system designs were probably first considered explicitly, the attitude of safety analysts has been to allocate an "almost perfect" reliability, i.e. probability $P \cong 1$, to passive systems and consequently ignore the need for their inclusion in PSA or, in general, nuclear power plant (NPP) reliability models. The argument was that a passive safety system has already a small unavailability to come into operation due to hardware failure and human error and that the likelihood of the occurrence of physical phenomena leading to pertinent failure modes of the system, once it comes into operation, can be considered zero as these phenomena rely entirely on the (deterministic) laws of

nature, thus having probability 1 of intended operation.

Since the 1990's, however, after observing some real deviations from intended operation (failure that control rods fall under gravity, stratification breaking natural convection, environmental phenomena diminishing radiation efficiency, etc.), passive systems were started to be considered like other engineered systems, i.e. through their physical performances under real conditions, and having reliability values $P < 1$. Consequently, a need for inclusion of passive systems and their reliability values in PSA arose.

This realization of "non-perfect reliabilities" for passive systems can, in principle, be verified in different ways for the different IAEA Categories:

- For Category A passive systems¹, structural reliability analysis methods can be applied.
- For Categories C and D², sufficient operating experience (statistical data)

¹ *Category A* systems are characterized by no signal inputs of "intelligence", no external power sources or forces, no moving mechanical parts or no moving working fluid. Examples are physical barriers and static structures (e.g. pipe wall, concrete building).

² *Category C*: characterized by no signal inputs of "intelligence", no external power sources or

is available in order to apply the classical tools of statistical reliability analysis.

Only for Category B systems, i.e. those which rely on natural forces and whose accident prevention and mitigation functions are, once the systems are started, not provided by means of external power sources (i.e. essentially thermo-hydraulic (T-H) systems), new methods have to be developed. Here, "non-perfect reliabilities" are generated due to the fact that the natural forces which drive the operation of the passive systems have a relatively small magnitude, thus enabling possible counter-forces, such as friction, to be of comparable, non-ignorable magnitude [2]. For such systems, a need to develop a specific quantitative reliability assessment method has been

forces, but moving mechanical parts, independent of presence of moving working fluids. The movement of the fluid is characterized as for Category B; mechanical movements are due to imbalances within the system (e.g. static pressure in check and relief valves, hydrostatic pressure in accumulators) and forces directly exerted by the process. Examples for Category C systems are check valves.

Category D addresses the transition area between active and passive where the execution of the safety function is made by means of passive methods as described for the previous categories, except that internal "intelligence" is not available here to initiate the passive process, but an external signal ("passive execution / active initiation"). Examples are scram systems.

recognized at EU level and the development work in a corresponding EU research project is described in Section 2.

2. An Approach to Quantify Reliability of T-H Passive Systems

To address the need to develop a method to quantitatively assess the reliability of Category B passive systems, a research project has been launched by the European Commission under its 5th Research Framework Program, called "Reliability Methods for Passive Systems" (RMPS), and successfully been concluded in early 2004 [3]. Main objective of RMPS was to develop a methodology to quantify the reliability of a T-H passive system. Applications were done on three passive safety systems: The isolation condenser system (ICS) of a BWR, the residual heat removal system of a PWR and the hydro-accumulator of a VVER.

The originality of RMPS is to gather methods coming from different disciplines (T-H, Structural Reliability, PSA and Monte Carlo simulation among others) and to further adapt and complete them in order to propose an efficient integrated methodology for assessing the reliability of a passive safety system.

The RMPS methodology consists of the following main steps:

- 1) Definition of the accident scenario of interest;
- 2) Characterisation of the passive safety system in terms of its mission, failure modes and success / failure criteria;
- 3) Modelling of the system by using a T-H computer code and performing best-estimate calculations³;
- 4) Identification and quantification of sources of uncertainties and determination of important variables by using expert judgement (EJ);
- 5) Identification of relevant parameters which affect accomplishment of system mission by using systematic EJ methods such as the Analytic Hierarchy Process (AHP) [4];
- 6) Quantification of uncertainties and their propagation through the T-H code (or a surrogate model obtained by means of, for example, response surface techniques) used to simulate the physical process and estimation of the passive system reliability (via common statistical estimation or via

³ Within RMPS, in order to validate reference calculations and to test different approaches to uncertainty analysis, the ICS has been modeled separately by the ATHLET, RELAP5 and CATHARE codes.

approximate methods such as FORM/SORM);

- 7) Incorporation of the estimated reliability of the passive system into the plant-specific PSA⁴.

The RMPS reliability assessment approach is based on the Resistance-Stress (R-S) model taken from Structural Reliability Analysis, where, in the present context, R and S represent a system's functional requirement (R) and state (S) and are characterized by their respective probability density functions. The structure is supposed to fail whenever the state does not fit the requirements. For example, water mass flow circulating through the system could be accounted for as physical quantity defining the (passive) system performance; the system could be considered to fail if this performance measure goes below a given reference value. In other words, the mission of the passive system defines which parameter values are considered a failure by comparing the corresponding probability density functions with the respective, deterministically defined safety criteria.

⁴ Within RMPS, this last point was, however, only touched and, due to project time constraints, no integration of the reliability assessment case studies into a real PSA model could be achieved.

Given a best estimate T-H code and a model of the (passive) system to be analysed, the performance function of this system according to its specified mission is:

$$M = \text{performance criterion} - \text{limit} \\ = g(X_1, X_2, \dots, X_n)$$

in which the X_i ($i=1, \dots, n$) are the n basic random input variables (input parameters, split up for methodological purposes in this project in design and critical parameters), and $g(\cdot)$ is the functional relationship between the random variables and the failure of the system [3]. The performance function can be defined such that the limit state, or failure surface, is given by $M = 0$. The failure event is defined as the space where $M < 0$, and the success event as the space where $M > 0$. Thus a probability of failure can be evaluated by the following integral:

$$P_f = \int_{M < 0} f_{\mathbf{x}}(\mathbf{x}) d\mathbf{x} , \quad (1)$$

where $f_{\mathbf{x}}(\mathbf{x})$ is the joint density function of X_1, X_2, \dots, X_n , and the integration is performed over the region where $M < 0$. Because each of the basic random variables has a unique distribution and they interact, the integral (1) cannot easily be evaluated. Two types of methods have been identified within RMPS to estimate the probability of

failure: The Monte Carlo simulation with or without variance reduction techniques and some approximate methods (FORM/SORM):

- *Direct Monte Carlo simulation techniques* can be used to estimate the probability of failure defined in equation (1) (or its complement to 1, the reliability). Monte Carlo simulation consists of drawing samples of the basic variables according to their probabilistic characteristics and then feeding them into the performance function. An estimate \hat{P}_f of the probability of failure P_f can be found by dividing the number of simulation cycles in which $g(.) < 0$ by the total number of simulation cycles N . As N approaches infinity, \hat{P}_f approaches the true probability of failure. The estimation accuracy can be evaluated in terms of its variance. For a small number of simulation cycles, the variance of \hat{P}_f can be quite large compared to the actual value of P_f . Additionally, as a rule of thumb, failure probabilities P_f demand sample sizes of at least $1/P_f$ in order to get acceptable estimates. Consequently, it may take a

large number of simulation cycles, mainly if the system is actually reliable ($P_f \approx 10^{-3} \Rightarrow N > 10^3$), to achieve a relevant accuracy and the amount of computer time needed will be large, up to several weeks, especially when each simulation cycle is performed by a T-H code.

- *Variance reduction techniques*, such as importance sampling, stratified sampling, Latin hypercube sampling, control variates, antithetic variates and directional simulation offer an increase in the efficiency and accuracy of the simulation-based assessment of the passive system reliability, providing acceptable estimate uncertainty ranges for small number of simulation cycles.
- *Approximate methods*, such as First- and Second-Orders Reliability Methods (FORM/SORM) consist of 4 steps:
 1. Transformation of the space of the basic random variables X_1, X_2, \dots, X_n into a space of standard normal variables ($N(\mathbf{0}, \mathbf{I})$);
 2. Determination, in this transformed space, of the point of minimum distance from the origin on the limit

state surface (this point is called the design point);

3. Approximation of the failure surface near the design point;
4. Computation of the failure probability corresponding to the approximate failure surface.

FORM and SORM apply only to problems where the set of basic variables is continuous. For small order probabilities, FORM/SORM are extremely efficient as compared to simulation methods. The calculation time is for FORM approximately linear in the number of basic variables and independent of the probability level. The drawback of these methods is that when the failure surface is not sufficiently smooth, problems arise in determining the design point. Additionally, they do not provide error estimates. Response surface methods can help and within RMPS a specific method has been developed to build and validate response surfaces.

- *Influence of choice of input distribution on output:* Knowledge uncertainty is the main source of uncertainty affecting as much design

parameters as critical parameters⁵. This fact forces PSA analysts to use EJ as a main source of information for assigning probability distributions. Experts some times disagree with each other and some other times change their opinion, as more information is available, so that, in many cases, the analysis of the system under different input parameter distributions deserves some attention. The codes used to calculate the T-H performance of a passive system may require several hours for each run. As the evaluation of the reliability of a passive system may require hundreds and even thousands of calculations, this poses a serious practical problem when estimating the effect of changes in the probabilistic distributions of the input parameters on the system reliability. Within RMPS, the efficiency of two methods has been assessed to measure the influence of input distribution changes in the means and distribution functions of the output variables (distribution sensitivity analysis), without running again the TH code:

⁵ Design parameters are those that come from the connection of the passive system with the rest of the system, while critical parameters are those that characterise the passive system behaviour and account for possible system failure causes.

the weighting and the rejection methods [5]. These methods are suitable for measuring the sensitivity to the change in one, several or all the input parameters, though with some restrictions. In some way, however, the results provided by these methods have to be considered "qualitative", since, although one gets quantitative estimates, no test is currently available to check for the statistical significance of the differences obtained.

3. Specific Conclusions

Regarding reliability evaluation, the strong reliance of passive safety systems on inherent physical principles makes quantification of the reliability of such systems difficult as compared to classical systems analysis. As discussed above, the main problems related to the generation of dependable reliability values for passive (Category B) safety system functions are:

- large T-H uncertainties in the system modeling,
- necessary large numbers of simulation cycles and thus long calculations times in practical applications,
- theoretical gaps in the development of uncertainty / sensitivity analysis

approaches, e.g. missing tests for significance.

One of the most important results from the studies performed so far is the confirmation of non-perfect reliabilities of passive safety systems (resulting unreliabilities in the order of 10^{-3} - 10^{-2}).

Future RTD efforts here should focus on systematic identification, quantification and reduction of uncertainties that appear in the reliability process as well as corresponding fundamental research in statistical methods. On this specific topic, DG JRC is participating in a new (November 2004) IAEA Coordinated Research Project on "Natural Circulation Phenomena, Modeling and Reliability of Passive Systems that Utilize Natural Circulation" with the main task to perform a systematic classification of uncertainties related to the modeling of natural circulation phenomena in passive systems.

Regarding inclusion of passive systems reliability estimates in future PSA studies, merging probabilities with T-H models, i.e. dynamic reliability, is necessary for realistic plant safety modeling since the operation of a passive

safety system in the context of all the other systems of a NPP is strongly dependent on time and its required mission time could be much larger than the 24 hours typically used in conventional PSA Level 1 applications.

Future RTD efforts here should focus on the further development of dynamic PSA models in order to make corresponding applications less time-consuming in terms of computational effort involved.

4. General Conclusions

PSA type of systems analyses have worked well for well defined engineered systems, such as NPPs, chemical process plants, space systems, incinerators, waste repositories. The way how the performance of such systems is estimated, e.g. their reliability, is essentially to collect sufficient general / specific operating experience from which specific failure probabilities are estimated and consider some effects of system complexity, such as redundancies.

However, our way of life in the Western World does not only rely on the safe performance of clearly defined "point

hazards", such as NPPs, but increasingly depends upon a complex, interdependent system of energy / transport / information infrastructures. These infrastructures are vulnerable to disruptions that can lead to cascading failures with serious consequences. Since hardly any classical operating experience data are available for such highly interconnected and often conceptually new systems, total reliability is dominated in such cases by performance reliability rather than functional reliability. Model and parameter uncertainties are of dominant influence here. New reliability assessment methods have to be developed for such applications and the type of approach developed within the RMPS project might be an interesting starting point not only in the context of innovative NPPs (which - though so far without any operating experience - are "classical" well defined engineering systems), but also for energy, transport and information infrastructures. Corresponding research is under development at DG JRC as a follow-up of the RMPS project described in this paper.

References

- [1] SAFETY RELATED TERMS FOR ADVANCED NUCLEAR PLANTS, TECDOC-626, IAEA, Vienna, 1991.
- [2] C. Kirchsteiger, R. Bolado, BEST LINKS BETWEEN PSA AND PASSIVE SAFETY SYSTEMS RELIABILITY, JRC Report, Petten, September 2004.
- [3] <http://www.energyrisks.jrc.nl/projects/RMPS/background.htm>
- [4] T.L. Saaty, THE ANALYTIC HIERARCHY PROCESS, McGraw-Hill, New York, 1980.
- [5] R. Bolado, NOTES ON TWO MONTE CARLO METHODS FOR ESTIMATING THE INFLUENCE OF DIFFERENT INPUT DISTRIBUTIONS ON THE OUTPUT DISTRIBUTION FROM A COMPUTER CODE SIMULATION, JRC Technical Note, Petten, April 2003.

The Organization Relationship for Construction Enterprise Resource Planning Project-Lessons Learned in Taiwan

Meng-Hsueh LEE ^a, H. Ping TSERNG ^b

a Ph.D. Student, Department of Civil Engineering, National Taiwan Univ., Taipei, Taiwan.

E-mail:D92521016@ntu.edu.tw

b Professor, Department of Civil Engineering, National Taiwan Univ., Taipei, Taiwan.

E-mail:hptserng@ce.ntu.edu.tw

Topic: Human and organizational behavior and errors

The Organization Relationship for Construction Enterprise Resource Planning Project-Lessons Learned in Taiwan

ABSTRACT

In recent years, there are many companies want to implement the ERP (Enterprise Resources Planning) in construction industry. However, only a few factory cases implement ERP, and only the enterprises involved in the process know the key factors. The implement project team is one of the key factors to influence the ERP project successfully. There are many kinds of the communication interfaces in the project. These interfaces include companies between consultants, the internal company? departments, and the external consultant? teams. If company understands the project organization relationship earlier, it will reduce the communication barrier and the probability of failing implementing ERP system. The paper will use IDEF0 (INTEGRATION DEFINITION FOR FUNCTION MODELING) to analyses the process when construction enterprises implement ERP system. Because the traditional flow analysis methods merely describes the input-output content, and they did not a very detail explanation about the interaction between flows. Therefore, the reference value is not very high. The paper mainly describes the real case which experience in Taiwan construction enterprise, explains the critical steps are needed. Finally, in order to clear and definite the organization when construction enterprise implement ERP system, this paper will compare several types about ERP project teams and discuss these organization relationship for the important procedures to successfully implement the ERP system.

Keywords: Enterprise Resource Planning, organization interface, Construction industry.

1: INTRIDUCTION

Enterprise Resource Planning (ERP) was originated in the manufacturing industry. It provides a general working environment for an enterprise to integrate its major business management functions with one single common database so that information can be shared and efficient communications can be achieved between management functions. Based on the needs of running a construction enterprise, ERP shows its potential for the construction industry. In recent years, there are many companies want to implement the ERP in construction industry. However, only a few factory cases implement ERP, and only the enterprises involved in the process know the key factors. These key factors include Clear strategic goals and understanding, Business Process Reengineering (BPR), Top management Support, Excellent project management, Data accuracy, Full-time implementation team, Extensive education and training, Construction sites consideration, Effective performance measures, Consultant vendor support, The Duration for implementation, The Preparation before implementation, Construction industries characteristics, and Compatibility for software and hardware. The implement project team is one of the key factors to influence the ERP project successfully. There are many kinds of the communication interfaces in the project team. These interfaces include companies between consultants, the internal company? departments (internal organization), and the external consultant? teams (external organization). If companies understand the project organization relationship earlier, it will reduce the communication barrier and the probability of failing implementing ERP system.

2: The limit and Methodology of the Research

The limit of the Research

(1) Due to there are few factories implemented the ERP system in the construction industry, it is impossible to collect amounts of research samples such as that in the manufacturing, electronics and information industry. Therefore, the research only focuses on few representative firms.

(2) Construction firms successfully implemented the ERP system had not exceeded one year, and still been pending in system adapting and transition stage. For the difficulty of analyzing their history information, finance and accounting forms, the research only can apply expert interviewing method to explore all kinds of problems and solutions involved in the implementing process.

(3) Although Construction Companies are core characters in the construction industry, the industrial behavior still includes architecture investment and contract work system. The scope of the research can be more extensive if studying in different characters within the construction life cycle. Though, for the restriction of the research, it focuses on proprietors, construction companies and professional contractors without the consulting firms and the architect offices.

(4) The construction company (General Constructor) had not entirely implemented the ERP system yet, the research only focuses on stages of plan to implement and partially implement progress, and applies literature reviewing, expert interviewing and practically participating.

The Function Analysis of IDEF0

This publication announces the adoption of the Integration Definition Function Modeling (IDEF0) as a Federal Information Processing Standard (FIPS). This standard is based on the Air Force Wright Aeronautical Laboratories Integrated Computer- Aided Manufacturing (ICAM) Architecture, Part II, Volume IV - Function Modeling Manual (IDEF0), June 1981.

This standard describes the IDEF0 modeling language (semantics and syntax), and associated rules and techniques, for developing structured graphical representations of a system or enterprise. Use of this standard permits the construction of models comprising system functions (activities, actions, processes, and operations), functional relationships, and data (information or objects) that support systems integration.

This standard is the reference authority for use by system or enterprise modelers required to utilize the IDEF0 modeling technique, by implementers in developing tools for implementing this technique, and by other computer professionals in understanding the precise syntactic and semantic rules of the standard (IDEF).

3: Literature review

There are many kinds of success factors will influence Public-Private partnerships in infrastructure development, include five main factors such as economic viability, appropriate risk allocation via reliable contractual arrangements, sound financial package, favorable investment environment and reliable concessionaire consortium with strong technical strength. The factor "strong and capable project team" is the most important sub factor of the main factors, "reliable concessionaire consortium with strong technical strength". However, the construction industry researches not only to discuss project team, but also to explore the interface management. In the

topic of interface management, there are three different types, physical, contractual and organizational. Interfaces within construction continue to cause problems within the construction process. Although these researches proved in construction industry how to manage a project team is a significant issue, but they had less result to demonstrate the organization relationship issue.

The agent problems analysis in construction industry

In construction industry, there are three types of principal-agent in organization internal relationship, such as listed company-employee (manager), unlisted company-employee, and public department-employee. The law's point of view of these three types is a part of employment contract; belong to the relation of employ-employee. But the economics' point of view is a type of principal-agent. However, there are four types of principal-agent between organization and organization, such as private company-general constructor, private company-architect, public department-general constructor, and public department-architect. The law's point of view of these two types about the relation between owner (private and public) and constructor belong to contract's agreement; another two types about the relation between owner and architect belong to authorization contract. These four types of the economics' point of view is a type of principal-agent. Please refer to Table 1.

The agent problems of the organization

The agent problems include the organization internal and which between organization. The organization internal problems are consuming privilege, avoid effort, non optimal decision-making, and collaborate with agents to cheat owner etc. Furthermore, the agent problems of organization between organizations are avoid effort, over design, jerry-build, undue design, and collaborate with agents to cheat owner etc. The reasons of these agent problems are information asymmetry and objective conflicts.

4: Case study

The Case A is a General Constructor which was established since 1976. This enterprise had traditional Chinese operate characteristic, with American and Japan business culture and modern management philosophy. This enterprise was choice People Soft System.

The topic of organization relationship for case A during the process of planning ERP had:

- What kind of special project organization structure should be had? Special project organization mutual work assign and why it will be duty?

- After implementing into ERP system, relevant ERP main system, software, hardware, and database maintenance by who is it responsible for to execute?
- Between the groups when the situation of having information asymmetry or the objective conflict, what kind of emergency mechanisms should be had?

Case A deals with the way of above-mentioned topics as follows:

- Implemented into the going on of the whole special project of ERP Consultant Company, including finance and accounting, information technology, human resources, administration system etc. If the system relate with engineering information system, the Construction Consultant Company should have the higher priority to respond, integrate and management this ERP project.
- No matter the main system of ERP, or relevant software technology and hardware equipments, even the extra systematic functions that develop and customize functions, the ERP Consultant Company should be given the main maintenance service.
- The ERP project is proceeding as planned the information asymmetry and objective conflict appears among the groups should be organized by the ERP project managers of both internal organizations (General Constructor) and external organizations (ERP Consultant Company, Construction Consultant Company, Software Technology Service Company, and Hardware Technology Service Company). However, the foundation of the coordination, in order to the working project while contracting, and every meeting is noted down and regarded as the main basis.

The Organization Relationship for Construction Enterprise Resource Planning Project

Internal Organizations

The internal organizations with the case study (the general constructor implements ERP project) are all of the company's departments. The internal organizations include all department due to the ERP project is connect all resources with all departments in the constructor company. Besides, the case invited a consultant from school in the ERP system planning stage. For these reason, the internal organizations of the research include construction engineering department, project actual site department, finance and accounting department, general administration and information technology department, human resource department, top management, and consultant.

- Construction engineering department? The major task are managing all projects' situation in headquarters, and detaching the engineers in the project.
- Project actual site department? The major tasks are managing the sub constructors in the actual site, and distribute the workmen.
- Finance and a ccounting department? The major tasks are controlling the cash flow in the constructor company and managing the projects' money with owners and sub constructor.
- General administration and information technology department? The major tasks are managing the administrations of the company's internal and external, and maintaining the original engineering information system.
- Human resource department? The major tasks are managing the employees' salaries and vacations.
- Top management? The major task is overall planning the departments and the projects of the company from the top management's vision.
- Consultant? The view of learning theory to give assistance the company planning, implementing, and constructing the ERP system.

External Organizations

The external organizations general mean the ERP consultant companies, which ones that discuss are organized by different service group in this research. On the other hand, this research doesn't discuss the different organizations inside the constructor company. The most ERP consultant companies were assistance mainly in manufacturers industry. But this research is discussing the company in the construction industry, and there is few construction companies implement ERP system. Therefore the construction company needs construction Consultant Company to help implement ERP system. For these reasons, the external organizations include ERP Consultant Company, Construction Consultant Company, Software Technology Service Company and, Hardware Technology Service Company.

- ERP Consultant Company? There are two types of ERP Consultant Company. The first one depends on ERP system develops company, and adds the consultants with finance, accounting, human resource, and manufacturing likes SAP, Oracle, People Soft and IBM. Another consultant company focuses on finance, accounting and information technology, besides the ERP system expert likes any ERP service agency.
- Construction Consultant Company? Because the ERP system major modules are focus on finance and accounting process, few functions focus on engineering and scheduling management process;

therefore need extra system for Construction Company. Furthermore, the ERP Consultant Company service experience almost in the manufacturing company result the Construction Company needs Construction Consultant Company in addition.

- Software Technology Service Company? There are two types of Software Technology Service Companies. The first one is the ERP system supplier, such as SAP, Oracle, and People Soft etc. The second is extra modules for ERP system, such as Knowledge Management (KM), Supply Chain Management (SCM), and Customer Relationship Management (CRM) etc.
- Hardware Technology Service Company? The main work is to supply the related hardware equipments for ERP project, such as server, router, personal computer, and notebook etc.

Analyze Construction Enterprise Resource Planning project organization relationship with IDEF0

In the past researches the project organization is one of the key factors in ERP project, but they didn't detail discuss the organization relationship neither the interface management problems between the organizations. Accordingly, this research will discuss the organization relationship when companies implement ERP system with IDEF0. In the IDEF0, ICOM are the main items to analyze the problem, ICOM individually represent four items, which include Input, Control, Output, and Mechanism. Please refer to Table 2 and Table 3.

The problems from interface management

Information asymmetry

The information asymmetry is not serious in the internal organization in ERP project. For example, the internal organizations in the case A were already have the communicated and cooperated experience more than twenty years. The case A has less information asymmetry problems than other company in youth. However, the information asymmetries usually occur from internal organization between external, and among the external organizations. Because the most Construction Company none understand the benefit if it implement ERP system, and the most ERP Consultant Company none understand the process in construction industry. It causes the information symmetry problems when construction Industry Company implements ERP system. Therefore, the Construction Consultant Company needs to solve the problem from information symmetries. Beside the problems between internal and external organization, another situation is occurring among the external organizations. For example, the construction company considers EIP module was

included and integrates easily to ERP system, but the ERP Consultant Company considers it was extra module in Case A. The foregoing problems will influence the schedule and enhance the communication cost in ERP project.

Objective conflicts

No matter internal or external organizations, it is easily occurring objective conflicts. The different demand from different departments is one of the objective conflicts in the internal organizations.

For example, the finance and accounting department need more detail income and outgo information to accurate control cash flow, but this information will need more extra job for project actual site department. In order to control cash flow, it will make the objective conflicts in internal organizations.

The objective conflicts between internal and external organization will occur the different cognitive for ERP project. For example, Construction Company considers some functions of ERP system should be a default service, but the ERP Consultant Company consider that should extra customizing or only rely on few manual process to solve. On one hand believe the information technology could solve all the problems; on the other hand consider some problem solutions are needed to more change the business process but more information technology. The foregoing problem of objective conflicts is emerging in an endless stream. Please refer to Table 4 and Table5.

The types of interface

There are several types of interface management in the research. The Case A originally needs to manage four interfaces in the ERP project, such as ERP Consultant Company, Construction Consultant Company, Software Technology Service Company, and Hardware Technology Service Company. Nevertheless, the Case A finally reduces the four interfaces to only one, which also reduces the interface management problems' probably.

More than two interfaces? When the Construction Company meet more than two interfaces while it implement ERP project, its probably because the ERP Consultant Company seldom has experience of implement ERP system thus it is difficult for them to integrate. Moreover, due to the Construction Consultant Company, Software Technology Service Company and Hardware Technology Service Company use their own systems so it's hard to manage and integrate. Therefore, the Construction Company has to be the manager of the interfaces and to take the risk of integrates failure.

Two interfaces: The two interfaces are ERP Consultant Company and Construction Consultant Company. Due to most ERP Consultant Companies use finance, accounting and manufacture as their management basis in order to service manufacturing industry, they rarely have enough knowledge in

construction industry. Thus, if they use the point of manufacturing to plan ERP system for construction industry, it may occur over design (add SCM and CRM system) and undue design (ignore the important of project management and scheduling control). Consequently, the Construction Consultant Company is the other interface as ERP Consultant Company.

One interface: If one of the ERP project external organizations could integrate the different interfaces, it will reduce four interfaces (ERP Consultant Company, Construction Consultant Company, Software Technology Service Company, and Hardware Technology Service Company) to one. It will help the Construction Company attention on the internal organization management and decrease the risk of failure of implement ERP system. Please refer to Figure 1.

5: Conclusion

The relationship between the organizations in the case of implement ERP system will be different to some extent because of relation of the contract. If the implement company signs the contract to an individual corporation itself, the management of the interface between them is sure to become an important issue. Take the increase of time cost of communication for instance; it will cost more if the amount of interface increases. If the construction company can transfer the management of interface of the corporation into the other firm, then the external interface management issues will be integrated by the firm which response for that part. Although the construction company can reduce a lot of problems while integrate the interface management issues to a main company, there are still two focal points especially need to consider. First, the professional background and teams of the integrated company must be good enough to deal with different interfaces. Second, the integrated company must have a long history or have a good word of mouth by handle these kinds of issues in order to avoid rescission in the process of providing service and to decrease the risk of failure of implement ERP system.

6: REFERENCES

- [1] Chang D. J., "The Study of Agent Problems in Construction Organization", National Taiwan University department of Civil Engineering, master thesis, July 1998.
- [2] Hans V., "Enterprise Resource Planning in a large construction firm: implementation analysis." Construction Management and Economics, Vol.21, July 2003, pp.511-521.

- [3] Integration definition for function modeling (IDEF0) .Draft federal information processing standards publication 183. <http://www.idef.com> (1993)
- [4] Meng-Hsueh LEE and H. Ping TSERNG, "Developing Analysis Models for Implementing Construction Enterprise Resource Planning System", ISARC, September 2004.
- [5] Shi, J. J., "Enterprise Resource Planning for Construction Business Management", Journal of Construction Engineering and Management", ASCE, March/April2003, pp.214 -221.
- [6] T. C. Pavitt and A. G. F. Gibb," Interface Management within Construction: In Particular, Building Facade", Journal of Construction Engineering and Management, January/February 2003, pp8-15.
- [7] Xueqing Zhang, "Critical Success Factors for Public-Private Partnerships in Infrastructure Development", Journal of Construction Engineering and Management, January 2005,pp3- 14.
- [8] Yu-Cheng LIN, Meng-Hsueh LEE and H. Ping TSERNG," Construction Enterprise Resource Planning Implementation: Critical Success Factors – Lesson Learning in Taiwan", ISARC, September 2003.

Table 1 The agent relationships and problems' researches definition table A

Constructio n industry	The types of Principal	The types of Principal-agent	The definition of cooperation relationships in Law and Economics		Agent Problems
Organizati on Internal	Listed company (private)	Employee (Manager)	Employment contract (The relation of Employ-Employee)	Agent relationship (Principal-Agent)	The behaviors of agents' consume privilege and avoid effort.
	Unlisted company (private)	Employee	Employment contract (The relation of Employ-Employee)	Agent relationship (Principal-Agent)	The behaviors of agents' lazy work and avoid effort.
	Government (public)	Employee (public servant)	Employment contract (The relation of Employ-Employee)	Agent relationship (Principal-Agent)	The behaviors of agents' lazy work and avoid effort.
Between Organizati on and Organizati on	Private company (private)	GC(General Constructor)	Contract's agreement (The relation of Owner-Constructor)	Agent relationship (Principal-Agent)	The behaviors of agents' jerry-build
		A/E (Architect/Engineer)	Authorization contract(The relation of Client-Agent)	Agent relationship (Principal-Agent)	The behaviors of agents' over design and undue design.
	Public department (public)	GC(General Constructor)	Contract's agreement (The relation of Owner-Constructor)	Agent relationship (Principal-Agent)	The behaviors of agents' jerry-build.
		A/E (Architect/Engineer)	Authorization contract(The relation of Client-Agent)	Agent relationship (Principal-Agent)	The behaviors of agents' over design and undue design.

Table 2 The items' description of IDEF0

Items		Note
I	Input	The Request for proposal (RFP) from all department of General Constructor
C	Control	Establish with the contract relation for each organization through contracting the agreement in ERP project
O	Output	Discuss the last objective tasks for ERP in contract through all ERP consultants and project members.
M	Mechanism	The members participate the ERP project include internal organization and external organization.

Table 3 The organization relationship of ERP project with IDEFO

Node A	No	The title of ERP organization ERP Project Organizations (Include internal and external)	Input Request For Proposal (RFP)	Control The relation of contract	Output The objective tasks in contract	Mechanism ERP Project team members	
A	1	ERP Project internal organizations (All departments of general constructor)	The functions of old information systems and the functions of future ERP system.	Employment contract (The relation of Employ-Em ployee)	The revision RFP in contract	The key members of internal organization	
A	11	Construction engineering department	Engineering information system	Employment contract	The demand of ERP system for objective tasks	The manager of Construction engineering department	
A	12	Project actual site department		(The relation of Employ-Em ployee)		The manager of Finance and accounting department	
A	13	Finance and accounting department	Finance and accounting system				
A	14	General administration and information technology department	General administration system				The manager of General administration and information technology department
A	15	Human resource department	Human resource system				The manager of Human resource department
A	16	Top management	Decision support system				Top management
A	17	Consultant	Academy and project practice experience				The basic system structure of engineering information system for ERP system
A	2	ERP Project external organizations (Each organization of ERP service firm)	The original functions of ERP system	Contract's agreement (The relation of Owner-Cons tructor)	The revision RFP in contract	The members of external organization	
A	21	ERP Consultant Company	The modules of ERP system	Contract's agreement	The demand of ERP system for objective tasks	The project manager of ERP Consultant Company	
A	22	Construction Consultant company	The engineering information system's function integrate to ERP system	(The relation of Owner-Cons tructor)		The manager of Construction Consultant Company	
A	23	Software Technology Service Company	The related software technology of ERP system			Software Technology Service Company	
A	24	Hardware Technology Service Company	The related hardware technology of ERP system			The demand of ERP system for hardware equipment	Hardware Technology Service Company

Table 4 The agent relationships and problems' researches definition table B

Construction industry	The types of Principal	The types of Principal-agent	The definition of cooperation relationships in Law and Economics		Agent Problems
Organization Internal	Listed company (private)	Employee (Manager)	Employment contract (The relation of Employ-Employee)	Agent relationship (Principal-Agent)	The behaviors of agents' consume privilege and avoid effort.
Between Organization and Organization	Private company (private)	Hardware Services Company	Contract's agreement (The relation of Owner-Constructor)	Agent relationship (Principal-Agent)	The behaviors of agents' over design and undue design.
		Software Services Company			
		ERP implement Services Company	Authorization contract (The relation of Client-Agent)	Agent relationship (Principal-Agent)	The behaviors of agents' jerry-build, over design and undue design.
		Construction industry Services Company			

Table 5 The case study for ERP system services contract table

ERP System Services	ERP implementing stage	ERP implement finish and maintain stage	
ERP Main System	By implement service consultant company integrate all relative contracts.	Is the implement service consultant company relative contract ending?	The maintenance of ERP main system belong the ERP system supplier?
ERP More Services			The maintenance of ERP more services belong the ERP more services supplier?
ERP Customize			The maintenance belong the customize contract?
Database			The maintenance belong the database supplier?

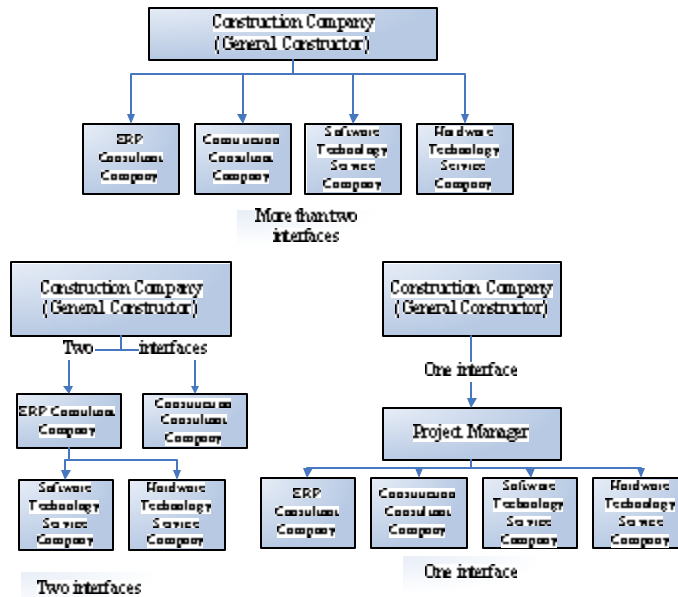


Figure 1 The types of interface

Value Judgment for Evaluating Sense of Security Provided by Nursing Care Robots Based on Prospect Theory under Uncertainty

Hiroyuki Tamura¹, Yoshitomo Miura² and Masahiro Inuiguchi³

TOPIC: Risk management and decision analysis

1 Faculty of Engineering, Kansai University, 3-3-35 Yamate-cho, Suita, Osaka 564-8680, Japan

PHONE/FAX: +81-6-6368-0829, E-MAIL: H.Tamura@kansai-u.ac.jp

2 Graduate School of Engineering Science, Osaka University, 1-3 Machikaneyama, Toyonaka, Osaka 560-8531, Japan

PHONE +81-6-6850-6353, E-MAIL: miura@inulab.sys.es.osaka-u.ac.jp

3 Graduate School of Engineering Science, Osaka University, 1-3 Machikaneyama, Toyonaka, Osaka 560-8531, Japan

PHONE +81-6-6850-6350, E-MAIL: inuiguti@sys.es.osaka-u.ac.jp

Value Judgment for Evaluating the Sense of Security Provided by Nursing Care Robots Based on Prospect Theory under Uncertainty

Hiroyuki Tamura/Kansai University, Yoshitomo Miura/Osaka University
and Masahiro Inuiguchi/Osaka University

Abstract

We aim at evaluating the value of sense of security in order to create more safe, secure and reliable society. For this purpose, we have tried to evaluate the value of sense of security of nursing care robots by using various utility theoretic approaches such as Expected Utility theory (EU), Prospect Theory (PT) and Cumulative Prospect Theory (CPT). We postulated some types of nursing care robots and evaluated the value of sense of security of them by using these approaches. As the result of comparison we found that PT is more appropriate for evaluating the value of sense of security of nursing care robots.

In this paper, we consider more practical cases. One of them is the case that we do not know whether a human nurse or a nursing care robot would take care of us. The other is the case that we do not know the type of nursing care robot that would take care of us. In these cases, we know basic probability for a set of outcomes but not for each outcome. For such cases, we propose an idea of Prospect Theory under Uncertainty (PTU) that is a powerful approach for modeling. We try to evaluate the value of sense of security by using the data obtained by the questionnaire collected from the people who have experienced to participate in the nursing care activities, and show that the idea of PTU describes people's preference and decision making quite well.

1. Introduction

Japan is currently an aging society composed largely of elderly people, and the proportion of the aged in the population is increasing year by year. This causes problems because the number of people who need care is increasing every year. It is estimated that more than

4% of Japanese will need care in 2025 [1]. However, the number of nurses is smaller than required [2]. In such a society, people increasingly turn to machines and tools for nursing care or welfare and some are already put to practical use. A wheelchair, nursing care bed and others are already put to practical use and are becoming more popular. However, more research and development of nursing care robots is urgently required because of the diversification of people who need care.

In our former study we assumed that certain types of nursing care robots were available and tried to evaluate the value of sense of security they provided. For this purpose, we used Expected Utility Theory (EU) [3], Prospect Theory (PT) [4] and Cumulative Prospect Theory (CPT) [5]. We conducted a survey of people who participated nursing care, and compared the results and showed that PT is the most suitable to evaluating the value of sense of security provided by nursing care robots among three utility theoretic approaches above.

In this paper we consider the case that we know total probability for some outcomes but we do not know probability for each outcome. In order to deal with such cases, we will propose PT under uncertainty (PTU) by using the idea of Value Function under Uncertainty (VFU) [6]. Moreover, we will try to evaluate the value of sense of security provided by nursing care robots by using PTU.

2. Nursing care robots

Robots that make some contribution to caring for people are referred to as "nursing care robots". Some nursing care robots are already on sale and in practical use, but most of these have a mechanical shape that is entirely different from human being, and their abilities are limited to a particular function. For example, they

help bedridden people to sit up in bed or take a meal. Moreover, they are too expensive for an individual to buy, so they are used only in some medical or nursing care institutions. On the other hand, more advanced nursing care robots are currently on the way of research and development. For example, some of them can perform a variety of actions and they are expected to respond to diverse needs. Others look like human being and can communicate with people, and they are expected to give people a sense of security. For nursing care robots, giving us a sense of security is an important prerequisite. If a robot does not give us a sense of security, it needs to be improved.

3. Former studies

In former studies we attempted to evaluate the value of sense of security that people felt in some different societies and compared the results. One was a society in which nursing care robots did not exist and the others were societies in which a certain type of them were popular.

Specifically, we assumed seven types of robots as shown in **Table 1**, and designated outcomes and their probabilities in **Table 2** based on statistical data [6,7], the attributes for evaluation as care level, sense of intimacy, cost and reserve for caregiver. Society 1 denotes the society in which nursing care robots do not exist and Society 2 denotes the society where they exist as shown in Table 2.

Table 1. Characteristics of robots

	Care level	Appearance	Cost per month
Robot A	Limited	Mechanical	6,000 yen
Robot B	Limited	Humanoid	6,000 yen
Robot C	Limited	Humanoid	30,000 yen
Robot D	Talk	Humanoid	6,000 yen
Robot E	Talk	Humanoid	30,000 yen
Robot F	General	Mechanical	30,000 yen
Robot G	General	Humanoid	30,000 yen

Table 2. Probability of obtaining each outcome

Outcome	Society 1	Society 2
No care	0.35	0.25
Care by family	0.35	0.35
Care by nurse	0.30	0.30
Care by robot	0	0.10

Next we considered two independences, Difference Independence (DI) and Weak Difference Independence (WDI) in order to enable to deal with the multiple attributes [8]. DI means that the difference in the strength of preference between two prospects is not affected by the fixed values of some attributes. WDI means that the ordering of difference in the strength of preference does not depend on the fixed values of some attributes. Then we evaluated the value of sense of security by using three methods introduced in Section 2, under each assumption, DI and WDI, respectively. An example of value judgment obtained is shown in **Table 3**.

Table 3. An example of value judgment

Robot	No	A	B	C
EU (DI)	0.597	0.618	0.620	0.594
EU (WDI)	0.825	0.832	0.838	0.830
PT (DI)	0.615	0.741	0.745	0.694
PT (WDI)	0.797	0.933	0.944	0.926
CPT (DI)	0.543	0.530	0.534	0.542
CPT (WDI)	0.698	0.754	0.765	0.753
Robot	D	E	F	G
EU (DI)	0.580	0.554	0.586	0.588
EU (WDI)	0.818	0.802	0.820	0.826
PT (DI)	0.667	0.615	0.678	0.682
PT (WDI)	0.903	0.872	0.901	0.918
CPT (DI)	0.519	0.468	0.530	0.534
CPT (WDI)	0.691	0.659	0.689	0.751

The individual concerned with Table 3 actually thought that the society of “No robot” was the worst, and the society of “Robot B” was the best. Except for “No robot”, she chose the society of “Robot E” as the worst. For convenience, the values concerned with the three alternatives are shown in boldface in Table 3. So we found that PT in WDI describes her preference the best. We were able to say that PT in WDI is the most suitable to evaluating the sense of security provided by nursing care robots because the results of other people were similar to hers.

4. Theory

We introduce some theories used in this paper in this section.

4.1 Prospect theory

PT [4] was proposed in order to explain people's decision making as follows:

- People's attitude for risk is loss averse.
- People feel that weight for very small probability is larger than itself.

We denote the prospect that yields outcome x^j with probability $p^j, j = 1, \dots, n$ by

$$l = (p_1, x^1; p_2, x^2; \dots; p_n, x^n). \quad (1)$$

In PT, the value V of the prospect (1) is evaluated by the evaluation function

$$V = \sum_{j=1}^n p(p_j)v(x^j) \quad (2)$$

where the value function v is convex and its curve is gentle in the gain domain, while it is concave and its curve is steeper in the loss domain, as shown in **Figure 1**. This shows that people in general are loss averse.

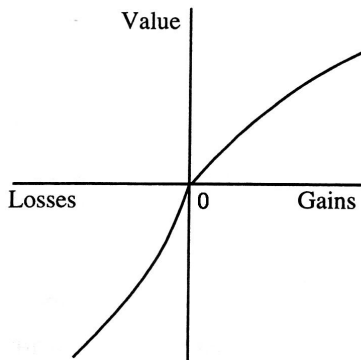


Figure 1. Value function

The weighting function p is a convex function as shown in **Figure 2** so small probability is weighted larger and middle or large probability is weighted smaller. However, this weighting function is not defined near the end point 0 and 1. The dotted line in Figure 2 shows for the case of EU model.

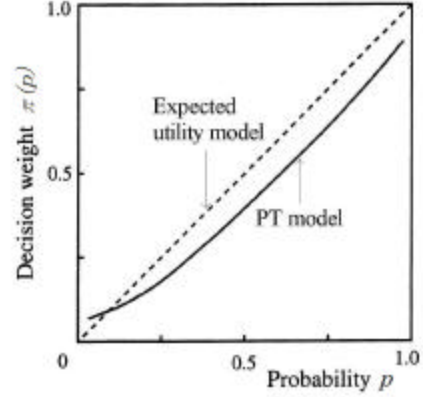


Figure 2. Weighting function

4.2 Prospect theory under uncertainty

We are not able to deal with the case where probability of occurrence for each event is unknown by PT. Here we use the idea of VFU [8] by the basic probability of Dempster-Shafer theory [9] and develop PT under uncertainty (PTU).

In Dempster-Shafer theory of probability [9] let $m(A_i)$ be basic probability which could be assigned by any subset A_i of Θ , where Θ denotes a set containing every possible element. The basic probability $m(A_i)$ can be regarded as a semimobile probability mass. Let $\Lambda = 2^\Theta$ be a set containing every subset of Θ . Then, the basic probability $m(A_i)$ is defined on Λ and takes a value contained in $[0, 1]$. When $m(A_i) > 0$, A_i is called the focal element or the set element and the following conditions hold:

$$m(A_i) = 0 \text{ if } A_i \text{ is empty} \quad (3)$$

$$\sum_{A_i \in \Lambda} m(A_i) = 1 \quad (4)$$

Let the value function in PTU based on this Dempster-Shafer basic probability be

$$f^*(B, \mathbf{m}) = p^*(\mathbf{m})v^*(B) \quad (5)$$

where B denotes a set element, m denotes the basic probability, p' denotes the weighting function for the basic probability, and v^* denotes the value function with respect to a set element. The set element B is a subset of $\Lambda=2^\Theta$.

For identifying v^* , we need to find the preference relations among set elements, which is not an easy task. If the number of elements contained in the set Θ is getting larger, it is not practical to find v^* . To cope with this difficulty we introduce an axiom of dominance as follows.

Axiom of Dominance 1. *In the set element B let the worst consequence be m_B and the best consequence be M_B . For any $B', B' \in \Lambda \in 2^\Theta$*

$$m_{B'} \prec m_B, M_{B'} \prec M_B \Rightarrow B' \prec B \quad (6)$$

and

$$m_{B'} \sim m_B, M_{B'} \sim M_B \Rightarrow B' \sim B \quad (7)$$

where $a \succ b$ denotes “ a is preferred to b ,” and $a \sim b$ denotes “ a is indifferent to b .”

Using Axiom of Dominance 1, we will restrict a set element B to

$$\Omega = \{(m, M) \in \Theta \times \Theta : m \prec M\} \quad (8)$$

where m and M denote the worst and the best consequence in the set element B , respectively. Then, equation (5) is reduced to

$$f^*(\Omega, m) = p'(m)v^*(\Omega) \quad (9)$$

Suppose we look at an index of pessimism $a(m, M)$, such that the following two alternatives are indifferent [10].

Alternative 1. One can receive m for the worst case and M for the best case. There exists no other information.

Alternative 2. One receives m with probability $a(m, M)$ and receives M with probability $1 - a(m, M)$, where $0 < a(m, M) < 1$.

If one is quite pessimistic, $a(m, M)$ becomes nearly equal to 1, and if one is quite optimistic $a(m, M)$ becomes nearly equal to zero. If we incorporate this pessimism index $a(m, M)$ in equation (9), the value function is obtained as

$$\begin{aligned} v^*(\Omega) &= v^*((m, M)) \\ &= a(m, M)v'(m) + (1 - a(m, M))v'(M) \end{aligned} \quad (10)$$

where v' denotes a value function for a single element.

However, there exist some cases that Axiom of Dominance 1 is unsuitable. Then we introduce Axiom of Dominance 2 [11] which is stricter than 1 as follows.

Axiom of Dominance 2. *Let the worst consequence be m_1 and the best consequence be M_1 in the set element B_1 , and let the worst consequence be m_2 and the best consequence be M_2 in the set element B_2 . Moreover, let the imaginary elements whose values are equal to the average values of B_1, B_2 be g_1, g_2 , respectively. Then*

$$m_1 \prec m_2, M_1 \prec M_2, g_1 \prec g_2 \Rightarrow B_1 \prec B_2 \quad (11)$$

and

$$m_1 \sim m_2, M_1 \sim M_2, g_1 \sim g_2 \Rightarrow B_1 \sim B_2 \quad (12)$$

where

$$v(g_1) = \frac{\sum_{i=1}^{n_1} v(a_i)}{n_1}, v(g_2) = \frac{\sum_{i=1}^{n_2} v(b_i)}{n_2},$$

n_1 denotes the number of the elements in the set element B_1 and n_2 denotes the number of the elements in the set element B_2 .

Axiom of Dominance 2 is too strict to use practically, so we try to relax it. Someone attaches importance to the best outcome and chooses an alternative, someone attaches importance to the worst outcome, and someone pays attention to the whole. We introduce the model that properly describes above situation [11].

Definition. Let the elements in the set element B be a_1, a_2, \dots, a_n such that $a_i \prec a_{i+1}, i=1, 2, \dots, n-1$, the value of element $a_i (i=1, 2, \dots, n)$ be $v(a_i)$ and the average value of elements $\sum_{i=1}^n v(a_i)/n$ be $v(g)$. Further, let the pessimism index decided by the question for the element $a_1 = m$ whose outcome is the worst and the element $a_n = M$ whose outcome is the best be $\mathbf{a}(m, M)$, we assume the value h of the set element B as follows.

$$h(B | \mathbf{a}) = a + b e^{-c\mathbf{a}(m, M)} \text{ if } v(g) \neq \frac{v(M) + v(m)}{2} \quad (13)$$

$$h(B | \mathbf{a}) = a + b\mathbf{a}(m, M) \text{ if } v(g) = \frac{v(M) + v(m)}{2} \quad (14)$$

where unknown parameters a, b, c are decided by

$$h(B | 0) = v(M), h(B | 0.5) = v(g), h(B | 1) = v(m).$$

We introduce Axiom of Dominance 3 in order to evaluate values based on the above definition as follows.

Axiom of Dominance 3.

$$h(B_1 | \mathbf{a}) < h(B_2 | \mathbf{a}) \Rightarrow B_1 \prec B_2 \quad (15)$$

and

$$h(B_1 | \mathbf{a}) = h(B_2 | \mathbf{a}) \Rightarrow B_1 \sim B_2 \quad (16)$$

By using Axiom of Dominance 3, we are able to write the value function in PTU as follows.

$$f^*(h(B | \mathbf{a}), \mathbf{m}) = \mathbf{p}'(\mathbf{m})h(B | \mathbf{a}) \quad (17)$$

We are able to properly describe senses of values of pessimistic people and optimistic people respectively by using equation (17).

We are able to evaluate the value V of the prospect that includes the case where probability of occurrence for each element is unknown but basic probability of occurrence for set elements are known by the evaluation

function

$$V = \sum_{j=1}^n \mathbf{p}(\mathbf{m}_j) v^*(B_j) \quad (18)$$

where \mathbf{p} denotes the weighting function of PT and v^* denotes the value function of VFU.

In the next section, we try to evaluate the value of sense of security provided by nursing care robots.

5. Experiment

We now attempt to evaluate the sense of security that people feel in two different situations and compare the results. One is a situation in which all probabilities for all outcomes are known and the other is a situation in which probabilities for some outcomes are unknown but the total probability for them is known. We designate following two cases as ones such that probabilities for some outcomes are unknown.

Case 1. You do not know which will care you, a human nurse or a nursing care robot, when you request nursing care center to care you.

Case 2. You do not know what type of robot will care you when you borrow a nursing care robot from nursing care center or government.

Subjects of this experiment are eleven people who live in Ikeda City or Minoo City in Osaka Prefecture, Japan. Seven of them participate nursing care and four of them have a member who needs care in their family. Their age is between twenties and fifties, and four of them are male.

5.1 Case 1

We designate outcomes and their probabilities in **Table 4** similar to Table 2 where No , Fa , Nu , Ro denote the outcomes “no care”, “care by family”, “care by nurse”, “care by robot”, respectively.

Then the value of Society 1 V_1 and the value of Society 2 V_2 are evaluated by the following equations

$$V_1 = \mathbf{p}(0.35)v(No) + \mathbf{p}(0.35)v(Fa) + \mathbf{p}(0.30)v(Nu), \\ V_2 = \mathbf{p}(0.25)v(No) + \mathbf{p}(0.35)v(Fa) + \mathbf{p}(0.40)v^*(Nu, Ro).$$

Table 4: Probability of obtaining each outcome

Outcome	Society 1	Society 2
<i>No</i>	0.35	0.25
<i>Fa</i>	0.35	0.35
<i>Nu</i>	0.30	0
<i>Nu or Ro</i>	0	0.40

Here $v^*(Nu, Ro)$ could be represented by using the pessimism index $\mathbf{a}(m, M)$ as

$$v^*(Nu, Ro) = \mathbf{a}(m, M)v(m) + (1 - \mathbf{a}(m, M))v(M)$$

where m denotes the worse one between Nu and Ro , M denotes the better one between them. Using these equations, we try to evaluate practically.

One typical example of results is shown in **Table 5**. Situation 1 denotes a situation in which all probabilities are known, as shown in Table 2. Situation 2 denotes a situation where some probabilities are unknown, as shown in Table 4.

Table 5: An example of results 1

Robot	Situation 1	Situation 2
No	0.768	0.768
A	0.854	0.720
B	0.858	0.730
C	0.834	0.702
D	0.824	0.674
E	0.794	0.627
F	0.885	0.757
G	0.888	0.766

This result shows that this individual prefers the societies where any nursing care robots exist than the society where nursing care robots do not exist when every probability is known, but his preference is reverse in the situation that some probabilities are unknown. It coincides with his actual preference. Similarly, for all individuals, results of evaluation experiment coincide with their actual preference, so we are able to say that PTU is a suitable method of evaluating the value of sense of security provided by nursing care robots in Case 1.

5.2 Case 2

We use outcomes and probabilities in Table 2 similar to former study, but in this case a type of robot who cares you is unknown. The value of Society 1 V_1 and the value of Society 2 V_2 are evaluated by the following equations

$$V_1 = \mathbf{p}(0.35)v(Nu) + \mathbf{p}(0.35)v(Fa) + \mathbf{p}(0.30)v(Nu),$$

$$V_2 = \mathbf{p}(0.25)v(Nu) + \mathbf{p}(0.35)v(Fa) + \mathbf{p}(0.30)v(Nu) + \mathbf{p}(0.10)v^*(Ro).$$

where Ro is a set element which consists of outcomes “care by robot A”, “care by robot B”, ..., “care by robot G”. Here $v^*(Ro)$ could be represented by using the pessimism index $\mathbf{a}(m, M)$ obtained by question for the worst robot and the best robot as

$$v^*(Ro) = h(Ro | \mathbf{a})$$

where h denotes the value function defined by equations (13) and (14). Result of the same individual as in Case 1 is shown in **Table 6**.

Table 6: An example of results 2

Robot	Value
No	0.768
A	0.854
B	0.858
C	0.834
D	0.824
E	0.794
F	0.885
G	0.888
Unknown	0.835

This result shows that he prefers the situation that a type of robot is unknown to the situation that he is cared by robot C, D, E, but he does not prefer the situation “unknown” than care by robot A, B, F, G. The value of “unknown” is lower than average of the values of robot A, B, ..., G. It coincides with his actual preference and every result agrees with each individual’s preference.

6. Conclusion

By using an idea of VFU, we could extend PT to PTU under uncertainty (PTU) and evaluate quantitatively the value of sense of security provided by nursing care robots with the case where probabilities for some outcomes are unknown. Furthermore, we showed that the results of evaluation coincide with actual individuals' preference well. We hope that PTU will be put to practical use in order to evaluate the value of sense of security provided by nursing care robots or something else that will be developed hereafter. We also found that people feel anxious if probabilities are not clear. It shows that publishing information is important to give people the sense of security.

In this paper we dealt with value judgment of the sense of security for an individual, but the value judgment for society is to be developed for further research.

Acknowledgement : This research was supported by the Ministry of Education, Culture, Sports, Science and Technology (MEXT) under Grant-in-Aid for Creative Scientific Research (Project No. 13GS0018).

References

- [1] National Institute of Population and Social Security Research, "Population Projection for Japan: 2001-2050," Jan. 2002; www.ipss.go.jp/
- [2] Japanese Economic Planning Agency, "The White Book of Nation's Life 1996," Nov. 1996; <http://wp.cao.go.jp/zenbun/seikatsu/wp-pl96/wp-pl96-000i1.html> (in Japanese)
- [3] J. von Neumann and O. Morgenstern, *Theory of Games and Economic Behavior*, Princeton University Press, 1944.
- [4] D. Kahneman and A. Tversky, "Prospect Theory: An Analysis of Decision under Risk," *Econometrica*, vol. 47, no. 2, Mar. 1979, pp. 263-291.
- [5] A. Tversky and D. Kahneman, "Advances in Prospect Theory: Cumulative Representation of Uncertainty," *Journal of Risk and Uncertainty*, vol. 5, no. 4, Oct. 1992, pp. 297-323.
- [6] Architec Office, "About Architecture and welfare," Oct. 1999, <http://www3.yomogi.or.jp/architec/kentiku&fukusi1.htm> (in Japanese)
- [7] The Mainichi Newspapers, "Mainichi Nursing Care News," Dec. 2002, www.kaigo-fukushi.com/shakai/200212/shakai2002121303.html (in Japanese)
- [8] K. Shell and E. Hall, eds., *Handbook of Industrial Automation*, Marcel Dekker, 2000.
- [9] G. Shafer, *A Mathematical Theory of Evidence*, Princeton University Press, 1976.
- [10] J. Jaffray, "Application of Linear Utility Theory to Belief Functions," *Proc. 2nd Int'l Conf. Information Processing and Management of Uncertainty in Knowledge-Based Systems (IPMU 88)*, 1988, pp. 1-8.
- [11] H. Tamura, H. Kitamura, I. Hatono and M. Umamo, "On a New Axiom of Dominance and Constructing a Measurable Value Function under Uncertainty –Evaluating Alternative Policies to Decrease Emission of Carbon Dioxide," *Transactions of the Institute of Systems, Control and Information Engineers*, vol. 8, No. 1, Jan. 1995, pp. 34-42. (in Japanese)

TITLE: Error Analysis in Hyper Omni Vision
AUTHOR: Tomohiro Mashita, Yoshio Iwai, Masahiko Yachida
TOPIC: Sensors, communications, and data fusion

Tomohiro Mashita
mashita@yachi-lab.sys.es.osaka-u.ac.jp
Graduate School of Engineering Science Osaka University

Yoshio Iwai
iwai@sys.es.osaka-u.ac.jp
Graduate School of Engineering Science Osaka University

Masahiko Yachida
yachida@sys.es.osaka-u.ac.jp
Graduate School of Engineering Science Osaka University

Yachida lab. Graduate School of Engineering Science
Osaka University 1-3, Machikaneyama, Toyonaka, Osaka
560-8531, JAPAN
(+81)(6)6850-6361
(+81)(6)6850-6341

Error Analysis in HyperOmni Vision

Tomohiro Mashita, Yoshio Iwai, Masahiko Yachida
Graduate School of Engineering Science, Osaka University
{mashita, iwai, yachida}@yachi-lab.sys.es.osaka-u.ac.jp

Abstract

It is important to analyze that the error in catadioptric cameras that have a single viewpoint in order to use them for measurement purposes. In this paper, we implement a simulation system for a catadioptric camera system and evaluate errors caused by the misalignment of rotation and translation between the camera and mirror. The catadioptric camera in our system consists of a hyperboloidal mirror and a perspective camera model. Our simulation system uses a hyperboloidal mirror model as the mirror model and a pinhole camera model as a camera model. In experiments, we calculate and evaluate viewpoint error and directional error caused by the misalignment of rotation and translation between the camera and mirror.

1 Introduction

Most catadioptric cameras are designed to have a single viewpoint. One advantage is that the catadioptric image can easily be transformed into a familiar perspective image. Another advantage is that algorithms for pinhole cameras can easily be applied to catadioptric cameras, which have a single viewpoint.

The disadvantage of catadioptric cameras is that alignment of the mirror and camera must be fixed exactly. If the alignment is not done correctly, the camera cannot maintain a single viewpoint and a single viewpoint model cannot be applied to it to obtain a geometrical relation between projected images. Misalignment problem causes various errors in systems using catadioptric cameras. Correcting misalignment differs according to the purpose of the camera is used for. In measurement applications, the camera's single viewpoint feature is not required, but the geometric arrangement between pixels, viewpoints, and rays should be correctly determined. In other words, the position of the camera and mirror should be exactly determined by calibration. In visualization applications, accurate alignment of the camera and mirror is not required and errors in viewpoint position and ray direction are within tolerance levels, so that the viewer does not have any sense of incongruity.

The errors caused by misalignment can be divided into two. The first is the error in viewpoint positions, and the other is error in the direction of a reflected rays. The

influence of these errors varies according to the depth of the object. Where the object is near the camera, error in viewpoint position affects the accuracy of measurement. Where the object is far from the camera, the error in ray direction affects the accuracy of measurement.

Because of these reasons, error analysis in catadioptric cameras that have a single viewpoint is important in order to use them for measurement purposes. In this paper, we implement a simulation system for a catadioptric camera that has a single viewpoint and also evaluate the effect of errors caused by misalignment of the camera and a mirror. Our simulation system uses a hyperboloidal mirror model, HyperOmniVision [1], as the mirror model and a pinhole camera model as the camera model.

1.1 Related Work

Many catadioptric camera systems have been proposed over the last decade. Typical catadioptric camera systems have been proposed by Nayar [2] and Yamazawa et al. [1]. The first uses an orthogonal camera model and a parabolic mirror. Yamazawa et al. uses a perspective camera model and a hyperboloidal mirror. A catadioptric camera that has non-single viewpoint has also been proposed [3].

Swaminathan et al. [4] have analyzed some characteristics of conic reflectors caused by misaligning the camera and mirror. The paper presents an in-depth analysis of the caustics [5] of catadioptric cameras with conic reflectors, a method of calibrating conic catadioptric systems, and a method of estimating their caustics from known camera motion. However, they do not analyze some characteristics of conic reflectors when the camera is rotated.

Much work has been done on developing methods to calibrate perspective camera [6][7][8] and catadioptric camera [9][10][11][12][13]. Geyer and Daniilidis [9] proposed a method of calibration to estimate intrinsic parameters of a catadioptric camera system that consists of a paraboloid mirror and an orthographic lens. Kang [10] also proposed a self-calibration method for a catadioptric camera system that consists of a paraboloid mirror and an orthographic lens. Strelow et al. [11] proposed a model for relation between the mirror and camera with 6 degrees of freedom (translation and rotation). They determined 6 parameters through nonlinear optimization. This has the advantage that translation and rotation parameters are simultaneously determined, but the disadvantage that the

accuracy of the estimated parameters is worse and depends on the initial values because of nonlinear optimization.

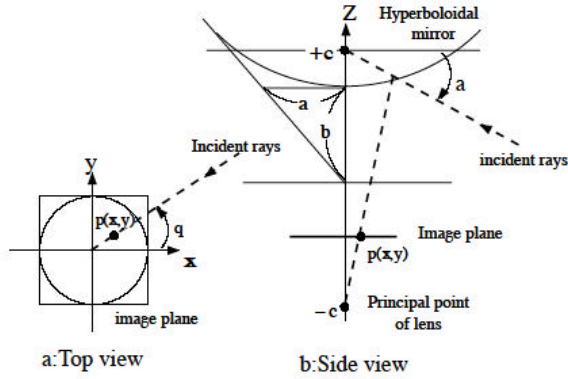


Fig. 1. HyperOmni Vision

2 Omnidirectional Camera: HyperOmni Vision

We use an omnidirectional image sensor as a catadioptric camera. This sensor covers a wide range of view and has the same optical characteristics of a common camera (single viewpoint), so we can easily transform the catadioptric image to a perspective image. We briefly explain the sensor below.

The sensor consists of a camera fixed upward and a hyperboloidal mirror fixed downward. The hyperboloidal plane of the mirror is expressed by Eq. 1 and has two focal points: $(0, 0, +c)$ and $(0, 0, -c)$. The hyperboloidal mirror is fixed at the upper focal point, $(0, 0, +c)$, and the focal point of the camera is fixed at the lower focal point, $(0, 0, -c)$ (Fig. 1). The image plane, x - y , is parallel to the XY -plane, and is fixed at $(0, 0, f-c)$. f is a focal length of the camera.

$$\frac{X^2 + Y^2}{a^2} - \frac{Z^2}{b^2} = -1, \quad (1)$$

$$c = \sqrt{a^2 + b^2}, \quad (2)$$

$$Y/X = y/x, \quad (3)$$

$$Z = \sqrt{X^2 + Y^2} \tan a + c, \quad (4)$$

$$a = \tan^{-1} \frac{(b^2 + c^2) \sin b - 2bc}{(b^2 - c^2) \cos b}, \quad (5)$$

$$b = \tan^{-1} \frac{f}{\sqrt{x^2 + y^2}}. \quad (6)$$

This is where a and b are parameters of the hyperboloidal plane, a is the depression angle, and b is the angle between the optical axis and projected point (x,y) .

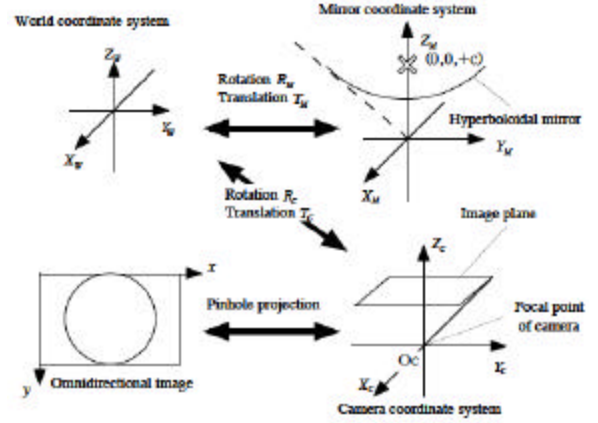


Fig. 2. Coordinate systems

3 Simulation System

In this section, we present a simulation system to analyze the error caused by misalignment of the camera and mirror. We cannot use the ideal model described in Sect. 2 because of misalignment. The simulation system uses four coordinate systems (image, camera, mirror, and world), and traces incident rays from the camera through coordinate transformation (Fig. 2).

3.1 Camera Model

The simulation system uses a perspective camera model as the camera model. Let $\tilde{\mathbf{x}} = (x, y, 1)^T$ and $\tilde{\mathbf{X}}_c = (X_c, Y_c, Z_c, 1)^T$ be the augmented vectors of points in the image coordinate system and in the camera coordinate system, respectively. The relation between $\tilde{\mathbf{x}}$ and $\tilde{\mathbf{X}}_c$ is expressed by the following equations:

$$\tilde{\mathbf{x}} = sA\tilde{\mathbf{X}}_c, \quad (7)$$

$$A = \begin{bmatrix} fk_x & fk_s & 0 & x_0 \\ 0 & fk_y & 0 & y_0 \\ 0 & 0 & 1 & 0 \end{bmatrix}, \quad (8)$$

where s is the scale factor, A is camera intrinsic matrix, f is the focal length, (x_0, y_0) is the image center, k_x and k_y are scale factors of pixel size, and k_s is the skewness of x and y axes. If the camera is an ideal perspective model, A is expressed as follows:

$$A = \begin{bmatrix} f & 0 & 0 & x_0 \\ 0 & f & 0 & y_0 \\ 0 & 0 & 1 & 0 \end{bmatrix}. \quad (9)$$

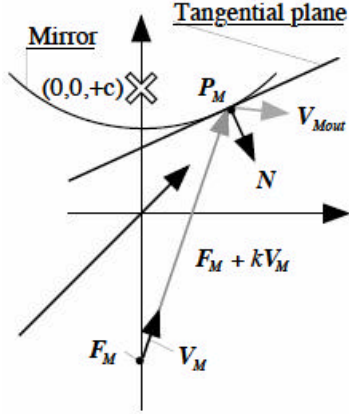


Fig. 3. Reflection in mirror coordinate system

3.2 Mirror Model

In this section, we explain the mirror coordinate system, mirror model, and reflection model. The hyperboloidal mirror expressed by Eq. 1 is used as a mirror model. The point, P_M of a ray from the camera intersecting with the mirror plane is calculated from the focal point of the camera in the mirror coordinate system, $F_M = (F_{MX}, F_{MY}, F_{MZ})^T$, the direction vector of a ray from the camera in the mirror coordinate system, $V_M = (V_{MX}, V_{MY}, V_{MZ})^T$, and Eq. 1. A ray from the camera can be defined as $F_M + kV_M$. Coefficient k at the intersection point, P_M , is calculated with the following equations:

$$k = \frac{-b_M \pm \sqrt{b_M^2 - a_M g_M}}{a_M} \quad (10)$$

$$a_M = \frac{V_{MX}^2 + V_{MY}^2}{a^2} - \frac{V_{MZ}^2}{b^2} \quad (11)$$

$$b_M = \frac{V_{MX} P_{MX} + V_{MY} P_{MY}}{a^2} - \frac{V_{MZ} P_{MZ}}{b^2} \quad (12)$$

$$g_M = \frac{P_{MX}^2 + P_{MY}^2}{a^2} - \frac{P_{MZ}^2}{b^2} + 1 \quad (13)$$

Let N be a normal vector of a mirror at intersection point P_M . Figure 3 shows the geometric relation between P_M , N , V_M , F_M , and the direction vector, $V_{M_{out}}$, of a ray reflected at intersection point P_M . N satisfies the following equation because of visibility:

$$(N, V_M) < 0, \quad (14)$$

where (\cdot) expresses the inner product. Equation 10 has two solutions, and we choose k which satisfies Eq. 14.

To calculate the tangential plane, Eq. 1 of a hyperboloidal plane is rewritten as

$$f(X_M, Y_M) = Z_M = \sqrt{b^2 \left(\frac{X_M^2 + Y_M^2}{a^2} + 1 \right)} \quad (Z_M > 0) \quad (15)$$

and partial derivatives are

$$f_{X_M} = \frac{bX_M}{a\sqrt{X_M^2 + Y_M^2 + a^2}} \quad (16)$$

$$f_{Y_M} = \frac{bY_M}{a\sqrt{X_M^2 + Y_M^2 + a^2}} \quad (17)$$

The normal vector, N , is

$$N = (f_{X_M}(P_M), f_{Y_M}(P_M), -1) \quad (18)$$

Finally, the direction vector, $V_{M_{out}}$, of a ray reflected at intersecting point P_M is calculated with the following equation:

$$V_{M_{out}} = V_M - 2N(N, V_M), \quad (19)$$

where V_M is the direction vector of a ray from the camera. The viewpoint of this ray is the intersecting point, P_M .

3.3 Ray Tracing

As previously mentioned, ray tracing is implemented by using coordinate transformation. A ray from the camera in the camera coordinate, V_C , and the focal point of the camera in the camera coordinate, F_C , are transformed to the world coordinate system by using rotation matrix R_W and translation vector T_C as follows:

$$V_W = R_C V_C, \quad (20)$$

$$F_W = R_C F_C + T_C. \quad (21)$$

Transformation from the world coordinate system to the mirror coordinate system are also accomplished with the following equations:

$$V_M = R_M V_W, \quad (22)$$

$$F_M = R_M F_W + T_M. \quad (23)$$

As mentioned in Sect. 3.2, a ray from the camera is reflected at intersection point P_M . The simulation system calculates a reflected ray, $V_{M_{out}}$, and a viewpoint of the reflected ray, which has the same position as intersection point P_M . The viewpoint and reflected ray in the world coordinate system are calculated with the following equations:

$$V_{W_{out}} = R_M^{-1} V_{M_{out}}, \quad (24)$$

$$P_W = R_M^{-1} (P_M - T_M). \quad (25)$$

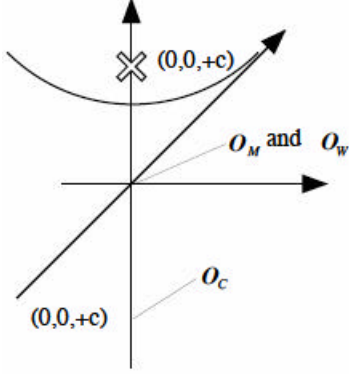


Fig. 4. Positions of coordinate systems

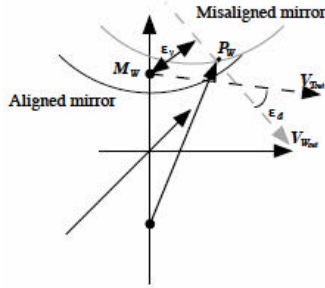


Fig. 5. The viewpoint error and the direction error

4 Experiments

We conducted experiments to evaluate estimation errors in the viewpoint and direction of a reflected ray, which were caused by misalignment between the camera and mirror. We used ideal positions for the camera and mirror as the ground truth in the experiments. Figure 4 shows the ground truth for each position of the coordinate systems. The parameters of the camera intrinsic matrix expressed in Eq. 9 were: $f=1000$, $x_0=250$, and $y_0=250$. The image was 500x500 pixels. These parameters were based on those of HyperOmni Vision [1].

Figure 5 shows the viewpoint error, e_v , and the direction error, e_d . These are calculated with the following equations:

$$e_v = \left| \mathbf{M}_w - \mathbf{P}_w + \mathbf{V}_{W_{out}} \left((-\mathbf{P}_w, \mathbf{V}_{W_{out}}) + (\mathbf{M}_w, \mathbf{V}_{W_{out}}) \right) \right| \quad (26)$$

$$e_d = \left| \cos^{-1} \left(\frac{|\mathbf{V}_{T_{out}}| |\mathbf{V}_{W_{out}}|}{(\mathbf{V}_{T_{out}}, \mathbf{V}_{W_{out}})} \right) \right|, \quad (27)$$

where $\mathbf{V}_{T_{out}}$ is the ground truth of the direction of a reflected ray and \mathbf{M}_w is the ground truth of the viewpoint, which is also the focal point of the mirror if the camera and mirror are correctly aligned. Variations in misalignment are caused by translation parallel to the Z and Y-axes and by rotating around the X-axis.

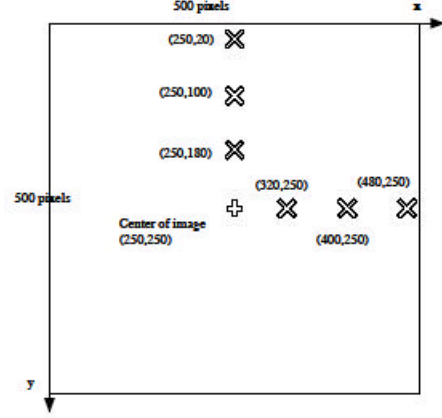


Fig. 6. The observation points

4.1 Error Distributions on Image Plane

The errors caused by misalignment are not constant on the image plane. In these experiments, we calculated the error distributions on the image plane. Figure 7 shows the error distributions. We can see that viewpoint error spreads from outside the image to the center and direction error spreads from the center of the image to the outside. Both errors caused by misalignment produced by translation parallel to the Y-axis are larger than errors caused by misalignment produced by translation parallel to the Z-axis.

4.2 Variation of Error

We did experiments on the relations between errors and variations in misalignment. In these, misalignment caused by translation parallel to the Y-axis was changed from 0 to 10.0 mm, misalignment caused by translation parallel to the Z-axis was changed from -10.0 to 10.0 mm, and misalignment of rotation was changed from 0.0 to 10.0 degrees around the X-axis. The system then calculated the errors at the observation points. Figure 8 shows the relations between each error and misalignment of rotation and translation. We can see that both direction and viewpoint error caused by misalignment due to translation parallel to the Z-axis is also smaller than the other errors. Direction error was larger than viewpoint error. The errors at inner observation points, (250,180) and (320,250) in Figs. 8 (b) and (f), are larger than the other observation points. However, the region near the center of the image is not used because the camera is projected into the region.

5 Conclusion

In this paper, we discussed the implementation of the simulation system for a catadioptric camera. Although our simulated HyperOmniVision consisted of a hyperboloidal mirror and pinhole camera model, it is easy to apply it to the catadioptric camera system consisting of a parabolic mirror and an orthogonal camera model. In the case of

parabolic mirror, we think that the camera model should not be an orthogonal camera but like a telecentric camera because an orthogonal camera is nonexistent. In a real catadioptric camera system, our system can be applied to calibration when both the rotation matrix and the translation vector between the camera and mirror are known or have been estimated.

In the experiment, we calculated and evaluated the viewpoint error and direction error caused by the misalignment of rotation and translation between the camera and mirror. The experimental results revealed that we need to address to misalignment parallel to the image plane and rotation around the X and Y-axes, when we align the camera and mirror.

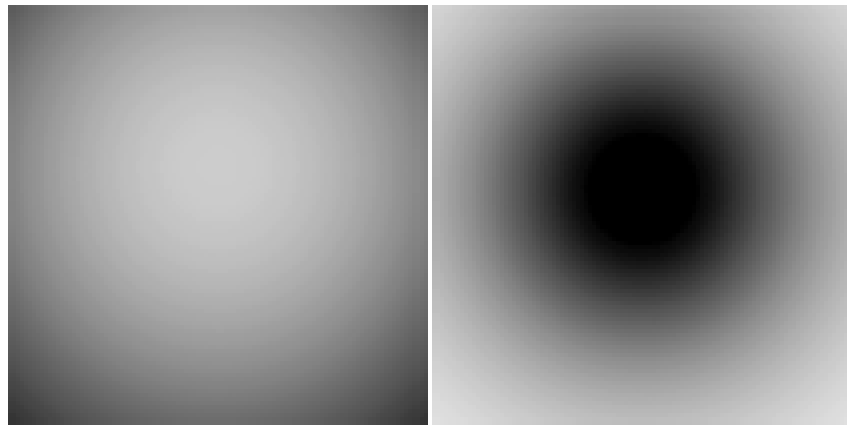
In future work, we intend to apply our simulation system to a catadioptric camera system consisting of a parabolic mirror and orthogonal camera model and experiment with calibrating catadioptric camera systems.

Acknowledgement

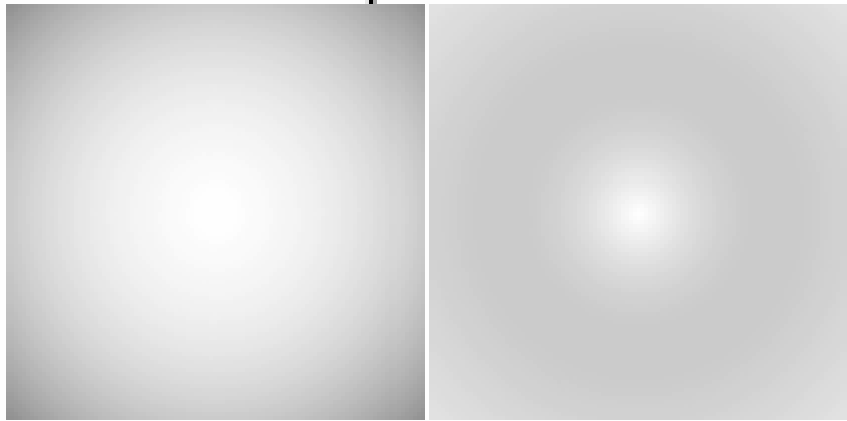
This research was supported (or founded) by the Japan Society for the Promotion of Science under Grant-in-Aid for Creative Scientific Research (Project No. 13GS0018).

References

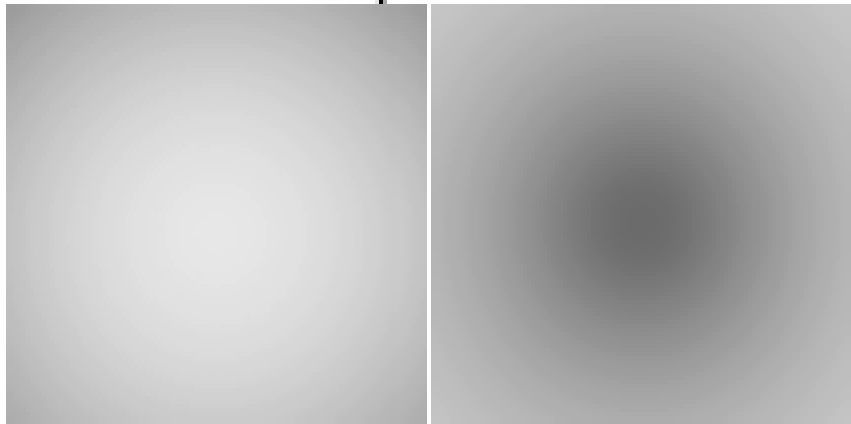
- [1] Yamazawa, K., Yagi, Y., Yachida, M., "Omnidirectional imaging with hyperboloidal projection", *IROS*. Vol. 2. pp. 1029-1034, 1993.
- [2] Nayar, S.K. "Catadioptric omnidirectional camera", *Proc. of IEEE Computer Vision and Pattern Recognition*. 482-488, 1997.
- [3] Srinivasan, M.V., "A new class of mirrors for wide angle imaging", *Omnivis*, 2003.
- [4] Swaminathan, R., Grossberg, M.D., Nayar, S.K., "Caustics of catadioptric cameras". *Proc. of IEEE International Conference on Computer Vision*, Vol. 2, pp. 2-9, 2001.
- [5] Bruce, J.W., Giblin, P.J., Gibson, C.G., "On caustics of plane curves", *The American Mathematical Monthly* 88 pp. 651-667, 1981.
- [6] Lenz, R., Tsai, R., "Techniques for calibration of the scale factor and image center for high accuracy 3-d machine vision metrology", *PAMI* Vol. 10 No. 5, pp. 713-720, 1988.
- [7] Yang, C., Sun, F., Hu, Z., "Planar conic based camera calibration". *Proc. of IEEE International Conference on Pattern Recognition*. Vol. 1, pp. 555-558, 2000.
- [8] Wu, H., Chen, Q., Wada, T., "Homography from conic intersection: Camera calibration based on arbitrary circular patterns", *IPSI Transactions on Computer Vision and Image Media* No. 139
- [9] Geyer, C., Daniilidis, K., "Catadioptric camera calibration", *Proc. of IEEE International Conference on Computer Vision*, pp. 398-404, 1999.
- [10] Kang, S.B., "Catadioptric self-calibration", *Proc. of IEEE Computer Vision and Pattern Recognition*, Vol. 1. pp. 201-207, 2000.
- [11] Stelow, D., Mishler, J., Koes, D., Singh, S. "Precise omnidirectional camera calibration", *Proc. of IEEE Computer Vision and Pattern Recognition*. Vol. 1, pp. 689-694, 2001.
- [12] Aliaga, D.G., "Accurate catadioptric calibration for real-time pose estimation of room-size environments", *Proc. IEEE International Conference on Computer Vision*, Vol. 1, pp.127-134, 2001.
- [13] Geyer, C., Daniilidis, K. "Paracatadioptric camera calibration", *PAMI* Vol. 24 pp. 687-695, 2002.



(a): Viewpoint error (b): Direction error
+5mm parallel to Y-axis

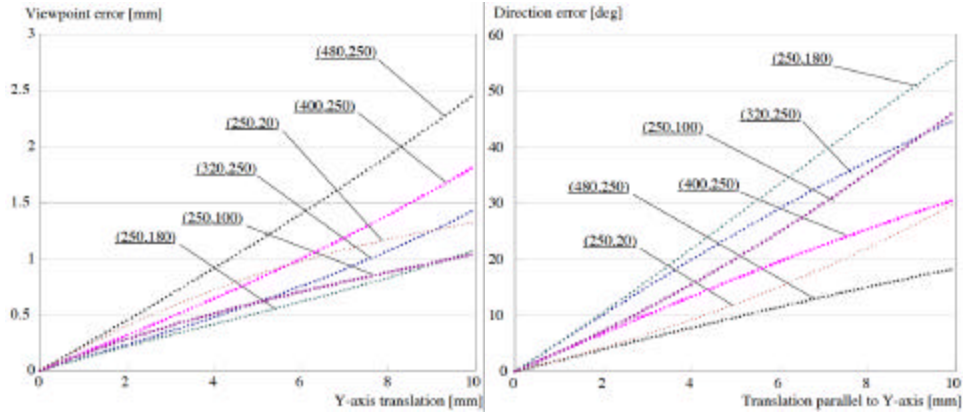


(c): Viewpoint error (d): Direction error
+10mm parallel to Z-axis



(e): Viewpoint error (f): Direction error
Three degrees rotation around X-axis

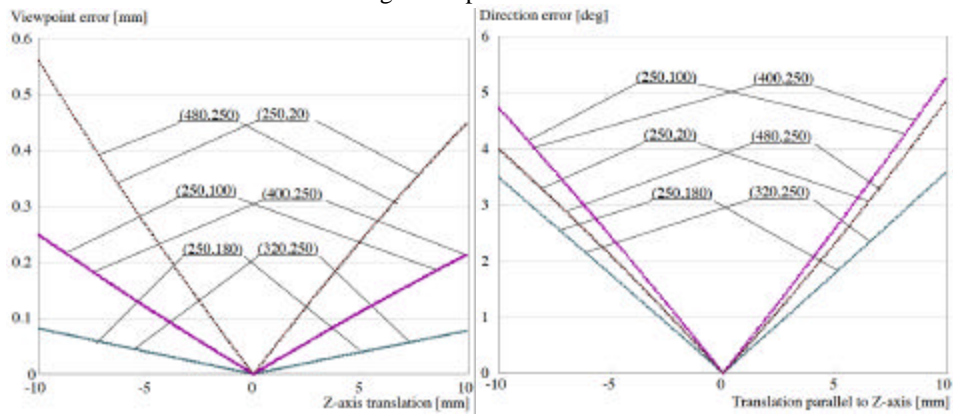
Fig. 7. Distributions of errors: The gray levels are progressively darker according to error i.e., error at pure white pixels is zero.



(a): Viewpoint error

(b): Direction error

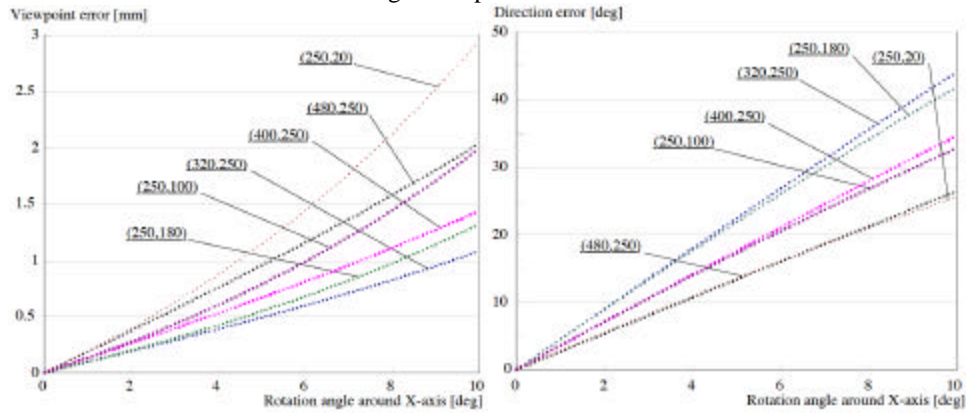
Misalignment parallel to Y-axis



(c): Viewpoint error

(d): Direction error

Misalignment parallel to Z-axis



(e): Viewpoint error

(f): Direction error

Misalignment of rotation around X-axis

Fig. 8. Variations in error

A Polynomial Time Algorithm for the Two-Sink Location Problem in a Tree Dynamic Network

Satoko MAMADA

Division of Mathematical Science for Social Systems,
Graduate School of Engineering Science, Osaka University,
Toyonaka, Osaka, 560-8531, Japan.

E-mail: mamada@inulab.sys.es.osaka-u.ac.jp

Phone: +81-6-6850-6353

Fax: +81-6-6850-6341

Kazuhisa MAKINO

Division of Mathematical Science for Social Systems,
Graduate School of Engineering Science, Osaka University,
Toyonaka, Osaka, 560-8531, Japan.

E-mail: makino@sys.es.osaka-u.ac.jp

Phone: +81-6-6850-6351

Fax: +81-6-6850-6341

Satoru FUJISHIGE

Research Institute for Mathematical Sciences, Kyoto University,
Kyoto, 606-8502, Japan.

E-mail: fujishig@kurims.kyoto-u.ac.jp

Phone: +81-75-753-7250

Fax: +81-75-753-7276

TOPIC: Networks

A Polynomial Time Algorithm for the Two-Sink Location Problem in a Tree Dynamic Network

abstract : We consider a sink location problem in a dynamic network as one of the basic studies on crisis management systems for evacuation guidance of residents against large-scale disasters. A dynamic network is defined by a directed graph $G = (V, A)$ with capacities $u(a)$ and transit times $\tau(a)$ for arcs $a \in A$. Given a dynamic network with initial supplies (representing residents) at vertices, the problem is to find a vertex set S of size k as a sink set in the network such that we can send all the initial supplies to S as quickly as possible. Motivated by evacuation plans, we restrict our attention to tree networks and flows such that all the supplies going through a common vertex are sent to a single sink, since everyone has to flee to a safety place (a sink) fairly and/or without confusion. It is known that the sink location problem with a single sink can be solved in $O(n \log^2 n)$ time, where n denotes the number of vertices in the network. In this paper we present an $O(n \log^3 n)$ time algorithm for the sink location problem with two sinks, i.e., $k = 2$.

1. Introduction

Recently, it has widely been recognized how important it is to establish crisis management systems against large-scale disasters such as big earthquakes. It is one of the most important issues in the crisis management against disasters to secure evacuation pathways and to effectively

guide residents to safety places.

In this paper, we adopt dynamic networks as a model for evacuation. Namely, we regard evacuation problems as flow problems on dynamic networks. Dynamic network flow problems have been considered in the literature (see, e.g., [1, 3]) and the multiple-source and multiple-sink dynamic network flow problem has been solved in strongly polynomial time [4].

A dynamic network is defined by a directed graph $G = (V, A)$ with a capacity function $u : A \rightarrow \mathbf{R}_+$ and a transit-time function $\tau : A \rightarrow \mathbf{R}_+$ on the arc set A . For example, if we consider building evacuation, vertices $v \in V$ model workplaces, hallways, stairwells, and so on, and arcs $a \in A$ model the links between these parts of the building. For an arc $a \in A$, $u(a)$ represents the number of people per unit time which can traverse the link corresponding to a , and $\tau(a)$ denotes the time it takes to traverse $a = (v, w)$ from v to w .

The quickest transshipment problem is defined by a dynamic network with several sources and sinks; each source has a specified supply and each sink has a specified demand. The problem is to send exactly the right amount of flow out of each source and into each sink in the minimum overall time. Here sources can be regarded as places where the people to evacuate are staying, and sinks can be regarded as emergency ex-

its. Hoppe and Tardos [4] constructed the only known polynomial time algorithm for the general problem.¹ Unfortunately, their algorithm requires polynomial time of high degree complexity, and hence is not practical.

In this paper, we restrict our attention to tree networks and consider flows such that all the supplies going through a common vertex are sent out from a single incident arc toward a single sink, since everyone has to flee to a safety place (a sink) fairly and without confusion. The problem when we want to optimally locate one sink can be solved in $O(n \log^2 n)$ time [5], where n is the number of vertices in the given network. Note that the assumption on flows is automatically satisfied in this case. The present paper shows that the problem with two sinks can be solved in $O(n \log^3 n)$ time by using an $O(n \log^2 n)$ algorithm [5].

The rest of the paper is organized as follows. The next section formally defines the problem and introduces some notations. Some definitions and preliminary results are given in Section 2. Section 3 briefly reviews the algorithm for our location problem with the single sink and considers our two-sink location problem. Finally, Section 4 concludes the paper.

¹ The continuous version of the quickest transshipment problem was solved by Fleischer and Tardos [2] in polynomial time.

2. Definitions and Preliminaries

We consider a dynamic network $\mathcal{N} = (T = (V, A), u, \tau, b)$, where T is a graph with a set V of vertices and a set A of arcs, $u : A \rightarrow \mathbf{R}_+$ is a capacity function, $\tau : A \rightarrow \mathbf{R}_+$ is a transit-time function, and $b : V \rightarrow \mathbf{R}_+$ is a supply function. Here \mathbf{R}_+ denotes the set of all nonnegative reals. For each arc $a \in A$ $c(a)$ denotes the upper limit for the rate of a flow that enters arc a per unit time, and $\tau(a)$ the time required for the transition through arc a , which does not depend on the flow rate. We assume that the undirected graph obtained from T by ignoring the orientation of arcs and then identifying parallel edges is a tree

The present paper addresses a problem of finding a sink pair $\{t_1, t_2\} \subseteq V$ such that we can send given initial supplies $b(v)$ ($v \in V \setminus \{t_1, t_2\}$) to the sinks t_1 and t_2 as quickly as possible. Here we assume that all the supplies going through a common vertex are sent to a single sink. It follows from the assumption that V can be partitioned into two disjoint sets V_1, V_2 such that for each $i = 1, 2$ the subgraph induced by V_i contains a single sink t_i and supplies in V_i are sent to t_i .

For any arc $a \in A$, any $\theta \in \mathbf{R}_+$, we denote by $f_a(\theta)$ the rate of a flow entering the arc a at time θ , which arrives at the head of a at time $\theta + \tau(a)$. We call $f_a(\theta)$ ($a \in A, \theta \in \mathbf{R}_+$) a *continuous dynamic flow* in T (with a sink set S) if it satisfies the following three conditions.

- (a) (Capacity constraints): For any arc $a \in A$

and $\theta \in \mathbf{R}_+$,

$$0 \leq f_a(\theta) \leq u(a).$$

- (b) (Flow conservation): For any $v \in V \setminus \{t_1, t_2\}$ and $\Theta \in \mathbf{R}$,

$$\sum_{a \in \delta^+ v} \int_0^\Theta f_a(\theta) d\theta - \sum_{a \in \delta^- v} \int_{\tau(a)}^\Theta f_a(\theta - \tau(a)) d\theta \leq b(v).$$

- (c) (Flow completion): There exists a time $\Theta \in \mathbf{R}_+$ such that

$$\sum_{a \in \Delta^-(S)} \int_{\tau(a)}^\Theta f_a(\theta - \tau(a)) d\theta - \sum_{a \in \Delta^+(S)} \int_0^\Theta f_a(\theta) d\theta = \sum_{v \in V \setminus S} b(v). \quad (2.1)$$

Here $\delta^+ v$ and $\delta^- v$ are, respectively, the set of arcs having v as their tails and heads, and $\Delta^+(S) = \{(v, w) \in A \mid v \in S, w \notin S\}$ and $\Delta^-(S) = \{(v, w) \in A \mid v \notin S, w \in S\}$. As seen in (b), we allow intermediate storage (or holding inventory) at each vertex.

Based on the assumption given above, we consider continuous dynamic flows that satisfy

- (d-1) For any arc $a = (t_i, w) \in A$ with $i = 1, 2$ and $\theta \in \mathbf{R}_+$, we have $f_a(\theta) = 0$,
- (d-2) For any arc $a = (v, w) \in A$, if $f_{a^*}(\theta^*) > 0$ for some $a^* \in \delta^+ v$ ($a^* \neq a$) and $\theta^* \in \mathbf{R}_+$, then $f_a(\theta) = 0$ for any $\theta \in \mathbf{R}_+$.

We call a flow satisfying (a), (b), (c), (d-1), and (d-2) *feasible*.

For a feasible (continuous dynamic) flow f , let θ_f denote the completion time for f , i.e., the minimum Θ in condition (c). For a sink set S

we denote by $C(S)$ the minimum θ_f for all feasible flows in \mathcal{N} with sink set S . Our problem is to compute a two-sink set $S = \{t_1, t_2\}$ that attains the minimum completion time $C(\{t_1, t_2\})$ among all two-sink sets in the given network \mathcal{N} .

3. Algorithm

In this section, we give an algorithm to solve the two-sink location problem described in the previous section.

3.1. Algorithm SINGLE-PHASE

Our algorithm for the two-sink location problem uses the algorithm SINGLE-PHASE described in [5]. SINGLE-PHASE outputs an optimal sink t that has the minimum completion time $C(\{t\})$ among all vertices of T . Then, T is regarded as an in-tree with root t , i.e., each edge of T is oriented toward the root t . Such an oriented tree with root t is denoted by $\vec{T}(t) = (V, \vec{E}(t))$. Each oriented edge in $\vec{E}(t)$ is denoted by the ordered pair of its end vertices and is called an arc. In this algorithm, we keep two tables, *Arriving Table* A_v and *Sending Table* S_v for each vertex $v \in V$. Arriving Table A_v represents the sum of the flow rates arriving at vertex v as a function of time θ , i.e.,

$$\sum_{e \in \vec{E}(t): e=(u,v)} f_e(\theta - \tau(e)) + \eta_\theta(v),$$

where $f_e(\theta) = 0$ holds for any $e \in \vec{E}(t)$ and $\theta < 0$, and $\eta_\theta(v) = \frac{b(v)}{\Delta}$ if $0 \leq \theta < \Delta$; otherwise 0. Here, Δ denotes a sufficiently small

positive constant. Intuitively, $\eta_\theta(v)$ (i.e., the area $\int_0^\infty \eta_\theta(v)d\theta$) denotes the initial supply at v . Sending Table S_v represents the rate of the flow leaving vertex v as a function of time θ , i.e.,

$$f_{(v,w)}(\theta),$$

where $(v, w) \in \vec{E}(t)$.

Let us consider a table $g : \mathbf{R}_+ \rightarrow \mathbf{R}_+$, which represents the flow rate in time $\theta \in \mathbf{R}_+$. Here, we assume $g(\theta) = 0$ for $\theta < 0$. Since our problem can be solved by sending out as much amount of flow as possible from each vertex to its parent if a candidate sink t is chosen in advance, we only consider the table g which is representable as

$$g(\theta) = \begin{cases} 0 & \text{if } \theta < \theta_1 \\ g(\theta_i) & \text{if } \theta_i \leq \theta < \theta_{i+1} \\ & \text{for } i = 1, \dots, k-1 \\ 0 & \text{if } \theta \geq \theta_k, \end{cases}$$

where $\theta_i < \theta_{i+1}$ and $g(\theta_i) \neq g(\theta_{i+1})$ for $i = 1, \dots, k$. Thus, we represent such tables g by a set of intervals (with their height), i.e.,

$$((-\infty, \theta_1), 0), ([\theta_i, \theta_{i+1}), g(\theta_i)) \quad (i = 1, 2, \dots, k),$$

where $\theta_{k+1} = +\infty$ and $g(\theta_k) = 0$. A time θ is called a *jump time* of g if $\lim_{x \rightarrow -0} g(\theta + x) \neq \lim_{x \rightarrow +0} g(\theta + x)$.

Figure 1 shows such a table g , where black circles denote $g(\theta_i)$'s at jump time θ_i 's.

Let us now describe the algorithm SINGLE-PHASE as follows.

Algorithm SINGLE-PHASE

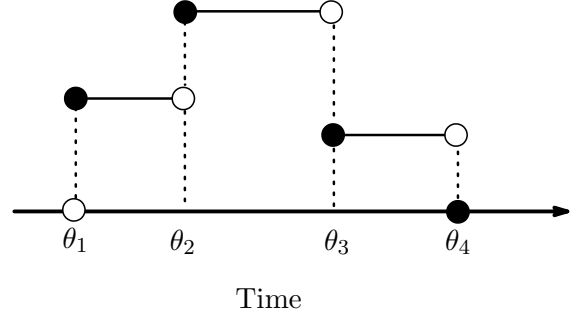


Figure 1: An example of a table that can be decomposed into intervals.

Input: A tree dynamic network $\mathcal{N} = (T = (V, E), c, \tau, b)$.

Output: An optimal sink t that has the minimum completion time $C(\{t\})$ among all vertices of T .

Step 0: Let $W := V$, and let L be the set of all leaves of T . For each $v \in L$, construct Arriving Table A_v .

Step 1: For each $v \in L$, construct from A_v Sending Table S_v to go through $(v, p(v))$, where $p(v)$ is an only vertex adjacent to v in T . Compute the time $Time(v, p(v))$ at which the flow based on S_v is completely sent to $p(v)$.

Step 2: Compute a vertex $v^* \in L$ minimizing $Time(v, p(v))$, i.e., $Time(v^*, p(v^*)) = \min_{v \in L} Time(v, p(v))$. Let $W := W \setminus \{v^*\}$ and $L := L \setminus \{v^*\}$.

If there exists a leaf v of $T[W]$ such that v is not contained in L ,

then:

- (1) Let $L := L \cup \{v\}$.
- (2) Construct Arriving Table A_v from the initial supply $\eta_\theta(v)$ and Sending Table $S_{v'}$ for the vertices v' that are adjacent to v in T and have already been removed from W .
- (3) Compute from A_v Sending Table S_v to go through $(v, p(v))$ where $p(v)$ is a vertex adjacent to v in $T[W]$, and compute $Time(v, p(v))$.

Step 3: If $|W| = 1$, then output $t \in W$ as an optimal sink. Otherwise, return to Step 2. \square

Here, $T[W]$ denotes a subtree of T induced by a vertex set W and it should be noted that Arriving Table A_v for a leaf v of the original $\vec{T}(t)$ represents the initial supply given at v , i.e., $A_v(0) = b(v)$ and $A_v(k) = 0$ for $k \neq 0$. It should also be noted that if the value of the left-hand side of (2.1) for a vertex $v(\neq t)$ is at least the capacity $u(v, v')$, then we put $f_k((v, v'), 0) = u(v, v')$ to attain the (quickest) completion time $C(\{t\})$. Also, note that $f_k((v, v'), 0) < u(v, v')$ only if $h_k(v) = 0$. This gives a procedure for constructing Sending Table S_v by using Arriving Table A_v . Since the problem can be solved by sending out as much amount of flow as possible from each vertex to its parent, we can see that algorithm SINGLE-PHASE correctly computes the completion time $C(\{t\})$ as well as A_v ($v \in V$) and S_v ($v \in V \setminus \{t\}$). Although we skip the details, we have an $O(n \log^2 n)$ -time algorithm for our problem [5].

3.2. The Two-Sink Location Problem

We can obtain a straightforward algorithm for the two-sink location problem as follows: for each arc $a \in A$, let T_a^1 and T_a^2 be the two subtrees of T obtained by cutting the given tree T at arc a and solve two single-sink location problems for T_a^1 and T_a^2 . The best sink pair among these solutions is an optimal sink pair. This gives an $O(n^2 \log^2 n)$ -time algorithm by repeated use of the $O(n \log^2 n)$ -time algorithm for a single-sink location problem. We show an $O(n \log^3 n)$ -time algorithm by using the information about the optimal cut location in the given tree that is obtained by solving the single-sink location problem for \mathcal{N} .

Let t be an optimal sink in T obtained by Algorithm SINGLE-PHASE and let $x = v_1$ be a vertex adjacent to t that sends the *last flow* to t , which is the flow that arrives at t last among all flows coming into t . Moreover, let v_2 be the vertex adjacent to v_1 that sends a last flow to v_1 . Repeating this process, we obtain a path $P_x = (v_1^x (= x), v_2^x, \dots, v_{\ell_x}^x (= \text{a leaf of } T))$. we call P_x the *x-last-flow-path*. By removing an edge $\{v, w\}$ from T , T is partitioned into two disjoint subtrees. We denote the one including v by $T_{(v,w)}^v$ and the other by $T_{(v,w)}^w$. Restricting the flow to $T_{(x,t)}^t$, let y be the vertex adjacent to t that sends the last flow in $T_{(x,t)}^t$. Then we obtain the *y-last-flow-path* $P_y = (v_1^y (= y), v_2^y, \dots, v_{\ell_y}^y (= \text{a leaf of } T))$ similarly as P_x . We call the path in T connecting the two leaves $v_{\ell_x}^x$ and $v_{\ell_y}^y$ the *last-flow-path* in T .

For any edge $\{u, v\}$ in T let $Time(u, v)$ be the minimum time to send supplies in $T_{(u,v)}^u$ to v .

Now, we have the following lemma.

Lemma 3.1: *There is an optimal sink pair $\{t_1, t_2\}$ such that t_1 lies in $T_{(x,t)}^x$ and t_2 lies in $T_{(x,t)}^t$.*

Proof. Let w be a vertex adjacent to x on the x -last-flow-path P_x . If we take $\{t, x\}$ as a sink pair in T , then

$$C(\{t, x\}) = \max\{Time(y, t), Time(w, x)\} \quad (3.1)$$

since t is an optimal single-sink location in T .

Consider a sink pair $\{t_1, t_2\}$ such that both t_1 and t_2 lie in $T_{(x,t)}^x$. Then, since t is an optimal single-sink location in T , we have

$$Time(t, x) \geq Time(x, t) \geq Time(w, x). \quad (3.2)$$

Also, by the definitions of x and y ,

$$Time(t, x) \geq Time(y, t). \quad (3.3)$$

It follows from (3.1), (3.2), and (3.3) that

$$\begin{aligned} C(\{t_1, t_2\}) &\geq Time(t, x) \geq \\ &\max\{Time(y, t), Time(w, x)\} = C(\{t, x\}). \end{aligned}$$

Hence, it suffices to consider the case when there is at most one of the sinks in the optimal sink-pair lies in $T_{(x,t)}^x$.

Moreover, consider a sink pair $\{t_1, t_2\}$ such that neither t_1 nor t_2 lies in $T_{(x,t)}^x$. For such a sink pair $\{t_1, t_2\}$ we have

$$\begin{aligned} C(\{t_1, t_2\}) &\geq Time(x, t) \geq \\ &\max\{Time(y, t), Time(w, x)\} = C(\{t, x\}). \end{aligned}$$

Therefore, there exists an optimal sink pair $\{t_1, t_2\}$ such that t_1 lies in $T_{(x,t)}^x$ and t_2 lies in $T_{(x,t)}^t$. \square

Lemma 3.2: *There is an optimal sink pair $\{t_1, t_2\}$ such that t_1 and t_2 lie in the last-flow-path P in T .*

Proof. From Lemma 3.1 there is an optimal sink-pair $\{t_1, t_2\}$ such that t_1 lies in $T_{(x,t)}^x$ and t_2 lies in $T_{(x,t)}^t$. Suppose that t_1 does not lie in P_x . Let v_k^x be the last vertex in P_x in the path going from x to t_1 in T . Also let u_1 be the vertex adjacent to v_k^x and lying in the path from v_k^x to t_1 (see Figure 2). Then, by the definition of the x -last-flow-path P_x ,

$$Time(v_{k+1}^x, v_k^x) \geq Time(u_1, v_k^x),$$

where note that v_k^x is not a leaf, due to the assumption. Hence we have

$$C(\{t_1, t_2\}) \geq C(\{v_k, t_2\}).$$

It follows that there is an optimal sink-pair $\{t_1, t_2\}$ such that t_1 lies in P_x and t_2 lies in $T_{(x,t)}^t$.

By the same argument we can further show that there is an optimal sink-pair $\{t_1, t_2\}$ such that t_1 lies in P_x and t_2 lies in the path from t to a terminal vertex $v_{\ell_y}^y$ of P_y . \square

By Lemma 3.2, our problem is reduced to the problem of optimally partitioning the last-flow-path P .

An optimal partition can be found as follows. We first find the last-flow-path P . Let P be given by a sequence (v_1, v_2, \dots, v_k) of vertices.

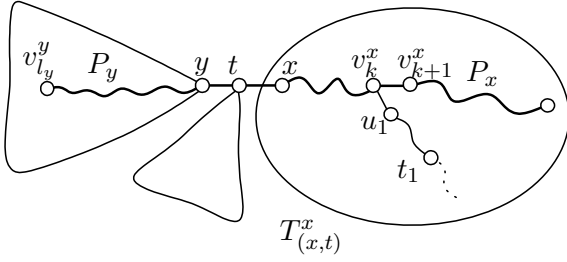


Figure 2: The component $T_{(x,t)}^x$.

For each $j = 1, 2, \dots, k-1$, let $\{t_1^j, t_2^j\}$ be a sink pair such that t_1^j and t_2^j are, respectively, optimal single-sinks of the two subtrees obtained by cutting T by edge $\{v_j, v_{j+1}\}$. Denote by $C_j(1)$ and $C_j(2)$ the completion times corresponding to sinks t_1^j and t_2^j , respectively. An optimal partition corresponds to j that attains the minimum of $\max\{C_j(1), C_j(2)\}$. Since $C_j(1)$ (resp., $C_j(2)$) is monotone non-decreasing (resp., non-increasing), we can determine the minimum of $\max\{C_j(1), C_j(2)\}$ by a binary search.

Now, an algorithm for the two-sink location problem is described as follows.

Algorithm TWO-SINK

Input: A tree dynamic network $\mathcal{N} = (T = (V, E), u, \tau, d)$.

Output: An optimal sink pair $\{t_1, t_2\}$ that has the minimum completion time $C(\{t_1, t_2\})$.

Step 1: Call Algorithm SINGLE-PHASE and construct a last-flow-path $P = (v_1, v_2, \dots, v_k)$.

Step 2: By means of the binary search, find $j \in \{1, 2, \dots, k-1\}$ that attains the minimum

of $\max\{C_j(1), C_j(2)\}$. Denote the obtained j and pair $\{t_1, t_2\}$ of optimal single-sinks by j^* and $\{t_1^*, t_2^*\}$.

Step 3: Output the sink pair $\{t_1^*, t_2^*\}$ and the completion time $C(\{t_1^*, t_2^*\}) = \max\{C_{j^*}(1), C_{j^*}(2)\}$ and halt. \square

Step 1 requires $O(n \log^2 n)$ time by using Algorithm SINGLE-SINK. Step 2 can be done in $O(n \log^3 n)$ time by Algorithm SINGLE-SINK and by the binary search. Hence Algorithm TWO-SINK computes a quickest flow and the completion time in $O(n \log^3 n)$ time.

Theorem 3.3: *Algorithm TWO-SINK solves the two-sink location problem in $O(n \log^3 n)$ time.*

4. Concluding Remarks

We have presented dynamic networks as a model for evacuation. When we restrict our attention to tree networks and flows such that all the supplies going through a common vertex are sent to a single sink, the problem is to compute an optimal pair $\{t_1, t_2\}$ of sinks such that all the supplies in V are sent to sinks t_1 and t_2 as quickly as possible. We have shown that the problem can be solved in $O(n \log^3 n)$ time, where n is the number of vertices in the given network. Further improvement over the complexity given here will be discussed elsewhere.

Finally, we note that the evacuation problem for dynamic flows can further be extended in

many directions. Some of them are (1) to find a sink to which we can send a flow of maximum value from sources within given fixed time, and (2) to consider the partition problem on general (non-tree) dynamic networks. These are left for future research.

References

- [1] J. E. Aronson: A survey of dynamic network flows. *Annals of Operations Research*, **20** (1989) 1-66.
- [2] L. Fleischer and É. Tardos: Efficient continuous-time dynamic network flow algorithms. *Operations Research Letters*, **23** (1998) 71-80.
- [3] L. R. Ford, Jr. and D. R. Fulkerson: *Flows in Networks* (Princeton University Press, Princeton, NJ, 1962).
- [4] B. Hoppe and É. Tardos: The quickest transshipment problem. *Mathematics of Operations Research*, **25** (2000) 36–62.
- [5] S. Mamada, T. Uno, K. Makino, and S. Fujishige: An $O(n \log^2 n)$ algorithm for the optimal sink location problem in dynamic tree networks, *Discrete Applied Mathematics*, to appear.

Model-Based Decision-Making Support for Problems With Conflicting Goals

Marek Makowski

International Institute for Applied Systems Analysis

A-2361 Laxenburg, Austria

marek@iiasa.ac.at

Abstract – *The paper presents selected issues of model-based support for solving complex problems. Such support requires an appropriate organization of the whole modeling process composed of a symbolic model specification, data collection, definition of model instances, diversified methods of analysis of model instances, and documentation of the whole process. The Structured Modeling Technology (SMT) developed for complex models and applied to support the whole modeling process is outlined. The main part of the paper deals with integrated methods of comprehensive model analysis, which support decision-makers with diversified ways of analysis of the underlying decision problem; one of these methods is presented in more detail, namely an extension of the reference point optimization, which supports an effective analysis of trade-offs between conflicting goals.*

Keywords: Structured modeling, decision support systems, multiple-criterion optimization, modeling systems and languages, model management, database management systems, object-oriented programming, large-scale optimization.

1 Introduction

Organizations need to solve complex problems efficiently, and in most cases this requires development, comprehensive analysis, and maintenance of models. Policy makers and almost all industrial companies, research, educational and other organizations are faced with problems of finding a best compromise between conflicting goals, such as costs versus performance and reliability of products and technologies, and the time to bring them to the market, life-time costs versus environmental impacts, or economic growth versus intergeneration fairness of a pension system, spatial and temporal allocation of costs of climate change mitigation versus ex ante and/or ex post risk management. These problems can be solved only if data, knowledge and information are not only available, but can be efficiently analyzed and shared, which typically implies use of models.

Making rational decisions for any complex problem requires various analyses of tradeoffs between conflicting goals (objectives, outcomes) that are used for measuring the results of applying various decisions in a wide range of ap-

plication domains. A typical decision problem has an infinite number of solutions, and users are interested in analyzing trade-offs between those that correspond to their preferences (assumptions, trade-offs), which is often called preferential structure of the user. A preferential structure typically induces partial ordering of solutions (characterized by values of goals) obtained for different combinations of values of decisions. Models can potentially provide better solutions for such problems, if an appropriate modeling technology is applied.

The rest of the paper is organized as follows. The next section presents the characteristics of models, and of modeling processes aimed at decision-making support for complex problems. Section 3 deals with an overview of structured modeling technology and its application to complex problems modeling. The main part of the paper, presented in Section 4 discusses modern methods of model analysis. The last section contains conclusions.

2 Modeling for decision support

Because of the unquestionable success of modeling in problem solving, various modeling paradigms have been intensively developed over the last few decades. In this, to a great extent case-study-driven process, a growing tendency to focus on specific methodologies and tools was observed. As a result, different types of models (characterized by types of variables and relations between them) were developed (e.g., static, dynamic, continuous, discrete, deterministic, stochastic, set-membership, fuzzy, soft constraints) with a view to best representing different problems by a selected type of model. Moreover, different methods of model analysis (e.g., simulation, optimization, soft simulation, multi-criteria model analysis) have been developed as the best-possible support for various types of model analyses for different purposes and/or users. Finally, because of the growing complexity of various computational tasks, solvers have become more and more specialized, even for what was originally the same type of mathematical programming problem. Each modeling paradigm embodies a great deal of accumulated knowledge, expertise, methodology, and modeling tools specialized for solving various problems peculiar

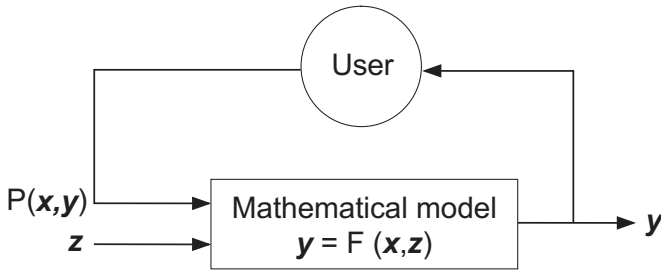


Figure 1: Structure of the use of a mathematical model for decision-making support.

to each modeling paradigm. These resources, however, are fragmented (available in diversified forms on heterogeneous hardware and software) and using more than one paradigm for the problem at hand is too expensive and time-consuming in practice. Thus, the challenge faced by the OR community is to convert the accumulated modeling knowledge and tools – which are now typically provided as closed modeling systems supporting specific modeling paradigms – into modeling environment that will enable sharing modeling resources (composed of models, data, and modeling tools) continuously contributed to global information networks.

A mathematical model describes the modeled problem by means of variables that are abstract representations of those elements of the problem that need to be considered in order to evaluate the consequences of implementation of a decision (usually represented by a vector composed of many variables). More precisely, such a model is typically developed using the following concepts:

- Decisions (inputs) x , which are controlled by the user;
- External decisions (inputs) z , which are not controlled by the user;
- Outcomes (outputs) y , used for measuring the consequences of the implementation of inputs;
- Auxiliary variables introduced for various reasons (e.g., to simplify model specification, or to allow for easier computational tasks); and
- Relations between decisions x and z , and outcomes y ; such relations are typically presented in the form:

$$y = F(x, z), \quad (1)$$

where $F(\cdot)$ is a vector of functions.

A structure of the use of a model for decision-making support is illustrated in Figure 1. The basic function of a DSS is to support the user in finding values for his/her decision variables x that will result in a solution of the problem that best fits his/her preferences. To achieve this one needs to:

- Develop and maintain a model that adequately represents relations (1);
- Organize a process of the model analysis, in which the user can specify and modify his/her preferences upon combining own experience and intuition with learning about the problem from analyses of various solutions.

These two issues are discussed in Sections 3 and 4.3, respectively.

3 Structured modeling

The complexity of problems, and the role of corresponding models in decision support are the two main factors that determine requirements for the type of modeling technology that differs substantially from the technologies successfully applied for modeling well-structured and relatively simple problems. In most publications that deal with modeling, small problems are used as an illustration of the modeling methods and tools presented. Often, these can also be applied to large problems. However, the complexity is characterized not primarily by the size, but rather by the structure of the problem and by the requirements for the corresponding modeling process.

3.1 Modeling process

Modeling is a network of activities, often referred to as a *modeling process*, or a *modeling lifecycle*. Such a process should be supported by modeling technology that is a craft of a systematic treatment of modeling tasks using a combination of pertinent elements of applied science, experience, intuition, and modeling resources, the latter being composed of knowledge encoded in models, data, and modeling tools.

Geoffrion presented in [4] a detailed specification of a modeling cycle. Here, we discuss the modeling cycle composed of more aggregated elements which correspond to the elements of the *Structured Modeling Technology* (SMT) outlined below:

- Analysis of the problem, including the role of a model in the corresponding decision-making process; and the development of the corresponding *model specification*.
- Collection and verification of *the data* to be used for the calculation of the model parameters.
- Definition of various *model instances* (composed of a model specification, and a selection of data defining its parameters).
- Diversified *analyses of the instances*.
- *Documentation* of the whole modeling process.

Often, a well organized modeling process provides more help to solving the given process than any specific result of the model analysis. Obviously, the quality of model-based support is determined by the weakest element of the modeling process. For simple problems it is possible for one person to develop and analyze a model using simple, general-purpose tools like a spreadsheet. However, any complex model is developed by several interdisciplinary teams, each contributing diversified pieces of knowledge that ultimately are organized in a mathematical model that can actually help to solve the problem. Thus, one needs a modeling technology that supports the whole process of modeling complex problems in a consistent way.

3.2 Structured Modeling Technology

SMT outlined here is based on two successful paradigms: the *Structured Modeling* (SM) paradigm developed by Geoffrion [3], which provides a proven methodological background, and the *Object-Oriented Programming* (OOP) paradigm which, combined with DBMS, XML, and the Web technologies, provides an efficient and robust implementation framework.

SMT is used through the Web interface, and all persistent elements of the modeling process are maintained by a DBMS. Thus the Web and a DBMS provide an integrating framework for collaborative work of interdisciplinary teams that use SMT applications for various elements of the modeling process.

Each model developed with SMT has its own *Data Warehouse* (DW). The DW handles not only data used for the computation of values of model parameters, but also all other persistent elements of the whole modeling process, including:

- Administrative data (about users, developers, administrators, access rights, etc.);
- A tree structure of updates defining various modifications of data;
- The specifications of elements of the modeling process, such as model specification, a selection of data (defined by a selection of updates), definitions of model instances;
- Results of various analyses of model instances.
- The documentation of the modeling process.

A more detailed presentation of SMT can be found in [8]. Here we only outline basic features of three SMT components, not including the model analysis, which is discussed in Section 4.3.

3.2.1 Model Specification

Model specification is a symbolic definition of the model composed of variables and algebraic relations between them. In order to efficiently handle large and complex models the specification exploits the power of OOP combined with core concepts of SM, such as sets, relations, hierarchy, primitive and compound entities. Primitive entities have attributes and functions common for the derived types, namely parameters, variables, and constraints (representing parametric relations between variables), each possessing additional attributes specific for each of them. Compound elements of the specification are composed of sets of primitive entities.

In other words, model specification provides parametric definitions of all variables and constraints, and is equivalent to a commonly used symbolic definition of a problem by a specification of variables and constraints in which all distinct collections of variables and constraints are declared. The sets of indices needed for the instantiation of collections are only declared (they are defined later during instantiations of a model).

3.2.2 Data

Data for large models comes from different sources (also as results from analyses of various models), and larger subsets of data are maintained by teams. SMT exploits the concept of *Data Warehouse* (DW) for supporting persistency and efficiency of data handling. The latter is achieved by defining a base dataset, and supporting incremental modifications of this set (which allows for avoiding duplications of large amounts of data needed in more traditional approaches requiring the storage of complete datasets even when only a small fraction of the data is modified).

The data structures of a DW are generated automatically from the model specification. This not only assures consistency between the declarations of the parameters in the model specification and the data used for their instantiations, but also saves substantial resources that would otherwise have been needed for preparing and maintaining data structures for any complex model.

Although SMT uses XML for data, it does so in a way that is different from that used in commonly known XML-based applications, which typically documents each data item separately. SMT uses XML only for meta data, which contain all the necessary information about the data structure (including types and units of each data element) and documentation; sparse or dense data structures are used depending on the sparsity characteristics of the corresponding data items. Therefore, the actual data is stored without any redundant information. Moreover, if necessary (e.g., for huge amounts of data) more efficient ways (e.g., based on BLOB or HFD) can be used to combine the advantages of a standard use of DBMSs with efficient handling of large amounts of numerical data.

3.2.3 Documentation

SMT exploits the XML capabilities for handling the documentation. XML is a data format for storing structured and semi-structured text, originally designed for publications on a variety of media. However, it can also be used for self-documenting various types of information that is exchanged between applications.

In SMT an XML document type is defined for enabling a single-source model symbolic specification that can be used for all relevant tasks of the whole modeling process. The documentation of other elements of the modeling process is done on different levels of detail. The basic information (such as date, user name, options requested for each object to be used) is automatically stored in the DW by each SMT application. Additionally, a user accessing a DB with privileges for data creation or modification is asked to write comments, which are logged. A more advanced documentation (e.g., automatic logging of changes in a way that allows for documenting the complete history of modifications, and optional undoing of the changes) can be included in applications that manipulate data.

4 Model analysis

Model analysis is probably the least-discussed element of the modeling process. This results from the focus that each modeling paradigm has on a specific type of analysis. However, the essence of model-based decision-making support is precisely the opposite; namely, to support various ways of model analysis, and to provide efficient tools for comparisons of various solutions.

4.1 Traditional OR approach

The (traditional) OR routine of representing a decision problem as a mathematical programming problem in the form:

$$\hat{x} = \arg \min_{x \in X_0} \mathcal{P}(x, F(x, z)), \quad (2)$$

which provides optimal decisions \hat{x} . However, this approach does not work for complex decision-making problems. The main reasons for that are:

- There is no unique representation of preferences $\mathcal{P}(\cdot)$;
- There is no unique definition of the set of admissible solutions X_0 (because X_0 is defined also by the bounds for values of the criteria not included in $\mathcal{P}(\cdot)$);
- Sensitivity analysis recommended for post-optimization problem analysis has very limited applicability to actual complex problems, see e.g., [9]; and
- Large optimization problems usually have many (typically, an infinite number of) very different solutions with almost the same value of the original goal function, see e.g., [7].

Thus, optimization in supporting decision making for solving complex problems has quite a different role from its function in some engineering applications (especially real-time control problems) or in very early implementations of OR for solving well-structured military or production planning problems. This point has already been clearly made e.g., by Ackoff [1], and by Chapman [2], who characterized the traditional way of using OR methods for solving problems as composed of the following five stages: describe the problem; formulate a model of the problem; solve the model; test the solution; and implement the solution. The shortcomings of such an approach are discussed in many other publications, see e.g., [9] and [14] for more details, and have been the main driving force for developing methods of model analysis that serve better the needs of decision makers.

4.2 Structured model analysis

The basic function of a model-based *Decision Support System* (DSS, illustrated in Fig. 1) is to support the user in finding values for his/her decision variables x that will result in a solution of the problem that best fits his/her preferences. A countless number of actual applications shows that to meet such requirements a well-organized model analysis phase of the modeling process is composed of several stages, see e.g., [9], each serving different needs. Thus, not only are different forms of $P(\cdot)$ typically used for the same problem, but also different instances of each of these forms are defined upon analyses of previously obtained solutions.

The analysis of the model instance is composed of a sequence of steps, each of which consists of:

1. Selection of the type of analysis, and the definition of the corresponding preferential structure, which takes different forms for different methods of model analysis, e.g., for:
 - Classical simulation, it is composed of given values of input variables;
 - Soft simulation, it is defined by desired values of decisions and by a measure of the distance between the actual and desired values of decisions;
 - Single criterion optimization, it is defined by a selected goal function and by optional additional constraints for the other (than that selected as the goal function) outcome variables;
 - Multicriteria model analysis, it is defined by an achievement scalarizing function, which represents the trade-offs between the criteria used for the evaluation of solutions.
2. Selection of a suitable solver, and specification of parameters that will be passed to a solver.
3. Generation of a computational task representing a mathematical programming problem, the solution of which best fits the user preferences.
4. Monitoring the progress of the computational task, especially if it requires a substantial amount of computing resources.
5. Translation of the results to a form that can be presented to the user.
6. Documenting and filing the results, and optional comments of the user.

Various specifications of the preferential structure support diversified analyses of the decision problem aimed at:

- Suggesting decisions for reaching specified goals;
- Analyses of trade-offs between conflicting goals; and
- Evaluations of consequences of decisions specified by the user.

The first two types of analyses are goal oriented and are discussed in Section 4.3. Now, we briefly comment on the third one, which focuses on the analysis of alternatives. For large problems it is difficult to specify values of decision variables without a prior knowledge of feasible alternatives, but such alternative solutions are provided by the goal-oriented model analysis, and users typically are interested in examining consequences of various modifications of such alternatives. A frequent problem with using the classical simulation is caused by infeasibility of the modified alternatives. The soft simulation methods provide the same functionality without the risk of getting infeasible solutions.

Several generalizations of the soft simulation are useful for a more comprehensive simulation-type analysis. We briefly outline three of them. The first, called *inverse simulation*, provides similar functionality in the space of outcome variables (i.e. the user specifies the desired values of outcome variables instead of the decision variables). The second, called *generalized inverse simulation* consists of a combination of the analysis provided by the soft and inverse

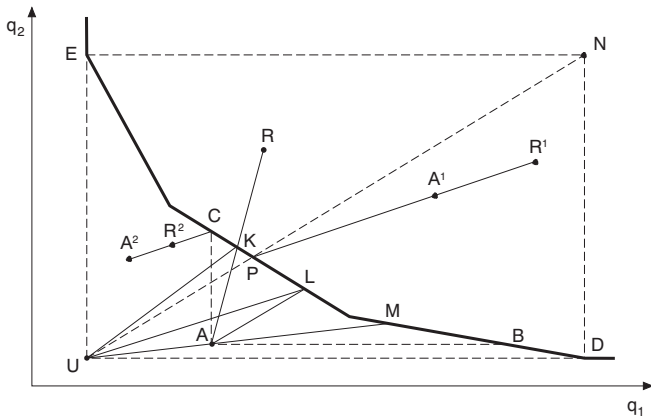


Figure 2: Trade-offs between criteria.

simulations. Finally, the *softly constrained inverse simulation* supports the analysis of trade-offs between goals (specified in a more general form as in the inverse simulation) and violations of a selected set of constraints (which are for this purpose treated as soft constraints). However, all these (and other) generalizations of the soft simulation are in fact specific applications of the multicriteria model analysis discussed below. A more detailed discussion of these issues is provided in [9].

4.3 Multicriteria model analysis

Traditional OR approaches are based on the assumption that the best solution of a decision problem is the one that maximizes a selected criterion. However, this assumption is true only for a specific class of well structured problems. Already almost 50 years ago Simon [12] demonstrated that such an assumption is wrong for most of actual decision making problems. Recent studies, see e.g., [11] confirm Simon's results.

A treatment of a decision-making problem as a single criterion optimization seems to be very attractive because offering a unique solution based on solid mathematical foundations is appealing; especially, if one considers that an abundant choice (even among discrete alternatives) typically creates problems, such as dissatisfaction or regret, see [10]. In reality, however, almost all actual decision problems have a large (or infinite) number of solutions typically evaluated with the help of conflicting criteria. Pareto-optimal solutions are not comparable in a mathematical programming sense, i.e., one can not formally decide which is better than another one. Thus, a choice of a solution depends on preferences of the user that implicitly define properties of the corresponding solution. Thus, in order to find a Pareto-efficient solution that corresponds best to user's preferences one needs to support the user in analysis of trade-offs between criteria.

The essence of problems related to trade-offs between criteria is illustrated in Fig. 2, which shows the Pareto set (segments between the points marked by E and D, respectively) for two minimized criteria. Each instance of the mul-

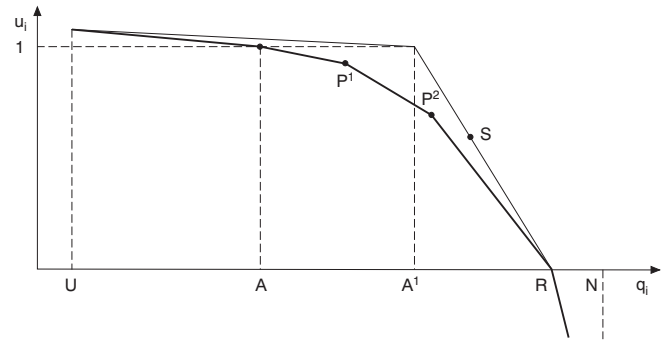


Figure 3: Component achievement scalarizing function.

ticriteria problem is converted into an auxiliary parametric single-objective problem, the solution of which provides a Pareto-optimal point having the desired properties. Different methods apply different conversions, but all commonly known methods can be interpreted in terms of the Achievement Scalarizing Function (ASF),¹ see [6] for details.

One of the most popular approaches to multicriteria optimization is based on the idea of converting a multicriteria problem into a single-criterion one by summing up weighted criteria. This approach is still popular because it is believed to be simple, intuitive, and reliable. However, in fact this approach is often contra-intuitive and not reliable, and has a number of other drawbacks as discussed in detail, e.g., in [7].

Most of the successful multicriteria optimization methods are based on the concept of the reference (aspiration) point, which is composed of the desired values of all criteria. Typically such a point is infeasible, thus one looks for a Pareto solution that is closest to this point. Obviously, for the Utopia point (composed of best values of all criteria, and marked by the letter U in Fig. 2), any of the Pareto-optimal points between points E and D can be obtained for various definitions of the distance between the aspiration point U and the Pareto set. Thus, for a unique selection of a Pareto solution one needs to define either another point (which together with the aspiration point define a direction) or an ASF that provides a unique selection of solution.

The first approach is exploited by the Aspiration-Reservation Based Decision Support (ARBDS) method, which requires a specification of two points, called aspiration and reservation, composed of the desired and the worst acceptable values of criteria, respectively. A well implemented ARBDS does not impose any restrictions on the feasibility of the aspiration nor of the reservation values. E.g., in Fig. 2 there are three pairs of aspiration and reservation points, denoted by $\{A, R\}$, $\{A^1, R^1\}$, and $\{A^2, R^2\}$, respectively. The corresponding Pareto-solutions are marked by K, P, and C, respectively. More details on ARBDS are provided in [5].

The second approach has been implemented in the

¹The concept of ASF was introduced by Wierzbicki see, e.g., [13, 14].

MCMA [5], which exploits an ASF is defined as:

$$ASF = \min_{1 \leq i \leq n} u_i(q_i, \bar{q}_i, \underline{q}_i) + \epsilon \sum_{i=1}^n u_i(q_i, \bar{q}_i, \underline{q}_i) \quad (3)$$

where $u_i(\cdot)$ denotes i -th Component Achievement Function (CAF), $q_i, \bar{q}_i, \underline{q}_i$, are the value, aspiration and reservation levels of i -th criterion, respectively; n is the number of criteria, and ϵ is a small positive number.

Two examples of CAFs are illustrated in Fig. 3. The first CAF is defined by four points, with values of the criterion, U, A¹, R, and N, corresponding to the values of utopia, aspiration, reservation, and nadir, respectively. The second CAF is defined by a modification of the first CAF, where the previously defined aspiration level A¹ was moved to the point A and two more points – P¹ and P² – were interactively defined.

Values of CAF have a very easy and intuitive interpretation in terms of the degree of satisfaction from the corresponding value of the criterion. Values of 1 and 0 indicate that the value of the criterion exactly meets the aspiration and reservation values, respectively. Values of CAF between 0 and 1 can be interpreted as the degree of *goodness* of the criterion value, i.e., to what extent this value is close to the aspiration level and far away from the reservation level. These interpretations correspond to the interpretation of the membership function of the Fuzzy Sets, which is discussed in [5].

By using an interactive tool for specification of the CAF illustrated in Fig. 3 such as MCMA [5] a user can analyze various parts of a Pareto set that best correspond to various preferences for trade-offs between criteria. These preferences are typically different for various stages of analysis, and are often modified substantially during the learning process, when aspiration and reservation levels for criteria values are confronted with the attainable solutions, which correspond best to the aspiration and reservation levels. In such an interactive learning process, a user gradually comes to recognize attainable goals that correspond best to his/her trade-offs.

5 Conclusions

Rational decision making is always based on a combination of knowledge, experience, and intuition. Models can represent a relevant part of knowledge, and appropriate methods of model analysis augment experience and intuition in the decision making process. However, one should never forget that there is no simple solution for any problem, which is truly complex. Thus a well organized modeling process can substantially help in finding better solutions but actually the final choice is always made by a decision maker.

Development of models for complex problems does, and will, require various elements of science, craftsmanship, and art (see, e.g. [14] for a collection of arguments that supports this statement). Moreover, development and comprehensive analysis of a complex model requires a substantial amount of time and other resources. SMT has been developed to provide a modeling environment supporting the whole modeling process, thus to increase the quality of modeling work and

to reduce the amount of the needed resources. While some features of SMT are already present in various modeling systems, SMT is probably the only modeling system that is fully integrated with DBMSs, and can actually be used for collaborative development and for the distributed use of complex models.

Thus, SMT effectively supports collaborative modeling (both model development and exploitation) by interdisciplinary teams working at distant locations. In particular, SMT supports the development of models with complex structures and huge amounts of data, and diversified analyses of such models; moreover, it provides automatic documentation of the whole modeling process. Thus, SMT promotes modeling quality and transparency, which are critically important for model-based support of decision-making, especially in environmental policy.

References

- [1] ACKOFF, R. The future of operational research is past. *Journal of OR Society* 30, 2 (1979), 93–104.
- [2] CHAPMAN, C. My two cents worth on how OR should develop. *Journal of Operational Research Society* 43, 7 (1992), 647–664.
- [3] GEOFFRION, A. An introduction to structured modeling. *Management Science* 33, 5 (1987), 547–588.
- [4] GEOFFRION, A. Integrated modeling systems. *Computer Science in Economics and Management* 2 (1989), 3–15.
- [5] GRANAT, J., AND MAKOWSKI, M. Interactive Specification and Analysis of Aspiration-Based Preferences. *European J. Oper. Res.* 122, 2 (2000), 469–485. available also as IIASA's RR-00-09.
- [6] MAKOWSKI, M. Methodology and a modular tool for multiple criteria analysis of LP models. Working Paper WP-94-102, International Institute for Applied Systems Analysis, Laxenburg, Austria, 1994. Available on-line from <http://www.iiasa.ac.at/~marek/pubs/>.
- [7] MAKOWSKI, M. Modeling techniques for complex environmental problems. In *Natural Environment Management and Applied Systems Analysis*, M. Makowski and H. Nakayama, Eds. International Institute for Applied Systems Analysis, Laxenburg, Austria, 2001, pp. 41–77. ISBN 3-7045-0140-9, available from <http://www.iiasa.ac.at/~marek/pubs/prepub.html>.
- [8] MAKOWSKI, M. A structured modeling technology. *European J. Oper. Res.* 168, 3 (2005). draft version available from <http://www.iiasa.ac.at/~marek/pubs/prepub.html>.
- [9] MAKOWSKI, M., AND WIERZBICKI, A. Modeling knowledge: Model-based decision support and soft computations. In *Applied Decision Support with Soft Computing*, X. Yu and J. Kacprzyk, Eds., vol. 124 of *Series: Studies in Fuzziness and Soft Computing*. Springer-Verlag, Berlin, New York, 2003, pp. 3–60. ISBN 3-540-02491-3, draft version available from <http://www.iiasa.ac.at/~marek/pubs/prepub.html>.
- [10] SCHWARTZ, B. The tyranny of choice. *Scientific American*, April (2004), 43–47.

- [11] SCHWARTZ, B., WARD, A., LYUBOMIRSKY, S., MONTEROSSO, J., WHITE, K., AND LEHMAN, D. Maximizing versus satisficing: Happiness is a matter of choice. *Journal of Personality and Social Psychology* 83, 5 (2002), 1178–1197.
- [12] SIMON, H. A behavioral model of rational choice. *Quarterly Journal of Economics* 69 (1955), 99–118.
- [13] WIERZBICKI, A. Basic properties of scalarizing functionals for multiobjective optimization. *Mathematische Operationsforschung und Statistik, s. Optimization* 8 (1977), 55–60.
- [14] WIERZBICKI, A., MAKOWSKI, M., AND WESSELS, J., Eds. *Model-Based Decision Support Methodology with Environmental Applications*. Series: Mathematical Modeling and Applications. Kluwer Academic Publishers, Dordrecht, 2000. ISBN 0-7923-6327-2.

Person Identification by Color Pattern Acquired in Visual Tracking

Yasushi MAE*, Naoki SASAO**, Yukinobu SAKAGUCHI***,
Tomohito TAKUBO***, Kenji INOUE***, and Tatsuo ARAI***

* Department of Human and Artificial Intelligence Systems,
Faculty of Engineering, University of Fukui
3-9-1 Bunkyo, Fukui-shi, Fukui, 910-8507, JAPAN
Tel: +81-776-27-8033, FAX: +81-776-27-8420
mae@rc.his.fukui-u.ac.jp

** Graduate School of Information Science
Nara Institute of Science and Technology
8916-5 Takayama, Ikoma, Nara, 630-0192, JAPAN
naoki-sa@is.naist.jp

*** Department of Systems Innovation,
Graduate School of Engineering Science, Osaka University
1-3 Machikaneyama, Toyonaka, Osaka, 560-8531, JAPAN
sakaguchi@arai-lab.sys.es.osaka-u.ac.jp
{ takubo, inoue, arai }@sys.es.osaka-u.ac.jp

TOPIC: Measurement, monitoring, and reliable control

Person Identification by Color Pattern Acquired in Visual Tracking

Abstract

The paper describes a method of visual tracking and identification of persons by person model composed of parts of the body and their surface color. The method acquires surface color of each part of the person model while tracking a person by a simple human shape model. The color pattern of the individual person is represented by the color of the parts. After acquiring color pattern of persons, the method tracks and identifies them by different acquired color patterns of individual person. The method is effective for monitoring who are doing what and where in daily life.

1: Introduction

For the purpose of creating a safe, secure and dependable space for living, it is important to understand who are doing what and where in daily environments. For monitoring and identification of persons, monitoring systems increase their performances by using not only fixed cameras but also moving cameras; the moving camera can eliminate blind spots of fixed cameras and monitor persons in detail by moving according to persons' motions (See Fig.1). It is also important monitored persons are not conscious about being monitored.

If an apparent face of a person on a monitored image is large enough, the person can be identified from the face. In this case many face recognition methods can be used for identification. The high-resolution image of the face of a person may be obtained by fixed cameras at appropriate positions. However, when a person is at far from any cameras, the identification of the person becomes difficult from the face. In that case, clothes color of a person is an effective cue for identification even other small features cannot be observed in detail. Since persons change their clothes every day, previously registered clothes color cannot be used for identification. Thus color pattern of body of person have to be acquired by monitoring systems everyday. There have many researches on tracking persons, for instance, [1, 2, 3 4]. There are no methods, however, for acquiring a color pattern of person while tracking and identification of persons from the acquired color model even when the person's face cannot be observed in high-resolution enough.

In the paper, we propose a method of visual tracking and identification of persons by person model composed of parts of the body and their surface color. The method acquires surface color of each part of the person model while tracking a person by a simple human shape model. After acquiring their color patterns, the method tracks them by acquired color pattern of the person model.

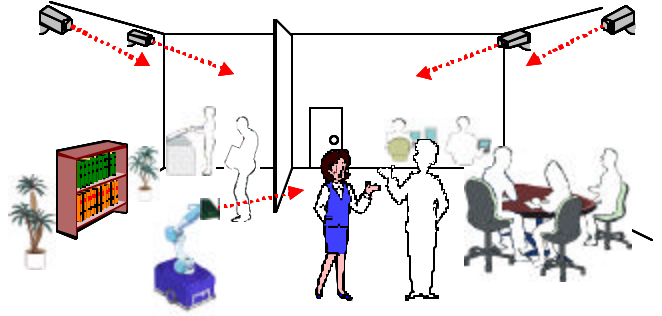


Figure 1. Modeling and Identification of persons by moving and fixed cameras in monitoring system.

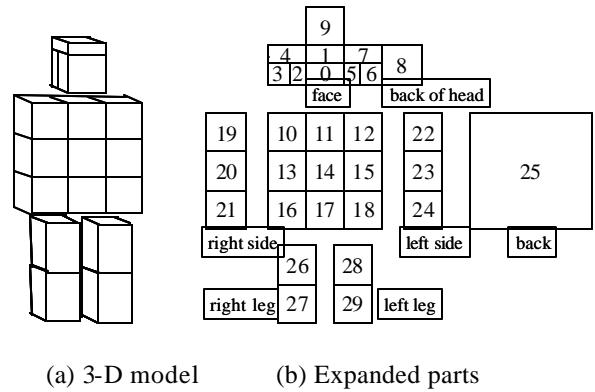


Figure 2. Person model

Then the tracked persons can be identified based on their color patterns. The method identifies persons at far distance from a camera by acquired color patterns even when the persons cannot be identified by their faces. Experimental results of tracking and identification of persons are shown. The proposed method is a basic technique for monitoring who are doing what and where in daily life.

2: Overview of Method

2.1: Person Model

Our generic person shape model consists of several parts of the body such as face, arm, leg (See Fig.2). Surface of a part has color model: R, G, B values and their variances. Let the color model of parts p be denoted by M_p ($p=0,1,\dots,29$) (See Fig.2). Initially, the values are unknown. Each color model of the body parts is obtained while tracking a person from different view points of the cameras.

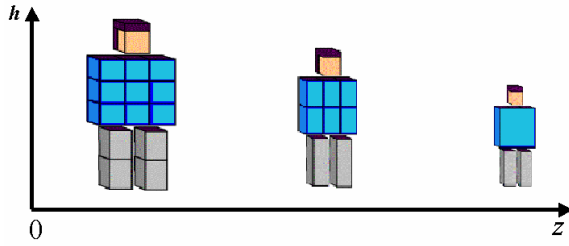


Figure 3. Different resolution levels depending on distance between person and camera



Figure 4. A moving camera for monitoring

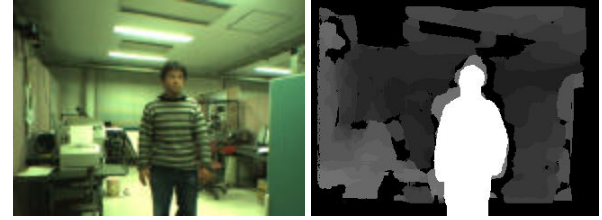
The resolution of the body parts changes depending on the distance between the camera and the person (See **Fig.3**). When the person is far from the camera, a large part is recomposed of several parts of the person model. For instance, large parts are *body*=(10,...,25) and *leg* = (26,...,29). The averages of R, G, B values of the component parts are used as the color model of the large part.

2.2: Moving Camera for Tracking

We have designed and built a mobile manipulator which can be used for monitoring persons (See **Fig.4**) [5, 6]. A precalibrated trinocular color camera unit is attached to the end of the arm of the mobile manipulator. The range data is obtained by calculating SAD(Sum of Absolute Distance) for every pixel in the image. The camera pose can be changed by moving the arm and the mobile platform to obtain appropriate view for monitoring persons. The camera attached to the arm is used as a moving camera for tracking a person in a monitoring system.

2.3: Outline of Tracking and Identification

First, regions composed of pixels with motion are extracted by background subtraction or frame difference. A person's head is detected based on the shape of the extracted motion regions by template matching of the silhouette of a head. The template of the silhouette of a head part is called simple human shape model. The color pattern of the person is acquired while tracking with a simple human shape model. To acquire color models of every body part, the position and the orientation of the person have to be estimated.



(a) input image (b) detected moving regions

Figure 5. Example of detected moving Regions

Next, the position and the orientation of the person are estimated from the head position, the range data at the breast, and his/her walking direction. The generic human shape model is fitted to the estimated position and orientation. R, G, B values, of the surface parts are sampled from the corresponding regions on the image. The color models are obtained from the sampled R,G,B values.

After enough number of R,G,B values are sampled, the color pattern of the person represented by the color models of the parts is used for detecting the individual person. If all the acquired color patterns of the persons in monitoring space are different, the tracked persons are identified from their color pattern even when the persons cannot be identified from their face.

3: Person Tracking by Silhouette of Head

3.1: Extraction of Moving Regions

To detect persons from the images of monitoring cameras, we first extract regions with motion caused by persons' motions in the image. To simplify the algorithm for person detection, we assume the camera does not move when the camera detects regions with persons' motions. We detect such moving regions by background subtraction or frame subtraction methods. When no moving objects are in the view for a long time, the view is recorded as a background image for background subtraction. In the other cases, the consecutive input images are used for frame subtraction.

Three images of the camera unit are denoted by I_1, I_2, I_3 , respectively. The image coordinate is denoted by $x = (x, y)$. An absolute value at (x, y) after subtraction of images is denoted by $?I_n(x, y)$. A binarized image $S_n(x, y)$ is obtained by thresholding $?I_n(x, y)$ for all pixels;

$$S_n(x, y) = \begin{cases} 1 & \text{if } \Delta I_n(x, y) \geq \text{threshold} \\ 0 & \text{otherwise.} \end{cases}$$

A set of pixels with $S_n(x, y) = 1$ represents the regions with motion. The suffix n indicates one of the three cameras. **Figure 5**(a) shows an input image. Extracted moving region is shown by white in fig.5(b). The moving region is obtained after several dilation and erosion processes. The other gray values indicate the distance from the camera to objects. The brighter regions indicate nearer objects.

3.2: Detection of Person's Head

We detect a head of a person to detect a moving direction of a tracking person. We use a silhouette of a head to detect a head region from extracted moving regions. The head silhouette template is represented by binarized image;

$$T(j, i) = \begin{cases} 1 & \text{if } (j, i) \text{ is on a silhouette} \\ 0 & \text{otherwise,} \end{cases}$$

where (j, i) indicates the coordinate on the template. We detect a part corresponding a head from the detected moving regions by matching to the head silhouette template. The image of the detected moving regions $S_1(x, y)$ is used as the input image to search for a silhouette of a head of a person. The head position on the image $x_h = (x_h, y_h)$ with the smallest SAD value which is lower than predetermined threshold is determined by

$$x_h = \arg \min_x \sum_{i=-\frac{M'}{2}}^{\frac{M'}{2}} \sum_{j=-\frac{N'}{2}}^{\frac{N'}{2}} |T(j, i) - S_1(x + j, y + i)|$$

The head silhouette template size is denoted by $M \times N$. By changing template size $M \times N$, template matching using a head silhouette works even when the distance between the person and the camera changes. In order to reduce calculation time, 15×15 pixels are used at the magnified positions and the other pixels are not used in SAD matching. The template size is selected automatically, which has the minimum SAD value. **Figure 6** shows a detected head part in tracking a person. The detected head part is overwritten by a red rectangle.

3.3: Calculation of 3-D Head Position

The distance to a person from a camera is determined from the range of the detected head position. The distance is determined by the average of the range in the neighborhood of the center of the template at the matched position. The neighborhood is determined by $M' \times N'$ rectangle region whose center corresponds to the center of the template. Let n denote the number of the pixels where $S_1(x, y) = 1$ in the neighborhood. Let $Z(x, y)$ denote the range at the pixel (x, y) . The distance to the person Z_p is determined by

$$Z_p = \frac{1}{n} \sum_{i=-\frac{M'}{2}}^{\frac{M'}{2}} \sum_{j=-\frac{N'}{2}}^{\frac{N'}{2}} S_1(x_h + j, y_h + i) Z(x_h + j, y_h + i)$$

Trajectory of a head position is obtained by tracking head position. **Figure 7** shows an overhead view of a trajectory of detected head positions. The detected positions are plotted by blue points. The consecutive measured positions are connected by a blue line segment. Then the moving direction of a person is determined by the head trajectory.



(a) Walking person far (b) Walking person near

Figure 6. Detected head part of a person

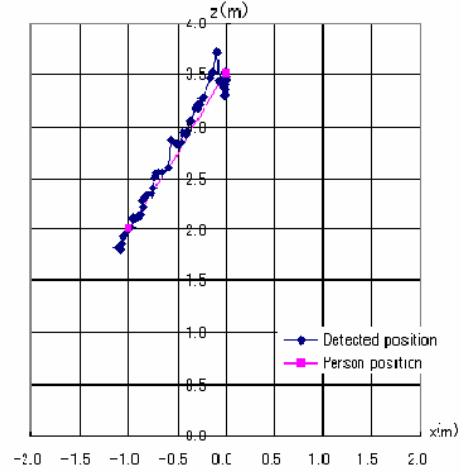


Figure 7. Head trajectory in walking

3.4: Acquisition of color pattern of person

To make color pattern of different directions, color pattern of person model is obtained while tracking a person with a simple person model. The orientation of the person is estimated and the color model of each part is obtained. The algorithm of acquisition of color model is described below.

A-1. Detection of person

Person region is detected by a method described in section 3. If a person region is detected, go to A-2. Otherwise A-1 is repeated until a person region is detected.

A-2. Estimation of distance to person

The distance to the person is calculated from the range data in the neighborhood of the center of the person region. If the distance is near enough, go to A-3. Otherwise go to A-1.

A-3. Estimation of orientation of person

The orientation of the person q (degree) for the line of sight of the camera is calculated using range data at the breast. The weighted least squared method is applied to the range data in 2-D space: horizontal and optical axes of the camera. The points nearer to the center of the breast have larger weight than the farther points. Go to A-4, A-5, A-6 depending on the estimated orientation.

A-4. Front or Back ($-15 \text{ degree} < q < 15 \text{ degree}$)

Front and back are distinguished from the moving direction of the person and the brightness of the face part. If the moving direction is toward the camera and the brightness is large enough, then it is estimated that the person faces the camera. If the moving direction is backward and the brightness is small, then it is estimated that the person faces backward. One of the two conditions is satisfied, R,G,B values are sampled for making color model of each apparent body part in the estimated orientation. Go to A-1.

A-5. Right side or Left side ($70 \text{ degree} < q < 90 \text{ degree}$ or $-90 \text{ degree} < q < -70 \text{ degree}$)

The right and left sides are distinguished from the moving direction of the person and the brightness of the head part. The brightness of the left head part is large enough and the moving direction is left, then it is estimated that the person faces the left. On the other hand, the brightness of the right head part is large enough and the moving direction is right, then it is estimated that the person faces the right. One of the two conditions is satisfied, R,G,B values are sampled for making color model of each apparent body part in the estimated orientation. Go to A-1.

A-6 Oblique orientation ($15 \text{ degree} < q < 70 \text{ degree}$ or $-70 \text{ degree} < q < -10 \text{ degree}$)

The orientation of the person is unstable, then nothing is done. Go to A-1.

Figure 8 shows examples when the color of a person is sampled. The sampled points are represented by yellow points. The positions correspond to the center of the parts on the person model. **Figure 8** (a),(b) show the persons with blue and red clothes facing the front and side direction to the camera. **Figure 9** shows an acquired color model of the person. The average colors of the parts are mapped to the corresponding parts of the person model.

4: Person Tracking and Identification by Acquired Color Pattern

4.1: Person Tracking by Acquired Color Pattern

After number of times of sampling color values for every body parts becomes large enough, acquired color models of persons can be used for identification in tracking them. The persons are identified by comparing their observed color pattern with their acquired color models.

Person model is recomposed by acquired person model depending on the distance. The color model of the recomposed person model is denoted by M'_p . If the person is far from the camera, the parts of the recomposed model are large (See **Fig.3**).



Figure 8. Acquisition of color model

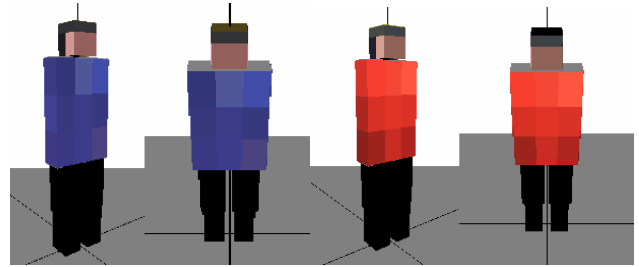


Figure 9. Acquired color pattern of person

In the experiment, person model in low-resolution is used initially for detecting persons at far distance projected onto the small region in the image. As a model in low-resolution, four body parts $p = (\text{face}, \text{hair}, \text{body}, \text{leg})$ are used. The four parts are defined as $\text{face}=(0,2,5)$, $\text{hair}=(1,3,4,6,7,8,9)$, $\text{body}=(10, \dots, 25)$, and $\text{leg} = (26, \dots, 29)$. Each color model of recomposed parts $M'_p = (M'_{\text{face}}, M'_{\text{hair}}, M'_{\text{body}}, M'_{\text{leg}})$ is recalculated by averaging the color vectors of composing parts.

The similarity of color pattern between input image and color model of every part of the person model is evaluated by inner product of vectors in the R,G,B color space. If every color model of parts M'_p satisfies the following condition, it is estimated that the person corresponding to the color pattern is found there.

$$M'_p \cdot I_p > th_p$$

where, I_p indicates R,G,B values at the pixel corresponding to the input image. The threshold th_p is determined to 0.995 experimentally.

The algorithm of tracking and identification of persons using acquired color model is described below.

B-1. Detection of Person by Acquired Model

If similar pattern of the person color model is found in the input image, the region with the similar pattern is detected as a person region, and go to B-2, otherwise B-1 is repeated.

B-2. Calculation of distance

Distance to the detected person is calculated by averaging range data in the 5×5 pixels neighborhood of the center of the body of the person model. Go to B-3.

B-3. Matching depending on distance

The resolution of the person model changes depending on the distance between the camera and the person. Go to B-1.

4.2: Experiment

We performed a simple experiment to track two persons by previously acquired color pattern. We call two persons A and B. Person A wears blue clothes and person B wears red clothes. Person A is walking from right to left, and person B is walking from left to right on the image (See Fig.10). A trinocular camera unit is set at the origin. The optical axis is along the z-axis. The two persons, A and B, walk across the z-axis at the same time, body A is occluded by body B at that time. They walk at usual speed. The persons are tracked by their color models acquired previously. In the experiment, only the body color is used for identification ($p=body=(10, \dots, 25)$). Trajectories of the two persons are shown in fig.11. In the figure, circle points represent the positions of person A and triangle points represent the positions of person B. We can see the two persons are tracked even they are crossing. They are identified from their acquired color patterns.

5: Conclusions

The paper proposes a method of acquisition of color model of persons for identification from clothes colors in monitoring systems. The person model consists of several parts of the body. Each part has color model. Each color of the body parts is obtained while tracking a person by the cameras in the monitoring system. The monitoring system identifies a person at far distance from a camera by acquired colors of the body parts even when the person cannot be identified from the face. The method is effective for monitoring multiple persons in human living environments.

We will develop our method to track multiple persons wearing various color clothes. In these difficult cases, when persons cannot be identified from their body color pattern, the moving camera moves near to the person for observing them in detail and identification by other features, for instance, their faces. Such motion generation of the moving camera is our future work.

Acknowledgements

This research was supported by the Japan Society for the Promotion of Science under Grand-in-Aid for Creative Scientific Research (Project No. 13S0018).



Figure 10. Two persons walk crosswise

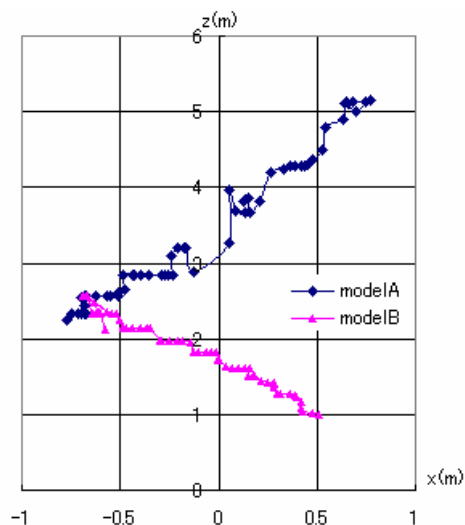


Figure 11. Trajectories of two persons

References

- [1] A.Nakazawa, et al.: "Human Tracking Using Distributed Vision Systems," 14th Inter. Conf. Pattern Recognition, 1998.
- [2] K.K.Lee, et al.: "Modeling of Human Walking Trajectories for Surveillance," Proc. of the 2003 IEEE/RSJ Intl. Conf. on Intelligent Robots and Systems, pp.1554-1559, 2003.
- [3] K.Uchida, et al.: "Probabilistic Method of Real-Time Person Detection Using Color Image Sequences," Proc. of the 2001 IEEE/RSJ Inter. Conf. on Intelligent Robots and Systems, pp.1983-1988, 2001.
- [4] S. Birchfield: "Elliptical Head Tracking Using Intensity Gradients and Color Histograms," Proceedings of the IEEE Conference on Computer Vision and Pattern Recognition, pp. 232-237, 1998.
- [5] Y. Mae, et al.: "Person Detection by Mobile-Manipulator for Monitoring" SICE Annual Conf. 2003, WAI-12-2, pp.2845-2850, 2003.
- [6] Y. Mae, et al.: "Head Detection and Tracking for Monitoring Human Behaviors," First Inter. Symp. On Systems & Human Science -For Safety, Security, and Dependability, pp.239-244, 2003.

Tracking Multiple Objects Occluding each other without Feature Extraction

Takayuki MORITANI, Shinsaku HIURA and Kosuke SATO

Graduate School of Engineering Science, Osaka University

1-3 Machikaneyama, Toyonaka, Osaka 560-8531, Japan

TEL: +81-6-6850-6371

FAX: +81-6-6850-6341

E-mail: shinsaku@sys.es.osaka-u.ac.jp

Topics: measurement, monitoring and reliable control

Tracking Multiple Objects Occluding each other without Feature Extraction

Takayuki Moritani, Shinsaku Hiura and Kosuke Sato
Graduate School of Engineering Science, Osaka University, Japan

Abstract

It's necessary to realize 3-D object motion tracking without feature extraction for monitoring general objects in an usual civil-life scene, because features observed on images much depend on the variety of the objects. The system must be also capable of multiple objects occluding each other, therefore we have proposed an appearance-based tracking method using multiple stereo cameras embedded on walls or ceilings. At first, stereo cameras measure the shape of the incoming object to prepare a CG model of the object. Then many images are generated from the model and compared with input images captured by the cameras. Motion parameter of the object is modified to minimize the difference between generated and captured images, and the parameter tracks the motion of the real object precisely when minimization is converged. Each stereo camera is connected to a corresponding PC, and most calculation is parallelized using the all PCs. We confirmed the ability of our method and achieved a 3DOFs real-time object tracking system using single camera, and 6DOFs tracking using four cameras at the rate of 5 frames/sec. At the image generating stage, occlusion is also simulated and we can easily handle the visible region of the object. Therefore, multiple objects occluding each other are correctly tracked using our system. Now we are improving the image generator using latest rendering hardware to accelerate the tracking speed.

1 Introduction

Object motion tracking is a task to estimate the pose and position of the object using a temporal sequence of the images. Especially it's more difficult but essential to estimate the spatial 3-D motion than 2-D motion in a plane. In existing method, both range and intensity images are used for motion analysis. Range images is very efficient for 3-D scene analysis[2], but real-time range sensors which have high performance for all of frame rate, accuracy and cost are not popular yet. Therefore intensity images captured by usual cameras are used in many studies of motion tracking. Armstrong et al. based on the concept of model-based vision and achieved polyhedral object tracking by extracting edges or corners from intensity images[3]. However, it's

difficult to extract features from curved objects such as sculpture and smooth textured surface because the extraction of the feature point is not robust.

Therefore, we expand the concept of model-based analysis to achieve top-down process[4] that uses shape and color information of the object, and propose a new tracking method without feature extraction. In advance, the shape of the object to be tracked is measured using rangefinder, and then a CG model is generated with color information for texture mapping. CG images are rendered with motion parameters to this CG model, which decide the pose and position of the object. These parameters are determined by minimizing the difference between these CG images and input images captured from cameras, and the motion tracking is achieved by iterations of this process. This method needs to get the 3-D object shape beforehand, but the range information is not measured in the tracking phase.

Contrary to the range images, the motion toward the optical axis can not be measured robustly using intensity images. In addition, it's hard to track multiple objects occluding each other from single viewpoint. We take advantage of multiple viewpoint camera system with a PC cluster to cover these weaknesses. For such systems, the overhead of the network transfer is very nuisance problem. In order to avoid this problem, calculation of the minimization is done in each PC, and reduced data is transferred and merged to estimate the object motion. This idea is based on a distributed least square method.

2 Principle of tracking

2.1 Gradient method

The image of a moving object changes as the pose and position of the object. If we can assume that the radiance of the object surface at each point is constant, the intensity value on each image is constant at the corresponding point. Therefore, well-known gradient constraint equation proposed by Horn[5] is described as

$$I(x, y, t) = I(x + \delta x, y + \delta y, t + \delta t). \quad (1)$$

To solve this equation for determining optical flow, Taylor expansion gives

$$\frac{\partial I}{\partial x} \frac{\delta x}{\delta t} + \frac{\partial I}{\partial y} \frac{\delta y}{\delta t} + \frac{\partial I}{\partial t} \simeq 0. \quad (2)$$

This equation only gives us a constraint between optical flow $(\delta x, \delta y)$ and the intensity change $\frac{\partial I}{\partial t}$, and it is obvious that this equation can not be solved without any additional constraint. Many researches are achieved for estimating optical flow by giving some constraints on an image plane, but it is not essential to solve the problem because such constraints are only for convenience and not related to the object motion itself. Therefore, we propose a direct estimation method of object motion based on gradient method.

Contrast to the equation(1), we can denote the image by the parameter of the object pose and position as

$$I = I(p_1, \dots, p_n). \quad (3)$$

Here n is degrees of freedom of the object motion. Similar to the equation(2), we can also expand equation(3) as

$$\frac{dI}{dt} \simeq \sum_{i=1}^n \frac{\partial I}{\partial p_i} \frac{dp_i}{dt}. \quad (4)$$

At a first sight of this equation, it is more difficult than equation(2) to solve because it has many unknown parameter. However, this constraint is common to the whole area on the image of the object, because the motion parameter p_i is common to the all pixels of the object image if the object is rigid body. Theoretically, the number of the pixels on the image of the object exceeds the degrees of freedom n , this equation can be solved using least squares method. Actually the number of pixels are much larger than the degrees of freedom to solve, therefore the motion can be directly estimated by using equation(4).

2.2 Calculation of motion parameters

We must prepare the derivative of the image with respect to the motion parameter $\partial I / \partial p_i$ to solve equation(4). This derivative can not be calculated only on the image plane because the shape of the object(depth of the scene) affects to the relationships between optical flow and the motion of the object. Therefore, we use a finite difference to calculate it as

$$\frac{\partial I}{\partial p_i} \simeq \frac{I(\dots, p_i + \frac{1}{2}\delta, \dots) - I(\dots, p_i - \frac{1}{2}\delta, \dots)}{\delta}. \quad (5)$$

If we have a precise CG model of the object and environment, we can generate images of any pose by rendering the object by using it. The way to prepare the model is described at section 2.3.

In this paper, we describe the method to track the motion of the rigid object. Therefore, the number of the parameters is 6, and equation(5) can be denoted as

$$\begin{aligned} I_{input} - I_0 & \simeq \frac{I_{+Xt} - I_{-Xt}}{\delta} \Delta X_t + \frac{I_{+Yt} - I_{-Yt}}{\delta} \Delta Y_t \\ & + \frac{I_{+Zt} - I_{-Zt}}{\delta} \Delta Z_t + \frac{I_{+Xr} - I_{-Xr}}{\delta} \Delta X_r \\ & + \frac{I_{+Yr} - I_{-Yr}}{\delta} \Delta Y_r + \frac{I_{+Zr} - I_{-Zr}}{\delta} \Delta Z_r. \end{aligned} \quad (6)$$

where I_{+Xt} denotes the vector of CG image with a slight shift of the object position along X axis, and I_{+Xr} is rotation, respectively. I_0 is a CG image of the original position of the object and I_{input} is the input image from the camera. Therefore, $\Delta X_t, \dots, \Delta Z_r$ can be calculated as the motion from the original position of CG image to the real object.

We can use least squares method to solve equation(6) as follows. At first, each variable is denoted as matrix form as

$$D = I_{input} - I_0 \quad (7)$$

$$G = \left[\frac{I_{+Xt} - I_{-Xt}}{\delta}, \dots, \frac{I_{+Zr} - I_{-Zr}}{\delta} \right] \quad (8)$$

$$E = [\Delta X_t, \Delta Y_t, \Delta Z_t, \Delta X_r, \Delta Y_r, \Delta Z_r]^T \quad (9)$$

and then we can rewrite equation(6) as

$$D \simeq GE. \quad (10)$$

Since the number of the row of matrix G is the same as the number of the pixels in the region of the object and it is much larger than the degrees of freedom of the object motion. Therefore we can solve this equation using least squares method as

$$E = (G^T G)^{-1} G^T D. \quad (11)$$

Motion parameter E calculated with equation(11) is used to generate next CG images, and the motion tracking is achieved by calculating parameter E repeatedly.

2.3 Rendering of aligned CG images

When the shape of the object to be tracked has already measured, CG images whose pose and position is as same as the real object must completely coincide with the real images. This complete match has two factors: geometric and photometric. In our system, the relation, that is camera parameter, between world coordinate (X, Y, Z) and camera coordinate (x_c, y_c) is

calculated by calibration in advance. Therefore, we can achieve the geometric match by this camera parameter and also the photometric match by mapping the texture captured from camera.

3 Multiple camera system

3.1 Calculation of motion parameters

Theoretically, the full rigid motion of the object can be estimated by using single camera as described in section 2.2. However, it is not so stable when the number of the motion parameter increases because some different motion looks similar from the camera. Therefore we use multiple cameras for estimating full motion of the object.

Here we assume a system with m cameras in this section. Each image from the camera is captured by a PC which is connected via LAN each other. To estimate the object pose and position, the summation of least square error calculated from all images must be minimized. In other words, the images taken by m cameras are simply connected each other, as

$$\begin{bmatrix} D_1 \\ \vdots \\ D_m \end{bmatrix} \simeq \begin{bmatrix} G_1 \\ \vdots \\ G_m \end{bmatrix} E. \quad (12)$$

Here D_1 is a subtraction between images from camera No.1 and corresponding CG images at original motion parameter, and the others respectively.

From a practical point of view, the calculation cost to solve equation(12) is not small because the number of row of each matrix is much larger than equation(10). The communication cost between PCs are also large, because each generated CG images must be transferred to the master PC. Therefore, we expand the equation of least squares method as

$$\begin{aligned} E &= \left(\begin{bmatrix} G_1 \\ \vdots \\ G_m \end{bmatrix}^T \begin{bmatrix} G_1 \\ \vdots \\ G_m \end{bmatrix} \right)^{-1} \\ &\quad \cdot \begin{bmatrix} G_1 \\ \vdots \\ G_m \end{bmatrix}^T \begin{bmatrix} D_1 \\ \vdots \\ D_m \end{bmatrix} \\ &= \left(\sum_{i=1}^m G_i^T G_i \right)^{-1} \cdot \sum_{i=1}^m G_i^T D_i. \end{aligned} \quad (13)$$

Here 6×6 matrix $G_i^T G_i$ and 6×1 vector $G_i^T D_i$ is calculated on each PC and the results are enough small to transfer via usual LAN. Master PC only calculates the summation and inversion of small matrices.

3.2 Evaluation method

In equation (11), $rank G = 6$ has equality if solution E exists. If matrix G has nearly $\mathbf{0}$ vector or linearly dependent vectors, solution E , that is motion parameters, is easily affected by error of matrix D . In this case, matrix G is unstable because the solution calculated with G^{-1} is much affected by various errors. Therefore, we evaluate the stability of $G^T G$ with condition number. Condition number(CN) as follows is known to be a measure of the stability,

$$CN(G^T G) = \frac{\max \lambda_i}{\min \lambda_i} \quad (14)$$

where λ_i ($i = 1, \dots, 6$) denotes eigen value of matrix $G^T G$. If $CN(G^T G)$ is close to 1, the more stable Matrix $G^T G$ is, and the more reliable motion parameters we will get. For example, CN of orthonormal matrix is 1, which is the most stable. Contrary, the larger $CN(G^T G)$ become, the more unstable Matrix $G^T G$ is. We show the evaluation experiment in the rear parts of section 5.2.

4 Tracking of multiple objects

It's natural that there are several objects to be tracked in usual scenes, therefore we need to achieve multiple object tracking with occlusion. In our method, we extract object regions from background by masking process, because change of background affects the stability of tracking if all pixels in the raw images captured from camera are used. Mask images are generated from the region of CG images. Hence, we can track multiple objects by applying our tracking principle to each object individually without the interference of the movement of other objects if the occlusion does not happen.

If occlusion occurs between some objects, we have to determine which object corresponds to each pixel. This problem is similar to the hidden surface removal, and the distance to the object from the viewpoint matters. Fortunately, CG models with 3-D information of all objects to be tracked have been already generated and labeled, so that it's easy to determine which is closer to the camera using depth buffer method. The part hidden by other objects is rendered as background in order to extract the region of target object. Figure 1 shows the result of the extracted object region. The region of occluded object (green wired model) is well extracted even if a part of the object is hidden by the front object (red wired model).



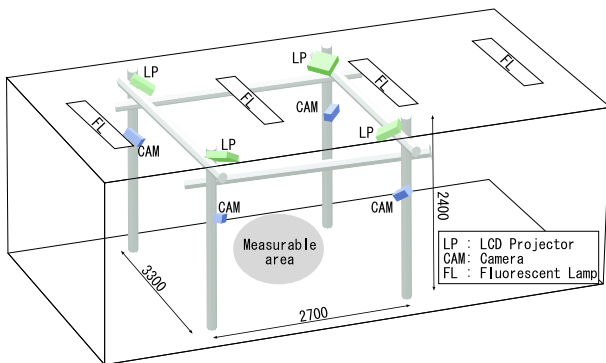
Figure 1: Object region extraction

5 Experiment and Evaluation

5.1 Object Tracking

The arrangement and specification of multiple camera system is shown in figure 2. At first each PC captures images, generates CG images and calculates covariance matrix as equation(13) independently, then transfers the matrix to the master PC. The master PC calculates the motion parameters and send them back to all client PCs for generation of new CG images in next step. The result of tracking is shown in figure 3. The motion tracking of 6 degrees of freedom is realized at the rate of 5 frames per second.

We also experimented multiple object tracking using basic single camera system. Figure 4 shows the result of two object tracking with 3 degrees of freedom movement. We can see that the rear object (green wired model) is tracked without interference of the front object (red wired model) even if occlusion happens as shown there. The stability of tracking is improved by using multiple camera system because the images with-



PC cluster: Pentium III 1.26 GHz \times 2
 GeForce2 MX440
 100Base-T Ethernet
 camera: EVI-20G (SONY)
 projector: ELP-703 (EPSON)
 1000 ANSI lm

Figure 2: System structure and specification

Table 1: Comparison of condition number

value δ	single	four
1.5, 0.5	87.8	13.8
3.0, 1.0	80.5	22.3
8.0, 3.0	97.2	19.9

value δ : amount of translation(cm) and rotation(deg.).

out occlusion are given from the other viewpoint.

5.2 Evaluation

Figure 5 shows the results of tracking accuracy evaluation. We placed the object shown in figure 3 on a slide stage and recorded the estimated position of the object when the optimization is converged, and also did the pose after rotating with a turn table. Both results show that it's very precise under the condition of the size of the object and the distance between the camera and the object.

Next we compared each CN of $G^T G$ calculated with images given by single and four camera system, which is described in section 3.2. The result is shown in table 1. Value δ denote the amount of translation and rotation of CG model moved hypothetically (in equation (5)) when we render CG images. The result means the stability of motion parameters given with multiple viewpoint images by least square method is improved because CNs calculated with multiple ones are smaller than those with single one. As a result, it means effective to use multiple viewpoint images.

5.3 Evaluation of difference between CG and input images

Our method has a weakness against the change of environmental light because it's based on texture mapping. Therefore, it's worth while evaluating the difference between real and CG images to investigate convergent accuracy affected by the change of intensity on images. We experimented on the rotation, which is



object size: $420 \times 280 \times 420$ mm (W×D×H), distance between object and camera: about 2m

Figure 3: Tracking with multiple camera system

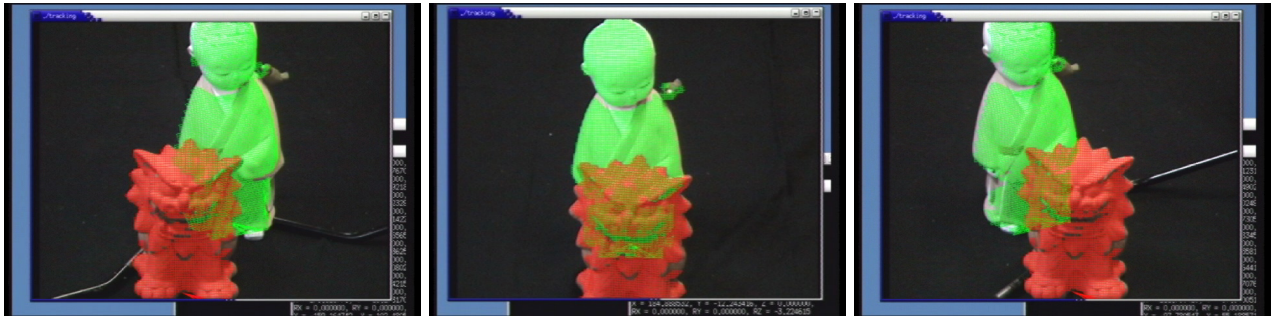


Figure 4: Tracking with occlusion

more varied than the translation by the change of light generated by motion of the object because of the shape and reflection property on the surface. We mapped the difference on the graph (figure 6) as rotating each of real object and CG model using the system, a turn table and object shown in figure 2 and 3. X-axis and Y-axis denote the rotating angle of real object and CG model, and Z-axis denotes average of absolute difference between real and CG images.

We can see in figure 6 that the difference does not increase so much on valley bottom, which means real

object and CG model were moved at the same amount, and the difference increases smoothly even when they were moved at the different amount, that is, V-shape is kept strictly. This means that convergence speed is almost constant and the reflection of high order does not affect on tracking too much.

6 Conclusion

We proposed a new simple principle to estimate the motion based on a model-based method and confirmed the ability of tracking of the multiple rigid objects with curved surface and smooth texture which occlude each other using multiple camera system. Our method can be understood as a multifactorial Newton optimization method with a raw image and has advantages that we need not to extract the features such as edges and corners from images and not to determine the congruent points. However, our method has a weakness that the change of environmental light affects on, we consider that this problem can be solved by generating CG images inclusive of the change after observing and modeling the change in environment light.

We have used rangefinders with cameras and projectors, which enables the measurement at high precision by active method. But we must project pattern light onto the tracking object, so that it takes some times to

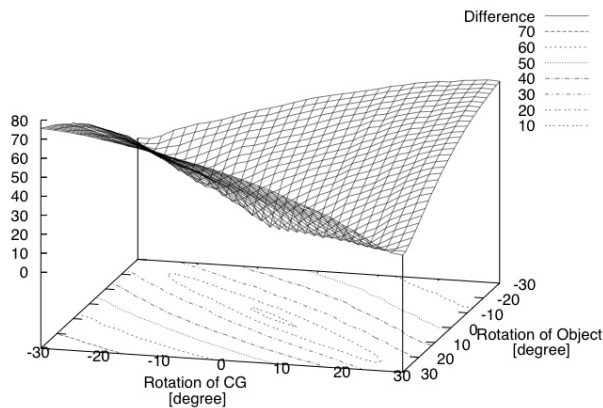


Figure 6: Difference between real and CG images

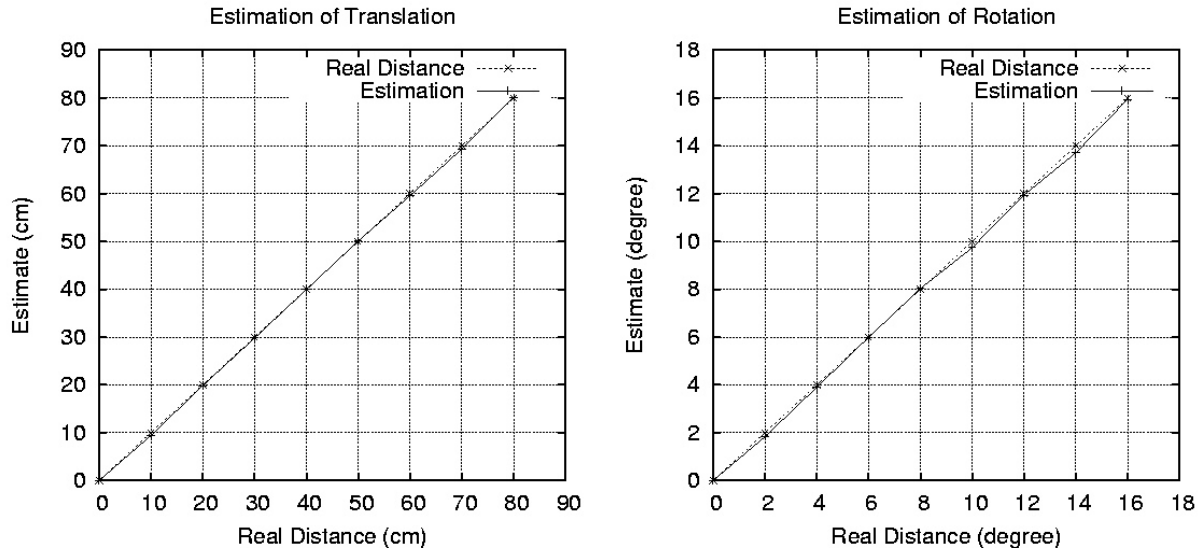


Figure 5: Evaluation of tracking accuracy

acquire the 3-D shape. Hence, it's difficult to measure the moving objects. In order to improve this problem, we are going to use stereoscopic cameras to get the 3-D information of the object. We consider that we don't need so precise 3-D shape to generate CG model because the color information of the object is the most important. In the future, we will confirm how the accuracy of the CG model affects on that of tracking, and built new tracking system with use of stereoscopic cameras without projectors.

References

- [1] T. Moritani, S. Hiura and K. Sato: "Visual Object Tracking Based on Multi-Viewpoint 3-D Gradient Method", 1st International Symposium on Systems & Human Science (SSR2003), pp.257-262, 2003
- [2] S. Hiura, A. Yamaguchi, K. Sato and S. Inokuchi: "Real-Time Tracking of Free-Form Objects by Range and Intensity Image Fusion", System and Computers in Japan, Vol.29, No.8, pp.19-27, 1998
- [3] M. Armstrong and A. Zisserman: "Robust object tracking", Proc. ACCV95 Vol.1, pp.58-62, 1995
- [4] D. Hogg: "Model-based Vision: a program to see a walking person", Image and Vision Computing, Vol.1 No.1, pp.5-20, 1983
- [5] B. Horn and E. Weldon: "Direct Methods for Recovering Motion", International Journal of Computer Vision, No.2, pp.51-76, 1988

Excavation and Recovery of Non-stockpile Munitions in China

Mr. Hiroshi Niho

Project Management Consultant PCI/JGC Joint Venture

ATTN: No.23 Building 1-23-7 Toranomon, Minatoku, Tokyo 105-0001 Japan

TEL: 03-3501-0544 FAX: 03-3501-0809

nihoh@pcitokyo.co.jp affiliation

Abstract:

The destruction of chemical weapons is going on by the chemical weapon prohibition treaty conclusion countries. In accordance with the memorandum and the understanding by GOJ and GOC regarding the abandoned chemical munitions in China, Japanese Cabinet Office proceeds with the Destruction Project of Abandoned Chemical Weapon in China. The abandoned chemical weapons are recognized in the north east provinces in China. And several hundred thousand munitions are buried in the twoburial pits at the Haerbaling area of Dunhua in Jiling Province. Abandoned chemical weapon destruction project is to excavate, classify and pack the buried munitions and finally destroy those in the destruction plant after the temporal storage. The careful handling is required in these processes to avoid the potential risk due to the explosive and chemical agent. So far, a series of proof-of-concept tests have been performed and the performance of the excavation system's main components, such as the munitions gripper, the soil retrieval subsystem consisting of the air injection and extraction nozzles, have been verified. With the recent technical innovations in the field of the telerobotic system, technologies of all of those are now readily available and a reliable telerobotic system can be developed and demonstrated shortly.

In this paper the outline of abandoned chemical weapon destruction project, excavation machine and soil removal system are addressed from the standpoint of Project Management Consultant who is supporting ACW office.

1. Introduction

From 1951 to 1963, several hundred thousands of abandoned chemical munitions were collected and buried by the

local government into the two burial pits that are located 43 km southeast of Dunhua City (Fig.1). These pits are relatively small in size and the distance between two pits is about 65meters. Two third of those munitions are buried in Pit No.1 and the remaining one third are buried in Pit No.2 .

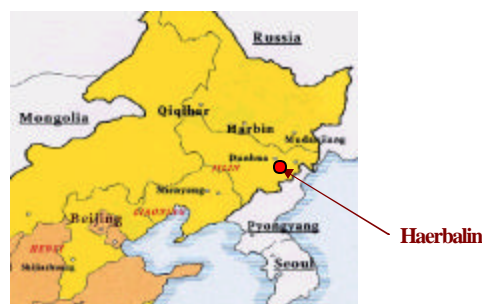


Fig.1 Location of Haerbaling

The International Treaty of Chemical Weapons convention and the Memorandum of Understanding by GOJ and JOC regarding the abandoned chemical munitions in China call for recovery of abandoned munitions from the two burial pits at the Haerbaling area of Dunhua in Jiling Province, China. Accordingly, GOJ began its initiatives to accomplish that objective, and in response to this initiative we proposed and designed the telerobotic system that makes it possible to safely dispose a huge amount of buried munitions efficiently and effectively. The system is designed to recover buried munitions with maximum excavation work efficiency while reducing the risk of munitions detonation and exposure to chemical agents to the minimum level.

2. Munitions

2.1 Condition of buried munitions

In 1995, the survey of burial pits and partial trial excavation

was carried out to check the condition of burial pits and buried munitions by the joint work of GOJ and GOC. The abandoned chemical munitions are buried in the inverted trapezoid pits and covered with the sandy soil of 3 meters in depth. According to the survey, the munitions were buried randomly and heavily rusted, but still have the enough strength to pick up by hands. The broken pieces of munitions, canisters, bombs, wooden case and other gavages are also buried in the pits.



Fig.2 Burial Pit

2.2 Type of Munitions

According to the survey on the abandoned chemical munitions which have been excavated and recovered in China, more than 90% of munitions are expected to be small in size and light in weight, and hence are relatively easy to handle with robotic systems. The shapes of munitions are as shown on Fig.3 and the percentage of those in the number of munitions in sizes and weights are as shown on Table 1.

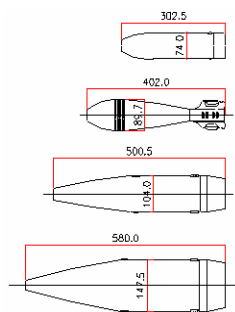


Fig.3 Shape of munitions

Diameter (mm)	Length (mm)	Weight per munition (kg)	Percentage in number (%)
75	302.5	5-6	22.4
90	392	5-6	70.9
105	485.5	16	4.9
150	556	32	1.8

Table 1 Sizes and weights of munitions

The percentages in the number of munitions in chemical agent types are expected to be as shown on Table 2. As indicated,

88 % are of chemical munitions type and 12 % are of conventional munitions type.

Chemical agent	Percentage in number
Mustard/Lewisite	60.4
Diphnylcyanosarsine	27.6
None (Conventional)	12.0

Table 2 Percentage of Chemical Munitions

2.3 Potential Risk

In addition to the potential risks of the explosion and the chemical agent as the chemical munitions, following potential risks should be taken into consideration when the facilities for excavation and recovery are planned.

- The sensitization of explosive by the composition of metal picrates.
- The leakage of chemical agent from the munitions.
- The unexploded munitions with fuse.
- The large scale explosion due to the sympathetic detonation.
- The dispersion of the chemical agents in the accident

3. Excavation, Recovery and Storage

3.1 Purposes

The purposes of excavation, recovery and storage system are to excavate the buried munitions from the pits, classify the type of munitions and pack into the air tight container to deliver those to the destruction plant to demilitarize the chemical munitions. The facilities for those purposes are built in the excavation area, the recovery area and the storage area.

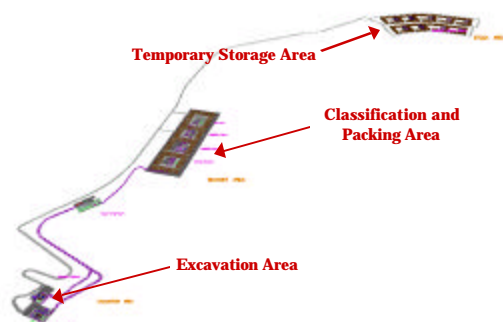


Fig.4 Bird's Eye View of Excavation and Recovery System

The buried munitions are excavated, decontaminated, washed

and numbered in the excavation area, and then temporarily stocked, inspected, classified and packed into the munition container in the recovery area and finally stocked in the temporary storage building in storage area. The layout of excavation, recovery and storage system is shown on Fig. 4.

3.2 Planning Conditions

The facilities for the excavation, the recovery and the temporary storage are planned on the following premises.

- The excavation and recovery work should be done safely within the certain time frame without any impact on the environment.
- The safety, the efficiency and the reliability of the equipment are the key factors in this project for the reason mentioned above.
- The automatic and remote control system is applied for the safety and the efficiency.
- At the same time, the rational combination of the remote control and human intervention is considered.
- The equipment and the technology should be reliable and commercially available in general. And the verification test should be carried out for the equipment and the technologies which should be developed for this project.

3.3 Facilities for Excavation and Recovery

Seven kinds of facilities are built in the excavation area, the recovery area and the temporal storage area. After the excavation, the munitions are put in the munition box, which is made of polypropylene (Fig. 5), and transported by the automatic guided vehicle (AGV) between those facilities and finally packed into the airtight munition container (Fig. 6).

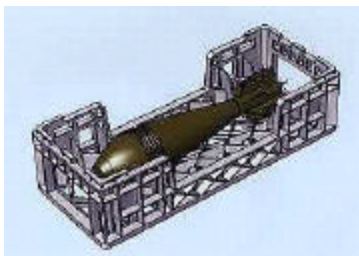


Fig.5 Munition Box

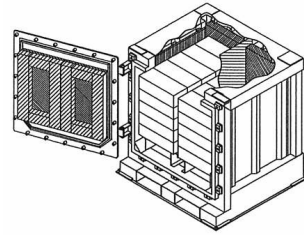


Fig.6 Munition Container

Following facilities are built in these areas.

1) Excavation building:

The excavation buildings are built over No.1 and No.2 Pits. The excavation machines and soil removal machines are installed in these buildings. The munitions, which are picked up from the burial pits, are transported to the munition treatment building by AGV through the corridor.

2) Munition treatment building:

The excavated munitions are decontaminated and/or washed, and then after confirming the non-leakage of chemical agent with the chemical agent detector, each munition is numbered for identification.

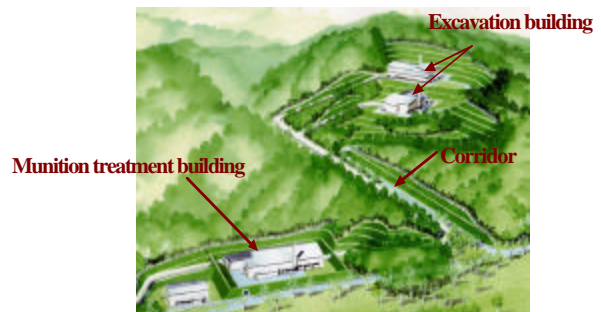


Fig.7 Excavation area

3) Temporary storage building:

The munitions are temporarily stocked in the automatic warehouse before delivering those to the classification buildings.

4) Classification building No.1:

The munitions are inspected and identified automatically with CCTV, weighing machine, X ray and neutron analyzers and then classified by the sorting machine.

5) Classification building No.2:

The munitions, which can't be identified automatically in the classification building No.1, are inspected and classified manually with X-ray and neutron analyzers.

6) Packing building:

The classified munitions are stocked temporarily in the automatic warehouse and then certain numbers of munitions of same type and size are packed into the respective container.

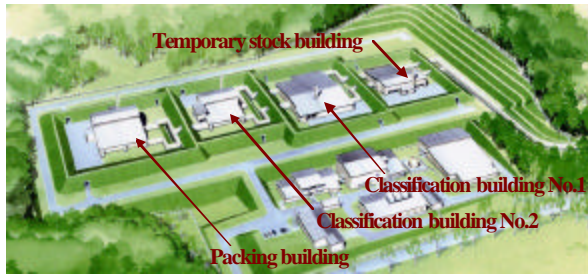


Fig.8 Recovery area

7) Temporary storage building:

The munition containers are transported to the temporary storage buildings by truck and stocked. The munition containers are handled manually with forklift in these buildings.



Fig.9 Storage area

8) Excavation control building and recovery control building:

All of the equipment in these facilities are operated and monitored from the remote control rooms in excavation control building and recovery control building except those in classification building No.2.

4. Excavation System

4.1 Basic Design concepts

The basic design concepts of the excavationsystem are:

- To adopt a robotic system to reduce manual excavation work as much as possible.
- To adopt a remote control system to ensure the safe excavation work.
- To adopt an automatic control as far as practically possible to ensure the efficient excavation work and to avoid the human error.

- To carry out the excavation work by human only for special cases when the use of a robotic system becomes inappropriate.

Even though a small number of abandoned chemical munitions in China have been excavated and recovered by human in the past, the robotic system can be utilized to re move munitions in Haerbaling safely and efficiently since a large amount of munitions is buried in a relatively small area. By applying a high performance telerobotic control to the robotic system, the excavation work becomes safer and more efficient, and can minimize human errors and reduce potential risks.

4.2 Functions

The functions of the excavation system are:

- To remove the soil without applying the impact on the munitions.
- To confirm the condition of exposed munitions whether those are free from the potential risks during the remote excavation work.
- To pick up the buried munitions safely.
- To transport the recovered munitions to the downstream facilities.
- To equipped with the other functions, such as water spray, chemical agent sensing, camera monitor, etc.

4.3 Layout

Buildings will be constructed at each burial pit to keep leaked chemical agents from being scattered into the air, thus making the environmental condition suitable for excavation work with a robotic system throughout the year. Two sets of a robotic system will be installed at Pit No.1 pit and one at Pit No.2. The munitions, which are excavated from the burial pit by the excavation robot, are put into the munition box and conveyed to the discharging point to AGV, which travels around the pit and transport the munitions to the next facilities for classification, sorting, packing and storage.

The soil removing machines of suction type, which extract the soil from the pit, are installed in the machinery room beside the burial pit. The soil is discharged into the soil drum.

The excavation robots, soil removing machines and AGV are controlled from the central control room in the excavation control building which is located 500m far from the excavation building. The bird's eye view of excavation building is shown on Fig.10.

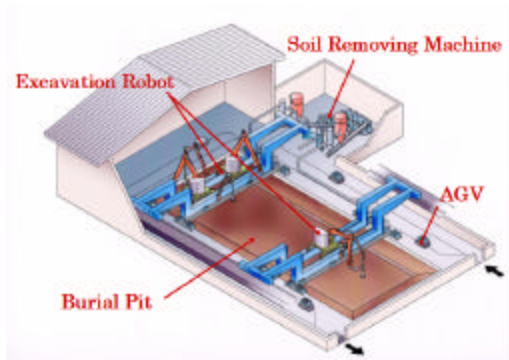


Fig.10 bird's eye view of excavation building

4.4 Soil removing

4.4.1 Functions

The abandoned chemical munitions might be piled up in the big inverted trapezoid pit at first and then the pit might be backfilled with the soil. The covered soil of 2-3m in depth, shall be removed by human before starting the excavation work of buried munitions. The soil removing system should remove the soil around the munitions without any harmful disturbance on the munitions, which have the potential risk of explosion due to the impact. The upper half of soil around the munitions shall be removed by the remote operation to the extent that the buried munitions can be visually confirmed through the CCTV monitors and the buried munitions can be gripped with the excavation robot.

4.4.2 Verification tests

The soil removal system is newly developed, because there is no past experience to introduce the soil removal system, which is applicable to this project. The design conditions of soil removal system are as described below.

- Munitions are buried in the sandy soil of weathering granite.
- Munitions are randomly placed.
- Soil should be removed with a telerobotic system.
- Soil should be removed without applying any harmful impact on the munitions
- Soil should be removed to such an extent that types and positions of munitions can be recognized with the automatic sensing system and the munitions can be gripped with the excavation robot.

The soil removal system of suction type was selected to meet such conditions. The soil suction nozzle is composed of a compressed air injection nozzle and an air extraction nozzle. At

first, the soil is loosened by injecting compressed air, and then extracted through the air extraction nozzle.

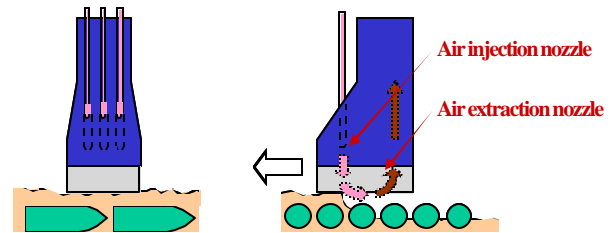


Fig.11 Soil Extracting Nozzle

The verification test was conducted in the following sequential steps:

- 1) Selected the suitable sandy soil having the same grain distribution as the one in Haerubaling.
- 2) Compacted the soil to simulate the same burial condition.
- 3) Conducted the fundamental test under various conditions and decided the construction of nozzle.
- 4) Conducted the total testing using mock-up munitions buried under the various conditions.
- 5) Examined the availability of water spray on the performance of soil removing.
- 6) Confirmed performance of the collision avoidance system between the nozzle and munitions.



Fig.12 Verification test machine

With this test setup, the performance of the soil removal system of a suction type was successfully demonstrated. Results of the test are as described below.

- By the combination of an injection nozzle and an extraction nozzle, the sandy soil of weathering granite can be removed effectively. It is less effective for the clay soil.
- The soil can be removed without any disturbance or impact on the buried munitions.

The water spray of small quantity is effective to loosen the compacted soil and to make the soil removing more efficient.



Fig.13 Soil removing test

4.4.3 Soil Removing Machine

The soil removing system is composed of a soil extracting nozzle, a soil separator, a dust collector, a blower and hoses & pipes. The soil is extracted from the pit and discharged into the soil container in machinery room. The flow diagram of soil removing system is as shown on Fig.14.

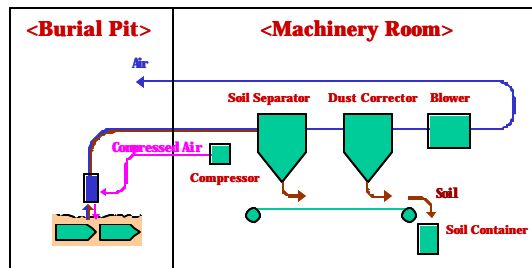


Fig.14 Flow diagram of soil removal system

4.4.4 Operation

The soil extracting nozzle and the hoses are fixed on the supporting arm, which is installed on the traveling bridge. The suction nozzle is gripped by the excavation robot during the soil removing operation and the soil extracting point is shifted by moving the suction nozzle with the manipulator of the excavation robot as shown on Fig.15.

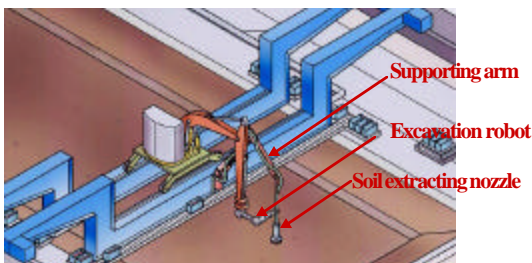


Fig.15 Soil removing operation

The collision avoidance system is provided to prevent the suction gripper from hitting the munitions in the pit.

4.5 Excavation

4.5.1 Functions

There are several key technologies, which have to be incorporated in the excavation robot to ensure the safe, efficient and reliable operation and to make it practically useful at Haerubaling site.

1) Gentle handling during gripping operation:

It is very important not to disturb the ambient munitions nor create the shocks to the munitions during gripping operation, because of the potential risk of fused munitions and metal picrate which are very sensitive against the shock.

2) Firm gripping of munition:

It is also important that the munition, which is once picked up with gripper, should not be dropped onto the burial pit to avoid the impact.

3) Easy gripping operation:

The type and construction of the gripper should be the one which is suitable for the telerobotic operation, because the telerobotic gripping operation is not so easy as it is considered in general.

4) Exact sensing of the munitions:

The exact sensing of location, direction and center of gravity of buried munitions should be done within the limited time frame.

5) Rational combination of automatic and manual operation:

We believe that the automatic operation combined with operator's judgment is the most reliable way to pick up the munitions safely and efficiently.

6) Suitable arrangement of camera and monitor:

Suitable arrangement of camera and monitor is important to recognize the condition and the location of buried munitions and to make the operation more efficient.

7) Sensing of chemical agent:

The chemical agent detector should be installed on the excavation robot to monitor the leakage of chemical agent.

8) Exact positioning of gripper:

The exact positioning of gripper by both automatic and manual operation is essential for the safe gripping operation.

9) Collision avoidance:

The collision avoidance system should be effective during the excavation operation.

4.5.2 Verification tests of gripper

There is no past experience to pick up the large number of buried munitions within the limited time frame. The existing telerobotic systems, which handle the explosive ordnance, are not available in this project. The excavation robot should be newly developed to fit this special case. For this purpose several kinds of gripper hand have been selected and tested to confirm the function needed as the gripper and to finalize the specification of it.

1) Magnet with flexible gripper

The concept of this type is to integrate the two different functions into one gripper to meet the requirement of adopting the autonomous control, gentle handling and reliability not to drop the munitions. The magnet is easiest way to pick up the object and accordingly easiest way to attain the autonomous control. After picking up the munitions by the magnet, three fingers, which are activated by the motor and wire, grasp the munitions gently not to drop it during the shifting motion to the munition box. The technical items which we have to confirm through the testing is whether the magnet of reasonable size can pick up the streamlined munitions covered with soil and rust and whether the flexible gripper can grip the munitions gently and tightly.

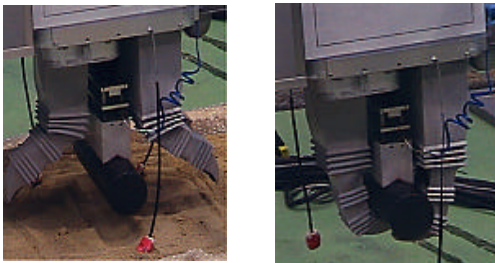


Fig.16 Magnet with flexible gripper

The rest result are:

- Enough magnetic force can be attained with the reasonable size of magnet. The size of magnet is 50mm in width and 150mm in length, and magnetic force is 235 N with 3 mm gap between magnet and the munitions surface, which corresponds about 4 times of the self weight of small size munitions.
- The magnet doesn't extract the surrounding object even gem clip.
- The magnet can pick up the munitions of which lower half is buried in the soil. This means that upper half of

surrounding soil should be removed by soil removal system.

- The flexible gripper can grasp the munition gently and tightly.
- The requirements on the accuracy for positioning magnet are confirmed.

2) Picking gripper

The picking gripper has been used in every industrial field as the gripper including the robots of explosive handling. The construction is simple and reliable. This type of gripper is workable to grip the munitions under the special burial condition by remote control. The testing was carried out to find out the best mechanism, shape of gripping finger and gripping procedure for each munition.

The testing was carried out by manufacturing the gripping hand of actual size and fitting it to the tip of link of power shovel. The munitions of actual size and weight are also manufactured for this test and buried in the soil.

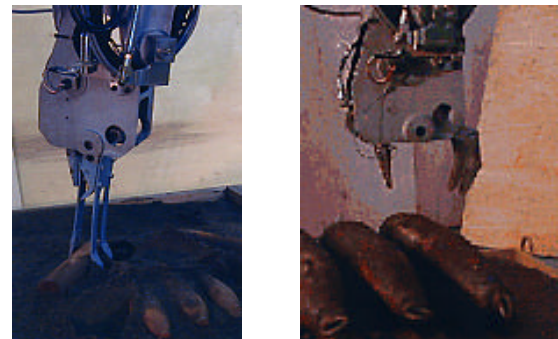


Fig.17. Magnet with flexible gripper

The test results are:

- The construction of two types of gripper is confirmed. One is a rigid type, which is suitable for gripping the larger munitions, and another is a flexible type, which is suitable for gripping the smaller munitions.
- Both types of munitions can grip the munitions tightly.
- The suitable gripping methods are confirmed for each case of burial condition and each munition.

3) Suction gripper

The suction gripper is widely used in the industrial field to pick up the handling material, and many kinds of suction pads are commercially available. But none of those are applicable for the rusty munitions adhered with soil. The verification test have

been carried out to develop the suction pad, which is applicable for the buried munitions, and to confirm the effectiveness of it for various occasions. The vacuum for suction gripper was made with compressed air and ejector.



Fig 18. Suction gripper

The test results are:

- The closed cell formed spongy is suitable for suction pad. (The bellows type suction pad is not applicable.)
- The suction gripper can lift the rusty shell, which is adhered with soil and have the groove.

4) Conclusion of verification test

The magnet gripper was the best selection, because the positioning of gripper on buried munition is easy, the disturbance to ambient munitions can be minimized and the munitions can be lifted up gently. However, the magnetic type could not be selected since there is a slight possibility of magnet inadvertently creating induced electrical current on the proximity fuse, which in turn may cause munitions to explode. (The proximity fuse was not developed by old Japanese army, but still there is a slight possibility of foreign-made proximity fuse being buried in the pits.)

The suction gripper is the alternatives, which has the same advantages as magnet gripper. The three fingers gripper with two knuckles is also used in combination with suction gripper to ensure the firm gripping after picking up the buried munition by suction gripper. Fig.19 shows the conceptual sketch of suction gripper with three fingers.

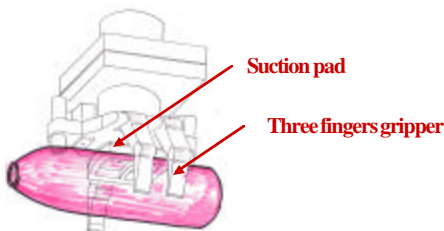


Fig 19. Suction gripper

4.5.3 Excavation Machine

The robotic systems are composed of the excavation robots, the traveling deck on which excavation robots are mounted, internal conveyor and the control system.

1) Excavation robot:

The excavation robot is composed of gripping hand, manipulator and a platform. Taking the reliability and the flexibility of operation into consideration, the construction like power shovel is planned to adopt a platform with some modification. The rough positioning of the gripping hand can be achieved by driving the traveling, revolving and luffing devices of the platform. The manipulator is installed at the tip of the lever of the platform for fine positioning of the gripping hands. The gripping hand is fitted at the tip of manipulator with the tool plate. The gentle gripping of buried munition is achieved by the harmonious control of the gripper and the manipulator.

2) Traveling deck:

The traveling deck travels alongside the pit and is composed of the bridge structure, traveling devices and the internal conveyor. The empty munition boxes are loaded on the internal conveyor from the AGV and conveyed to the excavation robot. The loaded munition boxes are conveyed to the discharging point and mounted onto the AGV.

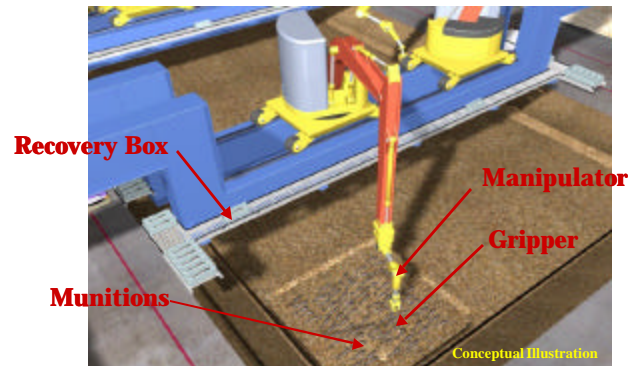


Fig.20 Bird's Eye View of Excavation Robot

3) Control system:

The robotic system for excavation and recovery is operated from the central control room. The operator operates the robotic systems by checking the site condition with CCTV and several other sensors and judging the correctness of telerobotic operation of robotic systems. When the operator judges that he should stop, change or modify the telerobotic operations, he can interrupt the

telerobotic operations at any time and correct it. The operator can also operate the robotic system under remote control mode with a joystick for any occasions when he feels that manual remote control is better suited for picking up the buried munitions than telerobotic control.

4.5.4 Operation

The operation sequences of excavation robot are:

- 1) After finishing the soil removal operation, 3D map of burial pit is created and displayed on the screen.
- 2) The 3D image data is further processed by the image recognition program and the munitions are discriminated and classified to each size. If the discrimination is erroneous, operator can correct it on the screen.
- 3) Operator selects the munition to be picked up by touching the screen or by the mouse.
- 4) The data of location, direction and position of center of gravity of the munition is generated and used to control the gripper and the manipulator.
- 5) When operator pushes the starting button, the gripper is shifted and stopped automatically above the munitions to be picked up. The gripper and finger are suitably positioned automatically.
- 6) After confirming the correctness of the position of the gripper through the video image and/or 3D image, operator pushes the button to start the automatic gripping operation. Operator is watching the video image during the gripping operation, and can interrupt at any time and can operate the excavation robot by remote manual control mode if necessary.
- 7) After gripping the munition, the munition is automatically lifted up and placed into the munition box.
- 8) The gripper returns to the original position automatically.
- 9) Repeat the operation from (3) to (8).
- 10) The collision avoidance system is always working during the operation.

5. Conclusion

Useful database had been obtained for the design of the gripping hand and the soil removal system through the experiments. Further, we will continue to work on validations of a total system of excavation robot by using the mock-up machine so as to enable the excavation operation by the telerobotic system.

Through those tests and validations, we believe we can develop a safe, reliable and efficient robotic system that can be used for the recovery of abandoned munitions from the two burial pits at the Haerbaling area of Dunhua in Jiling Province, China.

6. References

- 1) Hiroshi Niho, Telerobotic System for Recovery of non-Stockpile Munitions in China, The international CW Demil conference, May 2002.
- 2) Hiroshi Niho, Telerobotic System for Recovery of non-Stockpile Munitions in China, The international CW Demil conference, May 2003.
- 3) The conditions of abandoned chemical weapons in China, An Aggregated Report of the Results of Investigations(1991-1996), Japan Institute of International Affairs, March 1998.
- 4) Technological Risk Assessment and Risk Management for Destruction Technology for Abandoned Chemical Weapons, Report of the National Committee for Restoration of Devastated Living Environments by Advanced Technology, Science Council of Japan, November 2002.
- 5) Technological Risk Assessment and Risk Management for Destruction Technology for Abandoned Chemical Weapons, Report of the National Committee for Restoration of Devastated Living Environments by Advanced Technology, Science Council of Japan, November 2002.
- 6) Hiroshi Niho, Excavation of Non-stockpile Munitions in China, International Symposium on System and Human Science -For Safety, Security and Dependability (SSR2003), November 2003.
- 7) Hiroshi Niho, Abundant Chemical Weapon Destruction Project, 10TH Construction Robot Symposium, Japan Robot Association, September 2004.

Assessment of Safety Regulation

by Social Simulation

Masaya Nagase

Engineered Environment Division, Course of Human and Engineered Environmental Studies,
Institute of Environmental Studies, Graduate School of Frontier Sciences, the University of Tokyo
Furuta Laboratory, Faculty of Engineering Bldg. 12, 7-3-1 Hongoh, Bunkyo, Tokyo, Japan (Zip code 113-0033)
Telephone and Fax number: +81 -3-5841-8923, E-mail: nagase@cse.k.u-tokyo.ac.jp

Prof. Kazuo Furuta

Department of Quantum Engineering and Systems Science,
School of Engineering, the University of Tokyo
Furuta Laboratory, Faculty of Engineering Bldg. 12, 7-3-1 Hongoh, Bunkyo, Tokyo, Japan (Zip code 113-0033)
Telephone and Fax number: +81 -3-5841-6965, E-mail: furuta@q.t.u-tokyo.ac.jp

TOPIC: Roles of simulation

Assessment of Safety Regulation by Social Simulation

Masaya Nagase (the University of Tokyo), Kazuo Furuta (the University of Tokyo)

Abstract

Following the worldwide trend of deregulation, safety regulation is under re-consideration, whereas various accidents still endanger our society. Some method that can take both production and safety management into account is therefore required to assess safety regulation. This research proposes a social simulation to assess influence of safety regulation on social utility.

The model used in this study is a multi-agent system where many production companies act and evolve. The model of each company contains elements related to both productivity and reliability. Safety regulation influences companies' activities as the environment. This simulation model is so flexible that it can be extended from simple to more complicated ones.

As a result of case simulations we found the following results. Firstly, the appropriate style of safety regulation depends on the loss of an accident. It depends also on maturity of the industry. Secondly, in a large and complicated industry, a certain regulation style improves the productivity as a whole. In a small and simple industry, regulation always has negative effects. Thirdly, non-regulation or specification-based regulation is superior in case of a small loss of accident. Penalty-based or performance-based regulation is superior in case of a very large loss of accident. However, in that case, companies cannot compensate the loss with any penalty due to an accident.

In conclusion, an effective method for assessment of safety regulation has been developed, and then several insights were shown in this research.

1: Introduction

The modern industrial society is built on high technologies and efficient production systems. These technologies and systems are operated by private companies, which strive toward profits. As promoters of free market economy claim, these efforts brought us the prosperity. However, we must also consider possible failures of companies for optimizing social utility. Moreover some social utility cannot be achieved only by free activities of companies. Therefore the government should regulate and limit some activities of the private sector. In this work we deal with safety regulation that prevents accidents caused by companies' activities.

The trend of deregulation began from the standpoint of importance to efficiency. The former General Affairs Agency, in its report "White Paper on Deregulation"¹, claims "Existing public regulation should be always under re-consideration about necessity, the way and contents. And then, if it lose necessity or has negative effects, it should be relaxed or repealed". Originally, only "economic regulation" was concerned because such regulation has apparently little reasonableness. So far "social regulation", which includes safety one, is thought indispensable for safe and secure society. However, safety regulation is now also under re-consideration. There are mainly two reasons why discussion of deregulation on safety has begun. Firstly, if safety regulation is too tight, they must degrade productivity and social utility. Secondly, an old style of regulation may ironically become an obstacle rather than an enhancer of safety.

At the same time public demands for safety is increasing. People become more and more severe on accidents. There are mainly two reasons for this trend. Firstly, since prosperity of the society is almost saturated, people become to care greatly about negative aspects of industrial activities. Secondly, because of growth of modern industries and development of new technologies, accidents have become complicated, widely expandable, and serious, so that they are now too difficult to understand their causes, impacts, and consequences.

From the above backgrounds, a new style of safety regulation must be introduced to take balance between productivity and safety. However it is little known how different regulation styles influence production and safety. The question of how to assess safety regulation is still open.

The objectives of this study are to provide a method to assess safety regulation and to propose an appropriate style of safety regulation. An approach of social simulation was employed. The most important point of our simulation model is that it can consider both production and safety management.

2: Related Studies

Since most of previous studies on safety are concerned only with safety issues of individual companies, they do not deal with systemic aspects of safety regulation.

Reliability engineering², which is widely applied in various industries, is of great value to estimate reliability of individual instruments, components, or systems. It is applicable to various failure modes and maintenance modes. Principles of reliability engineering are the basis of this research, because our simulation model is composed of multiple instruments.

Human reliability assessment³, which is originated from reliability assessment of hardware, focuses on

human activities that may affect system safety. It is essential to consider accidents or failures caused by human activities. This aspect of human reliability can be included in reliability of individual instrument.

Recent disastrous accidents always have some grounds in organizational issues. James Reason, in his book "Managing the Risks of Organizational Accidents"⁴, analyzed accidents of this type, organizational accidents. He discusses that organizations are motivated both to production and safety management but that they are liable to disrespect safety management. He did not show any concrete method, however, to assess these effects.

3: Simulation Model

We will begin by introducing our simulation model. We use "term" as a unit time interval in simulation, and "resource(s)" as economic goods.

Our artificial society is a sort of multi-agent system, which contains many companies as agents, and safety regulation works as the environment. The companies are motivated to gain profits, and the safety regulation influences them equally. Each company is composed of "devices" that have some attributes determining productivity and reliability. Some companies may fail to cause an accident, and they will be replaced by new ones following the genetic algorithm.

The outline of this simulation is as follows.

1. Generate a population of companies at random.
2. All companies operate their own facility for production to increase or decrease their capital resources as a consequence.
3. All companies crashed are replaced with new ones following the genetic algorithm.
4. Repeat from Step 2.

3.1: Device

Devices are virtual but basic elements of this model. Every production company is somewhat similar, and their function can be represented that a company receives some inputs, transforms them, and emits some outputs. In the same way, a device receives input resource Z and emits output resource Z' . The input Z is transformed into the output Z' . In the transformation some cost C is consumed. If the device fails, Z' is smaller than Z . Concrete definition of a device can be given by specifying its transformation function.

3.2: Instrument

Instruments are concrete devices with specification. Specification of an instrument is related to its productivity and reliability. An instrument has a "status" that represents the state of its operation. If the status is in "failure", the instrument consumes the inputs Z but generates no outputs. Otherwise, if the status is in "normal", the input Z is transformed into $Z(1+V)$. Here, V is a property that represents the productivity of the instrument. The status of an instrument changes following another property R , which represents the reliability of the instrument. R can be a function of term t , and it is represented as $R(t)$. The status of an instrument is in normal with probability R . This means the status is in failure with probability $1-R$. The status changes term by term independently. Although the operation cost C of an instrument can be determined independently from other properties, it may depend on V and R .

3.3: Unit

A unit contains one device and it is linked to other units. The link is unidirectional. There are two kinds of links, an input link and an output link. A unit can temporarily store resources received from input links. The unit then transforms the resources in the containing

device, divides the transformed resources equally, and finally emits them into output links.

There are two types of characteristic links. Ordinary links form an AND gate that is used to compose a cascade line of units, while dynamic links form an OR gate. A dynamic link responds to unit failure. If the device contained in a unit fails, any dynamic link connected to the unit is automatically suspended during the term of failure, and waste of resources can be avoided consequently.

3.4: Line

A line contains units and it organizes them in a network, where each unit is a node. A line has two special units, the input unit and the output unit. The former corresponds to the input gate of a device, and the latter to the output gate. The operation cost of a line is the total costs of the all devices contained in the line.

Because of the characteristic of a device, a line must be organized as such that all resources that enter the input unit flow out from the output unit. No units are allowed to be isolated from the resource flow. In addition, the input unit must not have direct links to the output unit.

3.5: Company

Companies are represented as agents in this society. Each company possesses the root device, and it receives a constant amount of resources Z into the root device. Then the company obtains profits PF , where $PF = Z' - Z - C$. Here Z' represents the output from the root device and C is the operation cost of the root device.

A company accumulates capital resources CP as follows.

$$CP(t) = \begin{cases} r\{CP(t-1) + PF(t)\} & (PF > 0) \\ CP(t-1) + PF(t) & (PF \leq 0) \end{cases}$$

We call r the reservation rate ($0 \leq r \leq 1$), which represents that a company do not stock all the profits, because it must distribute dividends or invest for researches, etc.

If the root device of a company falls in failure, it is interpreted as an accident of the company.

3.6: Safety Regulation

Safety regulation is specified by two aspects: when they work (timing), and how they work (form).

Timing of influence in safety regulation has following three options. Proactive regulation affects companies when they are generated, reactive regulation when they caused accidents, and scheduled regulation with some periodic intervals.

Forms of safety regulation are threefold. Specification-based regulation restricts available devices, performance-based regulation restricts the reliability of the root device, and penalty-based regulation punishes companies caused an accident. If a company violates regulation, they must pay certain amount of fine.

4: Genetic algorithm

The genetic algorithm⁵ replaces companies like natural selection in the market. The elements of the genetic algorithm in this research are:

1. selection of adapted companies,
2. genetic coding of a company,
3. crossover,
4. mutation.

4.1: Selection of Companies

In this simulation the lifetime of a company is not limited. A company can subsist as long as its capital resources (CP) remain. If its CP is exhausted, the company is replaced with a new one. Parents of a new

company are selected by the adaptation proportional method. The degree of adaptation is proportional to the amount of stored capital resources.

4.2: Genetic Coding (Genotype)

In this model the root device determines the characteristics of the company. Accordingly a genetic code is defined for a line. Note that an instrument can be replaced with a line containing only one unit.

A genetic code is composed of a network gene and a node gene. The former corresponds to a network of line, and the latter to devices contained in units. Here, N stands for the number of units in a line.

A network gene $B(I, J)$ is determined as follows. Firstly all units are ordered and numbered serially with the input unit at the first (0) and the output unit at the last ($N+1$). Secondly, each allele $B(I, J)$ is set 1 if there exists a link from Unit I to Unit J ($0 \leq I < J \leq N+1$). Otherwise, it is set 0. A node gene $D(I)$ is determined such that the ID name of the device contained in Unit I ($0 < I \leq N$) is set at $D(I)$.

4.3: Crossover

The root device of a new company is generated by crossover. Every property is inherited from one of two parents except capital resources, which is reset to zero.

Crossover is executed as follows. Firstly, the direction of crossover is decided. There are two directions of crossover, row or column. Since crossovers in the both directions are similar, here we explain only for the row direction. Secondly, the crossover location (P, Q) is decided at random ($0 \leq P < Q \leq S$). Thirdly, following the direction and the location chosen, a new genetic code is generated.

Suppose $B_1(I, J)$ and $D_1(I)$ are the genetic codes of Parent 1, $B_2(I, J)$ and $D_2(I)$ are those of Parent 2, $B(I, J)$

and $D(I)$ are those of the new company. The new gene is generated as follows:

$$B(I, J) = \begin{cases} B_1(I, J) & (I < P; I = P, J \leq Q) \\ B_2(I, J) & (I > P; I = P, J > Q) \end{cases}$$

$$D(I) = \begin{cases} D_1(I) & (I \leq P) \\ D_2(I) & (I > P) \end{cases}$$

In case of crossover in the column direction, P and Q are to be interchanged. For simplicity, explanation of crossover between genes of different sizes is skipped here.

4.4: Mutation

Finally the new genetic code is mutated. Mutation can be applied to surviving companies. There are following three options of mutation.

LINK-SWITCH: A randomly selected bit of $B(I, J)$ is switched over in every row. This means some $B(I, J)$ is modified to $1-B(I, J)$.

NODE-SWITCH: A randomly selected device of $D(I)$ is replaced with some other device. A new device is chosen from all available devices existing in the society.

SCALE-CHANGE^a: The size of the genetic code is increased or decreased.

RESUME: A fatal gene is resumed if any. If $B(I, K)$ is zero for all K , one of those is changed to 1. If $B(K, I)$ is zero for all K , one of those is changed to 1. $B(0, N+1)$ is changed to 0.

5: Society without Regulation

In the following simulations, if unmentioned, each simulation runs until 250 terms and is repeated 100 times. Values in figures are the averages of 100 runs and shown with 95% confidence intervals. Each society contains 100 companies. The reservation rate is fixed 0.8. A company is equipped with a line of certain size as the

root device. We call the size of the line the size of the company. A line contains instruments only. Available instruments are determined in advance.

First we studied artificial societies with no regulation. All companies in these societies do business completely free. We can find fundamental characteristics of the model with these experiments.

Three properties are determined for instruments: productivity V , reliability R , and cost deflector Cd . Each property has two types: A and B . Type A is superior to Type B . These are shown in Table 1.

Item	Value
V	$V_A=0.2, V_B=0.1$
R	$R_A=0.99, R_B=0.9$
CD	$Cd_A=-0.8, Cd_B=-0.2$

Table 1: Properties-1

Here, cost C is defined as follows:

$$C = (1 + V)R + Cd$$

Characteristics of an instrument are decided by combinations shown in Table 2. The restriction that excludes both V_A and R_A represents trade-off relationship between productivity and reliability.

Item	Combination
1_A	V_A, R_B, Cd_A
1_B	V_A, R_B, Cd_B
2_A	V_B, R_A, Cd_A
2_B	V_B, R_A, Cd_B
3_A	V_B, R_B, Cd_A
3_B	V_B, R_B, Cd_B

Table 2: Properties Combination-1

Four cases of societies without regulation were simulated and time dependent performance was examined: company size of 5 without mutation, 10 without mutation, 5 with mutation, and 10 with mutation. Constant resources for a root device are same as the size.

5.1: Change of Performance

Change of expectation and reliability is shown in Figure 1 and Figure 2. Expectation means an expected value of profits of a company taking probability of an

^a This option is not applied to the following cases.

accident into consideration. These values were evaluated at the end of each term, which include companies crashed at the term.

These figures show that the larger companies become the higher expectation but the lower reliability they obtain. The reason is that a large company can create a long cascade of devices to gain more profits but the probability of an accident gets high owing to the large number of devices in the cascade.

We can also find that mutation reduces expectation but does not reduce reliability. The reason why mutation reduces expectation is that companies cannot sustain the optimum level of operation, because they are enforced to select Type b instruments. The reason why mutation does not reduce reliability is that companies of low reliability are likely to crash and to be replaced.

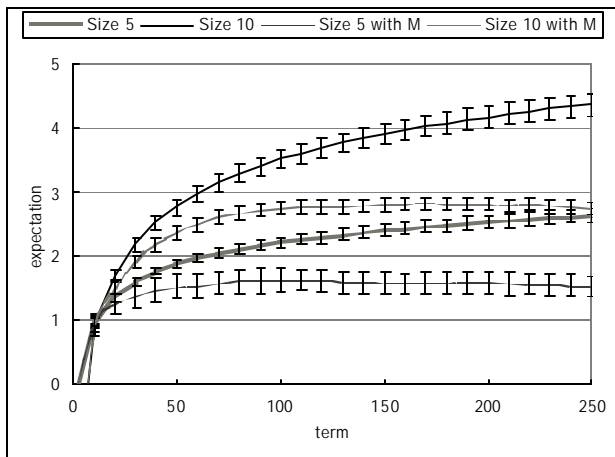


Figure 1: Change of Expectation

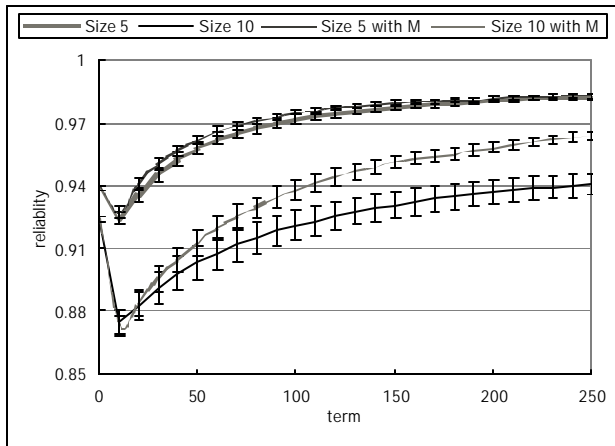


Figure 2: Change of Reliability

5.2: Gaps between Actual and Estimation

There exists a gap between the actual performance of companies survived and their estimated performance. Here, such a gap in reliability is defined as $G_R = E/(1-R)$, where E represents the statistical probability of an accident.

The gap of reliability is shown in Figure 3. Estimated performance in reliability is always inferior to the actual reliability, especially in with mutation. It is because a company is likely to crash and be replaced if it causes an accident. And these accidents are caused frequently in with mutation. This means, safety performance in a company survived is always inferior to appearance. Still, related with the previous result that mutation does not reduce reliability, this gap can be understood as results of improvement.

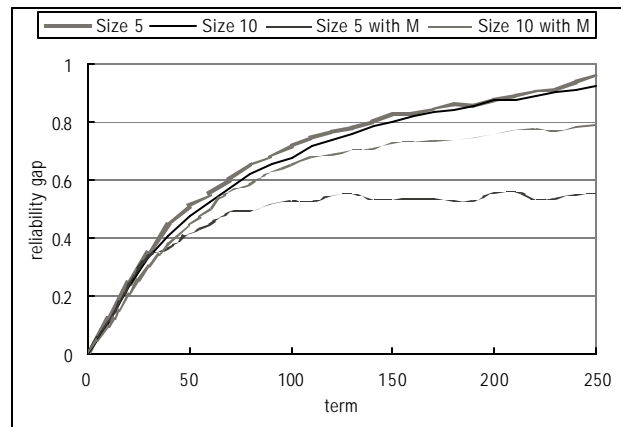


Figure 3: Reliability Gap

6: Penalty-based Regulation

Societies with penalty-based regulation were simulated to analyze effects of penalty on social utility. Two cases were assumed: company size of 5 and 10 without mutation. Various penalties are tested for these two cases while available instruments are the same as in Chapter 5.

6.1: Impact of Penalty on Performance

Expectation and reliability are shown in Figure 4 and Figure 5 for various penalty levels. Figure 5 shows that the larger penalty results in the higher reliability in the both cases, because a large penalty increases a risk of an accident and the importance of reliability.

Increase of reliability saturates above a certain penalty level, because any penalty level works in the same manner if it exceeds above the capacity of a company^b.

Figure 4 shows that the larger penalty results in the lower expectation with a company size of 5. With company size of 10, however, expectation gets maximum at a certain penalty level. Without penalty some insufficient companies can survive. This means that a certain penalty level promotes optimization of productivity in a large-scale industry.

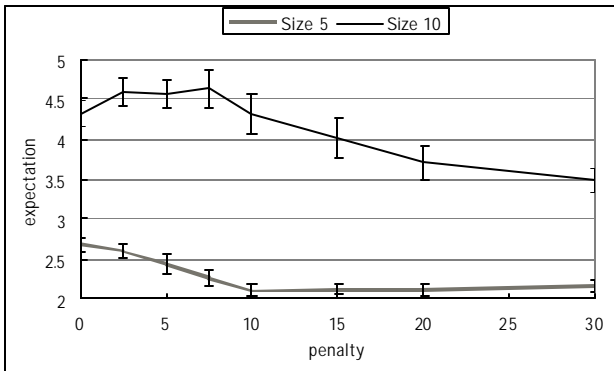


Figure 4: Expectation in Various Penalties

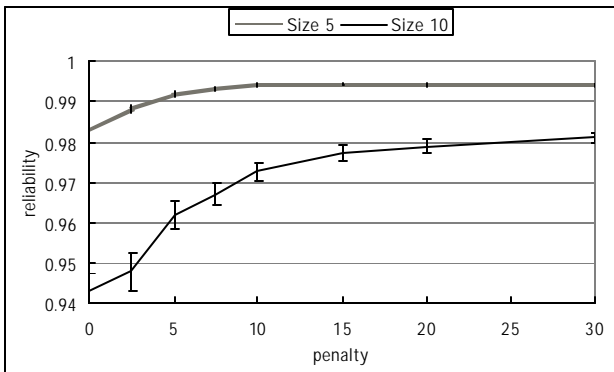


Figure 5: Reliability in Various Penalties

6.2: Impact of Penalty on Social Utility

To clearly assess the trade-off relationship between expectation P_E and reliability R , reliability should be converted into some resource measure that is the same as expectation (profits). For this purpose social utility U is defined as $U = P_E - L(I - R)$, where L is the loss for the society due to an accident.

This means, when L is large, companies should take efforts to decrease the probability of an accident even if their productivity will decrease a lot.

Social utility with various losses of an accident is shown in Figure 6 and Figure 7. We can find that the more loss is expected due to an accident the larger penalty should be imposed to obtain the maximum social utility. We can obtain the optimum curve of utility for considered regulation by combining these lines.

Based on these results, no penalty is required in case the expected loss of an accident is small and the scale of industry is also small. However, in case the scale of industry is large, certain penalty should be imposed. In case the expected loss of an accident is very large, penalty for an accident should be severe. Otherwise, it is impossible for a company to compensate the loss for any penalty.

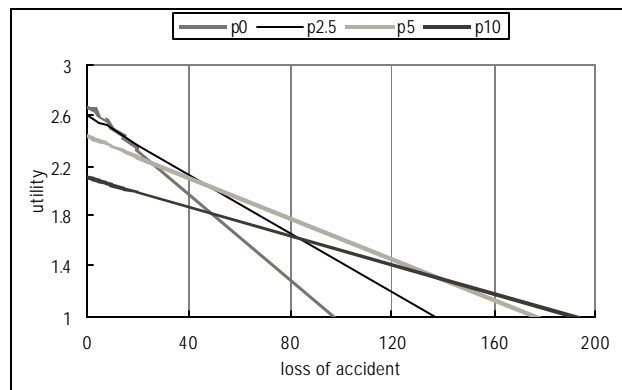


Figure 6: Social Utility for Company Size of 5

^b The average capital resource is about 8-10 for a company size of 5, and about 12-18 for 10.

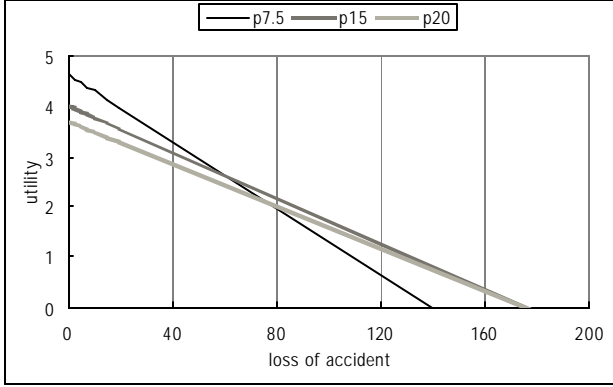


Figure 7: Social Utility for Company Size of 10

7: Societies with Various Regulation Styles

Various regulation styles are compared next. We considered five regulation styles: non-regulation (*Free*), penalty-based regulation with punishment for an accident (*Penalty*), specification-based regulation that enforces companies to use A -type instruments only (*Ra*), specification-based regulation that enforces companies to use X_5 instruments only (*Mainte*), and performance-based regulation that enforces companies to keep the reliability over 0.98 (*R0.98*). The fine of violation was fixed 5 for every case.

Conditions of simulations are as follows. Five properties are determined for instruments: productivity V_X , reliability at the beginning R_0 , reliability deterioration rate D_X , maintenance period M_X , and cost deflector Cd . These are shown in Table 3.

Item	Value
V_X	$V_A=0.2, V_B=0.1$
R_0	$R_0=1.0$
D_X	$D_A=0.002, D_B=0.02$
M_X	$M_0(=0), M_5=5$
Cd	$Cd=-0.8$

Table 3: Properties-2

Reliability R of an instrument changes as follows:

$$R = R_0 - tD_X$$

Here, t is the terms after the previous maintenance or repair. If maintenance or repair after an accident has been performed, t is reset to zero.

M has two options: M_0 and M_5 . M_0 corresponds to no

maintenance. M_5 corresponds to periodic maintenance that maintenance is executed every 5 term and t is reset to zero. Repair is executed in each case. Maintenance or repair costs 5 times of operation cost C . Here, cost C is defined as follows:

$$C = (1 + V_X)(R_0 - 5D_X) + Cd$$

Characteristics of an instrument are determined by combinations shown in Table 4.

Item	Combination
A_5	V_B, R_0, D_A, M_5, Cd
A_0	V_B, R_0, D_A, M_0, Cd
B_5	V_A, R_0, D_B, M_5, Cd
B_0	V_A, R_0, D_B, M_0, Cd

Table 4: Properties Combination-2

The size of companies is 5, and no mutation is applied to companies survived. Constant resource for a root device is 10.

7.1: Various Regulation Styles and Performance

Change of expectation for various regulation styles is shown in Figure 8. Here, expectation takes cost of maintenance and repair into consideration. Case *Free*, *Penalty*, and *Mainte* obtain high expectation. *Ra* and *R0.98* stay in low level. Each regulation affects companies so strong that genes only with very low productivity can survive.

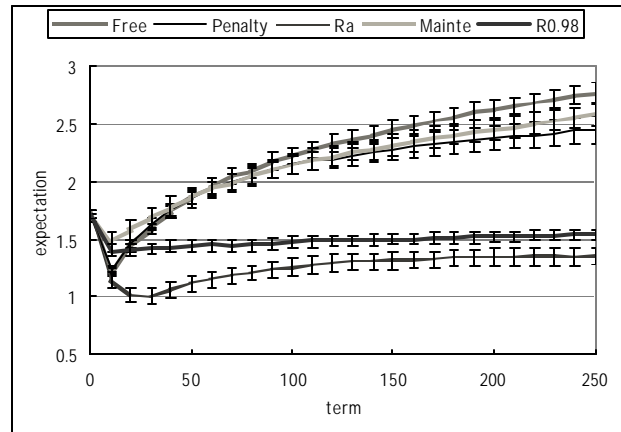


Figure 8: Regulation Style and Change of Expectation

Change of reliability for various regulation styles is

shown in Figure 9. Case *R0.98* obtains the highest reliability. Performance-based regulation promotes the best safety, because it directly selects genes with high reliability. *Ra* keeps the second level almost consistently. *Penalty* falls in early few terms but increases gradually to the level of *Ra*. Reliability of *Free* and *Mainte* stay in low level.

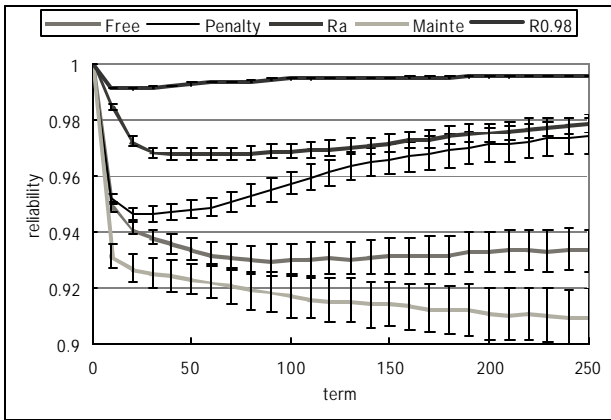


Figure 9: Regulation Style and Change of Reliability

There exists a gap between actual performance of the society and its estimated performance of the present time.

In Figure 10 and Figure 11, “estimated” represents estimated performance at the end of the simulation, and “actual” represents the statistic average of the total results in the society. We can find gaps especially in reliability of *Mainte*. These gaps should be considered as in the next section.

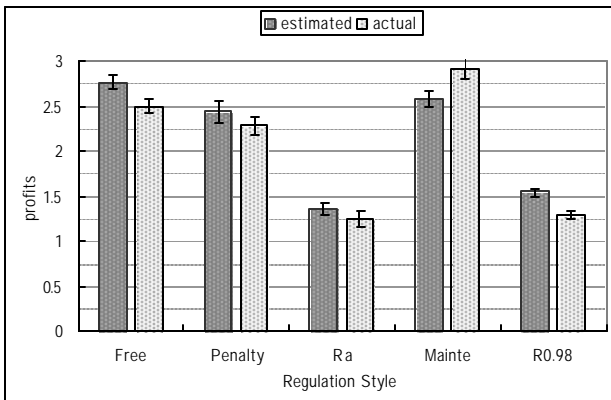


Figure 10: Regulation Style and Profits Gap

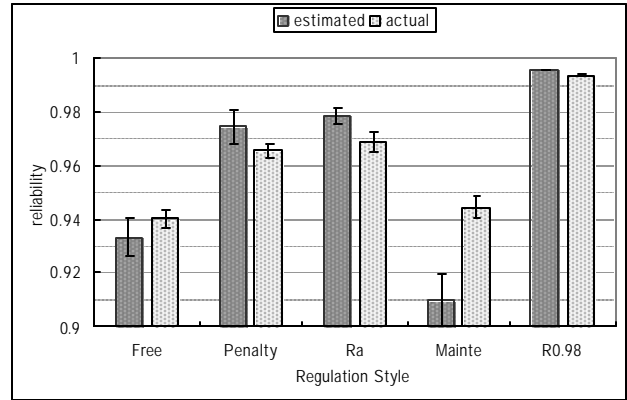


Figure 11: Regulation Style and Reliability Gap

7.2: Various Regulation Styles and Social Utility

Social utility is shown in Figure 12 and Figure 13. The former uses the estimated performance while the latter uses the actual one. From the result of Figure 12, the appropriate style is non-regulation in case the estimated loss of an accident is small, penalty-based regulation in case middle, and performance-based regulation in case large. Neither of specification-based regulation has any superiority over them. However, from the result of Figure 13, specification-based regulation *Mainte* is superior to non-regulation.

Figure 12 shows the best way at the present time while Figure 13 shows it as a whole. Regulation that works well till then does not necessarily work after that. In other words, an appropriate style of regulation sometimes depends on maturity of the industry.

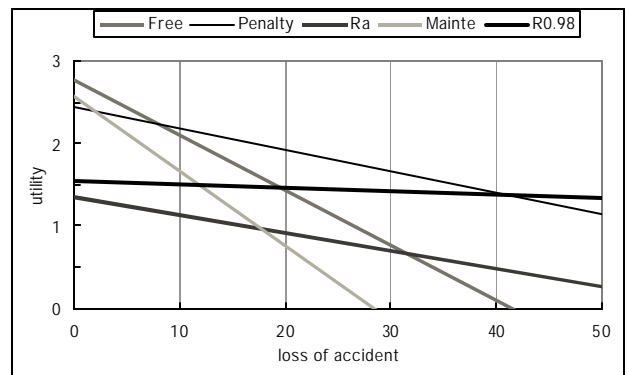


Figure 12: Regulation Style and Social Utility with Estimated Performance

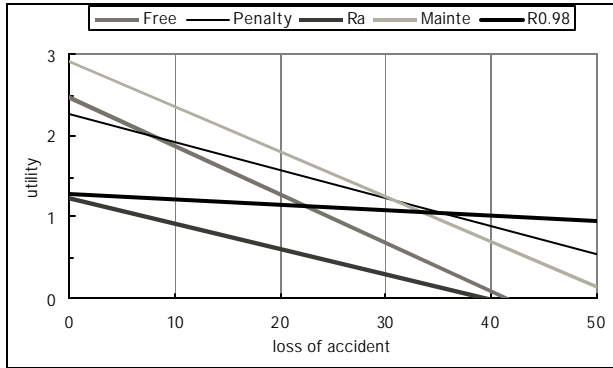


Figure 13: Regulation Style and Social Utility with Actual Performance

8: Conclusion

An effective method for assessment of safety regulation was developed and demonstrated, and then some insights were shown for an appropriate style of safety regulation.

8.1: General Characteristics

We found the following results about general characteristics from these simulations.

1. Positive reforms in a successful organization can be an obstacle against productivity but sometimes improve safety performance.
2. Safety performance in a company survived is always inferior to appearance but this gap can be results of improvement.

8.2: Remarks about Safety Regulation

We will make the following remarks about safety regulation.

1. An appropriate style of safety regulation depends on the expected loss of an accident. It may depend also on maturity of the industry.

2. In a large or complicated industry, certain safety regulation improves productivity of companies. In a small or simple industry, regulation is always an obstacle.
3. Non-regulation or specification-based regulation is superior for a small loss of an accident.
4. Penalty-based or performance-based regulation is superior for a large loss of an accident. Companies, however, cannot compensate the loss with any fine.

8.3: Future Work

Other styles of regulation in various conditions will be simulated. New properties will be introduced to instruments.

Expansion in this model is easy because of the flexibility.

References

- ¹ The General Affairs Agency (Japan), *White Paper on Deregulation [Kiseikanwa Hakusyo]*, 1998, chap. 6 (in Japanese).
- ² Hiroshi Shiomi, *Introduction to Reliability Engineering [Shinraisei-Kohgaku Nyuhmon]*, Maruzen, 1982 (in Japanese).
- ³ Kazuo Furuta, *Process Cognition Engineering [Purosesu-Ninchi-Kohgaku]*, Kaibundo, 1998 (in Japanese).
- ⁴ James Reason, *Managing the Risks of Organizational Accidents*, Ashgate, 1997.
- ⁵ David E. Goldberg, *Genetic Algorithms in Search, Optimization, and Machine Learning*, 1989.

Wide Area Recognition for Safety and Security Preserving Robots

Shun NISHIDE*, Tomohito TAKUBO*, Kenji INOUE*, Tatsuo ARAI*

* Division of Systems and Applied Informatics, Department of Systems Innovation,
Graduate School of Engineering Science, Osaka University
1-3 Machikaneyama, Toyonaka, Osaka, 560-8531, JAPAN
Tel: +81-6-6850-6368, FAX: +81-6-6850-6341
{nishide, takubo}@arai-lab.sys.es.osaka-u.ac.jp
{inoue, arai}@sys.es.osaka-u.ac.jp

TOPIC: Measurement, monitoring, and reliable control

Wide Area Recognition for Safety and Security Preserving Robots

Abstract

Robots intended to work for creating safe and secure society require quick recognition of a wide area of view. Compared to stationary robots, mobile robots possess higher advantages in terms of adaptation to the constantly changing environment. In this paper, a wide area recognition technique for mobile robots using Hybrid Motion Stereo is proposed.

The proposed technique consists of two computation phases: computation of positional information by stereo vision in areas visible in more than two cameras and computation of positional information by motion stereo in areas visible in only a single camera. As against the constantly computable stereo vision, computation by motion stereo requires given camera motion to extract positional information. Estimation of camera motion can be achieved by calculating the movements of immobile objects by stereo vision. Determination of immobile objects can be achieved by calculating the median of the movements of points, assuming there are no rotational camera motions. By these means, the 3D positions of the whole field of view can be recovered.

Experimental results represent recovery of 3D positions of a wide field of view. The computed results computed by motion stereo show substantial precision contrasted with those by stereo vision. Evaluation of the computation time denotes the capability of the proposed technique for practical use. Thus, recognition of wide area with reasonable computation time, which is crucial for robots that deal with safety and security, has been accomplished with Hybrid Motion Stereo.

1. Introduction

Creation of a safe and secure society has been a common goal for researchers in every field. Despite their efforts, there are numerous issues left to be overcome. High-tech empedience is yet far from giving consideration to the disabled and the senior. The increasing number of crimes, whether it be as large as terrorism or as small as purse snatching, has put civilians into anxiety. To contribute to the accomplishment of these goals, researchers in the robotic field have called into account the introduction of robots into the human society.

Researches on robots intended to work for safety and security have been performed over the last few years. A wheelchair supporting humanoid robot can lead to the creation of a friendly society for the disabled[1]. A monitoring system by mobile robots can help in early detection of crimes[2]. However, these systems require precise and broad recognition of the environment as a fundamental premise so as not to endanger the lives of the people around.

Cameras have been the researchers' favorite tools in the objective of environmental recognition. The two most common methods of computation of the 3D positions of the environment are stereo vision and motion stereo. Stereo vision possesses high precision, while it is unable to acquire information contained in only a single camera. Motion stereo is capable of acquiring 3D information of the whole camera view, while its precision is completely dependent on the precision of camera motion computation. The proposed technique, Hybrid Motion Stereo, which combines the two computation methods, is capable of acquiring the 3D positions of objects of the whole field of view with substantial precision. The comparison of the results between stereo vision and motion stereo has been performed in this paper.

2. Hybrid Motion Stereo

Stereo vision and motion stereo have been the two most popular methods of 3D position computation using cameras. Stereo vision computes the 3D positions with high precision for its use of several cameras which minimizes the errors derived in the process of computation in each camera. Motion stereo requires means of estimating the camera motion, which is often difficult for mobile robots. Techniques of camera motion estimation for wheeled robots have been proposed using the calculation of odometry. However the slips and free spins of the wheels caused by the roughness of the surface impose quite an arduous challenge. For legged robots, calculation of direct kinematics can be used to estimate the camera motion with high precision. However, miscalculations occur due to the slips of the feet caused by every step of the robot. Hybrid Motion Stereo uses only the information contained in the cameras retaining robustness to these disturbances.

By using several cameras, the field of view can be divided into two groups, namely, areas visible in more than two cameras (MCVA: Multiple Camera Visible Area) and areas visible in only a single camera (SCVA: Single Camera Visible Area). 3D information contained in MCVA can be computed by stereo vision, while those contained in SCVA require camera motion to be calculated by motion stereo. Hybrid Motion Stereo uses the computed results of stereo vision to estimate the motion of the camera. The concept of Hybrid Motion Stereo is shown in Fig. 1.

MCVA can be assumed to be the focused area of the robot, while SCVA can be considered to be the peripheral area. Information contained in MCVA should be used for main tasks, such as manipulation tasks or navigation tasks. Those contained in SCVA can be used for perception of

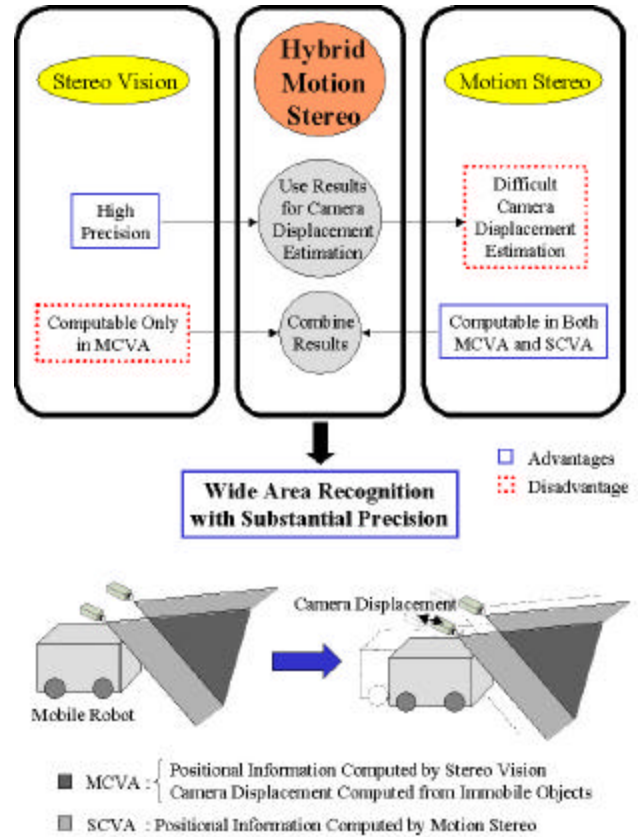


Fig. 1 : Concept of Hybrid Motion Stereo

obstacles, which should be avoided during the execution of the main task. An example of such tasks is a stair climbing task. The robot is required to compute the 3D positions of each step with high precision so as not to make a false step. Simultaneously the robot should locate people walking down the stairs as quick as possible in order to avoid collision. An approximate location of the people should be sufficient if they are to be located in SCVA, since they can be assumed to be in a distant location. Therefore, computation by motion stereo does not demand as much precision as stereo vision.

2.1 Estimation of Camera Motion

Precision in computation of motion stereo depends mainly on the precision of camera motion estimation. In

order to acquire substantial precision using motion stereo, the camera motion estimation should be performed as accurate as possible.

Camera coordinates move according to the camera motions since they are fixed to the cameras. Therefore, the motions of stationary objects in the images are the direct opposite of the camera motions. Although here are 6 DOF (X, Y, Z, Roll, Pitch, Yaw) in the movements of the cameras, the translational movements (X, Y, Z) can be determined with the movement of a single stationary point. Assume that a stationary point has been computed $[X_1, Y_1, Z_1]$ at time t , and $[X_1 + dX, Y_1 + dY, Z_1 + dZ]$ at time $t + dt$. Since the camera motion is the direct opposite of the movements of stationary points, the translational camera motion can be estimated $[-dX, -dY, -dZ]$. However, rotational movements (Roll, Pitch, Yaw) require the movement of one stationary point for the estimation of 1 DOF of the movement. Therefore, to estimate the whole camera motion, computation of the movements of 4 stationary points are necessary. For simplicity, we will assume that there are no rotational camera motions.

The computation of camera motion requires a method to detect stationary points. Here, we will assume that the environment is composed of a majority of stationary objects. Since the backgrounds of most scenery are immobile, this can be considered to be a valid assumption. Under this assumption, the median of the movements of points gives a good estimation of the camera motion.

2.2 Algorithm

In order to compute the 3D positions using motion stereo, the points must be tracked between each sequential images. Since a large amount of time consumes to track all of the points in the image, we have focused on computing the 3D positions of only the feature points. The

flow chart of the algorithm is shown in Fig. 2.

The 3D positions of feature points in MCVA are computed constantly while those in SCVA can only be computed when the camera motion has been estimated. To replenish feature points which have fallen out of view, or diminished due to large camera motions making them untraceable, a renewal of feature points is performed once in a while.

3. Experiment Using a Humanoid Robot

To compare the precision of computation by motion stereo and stereo vision, the authors have implemented the proposed technique into the humanoid robot HRP-2. The vision system of HRP-2 consists of three cameras equipped on the head. We will name each camera as stated in Fig. 3. The camera coordinate system Σ_C is set as stated: the X axis faces in the lateral direction to the right of the robot, the Y axis faces in the longitudinal direction downwards, and the Z axis faces in the perspective direction, which the robot faces. The origin of

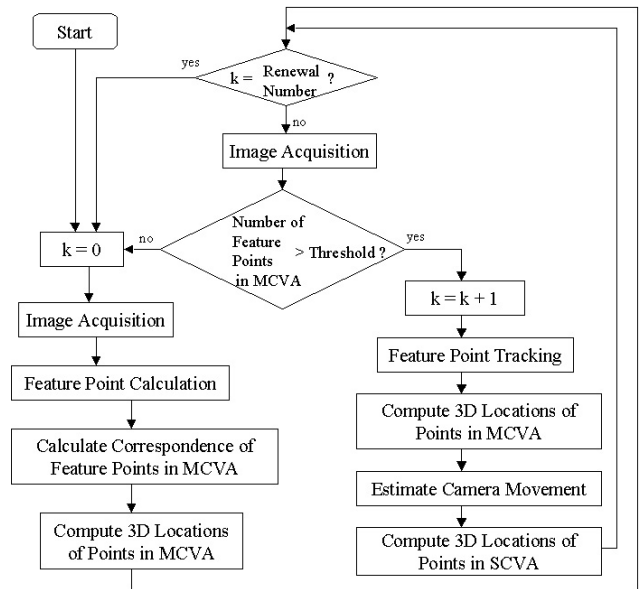


Fig. 2 : Flow Chart of the Proposed Technique

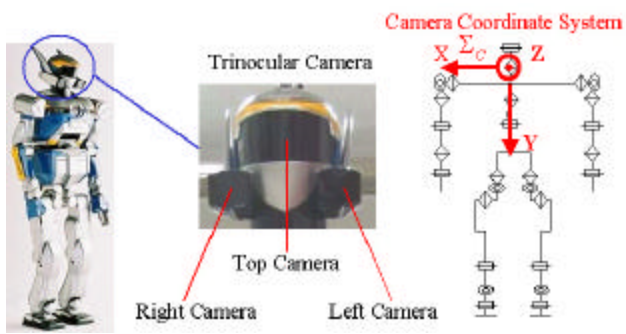


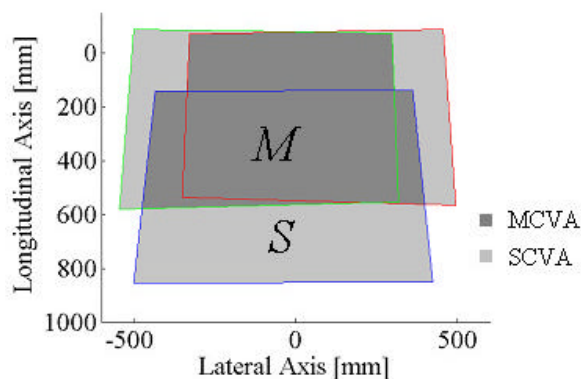
Fig. 3 : Vision System of HRP-2

the camera coordinate system is set at the neck joint.

3.1 Camera Configuration and the Field of View

Since humanoid robots possess the ability to perform both manipulation and navigation tasks, the cameras are set so that a wide area of view can be acquired to compute the information necessary for manipulation tasks. To be more precise, the area of MCVA is sufficiently large in the space where the humanoid's arm can move. Thus, high precision can be acquired for manipulation tasks, which usually requires higher precision than navigation tasks.

Fig. 4 shows the ratio of the whole field of view, and MCVA. Fig. 4(a) shows the computable areas 1500[mm]



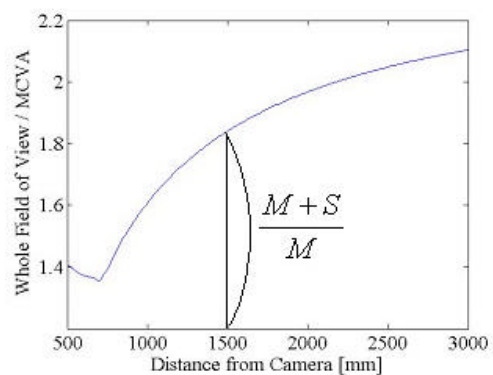
(a) Area of MCVA and SCVA for Z=1500[mm]

far from the camera. The light gray area represents SCVA, which is computable only by motion stereo. The dark gray area represents MCVA, which is computable by both motion stereo and stereo vision. We will define the area of MCVA as M and SCVA as S . Hybrid Motion Stereo is capable of computing both MCVA and SCVA, while stereo vision can only compute MCVA. Therefore, using Hybrid Motion Stereo, the computable area rises to $(M + S)/M$ times compared to stereo vision.

The size of the areas, M and S depends on the distance from the camera. Fig. 4(b) shows the relationship between the distance from the camera and the proportion of the whole field of view to MCVA, in other words, $(M + S)/M$. The graph states the effectivity of Hybrid Motion Stereo. Hybrid Motion Stereo is effective throughout the space, since the computable area increases by about 140% to 210% compared to stereo vision.

3.2 Comparison of Stereo with Motion Stereo

To evaluate the precision of computation by motion stereo, the authors have computed the feature points in MCVA by both stereo vision and motion stereo. The environment has been composed with 3 boxes with



(b) Relationship Between the Distance from the Camera and the Proportion of the Whole Field of View to MCVA

Fig. 4 : Proportion of MCVA to the Whole Field of View

checkerboard patterns on each face. The boxes are placed approximately 1 meter from the robot. The images of each camera are presented in Fig. 5. The white points in Fig. 5 indicate the calculated feature points in the images.

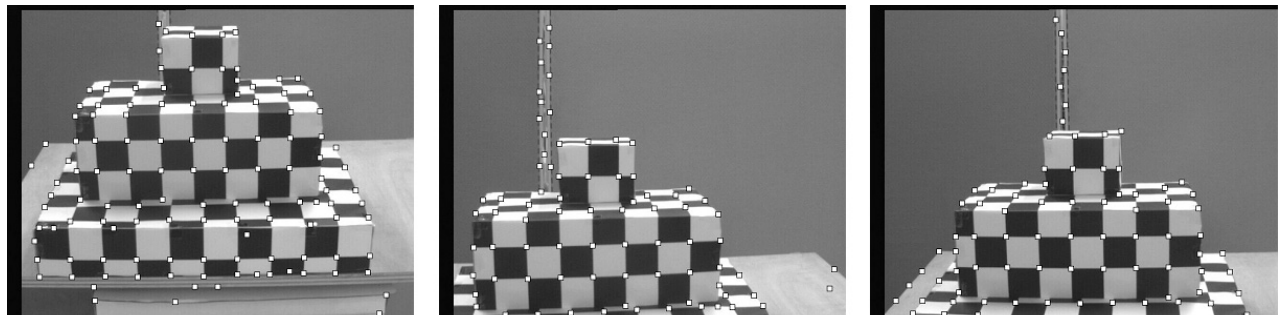
Calculation of feature points have been done using the method proposed by Shi and Tomasi[3]. Feature point tracking techniques using the pyramid implementation algorithm possesses high quality with a small amount of time[4][5]. The authors have implemented these techniques for the realization of Hybrid Motion Stereo. The computation time of the 3D positions of the feature points, neglecting the time cost for image acquisition, is approximately 0.1[s].

The computed absolute errors between stereo vision and motion stereo are shown in Fig. 6. The average errors

are presented in Table 1. From these results, it can be seen that the perspective errors are the maximum among the three. Considering that computation by stereo vision possesses considerably high precision, these errors can be assumed to be the errors in computation by motion stereo from the actual position of the objects. Although these errors cannot be tolerated for use in performing tasks such as manipulation and navigation, they are substantial for

	Absolute Average Error [mm]
Lateral Axis	41.7
Longitudinal Axis	64.8
Perspective Axis	105.9

Table 1 : Absolute Average Errors Between Stereo Vision and Motion Stereo

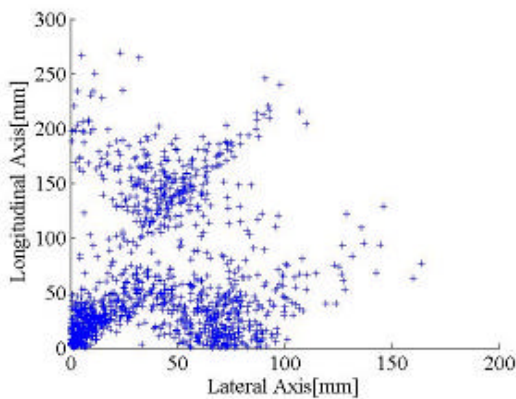


(a) Top Camera

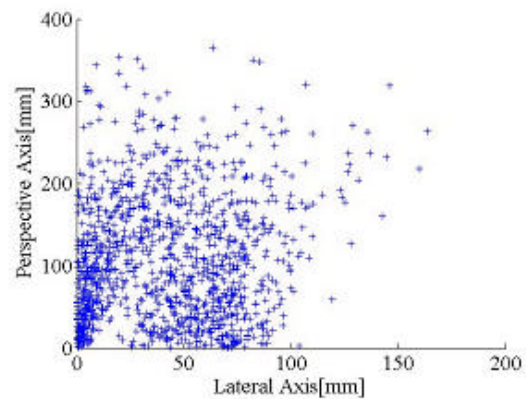
(b) Right Camera

(c) Left Camera

Fig. 5 : Images of Each Camera



(a) Lateral and Longitudinal Errors



(b) Lateral and Perspective Errors

Fig. 6 : Absolute Errors in Computation by Stereo Vision and Motion Stereo

acquiring the approximate locations of obstacles which come into sight.

Conclusion

In this paper, a wide-area recognition technique for mobile robots has been proposed using Hybrid Motion Stereo. By denoting the positioning of computation by motion stereo, the authors have presented applications in which Hybrid Motion Stereo can be used. The comparisons of the results by stereo vision and motion stereo indicates the effectivity of the proposed technique to various applications. The computation time proves to be substantial for real-time control.

Future works involve means of reducing the errors by motion stereo for advanced applications. Comparison of the results with the priors can help rectify the errors induced from mistracked feature points. For example, comparison of the results between several sequential frames and selecting the most suitable may reject miscomputed results. However, a method to select the most suitable result will be necessary. Considerations of rotational motions of the cameras must be done in order to develop the method into a more sophisticated technique. Here, a strategy to detect 4 immobile points, which cannot be performed by using the median, will be required. Detection of moving objects in SCVA and estimation of their movements will then be called into account after the precision of computation by motion stereo has been raised.

Acknowledgment

The authors would like to thank Prof. Yasushi Mae at Fukui University for providing valuable advices in the realization of the proposed technique. This work was supported by MEXT under Grant-in-Aid for Creative Scientific Research (Project No. 13GS0018).

References

- [1] K. Sakata, K. Inoue, T. Takubo, A. Arai, Y. Mae, "Proposal of Wheelchair Support System Using Humanoid Robots for Creating SSR Society," Int. Symposium on Systems & Human Science – For Safety, Security, and Dependability, pp. 53-58, 2003.
- [2] Y. Mae, N. Sasao, Y. Sakaguchi, K. Inoue, T. Arai, "Head Detection and Tracking for Monitoring Human Behaviors," Int. Symposium on Systems & Human Science – For Safety, Security, and Dependability, pp. 239-244, 2003.
- [3] J. Shi, C. Tomasi, "Good Features to Track," In Proc. of the IEEE Conference on Computer Vision and Pattern Recognition (CVPR), pp. 593-600, 1994.
- [4] J. Bouguet, "Pyramidal Implementation of the Lucas Kanade Feature Tracker Description of the algorithm," Intel Corporation, Microprocessor Research Labs. OpenCV Documents, 1999.
- [5] B. D. Lucas, T. Kanade, "An Iterative Image Registration Technique with an Application to Stereo Vision," In Proc. of Image Understanding Workshop, pp. 121-130, 1981.

Title: Human Modeling of Residents' Response in Nuclear Disaster

Author1: Tatsuya Shimizu

Address: 2-11-16, Yayoi, Bunkyo-Ku, Tokyo, 113-0033, Japan

Phone&Fax: +81-3-5841-8923(phone& fax)

Email: shimizu@cse.k.u-tokyo.ac.jp

Affiliation: Institute of Environmental Studies, the University of Tokyo, Japan

Author2: Taro Kanno

Address: 2-5-1, Atago, Minato-Ku, Tokyo, 105-6218, Japan

Phone&Fax: +81-3-6402-7578(fax), +81-3-5404-2893 (phone)

Email: kanno@diras.q.t.u-tokyo.ac.jp

Affiliation: Research Institute of Science and Technology for Society, Japan

Author3: Kazuo Furuta

Address: 7-3-1, Hongo, Bunkyo-Ku, Tokyo, 113-8656, Japan

Phone&Fax: +81-3-5841-6965(phone), +81-3-5841-8628(fax)

Email: furuta@q.t.u-tokyo.ac.jp

Affiliation: Department of Quantum Engineering and Systems Science, the University of Tokyo, Japan

Topic: Human and organizational behavior and errors

Human Modeling of Residents' Response in Nuclear Disaster

Tatsuya Shimizu*, Taro Kanno**, and Kazuo Furuta***

* Institute of Environmental Studies, the University of Tokyo, Japan

** Research Institute of Science and Technology for Society, Japan

***Department of Quantum Engineering and Systems Science, the University of Tokyo, Japan

Abstract

This research presents a human model of residents in a nuclear disaster, focusing on resident's decision-making process of several actions between receipts of information and real actions. The model uses probabilistic reasoning with a Bayesian network in situation assessment. Resident's action is determined by the balance between the awareness of the need to evacuate, which is derived from the probabilistic reasoning, and mental barriers to evacuate. We developed a simulation system of residents' behavior based on the model, and we carried out some test simulations. We confirmed that this model matches the qualitative features from our previous study and can incorporate various factors. The final aim of this study is to integrate the simulation system into a Multi-Agent SimulaTor of Emergency Response in nuclear Disaster (MASTERD) that considers various factors of disasters such as disaster phenomena, organizational activities, and resident behavior. The simulator of this study provides information on residents to the integrated simulation.

1: Introduction

Since the disastrous nuclear accident in JCO (1999), nuclear disaster preparedness plan has been improved rapidly in Japan. Though all the reforms were based on the lessons from the accident, it is difficult to understand and

assess how this new system will function in an actual emergency. In order to understand and assess the entire performance of emergency response and preparedness, lots of factors including not only accident phenomena but also human behaviors such as evacuation, communication, and coordination among different organizations, should be considered. Among them, efficiency and effectiveness in evacuation is important in particular, because in a nuclear disaster, 1) disaster information cannot be perceived directly by residents, 2) no damages on physical infrastructures will be caused, and 3) the most serious threat is the exposure of residents to radiation. One of the important factors in designing evacuation scheme is human behavior in an emergency, and many works have been done on resident model of evacuation. Most of them, however, did not deal with a decision-making process of a resident in a disaster. This research aims to construct a simulation model of resident's behavior in a nuclear disaster, focusing on resident's decision-making of several actions between receipts of information and real actions, and to simulate human behaviors under various settings.

In the next section, we introduce the qualitative model of resident behavior in nuclear disaster. In Section 3, we explain the architecture of our simulation system. In Section 4, the details of the implementation of the model are described. In Section 5, some results of a test simulation are shown and discussion is given, then conclusion is given in Section 6.

2: A Qualitative Model of Resident Behavior in Nuclear Disaster

In the previous study, we developed a qualitative model of resident behavior in nuclear disasters from a case analysis of past disasters [1]. This model is based on the conventional Stimulus-Organism-Response model of a human information processor, which consists of three steps in behaving: information input, situation judgment, and action execution. Figure 1 shows the outline of the model. The step of input includes the process of obtaining relevant information, judgment of trustworthiness of the information, and comprehending the contents. The next step includes recognition of danger, fear, and so on. The final step includes decision of an action and its execution. Probable actions that residents in an emergency will take are classified into two types: communication behavior, and evacuation behavior. Communication behavior includes active communications such as telling information to neighbors, making inquiries to the public office. Evacuative behavior includes evacuation and sheltering.

We also extracted the influencing factors of behavior in each step of the SO-R model from the case analysis. Table 1 shows the influencing factors confirmed in this work. Qualitative features of influence then have been studied. The following are some examples.

- Direct instruction of evacuation is more likely to arouse recognition of urgency.
- Seeing evacuation of others is likely to induce evacuation action.
- When the number of information media is few, trustworthiness of the received information is low.
- Information obtained through a private channel is more likely to be trusted than that obtained through a public channel.
- A family of a small size is likely to get less information.

- Elderly people show more reactive behavior in evacuation.

We developed a simulation model of resident behavior based on these features.

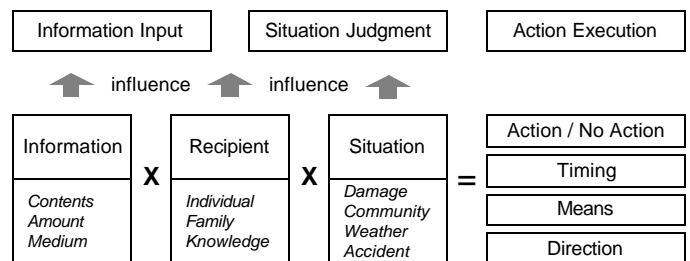


Figure 1 S-O-R model of resident behavior

Attribute of Information	Contents (Inclusion of instruction etc.)
	Amount (Number and Frequency)
	Medium (Source and Channel)
Attribute of Recipient	Individual (Sex and Age, etc.)
	Family (Family size, etc.)
	Knowledge (Past experience, etc.)
Attribute of Situation	Damage(Danger in the neighborhood)
	Community (Solidarity)
	Weather (Weather, Wind condition)
	Accident (Time, Facility etc.)

Table 1 Influencing factor of evacuation behavior

3: PRIMA

We implemented the model and developed a simulation system of resident behavior in nuclear disasters (PRIMA: Probabilistic Reasoning In Making A decision). We developed PRIMA as a distributed object based on CORBA (Common Object Request Broker Architecture), aiming to install it as a component of an integrated simulation system of emergency response we are now developing (Multi-Agent SimulaTor of Emergency Response in nuclear Disaster: MASTERD) [2]. Figure 2 shows the architecture of PRIMA. PRIMA consists of four modules;

Scenario Manager Information Control Center, Inference module and a Viewer.

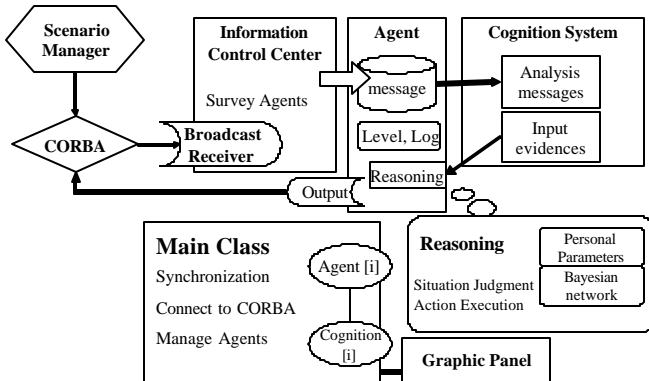


Figure 2 System Architecture of PRIMA

3.1: Scenario Manager

This module transmits input messages to PRIMA. The input message corresponds to an announcement from local governments or mass media by various media such as TVs, radios, and loudspeaker vans. It loads a scenario file and sends to the Information Control Center of PRIMA. Figure 3 shows an example of the input message. PRIMA was designed to receive input messages also from other modules of MASTERD in an integrated simulation.

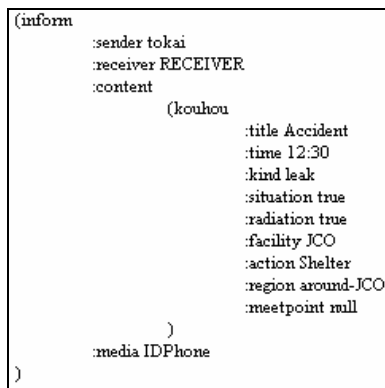


Figure 3 Example of messages from Scenario Manager

3.2: Information Control Center

Having Received messages from the Scenario Manager, the Information Control Center searches agents who can

receive the message by examining attention level and whether he/she is able to receive it by the media that broadcasts it, and deliver the message to the agent who fulfills the conditions. This module corresponds to the Information Input step of the Resident model.

3.3: Inference Module

A received message is parsed and it changes the values of corresponding nodes (evidence nodes) of the Bayesian network of situation judgment. Then, the values of all the nodes are updated and a behavior is determined. We will explain how to determine the behavior next.

3.4: Viewer

We developed a viewer to visualize the state of each resident. Figure 4 shows an overview of the viewer. Each resident is expressed as a circle. The color of the upper half of the circle represents an evacuation behavior; green means no action, orange means sheltering, and red means evacuation. The lower left is a flag for acquisition of messages. Red means success and blue means failure to get information (increase attention level). The lower right is a flag for communication behavior. Pink is for communication between family members, and green is for inquiries to the public office.

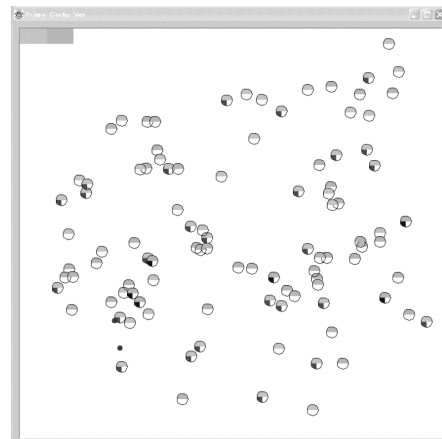


Figure 4 Viewer of PRIMA

reasoning with uncertain knowledge [3].

4: Implementation of the Resident Model

In this section, we will explain a simulation model of residents based on the conceptual model explained in Section 2.

4.1: Information Input

We used attention levels for filtering broadcasted information in order to model the information input step of the S-O-R model. When one resident get a chance to get information, whether he/she can get the information depends on his/her attention level: he/she receives only the information above the threshold to receive it. The attention level depends on one's past experience of similar disaster and awareness, and can change depending on the situations. Table 2 shows when the attention level changes.

Resulting from the increase of the attention level, one comes to be able to get information from other people or some media.

	Conditions to change attention level
Increase	Fail to recognize information
	Have not decided his/her behavior yet
	Get message from his/her family
Decrease	Know end of an accident
	Judge not to act.
	Finish evacuative action and telling information to his/her family

Table 2 Changes of Attention Level

4.2: Situation Judgment

We use probabilistic reasoning with a Bayesian network in resident's situation assessment. Bayesian network is a probability-based method and suits for representing and

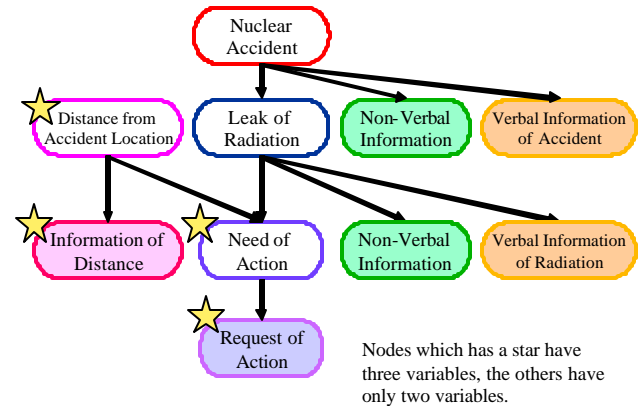


Figure 5 Bayesian network of situation judgment

4.2.1 Architecture of Network. Figure 5 shows the network of situation-awareness in a nuclear disaster. The network consists of situation nodes and various information nodes. Situation nodes ("Nuclear Accident", "Leak of Radiation", "Distance from Accident Location", and "Need of Action") express disaster situation that resident believes. Furthermore, various information nodes are connected to situation nodes as their child nodes. Information nodes are also leaf nodes of the network. The architecture of the network comes from qualitative causal association of situation awareness. Each child node has a conditional probability matrix of their parent nodes. Without any evidence and information, values of variables are calculated from their parent node by these conditional probability matrixes.

4.2.2 Input information. Ash nodes in Figure 5 are information nodes. Information nodes consist of not only information from mass media and public offices, but also a surrounding situation which reminds residents the outbreak of an accident and so on. Moreover, when he/she knows location of the accident, he/she reasons the distance from it and the value of the evidence node (Distance from Accident Location) is entered to the belief network. . When a resident

gets messages, evidence value is entered to each related node and the probability of each node is calculated by bottom-up and top-down reasoning with the conditional probability matrix. To represent that trustworthiness of the received information is low because of the number of information media is small, we used evidences that have phased value. The first information cannot increase the value to 100% (such as 90%), repetitious information can make the value 100%.

4.2.3 Output Results. A result of “Need of Action” means a belief of a resident which action should take. The belief probability of this node is transmitted to the next step to be corrected by the action barrier.

4.3: Action Execution

Evacuation behavior involves three actions: evacuate, shelter, and no-action. Based on the value of the node “Need of Action” of the Bayesian network, the next action is determined. Several factors influence the final decision of action. The final decision whether he/she moves into action depends on the corrected value of “Need of Action” by the coefficient.

Communication behavior has two types of action: tell and request information. We considered only communication between family members and inquiries to the public office as communication behavior at this stage. When a resident’s attention level is substantially high and he/she has full confidence in his/her situation judgment, then he/she comes to make contact with his/her family and tell his/her own information. Recipient treats this message as hearsay. When a resident has not full confidence in his situation judgment in spite of high attention level, he comes to make an inquiry at the public office or his/her family. If we consider communication with someone outside the family that has not been implemented at this stage, a small world network of residents should be used.

5: Experiment

We carried out a test simulation to validate the resident model. We made an input message set based on the actual announcements made in the JCO accident. The target of the simulation was 200 residents in 1km from the facility.

5.1: Result and Discussion

From the simulation, we observed that the values of the network of each resident gradually changed as he/she acquired information and a communication behavior or an evacuation behavior was determined. Figure 6 shows an example of transition of probability in the agent. Most of the residents followed the order of evacuation. On the other hand, some residents had already made a decision to evacuate or shelter before receiving the order and some had not evacuated because of the delay of information acquisition or the effects of action barriers. These results match those of post-disaster questionnaire surveys [4, 5] In addition, it was observed that an action and its timing depended on personal parameters. From now on, it is necessary to fine-tune conditional probability matrixes and initial probabilities of the network and improve the structure of the network to better match the results of the questionnaire surveys.

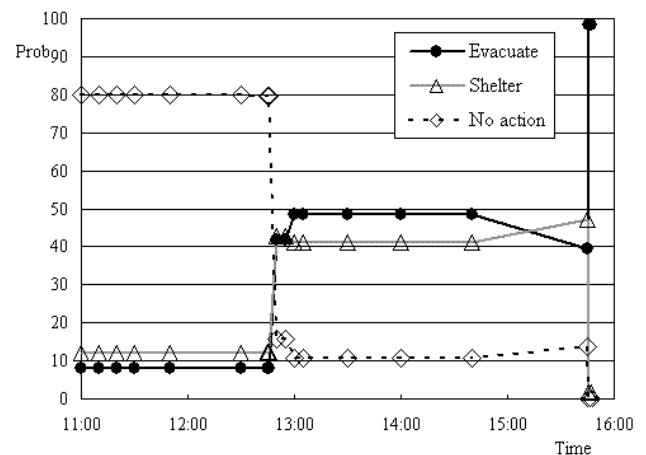


Figure 6 Transition of the probability of the agent

6: Conclusion

We developed a human model of residents in a nuclear disaster, focusing on resident's decision-making process of several actions between receipts of information and real actions. The model uses probabilistic reasoning with a Bayesian network in situation assessment. Resident's action is determined by the balance between the awareness of the need to evacuate, which is derived from the probabilistic reasoning, and mental barriers to evacuate.

We developed a simulation system of resident behavior based on the model, and we carried out some test simulations. We confirmed that this model matches the qualitative features from our previous study and can incorporate various factors. The simulation system of this study was developed as a component of an integrated simulation of emergency response in nuclear disasters (MASTERD). In the next stage, we plan to carry out an integrated simulation that considers various factors of disasters including disaster phenomena, organizational activities, and resident behavior.

References

- 1) K. Furuta, T. Kanno, E. Yagi, and Y. Shuto, "Socio-Technological Study for Establishing Comprehensive Nuclear Safety System, Proc. 11th. Int'l Conf. Nuclear Engineering (ICONE11), 2003.
- 2) T. Kanno, Y. Morimoto, and K. Furuta, "Multi-agent Simulation System of Emergency Response in Nuclear Disaster", Proc. 7th. Int'l Conf. Probabilistic Safety Assessment and Management (PSAM7), 2004, pp. 389-394.
- 3) Judea Pearl, 1998, Probabilistic Reasoning in Intelligent Systems: Networks of Plausible Inference.
- 4) M. Umemoto, K. Kobayashi, T. Ishigami, and M. Watanabe, "The Inhabitants' Receiving Disaster

Information and Their Reaction at the JCO Criticality Accident in Tokai-mura", Proc. Symp. Inst. Social Safety Science, 2000, Vol.10, pp 113-116 (in Japanese).

- 5) Hiroi O., et al., 2001, The Information Dissemination and Behaviors of the Inhabitants in the Criticality Accident of JCO Co's Uranium Processing Facility in 1999, The Research bulletin of the Institute of Socio-Information and Communication Studies, the University of Tokyo, 15, pp. 237-406 (in Japanese).

Wheelchair User Support System Using Humanoid Robots
- User Interface Using Smart Handy Device -

Kotaro Sakata *, Tomohito Takubo *, Shun Nishide *, Kenji Inoue *, Tatsuo Arai*

* Division of Systems and Applied Informatics, Department of Systems Innovation,
Graduate School of Engineering Science, Osaka University
1-3 Machikaneyama, Toyonaka, Osaka, 560-8531, JAPAN
Tel: +81-6-6850-6367, FAX: +81-6-6850-6341
{sakata, takubo, nishide}@arai-lab.sys.es.osaka-u.ac.jp
{inoue, arai}@sys.es.osaka-u.ac.jp

TOPIC: Robotics

Wheelchair User Support System Using Humanoid Robots

- User Interface Using Smart Handy Device -

Abstract

For creating safe, secure and reliable (SSR) society, a concept of wheelchair user support system using humanoid robots has been proposed; humanoid robots exist in our environment and provide both of mobility and manipulation supports for the wheelchair users. This is because wheelchair users arms cannot reach for wide space. We apply a real life-size humanoid robot HRP-2 to support for wheelchair users. The main characteristic of this system is that existing wheelchairs don't need any modification.

It is essential for this system to have an interactive human-robot interface to execute various tasks easily. We developed the user interface using handy device for wheelchair user support system. Wheelchair users give instructions to humanoid robots using GUI (Graphic User Interface) on their handy devices. 3 parts constitute their display; menu window, view window and operation window. Users select the task on menu window, get the environmental information from view window, and instruct to the system on operation window.

This paper discusses the concept of this interface and describes a fetch task execution using this interface as an operation example. This is because fetch tasks will happen quite often in the interactions between robots and humans in daily life.

1. Introduction

Since the kinematical structure of humanoid robots is similar to that of humans, humanoid robots are expected to work instead of humans in the same environment. In

recent years, as the technologies of humanoid robots have progressed, some applications of humanoid robots are being investigated. As the outstanding attempt, Ministry of Economy, Trade and Industry of Japan has promoted the Humanoid Robotics Project (HRP) [1] since 1998 Japanese fiscal year (JFY) for five years. In this project, some applications of humanoid robots – operating industrial vehicles [2], maintenance tasks of industrial plants [3], cooperative works by a human and a humanoid robot [4], and so on – have been developed.

By the way, it is the highest priority issue to create safe, secure and reliable (SSR) society in modern society. For the purpose of creating SSR society, we have proposed an integrated system of monitoring and support system [5-6]. The monitoring system finds the sign of problem quickly in the environment by watching wide area in detail using many fixed or moving cameras. The support system prevents the danger from occurring or copes with the occurring danger rapidly, thus reducing damage to the minimum; in the present project, humanoid robots are used as supporting devices. This is because humanoid robots can move in our environment and use some tools and machines as humans do. In this way, this integrated system can offer safe environment to us, and we feel security and comfort in the environment. Our project aims at conceptual design of such monitoring and support system and making a prototype of the system.

It is important for us to focus on everyone including elderly people and handicapped persons, for creating SSR society. Especially, elderly people and handicapped persons require the life support. Taking these points into account, we focus on the wheelchair users. We have proposed the wheelchair user support system using

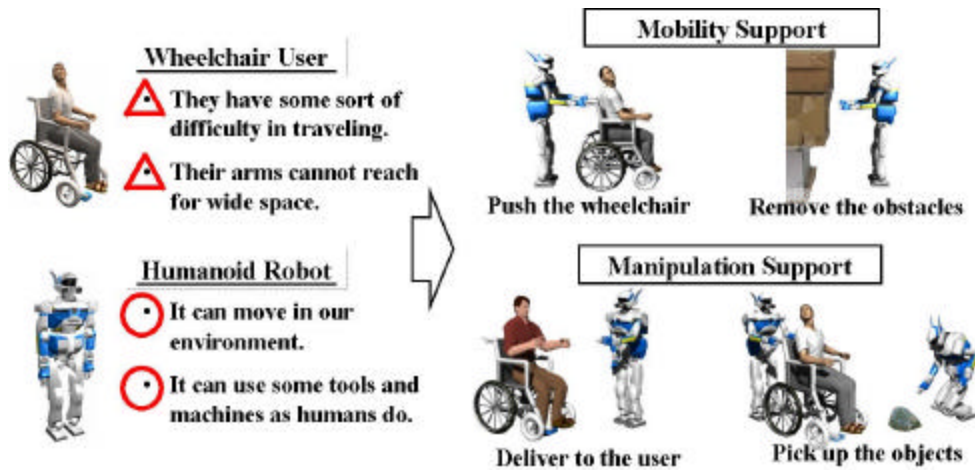


Fig.1. Concept of wheelchair user support by humanoid robots.

humanoid robots as concrete application of humanoid robots [7] (Fig. 1). The remarkable characteristic of this proposal system is to provide the total support of mobility and manipulation for wheelchair users.

When we study human-robot coexisting system, it is important for us to have human-centered view. This is why, in this project, we have focused wheelchair vibrations on mobility support [8], and evaluated the influence of pick and place motion of humanoid robot to human sense of security [9].

Furthermore, this support system needs human-robot interface, because a humanoid robot is not completely autonomous. In this study, we developed the user interface using handy device.

The rest of this paper is organized as follows; Section 2 describes the related work on user interfaces for robots. Section 3 clarifies the architecture of the user interface we developed. Finally, we show the operation example on fetch task in section 4.

2. Related Work

There are some researches on user interfaces for coexisting robots. Nishiyama et al. [10] developed a user

interface for humanoid service robot system. The operator wears the HMD, and controls the joystick to move the humanoid robot. At variance with this research, we do not intend to use an exclusive use device such as the HMD and the joystick for the user interface. Lundberg et al. [11] created a robot system which has user interface using PDA in order to examine the possibilities to aid soldier or rescue workers with transportation and exploration tasks. This interface performs mainly for drive of robot. But we want to develop user interface for both mobility and manipulation support. Aizawa et al. [12-13] proposed an intelligent robot system MARY (Mobile Assistant Robot for You) which has a human-machine interface using GUI on a fixed touch-sensitive panel in order to execute various tasks. We developed the user interface using handy device so that wheelchair users can use the support system by any time.

3. User Interface

Basic concepts of wheelchair user support system using humanoid robots are as follows:

- A robot performs both mobility and manipulation support.

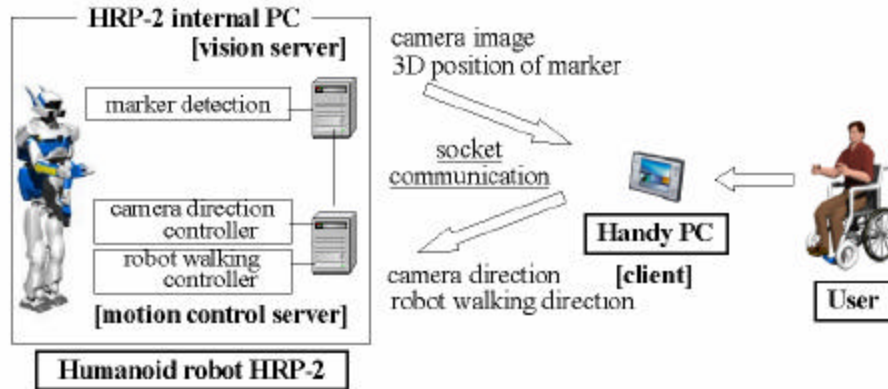


Fig.2. System configuration.

- A robot is not completely autonomous.
 - An existing wheelchair does not need any modification.
 - This system does not need any exclusive use device.
- According to these concepts, we use handy PC for the user interface. Users communicate with robots through the intermediary of GUI on handy PC.

3.1 System Configuration

Fig.2 shows an overview of this user interface using handy device. We selected the touch screen as the interaction media during the design phase. In addition, we have chosen Visual C++ to create the GUI. The combination of touch screen and small size means some kind of PDA, we used a SONY VAIO type U. The VAIO type U is 108[mm] height, 167[mm] width and 550[g] weight, and has touch-sensitive LCD panel (800*600[pixel]) and runs the Microsoft Windows XP operating system. We use a socket communication with TCP (Transmission Control Protocol) for communication between humanoid robot and handy device.

3.2 Humanoid Robot HRP-2

In this support system, the humanoid robot HRP-2 [14] is used as life supporting robot. The snapshots of this humanoid robot HRP-2 are shown in Fig. 3. This robot is the final version of humanoid robotics platform of the Humanoid Robotics Project (HRP), and it is 1539[mm] height, 621[mm] width, 58.0[kg] weight, 30 degrees of freedom (D.O.F.) includes 2 D.O.F. for waist, contains computers and batteries in its body. In addition, this robot has a stereo vision system composed of 3-eye CCD cameras and 2D.O.F. for its head that corresponds to pan/tilt. Two horizontal cameras are separated by 120[mm], and the third camera is 60[mm] upper than them.

3.3 GUI Design

In this system, the GUI on handy device has three parts; menu window, view window and operation window. Fig.4 shows the example of this screen snapshot.

(1) Menu Window

This window has the buttons for each tasks of mobility and manipulation support. In response to the selected button, view window and operation window show the corresponding contents.

(2) View Window

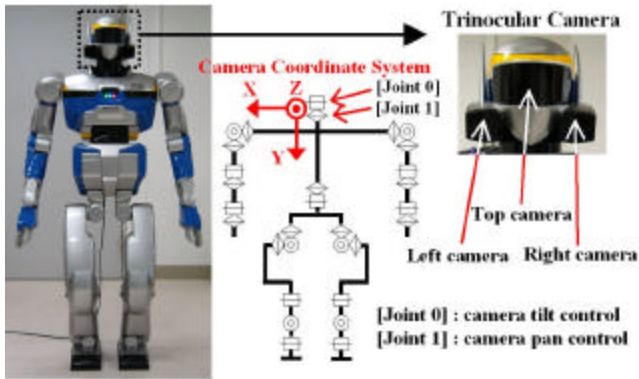


Fig.3. Humanoid robot HRP-2 that has 3-eye CCD stereo camera.

This window has two domains. The left domain shows the reduced-size (320*243[pixel]) image of the humanoid robot camera image (640*486[pixel]) in real time. This camera is pan/tilt controllable, by instructing on operation window. If the marker of the object is detected, the right domain shows the x-y window coordinate and the X-Y-Z camera coordinate of the marker.

(3) Operation Window

When users work with this window, they can instruct to control pan/tilt of humanoid robot camera, drive a humanoid robot and so on. Fig.5 shows the operation window for pan/tilt camera control and manual drive of robot.

In addition to above-mentioned windows, if necessary, dialog boxes display in order to confirm the validity of the process.

3.4 Three Dimensional Visual Processing

A position computation function is necessary for humanoid robots to grasp and carry an object. A marker has been placed to locate the position of the grasping point. Using the function in OpenCV [15], which detects a 2*2 checker board, the first camera determines the image coordinates of the marker. The coordinates are projected

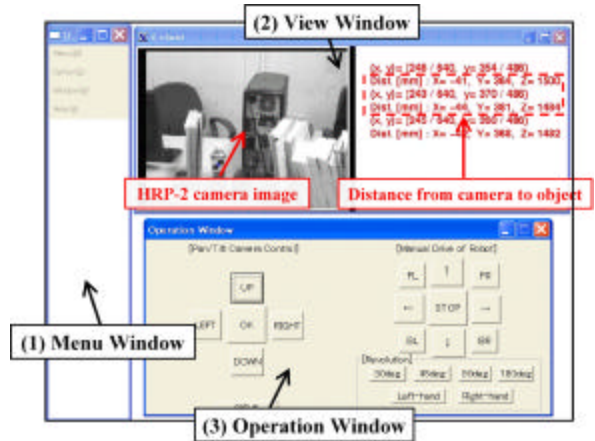


Fig.4. Handy device screen.

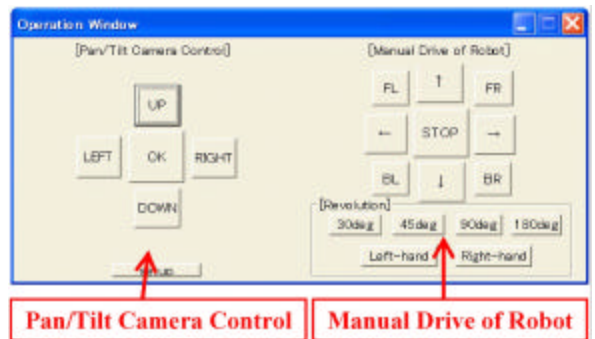
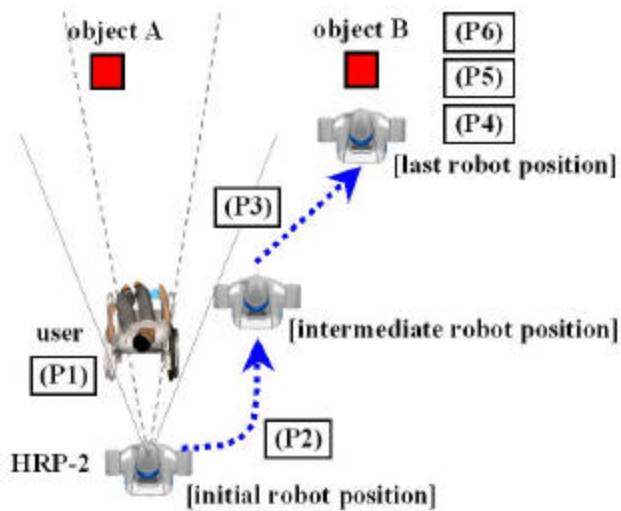


Fig.5. Operation window.

onto the second camera image creating the epipolar line, searching the coordinates of the marker above. The coordinates of the first and second camera are then projected onto the third camera to avoid mismatching. The image coordinates create 6 constraints to the 3 unknown three dimensional coordinates in real space. Using Least Square Method, the errors are minimized recovering the 3 coordinates. The grasping point was calculated within 5[mm] error using this algorithm.

4. Operation Examples

In this section, we describe the working of this user interface according to the following scenario. This scenario takes fetch tasks for instance. The fetch task



- (P1) Select the task
- (P2) Move next to the user
- (P3) Move to the front of the object
- (P4) Control the camera direction
- (P5) Measure the distance to the object
- (P6) Grasp the object

Fig.6. Task execution procedures (over view).

means that a humanoid robot goes and gets an object that the user specifies. Fig.6 shows the procedures of fetch task execution.

(P1) Select the task

The user selects the fetch task button on menu window. In response to this button, operation window shows the corresponding contents.

(P2) Move next to the user

The humanoid robot moves next to the user, because the system prevents the user making dead zone of the humanoid camera image and the humanoid robot conflicting the user on (P3).

(P3) Move to the front of the object

If the arms of the humanoid robot cannot reach the object, it moves to the front of the object.

(P4) Control the camera direction

The user controls the camera direction so that the object comes into view.

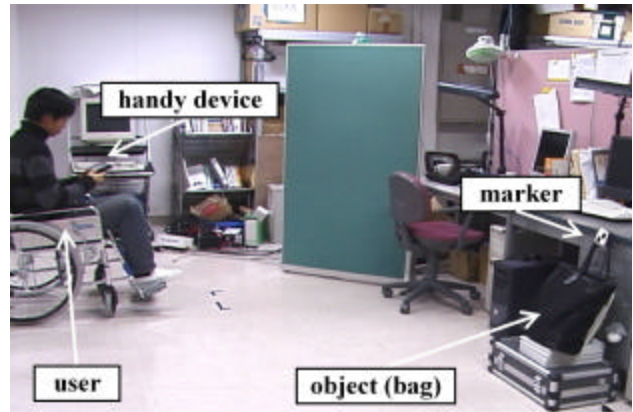


Fig.7. Experimental condition.

(P5) Measure the distance to an object

If the vision system detects the marker of the object, it measures the distance from the camera to the object.

(P6) Grasp the object

Using the results of the position computation (P5), the humanoid robot grasps the object.

We demonstrated the working of this system according to the above (P1)-(P5). The experimental condition is shown in Fig.7. The user desires the humanoid robot to go and get the bag that has the marker. Fig.8 shows the snapshots of this experiment. Fig.9 shows the snapshots of view window on handy device screen. From Fig.9, it is ascertained that the camera detected the marker and calculated the position of it.

5. Conclusion

This paper discussed the architecture of the user interface for wheelchair user support system using humanoid robots. In this interface, wheelchair users give instructions to humanoid robots using GUI on their handy devices. Then we described the operation examples, taking the fetch task as an example.

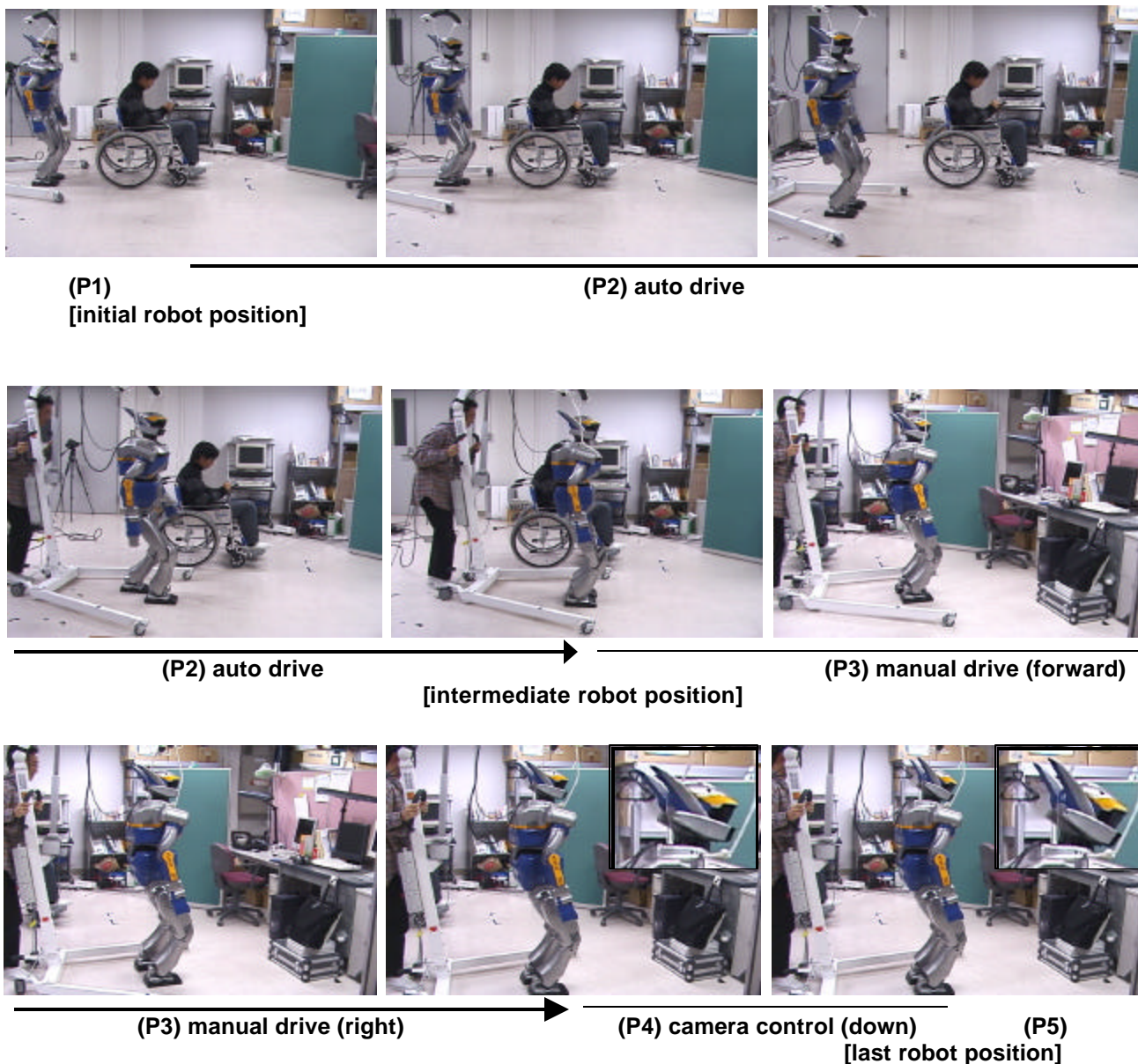


Fig.8. Snapshots of operation example on fetch task.

In future work, we will take usability a step further and evaluate the task execution using this interface.

Acknowledgment

This research was supported by the Japan Society for the Promotion of Science under Grant-in-Aid for Creative

Scientific Research (Project No. 13GS0018). The authors would like to express sincere thanks to them for financial supports.

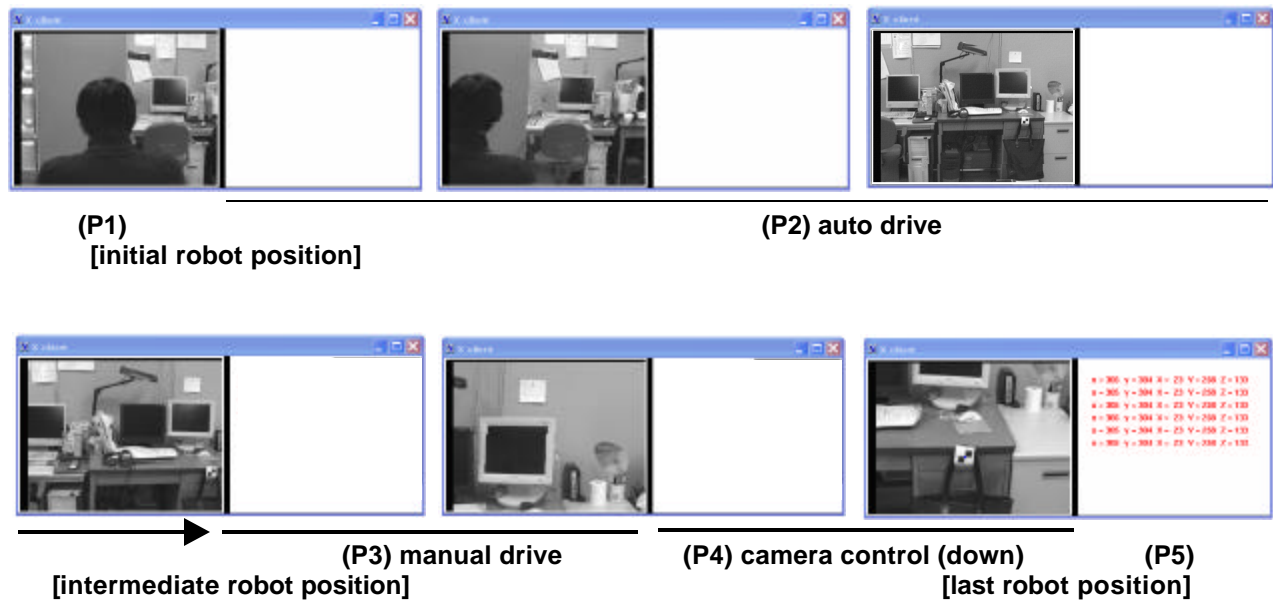


Fig.9. Snapshots of view window on handy device screen.

References

- [1] H. Inoue et al., "HRP: Humanoid Robotics Project of METI," Proc. of the First IEEE/RAS Int. Conf. on Humanoid Robots (Humanoids 2000), 2000.
- [2] H. Hasunuma et al., "A Tele-operated Humanoid Robot Drives a Backhoe," Proc. of IEEE Int. Conf. on Robotics and Automation (ICRA 2003), pp.2998-3004, 2003.
- [3] N. Kawauchi et al., "A Plant Maintenance Humanoid Robot System," Proc. of IEEE Int. Conf. on Robotics and Automation (ICRA 2003), pp.2973-2978, 2003.
- [4] K. Yokoyama et al., "Cooperative Works by a Human and a Humanoid Robot," Proc. of IEEE Int. Conf. on Robotics and Automation (ICRA 2003), pp.2985-2991, 2003.
- [5] K. Inoue et al., "Fundamental Study on Human Support System Using Humanoid Robots for Creating SSR Society," Proc. of SICE Annual Conference 2002 (SICE 2002), 2002.
- [6] K. Sakata et al.: "Human Support System Using Humanoid Robots for Safe, Secure and Reliable Society: Feasibility Study on Robotics Application for Safety and Security", Proc. of the 20th Annual Conference of the Robotics Society of Japan (RSJ 2002), 2002 (in Japanese).
- [7] K. Sakata et al.: "Proposal of Wheelchair User Support System Using Humanoid Robots for Creating SSR society", Proc. of 1st International Symposium on Systems & Human Science -For Safety, Security, and Dependability- (SSR2003), pp.53-58, 2003.
- [8] K. Sakata et al.: "Wheelchair User Support System Using Humanoid Robots -System Concept and Experiments on Pushing Wheelchair-", Proc. of SICE Annual Conference 2004 (SICE2004), 2004.
- [9] K. Sakata et al., "Psychological Evaluation on Shape and Motions of Real Humanoid Robot," Proc. of the 2004 IEEE International Workshop on Robot and Human Interactive Communication (Ro-Man2004), 2004.

- [10] T. Nishiyama et al., "Development of User Interface for Humanoid Service Robot System," Proc. of IEEE Int. Conf. on Robotics and Automation (ICRA 2003), 2003.
- [11] C. Lundberg et al., "PDA interface for a field robot," Proc. of IEEE Int. Conf. on Intelligent Robots and Systems (IROS 2003), 2003.
- [12] S. Aizawa and K. Kosuge, "Life Support System - Mary-," Proc. of the 20th Annual Conference of the Robotics Society of Japan (RSJ 2002), 2002 (in Japanese).
- [13] S. Aizawa and K. Kosuge, "Life Support Robot System -MARY- 2nd Report: Multiple Task Execution," Proc. of the JSME ROBOMECH 2003 Conference (ROBOMECH 2003), 2003 (in Japanese).
- [14] K. Kaneko et al., "Humanoid Robot HRP-2," Proc. of IEEE Int. Conf. on Robotics and Automation (ICRA 2004), 2004.
- [15] <http://sourceforge.net/projects/opencvlibrary/>

Application on Ubiquitous Functions for Human Life

Kenichi Ohara†, Kohtaro Ohba*, Kim Bong Kuen*, Shigeoki Hirai,* Kazuo Tanie*

* Intelligent Systems Research Institute,

National Institute of Advanced Industrial Science and Technology (AIST).

Address: AIST Central2 1-1-1 Umezono, Tsukuba, Ibaraki, 305-8568, Japan

Telephone: +81-29-861-3494

FAX: +81-29-861-3493

E-mail: {k.ohba, bk.kim, s.hirai, tanie.k}@aist.go.jp

† University of Tsukuba, JAPAN

Address: 1-1-1 Tennodai, Tsukuba-shi Ibaraki-ken, 305-8577, Japan

Telephone.:+81-29-853-2111

E-mail: k-ohara@aist.go.jp

Topic:

Ubiquitous Computing, RFID Tag, Sensor-net, Home Security and Safety, Distributed System

Application on Ubiquitous Functions for Human Life

Abstract: In this paper, the concept of “Ubiquitous Functions” and the “Ubiquitous Functions Activate Module” are proposed to support the human living in the real human life environments.

Recently, the concept of ubiquitous acts one of the important factors on not only on the information science, but also on the robotics. Unfortunately the general criteria to treat these ubiquitous systems had not proposed yet.

At first, the concept of “Ubiquitous Functions” is proposed to treat the space distributed objects focusing on the function of the object itself. Secondly, “Ubiquitous Functions Activate Module” designed to realize the “Ubiquitous Functions” for the human life activities. Several applications for human life show the validity of our propose concept. Furthermore, the typical robots in the human life environments with the ubiquitous functions activate modules is discussed. Finally, we have successfully shown the effectiveness of the proposed scheme in several real environmental examples.

1. Introduction

Recently, the quality of life (QOL) is one of the important keyword in science technology, such as in the medical science, information science, and robotics. But the most of the difficulty for the QOL with robotics might be coursed by that the human life environment is quite complicated.

Up to now, a lot of robots which work with human as a proxy had been investigated. The current robot recognizes the environment with several types of sensor setups which was installed in the robot. And, the number of sensors could improve the recognition accuracy, but require complicated wired setup and more calculation costs. Because of these difficulties on the sensor setup, the QOL improvement had discussed to be hard work in the robotics societies.

On the other hand, there is one movement on the monitoring the human daily life with a lot of sensors in the human life environments. The sensors, which are distributed to the space, provide the human some efficient information and service for the human life,

such as health monitoring. Each of these sensors in the space has small functions. However, combination of these sensors could give us quite important information to achieve the high QOL.

In this paper, at first, the concept of “Ubiquitous Functions”[1], which includes the distributed sensors and actuators in the environments, is proposed to support the human and to obtain the high QOL. Secondly, the “Ubiquitous Functions Activate Module” is proposed, which is one of the key modules to realize the ubiquitous functions criteria. In other words, this “ubiquitous functions” is not only useful for human but also for robot, which is working for human support work in the real human life environments. Finally, we introduce some applications which use ubiquitous functions activate module.

2. Ubiquitous Functions

To discuss the functions in ubiquitous environments, a new concept to treat these ubiquitous modules/systems must be required.

The “affordance” concept is treated all substance objects as the informative active, and describes the relationship between objects in psychological manner. However, for the network based robotics, substance and non-substance itself is quite important. And the interactive relationship between objects is also important; which might be active or passive relationship.

In this section, we would like to propose the “Ubiquitous Functions” criteria, which is the conceptual criterion focused on the original functions of substance and non-substance objects, to make it clear the relation of ubiquitous network and substances; human, objects and space, which is based on the interactive relationship, i.e. functions.

2-1 What is Ubiquitous Functions?

In the human life, there are human, space, and object with some functions. Thus, “One” which has the function is defined, “Ubiquitous Functions”.

For example, desk and chair has several functions, such as reading and writing space for human in Fig.1 (b). Another function could be applicable on the desk and chair, such as for sleeping space as same as a bed. However this is not an original function, which the designer had initially implemented. These functions are basically passive functions, which means the functions never happened by themselves. In this sense, original passive function by designer is quite important factors as its functions.

In the opposite site, actuators might have active functions by itself in Fig.1 (a). However the body parts of the actuator might have passive functions. In this sense, substance active objects might have the active parts and passive parts, basically as shown in Fig.2 (a).

In a word, it is important work in "Ubiquitous

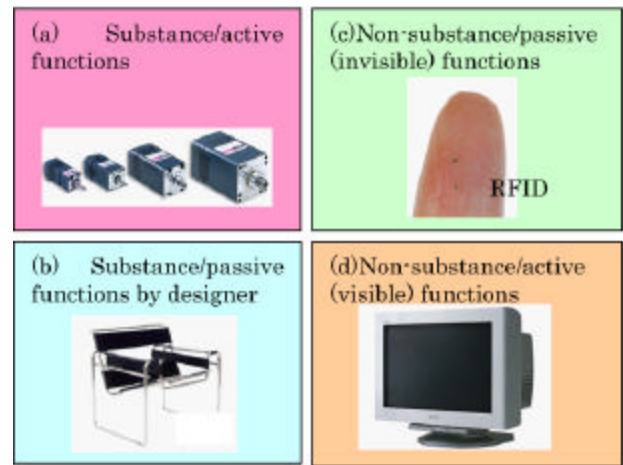


Fig.1 Classification of the functions

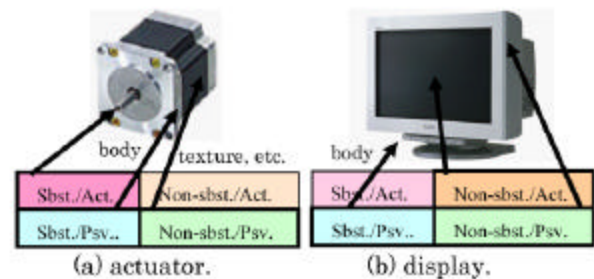


Fig.2 Basic functions of the objects

Functions" to analyze the function of the objects.

2-2 Functions on non-substance

In other site, non-substance information has also ubiquitous functions. For examples, the display could show the non-substance information with CG or text data. In the case of non-substance objects, active and passive is difficult to define. However we define the active and passive definition on non-substance as visible and invisible, respectively. Then, the display might be categorized in the non-substance active functions in Fig.1 (d). Here, the non-substance objects could have

substance parts, which might include the passive or active/passive functions as shown in Fig.2 (b). Also, the non-substance active objects could have the non-substance passive parts, such as the texture on the body.

As an example, let's discussed in the case of RFID, which is one of hot topics in the business field of physical distribution. The RFID could make the mobility of the non-substance information on the substance objects. RFID originally have only the passive non-substance functions in Fig.1(c). But once putting a RFID on an object, which has originally a passive substance function, the object could have two functions; the passive substance and the non-substance functions.

2-3 Example cases on Ubiquitous Functions

For example shown in Fig.3, in the case of a robot, robot have several ubiquitous functions parts, i.e. substance/active functions; actuators, substance/passive functions; body itself, non-substance/active functions; visible body texture and display, and non-substance/passive; sensors.

2-4 Function Design

For another example shown in Fig.4, the door itself has substance passive functions. But installing the activate module, such as a motor, the substance active function object; automatic door, could be obtained. To append other functions, the total design is quite important.

3. Ubiquitous Functions Activate Module

Recently, the research on Ubiquitous Computing is one of the hot topics in the information science. These

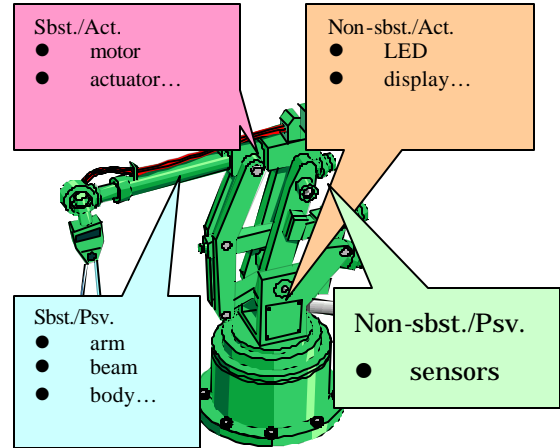


Fig.3 Example cases on Ubiquitous Functions

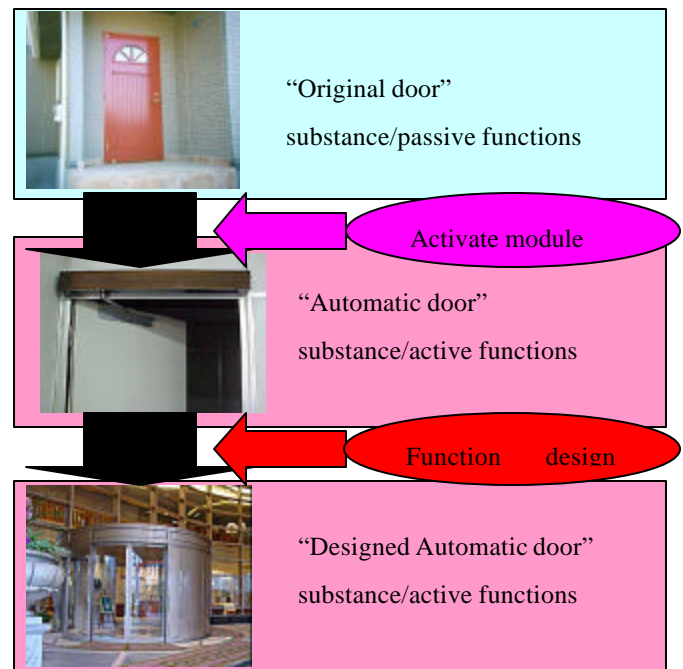


Fig.4 Functions change and design.

researches distribute a small computer to the space, then person can acquire information from anywhere at any time.

The typical types of the ubiquitous computing might be the RFID module and the sensor network module.

The comparison between each characteristics of each module is shown in Fig.5 and Table.1.

The RFID module has the following characteristics.

- Few Functions (Only transmission)
- Low power consumption
- Short communication distance

The sensor net module has the following features in one side.

- Input Functions
- Reception and Transmission functions
- Long communication distance
- High power consumption

Both the RFID and the sensor net modules have goodness and drawback for particular applications, i.e. the ubiquitous functions for human life. The following functions are supposed to be necessary for the ubiquitous functions for human and robot.

- Input/Output Functions
- Low power consumption
- Reception and Transmission functions
- Long communication distance

With some discussion above, the design for the ubiquitous function is decided. Figure.6 shows the “Ubiquitous Functions Activate Module (UFAM)” and the spec of this module in Tbl.2

The UFAM is composed of the reception/transmission module and a micro computer. And electric power is

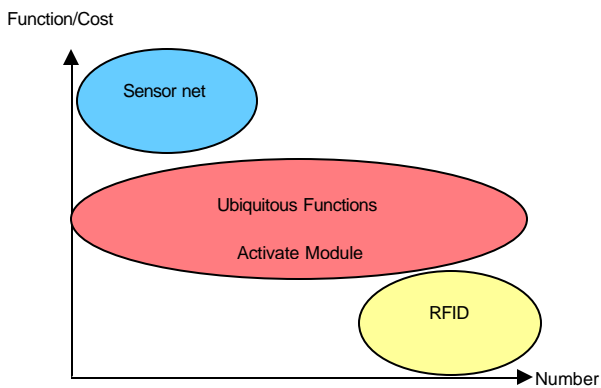


Fig.5 Comparison between RFID and sensor-net

supplied by the button type battery (3V) .Using this battery, UFAM can up and run for a year (in the case of 5 seconds interval). And the size of the UFAM is very small (excluded the antenna). Moreover, UFMA has the I/O port in five bits, programmable, and high sensitivity.

Table.1 Comparison with RFID, UFAM, SN

	RFID	Ubiquitous Functions Activate module	Sensor Net
Cost	Cheap	Cheap	Expensive
IO	None	Input/Output	Input only
Power Consumption	Passive; none Active; low	Low (More than one year)	High
OS	None	None	TinyOS (MICA)
Programmable	No	Yes	Yes
Numbers in environments	Large	Large	Small

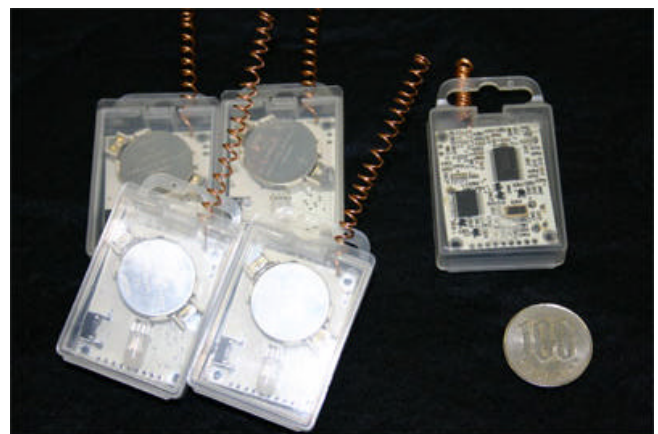
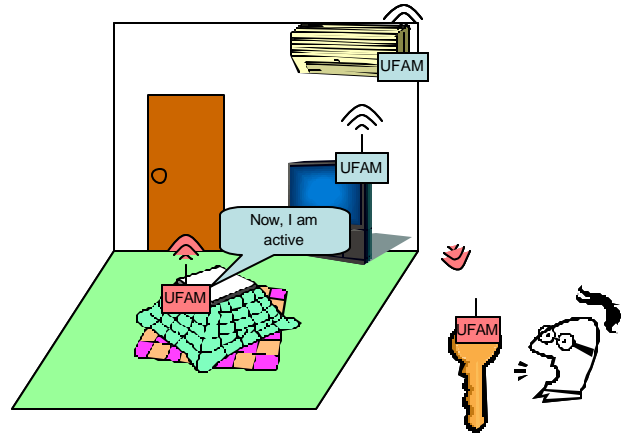


Fig.6 Ubiquitous Functions Activate Module

Table.2 Spec of the UFAM

CPU	PIC16F627A
Clock	4MHz
Transmission/Reception IC	TA32305FN
Baud rate(TX/RX)	9600bps
I/O Device	Switch, LED
Free I/O port	I/O(5bit)
Battery	3V(Button Type)



(a) Emergency call from fireplace with a coverlet to the key

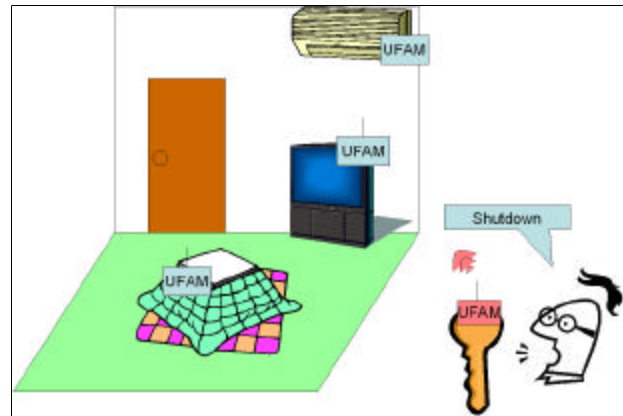
4. Application Examples for UFAM

4-1 Home Safety and Security

Now, in the field of the home security, monitoring services are quite important issues for the human life. But the every facility, such as door, window, gas, TV, heater, air conditioner, etc., are distributed in the home, and it require much costs to connect each other by wire to monitor all of them.

Using our UFAM, the status of each facility could be reported to the resident, with just install the UFAM to each facility, as shown in Fig.7 (a). The resident could obtain the status on another UFAM such as on the key or mobile phone.

Furthermore, using our UFAM, the command for each facility could be happened on the UFAM with resident, as shown in Fig.7 (b). If the resident want to shutdown these facilities, which is still on, the UFAM on the resident side could control the UFMA on the site of facility.



(b) Stop Signal from the key to fireplace with a coverlet.

Fig.7 Home Safety service using UFAM

4-2 Robot Control System

(a) Our past work; “Knowledge Distributed Robot Control Scheme”

At first, before showing the application example on the

robot control system with UFAM, our past work is briefly reviewed.

The “knowledge distributed robot control” scheme [2] was proposed in our past work, which could solve the robot problems on the real application in human life.

The typical model-based approach for the robot in real environments requires much knowledge pre-installed in the robot to recognize and operate objects in real environments. But in the real environments, the unknown objects are often appeared. Furthermore, to treat all of the objects in human life, each model of these objects should be reconstructed.

The “knowledge distributed robot control” scheme has

two key concepts. One is each model of the objects could be obtained from the manufacturer, which had originally made the products, via the IC tag. Second is these information is located in the distributed manner.

Generally speaking, this criteria described the how to reduce the robot management in the human life real situation with the knowledge distribution scheme.

(b) Ubiquitous Robotics

In our past work, only the knowledge for the standalone robot was distributed. The concept of “ubiquitous robot” could distribute its elements with the UFAM, such as sensors and actuators in the real environmental space.

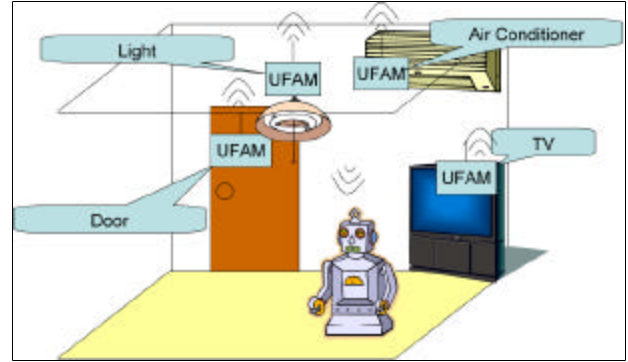
Then, the standalone robot, which supports the human in real environments, could obtain the sensor information, when the robot needs the particular information from the environments, as shown in Fig.8 (a). This ubiquitous sensor manner has some possibility to increase the accuracy on the sensor. And these constructed environments allow the robot without sensor inside.

Furthermore, using our UFAM, the robot could activate the actuator on the environments, as shown in Fig.8 (b). For example, if the robot require light source to recognize some object in the space, the robot could make command to the light module to turn it on.

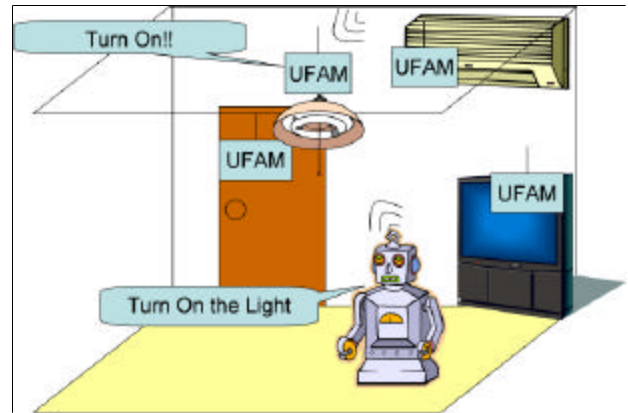
We define the distributed type of robot as the “ubiquitous robot”, in which each robot element is distributed in the space, and connected each other with unwired manner.

5. Conclusion

In this paper, the “Ubiquitous Functions” criteria had proposed, and the “Ubiquitous Functions Activate Module” was informed to apply to use the ubiquitous functions criteria in real applications. Several discussions



(a) Sending of information to the robot



(b) Transmission of demand from robot to Light

Fig.8 UFAM Application example for the robot

on real application usage show the validity of our criteria and module.

References

[1]K.Ohba,K.Ohara,T.Tanikawa,S.Hirai,K.tanie, “Ubiquitous Functions”,. Workshop on the IEEE/RSJ Int. Conf. on Robots and Systems, Sendai Japan,2004

[2]N.Y. Chong, H. Hongu, M. Miyazaki, K. Takemura, K. Ohara, K. Ohba, S. Hirai, K. Tanie, “Robots on Self-Organizing Knowledge Networks,” Proc. IEEE Int. Conf. on Robotics and Automation, 2004

Title: Malfunction diagnosis of the feedback system based on the gap metric

Name: Keita Suzuki* e-mail suzuki@ft-lab.sys.es.osaka-u.ac.jp
Osamu Kaneko* e-mail kaneko@sys.es.osaka-u.ac.jp
Takao Fujii* e-mail fujii@sys.es.osaka-u.ac.jp

Presenter Keita Suzuki

Affiliation* Graduate School of Engineering Science
Department of Systems Innovation
Division of Systems Science and Applied Informatics, Osaka
University

Tel. +81-6-6850-6358

Fax +81-6-6850-6341

Address Machikaneyama 1-3, Toyonaka, Osaka 560-8531, Japan
Graduate School of Engineering Science
Department of Systems Innovation
Division of Systems Science and Applied Informatics

Topic Evaluation and diagnosis of complex systems

Malfunction diagnosis of the feedback system based on the gap metric

K. Suzuki¹, O. Kaneko² and T. Fujii³

Graduate School of Engineering Science,
Osaka University, Machikaneyama 1-3,
Toyonaka, Osaka 560-8531, Japan

¹ suzuki@ft-lab.svs.es.osaka-u.ac.jp, ² kaneko@sys.es.osaka-u.ac.jp, ³ fujii@sys.es.osaka-u.ac.jp

Abstract: In this paper, we propose a new approach to the malfunction diagnosis problem for feedback systems based on the controller information. We define a fault as any loss of stability of the closed loop system, and a malfunction as a variation from the nominal situation that will develop into the fault, respectively. We supervise and evaluate the variation periodically, and avoid the occurrence of those faults in which gradual changes of plant dynamics result. First, in the supervision, the plant variation is obtained by using a plant model estimated by the closed loop identification scheme proposed by Dasgupta *et. al.* [14]. Second, the evaluation is achieved by comparing the stability margin of the initial feedback system with the plant variation after the occurrence of any malfunction from the view point of stability of the closed loop system. The gap metric, which is closely related to the stability, is used in order to compare the above two values, and the model variation is captured in terms of the gap metric. However, the exact plant model is unknown, so its upper bound is estimated by using the set membership identification [4, 12, 1] in the Dasgupta's framework. This comparison makes it possible to quantify the reliability of the feedback system.

Keywords: fault diagnosis, malfunction, gap metric

1. Introduction

Recent development of process technology has enhanced the productivity of various manufacturing processes and at the same time increased the complexity of their operations. This certainly enables us to meet increasing requirements of the process, but causes the vulnerability even to a slight fault because of the high complexity. As a result, strong demand for fault diagnosis with high availability, reliability, and safety has greatly increased on industrial processes day by day.

The fault diagnosis problem has been studied since the late seventies [3], and many approaches have been proposed since then. They can be divided into two main approaches from the viewpoint of the treatment of faults. One deals with a fault as some additive signal, and reduces the fault diagnosis problem to a design problem of a filter that identifies the additive signal. The other deals with a fault as a variation of the plant model, and reduces the fault diagnosis problem to an identification problem. In the case of the former, being a main approach, many methods are proposed [5,17] by this approach, but these methods provide the information only after the fault occurrence. In addition, these methods do not consider the influence of the fault on the closed loop system because the filter is designed such that

both the control input and the output do not affect the filter output. On the contrary, the latter is intuitive, however, such approaches rarely exist because it is difficult to determine a threshold whether the system is fault or not. The difficulty is due to the difficulty in finding a criterion measuring the distance between the two models before and after the fault occurrence.

The gap metric [2] is a powerful criterion that measures the gap between two linear dynamical systems, and is closely related to robust stability. Therefore, it is prospective that the gap metric is a useful criterion for the fault diagnosis problem because the difference between two models before and after the fault is measured, as far as a fault is dealt with as a model variation.

On the other hand, we need to consider the actual situation in manufacturing where the model-based control is rarely used, when the plant model is hardly available. This means that available information is the information on the controller alone, so the fault diagnosis using the controller information alone is required.

Therefore, we propose a new approach to the fault diagnosis problem for a feedback system based on the controller information alone. We define the fault as the loss of stability of the closed loop system, and the malfunction as the variation from the normal situation that will develop into the fault, respectively. We try to avoid the fault

occurrence in which gradual changes of plant dynamics result, by supervising and evaluating the malfunction periodically. In the supervision, the plant variation is obtained by estimating a model through the closed loop identification scheme proposed by Dasgupta [14]. The evaluation is achieved by comparing the stability margin of the initial feedback system with the system variation after the occurrence of any malfunction from the view point of stability of the closed loop system. The gap metric is used to capture the model variation. We aim to give such information that enables us to predict the fault occurrence based on the evaluation result.

In section 2, we introduce the gap metric and stability margin of closed loop system, and define the malfunction as well as the fault from the view point of closed loop stability. We state our problem in section 3, and describe a method to extract the feature of the malfunction occurrence in section 4. In section 5, we describe the evaluation of the feature. Lastly, we give some illustrative examples.

2. Preliminary

2.1 Gap metric

In order to evaluate the closeness between two systems, Vidyasagar [8] and El-Sakkary [2] proposed the graph metric and the gap metric as the distance inducing the graph topology, respectively. The gap metric is closely related to the robust stabilization problem, and is defined as follows.

Definition 1. The gap metric between two systems between $P_1(s)$ and $P_2(s)$ is defined by

$$\delta(P_1, P_2) = \|\Pi_{G(P_1)} - \Pi_{G(P_2)}\|, \quad (1)$$

Here $G(P)$ is the graph of the operator P , and is in the subspace of $H_2 \times H_2$, while $\Pi_{G(P)}$ is the orthogonal projection onto $G(P)$, where $\|k\|$ is the operator norm. The gap metric is characterized as follows [15]:

Lemma1. (N_1, D_1) and (N_2, D_2) are normalized right coprime factorizations of P_1, P_2 , respectively, and A_i is defined by

$$A_i = \begin{bmatrix} D_i \\ N_i \end{bmatrix}, \quad i = 1, 2$$

Then the gap between P_1 and P_2 is characterized as follows:

$$\delta(P_1, P_2) = \max \{ \bar{\delta}(P_1, P_2), \bar{\delta}(P_2, P_1) \}, \quad (2)$$

where the *directed gap* is defined by

$$\bar{\delta}(P_1, P_2) = \inf \{ \|A_1 - A_2 Q\|_\infty \mid Q \in RH_\infty \}$$

2.2 Stability margin

The following volume is introduced for the closed system $F(P, C)$ as shown in Fig.1.

$$b_{PC} = \left\| \begin{bmatrix} I \\ P \end{bmatrix} (I + CP)^{-1} \begin{bmatrix} I & C \end{bmatrix} \right\|_\infty^{-1} \quad (3)$$

This volume is defined as stability margin in [7]. The volume is used as "stability margin" in this paper be low.

2.3 Definition of fault

We need to define the fault so that we can deal with the fault diagnosis problem. Simani *et. al.* define "Fault" as unacceptable system variation [13]. For a feedback system, the variation means the loss of the stability. In addition, we define a "Malfunction" as a change from normal condition. Here "normal" condition means the situation where no model change exists from the nominal model. We assume the malfunction causes the fault. The definitions mentioned above are shown in Table 1.

Class of change	Definition of change
Malfunction	Model variation from the nominal model
fault	Loss of stability of the closed loop system

Table 1: Definition of fault

3. Problem formulation

The robust control system and the general feedback system have the same criterion as far as the closed loop stability is concerned. The difference between them lies in whether the stability is assured or not. Therefore, it is not true that the feedback system has no robustness, but the robustness is not merely quantified for the feedback system. Therefore, we consider the following problem.

Problem: Quantify the stability of a feedback system which is designed without quantification of the stability, and use the resulting value as the criterion measuring the reliability of the system.

For this aim, the gap metric is one powerful measure. The gap metric is closely related to the robust stabilization problem, and it is a useful measure for the stability of the closed loop system. Now, we consider the feedback system as shown in Fig. 1, where P is a true plant, P_0 is a nominal plant, C is a controller which stabilize the closed loop system consisting of P, C (denoted by $F(P, C)$ below), and \tilde{P} is the plant after malfunctions occur.

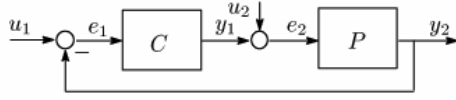


Figure 1: Feedback system

Then, we consider the quantification of the reliability of the closed system from the view point of the stability by using the gap metric. The procedure is described as follows:

- Step 1** Calculate the stability margin of $F(P_0, C)$, and estimate the upper bound of the gap between the nominal plant P_0 and the changed plant \tilde{P} .
- Step 2** Based on these two values, evaluate the reliability of the closed loop system $F(\tilde{P}, C)$ after the malfunction occurrence for the initial closed loop system $F(P_0, C)$ from the view point of stability, and quantify it.

The approach consists of extraction and evaluation of the feature indicating the malfunction occurrence. The details of each step are described in section 4 and 5, respectively.

4. Step 1 : Extraction of feature

We focus on the gap metric as the feature indicating the malfunction occurrence. First, the relation between the gap metric and the stability of the closed loop system is described.

4.1 Gap metric and the stability condition at the closed loop system

The stability condition characterized by the gap metric is well known [16].

Corollary 1. Let the right coprime factorizations (describe RCF below) of the two model P, \tilde{P} be $P=ND^{-1}$, $\tilde{P}=(N + \Delta N)(D + \Delta D)^{-1}$. Here, $\Delta N, \Delta D \in RH_\infty$ and $F(P, C)$ are stable. Then $F(\tilde{P}, C)$ is stable if

$$\delta(P, \tilde{P}) < b_{PC}$$

Our aim is to measure the gap between the true model and the nominal one, and to evaluate it by using *Corollary 1*. However, the true model is unknown, so the bound of the gap needs to be estimated. For this aim, the identification method based on the coprime factorization is desirable. Therefore, in the next subsection, we focus on the framework of closed loop identification by Dasgupta [14], and describe the strategy to estimate

the bound of the gap by using the framework, concretely.

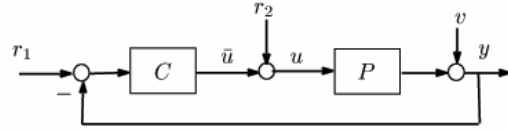


Figure 2: Original feedback system

4.2 Closed loop identification and the uncertainty bound estimation

We describe how to estimate the bound of the uncertainty represented by RCF. First, the closed loop identification is implemented by using the framework of the closed loop identification based on RCF [14]¹. Second, in process of the identification, the bound of the modeling error is estimated by using set-membership identification, and the uncertainty bound of the gap is calculated.

4.2.1 Closed loop identification

The framework of the closed loop identification [14] consists of two steps basically. Let the plant be represented by $P=ND^{-1}$. By using the input/output data (u, y) and the latent variable x , N is estimated based on the data (y, x) in the first step, and in the second step, D is estimated based on the data (u, x) . In this framework, it is assumed that the controller and its RCF and left coprime factorization (LCF), $C = U_r V_r^{-1} = V_l^{-1} U_l$, are known. Then the plant is parameterized as $P=(N_r + VrR)(D_r - U_r R)^{-1}$ by using RCF and LCF of the controller as well as the free parameter R . After all, the estimation

¹In the literature [14], the identification framework of nonlinear time-varying systems is dealt with, but the framework is applicable to linear time-invariant systems, therefore we use it directly. The detail is described in the following.

The closed system considered here is shown in Fig.2. Here r_1, r_2 are the references, and v, u, y are the noise, the control input, and the output, respectively. This is equally transformed to Fig.3.

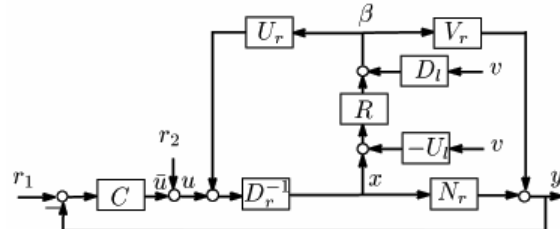


Figure 3: Linear right-coprime factorization based representation

Thus, the relation between x, u and y is as follows:

$$x=V_r R^2+U_r I \quad (4)$$

$$y=(V_r R+N_r)x+V_r(D_I-RU_I)v \quad (5)$$

$$u=(D_r-U_r R)x-(D_I-RU_I)v \quad (6)$$

where $R \in \mathbb{R}^{n \times n}$, and N_r, D_r, N_I, D_I are coprime factors satisfying the following relations.

$$\begin{aligned} U_I N_r + V_I D_r \\ N_I U_r + D_I V_r \\ D_r V_I + U_r N_I = I \end{aligned} \quad (7c)$$

$$N_r U_I + V_r D_I = I \quad (7d)$$

$$D_r U_I = U_r D_I \Leftrightarrow U_I D_I^{-1} = D_r^{-1} U_r \quad (7e)$$

$$N_r V_I = V_r N_I \Leftrightarrow N_I V_I^{-1} = V_r^{-1} N_r \quad (7e)$$

In the first step, x is prepared using the equation (4), and then the estimate $V_r \hat{R} + N_r$ of $V_r R + N_r$ is obtained by using the equation (5) based on the data (y, x) . In the second step, the estimate $D_r - U_r \hat{R}$ of $D_r - U_r R$ is obtained by using the equation (6) based on the data (u, x) . The uncertainty of the model obtained above is

$$\left\| \begin{bmatrix} \Delta D \\ \Delta N \end{bmatrix} \right\|_{\infty} = \left\| \begin{bmatrix} V_r(R - \hat{R}) \\ -U_r(R - \hat{R}) \end{bmatrix} \right\|_{\infty} \quad (8)$$

The uncertainty depends on the estimation accuracy of R . From *Corollary 1*, it is clear that the right side of the equation (8) limits the gap $\delta(P, \hat{P})$ between the true plant P and its estimate \hat{P} . Therefore, we estimate the bound of the right side of (8).

4.2.2 The uncertainty bound estimation by set-membership identification

Set-membership identification provides not only the nominal model but also the model set by ellipsoid approximation of the area of the model distribution [12]. In addition, it provides the bound of the modeling error by using the error data [4,1]. Now, it is assumed that the nominal model is obtained according to the above strategy, and by using set-membership identification the error is estimated as follows:

$$e(t) = \hat{\Delta}_m(z)u(t) + w(t), |w(t)| < c,$$

where $e(t), u(t), w(t), c$ are the error, the input, the unknown disturbance, and its bound, respectively. $\hat{\Delta}_m$ is the estimated error model with m dimensions. Then, the bound of the modeling error is $|\hat{\Delta}_m(e^{j\omega})| + E_I$, where E_I is the radius of the long axis of ellipsoid. Thus when the bounds in step 1 and 2 are described as b_N, b_D , respectively, the bound of (8) is obtained as follows:

$$\left\| \begin{bmatrix} V_r(R - \hat{R}) \\ -U_r(R - \hat{R}) \end{bmatrix} \right\|_{\infty} \leq \sqrt{2} \max\{b_N, b_D\} \quad (9)$$

5. Step 2 : Extraction of feature

In this section, the bound of the right side of the equation (9) is evaluated. Using the identification scheme, and the evaluation technique mentioned below can provide the useful information for the prediction of the fault.

Let $P, P_0, \tilde{P}, \tilde{P}_0$ be the initial true plant, the initial nominal model, the true plant after some changes and the nominal model after some changes, respectively. When the gap metric $\delta(P_0, \tilde{P}_0)$ is replaced as follows:

$$\tilde{b}_c = \delta(P_0, \tilde{P}_0) \quad (10)$$

then the gap $\delta(P_0, \tilde{P})$ satisfies the following relation because of the property of metric

$$\begin{aligned} \delta(P_0, \tilde{P}) &\leq \delta(P_0, \tilde{P}_0) + \delta(\tilde{P}_0, \tilde{P}) \\ &\leq \tilde{b}_e + \tilde{b}_c \end{aligned} \quad (11)$$

where the bound \tilde{b}_e is obtained as the right side of the equation (9) in each identification. Then the gap metric between the initial nominal model and the true plant model after some changes is bounded by the right side of the equation (11). Let the acceptable change of the controller C designed based on the initial nominal model P_0 be denoted by $b_{P,C}^0$. Then, if

$$\tilde{b}_e + \tilde{b}_c < b_{P,C}^0 \quad (12)$$

holds, then the true plant after some changes \tilde{P} is also stabilized by the controller C . Let us now apply this property to malfunction diagnosis. When the bound $\tilde{b}_e + \tilde{b}_c$ approaches $b_{P,C}^0$, then the stability margin of the closed loop system is not assured at the limit. From this point, as well as the equation (11) and (12), the reliability index σ should be defined in order to normalize the above property such that the ratio of the bound $\tilde{b}_e + \tilde{b}_c$ to the initial stability margin $b_{P,C}^0$ becomes lower than one while the stability is assured.

$$\sigma = 1 - \frac{\tilde{b}_e + \tilde{b}_c}{b_{P,C}^0} \quad (13)$$

The above discussion is summarized as follows:

Theorem 1. Let $P, P_0, \tilde{P}, \tilde{P}_0$ be the initial true plant, the initial nominal model, the true plant after some changes and the nominal model after some changes, respectively, and P be stabilized by the controller C . Then the closed loop system $F(\tilde{P}, C)$ does not achieve fault if the equation (11) holds.

Proof. From the equations (11),(12), the relation $\tilde{b}_e + \tilde{b}_c < b_{P,C}^0$ holds. Therefore, from *Corollary*

1, if (12) holds, the closed system $F(\tilde{P}, C)$ is stable, that is, does not achieve fault.

Remark 1. The remarkable point of the proposed method is to evaluate the variation with any malfunction occurrence from the view point of the stability of the closed loop system, and to quantify the reliability. This property provides the useful information such that we can predict the fault occurrence.

Remark 2. Theorem 1 is the sufficient condition in order that the closed loop system is stable. Therefore, even if Theorem 1 does not hold, the closed loop system does not necessarily achieve fault, but the conservativeness is acceptable for the purpose of the fault prediction.

Remark 3. The proposed method is implemented based on the estimated model, so the diagnosis accuracy depends on the accuracy of the identification. For example, if the modeling error bound \tilde{b}_e is larger than the initial stability margin $b_{P,C}^0$, then the reliability index (13) has no meaning. Therefore, $\tilde{b}_e < b_{P,C}^0$ should be presupposed in the proposed method.

The algorithm of the proposed method is as follows:

Step1. Calculate the initial stability margin

$b_{P,C}^0$

Step2. Estimate the plant model represented by RCF according to the closed loop identification framework [14], obtain the modeling error bound according to set-membership identification method, and calculate the bound (11)

Step3. Calculate the reliability index (13), return to Step 2

6. Numerical example

We illustrate the efficiency of the proposed method. Below, the true model is assumed to change gradually, and the variation occurs at the plant. First, the changed plant is identified according to the framework mentioned in section 4.2, and the bound of the modeling error is estimated. We state the remarkable points about the identification implementation. The reference r_1 is chosen as an M sequence signal, and r_2 as zero for simplicity. It is clear from the equations (5),(6) that the color noise mixes in the data used in the identification. However, if the model is identified as the nominal model with noise by using ARX and so on, this problem can be avoided. We thus use ARX here. Second, the reliability index

of (13) is calculated by using the bound of the modeling error. We show that iteration of these operations and supervision of the variation of the reliability index makes it possible to predict the fault. We derive here the case where the nominal model is already obtained. If the nominal model is not yet obtained, we need to estimate it according to the closed loop identification framework.

Let $P, P_0, \tilde{P}, \tilde{P}_0$ be the initial true plant, the initial nominal model, the true plant after some changes and the nominal model after some changes, respectively. The nominal model and the controller stabilizing the closed loop system $F(P_0, C)$ are given as follows:

$$P_0(s) = \frac{s+1}{(s-1)(s+2)}, \quad (14)$$

$$C(s) = \frac{12(s+2)}{(s+1)(s+6)}, \quad (15)$$

where the normalized RCF of the plant (N_r, D_r) and (U_r, V_r) satisfying Bezout equation $U_r N_r + V_r D_r = 1$ are given as follows:

$$N_r(s) = \frac{s+1}{(s+2)(s+3)}, \quad D_r(s) = \frac{s-1}{s+3}$$

$$U_r(s) = \frac{12}{(s+1)}, \quad V_r(s) = \frac{s+6}{s+2}$$

From (14),(15) the initial stability margin of $F(P_0, C)$:

$$b_{PC}^0 = \left\| \begin{bmatrix} I \\ P_0 \end{bmatrix} (I + CP_0)^{-1} [I \quad C] \right\|_{\infty}^{-1}. \quad (16)$$

is computed as $b_{P,C}^0 = 0.2271$. We then increase the unstable pole 1 by +0.01 every step, and estimate the bound of the modeling error. Here, we estimate the bound \tilde{b}_e according to the identification framework derived in section 4.2, and calculate the gap \tilde{b}_c by using the estimated model, which yields the right side bound (11). The reliability index (13) is calculated based on $b_{P,C}^0, \tilde{b}_e + \tilde{b}$ obtained above. These operations are iterated 50 times, and the resulting variation of the reliability index is supervised as shown in Fig.4, where the horizontal axis is the unstable pole change.

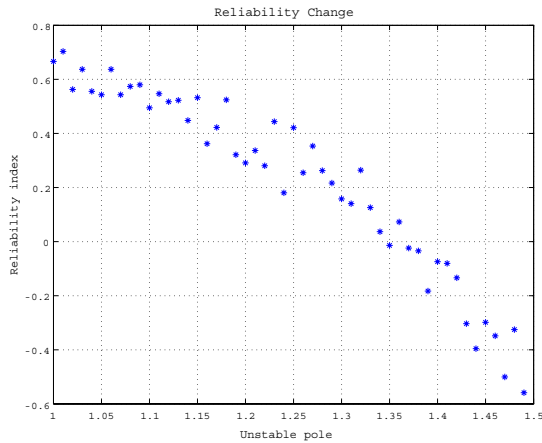


Figure 4: Reliability index

Figure 4 shows the gradual degradation of the reliability of the closed loop system. This result enables us to predict the development of model variation into closed-loop instability, that is, fault.

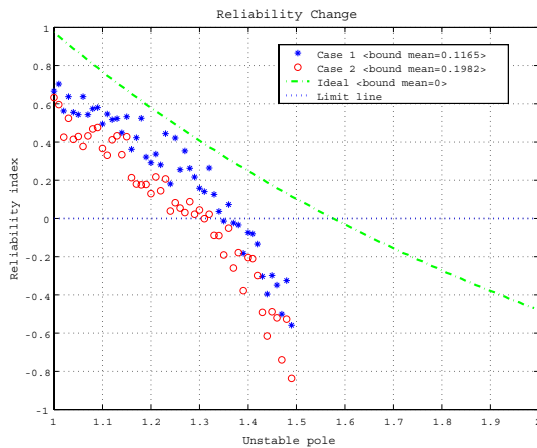


Figure 5: Diagnosis precision

In addition, the reliability changes for three cases: Case 1) the case with good modeling accuracy, Case 2) the case with bad modeling accuracy, Case 3) the case with no modeling error (Ideal) are compared in order to show that the proposed method depends on the modeling accuracy. The result is shown in Fig.5, where the asterisk (Case1) is the case where the average of the modeling error at 50 times is 0.1165, the circle (Case2) is the case where that is 0.1982, the chained line is the case where no modeling error exists (Case 3), and the dotted line is the stability limit of the closed loop system $F(P_0, C)$.

We can see from Fig.5 that in Case 2 the reliability crosses over the dotted line earlier than in Case 1, so Case 2 is more conservative than Case 1.

In addition, comparing Case 1 with Case 3 informs us the conservativeness of Case 1, but this conservativeness is acceptable for the purpose of fault prediction.

7. Conclusion

In this paper, we have proposed a malfunction diagnosis method based on a new framework, which differs from the usual one based on the filter design. We define the fault as the loss of stability of the closed loop system, and the malfunction as the variation from the normal situation that will develop into the fault, respectively. Under these definitions, we evaluate the reliability of the closed loop system by measuring the degree of the change. The extraction of the feature consists of the closed loop identification and the set-membership estimation of the modeling error. The evaluation of the feature is implemented based on the gap metric and robust stability, from which we obtained a simple sufficient condition such that the system is not fault. The result enables us to grasp the pre-information about a fault and to predict such a fault that is caused by the gradual change like aging. Finally, we showed the efficiency of the proposed method by the numerical example.

Acknowledgement

This research was supported by the Japan Society for the Promotion of Science under Grant-in-Aid for Creative Scientific Research (Project No. 13GS0018)

References

- [1] A. Sano, "Recent issue about system identification", *SICE seminar -system identification for control- introduction*, pp.31-44, 1995 (in Japanese)
- [2] A. K. El-Sakkary, "The Gap Metric : Robustness of Stabilization of Feedback Systems", *IEEE Trans. Autom. Contr.*, Vol.30, No.3, pp.240-247, 1985
- [3] A. S. Willsky, "A Survey of Design Methods for Failure Detection in Dynamic Systems", *Automatica*, Vol.12, No.6, pp.601-611, 1976
- [4] B. Wahlberg and L. Ljung, "Hard frequency- domain model error bounds from least squares like identification techniques", *IEEE Trans. Autom. Contr.*, Vol.37, No.7, pp.900-912, 1992
- [5] C. Commault, J. M. Dion, O. Sename & R. Mouton, "Observer-Based Fault Detection and Isolation for Structured

- Systems”, *IEEE Trans. Autom. Contr.*, Vol.47, No.12, 2002
- [6] F. R. Hansen and G. F. Franklin, ”On A Fractional Representation Approach To Closed-loop Experiment Design”, In *Proc. American Control Conf.*, Atlanta, GA, pp.1319-1320, 1988
- [7] H. Maeda, ”Graph Topology and Robust Control”, *Systems, Control and Information*, Vol.35, No.5, pp.278-286, 1991
- [8] M. Vidyasagar, ”The Graph Metric for Unstable Plants and Robustness Estimates for Feedback Stability”, *IEEE Trans. Autom. Contr.*, Vol.29, No.5, pp.403-418, 1984
- [9] M. Vidyasagar, ”Control System Synthesis : A Factorization Approach”, MIT Press, Cambridge, MA, 1985
- [10] P. M. J. Van Den Hof and R. J. P. Schrama, ”An Indirect Method for Transfer Function Estimation from Closed Loop Data”, *Automatica*, Vol.29, No.6, pp.1523-1527, 1993
- [11] P. Zhang, S. X. Ding, G. Z. Wang, D. H. Zou and E. L. Ding, ”Observer-based approaches to fault detection in multirate sampled-data systems”, *The 4th ASCC*, 2002
- [12] R. L. Kosut, M. K. Lau, and S. P. Boyd, ”Set- Membership Identification of Systems with Parametric and Nonparametric Uncertainty”, *IEEE Trans. Autom. Contr.*, Vol.37, No.7, pp.929-941, 1992
- [13] S. Simani, C. Fantuzzi and R. J. Patton, ”Model-based Fault Diagnosis in Dynamic Systems Using Identification Techniques”, Springer, 2002
- [14] S. Dasgupta and B. D. O. Anderson, ”A Parameterization for the Closed-loop Identification of Nonlinear Time-varying Systems”, *Automatica*, Vol.32, No.10, pp.1349-1360, 1996
- [15] T. T. Georgiou, ”On the Computation of the Gap Metric”, *Syst. Control Lett.*, Vol.11, pp.253-257, 1988
- [16] T. T. Georgiou and M. C. Smith, ”Optimal Robustness in the Gap Metric”, *IEEE Trans. Autom. Contr.*, Vol.35, No.6, pp.673-686, 1990
- [17] X. Ding and P. M. Frank, ”Fault detection via factorization approach”, *Syst. Control Lett.*, Vol.14, No.5, pp.431-436, 1990

Construction Productivity Loss and Worker's Behavior Caused by Work Space Conflict

Topic: Risk management and decision analysis

Li-Wen Wu¹/ National Taiwan University

Sy-Jye Guo²/ National Taiwan University

¹Dep. Of Civil Engineering Construction Engineering & Management NTU, PH.D Student, No.1 Sec.4, Roosevelt Road. , Taipei, 106 Taiwan ,R.O.C.,(886)928592269, Fax number:(886)2366-1640,e-mail address: d92521009@ntu.edu.tw

² Dep. Of Civil Engineering Construction Engineering & Management NTU, Professor, No.1 Sec.4, Roosevelt Road. , Taipei, 106 Taiwan, R.O.C., e-mail address: sjguo@ce.ntu.edu.tw

Construction Productivity Loss and Worker's Behavior Caused by Work Space Conflict

Abstract

In construction sites, different trades may interfere with one another while working in the same space. Thus, these space conflicts affect the productivity and worker's behavior directly. These situations would prolong the estimated schedule of the construction and decrease the workers' morale. With the assumption of constructing a standard floor 14 days for cast-in-space building construction, this study directly analyzes the relationship of productivity loss and worker's behavior. Try to explain the behavior of the workers caused by workspace conflict. Also, the fuzzy verbal questionnaires were adopted in the interviews and the interviews were recorded in the form of fuzzy intersection. After applying the fuzzy statistics, the productivity loss parameter of each fuzzy verbal variable

was produced.

Conclusively, the result of this study can be applied in Construction Management Information System to serve as a quantitative parameter and can be treated as a main resource for decision making of construction manager. Also, the investigation of these questionnaires can find the critical factors causing that the workers at the construction site work uncomfortably and feel ill mentally. The manager of the project can find the improving strategy according to the critical factors above. Most importantly, the result of this study will be obtained the solution of the relationship of productivity and worker's behavior caused by work space conflict.

1: Introduction

To satisfy the special need and demand of the construction project, we have been asked to have schedule expediting performance. However, it generates the interfaces of work space conflicts because different trades may enter the work area at the same time. Conflicts not only cause the work space of each worker crowded but only cause waiting behaviors happen. It causes workers wait and feel unsatisfied mentally, eventually makes the productivity reduce and even brings about the schedule of the project delayed.

According to Thabet's and Beliveau's theory, the foundation of this study was based on literatures review, field observation and interviews with the construction

workers on the job site. With the same assumption of constructing a standard floor 14 days for cast-in-space building construction, this study directly analyzes the relationship of productivity and waiting behavior. Besides, the fuzzy verbal questionnaires were adopted in the interviews according to the waiting behavior types, and the interviews were recorded in the form of fuzzy intersection. After applying the fuzzy statistics, the productivity loss parameter of each fuzzy verbal variable was produced.

Although there are many literatures discussing the relationship of productivity and schedule, they never

quantify the relationship of productivity and waiting behavior of the different trades. Therefore, it is important to quantify the waiting behavior of the different trades into productivity loss function. The three main purposes of the study are described below:

(1) Among all the conflict points, it will cause different waiting situation and productivity loss trades between different trades and construction types.

(2) Simulate the productivity loss for working crowded and waiting behaviors and combine those two factors into establishing a management rule for controlling the productivity loss.

2: Related research

There are lots of researches discussing the types of construction space, but the article from Riley and Sanvido has been commonly quoted. In this section, we will discuss the type of construction space and the relationship between the working space and working productivity loss.

2.1: Types of construction space

Riley and Sanvido define twelve different kind of types of construction space, and they could be divided into two categories.

(1) Areas: space occupied by activity work elements for a period of time.

(2) Paths: space required for the movement of material, people, and other resources.

- i. Layout area: The space required to determine the position of a material to be placed by an activity.
- ii. Unloading area: The space occupied or required by material-handling resources to place materials onto floors at access points.
- iii. Material path: The space required to move a particular material from unloading areas to storage areas and

work areas.

- iv. Staging area: The space required to temporarily arrange materials near work areas for short intervals of time.
- v. Personnel path: The path required for workers to travel between access points, material storage areas, and work areas.
- vi. Storage area: The space required to keep material or tools from the time delivered to site to the time of use.
- vii. Prefabrication area: The space used to prepare, shape, prefabricate, or assemble materials.
- viii. Work area: The space required for crews to install materials.
- ix. Tool and equipment area: Space occupied by a resource or temporary facility, which is used to support other activity work elements.
- x. Debris path: The space needed for the disposal of scrap material and packaging.
- xi. Hazard area: Space that is unusable due to health hazards or other dangers created by construction activities.
- xii. Protected area: Spaces that are used to protect material in place.

2.2: Space behavior pattern

From Riley and Sanvido 1995, when the order of space occupied between different trades are decided, we could then define space behavior pattern of each space type. For each “process-space type”, a subset of “process-space-patterns” describes how crews typically use space over time to perform work element. “Product-space-type” patterns describe the effects of completed work on space. The purpose of modeling this behavior is to define relationships between activities with different patterns and to predict the space needed for

activity work elements.

Space type		Space behavior patterns
Process-space	Work area	Linear
		Random
		Horizontal Unit/Area
		Vertical Units
		Spiral
		Building Face
	Storage area	Bulk storage
		Distributed storage
		Proximity storage
		Remote storage
Product-space	Layout area	Create space
		Remove space
		Enclose space
		Partition space
		Direct Impact
		No Impact

Table 2.1 Space behavior patterns

2.3: The definition of space conflict

The definition of space conflict has been cited fundamentally is from research of Riley and Sanvido (1995). The definition is that when two working activity space are superimposed, we call the overlapping space as space conflict (or time-space conflict). (See Fig. 2-1)

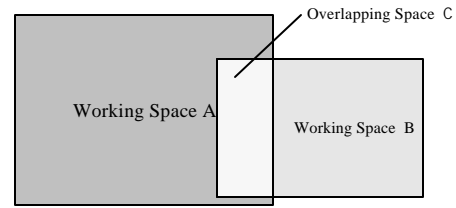


Fig.2-1 the definition of the conflict

2.4: Congestion Index and productivity

From Smith (1998), it mentioned the productivity of workers is directly affected by the congestion they felt. As to evaluate the level of congestion the workers felt, Smith defined Congestion Index.

$$\text{Congestion Index} \equiv \frac{\text{working area}}{\text{working population}} \dots\dots\text{Eq.2-1}$$

When each worker can occupy the working space area which is larger than 30m², there is no affection to working productivity. However, each worker should occupy at least 10 m², and it would cause the productivity loss 46 to 65%. Smith concludes that it would be avoided to let too many workers stay at the same working area, because it caused conflict between each other.

2.5: Space capacity factor and productivity

From Thabet and Beliveau (1994), it mentioned that it will lead unsafe working environment? working process pause? delay and argument between different trades when the useful space is restricted under scheduled working process. All these would cause minus loss to working productivity. When the useful space is less than the demand, the productivity of workers and equipment will decrease with reduced useful working space.

So, it comes the concept of space capacity factor (SCF) and we use SCF as a method to measure the

proportion of working space demand and working space useful. It is the equation of SCF.

$$SCF \equiv \frac{\text{working space demand}}{\text{working space useful}} \dots\dots\dots \text{Eq.2-2}$$

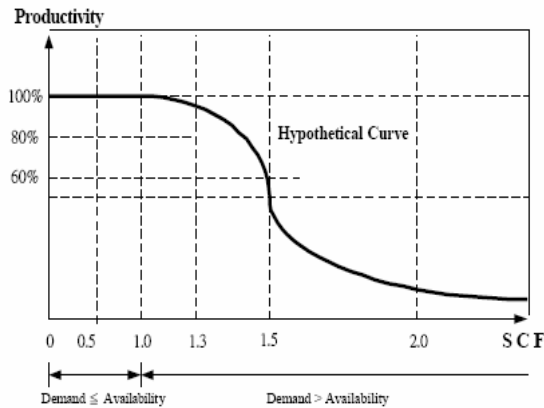


Fig. 2-2 SCF and productivity Diagram

3. Motivated Case

In this research, we emphasis on investigate when and how the space conflict happened in a typically 14-days R.C. one-floor construction project between different trades. For an advanced study, we take the 14-days R.C. one-floor construction project as the motivated case and define the assumptions:

- (1) In the reason of moldboard removal, we usually take 14 days as the R.C. one-floor construction cycle. In this paper, we analyze the space conflict process under this circumstance.
- (2) We look into the conflict of insufficient space coming form congestion of different activities
- (3) We investigate the conflict of different working space superimposed coming form overlapping time-schedule of different activities.
- (4) In this paper, we don't consider the division-construction.

3.1: Types of construction space simplified

In Riley and Sanvido (1995), there are twelve different kinds of types of construction space defined. In this paper, we simplify them into four types:

- i. Working area: The space occupied for workers to complete the assigned activity.
- ii. Tool and equipment area: Space occupied by a resource and space occupied when it works
- iii. Layout area: The space required to determine the position of a material to be placed by an activity.
- iv. Path area: The space needed for the transportation between different activities.

3.2: The construction process of a standard R.C. floor

Generally constructing the building with traditional moldboard, without system moldboard, we will pour the concrete from column? wal? beam to floor slab at one time. First of all, setting-out of survey begins. Then, workers can set the column steels and Stirrup. Hydroelectrical equipment distribution comes after Stirrup and then seals the molds. Outer wall mold constructed is following, then steel-setup of the wall ? hydroelectrical equipment distribution of the wall and inner wall mold constructed is coming after in turns. Continuously, plate and column molds constructed by moldboard workers and beam and plate steel constructed by steel workers. Finally, after inspection the pouring of the concrete commence.(see Fig.3-1)

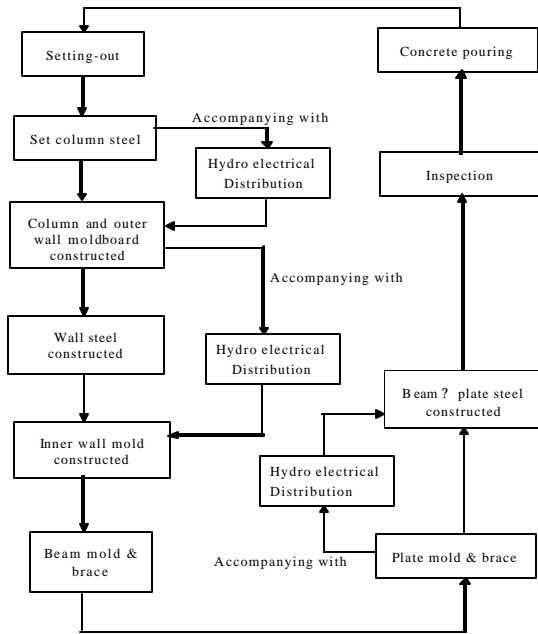


Fig.3-1 the construction process of standard R.C. floor

4. Analysis of space conflict and productivity loss function

4.1: The space conflict

By observation on site and records before, we can make up the standard time schedule of the 14-days R.C. one-floor construction project. In the 14 days process, we can easily find few different level conflicts in day 2, day 3, day 4, day 8, day 9, day 10, day 12. We can find six conflict spots in turns (see Fig 4-1). In this paper, we regard congestion as the main reason causes working productivity loss.

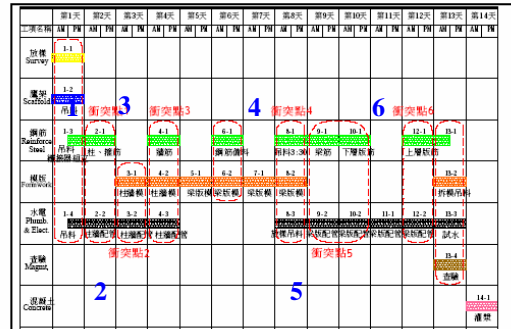


Fig 4-1 the conflict spots

4.2: The establish of the productivity-loss function

(1)The theorem of productivity-loss function

In this paper, we use productivity-loss function as a quantitative tool to evaluate the congestion affection to productivity. Also, we use fuzzy function to compile statistics of the questionnaires. Fuzzy function (also identified by the term “linguistic function”) is a function to which either numerical values or literal descriptions can be associated. Almost every numerical function can be transformed into fuzzy functions, by associating some descriptive attributes to the definition values which can then sum them up. In this paper, we use fuzzy variables to describe spacious, little crowd, c crowd, strongly crowd and completely crowd. Therefore, in face of qualitative assessment, we usually use fuzzy function as a quantitative tool to express the original thought of assessment.

(2) Productivity loss function

Here are the three steps to establish the function:

- i. Define the fuzzy variables and assess grade of membership between different trades caused by congestion.
- ii. Make up the fuzzy verbal questionnaires
- iii. Use matrix method to calculate the productivity loss and linear regression equation adjusted

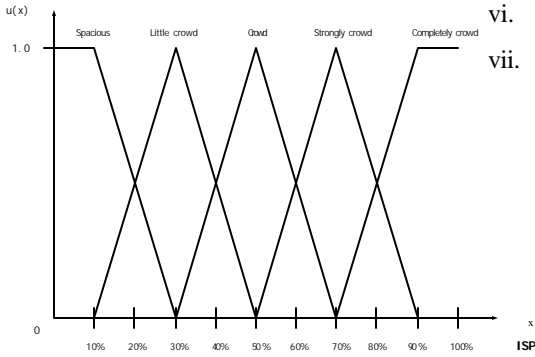


Fig. 4-2 the membership curve

After defining the membership function, we use fuzzy verbal questionnaire to investigate. Then we use questionnaire data to analysis and calculate. So, we employ the basic matrix method calculation concept to analysis and compile statistics. Here are the steps:

- i. the value of SCF or ISP can be expressed as a five-grade fuzzy set S
(x1.x2.x3.x4 and x5 are fuzzy variables)

$$S = \sum_{n=1}^5 \mu_S(x_n) / x_n \dots\dots Eq.4-1$$

Regard S as a 1*5 matrix.

- ii. By questionnaire data, the mean (reduce value) of each fuzzy verbal expectation variables are obtained.

$$P = \begin{bmatrix} p_1 \\ p_2 \\ p_3 \\ p_4 \\ p_5 \end{bmatrix} \dots\dots\dots Eq.4-2$$

Regard P as a 1*5 matrix.

- iii. The PL (productivity loss) is equal to S * P%
- iv. Each SCF or ISP value can find a reduce value corresponding. Draw each spot on X-Y diagram.
- v. To simplify the curve of the diagram, we select 100 SCF or ISP values form 0 to 100%, then find reduce value corresponding.

Continuously, use regression analysis to conclude the fit curve as productivity loss function curve.

(3) Questionnaire specimens

We investigated the leader hotel from national Taiwan University. The construction site is fitted in with the 14-days R.C. one-floor construction, corresponding to our assumption above. Questionnaire specimens are including construction company managers? professional technical workers? usual workers . There are 74 people investigated and proved validly.

5. The productivity loss caused by the conflicts of congestion behavior

- (1) The productivity loss caused by a single trade under restricted space

To evaluate the grade of membership by a single trade, we replace SCF value with five-grade fuzzy set S. Five grades are spacious, little crowd, crowd, strongly crowd and completely crowd. In this paper, we can conclude the productivity loss functions of moldboard construction? steel construction and hydroelectrical equipment construction under restricted space. Here we take moldboard construction for example. By the results of questionnaires, we calculate the data and regression line into Fig 4-1. We know then productivity loss will vary 25% to 50% in completely crowd membership, averagely 37%. When SCF value is between 1.0 to 1.25, SPSI value is 41.4; 1.25 to 1.50, SPSI value is 34.0; 1.50 to 1.75, SPSI value is 37.2 1.75 to 2.00, SPSI value is 33.8. Between 1.0 to 1.25, productivity will lose 0.414% Here is the equation of the regression line:

$$y = -13.404x^2 + 84.871x - 71.495$$

y is percentage of productivity loss , x is SCF value-----Eq. 5-1

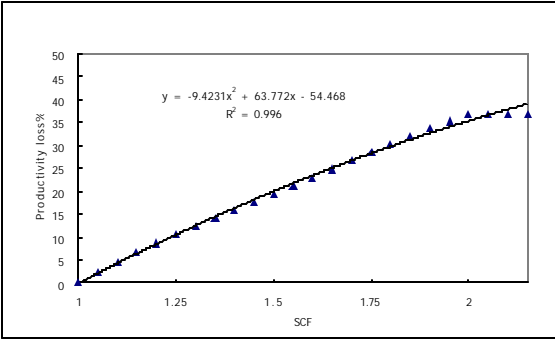


Fig. 5-1 moldboard construction regression curve

(2) The productivity loss caused by different trades under restricted space

To evaluate the grade of membership by different trades, we replace ISP value with five-grade fuzzy set S. Five grades are rarely overlapping, little overlapping, overlapping, strongly overlapping and completely overlapping.

$$\text{ISF}(\text{interference space percentage}) \equiv \frac{\text{overlapping space between activities}}{\text{own activity space}} \quad \text{Eq.5-2}$$

In this paper, we can conclude the productivity loss functions of six different conflict spots. Here we take the first one for example. First conflict spot: column steel set-up (steel construction) and column hydro electrical pipeline setup (hydro electrical equipment construction).

By the results of questionnaires, we calculate the data and regression line into Fig.5-2. We know then productivity loss will vary 34.6% to 47% in completely crowd membership, averagely 41%. When ISP value is between 10% to 30%, SPSI value is 0.34; 30% ~ 50%, SPSI value is 0.58; 50% ~ 70%, SPSI value is 0.45; 70% ~ 90%, SPSI value is 0.55. Between 10% to 30%, productivity will lose 0.58%. Here is the equation of the regression line:

$$y = -1E-09x^6 + 3E-07x^5 - 3E-05x^4 + 0.0016x^3 - 0.0279x^2 + 0.4163x$$

y is percentage of productivity loss, x is ISP value Eq. 5-3

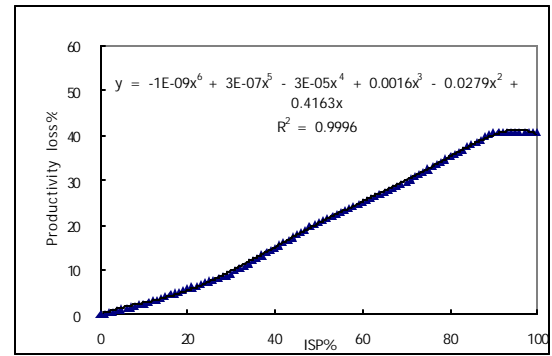


Fig.5-2 the conflict spot 1 regression curve

6: conclusion

(1) To generalize the space conflict type of R.C. building

In this paper, we use typically 14-days R.C. one-floor construction project for a motivated case. In the 14-days construction cycle, we investigated when and how conflicts happened. It improved the conflict analysis to consider the path and layout areas.

(2) Establishing the fuzzy verbal function to establish space conflict framework

In this paper, we define fuzzy verbal variables to five grades and establish ISF and ISP membership function, using productivity-loss function as a quantitative tool to evaluate the congestion affection to productivity.

(3) Establishing the productivity loss function and curve under restricted space

In this paper, we separately discuss the productivity loss caused by a single trade and different trades. The result can be viewed as a quantitative tool for space scheduling to solve the problem of lack of parameters.

7: Reference

1. Riley, D.R. and Sanvido, V.E., "Patterns of construction-space use in multistory buildings." *Journal of Construction Engineering and Management*, ASCE, 121(4), pp.464-473. (1995).
2. Sanders, S.R., Thomas, H.R. and Smith, G.R., "An analysis of factors affecting labor productivity in masonry construction." PTI # 9003, Pennsylvania State University, University Park, PA (1989).
3. Smith, A. G., "Increasing Onsite Production" *AACE Transactions* K.4. 1- K.4.14 (1987).
4. Thabet, W.Y. and Beliveau, Y.J., "Modeling work space to schedule repetitive floors in multistory buildings." *Journal of Construction Engineering and Management*, ASCE, 120(4), pp.96-116, (1994).

**Structural Modeling and Decision Support for Dissolving Uneasiness
Using Revised DEMATEL Methods**

Hiroyuki TAMURA¹ and Katsuhiro AKAZAWA²

¹ Faculty of Engineering, Kansai University, Suita, Osaka 564-8680, JAPAN

Phone and FAX: +81-6-6368-0829

<H.Tamura@kansai-u.ac.jp>

² Faculty of Life and Environmental Science, Shimane University, Matsue 690-8504,

JAPAN

Phone and FAX: +81-852-32-6530

<akazawa@life.shimane-u.ac.jp>

TOPIC: Keynote

Structural Modeling and Decision Support for Dissolving Uneasiness Using Revised DEMATEL Methods

Hiroyuki TAMURA¹ and Katsuhiro AKAZAWA²

¹ Faculty of Engineering, Kansai University, Suita, Osaka 564-8680, JAPAN

² Faculty of Life and Environmental Science, Shimane University, Matsue 690-8504, JAPAN

Abstract

In this paper we describe two revised DEMATEL (DEcision MAKing Trial and Evaluation Laboratory) methods. One is called "DEMATEL with Composite Importance" and the other is called "Stochastic DEMATEL," to extract structural model of a complex problematique and to represent the priority of each factor taking into account the uncertainty of structure.

From numerical experiments and experimental analyses, the following results are obtained: (1) Composite importance represents the useful information for deciding the priority of each factor. (2) When the structure is uncertain, stochastic DEMATEL could extract the features of structure by the degree of dispatching influences and the degree of central role. (3) Stochastic composite importance could express the uncertainty of priority and decide the priority taking into account the attitude of the decision maker; pessimistic, neutral or optimistic.

Key Words: *Safe, secure and reliable (SSR) society; Structural modeling; DEMATEL; Composite importance; Stochastic DEMATEL; Stochastic composite importance*

1. Introduction

DEMATEL (DEcision MAKing Trial and Evaluation Laboratory) has been widely used to extract a problem structure of a complex problematique [1-3]. By using DEMATEL we

could quantitatively extract interrelationship among multiple factors contained in the problematique. In this case not only the direct influences but also the indirect influences among multiple factors are taken into account. Furthermore, we could find the dispatching factors that will rather affect the other factors, the receiving factors that will be rather affected by the other factors, the central factors that the intensity of sum of dispatching and receiving influences is big, and so forth.

It is important and useful to get the structural model of a problematique from which we could find the priority among multiple strategies to improve the structure. This is the main aim of DEMATEL. However, the conventional DEMATEL [1] is insufficient to obtain significant implication of the priority of the strategies for decision making as follows:

- 1) Shortage of information on the importance of each factor

Suppose we got three factors; "to get enough income", "to get successor", "to improve productivity", in the problematique of agriculture. The decision maker is trying to find the order of priority among these three factors. Suppose the conventional DEMATEL found that "to improve productivity" is the most influential factor to improve the problem structure. However, if "to get successor" is the most important factor in the future agricultural problem, this factor should be the first priority for the strategic planning of agriculture. In the conventional DEMATEL it is hard to find the superiority of factors, since we could get only interrelationship of factors contained in the problematique. To overcome

this difficulty we proposed a new criterion “Composite Importance (CI)” [4] combining the interrelationship of factors and the importance of each factor.

2) Shortage of flexibility to describe structural uncertainty

Conventional DEMATEL describes the deterministic interrelationship among factors contained in the problematique. However, the strength of the interrelation among factors may be dependent on the various situations, and uncertainty may arise on the factors taken into account. For example, in the agricultural problematique, “to improve productivity” may contribute “to get enough income”, but to what extent may be dependent on each farmhouse. “To get enough income” may contribute “to get successor” uniformly, and so forth.

In this paper in the context of finding priority among multiple strategies to improve the structure of the problematique, we aim at three objectives as follows:

- (1) We show how to compute composite importance to find the priority of dissolving uneasy factor.
- (2) We show a stochastic DEMATEL to deal with flexible interrelationship among factors in the problematique, and we show usefulness and future problem of stochastic DEMATEL through an empirical analysis of ordinary consumers’ and food specialists’ uneasiness over foods when we deal with structural modeling of uneasy factors on foods.
- (3) Using the information of stochastic composite importance (SCI) we try to find the priority of dissolving uneasy factors on foods.

2. DEMATEL with Composite Importance

2.1 Outline of DEMATEL

Suppose, in a complex problematique composed of n factors, binary relations and the strength of each relation are investigated. An

example of binary relation is such that “How much would it contribute to resolve factor j by resolving factor i ?” We would get $n \times n$ adjacent matrix X that is called the direct matrix. The (i, j) element x_{ij} of this matrix denotes the amount of direct influence from factor i to factor j . If the direct matrix X is normalized as $X_r = IX$, by using $I = 1/(\text{the largest row sum of } X)$, we would obtain

$$X^f = X_r + X_r^2 + \dots = X_r(I - X_r)^{-1} \quad (1)$$

Matrix X^f is called the direct/indirect matrix. The (i, j) element x^f_{ij} of the direct/indirect matrix denotes the amount of direct and indirect influence from factor i to factor j .

Suppose D_i denotes the row sum of i -th row of matrix X^f . Then, D_i shows the sum of influence dispatching from factor i to the other factors both directly and indirectly. Suppose R_i denotes the column sum of i -th column of matrix X^f . Then, R_i shows the sum of influence that factor i is receiving from the other factors. Furthermore, the sum of row sum and column sum $(D_i + R_i)$ shows the index representing the strength of influence both dispatching and receiving, that is, $(D_i + R_i)$ shows the degree of central role that the factor i plays in the problematique. If $(D_i - R_i)$ is positive, then the factor i is rather dispatching the influence to the other factors, and if negative, then the factor i is rather receiving the influence from the other factors. We call D_i , R_i , $(D_i + R_i)$ and $(D_i - R_i)$ the degree of dispatching influences, the degree of receiving influences, the degree of central role and the degree of cause, respectively.

There exist many case studies [5-10] of DEMATEL to get an appropriate structural model. Some of them are trying to get a structural model identifying the central factors and the causing factors based on the evaluation of the degree of central role and the degree of cause. The degree of cause denotes

whether the factor is rather cause or effect. It does not reflect the amount of dispatching or receiving influence. Since the objective of this paper is to find the priority of the strategy to improve the overall structure, we turn our attention to the degree of dispatching influences.

2.2 Composite Importance

Suppose based on the degree of dispatching influences we found a factor that may contribute to improve the overall structure. In this case to resolve this factor is not necessarily the best choice, since the factor that could contribute to resolve some important factors may be more efficient to resolve even if it may not contribute to improve overall structure. Since the original DEMATEL is not taking into account the importance of each factor itself, it is not possible to evaluate the priority among the factors. Similarly, it is not possible to evaluate the priority of each factor by just looking at the importance of each factor. We need to take into account both the strength of relationships among factors and the importance of each factor. To reflect both viewpoint we proposed the composite importance z as [4]

$$z = y_r + X^f y_r = (I + X^f) y_r \quad (2)$$

where y_r denotes the normalized n -dimensional vector of y that denotes n -dimensional vector composed of the importance of each factor, where “normalized” means to divide each element of y by the largest element in y .

2.3 A Simple Numerical Experiment

Suppose an overall structure is composed of three factors a , b and c , and the direct matrix is given by

$$X_e = \begin{bmatrix} 0 & 2 & 1 \\ 1 & 0 & 0 \\ 0 & 1 & 0 \end{bmatrix}$$

In this structure factors a and b are mutually

influenced, factor c is influenced by factor a , and factor b is influenced by factor c . Therefore, factor b is influenced by factor a both directly and indirectly. The intensity of direct influence is the largest from factor a to factor b .

As the degree of dispatching influences and the degree of central role, we obtained for factor a : 1.85 and 2.80, for factor b : 0.95 and 2.80 and for factor c : 0.65 and 1.30. As for the degree of dispatching influences, factor a is the largest and factor b is the next. Both factors a and b are the central factors, factor a is a cause factor and factor b is an effect factor.

Next, to see the sensitivity of composite importance of each factor with respect to the importance change of some factor, the normalized importance of factor a and b are fixed to 0.1 and that of factor c is changed from 0.1 to 1 with the increment of 0.1.

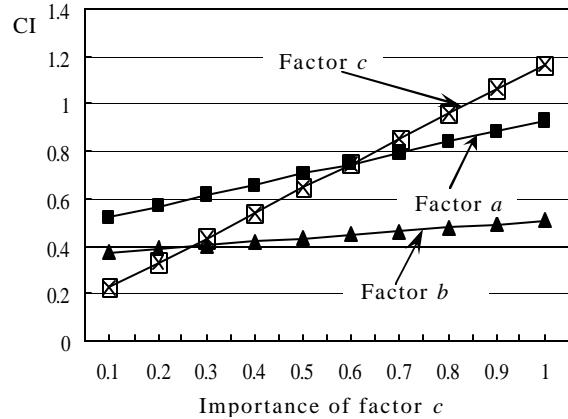


Fig. 1 Sensitivity of Composite Importance CI.

Fig. 1 shows the result for this computation. When the importance of all the factors a , b and c are 0.1, the composite importance for factor a is the largest then for factor b and factor c . This result implies that the composite importance reflects the degree of dispatching influences. When the importance of factor c is increased gradually, the composite importance of each factor is increased gradually and the increment for factor c is the largest. This result implies that the composite importance reflects the importance of each factor. The

reason why the composite importance of factors a and b is increased despite the importance of both factors are fixed, is that by increasing the importance of factor c the composite importance of each factor which will affect factor c is increased. The reason why the increment of composite importance of factor a is larger than for factor b is that the direct/indirect influence from factor a to factor c is larger than from factor b to factor c .

These results show that the composite importance reflects both the amount of interrelation among multiple factors and the importance of each factor, and offers important information to decide the priority of each factor.

3. Structural Modeling of Uneasy Factors by the DEMATEL with Composite Importance

3.1 Data Obtained from the Respondents

We asked respondents to answer two kinds of questionnaire: Questionnaire A and Questionnaire B, for extracting and analyzing uneasy factors in our life. In Questionnaire A we tried to extract the uneasy factors. In Questionnaire B we asked the questions on binary relations on each pair of factors. Questionnaire B is designed based on the factors extracted in Questionnaire A.

In Questionnaire A we asked questions to 42 respondents on the uneasy factors. As the result, we could extract two kinds of factors: one kind is private factors of respondents and the other kind is societal factors. We found that private factors depend upon the respon-

<p>Do you feel uneasy for your career to pursue?</p> <p>1. I feel quite uneasy.</p> <p>2. I feel very uneasy.</p> <p>3. I feel uneasy.</p> <p>4. I do not feel uneasy so much.</p> <p>5. I do not feel uneasy at all.</p>

Fig. 2 An example of questions on the importance of each factor.

dents' social standing: university students, unmarried adults and married adults.

In Questionnaire B the importance of each factor is asked to the respondents by 5-grade evaluation as shown in **Fig. 2** where we adopted 10 people each for university students, unmarried adults and married adults. In this questionnaire the importance of each factor implies the degree of feeling uneasy for each factor. Then, the strength of relation is asked by 3-grade evaluation. In detail, we obtained information on the binary relations between two private factors, between two societal factors and a societal factor to a private factor. **Fig. 3** shows an example of questions on the strength of relation between two factors.

3.2 Structural Models among Uneasy Factors

Structural models for private factors are shown in **Fig. 4** In this figure thick arrow is drawn from factor i to factor j if x_{ij} is greater than or equal to 0.15, thin arrow if x_{ij} is between 0.1 and 0.15, and no arrow if x_{ij} is less than 0.1. Each factor is circled by a thick line if the importance y_i of factor i is greater than or equal to 0.55, by a thin line if y_i is between 0.45 and 0.55, and by a dotted line if y_i is less than 0.45. Under each factor the values of (D_i+R_i) and (D_i-R_i) are shown.

From **Fig. 4** we found the following information for private factors of university students.

- 1) "Ability/character" got the highest $(D-R)$ value, that is, this is the main influence dispatching factor that will affect other factors. This means that by resolving the

<p>How much would it help in order to resolve the uneasiness for pension system by resolving the uneasiness for your career to pursue?</p> <p>1. I think it would help very much.</p> <p>2. I think it would help fairly well.</p> <p>3. I don't think it would help at all.</p> <p>4. I don't know.</p>
--

Fig. 3 An example of questions on the strength of relation between two factors.

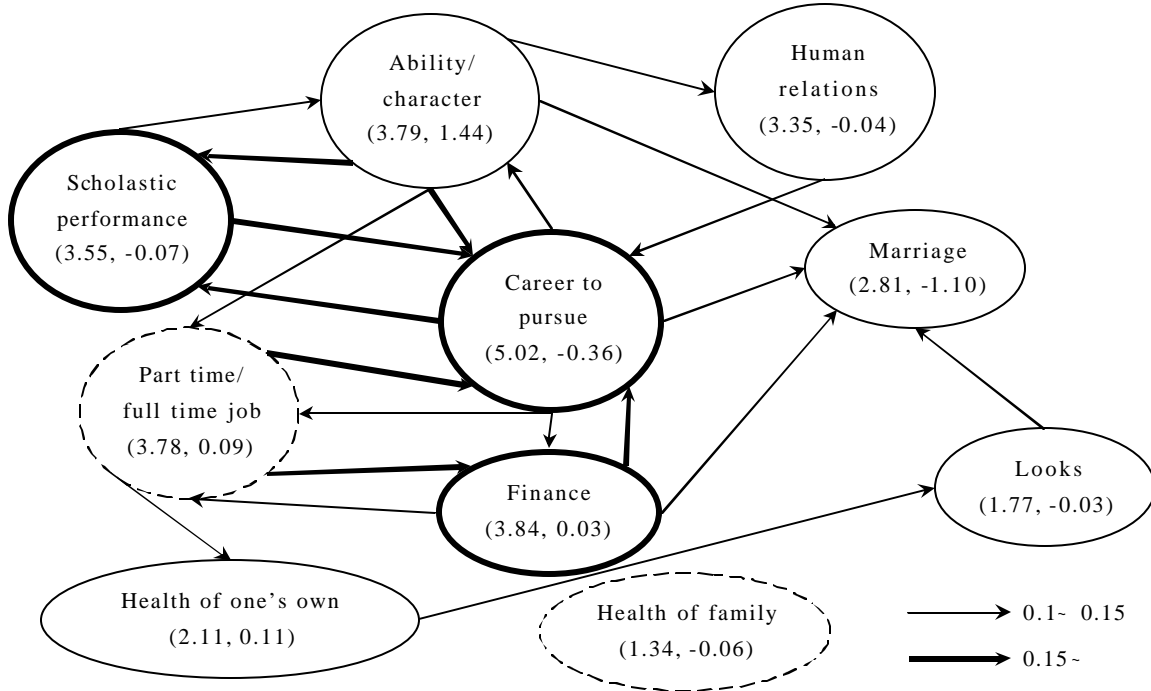


Fig. 4 Structural model for private factor of university students.

uneasiness on “ability/character” the uneasiness on “human relations”, “marriage” and “part time/full time job” will be improved very much. That is, “ability/character” plays central role among many other factors.

- 2) “Marriage” got the lowest ($D-R$) value, that is, this is the main factor of receiving influence from other factors. This means that by resolving the uneasiness on “marriage” it will not affect other factors, but resolving the uneasiness on “career to pursue”, “ability/character”, “looks” and “finance” will help to resolve the uneasiness on “marriage.”
- 3) ($D+R$) value of “career to pursue” is high. This means that “career to pursue” has strong connection with other factors and plays central role. Especially, it will receive big influence from “scholastic performance”, “finance” and “part time/full time job.”
- 4) ($D+R$) value of “health of family” is low. This means that “health of family” is neither an influence dispatching factor nor an influence receiving factor.

3.3 Composite Importance of Each Factor

In 3.2 we obtained structural models of factors that prevent safety and security in our life, and found factors with high ($D+R$) value that play central role, factors with high ($D-R$) value that mainly dispatch influence to the other factors, factors with low ($D-R$) value that mainly receive influence from the other factors, and so forth. However, from these discussions we cannot find effective factors to be resolved in order to create future safe, secure and reliable (SSR) society. For this purpose we evaluated eqn. (2) the composite importance of each factor to be resolved in order to realize SSR society. **Fig. 5** shows the

□ Composite importance ■ Degree of dispatching influence

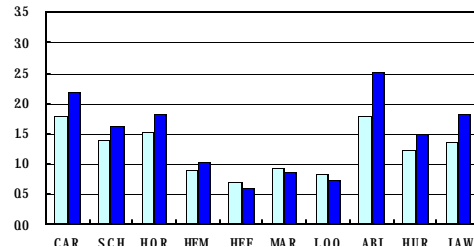


Fig. 5 Composite importance and the degree of dispatching influence.

results obtained for this purpose. In this figure the composite importance and the degree of dispatching influence of each private factor are shown. For university students, the composite importance of “ability/character” and “career to pursue”, is high. Therefore, resolving the uneasiness for these factors is effective to resolve the uneasiness for the other factors for them.

4. Stochastic DEMATEL

4.1 Stochastic Direct Matrix

In the ordinary DEMATEL the direct influence from factor i to factor j is written in the (i,j) element x_{ij} of the direct matrix X . Suppose the structure of the problematique is uncertain and x_{ij} is a random variable. Furthermore, suppose the stochastic parameter values of x_{ij} are different for different pairs of i and j . When each element of the direct matrix is a random variable, each element of the direct/indirect matrix X^f is also a random variable. Furthermore, the composite importance z is also a random variable. Therefore, it is necessary to extend the ordinary DEMATEL to deal with uncertainty in the problem structure. We propose a stochastic DEMATEL in which we could take care of various uncertainties in the problem structure.

In this stochastic DEMATEL it is postulated that we describe the amount of direct influence by expectation and the amount of uncertainty by variance and the shape of distribution. Suppose we got $n \times n$ direct matrix X and the matrix E of probability density function as

$$E = \begin{bmatrix} g_{11}(x|\mathbf{q}_{11}) \cdots g_{1n}(x|\mathbf{q}_{1n}) \\ \vdots & \ddots & \vdots \\ g_{n1}(x|\mathbf{q}_{n1}) \cdots g_{nn}(x|\mathbf{q}_{nn}) \end{bmatrix} \quad (3)$$

where $g_{ij}(x|\mathbf{q}_{ij})$ denotes the probability density function of direct influence from

factor i to factor j , and \mathbf{q}_{ij} denotes the parameters of this probability distribution including expectation and variance of the random variable x_{ij} .

Let G_X be a set of stochastic direct matrices X^s generated by a Monte Carlo method from the direct matrix X with probabilistic information. Then, we obtain

$$G_X = \{X_1^s, X_2^s, \dots, X_t^s\}. \quad (4)$$

In the stochastic DEMATEL we need to collect the information on the variance as well as on the expectation of influence. Possible methods to collect information on variance are as follows:

Method 1: We ask a respondent the best value and the worst value, by asking “How much would it contribute to resolve factor j at most by resolving factor i , and how much would it contribute to resolve factor j at least by resolving factor i ?” From the best value and the worst value we could estimate the variance.

Method 2: We ask multiple respondents on the value of direct matrix and compute the variance from these multiple direct matrices.

Method 3: We combine Method 1 and Method 2. We ask each respondent the best value and the worst value of each element of the direct matrix. Then, we aggregate these data and estimate the variance of each element of the direct matrix.

4.2 Manipulation in Stochastic DEMATEL and Stochastic Composite Importance

We normalize the stochastic direct matrix as

$$X_r^s = I_2 X^s \quad (5)$$

where $I_2 = 1 / (\text{the largest row sum of } X^s)$. Then we obtain

$$X^{sf} = X_r^s + (X_r^s)^2 + \dots = X_r^s (I - X_r^s)^{-1} \quad (6)$$

where X^{sf} denotes a stochastic direct/indirect matrix that has the same property as the ordinary direct/indirect matrix. If we obtain

X^{sf} for all X^s contained in G_X , we obtain a set G_{XF} of stochastic direct/indirect matrix as

$$G_{XF} = \{X_1^{sf}, X_2^{sf}, \dots, X_t^{sf}\} \quad (7)$$

Stochastic composite importance (SCI) is obtained as

$$z^s = y_r + X^{sf} y_r = (I + X^{sf}) y_r. \quad (8)$$

The set G_Z of SCI is obtained as

$$G_Z = \{z_1^s, z_2^s, \dots, z_t^s\}. \quad (9)$$

Furthermore, we could obtain the set of the degree of dispatching, the set of the degree of receiving, the set of the degree of central role and the set of the degree of cause, respectively.

In the DEMATEL with composite importance we could decide the priority of each factor based on the value of composite importance itself. In the stochastic DEMATEL we use three stochastic decision principles as follows:

- (1) **Expectation principle:** We decide the priority based on the expected value or median of SCI.
- (2) **Max-min principle:** We decide the priority of each factor by maximizing the worst value (either 2.5 percentile or 25 percentile) of SCI. This principle reflects a pessimistic decision.
- (3) **Max-max principle:** We decide the priority of each factor by maximizing the best value (either 75 percentile or 97.5 percentile) of SCI. This principle reflects an optimistic decision.

The stochastic DEMATEL could describe the uncertainty of the structure of complex problematique, could describe the uncertainty of priority by SCI and could decide the priority of each factor reflecting the decision makers attitude whether he/she is pessimistic, neutral or optimistic.

4.3 A Simple Numerical Experiment

Suppose the structure of the simple

numerical example shown in 2.3 is uncertain. Suppose besides the information on expectation given by the direct matrix, variance for each element is given by

$$Var_e = \begin{bmatrix} 0 & 0.04 & 0.04 \\ 0.04 & 0 & 0 \\ 0 & 0.04 & 0 \end{bmatrix}$$

where the dispersion of the influence from factor a to factor b is assumed to be relatively small. It is assumed that cutting normal distribution between zero and infinity is assumed for probability density function.

We generated 1,000 elements in a set G_X by using Monte Carlo method. Then, for each element of the set G_X , that is, for each stochastic direct matrix X_i^{sf} ($i=1, 2, \dots, 1000$), we could obtain stochastic direct/indirect matrix and we could constitute a set G_{XF} .

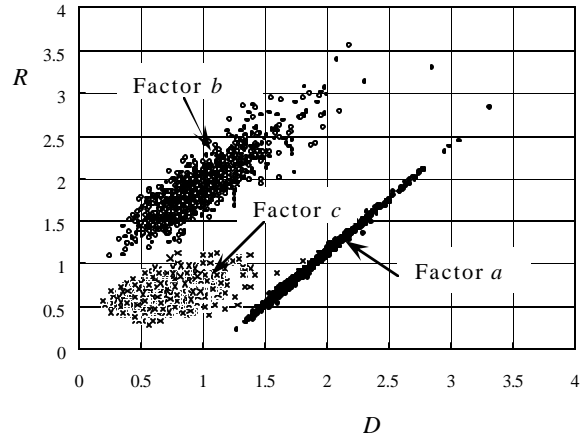


Fig. 6 Degree of dispatching influences and degree of receiving influences.

Fig. 6 shows the degree of dispatching influences and the degree of receiving influences obtained from the stochastic direct/indirect matrices. As seen in this figure the degree of dispatching influences of factor a is big and the degree of receiving influences of factor b is big. As the expectation (and the variance in the parenthesis) of the degree of dispatching influences and the degree of receiving influences we obtained for factor a : 1.8907 (0.0694), 1.0006 (0.1079), for factor b : 0.9936 (0.0966), 1.9064 (0.1167) and for

factor c : 0.6805 (0.0418), 0.6577 (0.0175).

For factor a and factor b we found a big positive correlation between the degree of dispatching influences and the degree of receiving influences especially for factor a . The reason is that for both factors when they affect the other factor, the influence is fed back to themselves directly. On the other hand for factor c since the influence is fed back to itself indirectly, we did not find a big correlation (correlation coefficient = 0.51) between the degree of dispatching influences and the degree of receiving influences.

In Fig. 6 we could draw many lines with gradient -1 . The points on the same line have the same degree of central role, and the point located upper right side has a bigger degree of central role than the points on the line. These lines denote the indifference lines of the degree of central role. By using these indifference lines we could find that factors a and b are the central factors. As the expectations of the degree of central role we found for factors a , b and c : 2.8914, 2.9000 and 1.3382, respectively.

Next, we draw a line passing through the origin with gradient 1 in Fig. 6. Then, the points located lower right side of this line are the “cause” factors and the points located upper left side of this line are the “effect” factors. This fact implies that in every stochastic direct/indirect matrix it is found that factor a is a cause factor and factor b is an effect factor. Factor c is a cause factor or effect factor case by case.

If we compare the degree of dispatching influences, the degree of receiving influences and the degree of central role for ordinary DEMATEL and for stochastic DEMATEL, these values are almost identical. The values for stochastic DEMATEL are slightly larger than those for the ordinary DEMATEL. If we could find a precise probability distribution function and if we could generate infinitely many random numbers precisely, the expectation for both DEMATELs should agree each other in principle.

We found that we could get a proper structural model of a complex problematique

under uncertainty by using the degree of dispatching influences and the degree of central role of the stochastic DEMATEL proposed in this paper.

5. Structural Modeling of Uneasy Factors by Stochastic DEMATEL

We use the data obtained from ordinary consumers and food specialists. For both groups 10 uneasy factors are chosen as follows:

1. Food additive (FAD)
2. Genetic recombined food (GRF)
3. Food forged display (FFD)
4. Agricultural chemical problem (AGC)
5. Imported food (IPF)
6. BSE problem (BSE)
7. Environmental hormones (EVH)
8. Carcinogenic (CAR)
9. Allergic (ALL)
10. Food poisoning (FPO)

Respondents to the questionnaire are 10 ordinary consumers and 10 food specialists. The importance of each factor is asked to the respondents by 5-grade evaluation where the importance of each factor means the degree of feeling uneasy for each factor. Then, the strength of binary relation for each pair of factors is asked by 3-grade evaluation. We look at the binary relation such that “How much would it contribute to resolve uneasy factor j by resolving uneasy factor i ?”

The direct matrix is obtained by averaging the data of 10 people on the strength of binary relations. The data for the importance of each factor are first normalized between 0 and 1 and then averaged for 10 people.

The dispersion of the data of the strength of binary relations obtained from the respondents are used as the variance of the strength of binary relations. This implies that the variations among people would induce structural uncertainty. The shape of the stochastic distribution is assumed to be cutting normal distribution defined on $[0, 1,000,000]$, since the data obtained from

respondents are all positive numbers. The number of stochastic direct matrices generated by random numbers are 1,000.

Structural model for uneasy factors of ordinary consumers is described as follows: The degree of central role for FFD (1.45) is high and FFD has the property of both cause factor and effect factor, but since the degree of cause for FFD (0.55) is positive, FFD is rather a cause factor. Actually, FAD, GRF, IPF, BSE and ALL are greatly affected by FFD.

The degree of central role for FFD (1.45) is the highest, and then IPF (1.33), EVH (1.24), GRF (0.941) and AGC (0.850). These factors are all cause factors. On the other hand CAR, ALL and FPO are completely effect factors. **Fig. 7** shows a structural model of uneasy factors for ordinary consumers.

Fig. 8 shows the degree of dispatching influence, and **Fig. 9** shows the stochastic composite importance (SCI), for ordinary consumer. In these figures, besides expected values, 2.5 percentile and 97.5 percentile data are also shown.

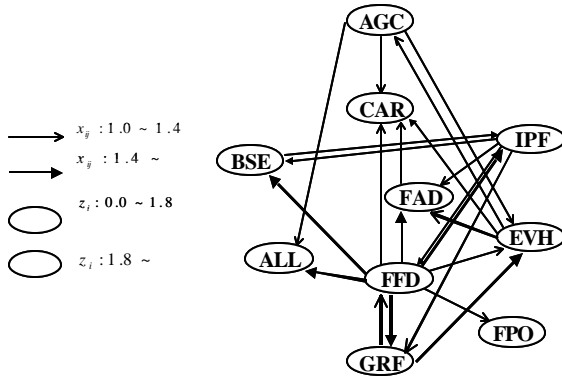


Fig. 7 Structural model of uneasy factors for ordinary consumers.

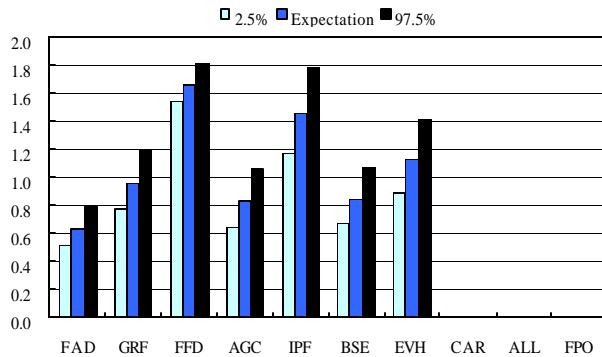


Fig. 8 Degree of dispatching influences for

ordinary consumers.

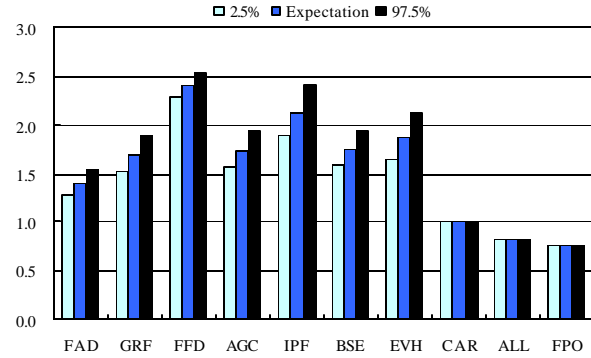


Fig. 9 Stochastic composite importance (SCI) for ordinary consumers.

The priority of uneasy factors to be resolved for ordinary consumers is as follows: FFD, IPF, EVH, BSE, AGC, GRF, FAD, CAR, ALL, FPO. These results are obtained from the computational results of stochastic composite importance.

6. Concluding Remarks

In this paper two revised DEMATEL methods are shown; DEMATEL with composite importance and a stochastic DEMATEL, for structural modeling of complex problematic. The stochastic DEMATEL is obtained by extending the deterministic variables in the DEMATEL with composite importance to random variables. Useful knowledge described in this study is as follows:

- (1) Composite importance could provide useful information for deciding the priority of factors to be resolved.
- (2) Stochastic DEMATEL could extract the characteristics of the structure even when there exist uncertainty in the structure.
- (3) Stochastic composite importance could decide the priority taking into account the attitude of the decision maker towards risk; pessimistic, neutral or optimistic.

It is demonstrated above that the stochastic DEMATEL and the information obtained by the SCI are quite useful for structural modeling of complex problematic.

For further study we need to develop a method of identifying appropriate probability distribution function or we need to develop a non-parametric approach. We also need to develop a method of collecting information on variance. For these purposes we need to experience more empirical analysis of various case studies.

Acknowledgement

This research was supported by the Ministry of Education, Culture, Sports, Science and Technology (MEXT) under Grant-in-Aid for Creative Scientific Research (Project No. 13GS0018).

References

- [1] E. Fontela and A. Gabus, "DEMATEL, Innovative Methods," Report No. 2 "Structural Analysis of the World Problematique (Methods)," Battelle Geneva Research Institute, 1974.
- [2] J.N. Warfield, *Societal Systems – Planning, Policy and Complexity*. New York: Wiley, 1976.
- [3] H. Tamura, ed.: *Large Scale Systems – Modeling, Control and Decision Making*. Tokyo: Shokodo, 1986. (in Japanese)
- [4] K. Akazawa, H. Nagata and H. Tamura: "Structural Modeling of Uneasy Factors for Creating Safe, Secure and Reliable Society," *J. Personal Finance and Economics*, Vol. 18, pp. 201-210, 2003. (in Japanese)
- [5] T. Yamagishi: *From Safe and Secure Society to Reliable Society*. Tokyo: Chukoshinsho, 1999. (in Japanese)
- [6] A. Yuzawa: "A State and Subjects of TMO Conception for City Core Vitalization Countermeasure – A Case Study of Maebashi TMO Conception," *Bulletin of Maebashi Institute of Technology*, Vol. 5, pp. 61-67 (2002).
- [7] I. Kimata: "Synthetic Preliminary Evaluation Analysis on Expectation of a Sewerage Improvement System in a Rural Community using the Decision Making and Evaluation Laboratory Method - Investigation of inhabitant consciousness of a sewerage improvement system (II)," *Trans. of JSIDRE*, Vol. 189, pp. 17-25 (1997). (in Japanese)
- [8] I. Kimata: "Synthetic Comparison Analysis of Inhabitant Consciousness between before and after Rural Community Sewerage Improvement Project in Hilled Rural Area," *Trans. of JSIDRE*, Vol. 213, pp. 119-127 (2001). (in Japanese)
- [9] M. Yamazaki, K. Ishibe, S. Yamashita, I. Miyamoto, M. Kurihara and H. Shindo: "An Analysis of Obstructive Factors to Welfare Service Using DEMATEL Method", *Reports of the Faculty of Engineering, Yamanashi University*, Vol. 48, pp. 25-30 (1997). (in Japanese)
- [10] Y. Zhou, Y. Kawamoto and Y. Honda: "A Study on Systematization of Tourism Development in China", *Mem. Fac. Eng. Fukui Univ.*, Vol. 49, No. 2, pp. 177-184 (2001). (in Japanese)